TESIS DE LA UNIVERSIDAD DE ZARAGOZA

2013

82

María José Clemente Oteo

Synthesis, characterization and study of supramolecular gel materials based on glycoamphiphiles

Departamento
Química Orgánica

Director/es
Fitremann, Juliette
Oriol Langa, Lluis T.

ISSN 2254-7606

Prensas de la Universidad
Universidad Zaragoza

Universidad Zaragoza
1542

Tesis Doctoral

SYNTHESIS, CHARACTERIZATION AND STUDY OF SUPRAMOLECULAR GEL MATERIALS BASED ON GLYCOAMPHIPHILES

Autor

María José Clemente Oteo

Director/es

Fitremann, Juliette
Oriol Langa, Lluis T.

UNIVERSIDAD DE ZARAGOZA

Química Orgánica

2013

SYNTHESIS, CHARACTERIZATION AND STUDY OF SUPRAMOLECULAR GEL MATERIALS BASED ON GLYCOAMPHIPHILES

María José Clemente Oteo

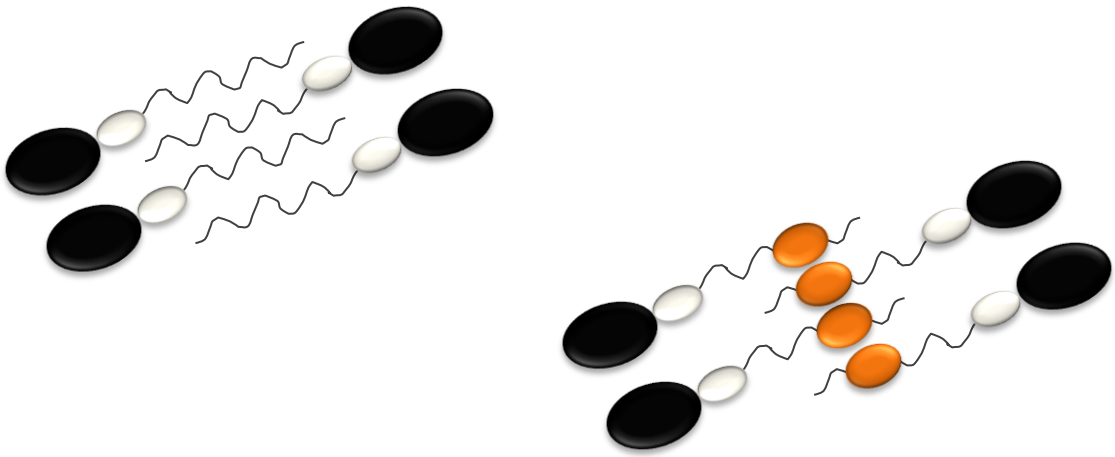

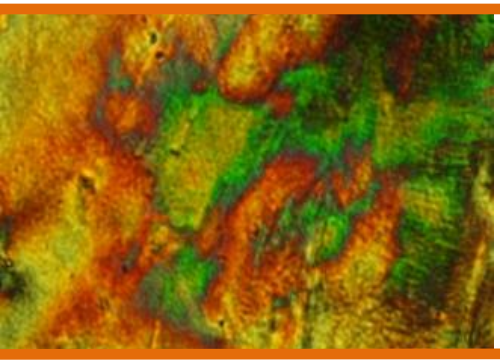

Departamento de Química Orgánica
Facultad de Ciencias-ICMA
Universidad de Zaragoza-CSIC

Departamento de Química Orgánica
Universidad Zaragoza

icma Instituto de Ciencia de Materiales de Aragón

CSIC

TESIS DOCTORAL

SYNTHESIS, CHARACTERIZATION AND STUDY OF SUPRAMOLECULAR GEL MATERIALS BASED ON GLYCOAMPHIPHILES

MARÍA JOSÉ CLEMENTE OTEO

Dpto. de Química Orgánica

Facultad de Ciencias- ICMA

Universidad de Zaragoza-CSIC

Zaragoza, marzo de 2013

Departamento de Química Orgánica
Universidad Zaragoza

icma Instituto de Ciencia de Materiales de Aragón

CSIC

TESIS DOCTORAL

SYNTHESIS, CHARACTERIZATION AND STUDY OF SUPRAMOLECULAR GEL MATERIALS BASED ON GLYCOAMPHIPHILES

Memoria presentada en la Universidad de Zaragoza para optar al grado de doctor

MARÍA JOSÉ CLEMENTE OTEO

Dpto. de Química Orgánica

Facultad de Ciencias- ICMA

Universidad de Zaragoza-CSIC

Zaragoza, marzo de 2013

Dr. LUIS T. ORIOL LANGA, Profesor Titular del Departamento de Química Orgánica perteneciente a la Facultad de Ciencias y al Instituto de Ciencia de Materiales de Aragón de la Universidad de Zaragoza-CSIC y Dra. JULIETTE FITREMANN chargée de recherche au CNRS,

HACEN CONSTAR:

Que el trabajo original titulado "SYNTHESIS, CHARACTERIZATION AND STUDY OF SUPRAMOLECULAR GEL MATERIALS BASED ON GLYCOAMPHIPHILES" ("Síntesis, caracterización y estudio de materiales derivados de moléculas basadas en azúcares para la formación de geles supramoleculares"), ha sido realizado bajo nuestra supervisión por Dña. MARÍA JOSÉ CLEMENTE OTEO en el Departamento de Química Orgánica de la Facultad de Ciencias y el Instituto de Ciencia de los Materiales de Aragón de la Universidad de Zaragoza-CSIC y en el laboratoire des IMRCP, Université Paul Sabatier y reune las condiciones para su presentación como tesis doctoral.

Zaragoza, a de marzo de 2013

Fdo: Dr. Luis T. Oriol Langa Fdo.: Dra. Juliette Fitremann

Departamento de Química Orgánica
Universidad Zaragoza

icma Instituto de Ciencia de Materiales de Aragón

CSIC

TRIBUNAL DESIGNADO PARA LA DEFENSA

DOCTORANDO: Dña. **María José Clemente Oteo**

TÍTULO DE LA TESIS: **SYNTHESIS, CHARACTERIZATION AND STUDY OF SUPRAMOLECULAR GEL MATERIALS BASED ON GLYCOAMPHIPHILES** ("Síntesis, caracterización y estudio de materiales derivados de moléculas basadas en azúcares para la formación de geles supramoleculares")

PRESIDENTE

SECRETARIO

VOCAL 1

VOCAL 2

VOCAL 3

SUPLENTE 1

SUPLENTE 2

El tribunal designado para calificar la Tesis Doctoral arriba indicada y reunido en la fecha indicada, una vez efectuado el acto de defensa por el doctorado, ha otorgado la calificación de:

En Zaragoza, a de de 2013

A mi familia

AGRADECIMIENTOS

Para el lector de esta tesis estas primeras páginas suponen el principio, sin embargo, para mí suponen el momento de volver la vista atrás a todos estos años de trabajo y esfuerzo y por ello quiero agradecer muy sinceramente la ayuda y colaboración prestadas por todas aquellas personas que han hecho posible no sólo el desarrollo de esta investigación sino también mi formación personal durante esta etapa de la vida.

En primer lugar he de dar las gracias a mis directores de tesis. Muchas gracias Luis Oriol por estar dispuesto a darme la oportunidad y la ayuda necesarias para no tirar por el "camino fácil" y hacer frente a las dificultades que han surgido durante este camino, he aprendido mucho. Gracias por dedicar tiempo a discutir en mis mil llamadas al despacho, por frenarme cuando los mares de dudas me asaltaban y hacerme ver que hay que "echar para adelante". Merci beaucoup Juliette Fritemann pour ton accueil dans mes premiers pas dans la thèse et aussi dans un pays étranger. Je voudrais te remercier pour ta patience et ton engagement.

En segundo lugar, quisiera agradecer a José Luis Serrano, director del grupo de Cristales Líquidos y Polímeros (CLIP), y a Monique Mouzac, directora del grupo des Polymères et organisation multi-échelles (POME), la posibilidad de haber formado parte de dos grupos de investigación en la Universidad de Zaragoza y en la Universidad Paul Sabatier de Toulose. En ambos casos ha sido una gran experiencia formativa.

Merci a tous les membres du IMRCP, en spécial au groupe POME (Anne Fraçoise, Barbara, Lacra, Elisabeth, Roland…), je garde un très bon souvenir de mon stage à Toulouse. También me gustaría dar las gracias a los españoles y demás amigos que allí conocí (Mar, Sheila, Alex, Olaia, Rita…) porque vosotros hicisteis que el salir de casa fuera un poquito menos duro.

Quisiera extender mi agradecimiento a los miembros del grupo CLIP, a Pilar Romero por estar siempre dispuesta a compartir su experiencia en RMN para resolver los sudokus de los azúcares, a Rosa Tejedor por su estimable ayuda con los geles azoicos, a Joaquín Barberá por su ayuda con los rayos X, a Blanca Ros por ser la profesora que guió mis primeros pasos en la química orgánica y al resto, porque ninguno os habéis librado de mis preguntas, gracias por intentar solucionarlas. Esto también es extensible al departamento porque más allá de nuestro grupo también he buscado ayuda.

Llega el momento de agradecer a los cristaleros, mis compañeros de laboratorio, por todo lo vivido en estos años, las risas, las conversaciones, en general todos los buenos momentos de viajes, cenas, cumpleaños, cines, jueves gastronómicos, deportes, bodas …etc (¡son tantos que no me caben!) y también por qué no, de las lágrimas, de los malos momentos y las dificultades, porque gracias a ellos ahora soy más fuerte.

Emma, has sido para mí como una hermana mayor tanto en nuestra aventura por Toulouse como aquí en Zaragoza, gracias por abrirme los ojos de vez en cuando y enchufarme dosis de energía positiva. Lucía, has sido una amiga, en lo bueno y en lo malo, gracias por todo lo compartido, que es mucho. Neli, gracias por tu iniciativa y tus ánimos especialmente en esta última etapa, Mada y Eva, habéis sido para mí un gran apoyo tanto en el laboratorio como fuera de él, Jordi, por aguantar mis gritos y por las bromas, Marta, quedan por delante muchos viajes por hacer…y a toda la gente de ciencias… por la desconexión en el laboratorio, comiendo y en el café (Melisa, Miguel C., Hugo, Ismael, Pedro…).

A las chicas INA… Isabel, por nuestras tertulias sobre geles y no geles, Julie y Lara, por vuestras conversaciones siempre interesantes y los momentos de deporte, Elisabetta por hacerme un hueco en tu casa en nuestro viaje a Italia. Alex y Eva G, por acogerme tan bien en mis excursiones allí. Un recuerdo para aquellos antiguos miembros del grupo que me ayudaron en los primeros momentos, cuando empecé siendo una TAD (Ana, Paco, Jesús…), también para los nuevos (Alberto, Bea, Jose…). Además quiero acordarme de aquellos que pasaron por el grupo y que aunque continuaron su camino, me regalaron su amistad (Carmina, Miguel L., Silvia, Theresa, Judith, Susana, Sara, André…).

Agradezco los estudios de microscopía realizados en el Servicio de Microscopia de la Universidad de Zaragoza y en el Laboratorio de Microscopía Avanzada (LMA) en el INA (Instituto de Nanociencia de Aragón) y las medidas realizadas de calorimetría.

A mis amigos y familia por vuestro apoyo fuera del trabajo. Laura siempre dispuesta a escucharme, Susana con su incondicional sonrisa, Rebeca, que aunque estés lejos y pase el tiempo, siempre serás una gran amiga y también al resto de vosotros. A mis compañeros de carrera (Raquel, Caco, Ramón, Cristina…) por esa gran época de estudiante.

A mi padre y mi abuela, que aunque ya no estaban en esta etapa de mi vida seguro que estarían muy orgullosos de su pequeña, a mi madre, que sí que ha estado a mi lado y me ha cuidado siempre, cuando lo necesitaba y cuando no. A mi hermana y mi cuñado, gracias por vuestra ayuda y compañía y sobre todo a mis sobris, que son los que siempre me hacen sonreír y a los que quiero con locura.

Gracias a todos por aportar vuestro grano de arena a esta gran montaña, que para mí ha sido esta tesis.

Finalmente, quiero agradecer la financiación económica que ha hecho posible la realización de este trabajo: al Fondo Social Europeo (Early Stage Research Nanotool Project, Marie Curie Actions program), al Fondo Europeo de Desarrollo Regional (FEDER) y al Gobierno de Aragón (proyecto MINECO MAT2011-27978-C02-01).

“Soy de las que piensan que la ciencia tiene una gran belleza. Un sabio en su laboratorio no es solamente un teórico, es también un niño colocado ante los fenómenos naturales que le impresionan como un cuento de hadas. No debemos creer que todo progreso científico se reduce a mecanismos, máquinas y engranajes, que de todas maneras, tienen su belleza propia. Tampoco creo que peligre en nuestro mundo la desaparición del espíritu de aventura. Si veo a mi alrededor algo vital es precisamente este espíritu de aventura emparentado con la curiosidad.”

Marie Curie (1867-1934)

“Ella está siempre en el horizonte. Me acerco dos pasos, ella se aleja dos pasos, camino diez pasos, y el horizonte se mueve diez pasos más allá. Por mucho que yo camine, nunca la alcanzaré. ¿Para qué sirve la utopía? para eso sirve, para caminar.

Eduardo Galeano (1940)

ÍNDICE

INTRODUCCIÓN

Este trabajo es fruto de una colaboración entre la Universidad Paul Sabatier y la Universidad de Zaragoza. El grupo de Toulouse tenía experiencia en materiales blandos, y en particular en derivados de sacarosa que habían mostrado su tendencia al autoensamblado y generación de geles supramoleculares. Por otro lado, la experiencia en materiales con fotorrespuesta derivados de azobenceno del grupo de Zaragoza se podía aprovechar para dotar a dichos materiales de una funcionalidad añadida. Con este primer objetivo compartido se diseñaron una serie inicial de glicolípidos basados en sacarosa que posteriormente fueron ampliándose a otros disacáridos. Con la experiencia adquirida en los mismos, y particularmente en los procedimientos sintéticos, se diseñó posteriormente una serie de materiales análogos que contienen azobenceno en su estructura y se estudió la fotorrespuesta. Constituyen una nueva línea de investigación en el grupo de cristales líquidos y polímeros, que había trabajado habitualmente en azopolímeros, y en menor extensión en compuestos de baja masa molecular, estos últimos con una estructura orgánica no anfífila, típica de cristales líquidos.

De acuerdo a esta sinergia surgió esta tesis doctoral que se ha desarrollado tanto en Toulouse como en Zaragoza, y que se presenta para optar a la mención de doctorado europeo. Como consecuencia, y de acuerdo a la normativa vigente de la Universidad de Zaragoza, la tesis ha sido escrita tanto en castellano como en inglés, idioma este que se ha utilizado para todos los capítulos de resultados y discusión obtenidos en los diferentes tipos de materiales estudiados.

La memoria se ha estructurado en los siguientes capítulos: geles supramoleculares basados en glicolípidos derivados de disacáridos y ácido palmítico, geles supramoleculares basados en glicoanfífilos derivados de azobenceno y estudio de moléculas anfífilas basadas en polietilenglicol y azobenceno.

1. ANTECEDENTES

1.1. Geles

1.1.1. *Definición y clasificación*

Los materiales blandos de tipo **gel**, no son sólo materiales interesantes por estar presentes en nuestra vida cotidiana en forma de cosméticos, alimentos, pinturas, adhesivos… etc. (**Fig. 1.1**) sino también por ser objeto de numerosos estudios estructurales así como de investigación para su aplicación en diferentes áreas tecnológicas.[1]

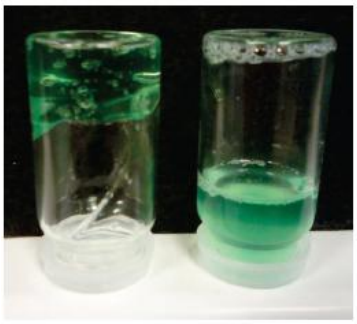

Fig. 1.1: Fotografía de un gel comercial usado como cosmético (izquierda) y transición de estado gel a sol al añadir NaCl (derecha).

Flory, describió en 1974 los geles como unas estructuras continuas con dimensiones macroscópicas que son permanentes en la escala del tiempo y que desde un punto de vista reológico se comportan como un sólido,[2] pero la creciente actividad investigadora en los últimos años en este campo y la posibilidad de clasificar los mismos en varias subclases, ha hecho que surjan numerosas y diversas explicaciones sobre qué es un gel. De hecho varios autores han comentado que un gel es más fácil de reconocer que de describir. Así podemos encontrar definiciones desde las más elaboradas, "los geles son estructuras viscoelásticas formadas por una red entrecruzada tridimensional y un disolvente, el cual es el componente mayoritario; la apariencia sólida del gel es el resultado de la oclusión y la adhesión del líquido en la superficie de la matriz sólida tridimensional; la formación de esta matriz es el resultado del entrecruzamiento de fibras poliméricas formadas a partir de la unión de las moléculas mediante interacciones físicas o químicas"[3], hasta las más simples, "si tiene apariencia de gelatina y al dar la

vuelta al recipiente donde se encuentra son capaces de mantener la forma bajo el estrés de su propio peso, es decir, no cae, se trata de un gel".[4]

Los geles, se pueden organizar atendiendo a diversos factores[3] (**Fig. 1.2**). Así se pueden clasificar según su origen, si se obtienen de recursos naturales o se sintetizan en el laboratorio; según su constitución, si son macromoleculares, es decir, que están constituidos por macromoléculas o si son supramoleculares. Los **geles de tipo supramolecular**, son aquellos que se forman por el auto-ensamblaje de moléculas de bajo peso molecular y son de los que nos ocuparemos a lo largo de este trabajo. Dentro de los geles macromoleculares, atendiendo al tipo de fuerza que dirige el entrecruzamiento se pueden especificar los geles de naturaleza covalente o no covalente. En los geles supramoleculares sólo existe el último tipo de entrecruzamiento, es decir, no covalente. Según el medio en el que se forman, se pueden obtener **organogeles**, si el disolvente usado es de naturaleza orgánica, **hidrogeles**, si el disolvente es agua o aerogeles, en el caso de que el medio sea un gas. Finalmente es posible obtener xerogeles, cuando el medio ha sido eliminado. Existen también moléculas gelificantes, llamadas gelificantes anfífilas, que son capaces de formar geles tanto en disolventes orgánicos como en agua.

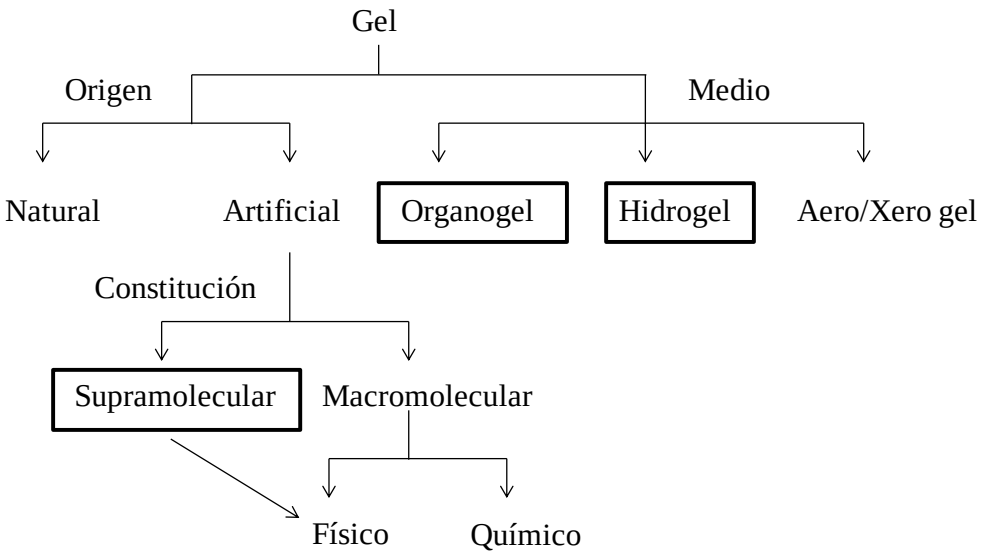

Fig. 1.2: Clasificación de los geles; **Ref [3].**

Los geles también se pueden clasificar según su estructura en diferentes subclases. Flory sugiere cuatro categorías:[2]

- Aquellos cuya estructura es lamelar bien ordenada (por ejemplo fosfolípidos).
- Aquellos formados por el entrecruzamiento covalente y desordenado de una red polimérica hinchada por un disolvente (por ejemplo resinas fenólicas y caucho).
- Aquellos formados por el entrecruzamiento de una red polimérica donde la interacción entre las cadenas no es covalente y existen regiones con cierto orden local (por ejemplo gelatinas).
- Aquellos formados a partir de estructuras donde la red está formada por fibras sin ningún orden.

Generalmente, los **geles supramoleculares** se incluyen dentro de este último tipo, los cuales se forman a partir de moléculas de bajo peso molecular (LMOGs: *Low Molecular Mass Organic Gelators*, con masa molar inferior a 3.000)[5] y que se auto-organizan en una red de forma fibrilar (SAFINs: *Self-Assembled Fibrillar Networks*).[6] Lo que caracteriza a estos geles es que la unión de sus moléculas gelificantes se produce mediante **interacciones de tipo no covalente**, como son los enlaces de hidrógeno, las interacciones π-π, interacciones dador-aceptor, fuerzas solvófobas, fuerzas de van der Waals… etc y pueden ser entendidos como "polímeros supramoleculares"[7] ya que están constituidos por unidades monoméricas que se ensamblan mediante interacciones secundarias direccionales y reversibles. Esta reversibilidad supone una ventaja frente a los geles formados con interacciones covalentes ya que se puede pasar de un estado fluido a un estado no fluido mediante la influencia de un estímulo externo, como por ejemplo, la temperatura, el pH o la luz.[3, 8]

Estos geles supramoleculares están teniendo en los últimos años una gran proyección de futuro por un doble interés. Por un lado, porque su estudio puede llegar a permitir comprender la estructuración fundamental de los agregados que se forman a diferentes escalas. Por otro, por sus posibles **aplicaciones tecnológicas**, como por ejemplo, en la liberación controlada de fármacos, la formación de plataformas para la regeneración de tejidos y la captura de partículas contaminantes.[9]

Las propiedades y caracterización de un gel dependen de varios factores como el modo de preparación, la temperatura de gelificación, el tiempo que permanecen estables, la

concentración de gelificante o ciertos criterios reológicos.[6] En cuanto a la forma de preparación, se han seguido distintos protocolos, como por ejemplo, calentar la mezcla del compuesto y del disolvente hasta completa disolución y posteriormente enfriar lenta o bruscamente hasta temperatura ambiente o incluso el uso de ultrasonidos para conseguir el gel. La **temperatura de transición gel-sol** ($T_{gel-sol}$), es la temperatura por encima de la cual se produce la rotura de los agregados auto-ensamblados y se obtiene un sistema fluido, por debajo de la misma se produce la gelificación. En cuanto a la estabilidad de los geles puede ser muy variada; existen ejemplos de geles que sólo son estables durante unas horas, mientras que otros pueden serlo durante años. La **concentración crítica de gelificante**, normalmente se expresa en porcentaje en peso en relación con el disolvente y da información de la mínima cantidad de moléculas capaces de atrapar la máxima cantidad de disolvente. Los **criterios reológicos** que se estudian dan idea de la viscosidad y viscoelasticidad del material, atendiendo a las magnitudes del módulo elástico G´ y el módulo viscoso G´´, pero no siempre es evidente asignar modelos teóricos y por lo tanto, es difícil predecir su comportamiento, ya que depende fuertemente del tipo de gelificante.

1.1.2. *Organización jerárquica de los geles*

El **auto-ensamblaje** de las moléculas para la formación de la red entrecruzada se produce mediante una aproximación *"bottom-up"*[10], donde los bloques (que son las moléculas) dan lugar a las organizaciones supramoleculares (que son las fibras) y como resultado, las propiedades del material final son diferentes a las de los bloques constituyentes.

Las propiedades macroscópicas del gel van a estar determinadas por la nano y micro-estructura de la red fibrilar. Para entender mejor el mecanismo de formación de un gel, Hamilton y Estroff, lo asemejan a una proteína, al fragmentar la red tridimensional en estructura primaria, secundaria y terciaria.[4]

En la **estructura primaria**, la escala considerada es de amstrongs a nanómetros y determina la interacción anisótropa en una o dos dimensiones, a un nivel molecular. A la hora de diseñar moléculas que sean capaces de gelificar, se ha de tener en cuenta que son necesarios en la estructura grupos que proporcionen interacciones de tipo no covalente, como son los enlaces de hidrógeno, por ejemplo a través de un grupo amida,

interacciones por empaquetamiento π-π o grupos cargados para provocar interacciones iónicas.[5c]

En la **estructura secundaria**, la escala considerada es de nanómetros a micrómetros y define la morfología de los agregados formados por autoensamblaje. Dependiendo de la estructura de la molécula y de variables como la concentración, pH, fuerza iónica… se obtienen diferentes agregados que construirán la estructura fibrilar entrecruzada y serán los que proporcionen rigidez a la misma. Para explicar el paso de estructura primaria a secundaria se han desarrollado varios modelos donde se describe el auto-ensamblaje que tiene lugar, como los que se explicarán a continuación.

Los geles supramoleculares, en la mayoría de los casos, están formados por **moléculas anfífilas**, es decir, aquellas que tienen una parte hidrófila bien diferenciada de una parte hidrófoba, que son capaces de formar distintos agregados en el disolvente. Para el estudio de la agregación en agua de moléculas anfífilas, Israelachivili[11] y sus colaboradores establecieron un parámetro *p*, llamado de empaquetamiento, atendiendo a la estructura de la molécula. En él se relaciona el área de la cadena hidrófoba con el área de la cabeza hidrófila, $p=v/a_o l$ (a_o es el área de la cabeza hidrófila, l la longitud efectiva de las cadenas hidrófobas y v es el volumen de las cadenas hidrófobas). El valor de *p* está relacionado con la morfología de los agregados como se puede ver en la **Fig. 1.3**.

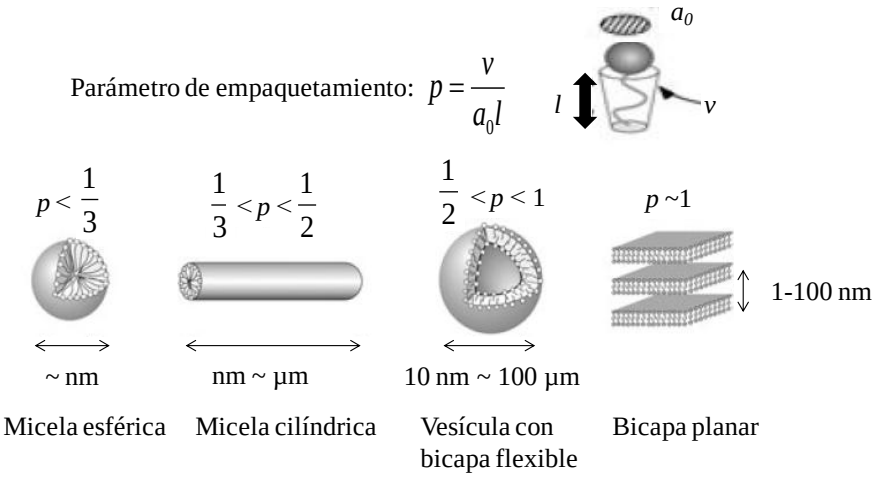

Fig. 1.3: Parámetro de empaquetamiento en moléculas anfífilas definido por Israelachivili; **Ref [12].**

Es importante señalar que pequeñas variaciones en la estructura de la molécula pueden inducir a grandes cambios de morfología. Este parámetro es útil para describir por qué una familia de moléculas se ensambla en forma de ciertos agregados. Sin embargo, es difícil predecir la morfología de los agregados de una molécula particular ya que este parámetro *p*, depende de la estructura molecular, pero además influyen en la forma de empaquetarse, otros factores, como el medio en el que se encuentra, la temperatura, el pH, la salinidad y la concentración.[12]

En el siguiente modelo, véase la **Fig. 1.4**, se representan mediante flechas posibles rutas de interconversión entre las distintas morfologías dependiendo de la concentración, el pH, la fuerza iónica…etc.

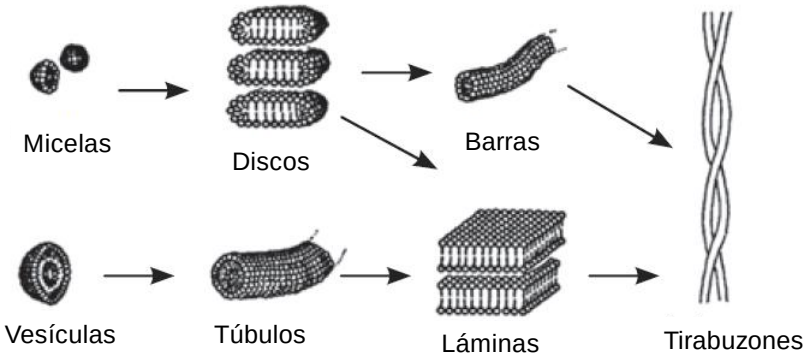

Fig. 1.4: Representación esquemática de los posibles agregados que pueden formarse en disolución mediante procesos de autoensamblaje; **Ref [4, 13].**

Si las moléculas anfífilas están basadas en nucleótidos, azúcares o péptidos, debido a la **quiralidad** de estas cabezas, se obtienen agregados helicoidales. Se han propuesto varios modelos para la formación de helicidad pero la más aceptada es aquella en la que las moléculas se empaquetan unas con otras con un ligero ángulo entre ellas, véase la **Fig. 1.5**.[14]

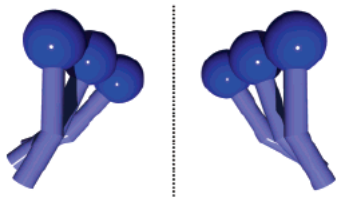

Fig. 1.5: Representación esquemática que muestra el ensamblaje molecular, en el cual, las moléculas se empaquetan con un ángulo distinto de 0 con respecto a su vecino más próximo; **Ref [14].**

Dentro de la variedad de agregados quirales, la mayoría de los descritos en la bibliografía pueden clasificarse en dos morfologías, cintas torsionadas (*"twisted ribbons"*) y cintas helicoidales (*"helical ribbon"*), dependiendo del ángulo de giro estas pueden dar lugar a nanotubos, véase la **Fig. 1.6**. En ocasiones no es fácil distinguir entre las dos morfologías.

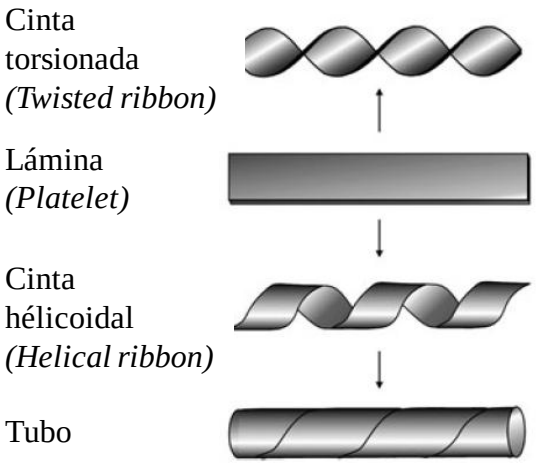

Fig. 1.6: Representación de la formación de cintas torsionadas, helicoidales y nanotubos; **Ref [14].**

Un modelo muy conocido es el propuesto por Boden y sus colaboradores,[15] donde utilizan como base la organización de las proteínas para explicar el autoensamblaje de

un hidrogelificante peptídico cuya morfología depende de la concentración, veáse la **Fig. 1.7**.

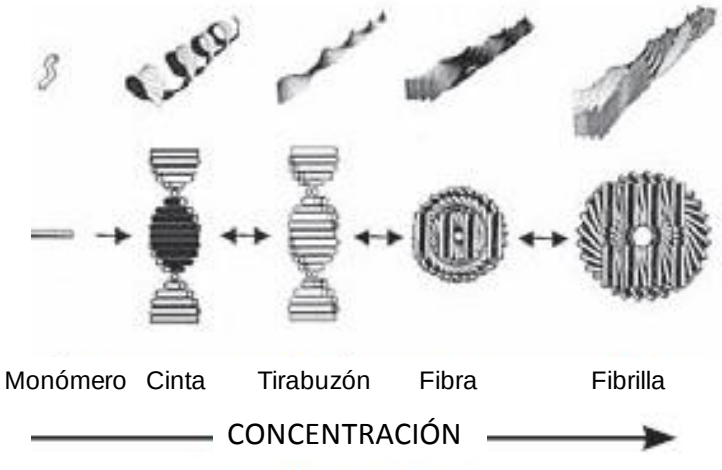

Fig. 1.7: Dependencia de la morfología con la concentración de un hidrogelificante de tipo varilla quiral; **Ref [15].**

Sin embargo, pese a los numerosos estudios físicos y matemáticos, todavía no se conoce bien la relación que existe en la combinación entre las partes hidrófobas e hidrófilas de una molécula para predecir el tamaño del agregado formado por el autoensamblaje ni tampoco se conoce bien la relación existente entre la quiralidad molecular y la quiralidad supramolecular.

En la **estructura terciaria**, la escala considerada es de micrómetros a milímetros y determina la interacción entre los agregados, es decir, el entrecruzamiento que da lugar a la red fibrilar tridimensional. Aquí son importantes los nodos necesarios para la estabilidad del gel y el grado de homogeneidad de los poros.

En resumen y tal y como se ha mencionado, los detalles de los modelos de formación de las estructuras fibrilares no están del todo claros, pero según diversos autores, el proceso de gelificación puede considerarse como una **agregación jerárquica**. Steed y sus colaboradores explican que esta organización consta de los siguientes pasos:[1]

1. Asociación de las moléculas individuales.
2. Formación de oligómeros por interacción entre las moléculas.

3. Formación de fibrillas de anchura molecular por extensión de los oligómeros.
4. Formación de fibras por la unión de varias fibrillas.
5. Interacción de las fibras en una red interconectada.
6. Inmobilización del disolvente en la red fibrilar, normalmente por efectos de la tensión superficial.

1.1.3. *Estructuras fibrilares autoensambladas quirales*

Como hemos visto en el apartado anterior, los geles están formados por la interconexión de estructuras fibrilares. Estas estructuras pueden finalmente formar macroscópicamente el gel o llegar a precipitar. Así pues, estudiar las fibras puede ayudar a comprender mejor la estructura del gel.

La preparación de las estructuras fibrilares es un procedimiento delicado debido a la naturaleza dinámica de la agregación supramolecular. Así mismo, la formación de las estructuras fibrilares para dar lugar a los geles también es importante. En los geles formados por estructuras fibrilares (tipo SAFIN), las características macroscópicas pueden depender de la forma de preparación. La gelificación es además, fuertemente dependiente de la concentración y la temperatura. Con una mayor concentración de gelificante, se pueden formar estructuras más sólidas, por el contrario con mayores temperaturas no se favorece la formación del gel, si no que se favorece el desorden individual de las moléculas y no la formación del agregado.[12]

La preparación y caracterización de estructuras fibrilares ha sido un tema muy estudiado, con especial interés en el caso de la existencia de **helicidad**.[10, 14] Las nanofibras helicoidales surgen de la agregación en una dimensión, poseen un diámetro nanométrico y una longitud mayor, incluso de micras. Además tienen helicidad supramolecular. Los monómeros pueden organizarse de una manera helicoidal en una fibra polimérica, pero también la fibra puede poseer helicidad por sí misma y estas dos helicidades no tienen por qué ser la misma.[10]

La helicidad se estudia mediante la combinación de distintas técnicas espectroscópicas y microscópicas, como dicroísmo circular (DC), microscopía electrónica de barrido (SEM) y de transmisión (TEM y cryo-TEM) y microscopía de fuerza atómica (AFM), que serán comentadas más adelante. Es esencial la combinación de estas técnicas

porque en ocasiones se pueden encontrar casos en los que no hay señal de DC mientras que en las técnicas microscópicas se observa cierta torsión, esto es debido a que la muestra puede contener una mezcla racémica de las dos helicidades.[16] Además, se pueden encontrar ejemplos de moléculas aquirales que pueden formar agregados fibrilares quirales[17] y casos en los que un sólo enantiómero da lugar a la mezcla de ambas hélicidades.[18]

Si bien es cierto que la relación entre la quiralidad molecular y la quiralidad supramolecular no está siempre clara, en general, la dirección de la fibra quiral está directamente relacionada con la quiralidad molecular, esto es, si un enantiómero forma hélices dextrógiras, normalmente, el otro forma hélices levógiras. Cuando se estudia el racemato, se pueden obtener agregados fibrilares con la mezcla de ambas helicidades[19] o también se pueden formar otro tipo de agregados. Este último caso, como se muestra en la **Fig. 1.8**, ocurre con un oligopéptido basado en lisina donde, en el racemato, se observan agregados globulares.[20] Normalmente en el racemato se suprime la capacidad de gelificación.[5c]

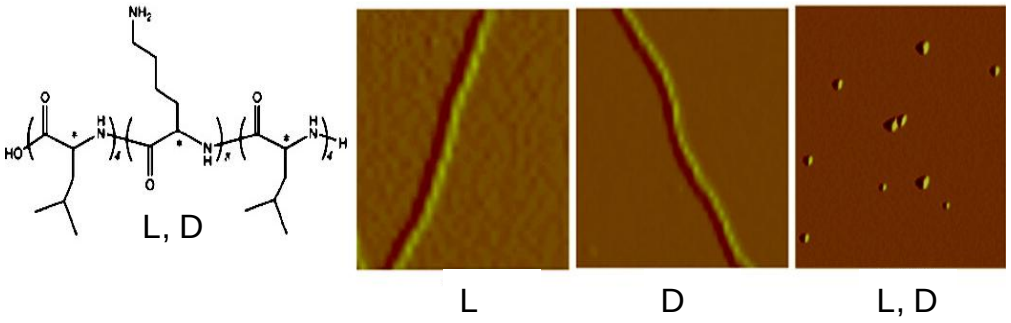

Fig. 1.8: Fotografías de AFM donde un oligopéptido con segmentos L-(lisina)$_8$ forma hélices levógiras, D-(lisina)$_8$ forma hélices dextrógiras y la mezcla racémica 1:1 no forma hélices sino agregados globulares; **Ref [20].**

También se ha estudiado la transferencia de quiralidad de una molécula quiral (sargento) que dirige la agregación quiral de otras (soldados) para la formación del agregado y el gel.[21]

1.1.4. *Moléculas gelificantes*

Normalmente, las **moléculas** de bajo peso molecular **capaces de gelificar** son aquellas que al encontrarse en una solución de un disolvente adecuado, en una concentración baja, que puede llegar a un valor mínimo de 0.1 % en peso aunque suele ser superior, se produce la agregación supramolecular y la correspondiente formación de una red fibrilar con propiedades macroscópicas de gel.

El número de moléculas que se pueden encontrar descritas en bibliografía capaces de gelificar es elevado y en muchas ocasiones, la obtención de los geles se ha producido de una manera accidental. Pese a la variedad estructural, las moléculas que servirán como piezas de construcción para la red cumplen una serie de características según Smith.[22]

1. Las moléculas han de ser parcialmente solubles en el disolvente elegido, pero no demasiado porque si no se solubilizarían.
2. Las moléculas han de ser parcialmente insolubles en el disolvente elegido, pero no demasiado porque si no precipitarían.
3. Las moléculas han de ser capaces de formar múltiples interacciones no covalentes entre ellas:

   En el caso de los organogeles, enlaces de hidrógeno e interacciones π-π.

   En el caso de los hidrogeles, enlaces de hidrógeno e interacciones hidrófobas.
4. Las interacciones no covalentes han de ser direccionales permitiendo el ensamblaje de la red de una forma anisótropa a escala nanométrica.

Existen ciertos grupos funcionales que normalmente se encuentran en las moléculas que gelifican y que favorecen la formación de interacciones no covalentes como son amidas y ureas, que tienen la capacidad de formar enlaces de hidrógeno; carbohidratos, que contienen múltiples grupos OH capaces también de formar enlaces de hidrógeno; esteroides y ácidos biliares que poseen superficies hidrofóbas; ácidos nucleicos, que forman interacciones π-π además de enlaces de hidrógeno, y largas cadenas alquílicas, que promueven interacciones van der Waals.

A continuación se describen distintos ejemplos de **moléculas gelificantes** como formadoras tanto de organogeles como de hidrogeles.

1.1.4.1. *Moléculas gelificantes que forman organogeles*

Al existir un amplio rango de estructuras químicas para los gelificantes, Weiss y Terech, realizaron una primera descripción de los **organogeles** supramoleculares donde agruparon las moléculas según su naturaleza química en diferentes categorías (de una manera subjetiva como comentan los propios autores):[5b]

- Derivados de **ácidos grasos**:

Son compuestos que derivan de ácidos grasos y por tanto, con largas cadenas alifáticas. Por ejemplo, el ácido 12-hidroxioctadecanoico (**Fig. 1.9**) y sus sales (como la de litio) se han usado durante décadas en la industria de los lubricantes ya que la red que forman estas moléculas es capaz de atrapar el aceite evitando la fricción en superficies metálicas.[23] Las estructuras formadas son helicoidales con helicidad levógira en el caso del D-ácido y con helicidad dextrógira en el caso del L-ácido. Las sales divalentes y trivalentes también se han usado en la industria de los lubricantes.

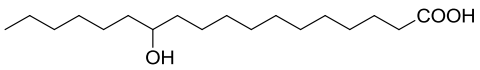

Fig. 1.9: Estructura química de 12-Hidroxioctadecanoico.

- Derivados de **esteroides** y derivados de esteroides con anillos aromáticos condensados:

El primer gelificante basado en esteroides, capaz de gelificar en hidrocarburos, fue descubierto por casualidad en el transcurso de una síntesis y es un radical libre, derivado de isoandrosteronas[24] (**Fig. 1.10**). La capacidad de gelificación varia con la funcionalización e insaturación en distintas posiciones, así se han obtenido varios gelificantes modificando el esteroide.

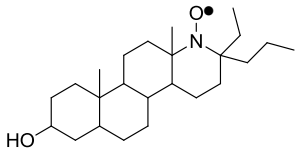

Fig. 1.10: Estructura química de un derivado de isoandrosteronas.

Así son capaces de gelificar aquellos compuestos que poseen un grupo aromático conectado con un grupo derivado de los esteroides, normalmente funcionalizado en la posición 3, mediante un grupo puente. Un ejemplo es el gel luminiscente de 4-(2-antriloxi)butanoato de colesterilo[25] (**Fig. 1.11**) , donde el grupo puente permite adoptar a la molécula, una configuración de varilla. Este compuesto además tiene comportamiento mesomorfo tanto termótropo como liótropo. Se ha confirmado, por la síntesis de distintos derivados que la conformación de los anillos aromáticos es un factor muy importante en la capacidad de gelificación.

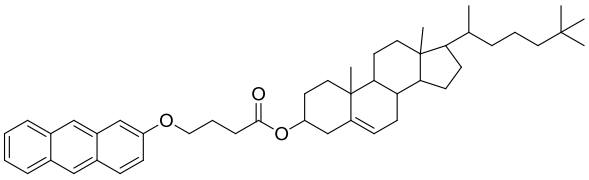

Fig. 1.11: Estructura química del gelificante 4-(2-antriloxi)butanoato de colesterilo.

- Derivados de **antraceno**:

Dentro de este grupo, se puede nombrar el 2,3-di-n-deciloxiantraceno (**Fig. 1.12**), que es capaz de gelificar en alcanos, alcoholes, aminas alifáticas y nitrilos.[26] Este compuesto es interesante por sus propiedades fotocrómicas.

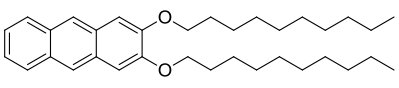

Fig. 1.12: Estructura química de 2,3-di-n-deciloxiantraceno.

- Derivados de **amida**:

Se incluyen aquí moléculas gelificantes que tienen grupos capaces de formar múltiples enlaces de hidrógeno gracias al grupo amida. En esta clasificación podemos encontrar oligómeros de α-aminoácidos, ciclodipéptidos… etc. Como ejemplo describimos el compuesto *N, N´, N´* -triesterariltrimesamida, (**Fig. 1.13**), en este caso una triamida, que es capaz de gelificar en disolventes como dimetilsulfóxido, dimetilformamida, diclorometano o nitrobenceno.

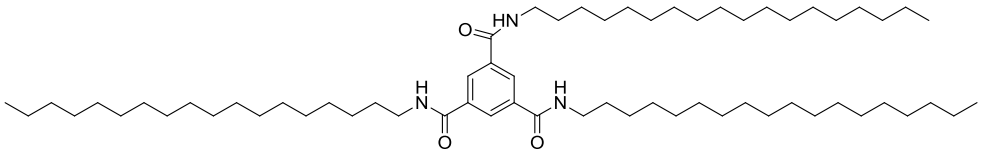

Fig. 1.13: Estructura química de *N, N´, N´´*-triesterariltrimesamida.

Weiss y Terech, clasificaron además otros tipos de moléculas que gelifican, como los compuestos **organometálicos**, por ejemplo las metaloporfirinas[27] y los **macrociclos**, por ejemplo los derivados de calixarenos.[28] Actualmente el número de organogelificantes es muy elevado y cada año aumentan las publicaciones relacionadas con ellos.

1.1.4.2. *Moléculas gelificantes que forman hidrogeles*

Para la gelificación en agua es necesario que las moléculas tengan por un lado, grupos hidrófobos para promover la agregación y por otro, grupos hidrófilos para proporcionar cierta solubilidad. Es difícil predecir la gelificación ya que no hay reglas exactas para el balance hidrofilia/hidrofobia, pero sí es cierto que dentro de una misma familia el número de carbonos de las cadenas alquílicas es importante en relación con la parte polar y que los grupos cargados facilitan la formación de geles y además pueden ser modulados por el pH.

Estroff y Hamilton clasificaron, en una primera revisión de hidrogeles supramoleculares, las moléculas "**hidrogelificantes**" según la posición del grupo polar de la siguiente manera:[4]

- **Anfílilos convencionales**:

Son aquellos que poseen una cabeza polar, formada, por ejemplo, por ácidos carboxílicos, aminoácidos, azúcares, fosfonatos o aminas cuaternarias, y una o dos colas hidrófobas, que pueden tener distinta largura, flexibilidad, saturación o ciclos (**Fig. 1.14**).

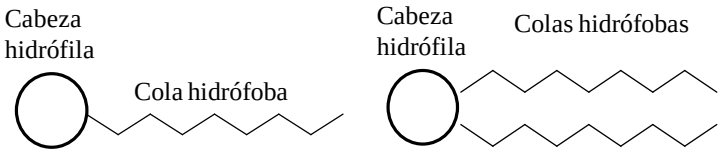

Fig. 1.14: Representación esquemática de la estructura de los anfífilos convencionales.

Muchos lípidos han sido estudiados como compuestos anfífilos gelificantes. Un ejemplo es la *N*-dodecilgluconamida (**Fig. 1.15**) estudiada por Fuhrhop y sus colaboradores.[29] A partir de esta estructura se han sintetizado diferentes diastereómeros que forman distintas morfologías, lo que sugiere que la geometría de la cabeza es responsable del empaquetamiento. También se han usado cadenas fluorocarbonadas[30] (**Fig. 1.15**), la cuales aportan rigidez, una concentración micelar crítica baja y una gran tendencia a autoensamblarse en agua.

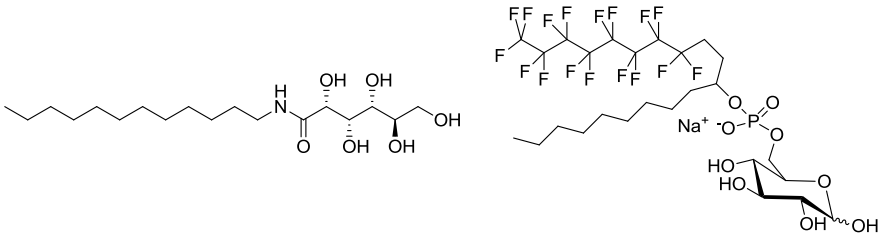

N-dodecilgluconamida Derivado de fluoroalcano

Fig. 1.15: Estructura química de *N*-dodecilgluconamida y un derivado de fluoroalcano.

- **Bolaanfifílos**:

En este grupo se incluyen aquellas moléculas que poseen dos cabezas polares unidas por una cola apolar (**Fig. 1.16**).

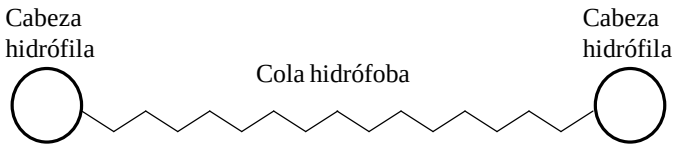

Fig. 1.16: Representación esquemática de la estructura de los compuestos bolaanfífilos.

Shimizu y sus colaboradores han trabajado ampliamente en el campo de los bolaanfifilos. En las cabezas polares han colocado nucleótidos,[31] aminoácidos[32] y azúcares.[33] Algunos son capaces de formar geles como el compuesto derivado de grupos desoxirribosa y fosfodiéster que se muestra en la **Fig. 1.17**, mientras que otros forman fibras por el autoensamblaje en agua que precipitan.

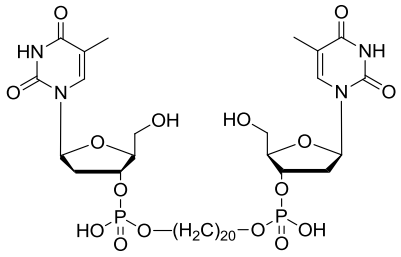

Fig. 1.17: Estructura química de un bolaanfífilo derivado de grupos desoxirribosa y fosfodiéster capaz de gelificar en agua.

- **Surfactantes tipo gemini**:

Son surfactantes que poseen una estructura general que sigue este esquema: cola flexible-ion-espaciador-ion-cola flexible (**Fig. 1.18**). Se caracterizan por tener una concentración micelar crítica inferior a la de los surfactantes comunes.

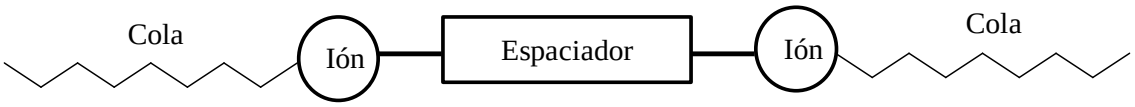

Fig. 1.18: Representación esquemática de un surfactante tipo gemini.

Menger[34] y sus colaboradores introdujeron este término y estudiaron varias familias de hidrogeles. En concreto con las moléculas con la estructura representada en la **Fig. 1.19**[35] se dedujo que la parte hidrófoba juega un papel muy importante en la gelificación. Variando la longitud de la cadena alquílica, el comportamiento de la molécula en agua es muy diferente. Por ejemplo, el derivado con una cadena de 18 átomos de carbono forma un gel; el que tiene una cadena con 10 átomos de carbono es capaz de hincharse pero no gelifica y el derivado de 9 átomos de carbono es soluble en agua

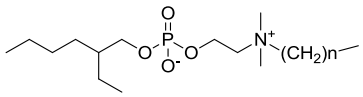

Fig. 1.19: Estructura química de surfactantes tipo gemini.

- **Otros**:

Dentro de esta clasificación se engloban aquellas moléculas que tienen un peso molecular algo más elevado pero que no llegan a considerase de tipo macromolecular.

Como ejemplos podríamos describir a los de tipo dendrítico, como es el caso de la molécula estudiada por Newkome y sus colaboradores[36] (**Fig. 1.20**), que estructuralmente es como un bolaanfífilo, donde los grupos OH dan cierta solubilidad y el espaciador permite las interacciones hidrófobas. Otro ejemplo muy interesante es el compuesto tripodal derivado del ácido cólico[37] que se describe en la **Fig. 1.20,** ya que es capaz de formar cavidades en las que se pueden atrapar moléculas.

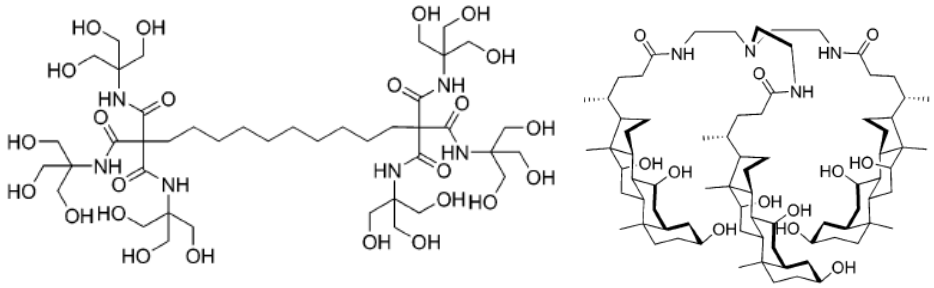

Molécula tipo dendrítica Derivado de ácido cólico tripodal

Fig. 1.20: Estructura química de una molécula tipo dendrítica y un derivado de ácido cólico tripodal.

Un grupo muy importante de moléculas gelificantes son los derivados de aminoácidos. Este grupo posee la combinación de efectos hidrófobos, debido a las cadenas laterales de los aminoácidos, junto a efectos hidrófilos, a causa de los puentes de hidrógeno procedentes de las uniones amida. Uno de los primeros ejemplos donde se estudió el autoensamblaje de derivados de aminoácidos fue el ácido *N*-dodecil-L-glutámico[38] capaz de gelificar a bajas temperaturas y bajos valores de pH, véase la **Fig. 1.21.a**. Otros ejemplos muy estudiados son los bolaanfífilos derivados de aminoácidos, como por ejemplo, el derivado de bis-urea que se muestra en la **Fig. 1.21.b**, que contienen grupos carboxílicos. Estos compuestos fueron estudiados por Estroff y Hamilton,[39] y podrían considerarse una mezcla de bolaanfífilo y un surfactante de tipo gemini. En este compuesto, las cadenas alquílicas proporcionan la capacidad de formar interacciones de tipo hidrófobo, la parte de la urea permite a las moléculas formar enlaces de hidrógeno y los grupos carboxílicos son capaces de establecer interacciones por enlaces de hidrógeno o se ionizan en función del pH, lo que hace a esta molécula sensible al pH. Este compuesto gelifica en agua a pH intermedios, a pH bajos forma vesículas y precipita en forma de fibras a pH altos. También se han sintetizado hidrogelificantes basados en β-péptidos.

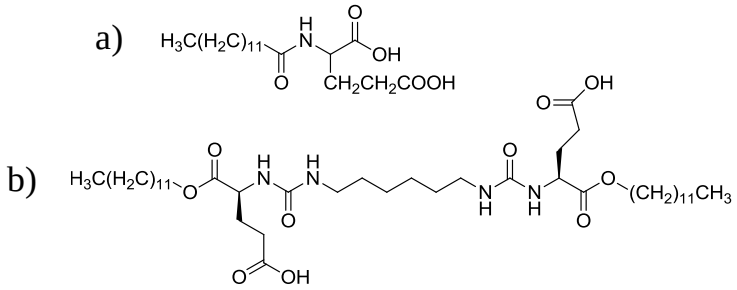

Fig. 1.21: Estructuras químicas derivadas de aminoácidos: a) ácido *N*-dodecil-L-glutámico, b) derivado de bis-urea con grupos carboxílicos.

En este capítulo, se ha considerado como otra clasificación aparte los compuestos que poseen azúcar, por tratarse de la estructura elegida para los gelificantes sintetizados durante este trabajo. La incorporación de los azúcares supone la adición de un interesante bloque soluble, ya que es biocompatible y puede dar lugar a materiales con aplicaciones médicas. De ellos se hablará en el **apartado 1.2**.

1.1.5. *Técnicas de estudio de los geles*

Para caracterizar los geles, es necesario estudiar su estructura desde la **escala molecular** a la **escala macroscópica** pasando por la **escala nanométrica**. Para el estudio de los geles se han utilizado una combinación de diferentes técnicas como las reológicas, microscopías avanzadas como las técnicas de microscopía electrónica o la de fuerza atómica, las espectroscopías y técnicas de difracción así como métodos de modelización. La información proporcionada por cada una de estas técnicas se ha de combinar, ya que las escalas de medida son diferentes y hay que tener especial cuidado cuando dichas medidas no pueden realizarse en las condiciones normales de gelificación, por ejemplo, si requieren el tratamiento o secado de la muestra, ya que la estructura sin disolvente puede colapsar y no ser exactamente la misma que en el medio húmedo o gel.[4, 5b]

La **temperatura de gelificación** se puede determinar mediante diferentes técnicas como la sencilla prueba del test del giro del tubo, los estudios de turbidez espectroscópica y el método de la caída de la bola,[40] así como también la reología, la calorimetría diferencial de barrido (DSC) y la resonancia magnética nuclear (RMN). Con la calorimetría

diferencial de barrido (DSC) se estudia el comportamiento de la muestra con el calor y se obtienen una serie de transiciones térmicas en función del tiempo correspondiente a la transformación del material del estado gel al sol y del sol a gel. A continuación se comentan las posibilidades que ofrecen algunas de las técnicas anteriormente mencionadas.

1.1.5.1. *Reología*

La reología permite describir propiedades macroscópicas del gel. En concreto, en el estudio reológico dinámico, se estudia la respuesta del material a un estrés oscilatorio, determinando variables como el **módulo elástico** (G´) y el **módulo viscoso** (G´´), y con ellas la **viscosidad**. En este tipo de materiales la elasticidad, medida con G´, será mayor que la energía disipada o comportamiento viscoso, determinado por G´´.[5b] La medida se realiza en una capa fina de gel que se encuentra entre un componente estacionario y otro móvil. Los tipos de platos estacionarios o móviles pueden ser distintos: paralelos, cilíndricos concéntricos, cono-plano… etc.

Estudiando los módulos en función de la frecuencia de oscilación, el estrés, la temperatura y la concentración del gelificante se puede caracterizar el gel.[4] Así se pueden describir como **geles tixotrópicos** aquellos que cuando se aplica suficiente estrés de una manera isoterma se forma una solución que revierte a gel al dejar de aplicar dicho estrés tras un tiempo de reposo. Los geles que poseen **reopexia** son aquellos en los que se produce la gelificación cuando existe una aceleración de la solidificación de una disolución a causa de movimientos suaves y regulares. Y los geles que poseen **sinéresis** son aquellos en los que se produce la expulsión de una parte del líquido con el paso del tiempo porque ha disminuido la cantidad de agregados pequeños y ha aumentado la cantidad de agregados grandes.[41]

En la **Fig. 1.22**, se puede observar diferentes experimentos para la caracterización por reología de un organogel en DMSO derivado de un gelificante cuya estructura química se representa en la **Fig. 1.22.a**. La **Fig. 1.22.b** muestra un experimento en el que se determina G´ y G´´ en función del estrés aplicado en el gel y donde se aplica una frecuencia de oscilación constante de 1Hz. El punto de corte entre G´y G´´, $\boldsymbol{\sigma_y}$ ("*yield stress*"), representa el punto donde al aplicar un determinado estrés el gel se rompe y comienza a fluir. En la **Fig. 1.22.c** se presenta un experimento donde, en esta ocasión, se

aplica un estrés constante de 3 Pa y se determina G´y G´´ en función de la frecuencia de oscilación. Tanto los valores de G´ como los de G´´ permanecen constantes de 0.1 a 10 Hz, lo que indica que estos parámetros son independientes de la frecuencia de oscilación. Hay que resaltar que G´ es superior en varios órdenes de magnitud a G´´, lo que ocurre siempre en el caso de los geles ya que son materiales más elásticos que viscosos.[42]

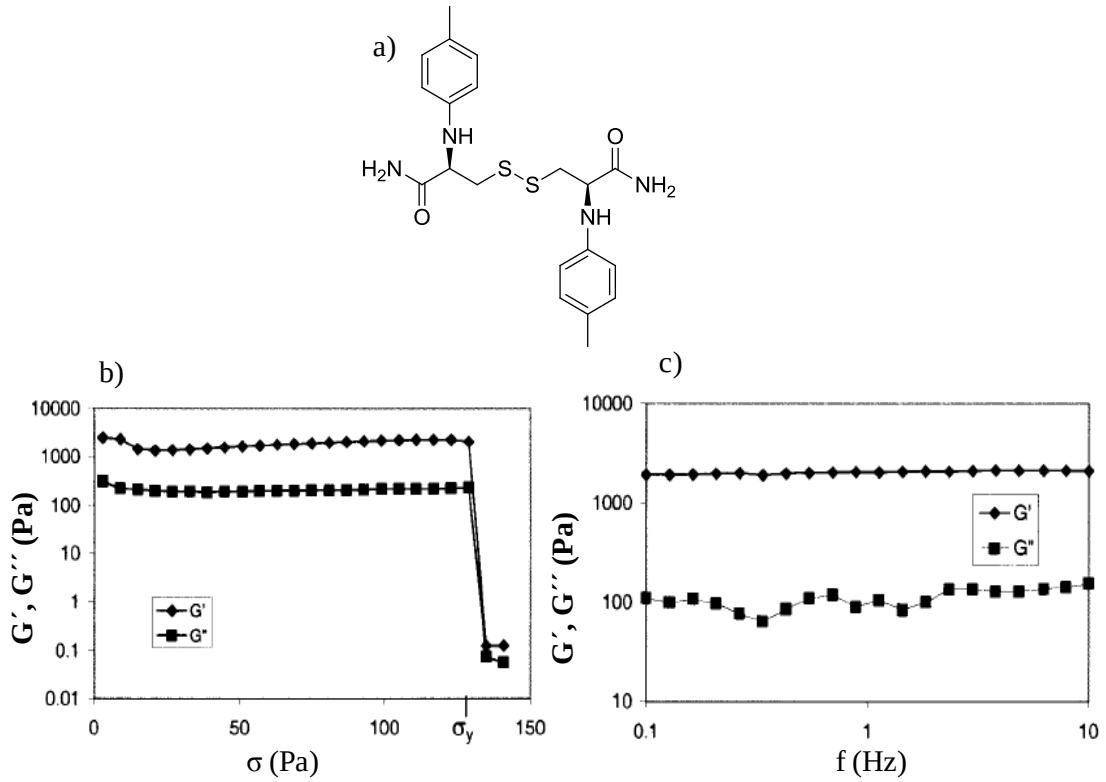

Fig. 1.22: Determinación de las propiedades reológicas de un organogel en DMSO a un 10% en peso: a) Estructura química de la molécula gelificante, b) Experimento de barrido de amplitud (Pa) a una frecuencia constante de 1Hz, c) Experimento de barrido de frecuencia (0,1-10 Hz) aplicando un estrés de 3 Pa; **Ref [42].**

1.1.5.2. *Microscopía avanzada*

Dentro de las técnicas microscópicas, la microscopía de fuerza atómica (AFM), la microscopía electrónica de barrido (SEM) y la microscopía electrónica de transmisión (TEM), en sus diferentes variantes, son muy útiles para el estudio de la estructura del gel en la escala del nanométro a la micra.

AFM es una técnica de alta resolución (con resolución lateral menor que un nanómetro), donde se pueden usar muestras con disolvente (en estado gel) pero para obtener una imagen mejor, se suelen secar tras la deposición en el sustrato, por lo que en ocasiones pueden introducirse modificaciones.[10]

En **TEM** y **SEM**, la resolución llega a los 0.2 nm, pero convencionalmente implica trabajar a alto vacío, lo que supone secar las muestras. Además en el caso del TEM, para la observación de productos orgánicos (**Fig. 1.23.a**) es necesaria la tinción negativa. La interacción de los agentes de tinción en ocasiones puede modificar la morfología de los agregados. En el caso del **SEM** se observa la topografía de la superficie de la muestra (**Fig. 1.23.b**). En los últimos años, se han desarrollado técnicas criogénicas, donde es posible vitrificar la muestra en etano líquido y trabajar a la temperatura del nitrógeno líquido para introducirla dentro del microscopio y así poder observar la muestra de una manera más cercana a su estructura en el disolvente, normalmente agua, ya que en disolventes orgánicos es más complicada la preparación. En la **Fig. 1.23.c** se muestra una imagen de **cryo-TEM**. También es posible realizar una crio-fractura para obtener capas más delgadas de muestra.[4] El **SEM ambiental** es una técnica que también permite observar la muestra sin necesidad de teñir y al poder variar las condiciones de temperatura, humedad y presión, se puede trabajar con el disolvente.

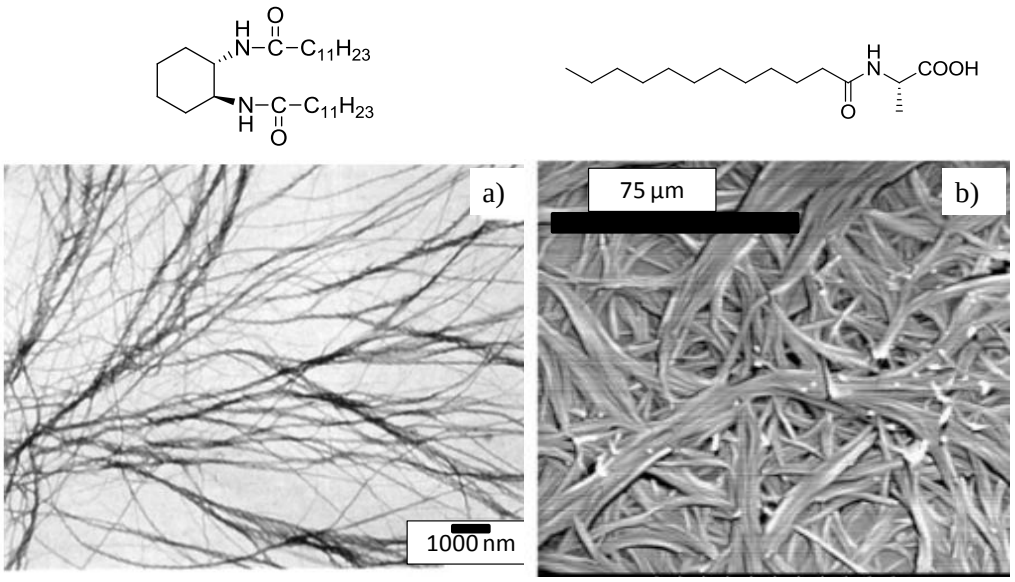

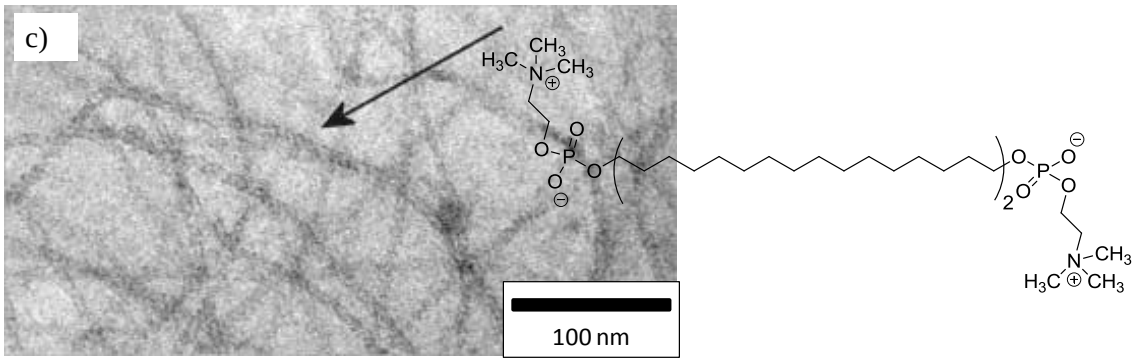

Fig. 1.23: a) Fotografía de TEM de las fibras obtenidas de un gel en acetonitrilo (1mM) de un derivado de (1R,2R)-1,2-ciclohexanciamina con tinción de ácido ósmico,[43] b) Imagen del xerogel del gel formado en tolueno (3,5 g L^{-1}) formado por la laurilamida derivada de L-alanina obtenido por SEM,[44] c) Imagen obtenida por cryo-TEM de las fibras obtenidas del gel en agua (0,03% en peso) del derivado bipolar de fosfocolina.[45]

1.1.5.3. *Técnicas espectroscópicas aplicadas a geles*

La resonancia magnética nuclear (RMN), el dicroísmo circular (CD), la espectroscopía infrarroja y en algunos casos la fluorescencia, son técnicas espectroscópicas que ayudan a entender la estructura primaria del gel, es decir, las interacciones a nivel molecular. Además estas técnicas son sensibles a la temperatura por lo que pueden servir para determinar temperaturas de gelificación.[4]

La **resonancia magnética nuclear** puede dar información de los enlaces formados durante la gelificación y de la temperatura de gelificación.[46] Además, las medidas de los tiempos de relajación pueden dar una idea de las partes de la molécula cuyos movimientos conformacionales o rotacionales disminuyen durante la gelificación.[47] Con medidas en estado sólido (*"solid state magic angle spinning"*) se pueden comparar los desplazamientos químicos de las señales con la disolución y así determinar un cambio en la agregación de las moléculas.[48]

Las medidas de espectroscopia **infrarroja** pueden, en ocasiones, confirmar la presencia de puentes de hidrógeno y determinar el estado de protonación de los ácidos carboxílicos, pero en el caso de las señales correspondientes al enlace NH, no se puede obtener información cuando se trata de hidrogeles ya que están ocultas por las bandas del OH del agua.[4]

Para obtener indicios de **helicidad** y por tanto de **quiralidad** en el material, se utiliza la técnica de **dicroísmo circular** donde la muestra se expone a luz circularmente polarizada. En el espectro resultante se obtiene una señal cuando se produce un **efecto Cotton**, es decir, un fenómeno de absorción desigual del haz dextrógiro y el haz levógiro, como resultado de la elipticidad de la luz transmitida. La señal de dicroísmo sólo se observa en la región donde la molécula es capaz de absorber en la región UV-vis. Si en la muestra existen dos cromóforos iguales y próximos en el espacio que constituyen un sistema quiral, sus momentos de transición electrónicos interactúan de tal manera que sus estados excitados se desdoblan en dos estados degenerados. Esta interacción supone lo que se denomina un **acoplamiento exciton** y en el espectro se refleja por la aparición de un par de bandas con signo opuesto.[5c, 10]

En esta técnica hay que tener especial cuidado con los "artefactos" que pueden producirse por tener un alineamiento macroscópico de sus momentos de transición, esto es dicroísmo lineal. En este caso, rotando la muestra puede comprobarse si hay influencia de dicroísmo lineal. En ocasiones, la ausencia de señal en DC no indica que la muestra no sea helicoidal ya que esta técnica mide de forma global y es posible que dentro de una misma muestra haya helicidades opuestas, para observar señal, una de las dos tendría que estar en exceso.[10]

En el caso de los geles, esta técnica además de dar información de la organización quiral puede proporcionar también la **temperatura de gelificación** realizando un estudio a temperatura variable. Si la señal está asociada a la organización supramolecular del gel, esta señal de dicroísmo puede desaparecer cuando se pasa de estado gel a sol.[5c] Un ejemplo de este tipo de estudio se ha realizado en un gel en butanol obtenido a partir de una molécula derivada del colesterol y un grupo azo[40] como se muestra en la **Fig. 1.24.** El gel tiene una banda de acoplamiento excitón a temperatura ambiente donde $\theta=0$, es decir, el punto de corte, coincide con $\lambda_{max}=310$ nm en el espectro de absorción. Cuando el gel se calienta a 60ºC, ya no se detecta esta señal.

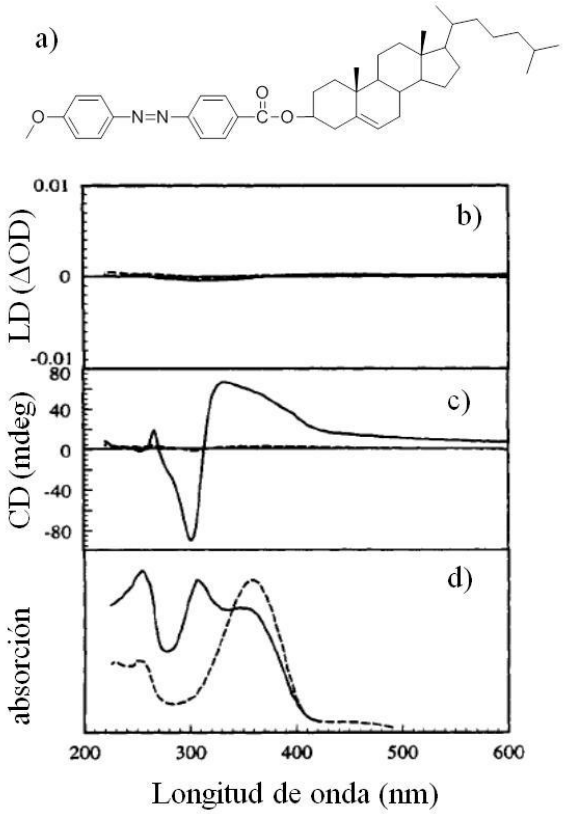

Fig. 1.24: Estudio a temperatura variable de un gel en butanol al 0,2% en peso: a) Estructura del gelificante derivado del colesterol y un azo, b) Espectro de dicroísmo lineal, c) Espectro de dicroísmo circular, d) Espectro de absorción. El estado gel se observa a 25ºC (—) y el estado disuelto se observa a 60ºC (---); **Ref [40].**

1.1.5.4. *Otras técnicas*

La difracción de rayos X puede usarse para la determinación de la estructura de los geles.[4] Las técnicas de **difracción a bajo ángulo** (SAXS) y la **dispersión de neutrones a bajo ángulo** (SANS) permiten determinar el empaquetamiento dentro de los agregados, pero para ello es necesario elegir un modelo (por ejemplo, micela tipo varilla), realizar un análisis matemático y después comparar los parámetros medidos con el modelo. También puede usarse para describir el papel del disolvente en la formación de las fibras.

Con la **difracción a alto ángulo en polvo** (XRD) se puede determinar el empaquetamiento de las moléculas, llegando a ver si se trata por ejemplo, de estructuras lamelares o hexagonales e incluso se puede determinar la conformación o interdigitalización de las cadenas alquílicas. La difracción a bajo ángulo, da información

de la repetición en las capas, mientras que la región de medio ángulo, es indicativa del empaquetamiento de las cadenas hidrocarbonadas.

Mediante SAXS se pueden realizar estudios en el gel directamente, sin embargo, con XRD la mayoría de los estudios que se han realizado han sido en seco (xerogel). El estudio de la estructura cristalina también puede dar idea de la estructura del gel, así se pueden comparar los posibles polimorfismos de la molécula gelificante con el rayos X en estado gel.[47]

No es fácil determinar la estructura de un gel, pero con el apoyo de **modelos** de minimización de niveles de energía y cálculos de dinámica molecular, es posible llegar a establecer la estructura primaria de las moléculas gelificantes.[4]

1.1.6. *Aplicaciones*

Los geles poliméricos se conocen desde hace cientos de años y sus aplicaciones son muy comunes. Sin embargo, en el campo de los geles supramoleculares, pese a que también han sido estudiados y usados en la industria desde hace mucho tiempo, (como por ejemplo, el sorbitol empleado como espesante alimenticio o las sales de ácidos grasos utilizados como lubricantes) ha sido en los últimos veinte años cuando, gracias a sus ventajas de **reversibilidad**, **control** y **biocompatibilidad** frente a los geles poliméricos, se han desarrollado otro tipo de aplicaciones principalmente en el campo de los **biomateriales**, los **materiales avanzados** ("*smart materials*") y los **dispositivos electrónicos.**[9]

Como ejemplos de algunas aplicaciones para geles supramoleculares se han de nombrar aquellos **organogeles** que se han usado para la **modificación en superficies**, ya que el empaquetamiento de las fibras, al evaporarse el disolvente, modifica la hidrofobicidad del material;[49] también se han usado organogeles para formar **poros** dentro de matrices poliméricas, así al mezclar moléculas de bajo peso molecular con disolventes capaces de polimerizar se forman canales en los polímeros tras la eliminación del gelificante.[50] Adicionalmente se han desarrollado **materiales sensibles a la luz**, este tipo de materiales será tratado más adelante en el **apartado 1.3**.

Se han desarrollado **dispositivos electrónicos,** formados por geles con metales (metalogeles),[51] aplicables a tecnologías basadas en luminiscencia, fotocatálisis o celdas

fotovoltaicas. También existen geles capaces de transportar electrones que permiten formar dispositivos de tamaño nanométrico en los que el autoensamblaje de las moléculas gelificantes facilita el transporte de energía,[52] o se han fabricado electrolitos con organogeles.[53]

Además se han estudiado sistemas que gelifican formando parte de **nanocomposites**, que mezclan compuestos orgánicos e inorgánicos. Como ejemplo, estos nanocomposites se han usado para controlar el crecimiento de nanopartículas de oro y plata.[54] Por último, en la **Fig. 1.25** se puede observar un **dispositivo electroóptico**[55] formado por una molécula gelificante (**1**) y una molécula cristal líquido (**2**), donde al aplicar un campo eléctrico el material pasa de un estado off donde hay dispersión de luz (opaco, A) a un estado donde hay transmisión de luz (transparente, B) como consecuencia de la orientación del cristal líquido bajo un campo eléctrico.

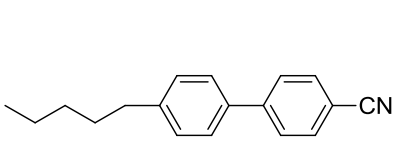

1

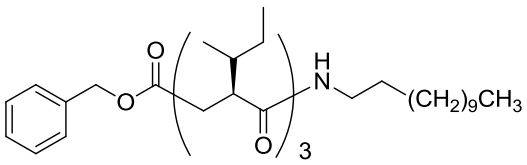

2

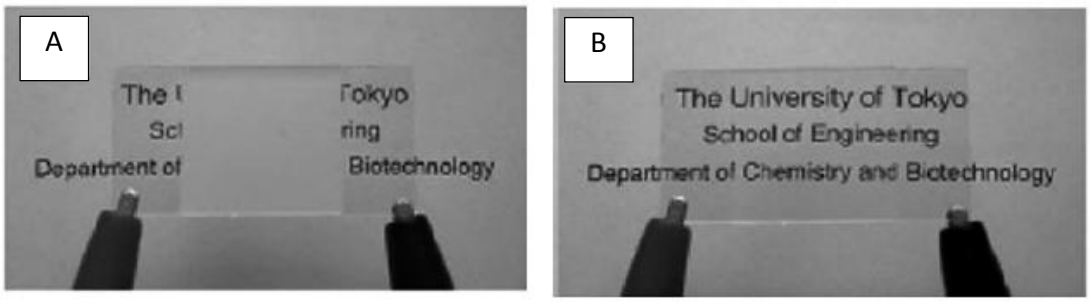

Fig. 1.25: Mezcla del cristal líquido (**1**) con un 0,2 % wt del gelificante (**2**), en estado de dispersión de la luz (**A**) y estado de transmisión de la luz (**B**); **Ref [55].**

Los **hidrogeles** por su parte, se han aplicado principalmente como biomateriales debido a su potencial biocompatibilidad y posible efecto biológico (como es el caso de los derivados de aminoácidos y los azúcares). Los hidrogeles supramoleculares son sistemas sintéticos que imitan estructuras biológicas, de ahí que se hayan usado para

explorar campos como la medicina regenerativa, el encapsulamiento y el crecimiento celular o la liberación controlada de fármacos.

En cuanto a la **medicina regenerativa**, se han realizado diversos estudios con nanofibras peptídicas donde éstas son usadas para la regeneración del sistema nervioso tanto en el cerebro, para la recuperación de la visión[56] (**Fig. 1.26),** como en la columna vertebral, para la recuperación de la movilidad.[57]

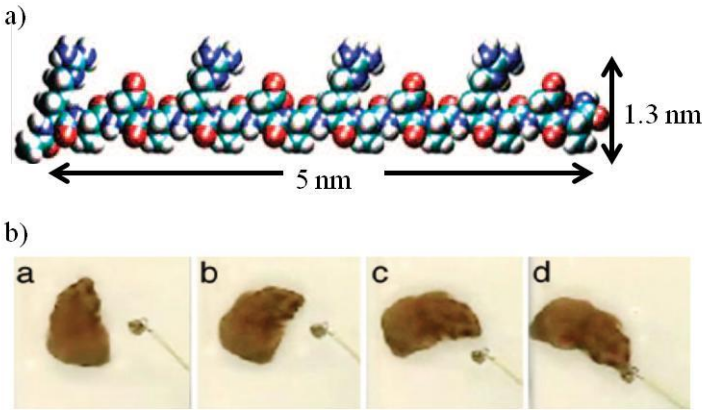

Fig. 1.26: a) Modelo molecular del péptido RADA 16-I, b) Tratamiento en el nervio óptico dañado de un hámster; **Ref [56].**

También se han usado hidrogeles para **encapsular células** en una matriz tridimensional con el objetivo de reparar tejidos como cartílagos[58] o promover la formación de estructuras vasculares.[59] En el campo de la **liberación controlada de fármacos**, existen ejemplos de hidrogeles basados en ibuprofeno, que liberan este medicamento gracias a la hidrólisis de enzimas.[60] Otros hidrogeles, son capaces de atrapar y liberar moléculas biológicas importantes, como es el caso de medicamentos para combatir la malaria.[61] Se han desarrollado también hidrogeles que son capaces de responder a **enzimas** específicos; así en el caso de un sistema enzimático fosfatas/quinasa se puede producir una gelificación reversible en agua.[62] Algunos hidrogeles también han sido capaces de encapsular enzimas para catalizar reacciones dentro de la matriz del propio gel.[63]

Los hidrogeles, como en el caso de los organogeles también se han usado, para hacer **nanocomposites**; así los hidrogelificantes pueden controlar la mineralización, como se ha estudiado en el caso del fosfato cálcico,[64] o pueden proporcionar el medio necesario

para el crecimiento de materiales inorgánicos, como ha sido el caso de la formación de cristales de calcita.[65]

La mayor parte de los ejemplos de aplicaciones con hidrogeles supramoleculares encontrados en la bibliografía han sido desarrollados con moléculas anfifílas de tipo peptídico. Sin embargo, existen otros estudios realizados con **derivados de moléculas azucaradas**. Como ejemplos, se pueden encontrar **sensores** capaces de detectar insulina,[66] realizados a partir de un monosacárido fluorescente basado en pireno o realizados a partir de esteres de aminoácidos glicosilados, los cuales pueden formar dispositivos semi-húmedos para la detección de péptidos/proteínas[67] o cationes.[68] En el campo de la **medicina regenerativa** un derivado de D-glucosamina es capaz de cicatrizar tejido cuando el hidrogel se aplica sobre una herida.[69] Alguno de estos ejemplos será visto más en detalle en el siguiente **apartado 1.2**.

1.2. Glicolípidos en ciencia de los materiales

Los **azúcares** son considerados, en ciencia de materiales, como un bloque soluble en agua capaz de proporcionar una librería de compuestos cuyas estructuras pueden resultar útiles en el campo de los ensamblajes moleculares e interesantes por su potencial biocompatibilidad. Entre estos derivados tenemos los glicolípidos.

1.2.1. *Glicolípidos*

Los **glicolípidos** son moléculas anfífilas, es decir, están constituidas por una parte hidrófoba o cola lipofílica y una parte hidrófila o cabeza polar, que contienen específicamente en sus cabezas polares mono u oligosacáridos. Son una importante clase de compuestos de origen natural que se encuentran implicados en eventos de reconocimiento celular, para reconocer hormonas, anticuerpos, virus u otras células. Los glicolípidos sintéticos pueden presentar algún inconveniente, ya que es posible que tengan más resistencia a la degradación y en algunos casos, incluso pueden resultar tóxicos.

Los glicolípidos pueden clasificarse en dos subgrupos:[70]

1) Los análogos a las membranas lipídicas: como ejemplos típicos encontramos los diacil glicoglicerolípidos y los dialquil glicoglicerolípidos (**Fig. 1.27**).

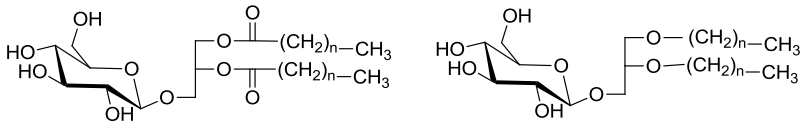

Fig. 1.27: Representación de la estructura molecular de los diacil glicoglicerolípidos y los dialquil glicoglicerolípidos.

2) Aquellos que poseen una sola cadena alquílica. También se pueden considerar tensioactivos o surfactantes basados en azúcares. Un ejemplo son los alquilglicósidos (**Fig. 1.28**).

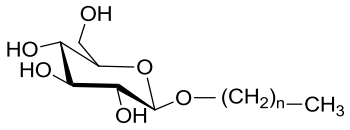

Fig. 1.28: Representación de la estructura molecular de un glicolípido con una sola cadena alquílica.

Este segundo grupo de compuestos está teniendo últimamente una importancia creciente por tratarse de surfactantes de bajo impacto ambiental. Si nos referimos a ciencia de materiales, los glicolípidos son compuestos ampliamente estudiados por sus características tanto como tensioactivos, como cristales líquidos e incluso, por ser moléculas de bajo peso molecular capaces de formar geles supramoleculares.

Como **tensioactivos**, estas moléculas tienden a formar capas monomoleculares o monocapas orientadas en las interfases, a bajas concentraciones, alterando las propiedades del sistema. Al aumentar la concentración en el seno de la disolución, pueden formar estructuras autoensambladas.[71] Como **cristales líquidos**, dada su estructura pueden microsegregar, donde por un lado, las cabezas polares forman enlaces de hidrógeno entre sí y por otro, las cadenas alquílicas se autoensamblan, dando lugar a mesofases tanto termótropas, por efecto de la temperatura, como liótropas, por el efecto del disolvente.[72] Los glicolípidos como cristales líquidos serán tratados más específicamente en el **apartado 1.4**.

En el caso de geles, el descubrimiento de que las moléculas glicolipídicas podían dar **geles supramoleculares**, ha sido relativamente reciente.[73] Los glicolípidos son moléculas que por su carácter anfífilo, tienen la capacidad de auto-ensamblarse y formar estructuras y así dependiendo de la concentración y de la cantidad de disolvente, pueden llegar a entrecruzarse y ocluir todo el líquido del medio.

Así pues, la característica principal para gelificar es la anfifília. Los diferentes tipos de moléculas glicoanfífilas capaces de gelificar, se pueden clasificar en dos tipos:[4] los **anfífilos convencionales**, con una sola cabeza polar y los **bolaanfífilos**, que poseen dos cabezas polares unidas por una cadena lipófila.

1.2.2. *Glicolípidos gelificantes*

A continuación se describen los principales ejemplos de moléculas gelificantes derivadas de azúcares que se pueden encontrar en la bibliografía.

1.2.2.1. *Anfífilos convencionales*

Dentro de los anfífilos convencionales podemos distinguir aquellos que tienen una cabeza azucarada de cadena abierta y aquellos que poseen azúcares cíclicos, siendo estos monosacáridos o disacáridos. También se mencionarán algunos ejemplos de moléculas gelificantes con azúcares modificados.

1.2.2.1.1. *Moléculas gelificantes con cabeza azucarada de cadena abierta*

Los primeros en describir un comportamiento gelificante en moléculas con azúcares en su estructura, fueron Pfannemüller y Welte.[73] Entre las distintas moléculas sintetizadas, las mostradas en la **Fig. 1.29** formaron geles en agua.

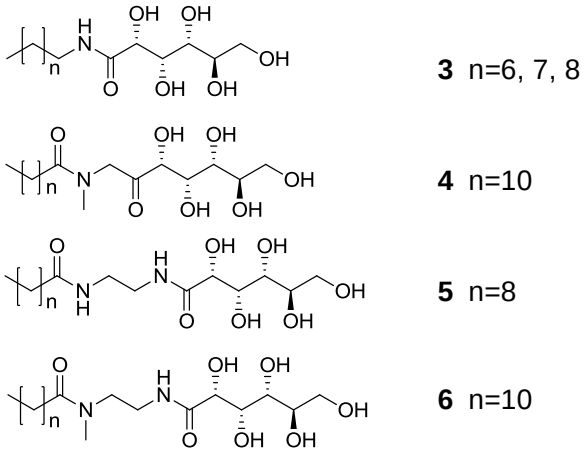

Fig. 1.29: Estructura química de los gelificantes estudiados por Pfannemüller y sus colaboradores.

La estructura **3**, es capaz de gelificar cuando n= 6, 7, 8, la estructura **5** es capaz de gelificar cuando n=8 y las estructuras metiladas **4** y **6** son capaces de gelificar cuando n=10. En los compuestos derivados de la estructura **3** se obtienen fibras dextrógiras

mientras que en el compuesto **5**, se obtienen cintas. Para **4** y **6**, se observan fibras helicoidales dextrógiras, en los dos casos. Estas fibras son las que dan soporte a la estructura del gel.

Comparando estos compuestos se puede observar que cuando se metila el nitrógeno, se aumenta la solubilidad debido a la ausencia de enlaces por puente de hidrógeno en el grupo amida. Según los autores, las interacciones que dan lugar al gel en este caso, no están dirigidas por los puentes de hidrógeno de la amida sino que son de tipo hidrofóbo aunque también participen las interacciones por enlaces de hidrógeno de los OH de la parte azucarada. Debido a esta falta de enlaces de hidrógeno en el grupo amida, las moléculas metiladas no están tan ordenadas y su capacidad para formar geles y estructuras quirales es menor.

Fuhrhop y sus colaboradores continuaron con el estudio del auto-ensamblaje de este tipo de moléculas con las **N-octil L- y D-gliconamidas**[29a, 74] y análogos (**Fig. 1.30**) las cuales se agregan para dar estructuras fibrilares y formar geles en agua. Mientras que los enantiómeros puros gelifican, los racematos forman placas que precipitan.

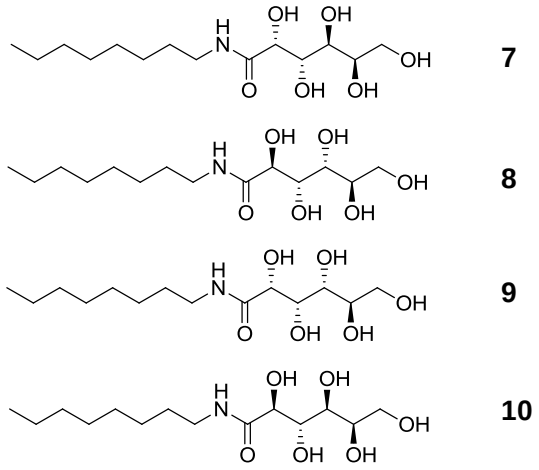

Fig. 1.30: Representación de las D-gliconamidas estudiadas por Fuhrhop y sus colaboradores.

La estructura de la **cabeza azucarada** influye en la gelificación. Así, tanto los derivados de D como L-**galactosa 7** forman geles en agua (en concentraciones bajas de 0.4-0.5 % en peso). Mientras que el enantiómero D da fibras levógiras, el enantiómero L da fibras

dextrógiras. Estos geles acuosos, son estables varias semanas pero a los meses precipitan en forma de cristales. Con derivados de **manosa 8** también se obtienen hidrogeles con ambos enantiómeros, pero las estructuras son cilíndricas. Con derivados de **glucosa 9** también se forman hidrogeles y se obtienen fibras dobles helicoidales, donde cada fibra tiene la anchura de una capa bimolecular y cada enantiómero tiene distinta orientación: en el enantiómero D la orientación es dextrógira y en el enantiómero L es levógira. Este gel precipita al cabo de un día. Finalmente los geles en agua de derivados de **talopiranosa 10** son inestables y están formados por fibras cortas y frágiles.

Recientemente, se ha añadido un surfactante (n-Laureth), véase **Fig. 1.31**, a las moléculas gelificantes de ***N*-octil-D-gluconamida** para impedir su cristalización.[75] Con la adición de este surfactante no sólo se consigue estabilizar el gel, sino que permite modificar sus propiedades mecánicas en varios órdenes de magnitud, variando la proporción de los compuestos

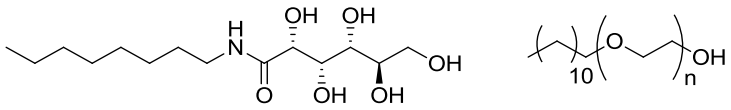

Fig. 1.31: Estructura química de *N*-octil-D-gluconamida y el surfactante n-Laureth (n= 4, 7, 12, 30).

Cintas y sus colaboradores, han trabajado con estructuras similares a los de Fuhrhop. Estudiaron una serie de compuestos como los mostrados en la **Fig. 1.32** donde las partes hidrófilas e hidrófobas se conectan vía ureido o bis ureido.[76] Los dos compuestos representados en la figura forman hidrogeles. Además se ha descrito su comportamiento cristal líquido liótropo, organizándose en fases lamelares o hexagonales con la adición de agua. Otros compuestos sintetizados en este trabajo con el grupo ureido formaron organogeles bajo la acción de ultrasonidos sin la necesidad de calentar.

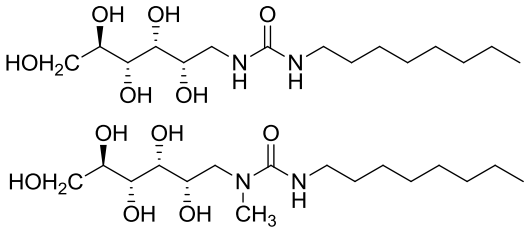

Fig. 1.32: Estructura química de moléculas gelificantes descritas por Cintas y sus colaboradores.

Sustituyendo la cadena carbonada por un grupo **pireno** también es posible obtener una librería de moléculas gelificantes homólogas pero con diferente estructura hidrófoba.[66] En concreto, la representada en la **Fig. 1.33** ha sido utilizada para detectar insulina en concentraciones de microgramos. Se ha demostrado mediante SEM que la insulina no rompe la organización del gel sino que se incorpora a la estructura fibrilar. Como consecuencia de la unión del azúcar y la insulina, se produce una modificación en la agregación del pireno lo que altera su fluorescencia; así este gel se puede utilizar como **sensor**.

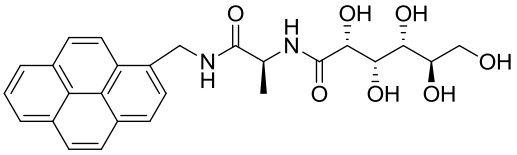

Fig. 1.33: Estructura del gelificante basado en pireno capaz de detectar insulina.

1.2.2.1.2. *Moléculas gelificantes con cabeza azucarada cíclica*

La utilización de derivados cíclicos en lugar de acíclicos se justifica porque son conformacionalmente más definidos, lo que imparte un carácter rígido a la molécula. La biocompatibilidad, la disponibilidad y el coste de los compuestos de partida hacen que sean atractivos para la síntesis de moléculas gelificantes.[77]

Uno de los primeros trabajos con anfífilos azucarados con cabeza cíclica descritos como hidrogelificantes fueron los **aril glicolípidos** estudiados por Shimizu y sus

colaboradores.[78] Estas moléculas se obtuvieron a partir de la glucosa y el cardanol, cuyas estructuras se representan en la **Fig. 1.34.** Se estudió una compleja mezcla con derivados de distintas cadenas insaturadas, en proporciones de **11** (29%) + **12** (16%) + **13** (50%) + **14** (5%), y se comparó con el compuesto **14**, donde la cadena está totalmente saturada. Tanto la mezcla como el compuesto **14**, se autoensamblan en agua para formar fibras helicoidales, pero sólo **14** forma un gel estable en una mezcla de alcohol/agua (1:1) o acetona/agua (1:1). En el caso de la mezcla con derivados de distintas cadenas insaturadas, los agregados fibrilares observados por TEM resultaron ser tubos y la difracción de rayos X permitió distinguir una organización lamelar interdigitada.

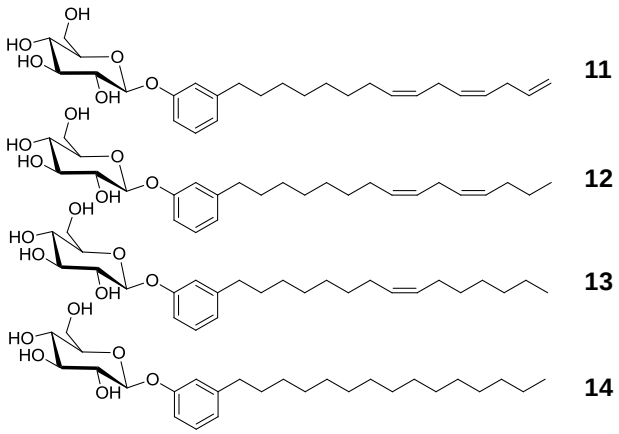

Fig. 1.34: Estructura de aril glicolipidos derivados del cardanol.

También el grupo de Shimizu en colaboración con el grupo de Shinkai, presentaron ese mismo año un trabajo realizado con una molécula, representada en la **Fig. 1.35**, obtenida sintéticamente, donde se introdujo además de la **glucosa,** un **grupo amida** y un **anillo aromático**, para favorecer el autoensamblaje de las moléculas y por tanto, la gelificación.[79]

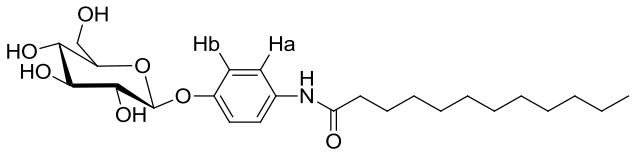

Fig. 1.35: Estructura química del derivado de glucosa con un grupo amida y un anillo aromático.

Esta nueva molécula resultó ser un buen gelificante capaz de formar geles tanto en disolventes orgánicos (THF, cloroformo, acetato de etilo y butanol) como en agua. Para formar el **hidrogel**, era necesaria la presencia de trazas de un disolvente orgánico (geles formados al 0,1% en peso en agua con 1% de metanol o etanol). Mediante estudios de microscopia electrónica, observaron que se forman fibras helicoidales levógiras. La difracción de rayos X del xerogel mostró una organización en **bicapa interdigitada** ya que el espesor de la capa resultó ser mayor que el ancho de la molécula. Al realizar el experimento de difracción de rayos X directamente en el gel se siguió observando la difracción correspondiente a esta bicapa lo que apuntó a que la organización es la misma tanto en el gel como en el xerogel. En la región de ángulo medio se observan unos picos agudos que dan idea de la fuerte organización de las cadenas alquílicas unidas por interacciones hidrófobas. Gracias a estudios de RMN de ^{1}H en mezclas de agua/metanol (**Fig. 1.36**), se pudo observar que a temperatura ambiente se obtienen unas señales de los H del anillo aromático (H_a y H_b) muy próximas, correspondientes al estado agregado (A) mientras que conforme se va calentando la muestra, estos picos van disminuyendo y aparecen unos nuevos picos correspondientes a los protones aromáticos de las especies en disolución (B) en equilibrio con los picos correspondientes a los protones aromáticos de los agregados.

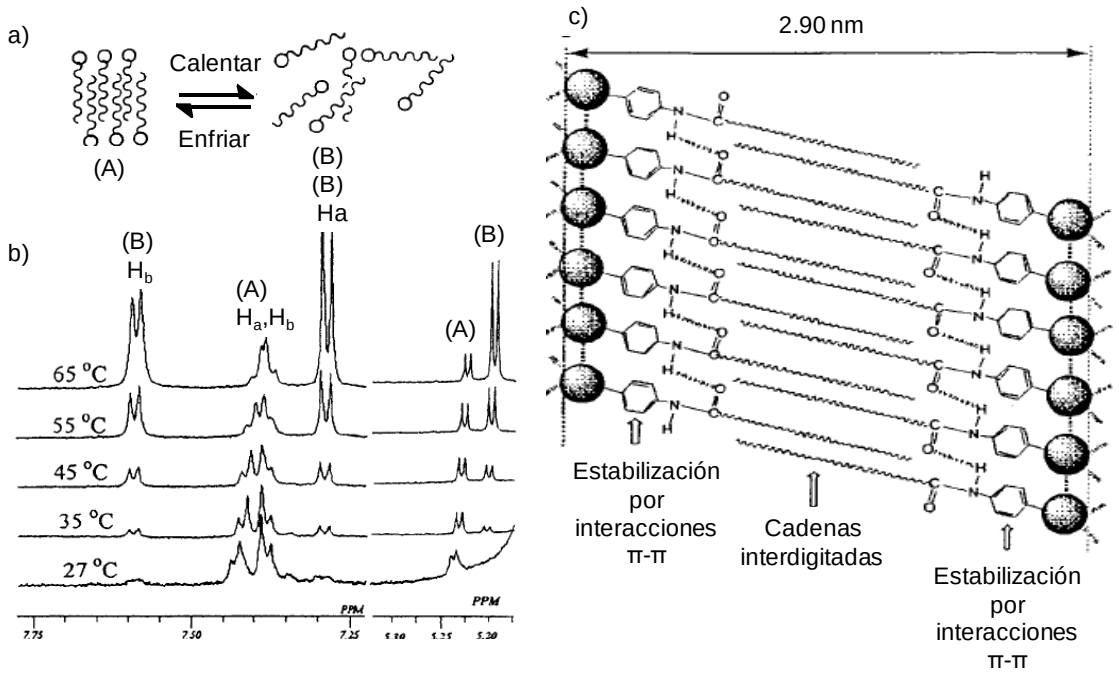

Fig. 1.36: a) Representación esquemática de la molécula descrita en la **Fig. 1.35** en estado agregado (**A**) y en disolución (**B**), b) Experimento de RMN de ^{1}H de un gel en D_2O y metanol-d_6 (1:1 v/v) de la molécula gelificante, c) Posible auto-ensamblaje en la microestrutura del hidrogel; **Ref [79].**

Los experimentos realizados, tanto de difracción de rayos X como de RMN, ponen en relieve que además de las interacciones por enlaces de hidrógeno de los OH de las cabezas azúcaradas, la interdigitalización de las cadenas alifáticas y el apilamiento π-π de los anillos aromáticos también participan en la formación de los hidrogeles.

En una publicación posterior, se estudió la misma estructura descrita anteriormente, pero con **galactosa** en la cabeza azucaradas en vez de glucosa. También se sintetizaron los correspondientes **bolaanfífilos** basados en glucosa y galactosa[80] (véase **Fig. 1.37**).

Como en el caso de la glucosa, la molécula con galactosa era capaz de gelificar en agua con pequeñas cantidades de disolventes orgánicos. Los bolaanfífilos también gelificaban en disolventes orgánicos y en agua, pero en este caso no era necesaria la adición de trazas de otro disolvente. Se advirtieron otras diferencias entre los anfífilos convencionales y los bolaanfifilos. Por ejemplo, estos segundos eran capaces de

gelificar a concentraciones más pequeñas, incluso de tan sólo 0.05% en peso, o que mientras los geles de una sola cabeza son opacos los bolaanfifílos son transparentes.

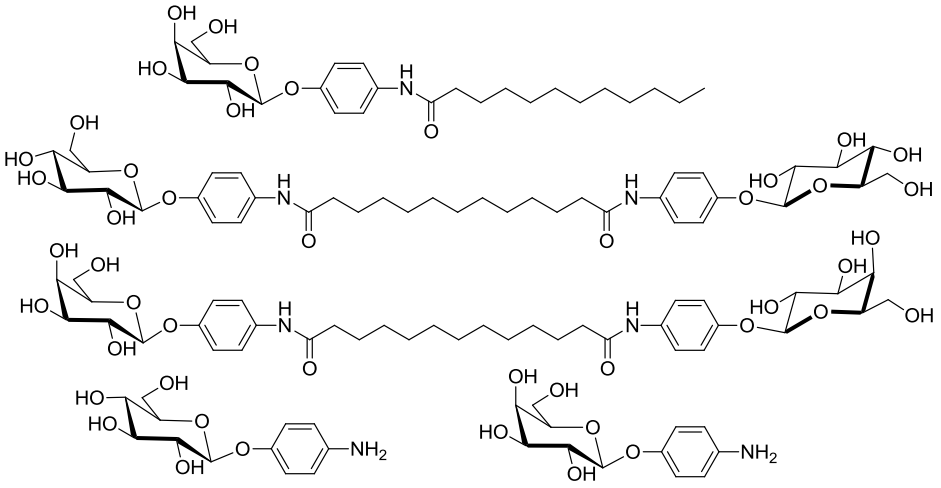

Fig. 1.37: Estructura del compuesto derivado de galactosa y los compuestos bolaanfífilos sintetizado por Shimizu, además de los *p*-aminofenil derivados de glucosa y galactosa.

Gracias a la señal de **DC**, se dedujo que los momentos dipolares de los anillos fenilo están orientados de una manera antihoraria en los agregados del gel ya que la señal tiene un signo negativo para el primer efecto Cotton, mientras que en una disolución de metanol no existía señal. En los estudios de **microscopía electrónica** (TEM y SEM) se observaron lamelas de 50-100 nm en los xerogeles de los bolaanfífilos y fibras de 20 nm en los de una sola cabeza.

Shimizu y Shinkai, utilizaron estos compuestos como **plantillas** "*templates"* para la formación de **nanotubos de sílice** mediante la **transcripción** de la estructura supramolecular de los gelificantes.[81] Además de las moléculas gelificantes, es necesaria la introducción de un grupo amino (*p*-aminofenil glucopiranósido y *p*-aminofenil galactopiranósido, **Fig. 1.37**), ya que este grupo tiene un papel importante en la polimerización de tetraetoxisilano (TEOS), muy posiblemente debido a la interacción de enlaces de hidrógeno entre la amina y las partículas de sílice oligoméricas cargadas negativamente. El TEOS se adsorbe sobre la superficie de las nanofibras de las moléculas gelificantes y allí es donde se produce su polimerización. Si se mezclan los

derivados de amina con las moléculas gelificantes se pueden obtener morfologías diferentes a cuando están solas, pero tras la reacción de polimerización del TEOS y la posterior calcinación de estas moléculas gelificantes (quedando sólo la estructura de silíceo) no se detectan cambios.

Una vez estudiado el cambio en la cabeza azucarada, Shimizu y su grupo, sintetizaron otra serie de moléculas, introduciendo en esta ocasión cambios en la cadena alifática,[82] véase la **Fig. 1.38.**

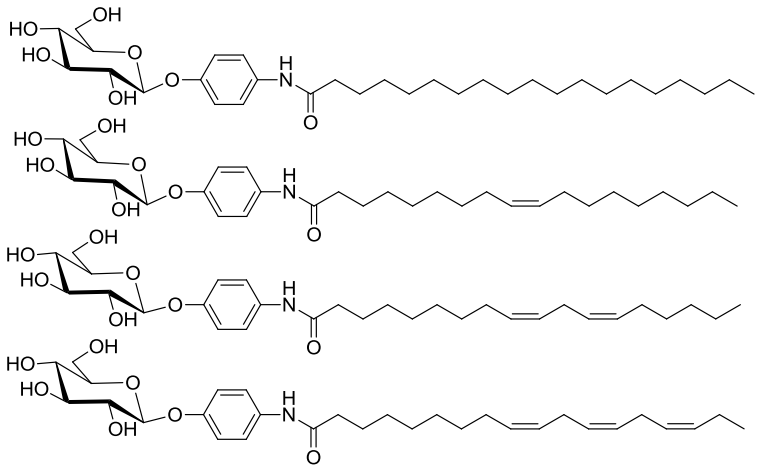

Fig. 1.38: Estructura química de los compuestos anfífilos derivados de glucosa y aminofenilo, descritos por Shimizu y sus colaboradores.

Partiendo de una cadena de 18 carbonos, compararon el comportamiento gelificante al introducir una, dos o tres insaturaciones en la cadena. Todas las moléculas resultaron formar agregados en agua (en la molécula con la cadena totalmente saturada fue necesario usar una mezcla agua/metanol). En el caso de que la cadena esté totalmente saturada o posea una insaturación se forman estructura fibrilares, mientras que cuando hay dos o tres insaturaciones, se forman tubos. El entramado de estas estructuras tubulares no es suficiente para provocar la gelificación.

Adicionalmente se ha realizado un estudio de agregación en agua de glucosilamidas, véase la **Fig. 1.39**, sin la presencia de un anillo aromático.[83] En este caso también se autoensamblan formando nanotubos huecos, sin embargo, no ha sido descrita la formación de hidrogeles.

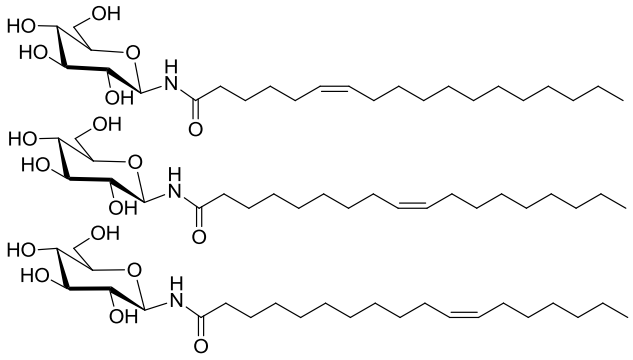

Fig. 1.39: Estructura química de las glucosilamidas estudiadas por Shimizu y sus colaboradores.

Kim y sus colaboradores continuaron con el estudio de moléculas basadas en **D-glucosamina** con la presencia de un grupo **naftol** y **fenilalanina**. Las moléculas de la **Fig. 1.40** han dado lugar a hidrogeles y estos han sido aplicados a la reparación de heridas.[84]

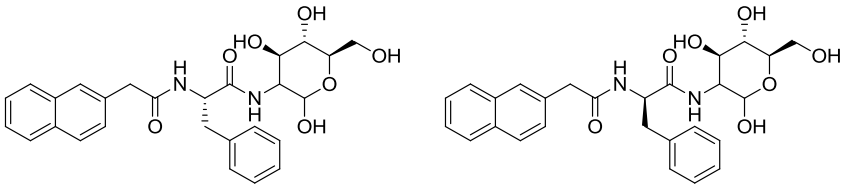

Fig. 1.40: Estructura química de Naftol-L-fenilalanina-D-glucosamina y Naftol-D-fenilalanina-D-glucosamina.

La rigidez de los anillos de naftaleno, ayudan a la gelificación. Por **espectroscopía de fluorescencia** y medidas de **absorción** se confirma el apilamiento de los grupos naftol y las señales de **DC** indican una organización muy parecida a la organización en láminas β de los péptidos. Además, los estudios de **propiedades reológicas** han mostrado diferencias en las propiedades mecánicas según deriven de D o L-fenilalanina. Estas características también se observan por **microscopía**: en el gel con L-fenilalanina hay una mayor densidad de fibras muy entrecruzadas, mientras que en el gel con D-fenilalanina los tamaños de las cintas son más uniformes siendo éstas más pequeñas y

rígidas. Como se ha comentado, estos geles supramoleculares se han aplicado con éxito a heridas, **previniendo** la formación de **cicatrices**. Tras realizar estudios de viabilidad celular eligieron el gel de D-fenilalanina para testarlo en ratones. No se observó toxicidad ni infecciones tras 18 días, además las cicatrices son más pequeñas y el proceso de cura es más rápido.

Recientemente el grupo de Wang, ha obtenido un nuevo hidrogel, utilizando la misma estructura en la parte hidrofóba que los hidrogeles anteriores, pero variando la cabeza polar, **Fig. 1.41**.[85] Han comprobado que su hidrogel sirve de matriz para la **adhesión y proliferación de células**, como los fibroblastos embrionarios de ratón: NIH 3T3 y los carcinomas humanos: Hep G2, AD293, HeLa. Los derivados con la misma parte hidrófoba pero con glucosa o lactosa como cabeza azucarada no gelifican.

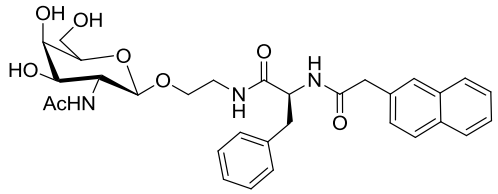

Fig. 1.41: Estructura química del compuesto gelificante glicosilado descrito por Wang y sus colaboradores.

El grupo de Möller utilizó las moléculas anfífilas azucaradas que se muestran en la **Fig. 1.42** para gelificar en disolventes orgánicos, con el objetivo de que sirvieran como **plantilla** para crear huecos en **matrices poliméricas**. Aprovechando su comportamiento gelificante, utilizan distintos metacrilatos como disolventes para formar una matriz que posteriormente polimerizan con luz UV.[86] Tras curar el material se obtuvieron láminas ultrafinas donde se observan estructuras fibrilares que coinciden con el tamaño de las moléculas gelificantes, sin embargo no se ha descrito su eliminación.

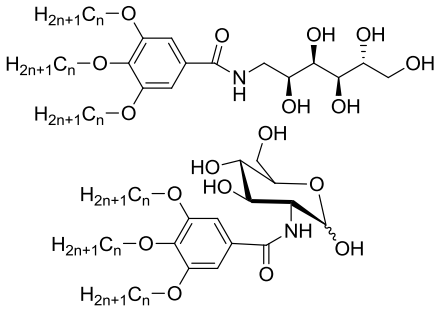

Fig. 1.42: Representación de las moléculas gelificantes utilizadas por Möller y sus colaboradores donde n=8, 12 y 16.

Otro ejemplo de los esfuerzos sintéticos realizados con este tipo de moléculas es el trabajo realizado por el grupo de Hamachi. Gracias a la optimización de una síntesis en fase sólida, prepararon una amplia librería de compuestos glicoanfifílos,[67, 87] dentro de la cual los compuestos de la **Fig. 1.43** forman hidrogeles. Algunos de ellos han sido aplicados con éxito en **sensores** y **encapsulación de células**.

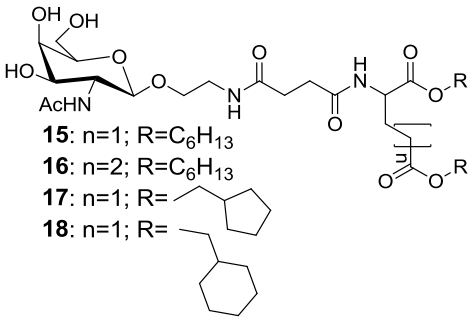

Fig. 1.43: Estructura química de los glicolipidos preparados por Hamachi y sus colaboradores capaces de gelificar en medio acuoso.

Atendiendo a la parte hidrófoba, se ha observado que aquellos compuestos que poseen anillos de cinco **17** o seis carbonos **18** gelifican mejor que aquellos que tienen una cadena alquílica lineal, llegando a gelificar incluso a una concentración de 0.15 % en peso.

El compuesto **17** es estable incluso a altas concentraciones de sal y además es capaz de atrapar mioglobina sin que pierda su actividad.[87b] Con este mismo compuesto, se han fabricado dispositivos que han servido como **sensores**.[68] La ventaja de usar estas matrices de tipo supramolecular es que se pueden inmovilizar receptores sin la necesidad de unirlos a un soporte y así no pierden la capacidad de reconocimiento que tienen en disolución. Las cavidades nanométricas sirven como zonas de reconocimiento en condiciones semi-húmedas y la relación señal/ruido mejora. El receptor se mezcla con la molécula gelificante y se forma el hidrogel, sobre éste se añade un analito (en este caso fosfato), que se difunde por la matriz. Se pueden entonces diseñar chips capaces de determinar varios analitos a la vez sin necesidad de separarlos y en cantidades muy pequeñas. En los chips, cada hidrogel puede tener un receptor distinto embebido en la matriz del gelificante.

El compuesto **18** por su parte tiene un comportamiento fuera de lo habitual, es capaz de **encogerse** y expulsar agua gracias al calentamiento en vez de la típica transición gel-sol. Los puentes de hidrógeno, en la cabeza azucarada, asisten el empaquetamiento de los anillos, de tal manera que las estructuras fibrilares resisten incluso temperaturas elevadas y así el gel se encoge pero no se solubiliza. Con este gel se han hecho pruebas de liberación de DNA, detectándose su fuga al aumentar la temperatura y también con bisfenol A, que queda atrapado en las cavidades y co-precipita con el gel al calentar. Se puede decir que este gel tiene la capacidad tanto de **encapsular** como de **liberar**.[88]

Se han formado también **microdispositivos semihúmedos péptido/proteína** donde, no sólo se puede detectar la presencia de analitos, sino que también se puede determinar la cantidad de los mismos.[89] En la **Fig. 1.44** se representa uno de estos dispositivos donde la reacción enzimática tiene lugar en las cavidades del hidrogel. En un primer momento, se deposita una disolución acuosa caliente del gel sobre un soporte y se deja enfriar para que se forme la estructura (**1**), posteriormente se añade un **péptido**, cuando lo que se quiere detectar es una determinada enzima, o un **enzima**, cuando lo que se quiere detectar es un determinado inhibidor (**2**). Por último, se adiciona el **analito problema** (**3**), siendo entonces un enzima o un inhibidor. Si además se inserta un fragmento fluorescente, se puede monitorizar la reacción por **fluorescencia**. Como ejemplos, se han utilizado glicosidasas, fosfatasas y proteasas.[68] Algunos dispositivos son capaces de

detectar y clasificar diferentes **bacterias** en función de sus análisis enzimáticos[90] y otros detectan **azúcares** unidos a proteínas.[91]

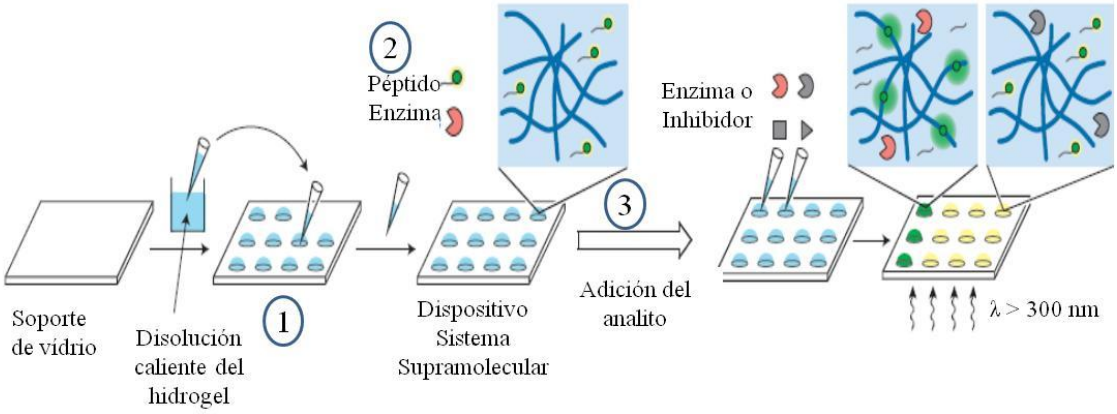

Fig. 1.44: Preparación de un dispositivo para la detección enzimática formado por el hidrogel del compuesto **18**; **Ref [68].**

Por el estudio realizado para la **liberación** de distintas **vitaminas**, cabe mencionar la formación de hidrogeles **sensibles al pH** que combinan el compuesto **18** con una molécula similar pero que en lugar de la cabeza azucarada posee un ácido carboxílico en su cabeza polar.[92]

En un paso más y siguiendo con este tipo de compuestos, Hamachi y su grupo modificaron la estructura de sus moléculas para obtener geles **sensibles a la luz** introduciendo amidas derivadas del ácido fumárico en el espaciador,[93] véase la **Fig. 1.45**.

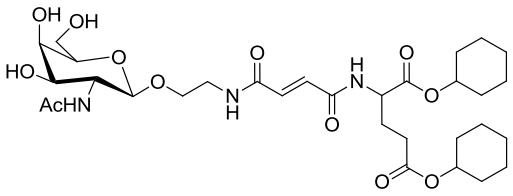

Fig. 1.45: Estructura química del gelificante con fumárico capaz de formar un hidrogel fotosensible.

Con esta molécula se obtiene un hidrogel transparente, a una concentración mínima de 0.05% en peso. Este gel puede irradiarse con luz UV de forma selectiva para que pase a sol en determinadas zonas. Esto sucede porque el fumárico (*trans*), se isomeriza a maleico (*cis*), rompiéndose con ello los enlaces de hidrógeno. Para que se dé esta transición, un 50% del isómero *trans* (fibras) ha de isomerizar, formándose vesículas. Es posible volver del estado sol al gel irradiando con luz visible en presencia de bromo. Este hidrogel se ha usado como dispositivo para **limitar el movimiento** rotatorio de F1-ATP y el movimiento de bacterias. Las F1-ATP o las bacterias no se pueden mover en el estado gel pero sí cuando es irradiado. Además se ha utilizado para construir **nano-reactores**, donde gracias al control con la luz se pueden producir reacciones enzimáticas dentro de gotas de tamaño nanométrico.[94]

También se ha introducido un ácido mucónico,[95] véase Fig. **1.46**, dando lugar a hidrogeles al 0.05%.

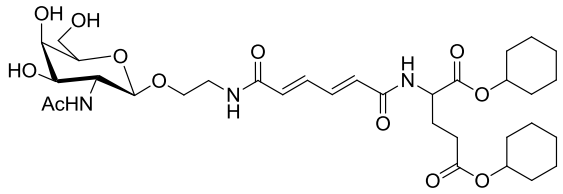

Fig. 1.46: Estructura química de la molécula gelificante derivada de N-acetil-glucosamina y ácido mucónico.

En este gel, gracias a un estudio realizado con nanoesferas de poliestireno, usadas en un principio para determinar el tamaño de poro, los autores descubrieron que se consigue una distribución más homogénea y dispersa del entramado fibroso cuando se añaden dichas nanoesferas. Esta ventaja la utilizaron para estudiar el hidrogel como matriz para **encapsular células**. Como se puede observar en la **Fig. 1.47**, en un ensayo con células T-humanas de tipo fibroblastos, se ha demostrado que las células se depositan cuando no hay hidrogel (**A**), con el hidrogel son capaces de distribuirse por la matriz (**B**) y con la adición de nanoesferas embebidas en el hidrogel se consigue una distribución aún más homogénea (**C**). Este último sistema no es citotóxico.

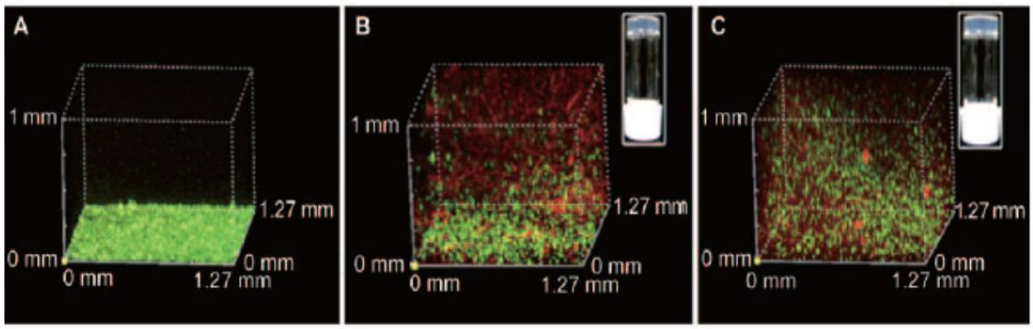

Fig. 1.47: Imágenes 3D por microscopía laser confocal espectral (CLSM) con células en medio (**A**), además con la presencia de 0.1% en peso del gelificante (**B**) y con la adición de nanoesferas (**C**); **Ref [95].**

1.2.2.1.3. *Moléculas gelificantes con cabeza azucarada disacárida*

En cuanto al estudio de hidrogeles con moléculas formadas por disacáridos como cabeza polar, los ejemplos en la bibliografía son limitados. Las moléculas de Bhattacharya y sus colaboradores,[77] están formadas por **lactosa** o **maltosa** unidas a una o dos **cadenas *N*-alquílicas**, véase la **Fig. 1.48**. Los compuestos con una sola cadena son capaces de gelificar en agua con la adición de metanol. Cuando hay dos cadenas también forman geles pero sus propiedades mecánicas son inferiores.

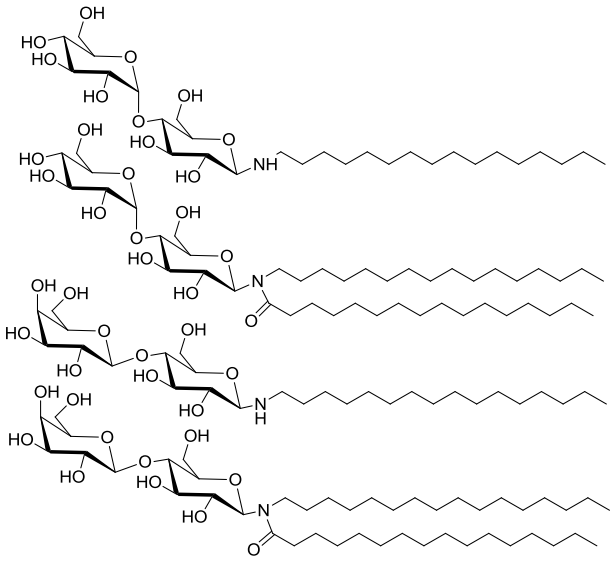

Fig. 1.48: Estructura química de los anfífilos derivados de *N*-alquil disacáridos.

La estructura observada en los geles es fibrilar, aunque en un trabajo posterior se buscó formar vesículas con estos compuestos.[96] Tanto en agua como con la adición de Cu^{2+} o Ni^{2+} se obtuvieron vesículas en suspensión en disoluciones frescas, pero con el tiempo (horas) se transforman en estructuras lamelares o tubulares. Con la adición de Cu^{2+}, en el caso de la lactosa unida a una sola cadena sí que se obtuvieron vesículas estables, ya que el cobre se coordina con el OH del C2 y la amina.

En el trabajo realizado por Rico-Lattes y sus colaboradores con glicolípidos, las moléculas que se muestran en la **Fig. 1.49** fueron capaces de gelificar en agua, para distintas concentraciones, desde 30 % en peso a 10 % en peso dependiendo del compuesto.[97] Estas moléculas derivan de la lactosa y tienen una cadena fluorocarbonada.

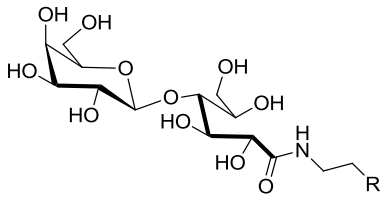

R= C_6F_{13} (mínima concentración gelificante 30 % en peso)
R= C_8F_{17} (mínima concentración gelificante 20 % en peso)
R= $C_{10}F_{21}$ (mínima concentración gelificante 10 % en peso)

Fig. 1.49: Estructura química de las moléculas hidrogelificantes derivadas de lactosa con una cadena alifática fluorocarbonada.

El último ejemplo de moléculas gelificantes basadas en disacáridos son los derivados de sacarosa y fenilalanina, sintetizados por Fitremann y colaboradores,[98] véase la **Fig. 1.50**. La mezcla de regioisómeros da lugar a un gel en agua al 2 % en peso, por tratarse de la base del trabajo realizado en esta tesis será comentado posteriormente en el siguiente capítulo.

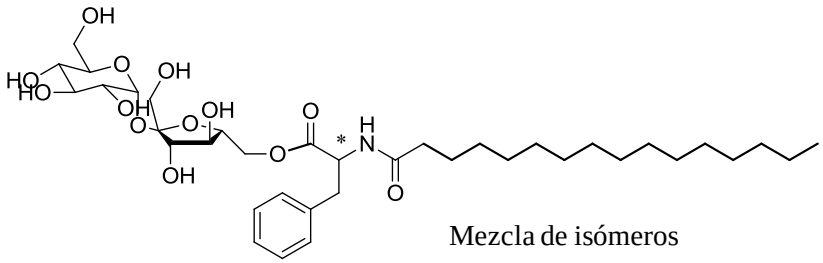

Fig. 1.50: Mezcla de isómeros de surcroésteres de N-palmitoilfenilalanina

1.2.2.1.4. *Otras moléculas gelificantes con azúcares modificados*

Además de los glicoanfifílos convencionales, existen otras moléculas gelificantes con azucares modificados en su estructura. Primero el grupo de Shinkai[99] y más tarde el grupo de Wang,[100] sintetizaron y estudiaron el comportamiento gelificante de benciliden-derivados de monosacáridos. En la **Fig. 1.51**, se han representado aquellos que gelifican en agua.

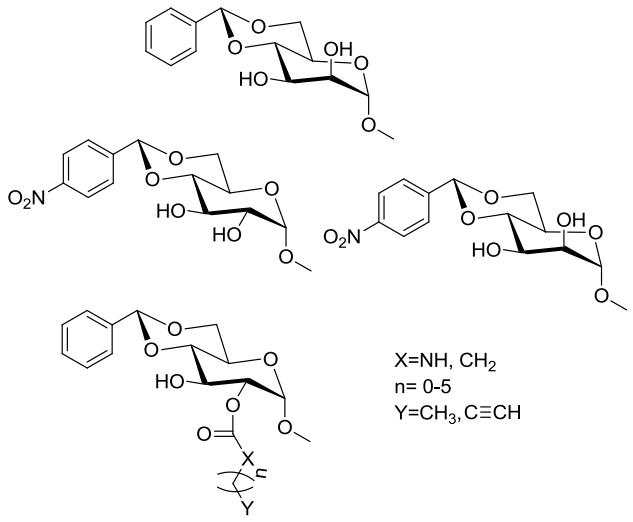

Fig. 1.51: Estructura química de moléculas gelificantes con azúcares modificados.

Construyeron toda una librería de compuestos con diferentes grupos unidos al azúcar por un enlace éster introduciendo además cadenas alquílicas de distintas longitudes, anillos, triples enlaces… etc. Estos derivados son capaces de gelificar en diferentes disolventes, tanto no polares, como aromáticos y polares próticos.

1.2.2.2. *Bolaanfífilos*

Los compuestos azúcarados anfífilos convencionales y en particular los derivados de monosacáridos han sido los más estudiados. No obstante, los compuestos que poseen dos cabezas polares, una en cada extremo de la estructura, también resultan ser buenos gelificantes.

Como ya se ha mencionado anteriormente, Shimizu y colaboradores, no sólo han trabajado en el estudio de anfífilos convencionales sino que también han sintetizado bolaanfífilos, como los representados en la **Fig. 1.37.** Además han descrito otros ejemplos donde dos cabezas azucaradas de **glucosa** están unidas por un puente alifático gracias a un enlace amida,[101] véase la **Fig. 1.52**.

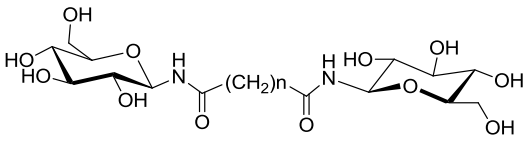

Fig. 1.52: Estructura química del bolaanfífilo formado por glucosilamidas con n=6, 9, 10, 11, 12, 13, 14.

En estos compuestos, que se diferencian por la distinta longitud de su cadena, se ha observado un **efecto par-impar** para su agregación en agua. Si la cadena alifática que sirve de puente tiene un número par de carbonos, los agregados se auto-ensamblan en forma de fibras mientras que si el número de carbonos es impar se obtienen sólidos amorfos, lo que pone de manifiesto la influencia de cualquier factor estructural a la hora de diseñar materiales gelificantes. En el caso de n=10 es capaz de gelificar.

Los autores han propuesto el modelo de organización que se muestra en la **Fig. 1.53** para la estructura fibrilar con n=12 basándose en medidas de difracción de RX, FT-IR y cálculos de longitud molecular. Se asume que las fibras están constituidas de estructuras en capas y que los periodos más largos medidos por RX corresponden a la anchura de una monocapa dentro de las fibras.

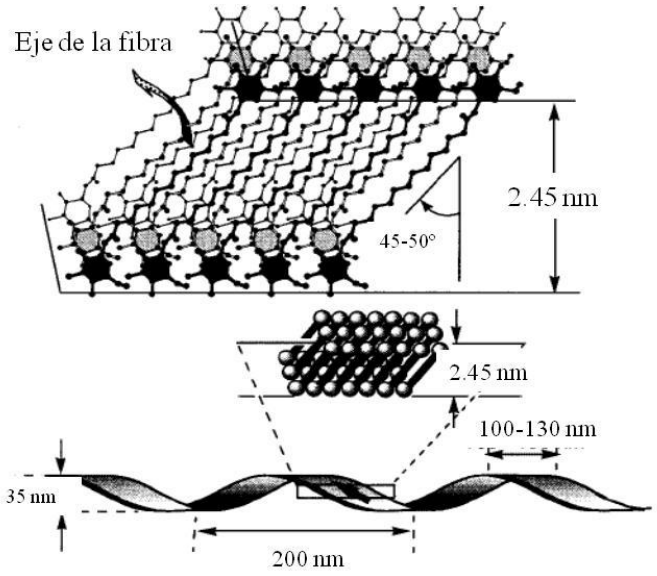

Fig. 1.53: Posible modelo de autoensamblaje del compuesto con n=12 en el que una fibra está compuesta de una monocapa laminar; **Ref [101].**

Se han sintetizado también compuestos similares a los de la **Fig. 1.52** pero con distintas cabezas azucaradas, de los cuales sólo con los derivados de 1-glucosamidas (n=12) y 1-galactosamidas (n=12) se obtienen geles, al realizar una mezcla 1:1 en agua/metanol.[33]

En un trabajo posterior, se introdujeron además triples enlaces en la cadena alifática para poder **polimerizar con luz UV**.[102] Si los grupos OH están protegidos con acetatos se obtienen organogeles en mezclas de acetato de etilo y hexano, mientras que si los grupos OH no están protegidos, se forman fibras en agua y THF. Al polimerizar dentro de las fibras, se ha podido comprobar que no existe cambio en la morfología y que se alcanza una cierta estabilización. En el caso de tener los OH desprotegidos, el empaquetamiento es mayor y se obtiene un mayor grado de polimerización que en el caso de tenerlos protegidos.

Con estos ejemplos de moléculas glicoanfífilas y los sistemas formados a partir de ellas, queda demostrado que los azúcares son útiles para el diseño molecular de nuevos geles que, normalmente, tienen estructura quiral. Sin embargo, el diseño de este tipo de estructuras no es sencillo ya que es necesario un balance adecuado entre las distintas interacciones (enlaces de hidrógeno, interacciones π-π e interacciones hidrófobas) para que se genere un auto-ensamblaje fibrilar que soporte la estructura del gel. En ocasiones es posible que incluso con un simple cambio en un carbono se pueda obtener un cambio

drástico en las propiedades de solubilidad y de morfología en las estructuras autoensambladas y por tanto en la gelificación.

1.3. Fotoquímica del azobenceno y aplicaciones a geles

Gracias a la reversibilidad de las interacciones no-covalentes que forman la estructura tridimensional de los geles supramoleculares éstos, son capaces de **responder** a estímulos externos.[3] Modulando estos **estímulos**, el material puede sufrir **modificaciones** en sus propiedades. Normalmente la modificación buscada es el paso de un estado no fluido a fluido (gel-sol) o viceversa, mediante el control de las uniones que mantienen el entramado. Esta modificación no siempre ocurre y el tipo de respuesta, va a depender del estímulo aplicado, afectando a la estructura a distintos niveles dentro de la organización supramolecular. De ahí que se puedan dar desde cambios a nivel molecular, en la geometría o extensión del ensamblaje y por lo tanto, provocar cambios en el tamaño o la forma de los agregados, hasta llegar a cambios en el tamaño o en las propiedades de las fibras. Así los geles, pueden también hincharse, cambiar de color o alterar sus propiedades de conductividad… etc.[103]

Además de las típicas respuestas a la temperatura o la aplicación de un estrés mecánico, los geles pueden modificarse con estímulos tanto de tipo **químico** como **físico**. Entre los geles capaces de responder a estímulos químicos, se pueden encontrar aquellos que responden a la formación de un complejo "host-guest",[104] a interacciones metal-ión[1] y a cambios en el pH.[105] Mediante un estímulo físico, como la **luz**, también se puede llegar a la transformación del material.

Dentro de los **geles fotosensibles**, Del Guerzo y Pozzo incluyen los geles luminiscentes[106] y los geles **foto-modificables** ("*fototunable"*).[103] En éstos últimos, la transformación se produce mediante un **proceso fotoquímico** y se consigue mediante la incorporación a nivel molecular de una parte fotosensible o bien, mediante la adición de un compuesto fotosensible en la red tridimensional. Este grupo fotosensible es el que proporciona la capacidad de alternar entre dos estados químicos diferentes, que poseen distintos espectro de absorción (fotocrómico). La alternancia se consigue gracias a la radiación electromagnética infrarroja, visible o ultra-violeta, irradiada en las longitudes de onda apropiadas. Algunos mecanismos por los que se puede producir esta modulación son isomerización *cis-trans*, tautomerización y apertura-cierre electrocíclico. El estado fotoinducido puede ser irreversible o reversible.[103]

Dentro de los distintos grupos fotocrómicos, el **azobenceno** se ha utilizado ampliamente en ciencia de los materiales. Al introducirlo en estructuras capaces de formar sistemas supramoleculares autoensamblados, se pueden inducir cambios por **isomerización fotoquímica** entre las especies ***trans* o E** y ***cis* o Z**. El isómero menos estable, Z, en algunos casos, puede llegar a predominar en el estado foto-estacionario y provocar modificaciones o disrupciones a nivel estructural. Así puede alcanzarse la transición gel-sol, mediante el paso de una especie gelificante E, a un isómero no gelificante, Z. Esta transición es reversible, pero en ocasiones, debido al buen empaquetamiento de los sistemas π-π del azobenceno en los agregados formados, no es posible la isomerización al *cis* y por tanto no se llega a producir cambios en la estructura del gel.[107]

Otros grupos fotocrómicos utilizados, que pueden inducir un fotocromismo reversible, son el antraceno,[108] benzopireno,[109] ditienilo[110]… etc. Por el contrario, la irradiación en derivados del maleico[111] o espiropirano,[112] en hidrogeles, o benzofenona,[113] en organogeles, producen cambios irreversibles en los sistemas gelificantes. Los hidrogeles fotosensibles son menos numerosos que los organogeles debido a la dificultad de introducir en su estructura partes sensibles a la luz ya que suelen ser bastante apolares.

En este capítulo nos vamos a centrar en el azobenceno como molécula fotocrómica y su aplicación a glicoanfífilos.

1.3.1. *Fotoisomerización del azobenceno*

El amplio uso de azobenzeno como **grupo fotosensible**[114] es debido a sus características de isomerización reversible, su alta estabilidad química y térmica y el hecho de que presenten una síntesis relativamente sencilla.

La molécula de azobenceno posee un orbital π deslocalizado a lo largo de toda la molécula y un orbital n que corresponde a los pares de los electrones no enlazantes de los átomos de nitrógeno.[115] La **interconversión reversible** del ***trans*-**azobenceno en su isómero ***cis***, es posible por **irradiación con luz** a una longitud de onda adecuada (generalmente luz UV con una longitud de onda correspondiente al máximo de la banda π-π* del *trans*-azobenzeno), dando lugar a una mezcla de ambos cuya composición depende de la longitud de onda y la temperatura. La transformación del ***cis*-**azobenceno a ***trans*-**azobenceno es un proceso reversible tanto por la luz (generalmente luz visible

en la banda n-π* donde el *cis* presenta mayor absorción) como térmicamente.[116] La isomerización térmica de la forma *cis* a la *trans* puede tener lugar incluso a temperatura ambiente y la vida media del isómero *cis* depende de los sustituyentes químicos del cromóforo azobenceno, del entorno en el que se encuentra y es menor conforme aumenta la temperatura.[117]

Se han propuesto varias explicaciones para el proceso de isomerización. La más apoyada es la que argumenta dos posibles **mecanismos**: rotación e inversión[118], véase la **Fig. 1.54**. El mecanismo de **rotación** consiste en un giro alrededor del enlace azo fuera del plano de la molécula, mientras que en el de **inversión** se produce un giro dentro del plano de la molécula de uno de los nitrógenos o de ambos a través de un estado estacionario híbrido de tipo sp. El mecanismo en el proceso de fotoisomerización depende de los sustituyentes del derivado de azobenceno y de la longitud de onda de la luz empleada en la fotoexcitación. En la isomerización térmica, el mecanismo de inversión es el dominante.[119]

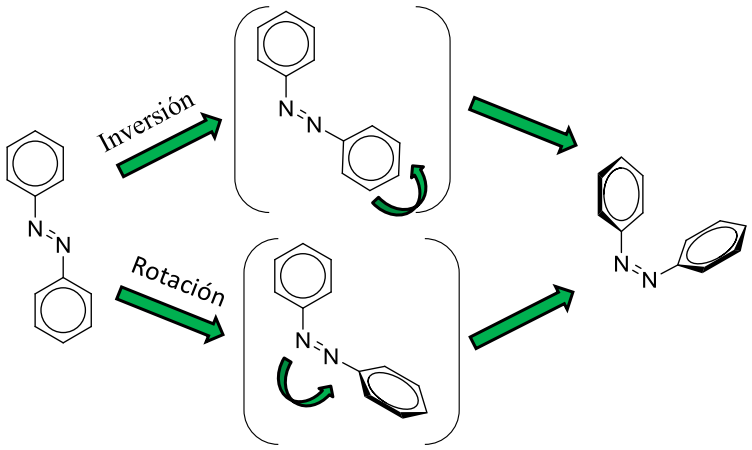

Fig. 1.54: Mecanismo de inversión (arriba) y de rotación (abajo) para la fotoisomerización *trans-cis* de azobencenos; **Ref [118].**

Esta isomerización va acompañada de un cambio en la estructura y en la polaridad. La distancia entre los átomos de carbono en posición *para* de los anillos de benceno disminuye desde 9,0 Å en el isómero *trans*, que es plano, a 5,5 Å en el isómero *cis*, con geometría curvada y no plano, véase la **Fig. 1.55**. Además se produce una variación en

el momento dipolar. El isómero *trans* no tiene momento dipolar neto, mientras que el isómero *cis* posee un momento dipolar de 3,0 D.[120]

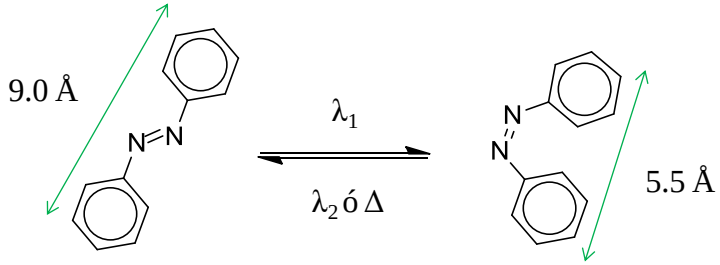

Fig. 1.55: Fotoisomerización *trans-cis-trans* del azobenceno.

La fotoisomerización estructural del grupo azobenceno da lugar a cambios en el espectro de absorción, **Fig. 1.56**. El isómero *trans* presenta una banda intensa en la región del UV-vis, a 340 nm, asociada a la transición **π-π***, y una débil en la región del visible, alrededor de 450 nm, correspondiente a la transició n-π* prohibida por simetría (que la intensidad no sea nula en el espectro del isómero *trans* se debe a distorsiones no planares de la molécula y a acoplamientos vibracionales). En el isómero *cis*, la transición n-**π*** está permitida y por ello la banda correspondiente es más intensa que en el isómero *trans*.[117a, 119]

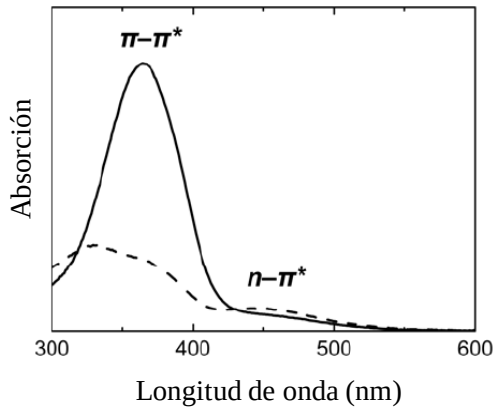

Fig. 1.56: Ejemplo típico del espectro de absorción de una película delgada de un derivado de azobenceno en su estructura en forma *trans* (línea continua) y después de la irradiación, *cis* (línea discontinua).

Además de la incorporación de distintos sustituyentes en el azobenceno, otro efecto que puede modificar las posiciones y las bandas de absorción de los compuestos es la tendencia a formar **agregados**. El apilamiento de los anillos aromáticos se produce de tal manera que los momentos dipolares de azobenceno quedan alineados. Los principales tipos de agregados son los denominados de tipo H y de tipo J, véase la **Fig. 1.57**. En los **agregados de tipo H** se produce un solapamiento completo de los grupos azobenceno. Por otra parte, cuando el ángulo de inclinación definido en la figura es lo suficientemente pequeño, el **agregado** es **de tipo J**. La formación de agregados de tipo H desplaza la banda de absorción principal hacia longitudes de onda menores mientras que en el caso de la formación de agregados J, se desplaza hacia mayores longitudes de onda.[121]

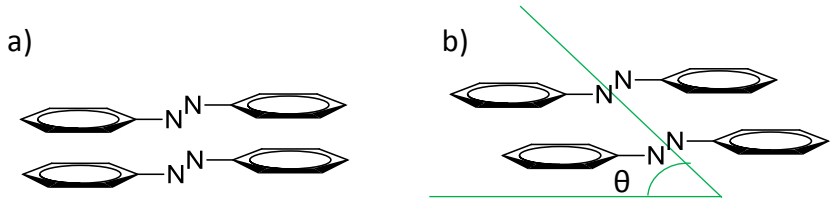

Fig. 1.57: Representación esquemática de los agregados tipo H (a) y J (b).

1.3.2. *Moléculas gelificantes fotosensibles con azobenceno en su estructura*

Dentro de los distintos **geles fotosensibles** podemos encontrar varios ejemplos de moléculas gelificantes con grupos **azobenceno** en su estructura, tanto organogeles como hidrogeles, aunque estos últimos en menor número. Además también se han realizado varios trabajos con mezcla de dos componentes, en el que uno de los dos era un derivado azobencénico.

1.3.2.1. *Organogeles con azobenceno en su estructura*

A continuación se presentan distintos ejemplos de organogeles encontrados en la bibliografía que contienen un grupo azoico en su estructura. Se han clasificado, de una forma no estricta, en función de un fragmento común distinto al azobenceno.

- **Derivados de colesterol:**

Uno de los primeros trabajos con moléculas gelificantes, donde se introdujo una unidad de azobenceno en la estructura, fue descrito por Shinkai[40, 122] y sus colaboradores. Sintetizaron los derivados de colesterol que se muestran en la **Fig. 1.58**. Estas moléculas, sin la parte azobencénica, se conocían anteriormente por sus propiedades como organogelificantes.[123]

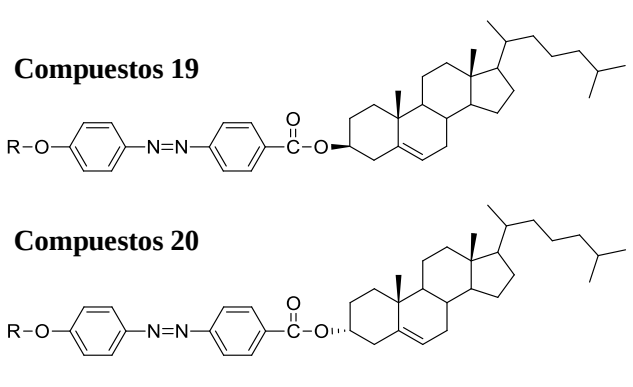

R= CH_3	**19Me**
R=C_2H_5	**19Et**
R= C_3H_7	**19Pr**
R= C_4H_9	**19Bu**
R= $C_{10}H_{21}$	**19Dec**
R= CH_3	**20Me**
R=C_2H_5	**20Et**
R= C_3H_7	**20Pr**
R= C_4H_9	**20Bu**
R= $C_{10}H_{21}$	**20Dec**

Fig. 1.58: Moléculas derivadas de colesterol con grupos azobenceno sintetizadas por Shinkai y sus colaboradores; **Ref [40].**

El objetivo era estudiar en primer lugar la organización que el grupo *trans*-azobenceno provocaba en la agregación, en segundo lugar, el control mediante irradiación de la transición sol-gel y en tercer lugar, la influencia en las temperaturas de gelificación y en la morforlogía de la introducción de distintos sustituyentes en el azobenceno.

Los derivados de *p*-alcoxiazobenzeno (**Fig. 1.58**, **compuestos 19 y 20**) actúan como gelificantes termosensibles en varios disolventes orgánicos. Dependiendo de la configuración del C3 del colesterol, cambian las propiedades de gelificación. Así, cuando hay una configuración S, **compuestos 19**, la gelificación tiene lugar en disolventes apolares y cuando la configuración es R, **compuestos 20**, la gelificación tiene lugar en disolventes polares. Además, en el caso de que la configuración sea S se ha observado un efecto par-impar en la longitud de las cadenas alifáticas, mientras que los derivados metoxi **19Me** y propiloxi **19Pr** gelifican en dietileter, los derivados de etoxi **19Et** y butoxi **19Bu**, no gelifican. En el caso de la configuración R, se han

obtenido resultados contrarios, ya que al aumentar el número de carbonos, aumenta la capacidad de gelificación. Como se puede observar en la **Fig. 1.59**, mediante DC, se ha observado que el estado sol no es activo, mientras que el estado gel sí lo es.

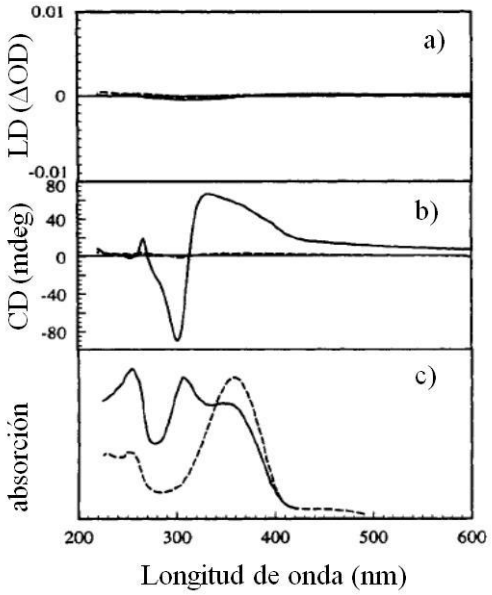

Fig. 1.59: Estudio del gelificante **19Me** en butanol al 0.2% en peso: a) Espectro de dicroísmo lineal, b) Espectro de dicroísmo circular, c) Espectro de absorción. El estado gel se observa a 25ºC (línea continua) y el estado disuelto se observa a 60ºC (línea discontinua); **Ref [40].**

El gel del ejemplo se forma en butanol al 0.2 % en peso del **compuesto 19Me**. La señal en UV-vis también cambia del estado sol al estado gel, se produce un desplazamiento del máximo a 360 nm en disolución a 310 nm en estado gel (**Fig. 1.59.c**). Para la señal de dicroísmo en estado gel, se han encontrado señales de acoplamiento exciton coincidiendo con $\lambda_{máx}$ en el estado gel (**Fig. 1.59.b**). Esto indica que las partes colestéricas se agregan en una dirección quiral específica impuesta por los azobencenos que interactúan entre ellos de una manera asimétrica.

De una manera accidental, se observó, que para algunos geles, dependiendo de su velocidad de enfriamiento, la señal de dicroísmo se invierte. Esto se puede observar en la **Fig. 1.60**, para un gel formado en etanol al 0.2% en peso del **compuesto 19Bu,** donde se ha obtenido una quiralidad opuesta, según la forma de hacer el gel.

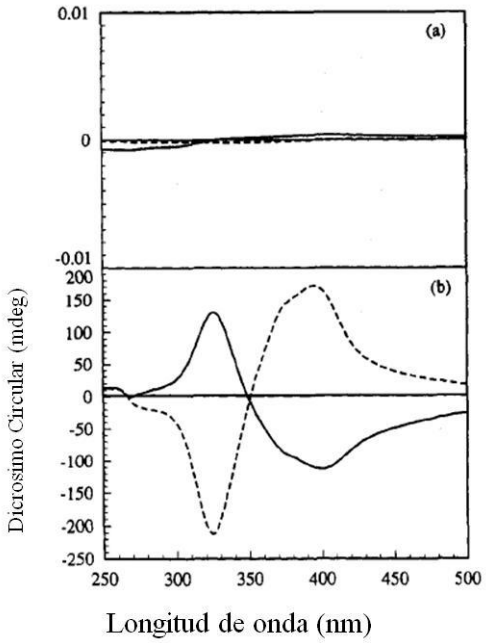

Fig. 1.60: a) Espectro de Dicroismo Lineal, b) Espectro de Dicroismo Circular de dos geles en etanol al 0.2 % en peso de **19Bu** medidos a 25ºC. Para un gel, la disolución a 60ºC se enfrió en un baño de hielo a 2ºC (línea continua), en el otro gel, la disolución a 60ºC se enfrió al aire a temperatura ambiente (línea discontinua); **Ref [40].**

En un gel de butanol (0.1 % wt) del **compuesto 19Me** se ha conseguido inducir la transición gel-sol por fotoisomerización *trans-cis*. Para ver si esta transición es reversible se realizaron experimentos de transmitancia, como se muestra en la **Fig. 1.61**. La transmitancia es del 97,8% para el isómero *trans* mientras que es del 100% para la mezcla *cis-trans*. Este experimento ha sido repetido varias veces obteniendo la misma reversibilidad.

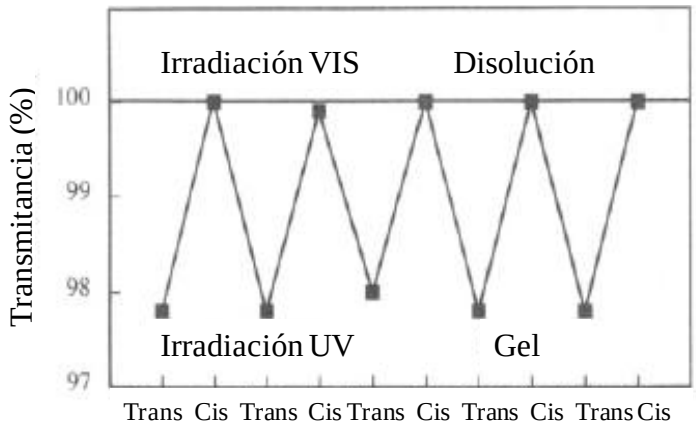

Fig. 1.61: a) Fotocontrol de la transición gel-sol de **19Me** (0.1% wt) en butanol medido a 25ºC. Luz UV (330 nm<λ<380 nm) y luz visible (λ>460 nm); **Ref [40].**

Si se estudia este fenómeno por DC, en una muestra del gel en butanol (0.2 % wt, a 25ºC), se observa que el estado gel tiene una señal de DC, mientras que irradiando con luz UV, se convierte en disolución y la señal desaparece. Al volver a irradiar con luz visible, el gel se vuelve a formar y se obtiene de nuevo una señal.

Además del grupo azo, Shinkai y sus colaboradores, introdujeron **éteres corona** a las moléculas gelificantes con colesterol (**Fig. 1.62**). Estos compuestos tienen, además de un grupo sensible a la luz, la capacidad de coordinarse a metales alcalinos (Li^+, Na^+, K^+, Rb^+) y sales de amonio. Estos iones son muy poco solubles en los disolventes de gelificación y cuando se acomplejan pasan a ser solubles. En los geles del compuesto **21** también pueden inducirse ciclos gel-sol mediante irradiación.[122]

Los compuestos de la **Fig. 1.62** son capaces de actuar como **plantillas** (*"templates"*) para la formación de estructuras de sílice.[124] Estas moléculas son capaces de gelificar en presencia de una disolución de tetraetoxisilano (TEOS)[125] y tras una policondensación del mismo sobre la supraestructura de los gelificantes, se forma una estructura de sílice. Posteriormente esta estructura queda hueca al eliminar los gelificantes por pirolisis. En los compuestos **23** y **24**, se estudió la estabilización por interacciones de tipo **"host-guest"** con la presencia de diaminas para formación de organogeles.[126]

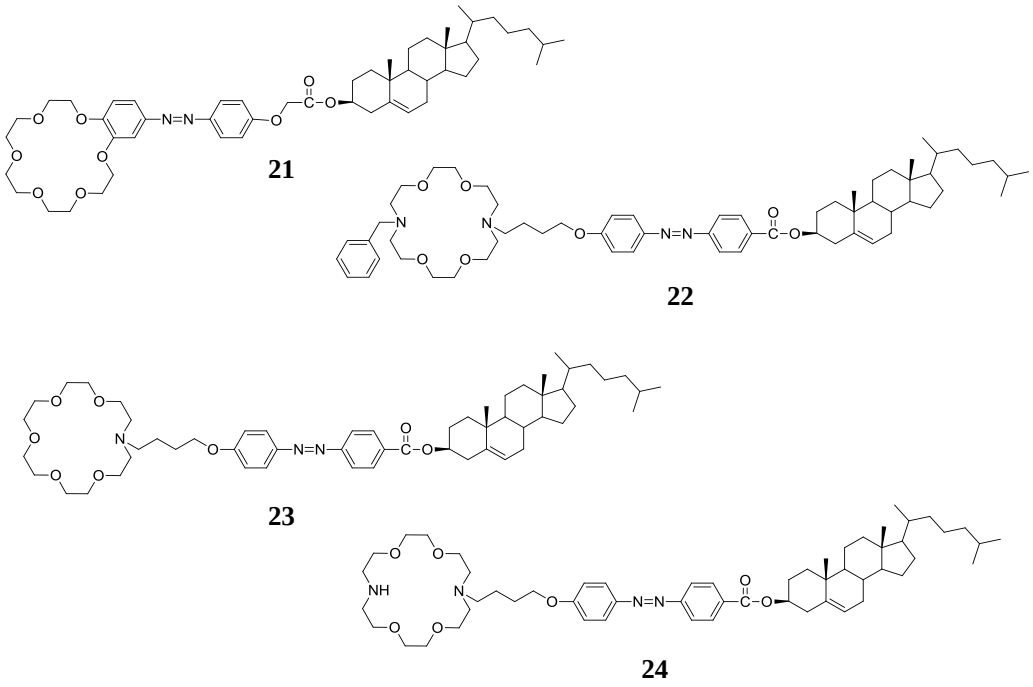

Fig. 1.62: Derivados de colesterol, azobenzeno y éteres corona sintetizados por Shinkai y sus colaboradores.

Otro compuesto similar a los anteriores, es el dímero de la **Fig. 1.63**, que contiene dos grupos colesterol y dos grupo azobenceno y es capaz de gelificar en 1-octanol, en un porcentaje de 5% en peso.[127] Mediante SEM y TEM se observan estructuras fibrilares y gracias a las medidas de sus diámetros, los autores proponen que la molécula adopta una configuración plegada. El gel tiene una señal negativa para el primer efecto Cotton en DC (visto el espectro de derecha a izquierda), indicando que los momentos dipolares tienden a organizarse de una manera antihoraria. Esta molécula también se utilizó como plantilla para la transcripción de la organización supramolecular en sílice, obteniéndose en este caso, huecos helicoidales, con un diámetro interno que coincide con el tamaño de la molécula plegada.

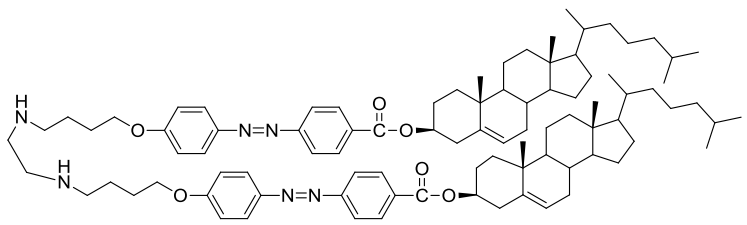

Fig. 1.63: Estructura dímera con azobenceno y colesterol descrito por Shinkai y sus colaboradores.

El siguiente ejemplo, es un derivado de azobenceno sustituido en posiciones 3, 3´ de forma simétrica con grupos colesterol en los extremos,[128] de acuerdo a la **Fig. 1.64**.

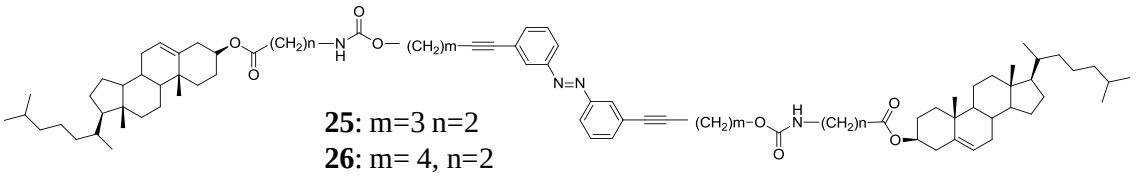

25: m=3 n=2
26: m= 4, n=2

Fig. 1.64: Compuestos derivados de azobenceno, uretano y colesterol descrito por Koumura, Tamaoki y sus colaboradores.

Los grupos uretano son los que permiten la formación de los enlaces de hidrógeno mientras que las partes colestéricas interaccionan por fuerzas de Van der Waals. Los dos compuestos **25** y **26**, forman geles en ciclohexano pero sólo la fotoisomerización de **26** es reversible. Estas transiciones son seguidas por FTIR, donde se observan los picos que indican la existencia de enlaces de hidrógeno antes de irradiar, que desaparecen al irradiar a 365 nm y reaparecen al formarse el gel de nuevo por irradiación a 388 nm. También por DC, la transición se traduce por la aparición de una señal en estado gel, en comparación con la disolución o el estado sol irradiado donde no la presentan.

- **Derivados de ureido:**

Otros ejemplos de organogeles azoicos, son los que han sido desarrollados a partir de la molécula gelificante ya conocida, 1,2-di(ureido)ciclohexano, incorporando en su estructura la unidad azoica.

En un primer estudio, realizado por Feringa, Van Esch y sus colaboradores, el compuesto de la **Fig. 1.65**, **compuesto 27,** se mezcló con una molécula análoga pero con el grupo azobenceno, **compuesto 28**, para estudiar el reconocimiento quiral de los agregados y los organogeles a los que la mezcla daba lugar.[129]

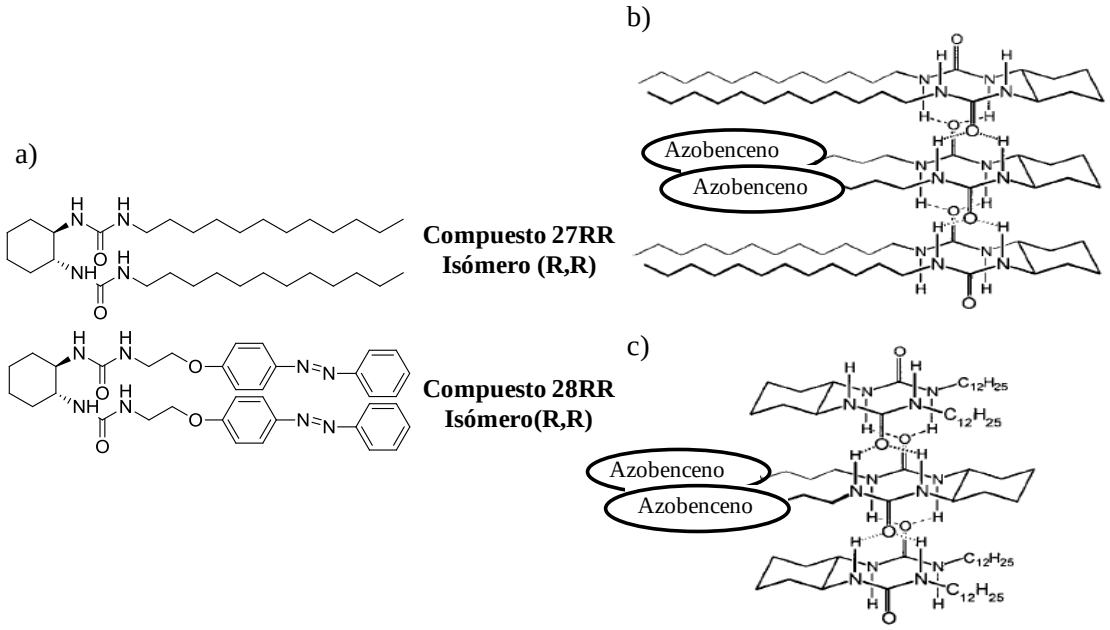

Fig. 1.65: a) Representación de la estructura química de los isómeros **RR** de los compuestos **27** y **28,** b) Modelo de la asociación de **27RR** con **28RR**, c) Modelo de asociación de **27SS** con **28RR**; **Ref [129].**

En la mezcla de los dos compuestos **27** y **28**, se ha comprobado que la formación de grandes agregados se ve afectada por la quiralidad de los compuestos. A partir de estudios de DC de los geles formados en butanol para las mezclas **27RR/28RR** y **27SS/28RR,** los autores han propuesto distintos modelos de asociación (**Fig. 1.65 b** y **c**). La disposición de la unidad azobencénica es diferente dependiendo de los isómeros que forman la estructura del gel. Así se ha observado que si los geles se irradian, tras la irradiación a 365 nm la isomerización es más lenta en el gel formado por **27SS/28RR** que en el de **27RR/28RR**, lo que puede significar que los azos están más expuestos al disolvente dentro del gel formado con **27SS** que en el gel procedente de **27RR**.

Kato y sus colaboradores, incorporaron en pequeñas cantidades una molécula gelificante **30** similar a la descrita anteriormente, en este caso con cianoazobenceno en el extremo a un cristal líquido **29**, véase la **Fig. 1.66**, para formar geles denominados "**geles cristal líquido**". [130]

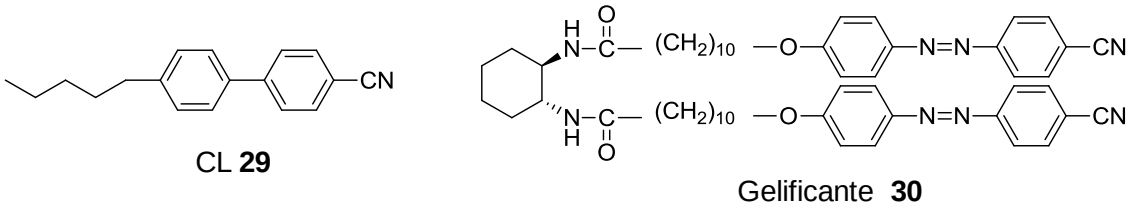

Fig. 1.66: Cristal líquido (CL) usado como disolvente y molécula gelificante derivada de cianoazobenceno utilizadas por Kato y sus colaboradores.

Mediante luz se pueden inducir dos estados diferentes de "geles cristal líquido", véase la **Fig. 1.67**. Al calentar la mezcla de gelificante y cristal líquido (3% en peso del gelificante en el CL, 64ºC) se obtiene un **líquido isótropo** (**A**) y al dejar enfriar se forma a temperatura ambiente un "**gel nemático**" (**B**), donde se ha formado la red tridimensional del gelificante (derivado de azobenceno) y el CL se encuentra en mesofase nemática.

Al irradiar con luz UV, se produce una isomerización en el gelificante y se obtiene una fase cristal líquido colestérica (**C**), donde el gelificante se encuentra disuelto y provoca que el CL presente fase colestérica inducida por la quiralidad del gelificante. Este paso de gel a sol, se demuestra mediante IR ya que después de la irradiación, en (**C**) las bandas NH y CO obtenidas son las que corresponden a grupos libres (3350-3450 y 1662 cm^{-1} respectivamente). Si se mantiene el sistema a temperatura ambiente o se irradia con luz visible débil, el estado *cis* del gelificante pasa a *trans* y se obtiene un "**gel colestérico**" (**D**), donde el gelificante se ha reorganizado manteniendo el orden colestérico del CL. Este "gel colestérico" es estable a temperatura ambiente pero si se calienta y se deja enfriar, se puede volver a obtener el "gel nemático". Esta metodología es aplicable al almacenamiento de información.

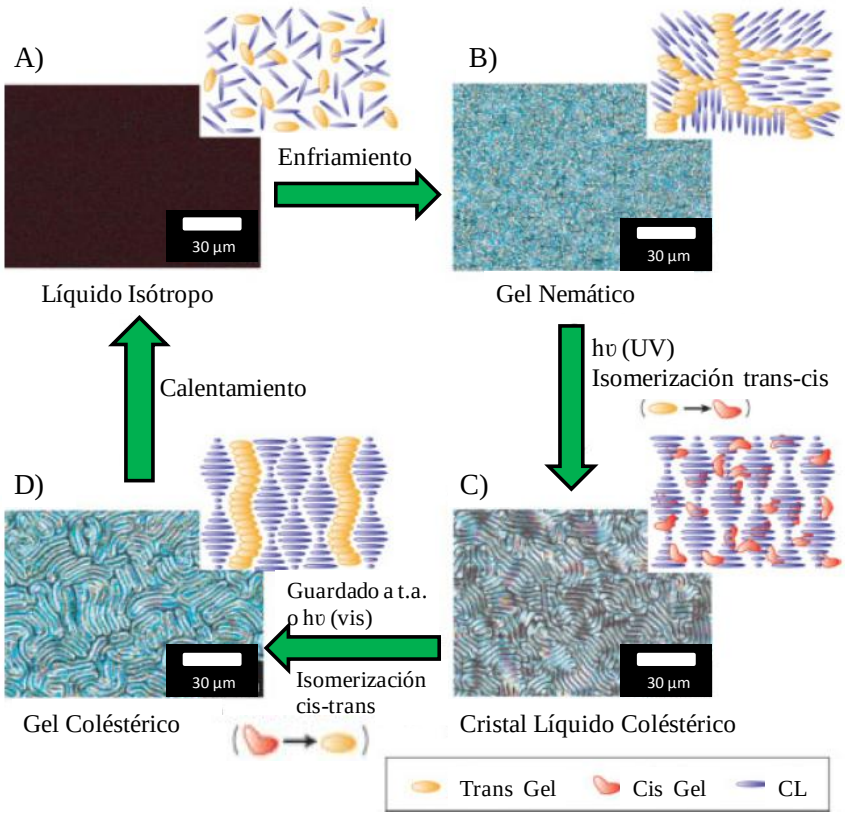

Fig. 1.67: Representación esquemática del tratamiento de una mezcla del CL y del gelificante **30** (3 % en peso) de la **Fig. 1.66**; **Ref [130]**.

El mismo grupo de Kato, estudió la capacidad de gelificación de la molécula azobencénica **30**, por sí sola, en distintos disolventes orgánicos (como en ciclohexanona que es el caso del gel representado en la **Fig. 1.68**) y la posibilidad de inducir un estado gel-sol en dichos geles mediante luz.[131]

Fig. 1.68: Gelificación del compuesto en ciclohexanona (20 gL^{-1}): a) antes de irradiar, b) estado sol después de la irradiación UV (λ= 365nm) durante 2h, c) estado gel después de irradiar el sol durante 1h con luz visible (λ= 436nm); **Ref [131]**.

El paso a sol inducido por la luz, puede deberse a dos posibles efectos, un **efecto estérico** provocado por el cambio de tamaño al pasar de *trans* a *cis* o un cambio en la **solubilidad** provocado por la distinta polaridad de los isómeros. Los autores comprobaron que una muestra irradiada rica en *cis*, es capaz de gelificar en dodecilbenceno aunque no en ciclohexanona. De este hecho, se puede deducir que también la forma *cis* es capaz de formar interacciones por enlaces de hidrógeno y gelificar. Por tanto, la causa probable de la transición es que se deba al cambio de la polaridad que induce un cambio de solubilidad en el disolvente de gelificación.

Van Esch, Feringa y sus colaboradores sintetizaron gelificantes azoicos basados en bisureas[107] como las mostradas en la **Fig. 1.69**. Ambos compuestos gelifican en diferentes disolventes orgánicos (tolueno, xileno…), pero mientras que los geles con el compuesto **31** son opacos y poco resistentes a la aplicación de un estrés mecánico, los geles del compuesto **32**, son transparentes y más resistentes. Los dos geles están formados por fibras pero en el gel derivado de **31**, estas fibras pueden observarse directamente con el microscopio óptico, mientras en el caso de los geles de **32**, su menor diámetro hace que tengan que ser detectados por microscopía electrónica.

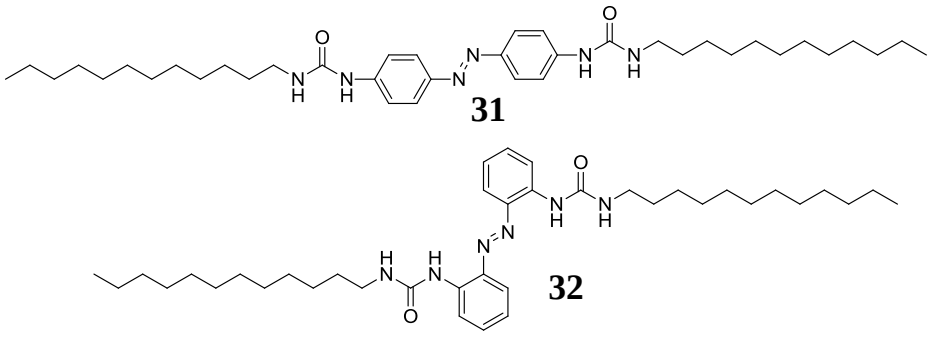

Fig. 1.69: Derivados de azobeceno y diurea.

Otro ejemplo de molécula organogelificante es el derivado tripodal con tres grupos ureido y tres azobencenos[132] que se muestra en la **Fig. 1.70**.

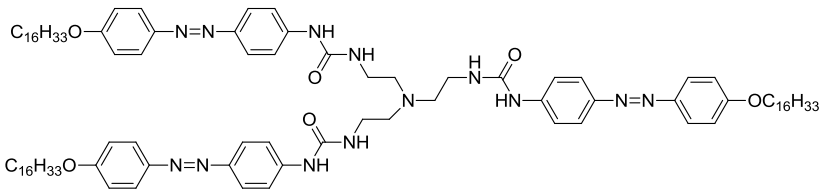

Fig. 1.70: Estructura de los compuestos tripodales con azo y ureido.

En este compuesto, la morfología formada depende mucho del disolvente. En xileno se obtiene una estructura que los autores denominan tipo "col" (*"cabbage like"*), en butanol se forman escamas regulares y en *N*-metilpirrolidina se forman arquitecturas que describen como tipo "flor". Todos los xerogeles tienen una estructura lamelar, sin embargo, poseen distinta capacidad de penetración del disolvente según las medidas del ángulo de contacto. Dependiendo del disolvente añadido, se puede cambiar la hidrofobicidad de la superficie de un xerogel depositado sobre un vidrio, aunque para ello sea necesario redisolver y calentar. Esto se puede hacer de forma reversible.

- **Derivados de amidas:**

Jung y sus colaboradores han descrito el comportamiento organogelificante de derivados de bisalanina,[133] como los mostrados en la **Fig. 1.71**, que tienen la particularidad de que el azobenceno se dispone como un sustituyente lateral.

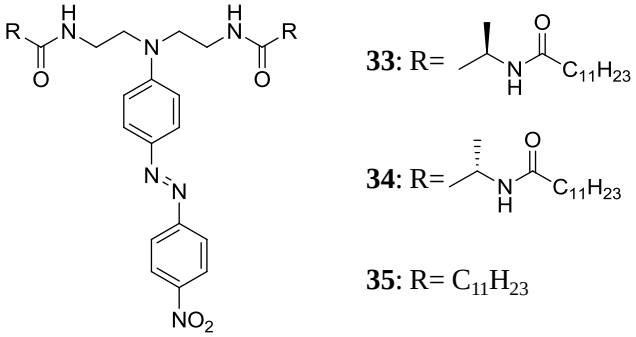

Fig. 1.71: Compuestos derivados de *p*-nitroazobenceno acoplados a bisalanina sintetizados por Jung y sus colaboradores.

Los geles en acetonitrilo del compuesto **33** (derivado de D-alanina) y **34** (derivado de L-alanina) son activos en DC, mientras que el gel en acetonitrilo de **35** (derivado aquiral) no presenta señal de DC. Los geles de **33** tienen un primer efecto Cotton positivo para la señal de acoplamiento excitón (visto el espectro de derecha a izquierda), lo que indica que los momentos dipolares de los azos vecinos están orientados de una manera horaria, mientras que en los geles de **34** tienen un primer efecto Cotton negativo para la señal de acoplamiento excitón. Gracias a la microscopía electrónica de barrido (SEM), se ha determinado que las fibras de **33** presentan una orientación dextrógira mientras que las fibras de **34** presentan una orientación levógira. Las fibras de **35** no presentan torsión.

Hanabusa y su grupo también estudiaron la unión de diferentes aminoácidos con derivados de azobenceno,[134] véase la **Fig. 1.72**. Los autores observaron en este caso que, con glicina, L-alanina y L-leucina no se forman buenos gelificantes, mientras que con L-isoleucina y L-valina sí. Los compuestos **36**-**40** son capaces de gelificar. Todos forman fibras y en el caso de **37** están torsionadas. Se ha estudiado el comportamiento de un gel en ciclohexanona de **37**, pero la transición a sol durante la irradiación no se produce porque las interacciones entre los agregados de tipo H son demasiado fuertes.

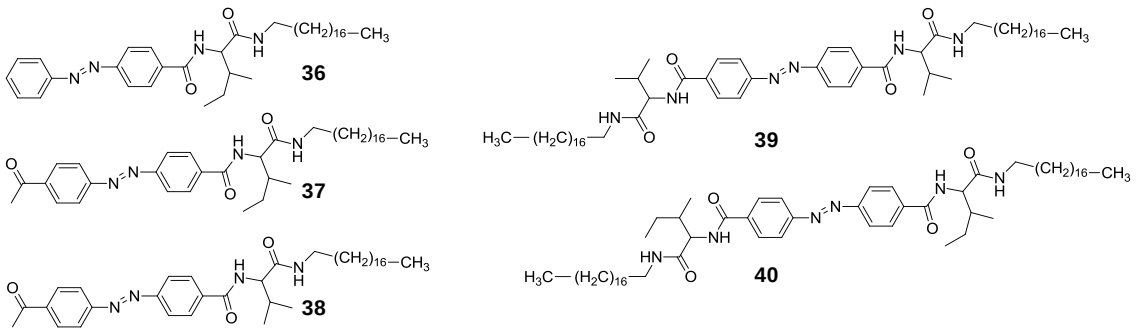

Fig. 1.72: Estructura de los compuestos con aminoácidos y derivados de azobenceno estudiados por Habanusa y sus colaboradores.

En un trabajo realizado por Stupp y sus colaboradores, donde estudiaban la helicidad en estructuras supramoleculares de distintos compuestos, observaron que existe una reducción en el paso de la hélice al irradiar con luz UV en un gel de clorohexano formado a partir de la molécula mostrada en la **Fig. 1.73,** con un derivado de azobenceno que se localiza en las partes exteriores de la fibra.[135]

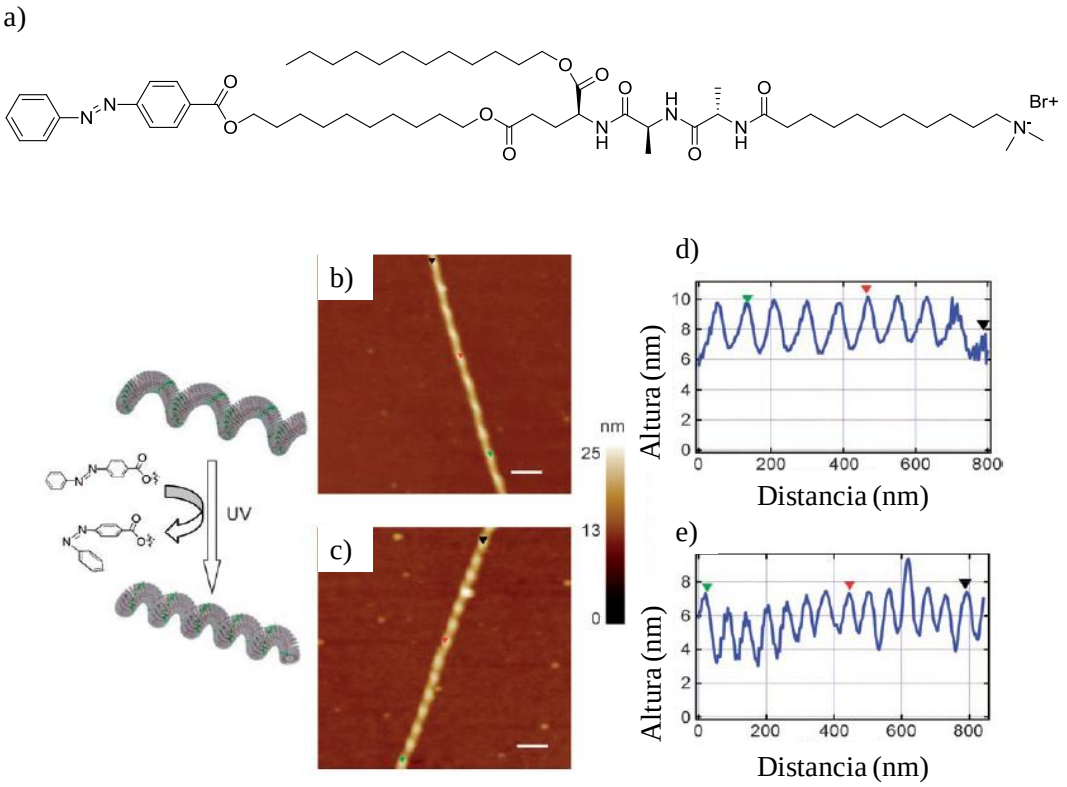

Fig. 1.73: a) Estructura molecular del gelificante. Imágenes de AFM (b y c) y sus perfiles de altura (d y e), respectivamente, antes y después de irradiar con luz UV; **Ref [135].**

Como el isómero *cis* es menos plano se puede producir un mayor retorcimiento y por tanto una reducción del paso de hélice. Antes de irradiar se obtuvo un paso de hélice de 78 nm y tras la irradiación, disminuye a 40-70 nm.

En los geles en los que el cromóforo forma agregados H, en ocasiones no se obtiene fotocromismo porque hay poco volumen libre disponible para la isomerización. Para forzar el paso a *cis* de los grupos azo del compuesto de la **Fig. 1.74** en geles de decalina, Miyasaka y sus colaboradores han llevado a cabo estudios de irradiación con un láser pulsado a 355nm.[136] En las irradiaciones en lámpara con distinta intensidad no consiguieron la isomerización, sin embargo, con un láser pulsado sí. Hay que destacar que en las pruebas que realizaron, el número de fotones con el pulso de laser no era mayor que en la irradiación normal durante un período determinado de tiempo, lo que da idea de que la densidad de fotones, es en realidad la que juega un papel importante en

la fotorreactividad del isómero *cis* en el estado gel. La isomerización *trans-cis* con un láser pulsado puede deberse a la producción simultánea de estados excitados de muchos azobencenos dando lugar a una excitación cooperativa.

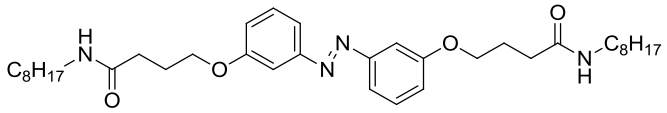

Fig. 1.74: Estructura química del gelificante azoico capaz de gelificar en decalina.

El siguiente ejemplo, derivado de hidracina con un grupo azobenceno, ha sido descrito recientemente, véase la **Fig. 1.75**. Esta molécula es capaz de gelificar en disolventes orgánicos (cloroformo, ciclohexano, tolueno).[137]

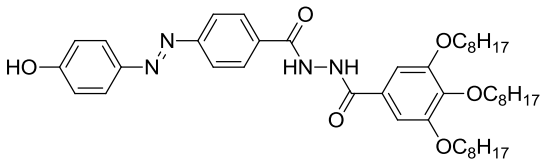

Fig. 1.75: Estructura química de la molécula gelificante derivada de hidracina y azobenceno.

El gel en cloroformo tiene una estructura fibrilar confirmada por TEM y mediante estudios de difracción de rayos X del xerogel, se ha comprobado que el empaquetamiento es columnar hexagonal con dos moléculas incluidas en la celda unidad. La fotoirradiación de este gel, provoca cambios morfológicos de fibras a vesículas, como se puede ver en la **Fig. 1.76**.

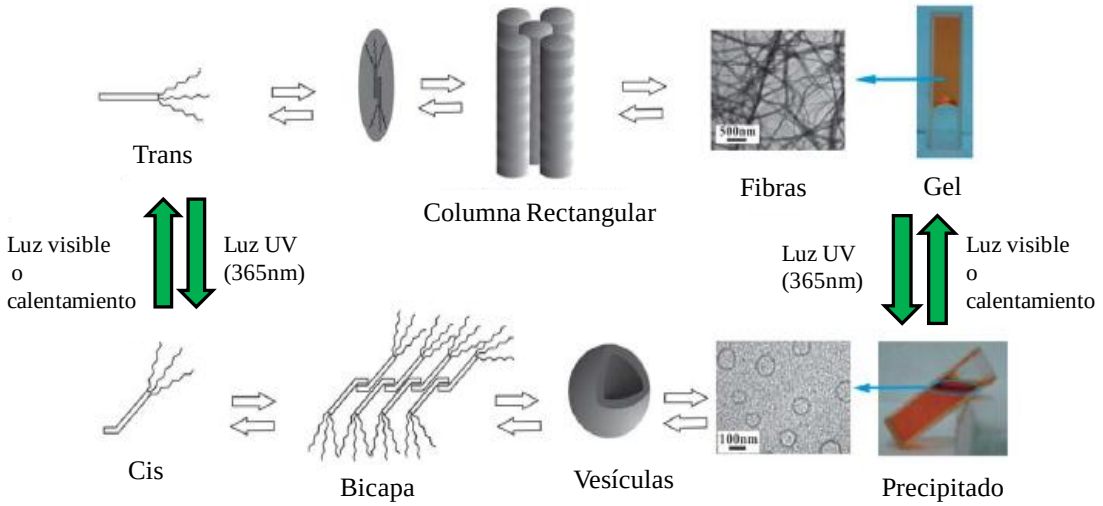

Fig. 1.76: Representación esquemática de la transformación por irradiación de los geles en cloroformo de la molécula de la **Fig. 1.75** (2.0 mg/mL); **Ref [137].**

Irradiando con luz UV (365 nm) el gel colapsa y se observa un precipitado, mientras que al irradiar con luz visible (455 nm) se restaura el gel. También se puede recuperar calentando o dejándolo en oscuridad. El precipitado obtenido tras la irradiación, se secó y observó por SEM; se trataba de vesículas. Los autores proponen para la transformación sufrida por la irradiación, un mecanismo donde en el estado *trans* la formación de nanofibras está permitida, gracias al apilamiento columnar, y al pasar a *cis* se forman bicapas y con ello vesículas (aunque en el transcurso de la isomerización también precipitan fragmentos de *trans* en forma de fibras). El disolvente juega un papel importante en la isomerización porque no se ha observado isomerización en los xerogeles o en los precipitados.

Liu y sus colaboradores han sintetizado y estudiado un lípido unido a un azo que forma organogeles, en los que la organización depende mucho del tipo de disolvente,[138] véase la **Fig. 1.77**.

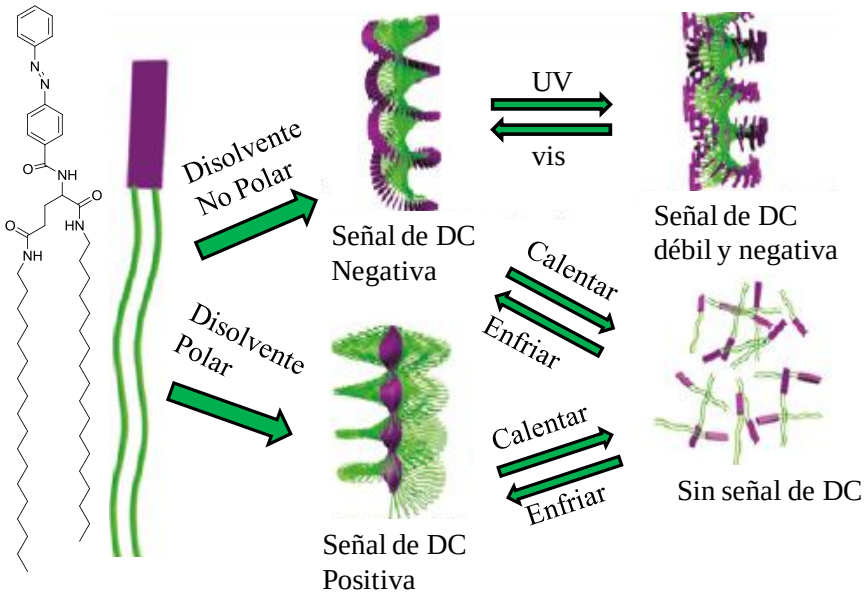

Fig. 1.77: Estructura del azo-lípido y explicación esquemática de su comportamiento en distintos disolventes según su polaridad; **Ref [138].**

Mientras que en DMSO (disolvente polar) se observan mediante microscopía electrónica fibras bien definidas, en dietiléter (disolvente no polar) las fibras no están bien definidas. Además, las señales en DC son positivas para disolventes polares mientras que en no polares se observa una señal negativa. El apilamiento π-π tampoco es igual en los dos sistemas, así mediante espectrocopia UV-vis, en los disolventes polares se observa una interacción más fuerte que en los no polares. De este hecho puede explicarse que los geles en disolventes polares no puedan fotoisomerizar. Sin embargo en tolueno, no polar, si se puede obtener la fotoisomerización.

- **Otros derivados:**

Una estructura capaz de gelificar en disolventes orgánicos que posee una parte azoica, es la estudiada por el grupo de Kato e Ikeda que consiste en un derivado quiral de azobenceno con un carbonato cíclico,[139] **Fig. 1.78**. La quiralidad juega un papel importante en la formación de las fibras y por tanto, en la capacidad de gelificar de estos compuestos, ya que el isómero RR, puede gelificar en alcoholes, éteres e hidrocarburos, sin embargo, el racemato no gelifica.

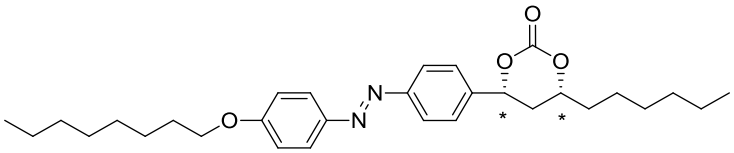

Fig. 1.78: Compuesto derivado azoico con carbonato cíclico.

En el caso de un derivado de diaminopirimidina,[140] como el que se muestra en la **Fig. 1.79**, se forman supraestructuras lamelares que forman organogeles.

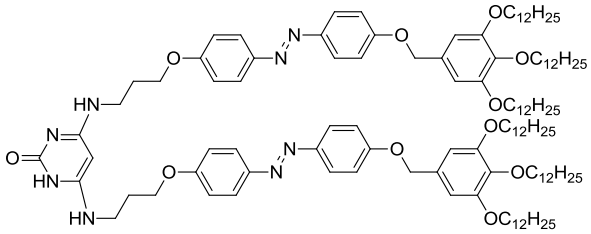

Fig.1.79: Derivados de diaminopiridina con azo en la estructura.

Mediante microscopía electrónica, se ha comprobado que a bajas concentraciones se forman fibras mientras que con disoluciones más concentradas, se forman láminas. En el estado gel en heptano, las unidades de azobenceno son fotorreactivas. Por absorción UV-vis se detecta que en estado gel sólo se produce un ligero desplazamiento hacia menores longitudes de onda comparado con una disolución. Esto indica que los grupos azos no tienen un fuerte empaquetamiento, por lo que es probable que se produzca una buena isomerización. La isomerización *trans-cis* induce el colapso de las estructuras lamelares en cintas más pequeñas y solubles que, incluso con largos tiempos de irradiación no desaparecen. Si se irradia con luz visible y se deja reposar un día se obtiene de nuevo el gel.

1.3.2.2. *Hidrogeles con azobenceno en su estructura*

Debido a la hidrofobicidad del grupo azo, son menos los casos en los que una molécula gelificante que contenga azo, sea capaz de gelificar en agua. Normalmente se suelen encontrar en este grupo de moléculas, aquellas que tienen un péptido o un azúcar

participando en la estructura como parte hidrófila. En el **apartado 1.3.3** se explicarán con más detalle aquellos gelificantes derivados de azúcares y azobenceno.

Como primer ejemplo, se describe un compuesto derivado azoico aniónico, estudiado por Tiller y sus colaboradores, que no posee péptidos ni azúcares, pero tiene carácter iónico. El compuesto de la **Fig. 1.80** es capaz de gelificar en agua a un 5 % en peso.[141] Por rayos X se ha establecido una organización lamelar en el xerogel. Al realizar cálculos se ha resuelto que el compuesto se encuentra preferentemente como el tautómero hidrazona y como la longitud de la fase lamelar es el doble de la molécula se deduce que forma una bicapa. Así las moléculas disponen sus grupos polares hacia fuera, forman agregados tubulares y con ellos estructuras porosas bien ordenadas. Se ha observado además que con el sólido liofilizado no era necesario calentar la muestra para obtener de nuevo el hidrogel, ya que al secarlo había mantenido la estructura.

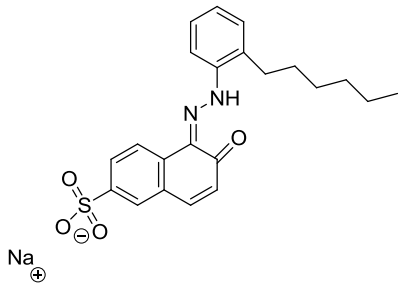

Fig. 1.80: Representación del compuesto azoico aniónico en su estrutura de hidrazona.

Los tripéptidos, derivados de trivalina, mostrados en la **Fig. 1.81**, gelifican en mezclas de un disolvente orgánico y agua.[142] En el gel del compuesto **41**, se puede inducir una transición reversible sol-gel mediante irradiación, sin embargo, en el compuesto **42** esto no ocurre.

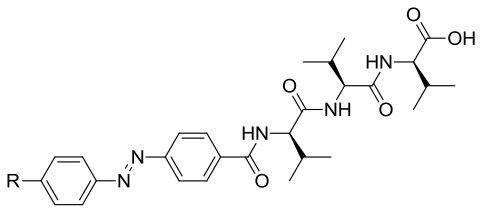

41: R=H
42: R=$(CH_3)N$-

Fig. 1.81: Tripeptidos derivados de trivalina.

El grupo de Xu, ha usado una reacción enzimática (con fosfatasa) para generar un hidrogelificante fotosensible[143] **44**, véase la **Fig. 1.82**. El precursor, **compuesto 43,** se ha sintetizado uniendo el grupo azobenceno a través de una cadena lateral de lisina.

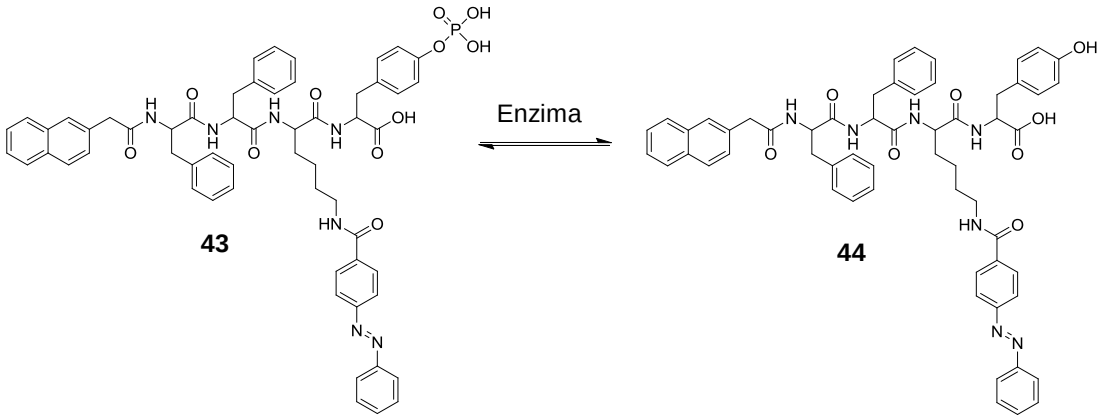

Fig. 1.82: Precursor **43** e hidrogelificante fotosensible **44** descrito por Xu y sus colaboradores; **Ref [143].**

En el hidrogel formado a una concentración de 0.8% en peso, que es transparente, se puede inducir la transición gel-sol al irradiar con luz UV (365nm) durante 35min. El gel se recupera con la exposición a la luz visible durante 12h. Esta transición gel-sol puede seguirse por la disminución de la señal de DC y cambios reológicos. El inconveniente de este gel es que se forma a pH 9.

Zhang y sus colaboradores han diseñado recientemente moléculas basadas en péptidos, capaces de gelificar en agua sin la ayuda de disolventes orgánicos. Estas contienen una parte peptídica además del azobenceno como unidad sensible a la luz,[144] como se puede ver en la estructura representativa de la **Fig. 1.83**.

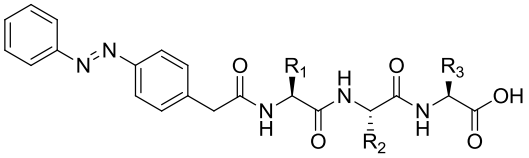

Fig. 1.83: Representación esquemática de la estructura química de tripéptidos con azobenceno estudiados por Zhang y sus colaboradores.

En primer lugar, sintetizaron una serie de dipéptidos unidos al grupo azobenceno y comprobaron que aquellos que poseen anillos aromáticos como la fenilalalina o la tirosina, son capaces de gelificar en agua a un pH apropiado, mientras que los derivados de aminoácidos con residuos catiónicos son desfavorables. Además, si estos aminoácidos no están directamente unidos al azo, la hidrogelificación es más efectiva. También se han sintetizado tripéptidos y otros péptidos bioactivos cortos para estudiar su gelificación.

No todos los tripéptidos que se han sintetizado muestran el mismo comportamiento ante la irradiación. En algunos de ellos se puede conseguir una transición gel-sol mientras que en otros casos la transición está impedida. Como se puede observar en la **Fig. 1.84**, el tripeptido **Azo-Gln-Phe-Ala** colapsa a los sólo 3 minutos de ser irradiado a 365nm y en 20 minutos se obtiene una disolución homogénea y no viscosa. A los dos días bajo luz visible, vuelve a gelificar. La presencia de los distintos isómeros, antes y después de la irradiación se ha comprobado por absorción UV-vis y mediante análisis por HPLC (**Fig. 1.84 b y c**). El gel del compuesto **Azo-Gln-Phe-Ala**, puede además encapsular la vitamina B12 sin que se desestabilice el gel. Sin irradiar, la liberación se produce por gradiente de concentraciones, pero con la irradiación se acelera el proceso.

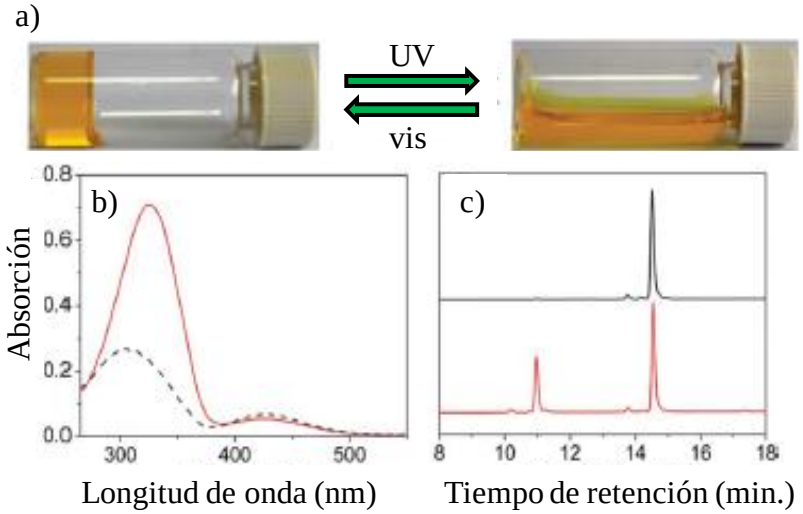

Fig. 1.84: a) Cambio con la irradiación en el hidrogel, b) Seguimiento mediante absorción UV-vis, antes de irradiar (línea roja) y después de irradiar (línea negra discontinua), c) Seguimiento mediante HPLC, antes de irradiar (arriba, sólo isómero *trans*) y después de irradiar (abajo, isómero *cis* y *trans*); **Ref [144].**

1.3.2.3. *Mezclas binarias gelificantes con un componente azobencénico*

Además de la incorporación del azo a la estructura del gelificante, el cromóforo se puede introducir realizando mezclas de dos componentes para formar el gel. En este apartado se comentan distintos ejemplos de estas mezclas y para su descripción se han dividido en organogeles e hidrogeles.

1.3.2.3.1. *Organogeles binarios*

Kitamura y sus colaboradores, han estudiado organogeles formados en hidrocarburos preparados a partir de la co-agregación de dímeros de melamina con un puente de azobenceno **45** y un derivado cianurato **46** o barbiturato **47** y **48**,[145] véase la **Fig. 1.85**.

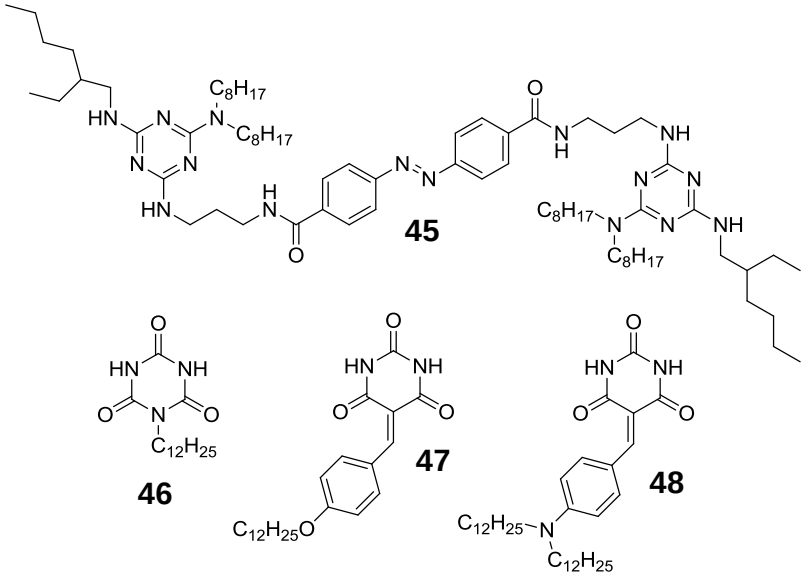

Fig. 1.85: Dímeros de melamina con un puente de azobenceno **45** y los derivados de cianurato **46** y barbiturato **47** y **48** con los que se co-agrega.

Mientras que la molécula azobencenica por sí misma no forma geles, al añadir cianurato o barbiturato sí que gelifica. De los estudios por IR se confirma que la agregación se produce por enlaces de hidrógeno, pero mediante estudios de UV-vis se demuestra que también hay una contribución de los azobencenos por sus interacciones π-π.

Los autores comparan estas moléculas con estudios previos realizados con derivados de melamina con puentes de dodecametileno co-agregados a cianurato o barbiturato.[146] Contrariamente a estos, los derivados azoicos no presentan dependencia con la molécula a la que se agregan (cianurato o barbiturato), obteniéndose en ambos casos estructuras fibrilares. Los geles con el derivado del azobenceno co-agregado son resistentes a la irradiación de luz ultravioleta debido a su fuerte empaquetamiento dentro de la estructura.

Continuando con esta línea de investigación, Kitamura y su grupo estudiaron otros geles en disolventes alifáticos de compuestos con forma de disco obtenidos también a partir de la co-agregación de melamina y cianurato o barbiturato, pero en esta ocasión la melamina tenía dos grupos azobenceno,[147] véase la **Fig. 1.86**.

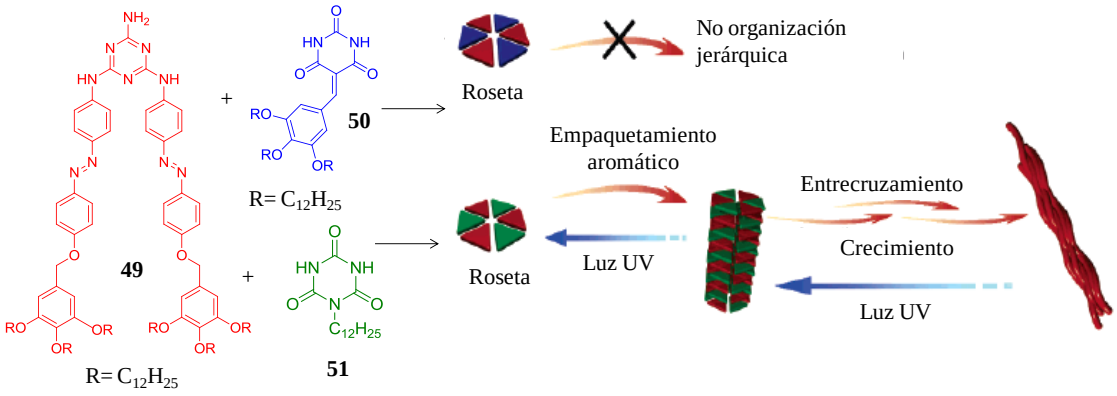

Fig. 1.86: Agregación de la azo-melamina **49** con los derivados de barbiturato **50** y cianurato **51; Ref [147].**

Mientras que la mezcla del derivado di-azoico de la melanina **49** con un derivado de barbiturato **50** no gelifica en disolventes alifáticos, la co-agregación con el derivado de cianurato **51** sí lo hace, en concreto, en ciclohexano. Los agregados del gel se construyen como rosetas unidas por enlaces de hidrógeno. El apilamiento de las rosetas da lugar a columnas por interacciones solvofóbicas y por interacciones entre los grupos aromáticos. Estas columnas se asocian en forma de fibras cilíndricas por la interacción entre las cadenas alifáticas.

Tanto en disolución como en gel se puede inducir un estado foto-estacionario reversible mediante irradiación. En estado gel (en ciclohexano), al irradiar un vial (1h) se pasa a una fase fluida con un incremento en el isómero *cis* del 34%. Tras irradiar, la solución ha de dejarse en la oscuridad durante dos días o bien irradiarse con luz visible y esperar 30h, lo que indica que es necesario un periodo de tiempo para la organización de los agregados.

Huang y sus colaboradores, también han trabajado con mezclas de dos componentes como los que se muestran en la **Fig. 1.87**. Son dos triamidas **52** y **54** o **53** y **54**, de las cuales una contiene una parte azoica[148] **52** o **53**. Se obtienen organogeles en 1,4-dioxano. En ellos se puede alcanzar un estado de fotoisomerización reversible pero sin romper el estado gel.

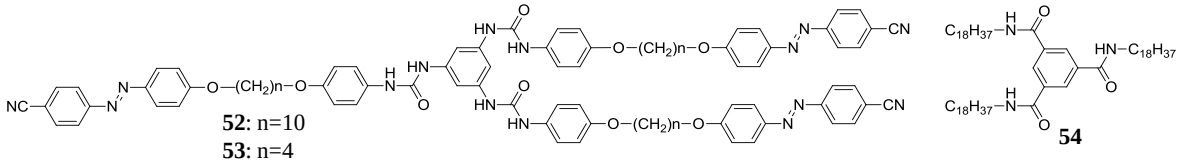

Fig. 1.87: Estructura química de los componentes para la mezcla de triamidas.

1.3.2.3.2. *Hidrogeles binarios*

En cuanto a la mezcla de dos componentes para la formación de hidrogeles, en la **Fig. 1.88** se pueden observar dos ejemplos basados en ciclodextrinas mezcladas con moléculas azoicas. En el caso de la γ-ciclodextrina **55**, al interaccionar mediante interacciones "*host-guest*" con un azo **56**, se forma un hidrogel.[149] Si se introducen distintos metales, esta capacidad de gelificar se modifica y pasa a un estado sol. En el segundo ejemplo, se describe un pseudorotaxano, formado por una molécula de PEG y una α-ciclodextrina **57** que gelifican en agua.[150] En este caso, la adición de un azobenceno **58** convierte el gel en estado sol. Si se irradia con luz UV se puede volver al estado gel y con la irradiación con luz visible se pasa de nuevo al estado sol. Esto ocurre por la competitividad que existe entre el PEG y la molécula azoica dentro de la cavidad de la ciclodextrina.

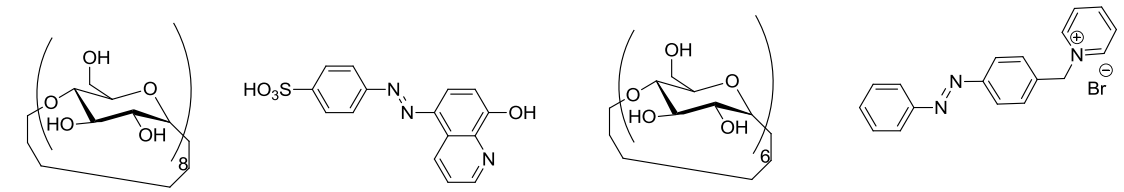

55: γ- ciclodextrina **56** **57**: α- ciclodextrina **58**

Fig. 1.88: Ciclodextrinas y compuestos azoicos para la formación de hidrogeles.

Como último ejemplo de mezclas para formar hidrogeles, hay que destacar el trabajo realizado por Liu y sus colaboradores, donde se mezcla un bolaanfifílo **59** con un ácido 4-fenilazobenzoico **60**,[151] véase la **Fig. 1.89**. El bolaanfífilo está basado en un derivado del ácido glutámico, que es capaz de auto-ensamblarse en nanotubos quirales y de gelificar en agua. Los nanotubos del enantiómero L tienen helicidad dextrógira y los del enantiómero D la tienen levógira. La mezcla de los dos componentes, se puede realizar de dos maneras distintas, siguiendo la denominación de los autores: a "**nivel supramolecular"** (**A**), donde el azo se dispersa en los nanotubos formados, y a "**nivel molecular"** (**B**), donde los dos compuestos se mezclan en caliente, véase **Fig. 1.89**.

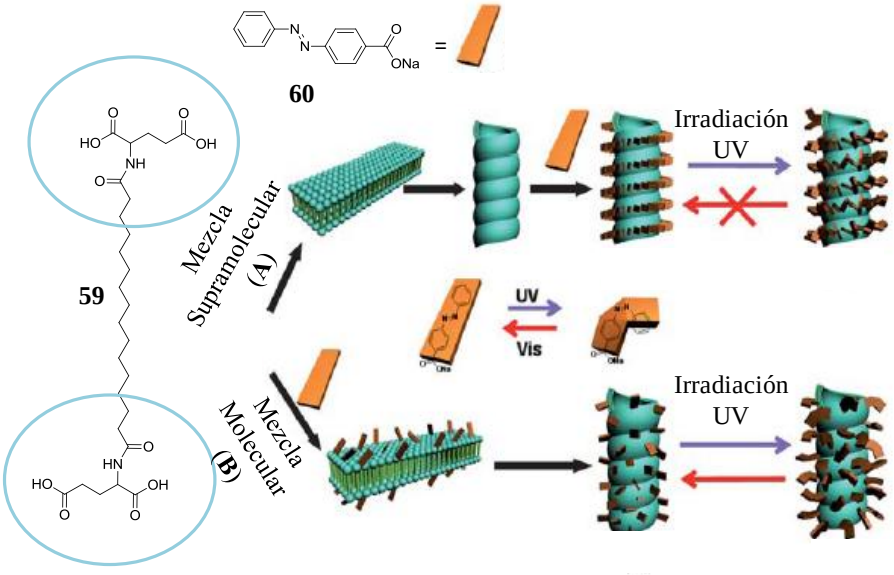

Fig. 1.89: Estructura de los dos componentes de la mezcla: el gelificante **59** y el dopante azoico **60** y representación de la organización de la mezcla a "**nivel supramolecular"** (**A**) y organización de la mezcla a **"nivel molecular"** (**B**)**; Ref [151].**

En estas mezclas se han estudiado las modificaciones obtenidas con la irradiación. En la mezcla a **"nivel supramolecular"** (**A**), por AFM se observan fibras prácticamente iguales antes y después de irradiar y en el espectro de absorción sí que se obtiene una reversibilidad *trans-cis-trans*, mientras que en la señal de DC no se observa recuperación de la señal. A partir de estos resultados los autores proponen que las moléculas de azo, en esta mezcla, se adsorben sobre la superficie del nanotubo por enlaces de hidrógeno e interacciones electrostáticas, así después de irradiar se produce una reorganización de las moléculas de azo sobre la superficie que no llegan a recuperar su organización original. Por el contrario, en la mezcla a **"nivel molecular"** (**B**), por AFM se detecta una dispersión de tamaños en los nanotubos al irradiar, y se observa también que existe reversibilidad tanto en el espectro de absorción como en la señal de DC. De acuerdo a esto, los autores proponen que, en este caso, el azo está embebido en la pared del nanotubo y entonces la organización es totalmente reversible.

1.3.3. *Moléculas gelificantes con azúcares y azobenceno en su estructura*

El número de gelificantes basados en azúcares como cabeza polar y que contienen azobenceno en su estructura descritos hasta la fecha se reduce considerablemente. A continuación se van a explicar diferentes gelificantes con estas características.

En primer lugar, es interesante comentar las moléculas anfífílas con azúcares y azobenceno mostradas en la **Fig. 1.90** que, aunque no han sido descritas como gelificantes, sí se ha estudiado su agregación en una mezcla de DMSO/Agua.[152] Al añadir agua a una disolución de estas moléculas en DMSO, se produce un desplazamiento en el máximo de absorción hacia menores longitudes de onda y un aumento de la intensidad. Además aparece una señal de DC asociada a una agregación quiral supramolecular.

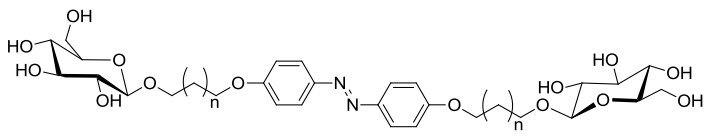

61: n=3 **62**:n=6 **63**: n=8

Fig. 1.90: Compuestos bolaanfifílicos derivados de glucosa y azobenceno.

Para el compuesto **63**, la formación de vesículas o fibras depende de las condiciones de preparación: las fibras son los agregados cinéticamente estables mientras que las vesículas son los agregados termodinámicamente estables. En el caso del compuesto **62**, se ha observado que al irradiar con luz UV, se puede pasar de una estructura en forma de vesículas (sin irradiar) a la formación de fibras (muestra irradiada). Si se irradia la muestra, esta vez con luz visible, o se calienta, vuelven a formase de nuevo las vesículas.

Shinkai y sus colaboradores, con su experiencia en organogeles e hidrogeles con azúcares, decidieron estudiar los derivados de azo-naftol (que actúa como parte hidrófoba) y azúcar (que actúa como parte hidrófila) que se muestran en la **Fig. 1.91.**[153] Los compuestos **64** y **65** son capaces de gelificar si previamente se solubiliza el compuesto en etanol. El compuesto **66**, en cambio, precipita incluso en la mezcla de disolventes.

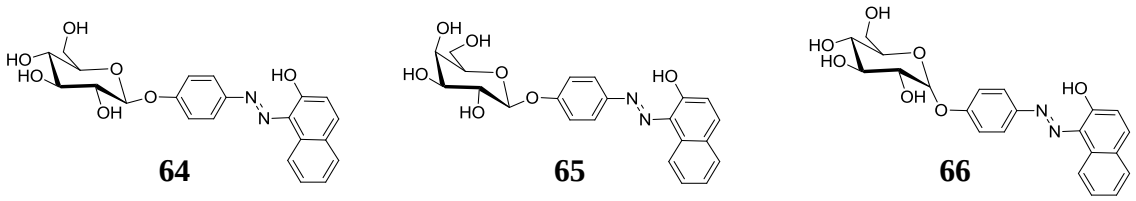

Fig. 1.91: Derivados de azo-naftol descritos por Shinkai y sus colaboradores.

Más tarde este mismo grupo, sintetizó y estudió el comportamiento de unas moléculas gelificantes bolaanfifílas,[154] véase la Fig. **1.92**, donde usan como cabezas polares distintos monosacáridosy como parte hidrófoba, segmentos de diazobenceno que participarán en la agregación por interacciones tipo π-π.

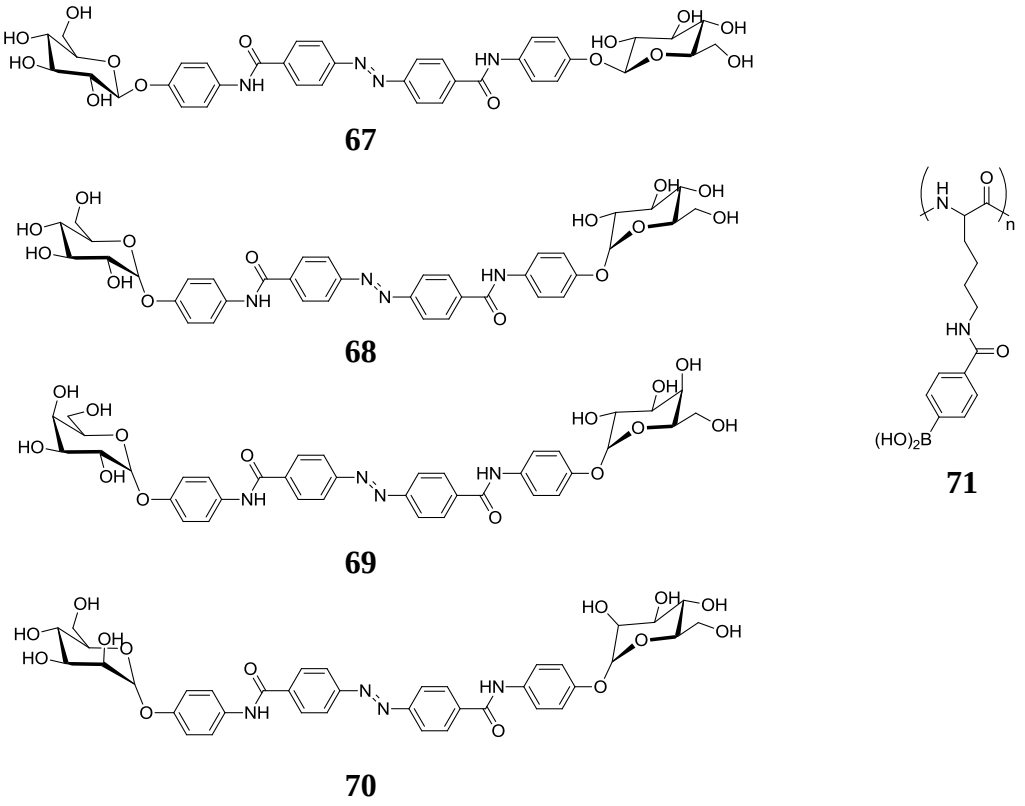

Fig. 1.92: Derivados de azúcar y azobencenos bolaanfifílicos **67**-**70** y polilisina modificada con un ácido borónico **71**.

De los compuestos de la **Fig. 1.92**, el **67** es el único capaz de gelificar sólo en agua a concentraciones inferiores a 0.1%. En mezclas DMSO/agua gelifican tanto **67** como **68**, estos geles son translúcidos. **69** y **70** no gelifican, de lo que se puede deducir que la capacidad de formar geles se ve afectado por el tipo de azúcar. Mientras que **67** y **68** poseen OH ecuatoriales, en **69** y **70** hay un grupo axial. La explicación de que **67** sea mejor gelificante puede deberse, según los autores, al hecho de que con β-glucosa la conformación más estable de la molécula es más planar y por tanto se favorece el apilamiento. Por TEM se han identificado los agregados formados: en el caso de los geles de **67** y **68** se observan fibras, mientras que en los precipitados de **69** y 7**0** se observan vesículas.

Si se añade a un gel de **68** una concentración creciente de polilisina modificada con ácido borónico **71**, se puede pasar del estado gel (estructura fibrilar) a un estado sol (vesículas) como se puede ver en la **Fig. 1.93**. Esto se produce gracias a las

interacciones específicas del ácido borónico con las partes azucaradas. La modificación es reversible y al añadir fructosa, que posee una gran afinidad por el ácido borónico, el estado sol vuelve al gel y la estructura vuelve de vesícula a fibra. Se puede realizar entonces, un control de la transición sol-gel a temperatura ambiente.[155]

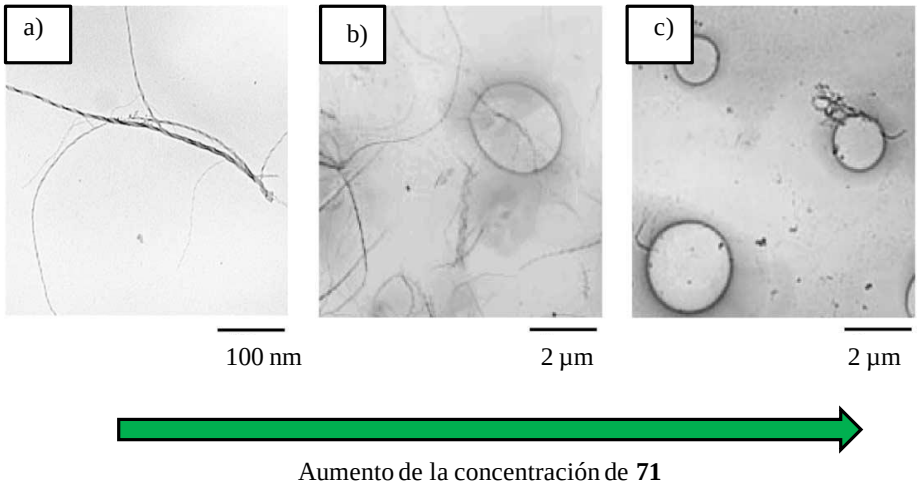

Fig. 1.93: 1.0 10^{-2} mol dm^{-3} de **68** en DMSO/agua (1:1). a) En ausencia de **71**, estado gel, observación de fibras, b) [**71**]= 2.0 unidades de monómero mmol dm^{-3}, estado gel, observación de fibras y vesículas, c) [**71**]= 3.0 unidades de monómero mmol dm^{-3}, estado sol, observación de vesículas; **Ref [155].**

El grupo de Bhattacharya, ha estudiado la gelificación en agua a varias concentraciones de pH y en presencia de sales, de una molécula derivada de azucares[156] como la descrita en la **Fig. 1.94.**

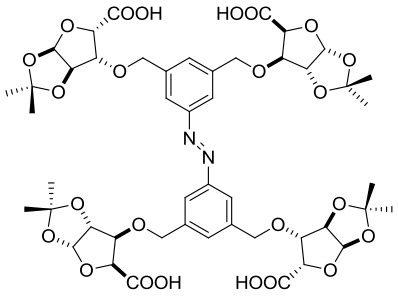

Fig. 1.94: Estructura del tretrámero basado en azúcar y azobenceno estudiado por Bhattacharya y sus colaboradores.

Los geles se forman en agua a una concentración de 0.1 % en peso con la adición de 10 µL de DMSO. La capacidad de gelificar de esta molécula se conserva para un rango de pH de 4-10 y se ha demostrado que la presencia de tampones inhibe la gelificación. Se han realizado estudios de fotoestabilidad mediante irradiación pero existe un empaquetamiento demasiado fuerte que no permite el paso al isómero *cis*. Siguiendo la absorción en UV-vis de una disolución de DMSO a la que se añade agua, se comprueba que se produce un desplazamiento hacia menores longitudes de onda, lo que indica que se forman agregados tipo H. Este fuerte empaquetamiento es el que impide el paso a sol.

Das, Ajayaghosh y sus colaboradores han sintetizado diferentes compuestos derivados de azúcar que son capaces de gelificar en disolventes aromáticos.[157] Como ejemplo, se describe en la **Fig. 1.95** un compuesto que actúa como "super-gelificante" al tener una concentración de gelificación mínima de 0.05 % en peso en tolueno. Estos geles son fotosensibles llegando a producirse una transición gel-sol con irradiación UV.

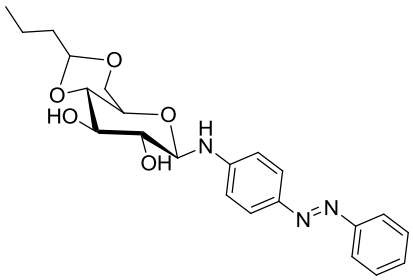

Fig. 1.95: Estructura de la molécula gelificante estudiada por Das, Ajayaghosh y sus colaboradores.

Otro interesante ejemplo de moléculas gelificantes basadas en azúcares y azobenceno, es el trabajo publicado por Huang y sus colaboradores.[158] El gelificante está formado por una cabeza azucarada alicíclica (gluconamida) y una cola hidrófoba con un grupo azobenceno, como se puede ver en la **Fig. 1.96**. Esta molécula gelifica en agua a una concentración de 20 mM y su microestructura está formada por dobles hélices helicoidales como se ha medido por TEM y cryo-TEM. Para ver la influencia de las distintas partes de la molécula, se han sintetizado compuestos homólogos pero con otros grupos polares en la cabeza sustituyendo al azúcar (aminas cuaternarias, carboxilatos o glicoles), pero con estos compuestos sólo se han obtenido micelas globulares o

vesículas. Además, han comprobado que la presencia del grupo butilo o hexilo es esencial para que se formen las dobles hélices, ya que si las cadenas son menores precipitan. Los autores, explican la formación de las hélices gracias el empaquetamiento girado de las partes azucaradas. Los enlaces de hidrógeno entre los azúcares son lo que permiten unir dos hélices.

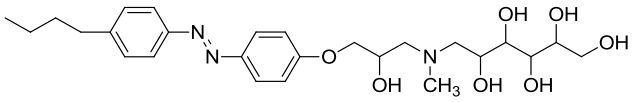

Fig. 1.96: Estructura de la molécula gelificante estudiada por Huang y sus colaboradores.

Muy recientemente, el grupo de Kitaoka ha publicado un estudio con moléculas derivadas de azobenceno y lactonas disacáridas,[159] véase la **Fig. 1.97**. Estas moléculas son capaces de gelificar en agua.

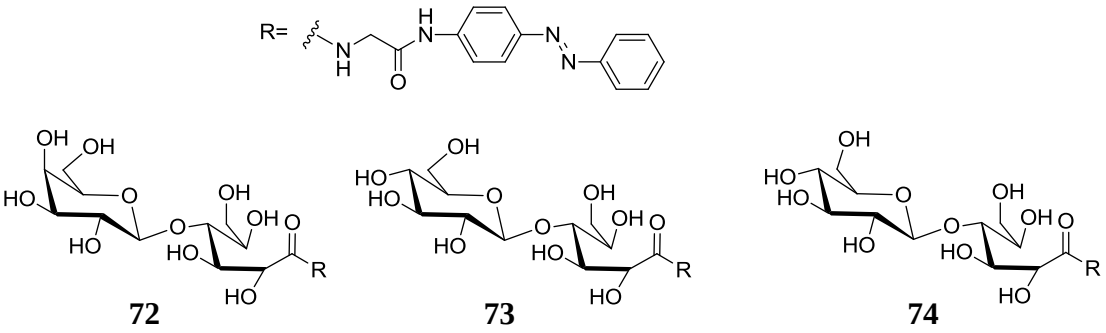

72 **73** **74**

Fig. 1.97: Estructura de las moléculas gelificantes estudiada por Kitaoka y sus colaboradores.

La orientación quiral de los grupos azobenceno medida por DC es diferente para cada hidrogel, así con el compuesto **72** (derivado de lactosa) presentan una orientación dextrógira, con el compuesto **73** (derivado de maltosa) presenta una orientación levógira y con el compuesto **74** (derivado de celobiosa) no hay quiralidad. De esto se pude deducir que la organización quiral del azobenceno depende tanto del enlace glicosídico como de la disposición estérica de los grupos OH en los carbohidratos. Los ensayos de

unión con lectinas y de adhesión celular revelan que las partes no reducidas se encuentran expuestas en la superficie de las fibras del hidrogel. Se puede producir una transición gel-sol por irradiación UV.

1.4. Cristales Líquidos

1.4.1. *Definición*

El estado **cristal líquido** aparece cuando el orden molecular de un compuesto es intermedio entre el sólido cristalino ordenado y un líquido desordenado. Las características fundamentales de estas fases combinan la **anisotropía** de propiedades del estado sólido y la **movilidad** y **fluidez** del líquido. Las ordenaciones moleculares de este tipo se llaman **fases cristal líquido** o **fases mesomorfas**, y los compuestos que muestran estas mesofases se denominan cristales líquidos o mesógenos.[160]

Se pueden encontrar cristales líquidos de dos tipos principales en función de cómo se genere la mesofase. En los cristales líquidos **termótropos** se genera por efecto de la temperatura. En los cristales líquidos **liótropos**, la mesofase se genera por efecto de un disolvente. Los que presentan ambos tipos de comportamientos se denominan **anfótropos**.

A continuación se realizará un breve repaso de los distintos cristales líquidos tanto termótropos, como liótropos; así como una descripción de varios ejemplos de glicolípidos y glicoanfífilos con azobenceno en su estructura, que poseen propiedades mesomorfas.

1.4.2. *Cristales Líquidos termótropos*

Dependiendo de la estabilidad termodinámica de la mesofase respecto a la fase sólida, la mesofase termótropa puede ser enantiótropa o monótropa. La **mesofase enantiótropa** es termodinámicamente estable y por tanto aparece tanto en el proceso de calentamiento desde la fase sólida como en el proceso de enfriamiento desde la fase de líquido isótropo. La **mesofase monótropa** es termodinámicamente metaestable y únicamente aparece en el proceso de enfriamiento desde la fase líquido isótropo como consecuencia de la histéresis en la cristalización.

Las **mesofases termótropas** se pueden clasificar principalmente en dos tipos atendiendo a la geometría de los mesógenos: mesofases de **tipo calamítico**, cuando las moléculas tienen forma de varilla y de **tipo discótico**, cuando las moléculas tienen forma de disco.[161]

Las mesofases más comunes en los cristales líquidos **calamíticos** son las de tipo nemático (N) o esméctico, siendo las esméctica A (SmA) y esméctica C (SmC), las más comunes como se muestra en la **Fig. 1.98.**

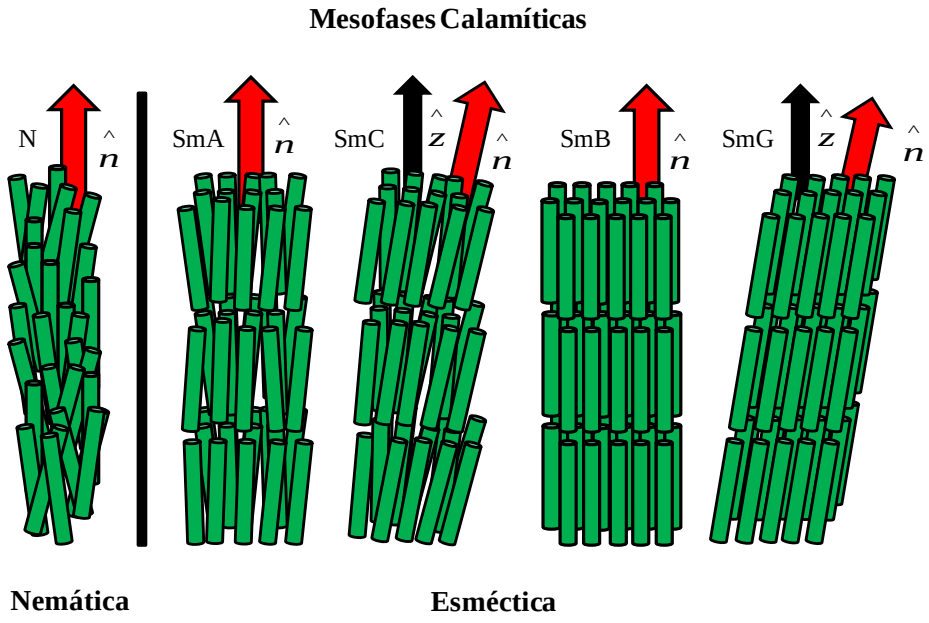

Fig. 1.98: Representación esquemática de las mesofases calamíticas más comunes.

La mesofase **nemática** (N) es la menos ordenada, ya que las moléculas no presentan orden posicional. En esta mesofase, los ejes largos moleculares están orientados en promedio en una misma dirección, definida por el vector director "n".

Las mesofases **esmécticas** se caracterizan porque las moléculas están organizadas en capas. Dos factores determinan los diferentes tipos de mesofases esmécticas. El primer factor es el orden posicional de las moléculas en cada capa, lo que da lugar a mesofases esmécticas menos ordenadas (SmA y SmC) donde no hay orden posicional en las capas o más ordenadas (SmB, SmG… etc), cuando sí existe. El segundo factor es la inclinación de las moléculas en las capas. Así las mesofases esmécticas pueden ser no inclinadas u ortogonales cuando en promedio el ángulo formado entre el vector director "n" y la normal a las capas "z" es nulo (SmA, SmB), o inclinadas cuando es distinto de cero (SmC, SmG,…etc). La mesofases esmécticas más frecuentes son la **SmA** (ortogonal) y la **SmC** (inclinada).

Existen además mesofases quirales por la introducción de quiralidad en la molécula. Las más estudiadas son la **nemática quiral** (**N***) conocida también como **colésterica** (**Ch**) y la **esméctica C quiral** (**SmC***), representadas en la **Fig. 1.99**. La quiralidad en las fases colestéricas aparece como consecuencia de que el vector director de las moléculas rota describiendo una hélice. La fase esméctica quiral se forma por el giro gradual de los vectores directores de cada capa, lo que nuevamente da lugar a una hélice.

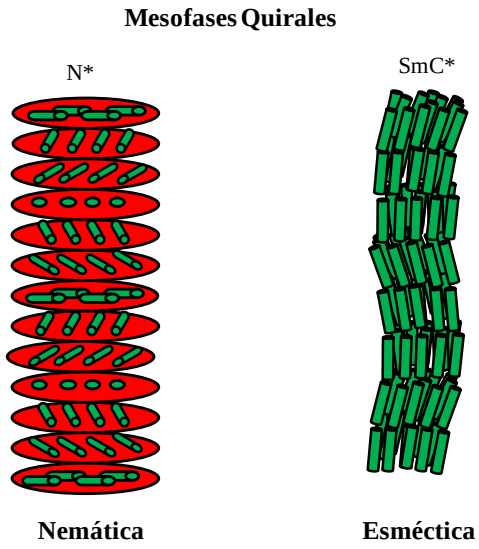

Fig. 1.99: Representación esquemática de las estructura de las mesofases quirales más comunes.

Las mesofases **discóticas** se clasifican en **mesofase nemática discótica** (**N_D**), donde las moléculas se distribuyen sin ningún tipo de orden posicional y sólo poseen orden orientacional, y **mesofases columnares**, donde las moléculas mantienen cierto grado de orden posicional, apilándose en columnas. Si las columnas no presentan ningún orden bidimensional, la mesofase columnar es de tipo **columnar nemática** (**Col_N**). Si por el contrario presentan algún tipo de organización bidimensional en el plano perpendicular a las columnas podemos encontrar la mesofase **columnar hexagonal** (**Col_h**), cuando la simetría de la red bidimensional es hexagonal, y la mesofase **columar rectangular** (**Col_r**), cuando la simetría es ortorrómbica. Este tipo de mesofases se representan en la **Fig. 1.100.**

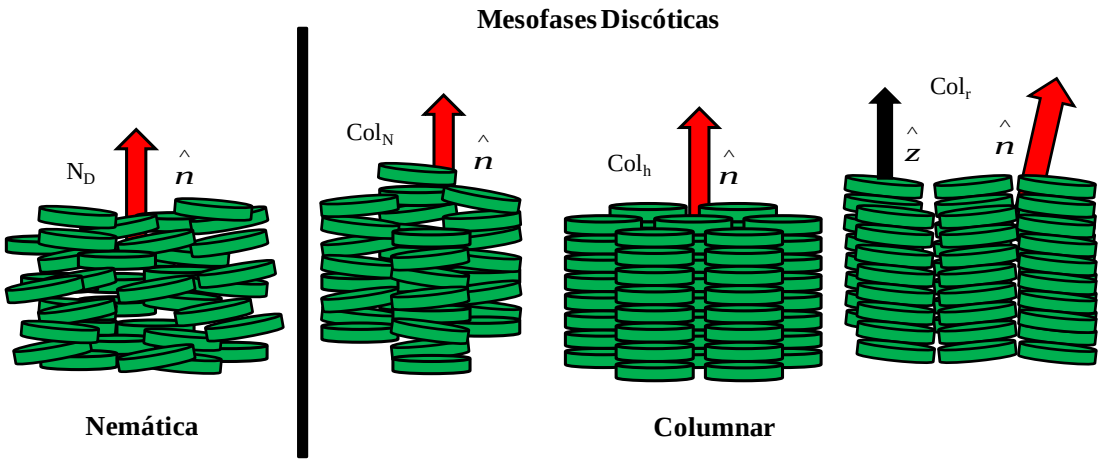

Fig. 1.100: Representación esquemática de las mesofases discóticas más comunes.

Existen moléculas con morfología diferente a la calamítica o discótica, como moléculas de tipo semidisco,[162] con forma piramidal,[163] con forma de V o banana[164]… etc.

1.4.3. *Cristales Líquidos liótropos*

En cuanto a los cristales líquidos de tipo **liótropo**, pueden encontrarse varias clases de fases, en general con textura característica debido a su birrefringencia, excepto la fase cúbica que no es birrefringente. Las fases liótropas se presentan secuencialmente y ocupan una región específica en el diagrama de fases.[161, 165]

Se pueden formar **fases normales**, donde las regiones polares están en contacto con el medio (disolvente) o **fases reversas** cuando las regiones en contacto con el medio son las apolares.

En la **fase lamelar** (**L*α***), **Fig. 1.101**, las moléculas se encuentran en forma de monocapas o bicapas, y se extienden en distancias largas. Estas capas formadas por las moléculas están separadas entre sí por capas de agua. Esta fase es similar a la mesofase SmA termótropa.

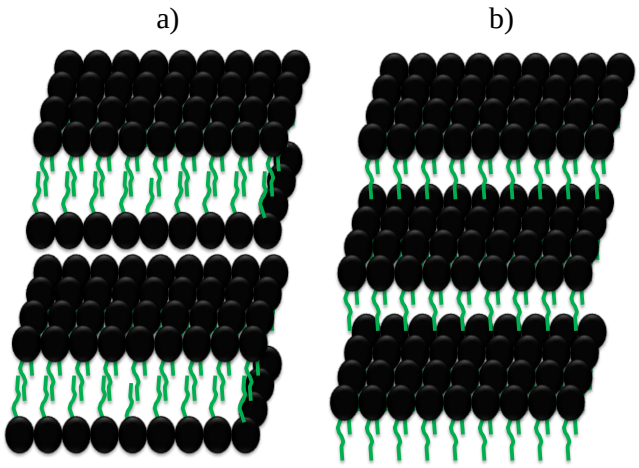

Fig. 1.101: a) Estructura lamelar (**L*α*)** en bicapa, b) estructura lamelar (**L*α*)** en monocapa; **Ref [161].**

La **fase hexagonal**, **Fig. 1.102**, está formada por agregados cilíndricos empaquetados de una manera hexagonal. Se denominan **H_1** si **es hexagonal normal** o **H_2** si es **hexagonal reversa**.

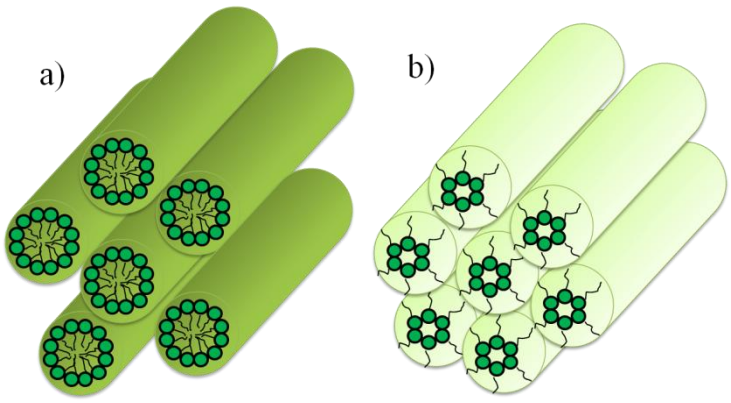

Fig. 1.102: a) fase H_1, hexagonal normal y b) fase H_2, hexagonal inversa; **Ref [161].**

En la **fase cúbica**, como su propio nombre indica, las micelas se organizan en una estructura de un cubo y existen tres formas de empaquetamiento: cúbica, cúbica centrada en la cara y cúbica centrada en el cuerpo. Son altamente viscosas y como se ha mencionado antes, no presentan textura birrefringente. Dentro de las fases cúbicas

encontramos la **fase I** (**Fig.1.103**), donde la agregación micelar es esférica, o la **fase V** (**Fig. 1.104**), donde los agregados son cilindros que están interconectados. Suponiendo un orden creciente de concentración, la fase I se localiza entre la solución micelar isótropa y la fase hexagonal, mientras que la fase V se localiza entre la fase hexagonal y la lamelar. Tanto I como V pueden ser normales o reversas, denominándose I_1 y V_1 las normales y I_2 y V_2 las reversas.

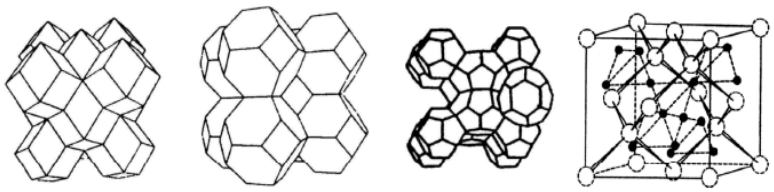

Fig. 1.103: Representación polihédrica que muestra la organización micelar para a) Pm3n, b) Im3m y c) Fm3m de la fase cúbica I_1, d) Fd3m en la fase I_2; **Ref [161].**

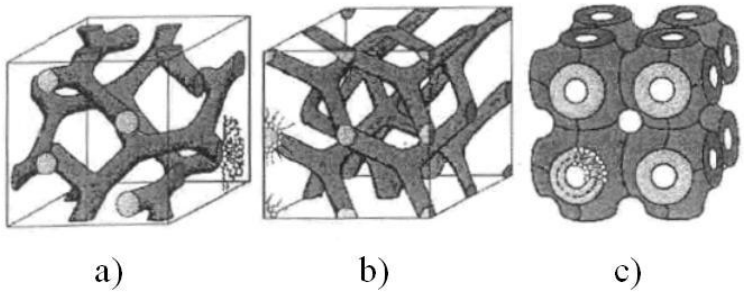

Fig. 1.104: Representación esquemática de las fases cúbicas discontinuas V, a) Ia3d, b) Pn3m y d) Im3m; **Ref [161].**

Las fases **nemáticas**, **Fig. 1.105**, ocurren entre la fase isótropa micelar y la fase hexagonal o lamelar. Son similares a la fase nemática termótropa y poseen texturas Schlieren. La $\mathbf{N_d}$, es una **fase nemática de tipo disco**, que está relacionada con la fase lamelar, y la $\mathbf{N_c}$, es una **fase nemática de tipo cilindro**, que está relacionada con la fase hexagonal. También existen fases liótropas **colestéricas** formadas por micelas giradas.

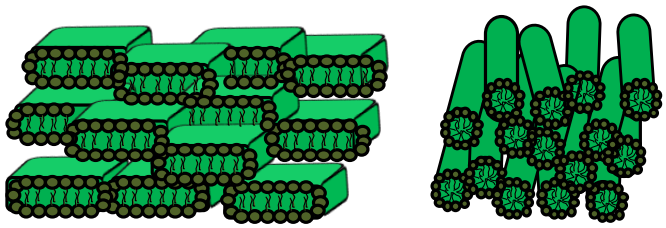

Fig. 1.105: Representación esquemática de las fases a) nemática tipo disco (N_d) y b) nemática tipo cilindro (N_c); **Ref [161].**

La **fase gel** (**L_β**) tiene una alta viscosidad debido a que la bicapa es muy rigida. Esta fase no ha de confundirse con los geles de tipo polimérico o supramolecular, ya que esta es una denominación referente a la organización en una fase, no al material. Las cadenas alquílicas de los surfactantes se encuentran en *todo-trans*. Hay tres tipos de fases, la **fase normal** donde la bicapa se encuentra normal al eje del cristal líquido y el grosor de la capa alquílica es dos veces la configuración *todo-trans* de la molécula, la **fase girada**, que se obtiene cuando la cabeza polar es mayor que la anchura de la cadena alquílica, y la **fase interdigitada**, que se encuentra en sistemas que tienen cadenas largas (**Fig 1.106**). La movilidad de las cadenas está muy restringida pero no así las capas de agua que tienen mucha movilidad.

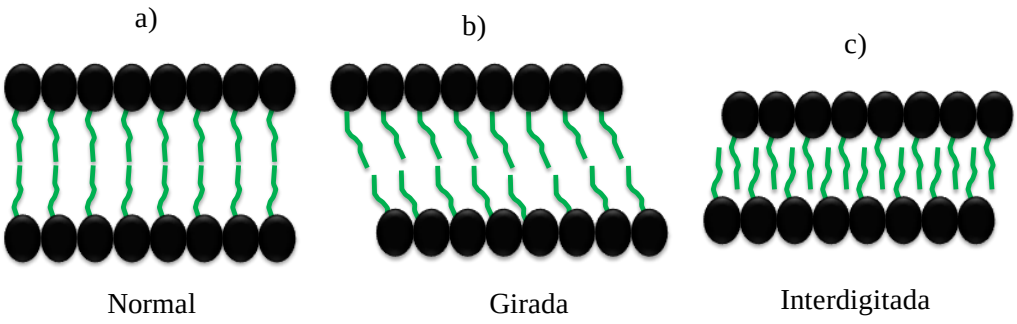

Fig. 1.106: Representación esquemática de posibles fases gel, a) normal, b) girada y c) interdigitada; **Ref [161].**

Por último, se describen también **fases intermedias**. En este grupo se clasifican distintas estructuras como la **tipo cinta**, entendiendo esta fase como una fase hexagonal distorsionada, **estructuras en capas con poros**, que puede considerarse como una fase lamelar distorsionada en la cual se encuentran defectos en la bicapa y **estructuras discontinuas,** siendo estructuras cúbicas distorsionadas.

1.4.4. *Métodos de caracterización y propiedades*

Las propiedades cristal líquido se estudian, en primera instancia, mediante **microscopía óptica de luz polarizada**, ya que estos compuestos poseen texturas características debido a su birrefringencia y mediante **calorimetría diferencial de barrido** (DSC), para determinar la entalpía y temperatura asociadas a las transiciones de fase que sufre el compuesto. Para el estudio del comportamiento liótropo en microscopía óptica , suele utilizarse, en primera instancia, el **método de contacto**.[72] Como se indica en la **Fig. 1.107**, éste consiste en colocar el material entre dos vidrios, calentar hasta líquido isótropo, dejar enfriar y entonces añadir una gota de disolvente, permitiendo que entre por capilaridad entre los vidrios y se cree un gradiente de concentración en la muestra para observar las diferentes fases en función del porcentaje de soluto. Es un método cualitativo, pero permite determinar las fases rápidamente.

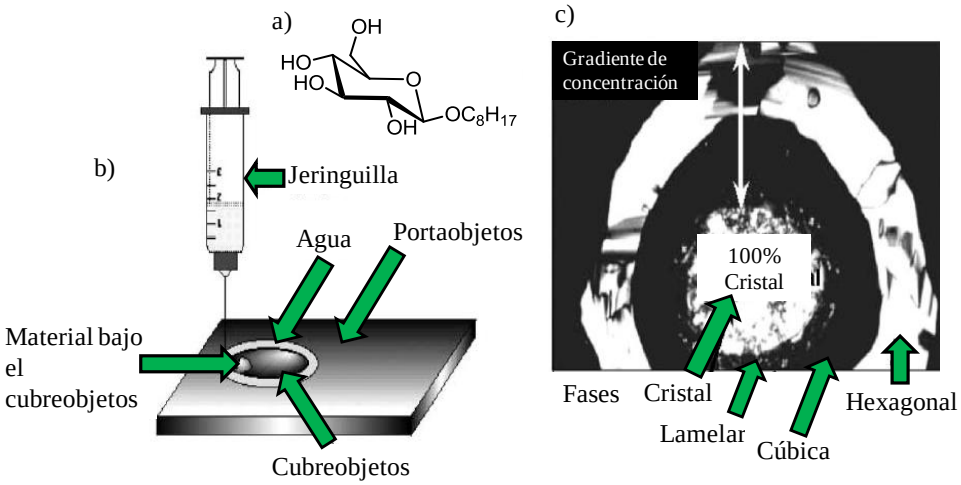

Fig. 1.107: Estudio del comportamiento liotropo del n-octil β-D-glucopiranósido disuelto en agua: a) Representación de su estructura, b) Representación esquemática del método de contacto, c) Fotografía donde se pueden ver las fases hexagonal, cúbica, lamelar y cristalina, en orden creciente de su concentración en agua; **Ref [72].**

1.4.5. *Glicolípidos y sus propiedades Cristal Líquido*

Los glicolípidos además de su conocida capacidad de formar agregados en agua pueden tener comportamiento como cristales líquidos. Esto se debe a que las cabezas polares son capaces de formar enlaces por puentes de hidrógeno entre sí, mientras que las cadenas alquílicas interaccionan entre ellas, dando lugar a regiones microsegregadas. Es común que algunos glicolípidos posean características anfótropas, es decir, que tengan un comportamiento tanto termótropo como liótropo.

Unas de las primeras familias estudiadas, en este tipo de compuestos, fueron los n-alquil glucopiranósidos,[72, 166] véase como ejemplo el n-octil β-D-glucopiranosido representado en la **Fig. 1.107**. En cuanto a su comportamiento termótropo, presentan fases esméticas A o como más tarde se concretó, A_d^* (en la fase esméctica A_d^*, las moléculas tienen una organización interdigitada), véase la **Fig. 1.108**.

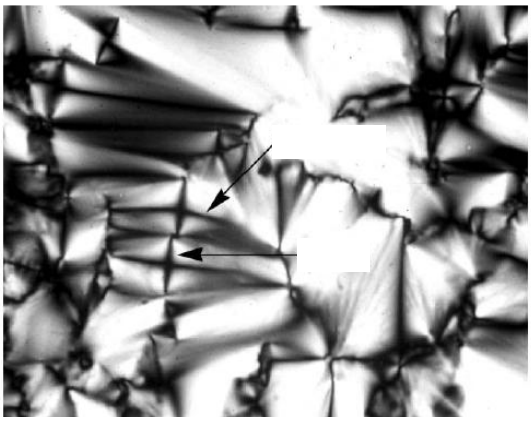

Fig. 1.108: Textura conico-focal de una fase esméctica A_d* del n-octil β-D-glucopiranósido (X100); **Ref [72].**

Además los n-alquil glucopiranósidos presentan mesofases liótropas. Éstas son diferentes atendiendo a la longitud de la cadena alquílica, véase la **Fig. 1.109**.

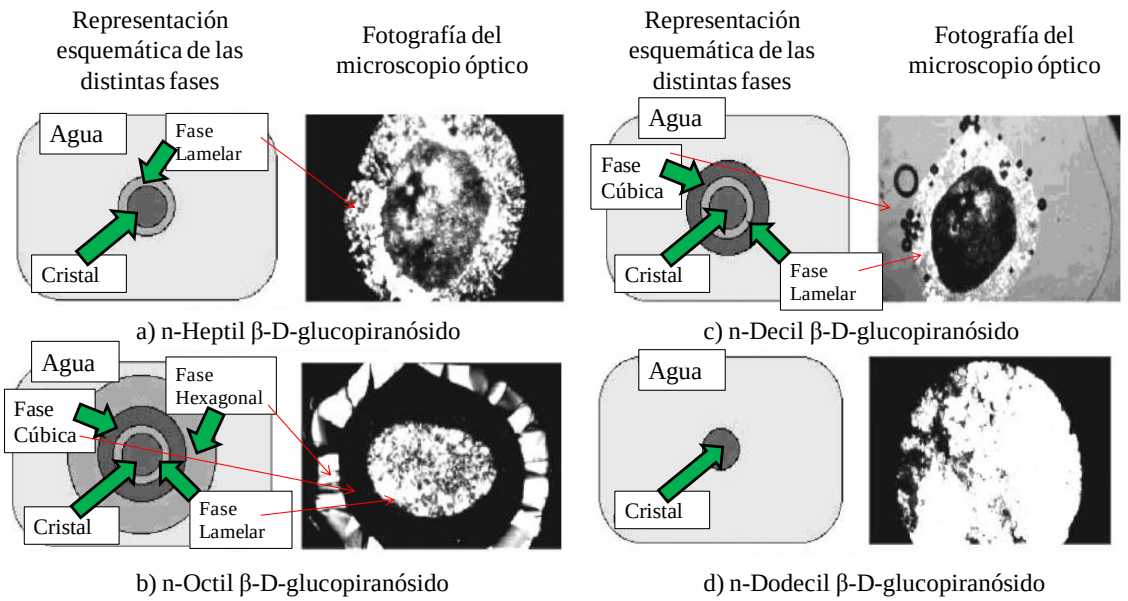

Fig. 1.109: Método de contacto para los derivados de n-alquil glucopiranósidos; **Ref [72].**

Para el n-heptil β-glucopiranósido se observa una fase lamelar, véase la **Fig. 1.109.a.** Para el n-octil β-glucopiranósido se observan la fase lamelar más la cúbica y la hexagonal, véase la **Fig. 1.109.b**. Para el n-decil β-glucopiranósido se observa la fase lamelar junto con la cúbica, véase la **Fig. 1.109.c** y para n-dodecil β-glucopiranósido, sin embargo, no se observan mesofases, véase la **Fig. 1.109.d**.

Posteriormente, el número de compuestos y mesofases caracterizadas han ido aumentando;[167] en la **Fig 1.110** se muestran algunos ejemplos de cristales líquidos termótropos basados en azúcares descritos hasta la fecha:

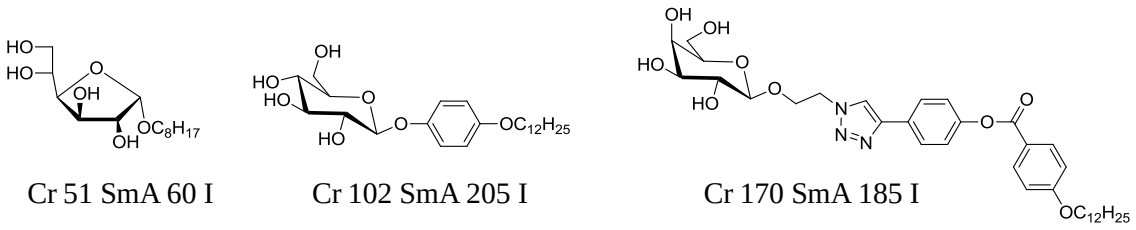

Cr 51 SmA 60 I Cr 102 SmA 205 I Cr 170 SmA 185 I

Fig. 1.110: Distintos ejemplos de estructuras químicas, temperaturas y fases de glicolípidos mesógenos: a) Derivados de furanosa, descritos por Goodby y sus colaboradores, **Ref [167d]**, b) Derivados de glucosa, descritos por Van Doren y sus

colaboradores, **Ref [167e]** y c) Derivados de galactosa, descritos por Hsu y sus colaboradores, **Ref [167f]**.

A pesar de que los glicolípidos mesógenos que poseen di- o polisacáridos en su cabeza polar[168] es aún relativamente pequeño, se pueden encontrar en la bibliografía algunos ejemplos[169] como los representados en la **Fig. 1.111**.

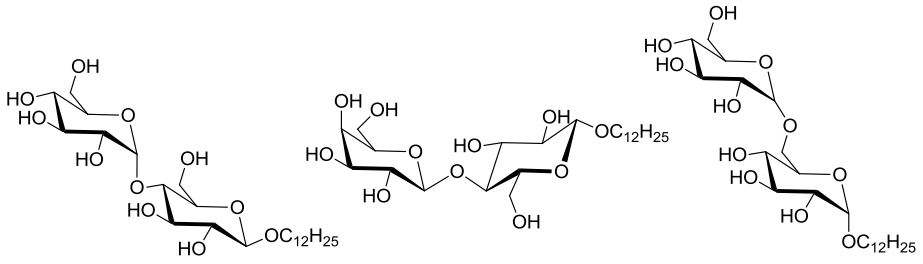

Cr 80 SmA^*_d 244 I Cr 183 SmA^*_d 246 I Cr 75 Cub 162 I

Fig. 1.111: Estructura química, temperatura y fases de los glicolípidos mesógenos descritos por Vill y sus colaboradores; **Ref [169].**

Aunque es difícil encontrar una relación estructura-actividad, dependiendo de factores como el tipo de cabeza azucarada y la posición o longuitud de la cadena del sustituyente, se han encontrado además de la esméctica, otro tipo de mesofases termótropas, como columnares o cúbicas. Los dos primeros ejemplos de la **Fig. 1.111** presentan mesofases esmécticas A_d^* mientras que el derivado de gentiobiosa tienen una mesofase cúbica. Comparando las distintas cabezas azucaradas, con la misma longitud de cadena en el sustituyente, se puede observar que las moléculas que forman las mesofases esmécticas tienen forma de varilla mientras que la molécula que tiene una mesofase cúbica, está más curvada.

En los derivados de O-(2-hidroxidodecil) sacarosa[170] de la **Fig. 1.112**, también se pueden encontrar distintas mesofases dependiendo de la posición en la que se encuentre el sustituyente. Como en el caso anterior, se puede encontrar una relación con la forma más o menos curvada de la molécula y la mesofase obtenida. Se forman fases SmA*

cuando el sustituyente está en posición **b**, **c**, **d**, **e**, **g**, cúbicas para **a** y columnares para **f** (véase la **Fig. 1.112** para establecer las posiciones de sustitución).

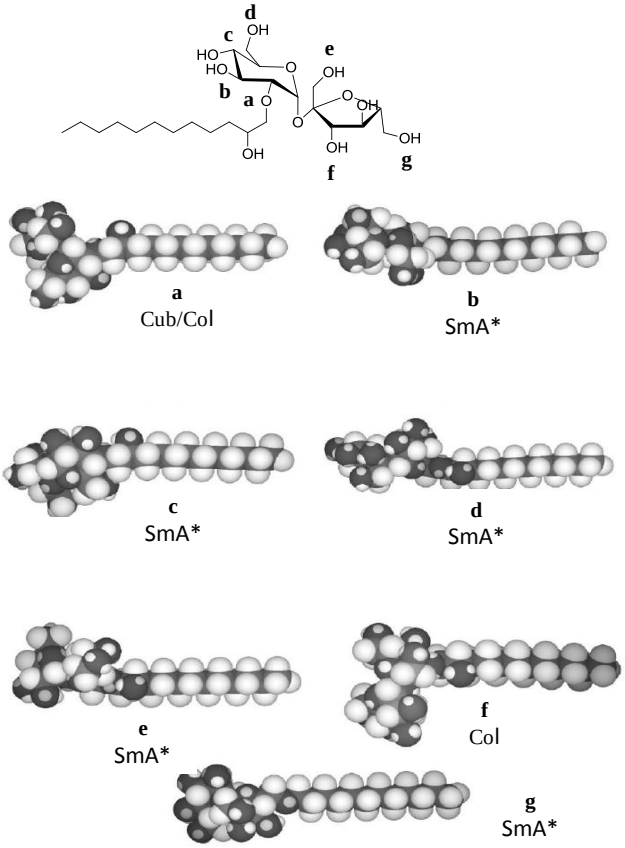

Fig. 1.112: Dependencia de la mesofase con la sustitución en los derivados de O-(2-hidroxidodecil) sacarosa; **Ref [170].**

En compuestos derivados de sacarosa con esteres de distinto tamaño (octanoil, decanoil, dodecanoil, hexadecanoil y octadecanoil),[171] si se compara 6-O-octanoilsacarosa y 6-O-octadecanoilsacarosa (**Fig. 1.113**) se observa que en la cadena más corta hay una fase columnar (la molécula está curvada) mientras que con la cadena larga se obtiene una fase lamelar (la molécula tiene más forma de varilla que la de cadena corta). Para 6-O-decanoilsacarosa, 6-O-dodecanoilsacarosa y 6-O-hexadecanoilsacarosa también se obtienen fases SmA*. Para los esteres sustituidos en posición 1´-O o 6´-O, el comportamiento es el mismo, para el derivado octanoilo se obtiene una fase columnar mientras que para el resto es esméctica.

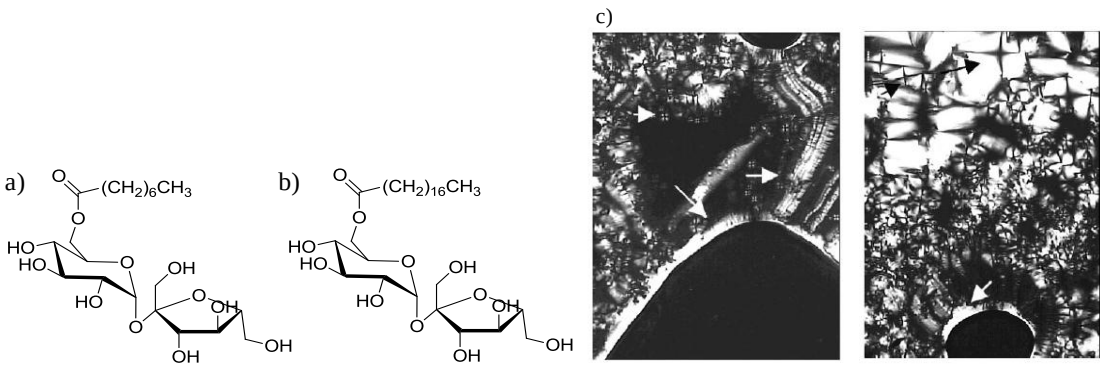

Fig. 1.113: Representación de (a) 6-O-octanoilsacarosa y (b) 6-O-octadecanoilsacarosa, c) defectos en la textura esméctica A* de 6-O-dodecanoilsacarosa; Ref **[171].**

Otro ejemplo, de estudios sobre el comportamiento cristal liquido termótropo y liótropo en glicolipidos con disacáridos (maltosa, melibiosa y lactosa), se ha realizado en compuestos unidos por un enlace amida a cadenas derivadas de ácidos grasos desde C_{11} hasta $C_{15,}$[172] **Fig. 1.114**. Todos ellos presentan una fase esméctica A, con temperaturas de transición a mesofase de 130ºC a 140ºC. La fase liótropa encontrada también ha sido lamelar, Lα. Para estudiar estos compuestos, por el método de contacto, ha sido necesario calentar la muestra una vez añadida la gota de agua para observar la mesofase.

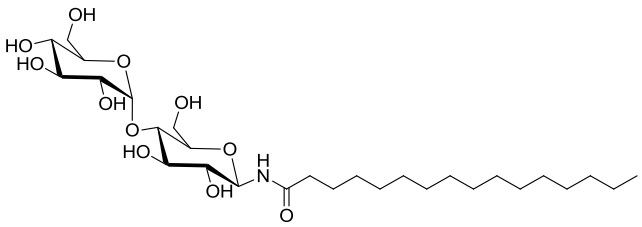

Fig. 1.114: Estructura química de un compuesto derivado de maltosa unido por un enlace amida a un cadena alquílica C_{15}**.**

1.4.6. *Azoglicoanfífilos y sus propiedades Cristal Líquido*

En compuestos glicolipídicos que poseen azobenzeno dentro de su estructura, también se han descrito mesofases de tipo cristal líquido, si bien son muy pocos los ejemplos descritos hasta la fecha.

En los derivados 4-(4´-*N*, *N*-didodecilaminofenildiazo)fenil- glicósidos,[173] cuando la parte azucarada es galactosa (**Fig. 1.115.a)**, lactosa o manosa, la fase que se obtiene es lamelar, véase la **Fig. 1.115.c**, mientras que con glucosa (**Fig. 1.115.b)**, la fase obtenida es columnar rectangular, véase la **Fig. 1.115.d**. Esta diferencia de organización en la mesofase puede explicarse porque la glucosa, a diferencia de los otros azúcares estudiados, tiene en posición ecuatorial todos sus grupos hidroxilos. Los autores proponen la organización que se muestra en las **Fig. 1.115** para la obtención de estas fases.

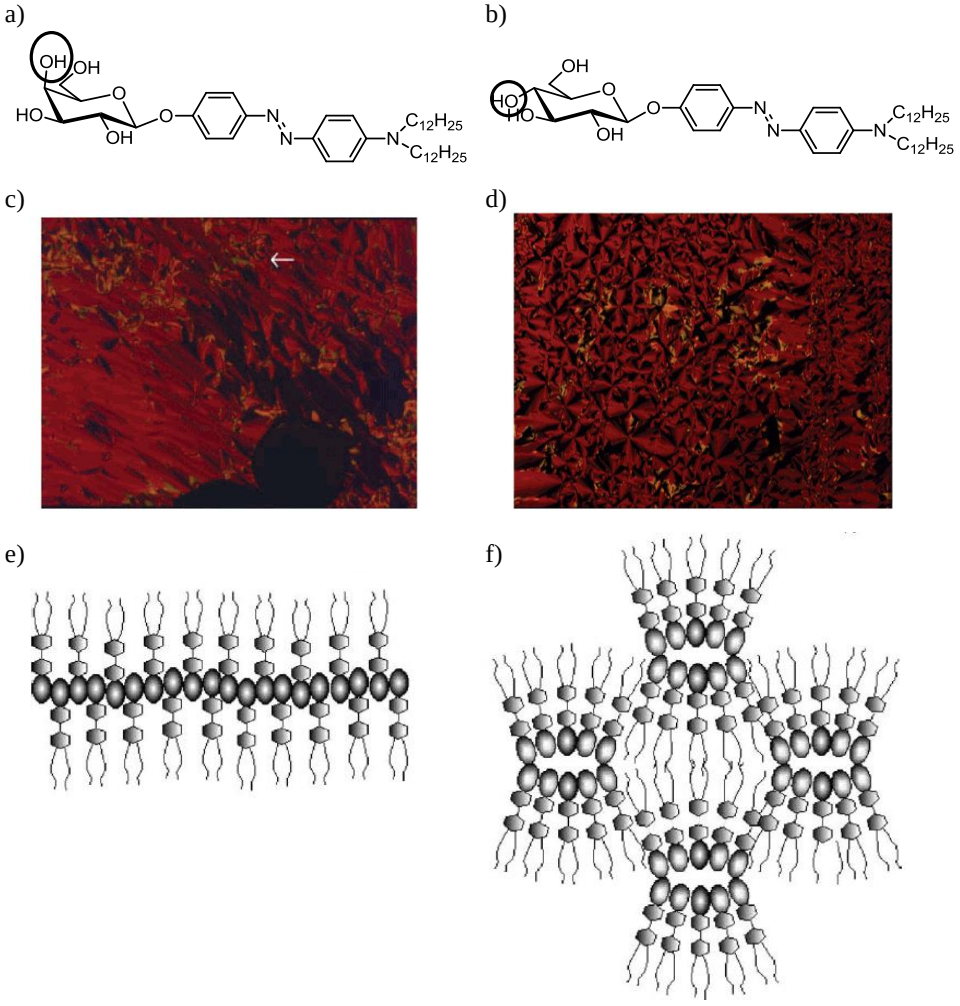

Fig. 1.115: Representación esquemática de los compuestos derivados de la galactosa (a) y de la glucosa (b). Fotografías de las mesofases, lamelar para la galactosa (c) y columnar para la glucosa (d). Representación esquemática de las fases lamelar para la galactosa (e) y columnar para la glucosa (f); **Ref. [173].**

En el caso de compuestos bolaanfifilos con un grupo azo en el centro de la cadena alquílica como el descrito en la **Fig. 1.116**, dependiendo de la longitud de dicha cadena, se puede encontrar una mesofase SmA para n=3, además de mesofases de tipo SmC* para n= 5, 6, 8, 10.[174] La combinación de las interacciones entre los azos y las cadenas alifáticas favorecen la torsión dentro de la organización.

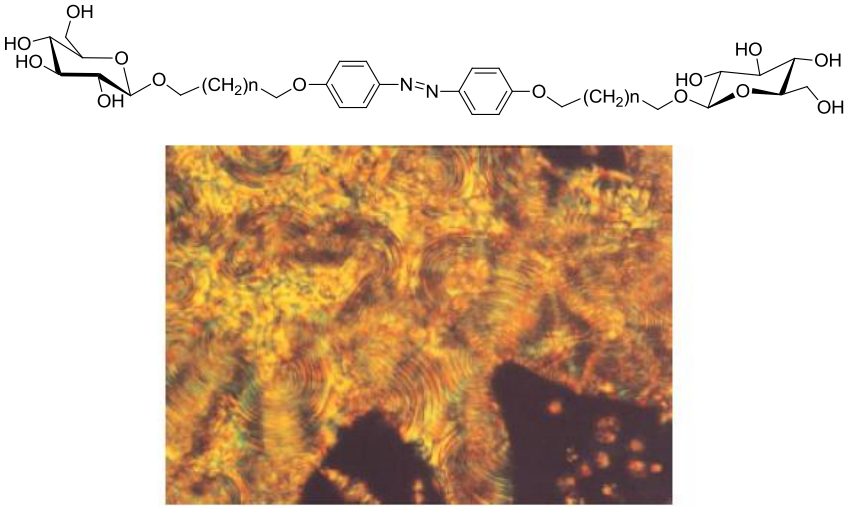

Fig. 1.116: Estructura química y fotografía de la textura SmC* para el compuesto con n=6 a 205ºC; **Ref [174].**

Con esta revisión bibliográfica sobre la estructura de moléculas anfifílas, especialmente con azúcar en su estructura y también con un grupo azobenzeno, se ha pretendido realizar una visión global de lo realizado antes y durante el trabajo de esta tesis.

1.5. Bibliografía

1. Piepenbrock, M. O. M.; Lloyd, G. O.; Clarke, N.; Steed, J. W., Metal- and Anion-Binding Supramolecular Gels. *Chem. Rev.* **2010,** *110* (4), 1960-2004.
2. Flory, P. J., Introductory Lecture. *Discuss of the Faraday Society* **1974,** *57*, 7-18.
3. Sangeetha, N. M.; Maitra, U., Supramolecular gels: Functions and uses. *Chem. Soc. Rev.* **2005,** *34* (10), 821-836.
4. Estroff, L. A.; Hamilton, A. D., Water gelation by small organic molecules. *Chem. Rev.* **2004,** *104* (3), 1201-1217.
5. (a) Abdallah, D. J.; Weiss, R. G., Organogels and low molecular mass organic gelators. *Adv. Mat.* **2000,** *12* (17), 1237-1247; (b) Terech, P.; Weiss, R. G., Low molecular mass gelators of organic liquids and the properties of their gels. *Chem. Rev.* **1997,** *97* (8), 3133-3159; (c) Smith, D. K., Lost in translation? Chirality effects in the self-assembly of nanostructured gel-phase materials. *Chem. Soc. Rev.* **2009,** *38* (3), 684-694; (d) Banerjee, S.; Das, R. K.; Maitra, U., Supramolecular gels 'in action'. *J. Mat. Chem.* **2009,** *19* (37), 6649-6687.
6. Weiss, R. G.; Terech, P., *Molecular gels*. Springer: Dordrecht, 2006.
7. (a) Brunsveld, L.; Folmer, B. J. B.; Meijer, E. W.; Sijbesma, R. P., Supramolecular polymers. *Chem. Rev.* **2001,** *101* (12), 4071-4097; (b) De Greef, T. F. A.; Smulders, M. M. J.; Wolffs, M.; Schenning, A.; Sijbesma, R. P.; Meijer, E. W., Supramolecular Polymerization. *Chem. Rev.* **2009,** *109* (11), 5687-5754.
8. Ajayaghosh, A.; Praveen, V. K.; Vijayakumar, C., Organogels as scaffolds for excitation energy transfer and light harvesting. *Chem. Soc. Rev.* **2008,** *37* (1), 109-122.
9. Hirst, A. R.; Escuder, B.; Miravet, J. F.; Smith, D. K., High-Tech Applications of Self-Assembling Supramolecular Nanostructured Gel-Phase Materials: From Regenerative Medicine to Electronic Devices. *Angew. Chem.-Int. Edit.* **2008,** *47* (42), 8002-8018.
10. Lee, C. C.; Grenier, C.; Meijer, E. W.; Schenning, A., Preparation and characterization of helical self-assembled nanofibers. *Chem. Soc. Rev.* **2009,** *38* (3), 671-683.
11. Israelachvili, J. N.; Mitchell, D. J.; Ninham, B. W., Theory of self-assembly of hydrocarbon amphiphiles into micelles and bilayers. *J. Chem. Soc.-Far. Trans. II* **1976,** *72*, 1525-1568.
12. Oda, R., Safin Gels with Amphiphilic Molecules. In *Molecular gels*, Weiss, R. G.; Terech, P., Eds. Springer: Dordrecht, 2006.
13. García Velázquez, D., Gelificadores multifuncionales de bajo peso molecular. Propiedades y aplicaciones de arquitecturas inteligentes. *Anales de la Química* **2010,** *106* (4), 257-267.
14. Shimizu, T.; Masuda, M.; Minamikawa, H., Supramolecular nanotube architectures based on amphiphilic molecules. *Chem. Rev.* **2005,** *105* (4), 1401-1443.
15. Aggeli, A.; Nyrkova, I. A.; Bell, M.; Harding, R.; Carrick, L.; McLeish, T. C. B.; Semenov, A. N.; Boden, N., Hierarchical self-assembly of chiral rod-like molecules as a model for peptide beta-sheet tapes, ribbons, fibrils, and fibers. *Proc. Nat. Acad. Sci. U. S. A.* **2001,** *98* (21), 11857-11862.
16. Spector, M. S.; Selinger, J. V.; Singh, A.; Rodriguez, J. M.; Price, R. R.; Schnur, J. M., Controlling the morphology of chiral lipid tubules. *Langmuir* **1998,** *14* (13), 3493-3500.

17. Shimizu, T.; Iwaura, R.; Masuda, M.; Hanada, T.; Yase, K., Internucleobase-interaction-directed self-assembly of nanofibers from homo- and heteroditopic 1,omega-nucleobase bolaamphiphiles. *J. Am. Chem. Soc.* **2001,** *123* (25), 5947-5955.
18. Thomas, B. N.; Lindemann, C. M.; Corcoran, R. C.; Cotant, C. L.; Kirsch, J. E.; Persichini, P. J., Phosphonate lipid tubules II. *J. Am. Chem. Soc.* **2002,** *124* (7), 1227-1233.
19. Messmore, B. W.; Sukerkar, P. A.; Stupp, S. I., Mirror image nanostructures. *J. Am. Chem. Soc.* **2005,** *127* (22), 7992-7993.
20. Koga, T.; Matsuoka, M.; Higashi, N., Structural control of self-assembled nanofibers by artificial beta-sheet peptides composed of D- or L-isomer. *J. Am. Chem. Soc.* **2005,** *127* (50), 17596-17597.
21. de Jong, J. J. D.; Tiemersma-Wegman, T. D.; van Esch, J. H.; Feringa, B. L., Dynamic chiral selection and amplification using photoresponsive organogelators. *J. Am. Chem. Soc.* **2005,** *127* (40), 13804-13805.
22. Smith, D. K., Molecular gels - underpinning nanoscale materials with organic chemistry - Preface. *Tetrahedron* **2007,** *63* (31), 7283-7284.
23. Polishuk, A. T., Properties and Performance-Charasteristics of Some Modern Lubricating Greases. *Lub. Engin.* **1977,** *33* (3), 133-138.
24. Martinborret, O.; Ramasseul, R.; Rassat, A., Nitroxide-89 - 17-alpha-Aza D-Homosteroidal Nitroxides. *Bulletin De La Societe Chimique De France Partie Ii-Chimie Moleculaire Organique et Biologique* **1979,** (7-8), 401-408.
25. Lin, Y. C.; Weiss, R. G., A novel gelator of organic liquids and the properties of its gels *Macromol.* **1987,** *20* (2), 414-417.
26. (a) Brotin, T.; Desvergne, J. P.; Fages, F.; Utermohlen, R.; Bonneau, R.; Bouaslaurent, H., Photostationary Fluorescence Emission And Time Resolved Spectroscopy Of Symmetrically Disubstituted Anthracenes on the Meso and Side Rings - The Unusual Behavior of the 1,4 Derivative. *Photochem. and Photobiol.* **1992,** *55* (3), 349-358; (b) Brotin, T.; Utermohlen, R.; Fages, F.; Bouaslaurent, H.; Desvergne, J. P., A Novel Small Molecular Luminiscent Gelling Agent For Alcohols. *J. Chem. Soc.-Chem. Commun.* **1991,** (6), 416-418.
27. Terech, P.; Gebel, G.; Ramasseul, R., Molecular rods in a zinc(II) porphyrin/cyclohexane physical gel: Neutron and X-ray scattering characterizations. *Langmuir* **1996,** *12* (18), 4321-4323.
28. (a) Aoki, M.; Murata, K.; Shinkai, S., Calixarene-Based Gelators Of Organic Fluids. *Chem. Lett.* **1991,** (10), 1715-1718; (b) Aoki, M.; Nakashima, K.; Kawabata, H.; Tsutsui, S.; Shinkai, S., Molecular Design and Characterizations of New Calixarene-Based Gelators of Organic Fluids. *J. Chem. Soc.-Perkin Trans. 2* **1993,** (3), 347-354.
29. (a) Fuhrhop, J. H.; Schnieder, P.; Rosenberg, J.; Boekema, E., The Chiral Bilayer Effect Stabilizes Micellar Fibers. *J. Am. Chem. Soc.* **1987,** *109* (11), 3387-3390; (b) Fuhrhop, J. H.; Svenson, S.; Boettcher, C.; Rossler, E.; Vieth, H. M., Long-lived Micellar N-Alkylaldonamide Fiber Gels- Solid-State NMR and Electron-Microscopic Studies. *J. Am. Chem. Soc.* **1990,** *112* (11), 4307-4312.
30. (a) Imae, T.; Funayama, K.; Krafft, M. P.; Giulieri, F.; Tada, T.; Matsumoto, T., Small-angle scattering and electron microscopy investigation of nanotubules made from a perfluoroalkylated glucophospholipid. *J. Coll. Interf. Sci.* **1999,** *212* (2), 330-337; (b) Pang, S. F.; Zhu, D. B., Pronounced hydrogel formation by the self-assembled aggregate of semifluorinated fatty acid. *Chem. Phys. Lett.* **2002,** *358* (5-6), 479-483.
31. Iwaura, R.; Yoshida, K.; Masuda, M.; Ohnishi-Kameyama, M.; Yoshida, M.; Shimizu, T., Oligonucleotide-templated self-assembly of nucleotide bolaamphiphiles:

DNA-like nanofibers edged by a double-helical arrangement of A-T base pairs. *Angew. Chem.-Int. Edit.* **2003,** *42* (9), 1009-1012.

32. (a) Kogiso, M.; Hanada, T.; Yase, K.; Shimizu, T., Intralayer hydrogen-bond-directed self-assembly of nano-fibers from dicarboxylic valylvaline bolaamphiphiles. *Chem. Commun.* **1998,** (17), 1791-1792; (b) Kogiso, M.; Ohnishi, S.; Yase, K.; Masuda, M.; Shimizu, T., Dicarboxylic oligopeptide bolaamphiphiles: Proton-triggered self-assembly of microtubes with loose solid surfaces. *Langmuir* **1998,** *14* (18), 4978-4986.

33. Nakazawa, I.; Masuda, M.; Okada, Y.; Hanada, T.; Yase, K.; Asai, M.; Shimizu, T., Spontaneous formation of helically twisted fibers from 2-glucosamide bolaamphiphiles: Energy-filtering transmission electron microscopic observation and even-odd effect of connecting bridge. *Langmuir* **1999,** *15* (14), 4757-4764.

34. Menger, F. M.; Littau, C. A., Gemini Surfactants- Synthesis and Properties. *J. Am. Chem. Soc.* **1991,** *113* (4), 1451-1452.

35. Menger, F. M.; Seredyuk, V. A.; Apkarian, R. P.; Wright, E. R., Colloidal assemblies of branched geminis studied by cryo-etch-HRSEM. *J. Am. Chem. Soc.* **2002,** *124* (42), 12408-12409.

36. Newkome, G. R.; Baker, G. R.; Arai, S.; Saunders, M. J.; Russo, P. S.; Theriot, K. J.; Moorefield, C. N.; Rogers, L. E.; Miller, J. E.; Lieux, T. R.; Murray, M. E.; Phillips, B.; Pascal, L., Cascade Molecules .6. Shynthesis and Characterization Of 2-Directional Cascade Molecules and Formation Of Aqueous Gels. *J. Am. Chem. Soc.* **1990,** *112* (23), 8458-8465.

37. Maitra, U.; Mukhopadhyay, S.; Sarkar, A.; Rao, P.; Indi, S. S., Hydrophobic pockets in a nonpolymeric aqueous gel: Observation of such a gelation process by color change. *Angew. Chem.-Int. Edit.* **2001,** *40* (12), 2281-2283.

38. Imae, T.; Takahashi, Y.; Muramatsu, H., Formation of fibrous Molecular assemblies by amino-acid Surfactants in water. *J. Am. Chem. Soc.* **1992,** *114* (9), 3414-3419.

39. (a) Estroff, L. A.; Hamilton, A. D., Effective gelation of water using a series of bis-urea dicarboxylic acids. *Angew. Chem.-Int. Edit.* **2000,** *39* (19), 3447-3450; (b) Estroff, L. A.; Leiserowitz, L.; Addadi, L.; Weiner, S.; Hamilton, A. D., Characterization of an organic hydrogel: A cryo-transmission electron microscopy and X-ray diffraction study. *Adv. Mat.* **2003,** *15* (1), 38-42.

40. Murata, K.; Aoki, M.; Suzuki, T.; Harada, T.; Kawabata, H.; Komori, T.; Ohseto, F.; Ueda, K.; Shinkai, S., Thermal and Ligth control of the Sol-Gel Phase-Transition in Cholesterol-Based Organic Gels- Novel Helical Aggregation Modes as detected by Circular-Dichroism and Electron-Microscopic Observation. *J. Am. Chem. Soc.* **1994,** *116* (15), 6664-6676.

41. Glosario de terminología Reológica. *Revista Iberoamericana de Polímeros* **2002,** *3* (2).

42. Menger, F. M.; Caran, K. L., Anatomy of a gel. Amino acid derivatives that rigidify water at submillimolar concentrations. *J. Am. Chem. Soc.* **2000,** *122* (47), 11679-11691.

43. Hanabusa, K.; Yamada, M.; Kimura, M.; Shirai, H., Prominent gelation and chiral aggregation of alkylamides derived from trans-1,2-diaminocyclohexane. *Ang. Chem.-Int. Ed. Eng.* **1996,** *35* (17), 1949-1951.

44. Bhattacharya, S.; Krishnan-Ghosh, Y., First report of phase selective gelation of oil from oil/water mixtures. Possible implications toward containing oil spills. *Chem. Commun.* **2001,** (2), 185-186.

45. Kohler, K.; Forster, G.; Hauser, A.; Dobner, B.; Heiser, U. F.; Ziethe, F.; Richter, W.; Steiniger, F.; Drechsler, M.; Stettin, H.; Blume, A., Self-assembly in a bipolar phosphocholine-water system: The formation of nanofibers and hydrogels. *Angew. Chem.-Int. Edit.* **2004,** *43* (2), 245-247.
46. Hirst, A. R.; Coates, I. A.; Boucheteau, T. R.; Miravet, J. F.; Escuder, B.; Castelletto, V.; Hamley, I. W.; Smith, D. K., Low-molecular-weight gelators: Elucidating the principles of gelation based on gelator solubility and a cooperative self-assembly model. *J. Am. Chem. Soc.* **2008,** *130* (28), 9113-9121.
47. Steed, J. W., Supramolecular gel chemistry: developments over the last decade. *Chem. Commun.* **2011,** *47* (5), 1379-1383.
48. (a) Escuder, B.; Llusar, M.; Miravet, J. F., Insight on the NMR study of supramolecular gels and its application to monitor molecular recognition on self-assembled fibers. *J. Org. Chem.* **2006,** *71* (20), 7747-7752; (b) Iqbal, S.; Rodriguez-Llansola, F.; Escuder, B.; Miravet, J. F.; Verbruggen, I.; Willem, R., HRMAS (1)H NMR as a tool for the study of supramolecular gels. *Soft Matt.* **2010,** *6* (9), 1875-1878; (c) Shapiro, Y. E., Structure and dynamics of hydrogels and organogels: An NMR spectroscopy approach. *Prog. Pol. Sci.* **2011,** *36* (9), 1184-1253.
49. Yamanaka, M.; Sada, K.; Miyata, M.; Hanabusa, K.; Nakano, K., Construction of superhydrophobic surfaces by fibrous aggregation of perfluoroalkyl chain-containing organogelators. *Chem .Commun* **2006,** (21), 2248-2250.
50. (a) Stendahl, J. C.; Li, L. M.; Zubarev, E. R.; Chen, Y. R.; Stupp, S. I., Toughening of polymers by self-assembling molecules. *Advanced Materials* **2002,** *14* (21), 1540-1543; (b) Zubarev, E. R.; Pralle, M. U.; Sone, E. D.; Stupp, S. I., Scaffolding of polymers by supramolecular nanoribbons. *Adv. Mat.* **2002,** *14* (3), 198-203.
51. (a) Kishimura, A.; Yamashita, T.; Aida, T., Phosphorescent organogels via "metallophilic" interactions for reversible RGB-color switching. *J. Am. Chem. Soc.* **2005,** *127* (1), 179-183; (b) Tu, T.; Assenmacher, W.; Peterlik, H.; Weisbarth, R.; Nieger, M.; Dotz, K. H., An air-stable organometallic low-molecular-mass gelator: Synthesis, aggregation, and catalytic application of a palladium pincer complex. *Angew. Chem.-Int. Edit.* **2007,** *46* (33), 6368-6371.
52. (a) Del Guerzo, A.; Olive, A. G. L.; Reichwagen, J.; Hopf, H.; Desvergne, J. P., Energy transfer in self-assembled n -acene fibers involving >= 100 donors per acceptor. *J. Am. Chem. Soc.* **2005,** *127* (51), 17984-17985; (b) Montalti, M.; Dolci, L. S.; Prodi, L.; Zaccheroni, N.; Stuart, M. C. A.; van Bommel, K. J. C.; Friggeri, A., Energy transfer from a fluorescent hydrogel to a hosted fluorophore. *Langmuir* **2006,** *22* (5), 2299-2303.
53. Kubo, W.; Kitamura, T.; Hanabusa, K.; Wada, Y.; Yanagida, S., Quasi-solid-state dye-sensitized solar cells using room temperature molten salts and a low molecular weight gelator. *Chem. Commun.* **2002,** (4), 374-375.
54. Vemula, P. K.; John, G., Smart amphiphiles: hydro/organogelators for in situ reduction of gold. *Chem. Commun.* **2006,** (21), 2218-2220.
55. Kato, T.; Mizoshita, N.; Kishimoto, K., Functional liquid-crystalline assemblies: Self-organized soft materials. *Angew. Chem.-Int. Edit.* **2006,** *45* (1), 38-68.
56. (a) Zhang, S. G.; Holmes, T. C.; Dipersio, C. M.; Hynes, R. O.; Su, X.; Rich, A., Self-Complementary Oligopeptide Matrices Support Mammalian-Cell Attachment. *Biomat.* **1995,** *16* (18), 1385-1393; (b) Holmes, T. C.; de Lacalle, S.; Su, X.; Liu, G. S.; Rich, A.; Zhang, S. G., Extensive neurite outgrowth and active synapse formation on self-assembling peptide scaffolds. *Proc. Nat. Acad. Sci. U. S. A.* **2000,** *97* (12), 6728-6733; (c) Ellis-Behnke, R. G.; Liang, Y. X.; You, S. W.; Tay, D. K. C.; Zhang, S. G.; So, K. F.; Schneider, G. E., Nano neuro knitting: Peptide nanofiber scaffold for brain

repair and axon regeneration with functional return of vision. *Proc. Nat. Acad. Sci. U. S. A.* **2006,** *103* (13), 5054-5059.
57. Silva, G. A.; Czeisler, C.; Niece, K. L.; Beniash, E.; Harrington, D. A.; Kessler, J. A.; Stupp, S. I., Selective differentiation of neural progenitor cells by high-epitope density nanofibers. *Science* **2004,** *303* (5662), 1352-1355.
58. Kisiday, J.; Jin, M.; Kurz, B.; Hung, H.; Semino, C.; Zhang, S.; Grodzinsky, A. J., Self-assembling peptide hydrogel fosters chondrocyte extracellular matrix production and cell division: Implications for cartilage tissue repair. *Proc. Nat. Acad. Sci. U. S. A.* **2002,** *99* (15), 9996-10001.
59. Davis, M. E.; Motion, J. P. M.; Narmoneva, D. A.; Takahashi, T.; Hakuno, D.; Kamm, R. D.; Zhang, S. G.; Lee, R. T., Injectable self-assembling peptide nanofibers create intramyocardial microenvironments for endothelial cells. *Circulation* **2005,** *111* (4), 442-450.
60. Bhuniya, S.; Seo, Y. J.; Kim, B. H., (S)-(+)-Ibuprofen-based hydrogelators: an approach toward anti-inflammatory drug delivery. *Tetrahedron Lett.* **2006,** *47* (40), 7153-7156.
61. Friggeri, A.; Feringa, B. L.; van Esch, J., Entrapment and release of quinoline derivatives using a hydrogel of a low molecular weight gelator. *J. Contr. Rel.* **2004,** *97* (2), 241-248.
62. Yang, Z. M.; Liang, G. L.; Wang, L.; Xu, B., Using a kinase/phosphatase switch to regulate a supramolecular hydrogel and forming the supramoleclar hydrogel in vivo. *J. Am. Chem. Soc.* **2006,** *128* (9), 3038-3043.
63. (a) Wang, Q. G.; Yang, Z. M.; Wang, L.; Ma, M. L.; Xu, B., Molecular hydrogel-immobilized enzymes exhibit superactivity and high stability in organic solvents. *Chem. Commun.* **2007,** (10), 1032-1034; (b) Wang, Q. G.; Yang, Z. M.; Zhang, X. Q.; Xiao, X. D.; Chang, C. K.; Xu, B., A supramolecular-hydrogel-encapsulated hemin as an artificial enzyme to mimic peroxidase. *Angew. Chem.-Int. Edit.* **2007,** *46* (23), 4285-4289.
64. Schnepp, Z. A. C.; Gonzalez-McQuire, R.; Mann, S., Hybrid biocomposites based on calcium phosphate mineralization of self-assembled supramolecular hydrogels. *Adv. Mat.* **2006,** *18* (14), 1869-1872.
65. Estroff, L. A.; Addadi, L.; Weiner, S.; Hamilton, A. D., An organic hydrogel as a matrix for the growth of calcite crystals. *Org. & Biomol. Chem.* **2004,** *2* (1), 137-141.
66. Bhuniya, S.; Kim, B. H., An insulin-sensing sugar-based fluorescent hydrogel. *Chem. Commun.* **2006,** (17), 1842-1844.
67. Mohan, S. R. K.; Hamachi, I., Synthesis of new supramolecular polymers based on glycosylated amino acid and their applications. *Curr.Org. Chem.* **2005,** *9* (5), 491-502.
68. Yoshimura, I.; Miyahara, Y.; Kasagi, N.; Yamane, H.; Ojida, A.; Hamachi, I., Molecular recognition in a supramolecular hydrogel to afford a semi-wet sensor chip. *J. Am. Chem. Soc.* **2004,** *126* (39), 12204-12205.
69. Yang, Z. M.; Xu, K. M.; Wang, L.; Gu, H. W.; Wei, H.; Zhang, M. J.; Xu, B., Self-assembly of small molecules affords multifunctional supramolecular hydrogels for topically treating simulated uranium wounds. *Chem. Commun.* **2005,** (35), 4414-4416.
70. Hato, M., Synthetic glycolipid/water systems. *Curr. Op. Coll. & Interf. Sci.* **2001,** *6* (3), 268-276.
71. Sanchez, M. Propiedades bioquímicas y biofísicas de ramnolípidos biotensioactivos. Universidad de Murcia, Murcia, 2010.
72. Goodby, J. W.; Gortz, V.; Cowling, S. J.; Mackenzie, G.; Martin, P.; Plusquellec, D.; Benvegnu, T.; Boullanger, P.; Lafont, D.; Queneau, Y.; Chambert, S.;

Fitremann, J., Thermotropic liquid crystalline glycolipids. *Chem. Soc. Rev.* **2007,** *36* (12), 1971-2032.
73. Pfannemuller, B.; Welte, W., Amphiphilic Properties of Synthetic Glycolipids Based on Amide Linkages. 1. Electron -Microscopic Studies on Aqueous Gels. *Chem. Phys. Lip.* **1985,** *37* (3), 227-240.
74. Fuhrhop, J. H.; Schnieder, P.; Boekema, E.; Helfrich, W., Lipid Bilayer Fibers from Diastereomeric and Enantiomeric N-Octylaldonamides. *J. Am. Chem. Soc.* **1988,** *110* (9), 2861-2867.
75. Buerkle, L. E.; Galleguillos, R.; Rowan, S. J., Nonionic surfactant-induced stabilization and tailorability of sugar-amphiphile hydrogels. *Soft Matt.* **2011,** *7* (15), 6984-6990.
76. Avalos, M.; Babiano, R.; Cintas, P.; Gomez-Carretero, A.; Jimenez, J. L.; Lozano, M.; Ortiz, A. L.; Palacios, J. C.; Pinazo, A., A family of hydrogels based on ureido-linked aminopolyol-derived amphiphiles and bolaamphiphiles: Synthesis, gelation under thermal and sonochemical stimuli, and mesomorphic characterization. *Chem.-a Eur. J.* **2008,** *14* (18), 5656-5669.
77. Bhattacharya, S.; Acharya, S. N. G., Pronounced hydrogel formation by the self-assembled aggregates of N-alkyl disaccharide amphiphiles. *Chem. Mat.* **1999,** *11* (12), 3504-3511.
78. John, G.; Masuda, M.; Okada, Y.; Yase, K.; Shimizu, T., Nanotube formation from renewable resources via coiled nanofibers. *Adv. Mater.* **2001,** *13* (10), 715-718.
79. Jung, J. H.; John, G.; Masuda, M.; Yoshida, K.; Shinkai, S.; Shimizu, T., Self-assembly of a sugar-based gelator in water: Its remarkable diversity in gelation ability and aggregate structure. *Langmuir* **2001,** *17* (23), 7229-7232.
80. Jung, J. H.; Shinkai, S.; Shimizu, T., Spectral characterization of self-assemblies of aldopyranoside amphiphilic gelators: What is the essential structural difference between simple amphiphiles and bolaamphiphiles? *Chem.-a Eur. J.* **2002,** *8* (12), 2684-2690.
81. Jung, J. H.; Lee, S. S.; Shinkai, S.; Iwaura, R.; Shimizu, T., Novel silica nanotubes using a library of carbohydrate gel assemblies as templates for sol-gel transcription in binary systems. *Bull. Korean Chem. Soc.* **2004,** *25* (1), 63-68.
82. Jung, J. H.; John, G.; Yoshida, K.; Shimizu, T., Self-assembling structures of long-chain phenyl glucoside influenced by the introduction of double bonds. *J. Am. Chem. Soc.* **2002,** *124* (36), 10674-10675.
83. Kamiya, S.; Minamikawa, H.; Jung, J. H.; Yang, B.; Masuda, M.; Shimizu, T., Molecular structure of glucopyranosylamide lipid and nanotube morphology. *Langmuir* **2005,** *21* (2), 743-750.
84. Yang, Z. M.; Liang, G. L.; Ma, M. L.; Abbah, A. S.; Lu, W. W.; Xu, B., D-glucosamine-based supramolecular hydrogels to improve wound healing. *Chem. Commun.* **2007,** (8), 843-845.
85. Wang, W. J.; Wang, H. M.; Ren, C. H.; Wang, J. Y.; Tan, M.; Shen, J.; Yang, Z. M.; Wang, P. G.; Wang, L., A saccharide-based supramolecular hydrogel for cell culture. *Carb. Res.* **2011,** *346* (8), 1013-1017.
86. Beginn, U.; Keinath, S.; Moller, M., New carbohydrate amphiphiles. 2. Gel formation and gel morphologies. *Macromol. Chem. and Phys.* **1998,** *199* (11), 2379-2384.
87. (a) Hamachi, I.; Kiyonaka, S.; Shinkai, S., Solid phase lipid synthesis (SPLS) for construction of an artificial glycolipid library. *Chem. Commun.* **2000,** (14), 1281-1282; (b) Kiyonaka, S.; Shinkai, S.; Hamachi, I., Combinatorial library of low molecular-

weight organo- and hydrogelators based on glycosylated amino acid derivatives by solid-phase synthesis. *Chem.-a Europ. J.* **2003,** *9* (4), 976-983.
88. Kiyonaka, S.; Sugiyasu, K.; Shinkai, S.; Hamachi, I., First thermally responsive supramolecular polymer based on glycosylated amino acid. *J. Am. Chem. Soc.* **2002,** *124* (37), 10954-10955.
89. (a) Kiyonaka, S.; Sada, K.; Yoshimura, I.; Shinkai, S.; Kato, N.; Hamachi, I., Semi-wet peptide/protein array using supramolecular hydrogel. *Nat. Mat.* **2004,** *3* (1), 58-64; (b) Yamaguchi, S.; Yoshimura, L.; Kohira, T.; Tamaru, S.; Hamachi, I., Cooperation between artificial receptors and supramolecular hydrogels for sensing and discriminating phosphate derivatives. *J. Am. Chem. Soc.* **2005,** *127* (33), 11835-11841.
90. Tamaru, S.; Kiyonaka, S.; Hamachi, I., Three distinct read-out modes for enzyme activity can operate in a semi-wet supramolecular hydrogel. *Chem.-a Eur. J.* **2005,** *11* (24), 7294-7304.
91. Koshi, Y.; Nakata, E.; Yamane, H.; Hamachi, I., A fluorescent lectin array using supramolecular hydrogel for simple detection and pattern profiling for various glycoconjugates. *J. Am. Chem. Soc.* **2006,** *128* (32), 10413-10422.
92. Zhou, S. L.; Matsumoto, S.; Tian, H. D.; Yamane, H.; Ojida, A.; Kiyonaka, S.; Hamachi, I., pH-Responsive shrinkage/swelling of a supramolecular hydrogel composed of two small amphiphilic molecules. *Chem.-a Eur. J.* **2005,** *11* (4), 1130-1136.
93. Matsumoto, S.; Yamaguchi, S.; Ueno, S.; Komatsu, H.; Ikeda, M.; Ishizuka, K.; Iko, Y.; Tabata, K. V.; Aoki, H.; Ito, S.; Noji, H.; Hamachi, I., Photo gel-sol/sol-gel transition and its patterning of a supramolecular hydrogel as stimuli-responsive biomaterials. *Chem.-a Eur. J.* **2008,** *14* (13), 3977-3986.
94. Matsumoto, S.; Yamaguchi, S.; Wada, A.; Matsui, T.; Ikeda, M.; Hamachi, I., Photo-responsive gel droplet as a nano- or pico-litre container comprising a supramolecular hydrogel. *Chem. Commun.* **2008,** (13), 1545-1547.
95. Ikeda, M.; Ueno, S.; Matsumoto, S.; Shimizu, Y.; Komatsu, H.; Kusumoto, K. I.; Hamachi, I., Three-Dimensional Encapsulation of Live Cells by Using a Hybrid Matrix of Nanoparticles in a Supramolecular Hydrogel. *Chem.-a Eur. J.* **2008,** *14* (34), 10808-10815.
96. Bhattacharya, S.; Acharya, S. N. G., Vesicle and tubular microstructure formation from synthetic sugar-linked amphiphiles. Evidence of vesicle formation from single-chain amphiphiles bearing a disaccharide headgroup. *Langmuir* **2000,** *16* (1), 87-97.
97. Emmanouil, V.; El Ghoul, M.; Andre-Barres, C.; Guidetti, B.; Rico-Lattes, I.; Lattes, A., Synthesis of new long-chain fluoroalkyl glycolipids: Relation of amphiphilic properties to morphology of supramolecular assemblies. *Langmuir* **1998,** *14* (19), 5389-5395.
98. Fitremann, J.; Bouchu, A.; Queneau, Y., Synthesis and gelling properties of N-palmitoyl-L-phenylalanine sucrose esters. *Langmuir* **2003,** *19* (23), 9981-9983.
99. (a) Yoza, K.; Ono, Y.; Yoshihara, K.; Akao, T.; Shinmori, H.; Takeuchi, M.; Shinkai, S.; Reinhoudt, D. N., Sugar-integrated gelators of organic fluids: on their versatility as building-blocks and diversity in superstructures. *Chem. Commun.* **1998,** (8), 907-908; (b) Yoza, K.; Amanokura, N.; Ono, Y.; Akao, T.; Shinmori, H.; Takeuchi, M.; Shinkai, S.; Reinhoudt, D. N., Sugar-integrated gelators of organic solvents - Their remarkable diversity in gelation ability and aggregate structure. *Chem.-a Eur. J.* **1999,** *5* (9), 2722-2729; (c) Gronwald, O.; Shinkai, S., 'Bifunctional' sugar-integrated gelators for organic solvents and water-on the role of nitro-substituents in 1-O-methyl-4,6-O-

(nitro benzylidene)-monosaccharides for the improvement of gelation ability. *J. Chem. Soc.-Perkin Trans. 2* **2001,** (10), 1933-1937.
100. (a) Wang, G. J.; Cheuk, S.; Williams, K.; Sharma, V.; Dakessian, L.; Thorton, Z., Synthesis and characterization of monosaccharide lipids as novel hydrogelators. *Carb. Res.* **2006,** *341* (6), 705-716; (b) Cheuk, S.; Stevens, E. D.; Wang, G., Synthesis and structural analysis of a series of D-glucose derivatives as low molecular weight gelators. *Carb. Res.* **2009,** *344* (4), 417-425; (c) Wang, G. J.; Cheuk, S.; Yang, H.; Goyal, N.; Reddy, P. V. N.; Hopkinson, B., Synthesis and Characterization of Monosaccharide-Derived Carbamates as Low-Molecular-Weight Gelators. *Langmuir* **2009,** *25* (15), 8696-8705; (d) Goyal, N.; Cheuk, S.; Wang, G. J., Synthesis and characterization of D-glucosamine-derived low molecular weight gelators. *Tetrahedron* **2010,** *66* (32), 5962-5971; (e) Wang, G. J.; Yang, H.; Cheuk, S.; Coleman, S., Synthesis and self-assembly of 1-deoxyglucose derivatives as low molecular weight organogelators. *Beilstein J. Org. Chem.* **2011,** *7*, 234-242.
101. (a) Shimizu, T.; Masuda, M., Stereochemical effect of even-odd connecting links on supramolecular assemblies made of 1-glucosamide bolaamphiphiles. *J. Am. Chem. Soc.* **1997,** *119* (12), 2812-2818; (b) Shimizu, T., Bottom-up synthesis and morphological control of high-axial-ratio nanostructures through molecular self-assembly. *Pol. J.* **2003,** *35* (1), 1-22.
102. Masuda, M.; Hanada, T.; Okada, Y.; Yase, K.; Shimizu, T., Polymerization in nanometer-sized fibers: Molecular packing order and polymerizability. *Macromol.* **2000,** *33* (25), 9233-9238.
103. Del Guerzo, A.; Pozzo, J. L., Photoresponsive Gels. In *Molecular gels*, Weiss, R. G.; Terech, P., Eds. Springer: Dordrecht, 2006.
104. (a) Hanabusa, K.; Miki, T.; Taguchi, Y.; Koyama, T.; Shirai, H., 2-Component, Small- Molecule Gelling Agents. *J. Chem. Soc.-Chem. Commun.* **1993,** (18), 1382-1384; (b) Inoue, K.; Ono, Y.; Kanekiyo, Y.; Ishi-i, T.; Yoshihara, K.; Shinkai, S., Design of new organic gelators stabilized by a host-guest interaction. *J. Org. Chem.* **1999,** *64* (8), 2933-2937.
105. (a) Pozzo, J. L.; Clavier, G. M.; Desvergne, J. P., Rational design of new acid-sensitive organogelators. *J. Mat. Chem.* **1998,** *8* (12), 2575-2577; (b) Deng, W.; Thompson, D. H., pH and cation-responsive supramolecular gels formed by cyclodextrin amines in DMSO. *Soft Matt.* **2010,** *6* (9), 1884-1887.
106. (a) Terech, P.; Coutin, A., Organic solutions of monomolecular organometallic threads. Nonlinear rheology and effects of end-capping species. *J. Phys.Chem. B* **2001,** *105* (24), 5670-5676; (b) Perez, A.; Serrano, J. L.; Sierra, T.; Ballesteros, A.; de Saa, D.; Barluenga, J., Control of Self-Assembly of a 3-Hexen-1,5-diyne Derivative: Toward Soft Materials with an Aggregation-Induced Enhancement in Emission. *J. Am. Chem. Soc.* **2011,** *133* (21), 8110-8113.
107. van der Laan, S.; Feringa, B. L.; Kellogg, R. M.; van Esch, J., Remarkable polymorphism in gels of new azobenzene bis-urea gelators. *Langmuir* **2002,** *18* (19), 7136-7140.
108. Ayabe, M.; Kishida, T.; Fujita, N.; Sada, K.; Shinkai, S., Binary organogelators which show light and temperature responsiveness. *Org. & Biomol. Chem.* **2003,** *1* (15), 2744-2747.
109. Ahmed, S. A.; Sallenave, X.; Fages, F.; Mieden-Gundert, G.; Muller, W. M.; Muller, U.; Vogtle, F.; Pozzo, J. L., Multiaddressable self-assembling organogelators based on 2H-chromene and N-acyl-1,omega-amino acid units. *Langmuir* **2002,** *18* (19), 7096-7101.

110. (a) de Jong, J. J. D.; Lucas, L. N.; Kellogg, R. M.; van Esch, J. H.; Feringa, B. L., Reversible optical transcription of supramolecular chirality into molecular chirality. *Science* **2004,** *304* (5668), 278-281; (b) Lucas, L. N.; van Esch, J.; Kellogg, R. M.; Feringa, B. L., Photocontrolled self-assembly of molecular switches. *Chem. Commun.* **2001,** (8), 759-760.
111. Frkanec, L.; Jokic, M.; Makarevic, J.; Wolsperger, K.; Zinic, M., Bis(PheOH) maleic acid amide-fumaric acid amide photoizomerization induces microsphere-to-gel fiber morphological transition: The photoinduced gelation system. *J. Am. Chem. Soc.* **2002,** *124* (33), 9716-9717.
112. Qiu, Z. J.; Yu, H. T.; Li, J. B.; Wang, Y.; Zhang, Y., Spiropyran-linked dipeptide forms supramolecular hydrogel with dual responses to light and to ligand-receptor interaction. *Chem. Commun.* **2009,** (23), 3342-3344.
113. Koshima, H.; Matsusaka, W.; Yu, H. T., Preparation and photoreaction of organogels based on benzophenone. *J. Photochem. Photobiol. a-Chem.* **2003,** *156* (1-3), 83-90.
114. (a) Kawata, S.; Kawata, Y., Three-dimensional optical data storage using photochromic materials. *Chem. Reviews* **2000,** *100* (5), 1777-1788; (b) Natansohn, A.; Rochon, P., Photoinduced motions in azo-containing polymers. *Chem. Rev.* **2002,** *102* (11), 4139-4175.
115. Wang, C. H.; Weiss, R. G., Thermal cis -> trans isomerization of covalently attached azobenzene groups in undrawn and drawn polyethylene films. Characterization and comparisons of occupied sites. *Macromol.* **2003,** *36* (11), 3833-3840.
116. Sato, M.; Kinoshita, T.; Takizawa, A.; Tsujita, Y., Photoinduced Conformational Transition of Polypeptides contraining Azobenzenesulfonate in the Side Chains. *Macromol.* **1988,** *21* (6), 1612-1616.
117. (a) Rau, H., *Photochromic Molecules and Systems*. Elsevier: Amsterdam, 1990; (b) Bieringer, T., *Holographic Data Storage- Photoadressable polymer*. Springer-Verlag: Berlín, 2000.
118. Zhao, Y.; Ikeda, T., *Smart Light-Responsive Materials*. Wiley: Hoboken, 2009.
119. Chang, C. W.; Lu, Y. C.; Wang, T. T.; Diau, E. W. G., Photoisomerization dynamics of azobenzene in solution with S-1 excitation: A femtosecond fluorescence anisotropy study. *J. Am. Chem. Soc.* **2004,** *126* (32), 10109-10118.
120. Kumar, G. S.; Neckers, D. C., Photochemistry of Azobenzene-Containing Polymers. *Chem. Rev.* **1989,** *89* (8), 1915-1925.
121. (a) Kempe, C.; Rutloh, M.; Stumpe, J., Photo-orientation of azobenzene side chain polymers parallel or perpendicular to the polarization of red HeNe light. *J. Phys.-Cond. Matt.* **2003,** *15* (11), S813-S823; (b) Zebger, I.; Rutloh, M.; Hoffmann, U.; Stumpe, J.; Siesler, H. W.; Hvilsted, S., Photoorientation of a liquid-crystalline polyester with azobenzene side groups: Effects of irradiation with linearly polarized red light after photochemical pretreatment. *Macromol.* **2003,** *36* (25), 9373-9382.
122. (a) Murata, K.; Aoki, M.; Nishi, T.; Ikeda, A.; Shinkai, S., New Cholesterol-Based Gelators with Light-Responsive and Metal-Responsive Functions. *J. Chem. Soc.-Chem. Commun.* **1991,** (24), 1715-1718; (b) Murata, K.; Aoki, M.; Shinkai, S., Sol-Gel Phase-Transition of Switch-Functionalized Cholesterol as detected by Circular Dichroism. *Chem. Lett.* **1992,** (5), 739-742.
123. (a) Lin, Y. C.; Weiss, R. G., A Novel Gelator of Organic Liquids and their properties of its Gels. *Macromol.* **1987,** *20* (2), 414-417; (b) Lin, Y.; Kachar, B.; Weiss, R. G., Novel Family of Gelators of Organic Fluids and the Structure of their Gels. *J. Am. Chem. Soc.* **1989,** *111* (15), 5542-5551; (c) Furman, I.; Weiss, R. G., Factors Influencing the Formation of Thermally Reversible Gels Comprised of Cholesteryl4-(2-

Anthryloxy)butanoate in Hexadecane, LOctanol, or Their Mixtures. *Langmuir* **1993,** *9* (8), 2084-2088.
124. (a) Ono, Y.; Nakashima, K.; Sano, M.; Kanekiyo, Y.; Inoue, K.; Hojo, J.; Shinkai, S., Organic gels are useful as a template for the preparation of hollow fiber silica. *Chem. Commun.* **1998,** (14), 1477-1478; (b) Jung, J. H.; Ono, Y.; Shinkai, S., Sol-gel polycondensation of tetraethoxysilane in a cholesterol-based organogel system results in chiral spiral silica. *Ang. Chem.-Int. Ed.* **2000,** *39* (10), 1862-1865.
125. Jung, J. H.; Ono, Y.; Shinkai, S., Novel silica structures which are prepared by transcription of various superstructures formed in organogels. *Langmuir* **2000,** *16* (4), 1643-1649.
126. Jung, J. H.; Ono, Y.; Shinkai, S., Organogels of azacrown-appended cholesterol derivatives can be stabilized by host-guest interactions. *Tetrahedron Lett.* **1999,** *40* (48), 8395-8399.
127. Jung, J. H.; Shinkai, S.; Shimizu, T., Nanometer-level sol-gel transcription of cholesterol assemblies into monodisperse inner helical hollows of the silica. *Chem. Mat.* **2003,** *15* (11), 2141-2145.
128. Koumura, N.; Kudo, M.; Tamaoki, N., Photocontrolled gel-to-sol-to-gel phase transitioning of meta-substituted azobenzene bisurethanes through the breaking and reforming of hydrogen bonds. *Langmuir* **2004,** *20* (23), 9897-9900.
129. de Loos, M.; van Esch, J.; Kellogg, R. M.; Feringa, B. L., Chiral recognition in bis-urea-based aggregates and organogels through cooperative interactions. *Ang. Chem.-Int. Ed.* **2001,** *40* (3), 613-616.
130. Moriyama, M.; Mizoshita, N.; Yokota, T.; Kishimoto, K.; Kato, T., Photoresponsive anisotropic soft solids: Liquid-crystalline physical gels based on a chiral photochromic gelator. *Adv. Mat.* **2003,** *15* (16), 1335-1338.
131. Moriyama, M.; Mizoshita, N.; Kato, T., Reversible on-off photo-switching of hydrogen bonding for self-assembled fibers comprising physical gels. *Bull. Chem. Soc. Jap.* **2006,** *79* (6), 962-964.
132. Zhou, Y. F.; Yi, T.; Li, T. C.; Zhou, Z. G.; Li, F. Y.; Huang, W.; Huang, C. H., Morphology and Wettability tunable two-dimensional superstructure assembled by hydrogen bonds and hydrophobic interactions. *Chem. Mat.* **2006,** *18* (13), 2974-2981.
133. Lee, S. J.; Lee, S. S.; Kim, J. S.; Lee, J. Y.; Jung, J. H., Mirror image nanostructures of new chromogenic azobenzene gels by introduction of alanine moiety. *Chem. Mat.* **2005,** *17* (26), 6517-6520.
134. Inoue, D.; Suzuki, M.; Shirai, H.; Hanabusa, K., Novel low-molecular-weight gelators based on azobenzene containing L-amino acids. *Bull. Chem. Soc. Jap.* **2005,** *78* (4), 721-726.
135. Li, L. S.; Jiang, H. Z.; Messmore, B. W.; Bull, S. R.; Stupp, S. I., A torsional strain mechanism to tune pitch in supramolecular helices. *Ang. Chem.-Int. Ed.* **2007,** *46* (31), 5873-5876.
136. Uchida, K.; Yamaguchi, S.; Yamada, H.; Akazawa, M.; Katayama, T.; Ishibashi, Y.; Miyasaka, H., Photoisomerization of an azobenzene gel by pulsed laser irradiation. *Chem. Commun.* **2009,** (29), 4420-4422.
137. Ran, X.; Wang, H. T.; Zhang, P.; Bai, B. L.; Zhao, C. X.; Yu, Z. X.; Li, M., Photo-induced fiber-vesicle morphological change in an organogel based on an azophenyl hydrazide derivative. *Soft Matt.* **2011,** *7* (18), 8561-8566.
138. Duan, P. F.; Li, Y. G.; Li, L. C.; Deng, J. G.; Liu, M. H., Multiresponsive Chiroptical Switch of an Azobenzene-Containing Lipid: Solvent, Temperature, and Photoregulated Supramolecular Chirality. *J. Phys. Chem. B* **2011,** *115* (13), 3322-3329.

139. Mamiya, J.; Kanie, K.; Hiyama, T.; Ikeda, T.; Kato, T., A rodlike organogelator: fibrous aggregation of azobenzene derivatives with a syn-chiral carbonate moiety. *Chem. Commun.* **2002,** (17), 1870-1871.
140. Yagai, S.; Iwashima, T.; Kishikawa, K.; Nakahara, S.; Karatsu, T.; Kitamura, A., Photoresponsive self-assembly and self-organization of hydrogen-bonded supramolecular tapes. *Chem.-a Eur. J.***2006,** *12* (15), 3984-3994.
141. (a) Bieser, A. M.; Tiller, J. C., Surface-induced hydrogelation. *Chem. Commun.* **2005,** (31), 3942-3944; (b) Bieser, A. M.; Tiller, J. C., Structure and properties of an exceptional low molecular weight hydrogelator. *J. Phys. Chem. B* **2007,** *111* (46), 13180-13187.
142. Matsuzawa, Y.; Tamaoki, N., Photoisomerization of Azobenzene Units Controls the Reversible Dispersion and Reorganization of Fibrous Self-Assembled Systems. *J. Phys. Chem. B* **2010,** *114* (4), 1586-1590.
143. Li, X. M.; Gao, Y.; Kuang, Y.; Xu, B., Enzymatic formation of a photoresponsive supramolecular hydrogel. *Chem.Commun.* **2010,** *46* (29), 5364-5366.
144. Huang, Y. C.; Qiu, Z. J.; Xu, Y. M.; Shi, J. F.; Lin, H. K.; Zhang, Y., Supramolecular hydrogels based on short peptides linked with conformational switch. *Org. & Biomol. Chem.* **2011,** *9* (7), 2149-2155.
145. Yagai, S.; Karatsu, T.; Kitamura, A., Melamine-barbiturate/cyanurate binary organogels possessing rigid azobenzene-tether moiety. *Langmuir* **2005,** *21* (24), 11048-11052.
146. (a) Yagai, S.; Higashi, M.; Karatsu, T.; Kitamura, A., Binary supramolecular gels based on bismelamine-cyanurate/barbiturate noncovalent polymers. *Chem. Mat.* **2004,** *16* (19), 3582-3585; (b) Yagai, S.; Higashi, M.; Karatsu, T.; Kitamura, A., Dye-assisted structural modulation of hydrogen-bonded binary supramolecular polymers. *Chem. Mat.s* **2005,** *17* (17), 4392-4398.
147. Yagai, S.; Nakajima, T.; Kishikawa, K.; Kohmoto, S.; Karatsu, T.; Kitamura, A., Hierarchical organization of photoresponsive hydrogen-bonded rosettes. *J. Am. Chem. Soc.* **2005,** *127* (31), 11134-11139.
148. Zhou, Y. F.; Xu, M.; Yi, T.; Xiao, S. Z.; Zhou, Z. G.; Li, F. Y.; Huang, C. H., Morphology-tunable and photoresponsive properties in a self-assembled two-component gel system. *Langmuir* **2007,** *23* (1), 202-208.
149. Park, J. S.; Jeong, S.; Ahn, B.; Kim, M.; Oh, W.; Kim, J., Selective response of cyclodextrin-dye hydrogel to metal ions. *J. Incl. Phen. Macrocyclic Chem.* **2011,** *71* (1-2), 79-86.
150. Liao, X. J.; Chen, G. S.; Liu, X. X.; Chen, W. X.; Chen, F.; Jiang, M., Photoresponsive Pseudopolyrotaxane Hydrogels Based on Competition of Host-Guest Interactions. *Ang. Chem.-Int. Ed.* **2010,** *49* (26), 4409-4413.
151. Cao, H.; Jiang, J.; Zhu, X. F.; Duan, P. F.; Liu, M. H., Hierarchical co-assembly of chiral lipid nanotubes with an azobenzene derivative: optical and chiroptical switching. *Soft Matt.* **2011,** *7* (10), 4654-4660.
152. Narayan, G.; Kumar, N. S. S.; Paul, S.; Srinivas, O.; Jayaraman, N.; Das, S., Aggregation and photores ponsive behavior of azobenzene-oligomethylene-glucopyranoside bolaamphiphiles. *J. Photochem. Photobiol. a-Chem.* **2007,** *189* (2-3), 405-413.
153. Amaike, M.; Kobayashi, H.; Shinkai, S., Molecular design of low molecular-weight aqueous gels bearing an azo-hydrazone tautomeric group useful as a solvent polarity probe. *Chem. Lett.* **2001,** (7), 620-621.
154. (a) Kobayashi, H.; Friggeri, A.; Koumoto, K.; Amaike, M.; Shinkai, S.; Reinhoudt, D. N., Molecular design of "super" hydrogelators: Understanding the

gelation process of azobenzene-based sugar derivatives in water. *Org. Lett.* **2002,** *4* (9), 1423-1426; (b) Kobayashi, H.; Koumoto, K.; Jung, J. H.; Shinkai, S., Sol-gel phase transition induced by fiber-vesicle structural changes in sugar-based bolaamphiphiles. *J. Chem. Soc.-Perkin Trans. 2* **2002,** (11), 1930-1936.
155. Shinkai, S.; Takeuchi, M., Molecular design of synthetic receptors with dynamic, imprinting, and allosteric functions. *Biosensors & Bioelectronics* **2004,** *20* (6), 1250-1259.
156. Srivastava, A.; Ghorai, S.; Bhattacharjya, A.; Bhattacharya, S., A tetrameric sugar-based azobenzene that gels water at various pH values and in the presence of salts. *J. Org. Chem.* **2005,** *70* (17), 6574-6582.
157. Rajaganesh, R.; Gopal, A.; Das, T. M.; Ajayaghosh, A., Synthesis and Properties of Amphiphilic Photoresponsive Gelators for Aromatic Solvents. *Org. Lett.* **2012,** *14* (3), 748-751.
158. Lin, Y. Y.; Wang, A. D.; Qiao, Y.; Gao, C.; Drechsler, M.; Ye, J. P.; Yan, Y.; Huang, J. B., Rationally designed helical nanofibers via multiple non-covalent interactions: fabrication and modulation. *Soft Matt.* **2010,** *6* (9), 2031-2036.
159. Ogawa, Y.; Yoshiyama, C.; Kitaoka, T., Helical Assembly of Azobenzene-Conjugated Carbohydrate Hydrogelators with Specific Affinity for Lectins. *Langmuir* **2012,** *28* (9), 4404-4412.
160. Collings P. J., H. M., Introduction to Liquid Crystalas. Chemistry and Physics. Francis, T., Ed. London, 1997.
161. Demus D., G. J. W., Gray G. W., Spiess H. W., Vill V., *Handbook of Liquid Crystals*. Weinheim, 1998.
162. Kishikawa, K.; Nakahara, S.; Nishikawa, Y.; Kohmoto, S.; Yamamoto, M., A ferroelectrically switchable columnar liquid crystal phase with achiral molecules: Superstructures and properties of liquid crystalline ureas. *J. Am. Chem. Soc.* **2005,** *127* (8), 2565-2571.
163. Zimmermann, H.; Bader, V.; Poupko, R.; Wachtel, E. J.; Luz, Z., Mesomorphism, isomerization, and dynamics in a new series of pyramidic liquid crystals. *J. Am. Chem. Soc.* **2002,** *124* (51), 15286-15301.
164. (a) Reddy, R. A.; Tschierske, C., Bent-core liquid crystals: polar order, superstructural chirality and spontaneous desymmetrisation in soft matter systems. *J. Mat. Chem.* **2006,** *16* (10), 907-961; (b) Ros, M. B.; Serrano, J. L.; de la Fuente, M. R.; Folcia, C. L., Banana-shaped liquid crystals: a new field to explore. *J. Mat. Chem.* **2005,** *15* (48), 5093-5098.
165. Burducea, G., *Romanian Reports in Physics*. 2004; Vol. I, p 66-86.
166. (a) Dorset, D. L.; Rosenbusch, J. P., Solid-State Properties Of Anomeric "1-O-Normal-Octyl-D-Glucopyranosides". *Chem. Phys. Lip.* **1981,** *29* (4), 299-307; (b) Carter, D. C.; Ruble, J. R.; Jeffrey, G. A., The Crystal-Structure of Heptyl 1-Thio-Alpha-D-Mannopyrano-side, a Liquid-Crystal Precursor. *Carb. Res.* **1982,** *102*, 59-67; (c) Jeffrey, G. A.; Bhattacharjee, S., Carbohydrate Liquid-Crystals .2. *Carb. Res.* **1983,** *115*, 53-58; (d) Goodby, J. W., Liquid-Crystal Phases Exhibited By Some Monossacharides. *Mol. Cryst. Liq. Cryst.* **1984,** *110* (1-4), 205-219; (e) Vill, V.; Bocker, T.; Thiem, J.; Fischer, F., Studies on Liquid-Crystalline Glycosides. *Liq. Cryst.* **1989,** *6* (3), 349-356; (f) Miethchen, R.; Holz, J.; Prade, H.; Liptak, A., Amphiphilic And Mesogenic Carbohydrates.2. Synthesis And Characterization Of Mono-O-(Normal-Alkyl)-D-Glucose Derivatives. *Tetrahedron* **1992,** *48* (15), 3061-3068.
167. (a) Vandoren, H. A.; Vandergeest, R.; Deruijter, C. F.; Kellogg, R. M.; Wynberg, H., The Scope and Limitations of Liquid-Crystalline Behavior in Monosaccharide Amphiphiles-Comparison of the Thermal-Behavior of Several

Homologous Series of D-Glucose Derived Compounds with an Amino-Linked Alkyl Chain. *Liq. Cryst.* **1990,** *8* (1), 109-121; (b) Vandoren, H. A.; Wingert, L. M., The Relationship Between The Molecular-Structure of Polyhydroxy Amphiphiles and Their Aggregation Behavior in Water .1. The Conctact Preparation Method as a Tool For Empirical-Studies. *Recueil Des Travaux Chimiques Des Pays-Bas-Journal of the Royal Netherlands Chemical Society* **1994,** *113* (4), 260-265; (c) Auvray, X.; Petipas, C.; Anthore, R.; Ricolattes, I.; Lattes, A., RX-Diffraction Study of The Ordered Lyotropic Phases Formed by Sugar-Based Surfactants. *Langmuir* **1995,** *11* (2), 433-439; (d) Goodby, J. W.; Haley, J. A.; Mackenzie, G.; Watson, M. J.; Plusquellec, D.; Ferrieres, V., Amphitropic liquid-crystalline properties of some novel alkyl furanosides. *J. Mat. Chem.* **1995,** *5* (12), 2209-2220; (e) Smits, E.; Engberts, J.; Kellogg, R. M.; VanDoren, H. A., Thermotropic and lyotropic liquid crystalline behaviour of 4-alkoxyphenyl beta-D-glucopyranosides. *Liq. Cryst.* **1997,** *23* (4), 481-488; (f) Ho, M. S.; Hsu, C. S., Synthesis and self-assembled nanostructures of novel chiral amphiphilic liquid crystals containing -beta-galactopyranoside end-groups. *Liq. Cryst.* **2010,** *37* (3), 293-301.

168. (a) Ma, Y. D.; Takada, A.; Sugiura, M.; Fukuda, T.; Miyamoto, T.; Watanabe, J., Thermotropic Liquid-Crystals Based On Oligosaccharides- N-Akyl-1-O-Beta-D-Cellobiosides. *Bull. Chem. Soc. Jap.* **1994,** *67* (2), 346-351; (b) von Minden, H. M.; Brandenburg, K.; Seydel, U.; Koch, M. H. J.; Garamus, V.; Willumeit, R.; Vill, V., Thermotropic and lyotropic properties of long chain alkyl glycopyranosides. Part II. Disaccharide headgroups. *Chem. Phys. Lip.* **2000,** *106* (2), 157-179.

169. Fischer, S.; Fischer, H.; Diele, S.; Pelzl, G.; Jankowski, K.; Schmidt, R. R.; Vill, V., On The Structure Of The Thermotropic Cubic Mesophases. *Liq. Cryst.* **1994,** *17* (6), 855-861.

170. Queneau, Y.; Gagnaire, J.; West, J. J.; Mackenzie, G.; Goodby, J. W., The effect of molecular shape on the liquid crystal properties of the mono-O-(2-hydroxydodecyl)sucroses. *J. Mat. Chem.* **2001,** *11* (11), 2839-2844.

171. Molinier, V.; Kouwer, P. H. J.; Fitremann, J.; Bouchu, A.; Mackenzie, G.; Queneau, Y.; Goodby, J. W., Self-organizing properties of monosubstituted sucrose fatty acid esters: The effects of chain length and unsaturation. *Chem.-a Eur. J.* **2006,** *12* (13), 3547-3557.

172. Gerber, S.; Wulf, M.; Milkereit, G.; Vill, V.; Howe, J.; Roessle, M.; Garidel, P.; Gutsmann, T.; Brandenburg, K., Phase diagrams of monoacylated amide-linked disaccharide glycolipids. *Chem. Phys. Lip.* **2009,** *158* (2), 118-130.

173. Laurent, N.; Lafont, D.; Dumoulin, F.; Boullanger, P.; Mackenzie, G.; Kouwer, P. H. J.; Goodby, J. W., Synthesis of amphiphilic phenylazophenyl glycosides and a study of their liquid crystal properties. *J. Am. Chem. Soc.* **2003,** *125* (50), 15499-15506.

174. Abraham, S.; Paul, S.; Narayan, G.; Prasad, S. K.; Rao, D. S. S.; Jayaraman, N.; Das, S., Observation of a chiral smectic phase in azobenzene-linked bolaamphiphiles containing free sugars. *Adv. Funct. Mater.* **2005,** *15* (10), 1579-1584.

2. OBJETIVOS Y PLANTEAMIENTO

2.1. Objetivo

El trabajo desarrollado en esta tesis se centra en el campo de los materiales blandos, y en concreto dentro de los geles supramoleculares. El objetivo general de esta tesis consiste en obtener nuevos materiales sensibles a la temperatura y a la luz a partir de moléculas gelificantes anfífilas, principalmente basadas en disacáridos como bloque hidrófilo. Se estudiará la influencia en la capacidad de gelificación de la estructura del gelificante y la organización y propiedades tanto de las moléculas como de los geles.

La estructura elegida para el diseño de estas moléculas gelificantes ha sido la siguiente:

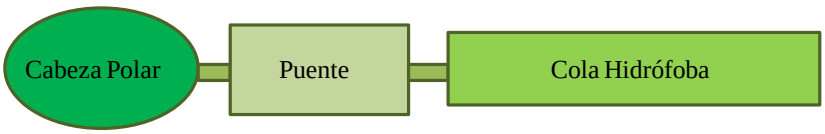

En la cabeza polar se va a trabajar con azúcares ya que es conocida su capacidad para autoensamblarse y por tanto son potencialmente buenos bloques para formar geles. La mayor parte de los trabajos previos se han focalizado en los monosacáridos, en concreto en la glucosa, a partir de cuyos derivados se obtienen hidrogeles en los que normalmente es necesario la utilización en pequeñas proporciones de un alcohol que ayude en la gelificación. Nuestro trabajo se basa principalmente en disacáridos. Por un lado, supone la introducción de un mayor número de grupos para formar enlaces de hidrógeno y esto podría dar lugar a la formación de estructuras más sólidas. Por otro lado, se aumenta la parte hidrófila para poder posteriormente introducir grupos hidrófobos y así mantener la proporción hidrofilia/hidrofobia adecuada. También se explora, de forma comparativa, el uso de derivados de polietilenglicol por tratarse de una molécula polar ampliamente usada en el campo de los materiales.

En cuanto a la parte apolar se ha utilizado un ácido graso para preparar glicolípidos y se ha querido explorar la posibilidad de introducir un grupo cromóforo para poder inducir el paso mediante luz entre dos isómeros de una forma reversible, lo que puede derivar en cambios de la estructura supramolecular y modificar la organización de las fibras formadas. Los ejemplos encontrados con moléculas anfífilas azucaradas fotosensibles son reducidos hasta la fecha.

Con estas modificaciones estructurales se ha querido estudiar la influencia de la relación hidrofilia-hidrofobia en la formación de agregados supramoleculares e investigar la posibilidad de gelificación.

Para cumplir los objetivos generales, los objetivos específicos han sido los siguientes:

A. Sintetizar y caracterizar moléculas anfífilas:

- Obtener moléculas anfifílas capaces de gelificar en agua basadas en un disacárido y un ácido graso:
    1. Estudiar la influencia de la variación en la conexión entre la parte polar y apolar: enlace amida o triazol.
    2. Estudiar la influencia de la variación en la cabeza polar: introducción de distintos disacáridos.
    3. Estudiar la influencia de la variación en la cadena apolar: adición de un aminoácido en la estructura.
- Obtener moléculas anfifílas sensibles a la luz capaces de gelificar basadas en un disacárido, un ácido graso y azobenceno y estudiar la influencia de las distintas posiciones del gupo cromóforo dentro de la cola apolar.
- Sintetizar distintas estructuras anfifílas, derivadas de un ácido graso y un azobenceno y determinar los cambios al introducir en la parte polar polietilenglicol o un disacárido, manteniendo fija la estructura de la cola apolar.
- Caracterizar los materiales y en particular las propiedades térmicas y cristal líquido de las moléculas anfifílas.

B. Estudiar las propiedades y la organización de los geles derivados:
    1. Estudiar la capacidad de gelificación en diversos disolventes, concentraciones mínimas de gelificación y temperaturas de gelificación.
    2. Estudiar la organización del gel mediante diversas técnicas: SEM, ESEM, TEM, cryoTEM y DC.

C. Estudiar la respuesta ante la irradiación de los geles potencialmente sensibles:
    1. Irradiar geles de un solo componente
    2. Irradiar geles formados por una mezcla binaria.

2.2. Planteamiento y nomenclatura

Este trabajo tiene como punto de partida los estudios realizados por Fitremann y sus colaboradores en los que demostraron que una mezcla de isómeros derivados de sucroésteres de *N*-palmitoilfenilalanina tenía características gelificantes, véase la **Fig. 2.1**. Este compuesto, en contacto con el agua, a una concentración mínima de un 2%, forma un gel que, debido a sus propiedades mecánicas, puede denominarse como tipo "clara de huevo" donde el módulo elástico es siempre mayor que el módulo viscoso y los valores absolutos de los mismos son bajos, y que además presenta tixotropía.

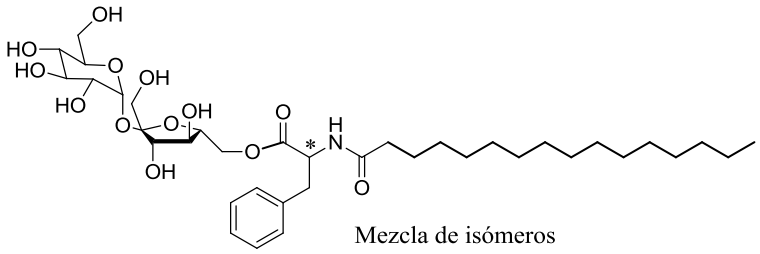

Fig. 2.1: Mezcla de isómeros de surcroésteres de N-palmitoilfenilalanina

Tomando como referencia esta estructura, el trabajo se dirige hacia la búsqueda de nuevos sistemas gelificantes. En un primer capítulo, se explica la utilización de diferentes rutas sintéticas para obtener moléculas gelificantes y se estudia la influencia de la estructura para la obtención de **hidrogeles**. Posteriormente se introduce un grupo fotoisomerizable, el azobenceno, para obtener **geles fotosensibles** y en la última parte del trabajo se han sintetizado y estudiado diferentes **organogeles**, manteniendo la presencia del grupo azoico.

2.2.1. *Geles Supramoleculares basados en glicolípidos derivados de disacáridos y ácido palmítico*

a) En un primer momento se realiza la síntesis de los sucroésteres de N-palmitoilfenilalanina, **Suc-OOC-Phe-C_{16}** y se estudia el material formado bajo distintas técnicas y condiciones.

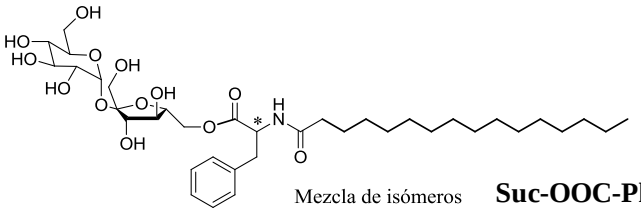

Mezcla de isómeros **Suc-OOC-Phe-C_{16}**

b) Posteriormente se selecciona la maltosa como el disacárido que constituiría la cabeza polar. Se sintetiza el análogo al compuesto anterior con fenilalanina y palmítico, uniendo la cabeza polar y la cola hidrófoba mediante un enlace amida, **Malt-NH-Phe-C_{16}** o mediante un anillo de triazol, **Malt-Tz-Phe-C_{16}** y sus análogos sin la presencia de fenilalanina, **Malt-NH-C_{16}** y **Malt-Tz-C_{16}**.

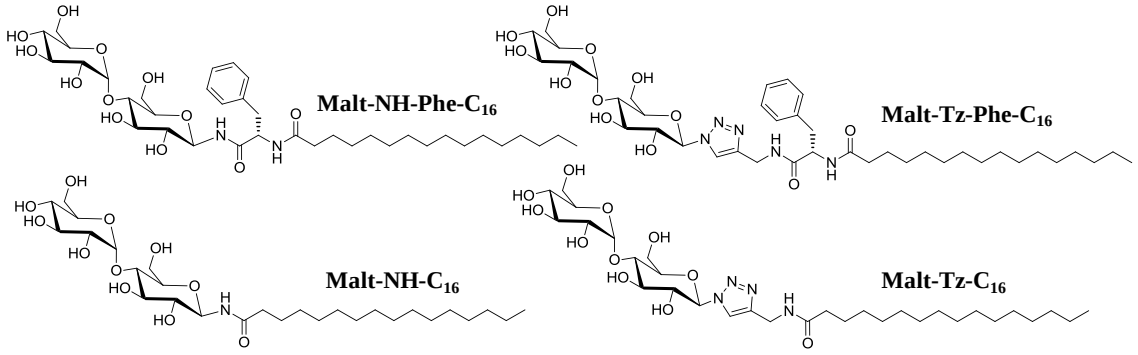

Malt-NH-Phe-C_{16}

Malt-Tz-Phe-C_{16}

Malt-NH-C_{16}

Malt-Tz-C_{16}

c) A continuación, se cambia la maltosa por otros disacáridos tomando como referencia la estructura **Malt-Tz-C_{16}** (que forma hidrogeles) y así observar posibles diferencias debidas a la cabeza polar.

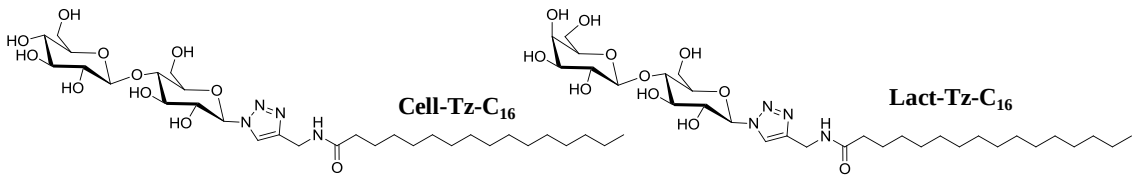

Cell-Tz-C_{16}

Lact-Tz-C_{16}

2.2.2. *Geles Supramoleculares derivados de glicolipidos con azobenceno*

a) Se utiliza la estrategia sintética de la cicloadición [3+2] azida-alquino catalizada con cobre, para obtener compuestos derivados de azobenceno, dispuesto en diferentes posiciones de la molécula gelificante.

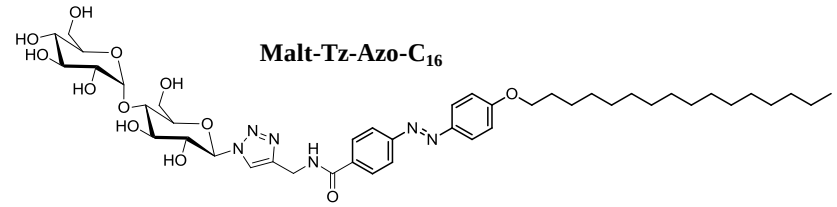

Malt-Tz-Azo-C_{16}

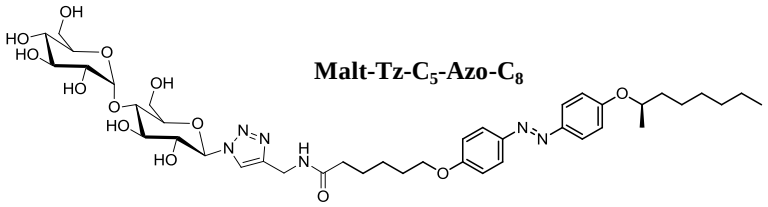

Malt-Tz-C_5-Azo-C_8

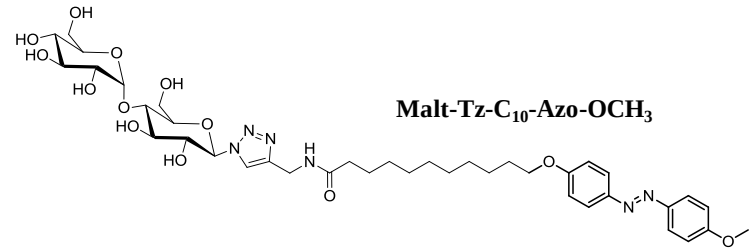

Malt-Tz-C_{10}-Azo-OCH_3

b) Estudio de mezclas binarias de un derivado de azobenceno con **Malt-Tz-C_{16}**:

Gel I: **Malt-Tz-C_{16}** + **Malt-Tz-C_5-Azo-C_8**

Gel II: **Malt-Tz-C_{16}** + **Malt-Tz-Azo-C_{16}**

2.2.3. *Moléculas anfifílilas con derivados de azobenceno y polietilenglicol*

a) Preparación de un derivado de azobenceno anfífilo

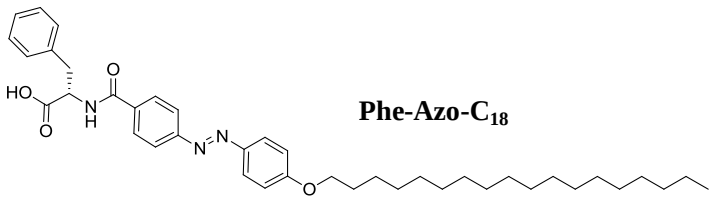

Phe-Azo-C_{18}

b) Introducción de una cabeza polar derivada de polietilenglicol para obtener modificaciones en la capacidad de gelificación. Síntesis de los compuestos **PEG_8-Phe-Azo-C_{18}** y **PEG_{16}-Phe-Azo-C_{18}**.

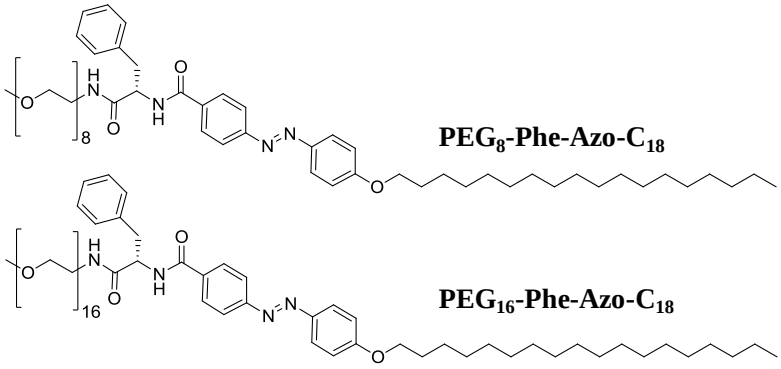

c) Síntesis de un análogo con cabeza polar derivada de maltosa, **Malt-Phe-Azo-C_{18},** para comparar con los derivados de polietilenglicol**.**

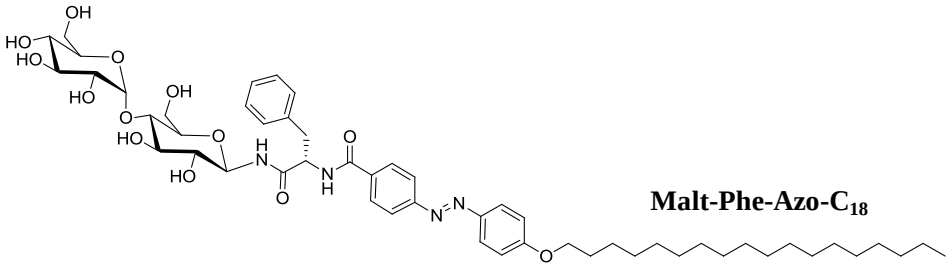

Los geles derivados de las moléculas sintetizadas se denominan como el compuesto del que proceden, indicando el porcentaje en peso y el disolvente en el que gelifican.

Este trabajo se ha realizado en colaboración con la Universidad Paul Sabatier de Toulouse, Francia, donde he realizado una estancia durante 18 meses. Cumpliendo con los requisitos para la obtención de un doctorado con mención europea, los capítulos que se presentan a continuación (que describen los principales resultados, discusión y conclusiones) han sido redactados en inglés.

3. SUPRAMOLECULAR GELS BASED ON GLYCOLIPIDS DERIVED FROM DISACCHARIDES AND PALMITIC ACID

3.1. Introduction

Amphiphilic molecules with a sugar polar head and a fatty hydrophobic chain can act as low molecular mass supramolecular hydrogelators. As it has been mentioned in previous chapters, in supramolecular gels, gelators form a cross-linked network by self-aggregation, which occurs through a combination of non-covalent interactions like H-bonding, π-π stacking, donor-acceptor interactions, solvophobic forces and van der Waals interactions. This self-assembly allows this kind of materials to be considered as supramolecular polymers.[1] In contrast to macromolecular gels, supramolecular gels can be cycled between free-flowing liquids and non-flowing materials by means of different stimuli, usually temperature. Depending on the gelator structure the reversibility can be triggered by other stimuli such as pH or irradiation.[2]

Carbohydrates are hydrophilic building blocks used in the preparation of hydrogelators[3] able to form multiple H-bonding due to their hydroxyl groups. First examples of glycolipids as hydrogelators were described on non-cyclic glycosyl derivatives.[4] Conventional single-head amphiphiles[5] and bolaamphiphiles[6] mainly based on monosaccharides, were subsequently described. They usually have the ability to gel in a mixture of water and alcohol or, in some cases, in only water. Cyclic forms of carbohydrates have multiple and directional hydroxyl groups and therefore they can give rise to a stronger cooperative network to support the self-assembled fibrous structure of the gel.

Stability and gel properties are strongly dependent on the molecular structure of the gelator. Different polar sugar heads, mainly mono[7] but also disaccharides[8] units have been used as hydrophilic part of gelators. The linker unit between hydrophilic and hydrophobic parts is also important. In this way, it has been reported that the presence of amide groups or the incorporation of π-π stacked rings also contributed to the cooperative interactions of glycoamphiphiles.[5b, 6b, 9] The gelation process is a consequence of a network resulting from the association of aggregates, which are formed by the *bottom-up* assembly of glycolipids. Amphiphilic hydrogels based on carbohydrates have been reported, for instance, as drug delivery systems or sensors[10] and for cell encapsulation.[11]

Apart from their ability to self-assemble in solvents, glycoamphiphiles can exhibit microsegregated regions due to the polar asymmetry of their structure and can consequently exhibit liquid crystal (LC) phases.[12] Thermotropic LC phases were first observed in alkyl glucopyranosides and these compounds are known to form smectic phases, similar to the lamellar phase formed in aqueous media.[13] Other mesophases such as cubic or columnar phases have been found later.[14] Most of the mesogenic glycolipids are based on monosaccharides.[13, 15] However only a few and examples having disaccharide head groups have been described so far.[14, 16]

In a previous study by Fitremann *et al.*, a mixture of isomers of ***N***-palmitoylphenylalanine sucroesters,[8b] obtained by direct esterification of sucrose, was reported to form an 'egg-white'-like gel. The chemical structure of these glycoamphiphiles (**Suc-OOC-Phe-C_{16}**) was taken as reference in this work, see **Scheme 3.1**.

The initial and direct synthesis of glycolipids, designed to fit the requirements of a possible industrial development, was also attempted in this work and lead to a mixture of isomers due to esterification in different positions. The gelification of this material could be less effective compared to a well-defined hydrogelator. For this reason, new synthetic strategies were explored to prepare well-defined hydrogelators having disaccharides as polar head and a hydrophobic alkyl chain derived from palmitoyl acid. Changes on the hydrophobic chain structure and the linker between the hydrophilic and hydrophobic part were performed as well as different disaccharides were used as sugar polar head. Finally, their gelation properties either in water or in mixtures of alcohol and water were tested in order to better know how the structure affects to gel properties.

The liquid crystalline properties of the amphiphilic materials have been characterized by polarizing optical microscopy (POM), thermogravimetric analysis (TGA) and differential scanning calorimetry (DSC). The supramolecular structures formed by the self-assembly have been studied by different microscopic techniques as scanning electron microscope (SEM), transmission electron microscopy (TEM), cryogenic transmission electron microscopy (cryo-TEM), environmental scanning electron microscope (ESEM) and atomic force microscopy (AFM). Micro and nano structures were measured on the dried gel (xerogel) as well as in hydrated conditions, close to real gel. The sol-gel transition temperature was also determined by differential scanning

calorimetry (DSC) and nuclear magnetic resonance (NMR). Chiral supramolecular arrangement was studied by circular dichroism (CD). The following sections have been divided according to the different type of glycolipids synthesized and studied in this part of the work.

3.2. Glycolipid derived from sucrose and palmitoyl acid

As mentioned above, a mixture of *N*-palmitoylphenylalanine sucrose esters is known to behave as hydrogelator. In order to investigate the organization and mechanical behavior of hydrogels derived from this type of materials, sucrose was directly esterified to obtain the aimed gelators.

3.2.1. *Synthesis*

Taking as reference the method described by Fitremann et *al.,* *N*-palmitoylphenylalanine sucrose esters (obtained from a racemate of D,L-phenyalanine) were synthesized by functionalization of unprotected sucrose as a direct method to obtain hydrogelators. Esterification was performed with *N*-palmitoylphenylalanine in the presence of *N, N´*-dicyclohexylcarbodiimide (DCC) and 4-(dimethylamino)pyridine (DMAP) in dimethylformamide (DMF), see **Scheme 3.1**. *N*-Palmitoylphenylalanine was first synthesized by a one pot reaction; the carboxylic group was activated by *N*-hydroxysuccinimide by means of a DCC coupling and then phenylalanine was added in a mixture of THF and water to have good solubility of both reagents. Yield was around 22% from easily available starting materials.

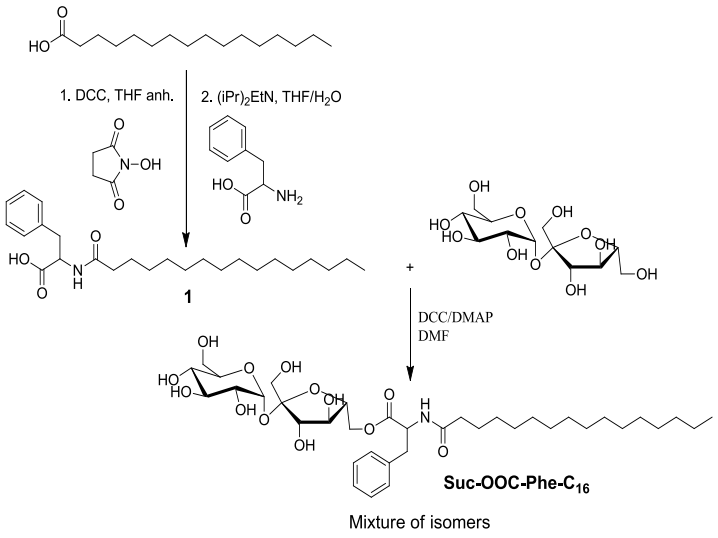

Scheme 3.1: Synthesis of a mixture of isomers of *N*-Palmitoylphenylalanine sucrose esters.

The reaction was monitored by HPLC with a column C8 and THF/MeOH/H_2O: 40/40/20 + 0.5 ml/L AcOH as eluent. When peak area at around 5 min (mixture of monoesters) did not increase anymore, reaction was considered completed. The reaction was stirred during 46 h. Finally, a complex mixture of different substitution degrees was obtained. Monoester fraction was purified by flash chromatography. The solid is highly hygroscopic and purification was performed with a mixture of solvents. In this fraction a mixture of regioisomers was obtained as white solid which was freeze-dried. Compounds were characterized by ^{1}H and ^{13}C NMR, IR and mass spectrometry to confirm the desired structure. In a previous work carried out in the Polymères et organization multi-échelle (POME) group at the Paul Sabatier University,[17] regioisomers of this mixture were separated and analyzed. Based on their results, when D,L phenylalanine was used as starting material, 3L/3D and 3´L/3´D were the main regioisomers; also 6L/6D, 1´L/1´D and 6´L/6´D could be identified.

3.2.2. *Thermal properties*

The liquid crystal (LC) properties of the sucroesters have been studied. As mentioned before there are a few reports about glycoamphiphiles based on a disaccharide as polar head. Molinier *et al.* described the self-organizing properties of monosubstituted sucrose fatty acid esters.[14b] They proved that lamellar phases predominated for higher fatty chains homologues, as for example palmitic derivatives, describing their thermotropic liquid crystals properties, see **Fig. 3.1.**

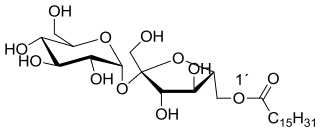

Mono-1´-substituted:
Cr 53.8 SmA* 209.5 I

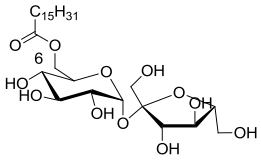

Mono-6-substituted:
Cr 72.4 SmA* 212 I

Figure 3.1: Transition temperatures of thermotropic mono-1´and mono-6 palmitic sucrose esters.

Besides glycolipids usually present lyotropic liquid crystal properties, since they have the ability to self-assemble in water.

Thermal and Thermotropic liquid crystal properties. The thermal degradation of the mixture of *N*-palmitoylphenylalanine sucrose esters (**Suc-OOC-Phe-C_{16}**) was first studied by TGA. Thermogravimetric curve for **Suc-OOC-Phe-C_{16}** displays a 5 % weight loss at 185ºC and onset temperature for decomposition associated to weight loss was detected at around 190ºC. The sample was first stored under vacuum and immediately analyzed. Observations by optical microscopy pointed to a texture change around 60ºC and isotropic state was observed from around 130 ºC to 160ºC. Decomposition was observed when some parts of the sample became brown around this point, most probably due to decomposition of the sugar unit. The texture of the mesophase observed by optical microscopy, see **Fig. 3.2**, can be assigned as smectic, on the basis of previous results on thermotropic glycolipids with similar structure.

A DSC study of the sample was performed by heating the compound two cycles to 120 ºC, see **Fig. 3.3**, in order to minimize the thermal decomposition of the samples and a third cycle to 170ºC to investigate decomposition process. First and second cycles were reproducible and only exhibit a jump of the baseline at 34ºC corresponding to a glass transition. However, in the third cycle on heating to 170ºC, the decomposition of the material was detected around 130ºC as an endothermic peak and subsequent decrease of the baseline.

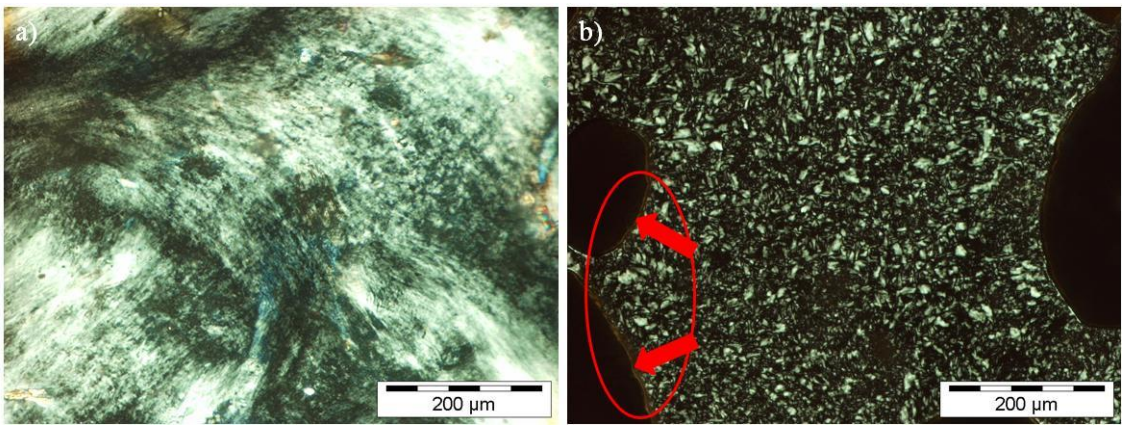

Fig. 3.2: Images of **Suc-OOC-Phe-C_{16}** by polarized optical microscope: a) Smectic mesophase at heating cycle, 80ºC in the heating process; b) mesophase at 85ºC in the cooling cycle of a sample previously heated up to 160ºC, partial brown decomposition was observed (brown region, see red arrows).

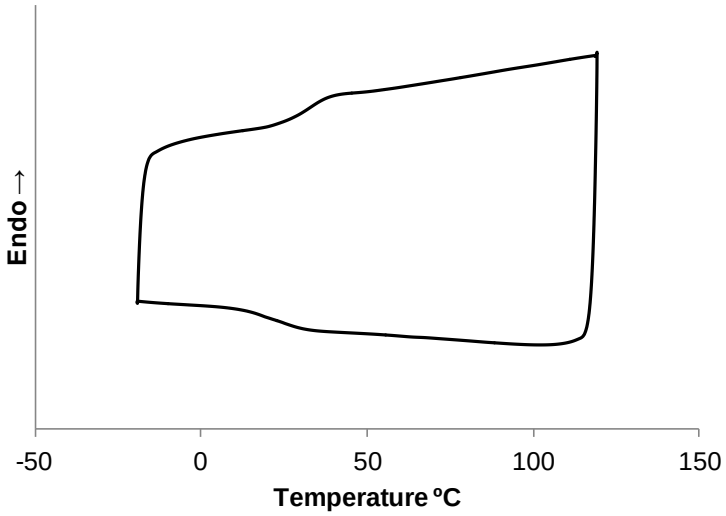

Fig. 3.3: Second cycle scan DSC profile in the solid state of **Suc-OOC-Phe-C_{16}**.

According to these results the mixture of isomers **Suc-OOC-Phe-C_{16}** is glassy at room temperature (RT) and presents a T_g at 34ºC into a smectic mesophase.

Lyotropic liquid crystal properties. The lyotropic properties of **Suc-OOC-Phe-C_{16}** were investigated by the contact method. The sample was heated to 120 ºC (mesophase) to avoid decomposition and then cooled to RT. A small amount of water was then placed on the slide at the edge of the cover glass and this completely surrounded the sample. Phases were observed by polarizing optical microscopy. A concentration effect was observed, as can be seen in **Fig. 3.4**. A birefringent lamellar texture appeared at RT (see **Fig. 3.4.a**) on a gradient of water from pure liquid to solid glass state from right to left. Heating the sample at 50ºC a dark zone appeared, one possibility to explain this non birefrigent part could be the occurrence of a cubic phase, which remains to be checked by other means (see **Fig. 3.4.c**).

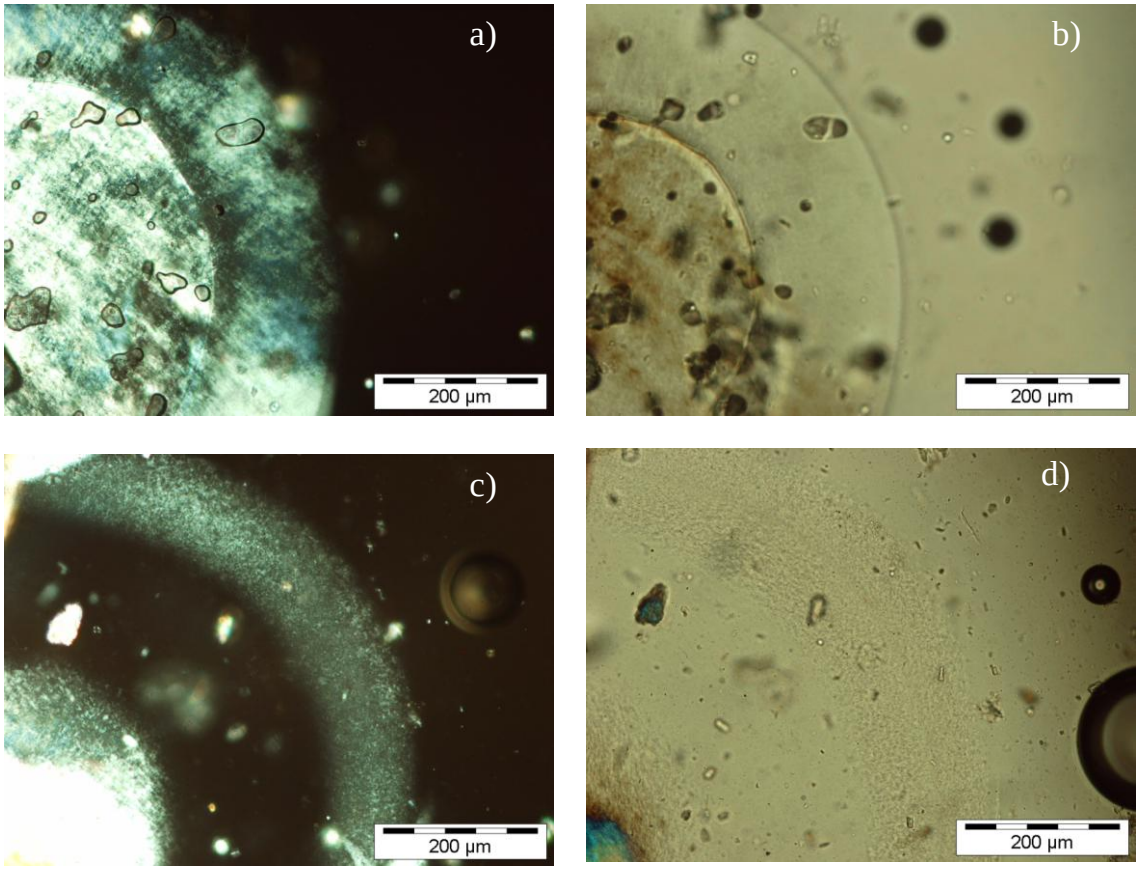

Fig. 3.4: Lyotropic phase observed by optical microscopy on a sample of **Suc-OOC-Phe-C_{16}** in water prepared by the contact method: a) at RT with polarizers, b) at RT without polarizers, c) at 50ºC with polarizers, d) at 50ºC without polarizers. The water concentration increases from right to left; the solid glycolipid is on the left side, bottom.

3.2.3. *Supramolecular Gels*

Suc-OOC-Phe-C_{16} sample was soluble in DMSO and methanol. However dispersion in water at 2 wt % give rise to transparent jellies that look like an "egg white", see **Fig. 3.5,** which flows by successive cohesive lumps when transferred from one recipe to another. The gel can be formed at RT with stirring or with slightly heating to favor solubilization. These results are in accordance with the previously described by Fitremann et *al*.[8b]

Fig. 3.5: Transparent gel of a mixture of regioisomers at 2 wt % in water.

Morphological gel characterization. In order to gain an insight into the organization of this material at different scales, several microscopic techniques have been carried out, as transmission electron microscopy (TEM), scanning electron microscope (SEM) and cryogenic transmission electron microscopy (cryo-TEM). These techniques give an idea about how gelator molecules form aggregates.

The self-assembled structure of the gels was investigated by TEM. Although the hydrogel of *N*-palmitoylphenylalanine sucrose esters is formed at 2 wt % in water, this concentration is too high to perform TEM observations. The gel was prepared stirring with a stirrer bar. When gel sample was diluted at 0.2 wt % in water and then observed by TEM, fibres can be detected, see **Fig. 3.6**. To prepare the sample a drop of the diluted solution was placed onto the grid and then was negatively stained with uranyl acetate (1 wt %). The grid was dried overnight.

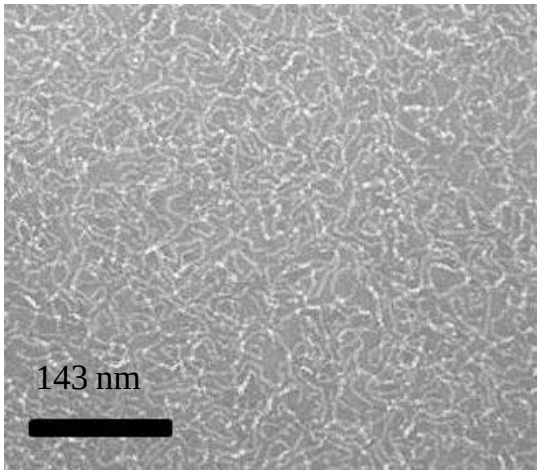

Fig. 3.6: TEM image of **Suc-OOC-Phe-C_{16}** (0.2 wt % in water).

The effects of stirring and heating the sample on the fiber morphology were investigated. Surprisingly, when a high stirring (9500 rpm for 30s) was applied at RT in a 0.2 wt % water sample of **Suc-OOC-Phe-C_{16}** by using a high dispersing and stirring system (Ultra-turrax homogenizer), longer fibres than by a simple mechanical stirring (stirrer bar), were obtained, see **Fig. 3.7**. If the sample was prepared by first heating at 80ºC for 30 min, to favor a solubilization of the sample, and subsequent stirring 30 s at 9500 rpm, shorter fibers were observed. Consequently, the formation of well defined and longer fibers seems to be favored by a high stirring at RT.

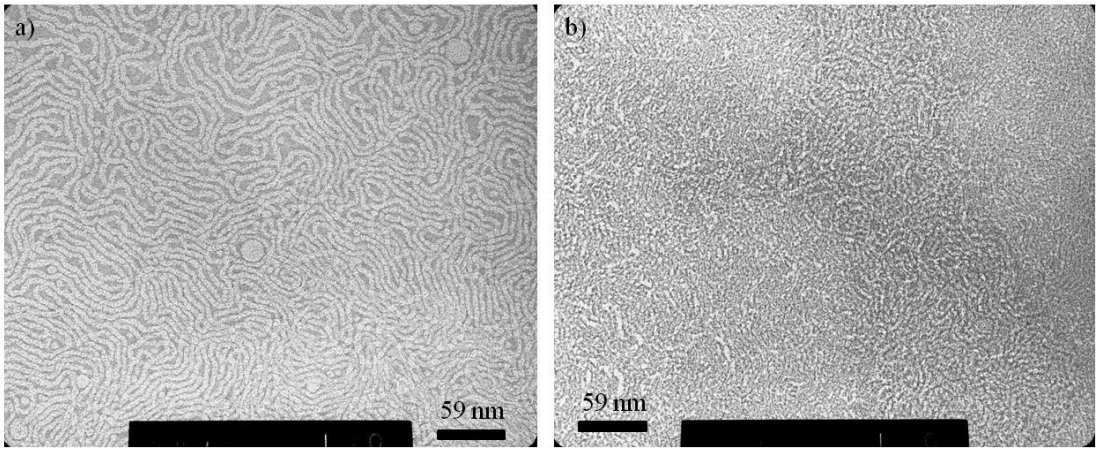

Fig. 3.7: TEM images of **Suc-OOC-Phe-C_{16}**: a) 0.2 wt % in water and stirred at 9500 rpm for 30 s, b) 0.2 wt % in water and heated at 80ºC for 30 min and after stirring 30 s at 9500 rpm.

Fibers found were approximately 12 nm thick, in all samples, but length depends on the preparation. Moreover some spherical aggregates have been observed at different areas of the same sample grid (see **Fig. 3.7.a**), with a diameter around 10-30 nm. Based on this observation it could be thought that fibrillar aggregates have a worm-like morphology.

By SEM direct measurements of the gel (without dilution) additional topological information is obtained. A drop of gel was fixed onto a glass and evaporated overnight. The sample was then coated with gold to make possible the SEM observation. The xerogel structure can give an idea about the organization of the 3D network.

As it is shown at **Fig. 3.8**, the xerogel is formed by several layers at the micrometer scale. In an expanded area, globular aggregates appear (**see Fig. 3.8.b**). These aggregates are not easy to measure and they have a wide size ranging from 25 to 100 nm.

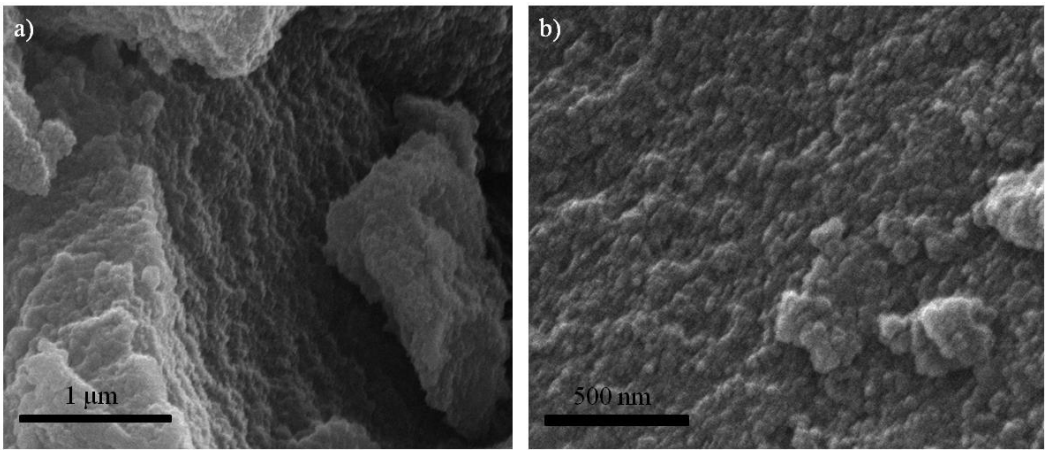

Fig. 3.8: a) SEM images of **Suc-OOC-Phe-C_{16}** gel 2 wt % in water, b) expanded area of a).

Cryo-TEM has been also used for the gel characterization. In this technique the drying and staining processes are avoided and a direct observation of the frozen gel (sample was vitrified in liquid ethane and observed at low temperature using liquid nitrogen). Cryo-TEM measurements show a fibrillar structure, see **Fig. 3.9**, and the diameters are around 10 nm. Since fibers are not cross-linked, a partial organization is observed.

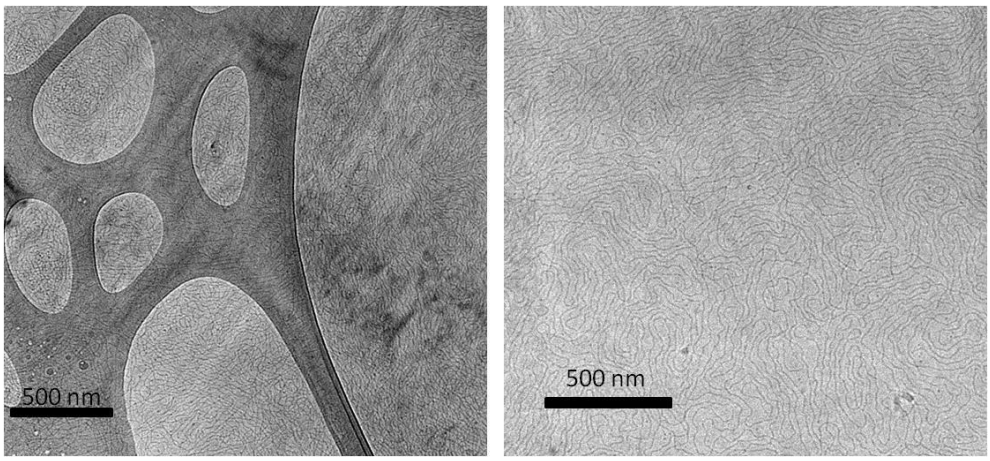

Fig. 3.9: a) CryoTEM image of **Suc-OOC-Phe-C_{16}** gel 2 wt % in water, b) central area of a hole of the same sample a).

Rheological properties. In order to define macroscopic properties of the gel, rheological experiments were performed. Previous works proved an increase of the viscosity by a factor of 200 compared to pure water at low stirring rate in **Suc-OOC-Phe-C_{16}** gel, 2 wt % in water.[8b] A partial thixotropy was evidenced by the recovery of the yield stress after several hours. In this section the viscoelastic behavior was tested by dynamic rheological measurements in order to quantify the elastic component.

First of all, the linear viscoelastic region was determined: the **storage** (G') and **loss** (G'') **moduli** were measured as a function of stress (0.1-500 Pa) at fixed frequencies (0.1, 1, 10, 100 Hz). In **Fig. 3.10** graphics at 0.1 Hz and 1 Hz are shown. The **linear viscoelastic region** was established in the region 0.1-0.5 Pa for fixed frequencies of 0.1-1 Hz (region was limited up to 0.5 Pa according to graphics of 10 and 100 Hz). For stress values up to this region the gel can break and begins to flow.

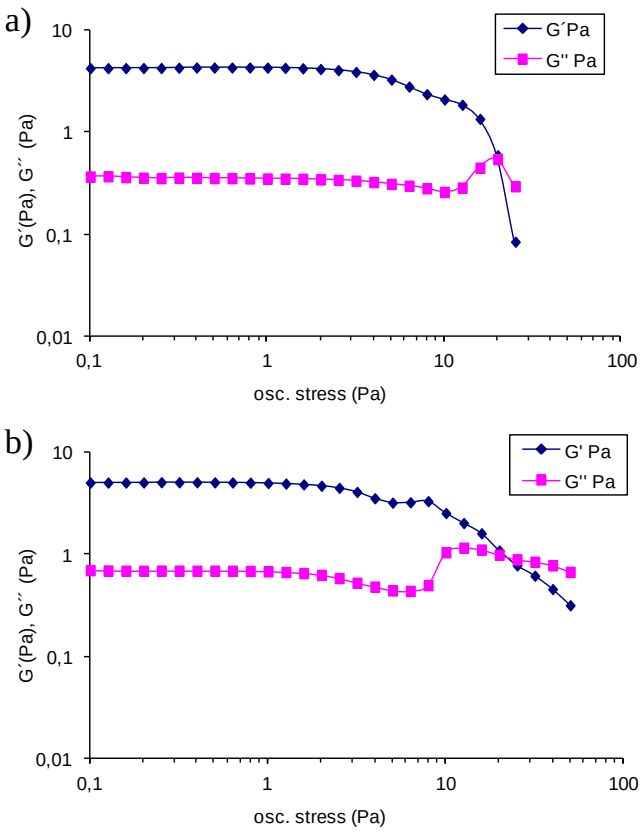

Fig. 3.10: a) Stress sweep (0.1-500 Pa) at fixed frequency of 0.1 Hz in a sample of **Suc-OOC-Phe-C_{16}** gel, 2 wt % in water stirred at 9500 rpm for 30 s, b) Stress sweep (0.1-500 Pa) at fixed frequency of 1 Hz in a sample of **Suc-OOC-Phe-C_{16}** gel, 2 wt % in water, stirred at 9500 rpm for 30 s.

As it have been establish, 0.1-0.5 Pa is the limit for the values of the fixed stress to measure curves of G´ and G´´ as a function of frequency. Then these curves were registered. **Fig. 3.11** shows two examples of these experiments at 0.1 and 0.5 Pa. G´ remains about 10 times higher than G´´ over the whole range of frequency from 0.01 to 100 Hz and consequently the material is more elastic than viscous, which is distinctive of a gel. G´ and G´´ cross over at very low frequency, nearly 10^{-3} Hz.

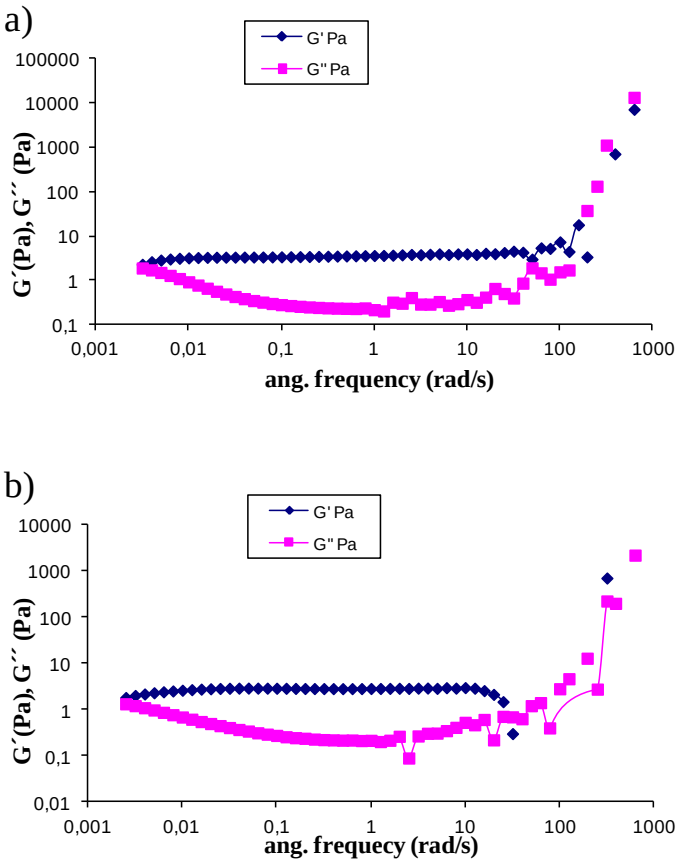

Fig. 3.11: a) Frequency sweep (100-0.0001 Hz) at fixed stress of 0.5 Pa in a sample of **Suc-OOC-Phe-C_{16}**, 2% water, stirred at 9500 rpm for 30 s, b) Frequency sweep (100-0.0001 Hz) at fixed stress of 0.1 Pa in a sample of **Suc-OOC-Phe-C_{16}**, 2% water, stirred at 9.500 rpm for 30 s.

As we can see in the graphics, the two modulus values are low as can be expected for these transparent jellies having an “egg white” like morphology. The influence of stirring the sample with the Ultra-turrax homogenizer on their rheological properties has

been checked and no clear differences are observed with respect to the native gel (without stirring, see **ref [8b]**).

An attempt to organize the fibers forming the hydrogel in one preferential direction by a mechanical orientation was carried out. The molecular combing technique[18] was applied to organize the fibers at the nanometric scale. This method was carried out in collaboration with the NanoBioSystem group in the LAAS laboratory, Toulouse (C. Vieu, A. Cerf).

Molecular combing is usually used to orient and stretch DNA molecules on a surface. A schematic design of this technique is represented in **Fig. 3.12**. The linear macromolecules can be anchored on several surfaces by their extremities or only sticked with high interactions. The solution moves and after the meniscus has receded, molecules are stretched and bound onto the surface.

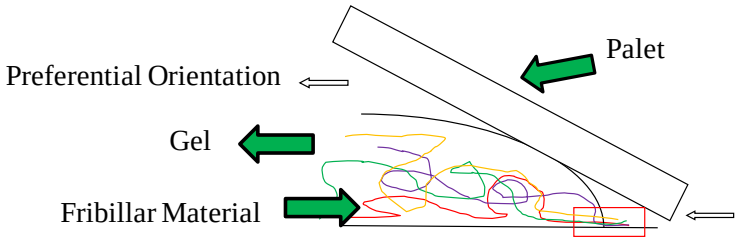

Fig. 3.12: Schematic representation of the molecular combing.

Different conditions were tested. Molecular combing was tried directly on a glass surface and on treated surfaces by microcontact printing with a poly(dimethylsiloxane) (PDMS) stamp (without or with patterns) in order to favor the anchoring of the sample. Finally, the surface was treated with octadecylchlorosilane (OTS) in order to anchor the hydrogel fibres on the glass defects and to align them on the hydrophobic parts (OTS). AFM is one of the techniques commonly used in other to check if combing is achieved. However, AFM showed a bulk agglomeration, but no fibers at the nanometer scale. For this reason TEM was chosen and the combing was made directly on the TEM grid, see **Fig. 3.13**. Moreover, different experimental conditions were tested by modifying the

concentration (0.02% and 0.002% in water) and different speeds of pallet movement (1, 10, 100 μm/s).

As conclusion, there was agglomeration on the sides, meniscus was broken by the viscosity of the sample and only a slight orientation was achieved, as can be seen in **Fig. 3.13.b**.

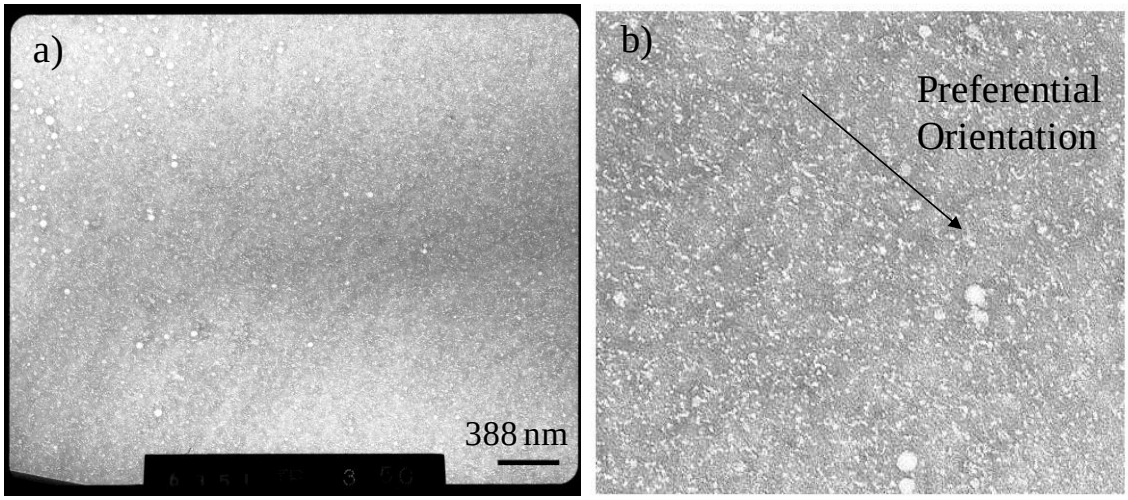

Fig. 3.13: a) 0.02 wt % in water of **Suc-OOC-Phe-C_{16}** 9.500 rpm for 30 s, combing speed 1mm/s, negative stained with uranyl acetate, b) a zoom of a) where a slight preferential orientation was observed.

When the structural information of all used techniques is compiled a clear conclusion about hydrogel organization does not arise. In fact, a fibrillar structure can be proposed from the TEM and cryo-TEM observations. However, SEM measurements did not confirm this conclusion and moreover by the application of capillary forces, in molecular combing, elongated smaller entities were found. With all this information, we might propose a fibrillar structure, probably formed by an association of worm like aggregates.

N-Palmitoylphenylalanine sucrose-esters form gels in water with an interesting rheological behavior, however this material is formed by a mixture of isomers and esterification can occur in different positions. In order to investigate new glycolipids with a well-defined chemical structure, other disaccharides and synthetic approaches

were selected as it is reported in the following sections using new linking groups with a higher hydrolytic resistance than the ester bond.

3.3. Glycolipids derived from maltose and palmitic acid

In this section, the synthesis, characterization and properties of four low molecular mass amphiphilic glycolipids will be described. The glycoamphiphiles have been prepared by linking a maltose polar head and a hydrophobic linear chain either by amidation or copper(I)-catalyzed azide-alkyne [3+2] cycloaddition. The liquid crystalline, gel properties and supramolecular organization of these amphiphilic molecules have been characterized by different techniques.

3.3.1. *Synthesis*

The synthesis of amphiphiles analogous to **Suc-OOC-Phe-C_{16}** was accomplished using maltose as starting material but linking the hydrophobic part to the sugar through an amide bond and taking advantage of the anomeric position to obtain a selective grafting of the hydrophobic tail on the C1 position of the sugar. According to this strategy the synthesis of **Malt-NH-C_{16}** and **Malt-NH-Phe-C_{16}** was first achieved. In both cases, the previous synthesis of maltosylamine and further amidation with palmitic acid or *N*-palmitoylphenylalanine was required.

In a first synthetic approach, maltose was reacted with ammonium carbonate[19] or with ammonium carbamate,[20] as ammonia donor, to synthesize maltosylamine **2**, see **scheme 3.2**. Excess of ammonia donor had to be added and product was precipitated and filtered under vacuum. Different temperatures (RT or heating up to 45ºC) and reaction times were tested.

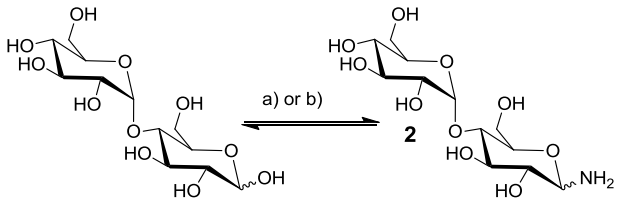

Scheme 3.2: Synthesis of maltosylamine **2**: a) with ammonium carbonate in DMSO, b) with ammonium carbamate in MeOH.

By using ammonium carbonate as ammonium donor, degradation of maltosylamine was observed. Ammonium carbamate was then tested because in this reaction a carbamic acid salt should be obtained and therefore is expected to be more stable; however degradation of the maltosylamine was also observed and *N*-maltosylcarbamate was found as side product. Due to these stability problems, maltosylamine was finally synthesized using ammonium carbonate but without isolation of the maltosylamine that was directly used in the next reaction step.

The subsequent amide formation for obtaining **Malt-NH-C$_{16}$** was performed using DCC as coupling agent. *N*-palmitoylphenylalanine was activated by N-hydroxysuccinimide to react with maltosylamine **2**, following the **scheme 3.3**.

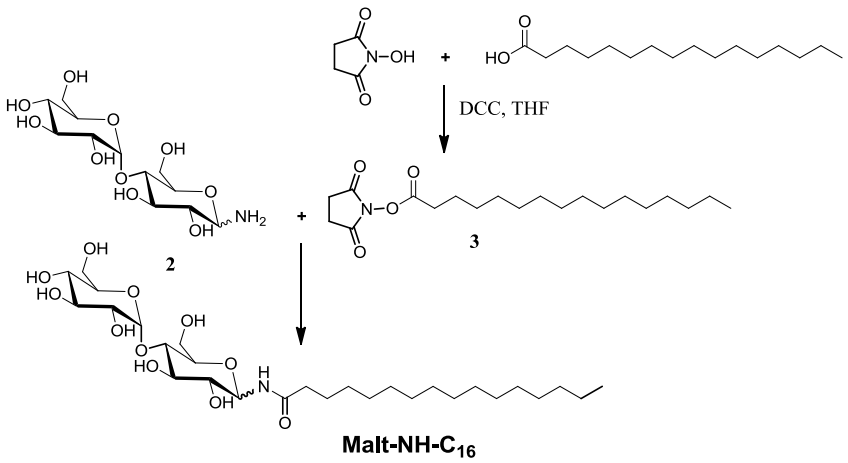

Scheme 3.3: Synthesis of **Malt-NH-C$_{16}$** by unprotected method.

Different conditions were tested; DMF and pyridine were used as solvents. Diisopropylethylamine or dimethylaminopyridine were added as co-reagents and sugar excess was added due to the degradation problems observed. Reaction was stirred for 2 days at RT and monitored by TLC (phosphomolybdic acid and ninhydrin as revelator). Even though the final product was not finally purified it was confirmed by mass spectrometry but yield of the reaction was lower than 5%. In the experimental section is described one example of the experimental conditions tested by this method, see section **3.7** for more details.

To obtain **Malt-NH-Phe-C$_{16}$**, two different reactions were tested, see **scheme 3.4**. On one hand, the carboxylic group of *N*-*L*-palmitoylphenylalanine was first activated by a

reaction with N-hydroxysuccinimide and then coupled with maltosylamine by DCC. On the other hand, DCC coupling was directly made with hydroxybenzotriazole as co-reagent.

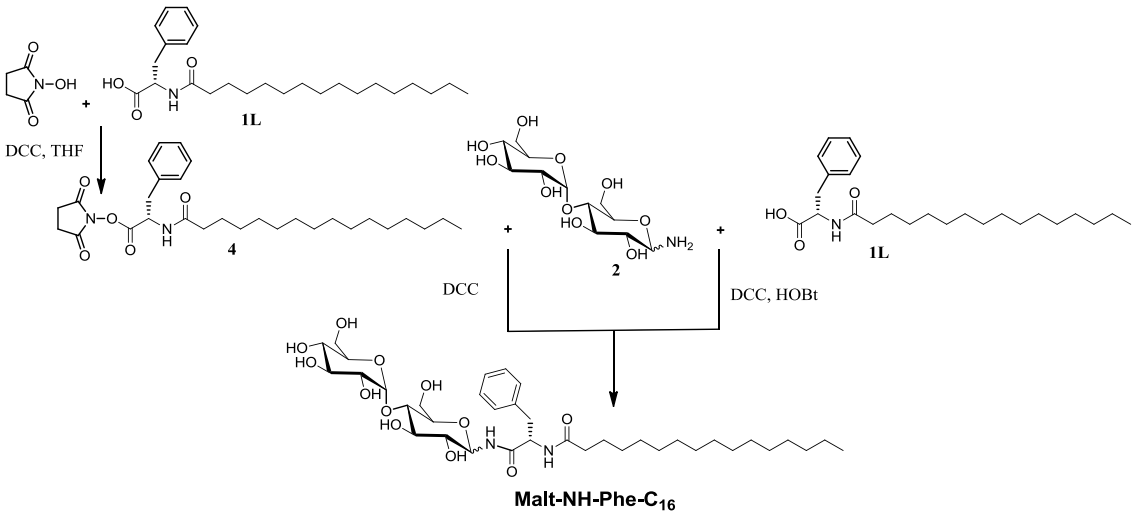

Scheme 3.4: Synthesis of **Malt-NH-Phe-C_{16}**

Different reaction conditions were also tested; DMF and pyridine were used as solvents, diisopropylethylamine or dimethylaminopyridine were added as co-reagents and sugar excess was added. Reaction was stirred at RT. In the experimental section, the conditions of one example for each method where the product was obtained, are described. See **section 3.7** for more details.

Reactions were monitored by HPLC. The reaction crude (0,1 mL crude reaction/5 mL HPLC eluent) was injected, using methanol/ water (82/18) + 0,5 mL/L acetic acid as eluent in a C8 column. Under these conditions appeared, on chromatograms, two peaks at around 11.5 and 15.5 min. In order to determinate the correspondence between compounds and peaks, HPLC was coupled with Mass Spectrometry (Service commun de spectrometrie de masse, ICT, Toulouse, Cathy Claparols). As example, a chromatogram of the reaction by direct coupling with DCC and hydroxybenzotriazole, described in experimental section, is shown on **Fig. 3.14**.

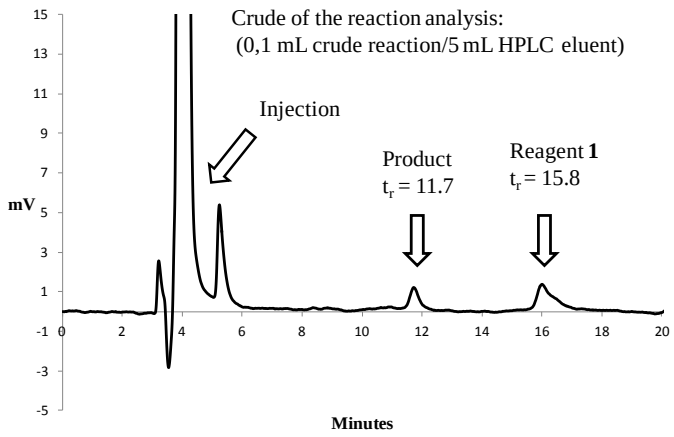

Fig. 3.14 Chromatogram of the MS-HPLC experiment.

Peak at around 11.5 corresponds to the desired product as was corroborated by Mass Spectrometry and peak around 15.5 mainly corresponds to reagent **1,** although the presence of other by-products were also identified, their mass peaks indicate that it could be related to the formation of amide or methylic ester derivatives of **1**. The evolution of this reaction was followed by HPLC but yields were around or lower than 5%. The compound had to be purified by preparative HPLC as attempts to purify it by flash chromatography were unsuccessful.

Preparative HPLC was performed using a X Bridge C18 column, with methanol 88% / TFA (1% water) 12 % as solvent by isocratic method (Service commun d´HPLC, ICT, Toulouse, Chantal Zedde). **Fig. 3.15** shows the analytical HPLC of the purified final product.

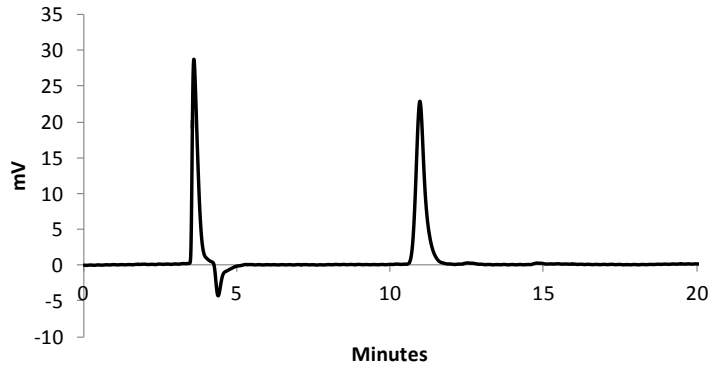

Fig. 3.15: Analytical HPLC after preparative HPLC chromatograms of **Malt-NH-Phe-C_{16}.**

Due to the difficulties found in the synthesis and purification of the target glycolipid by this approach, we finally decided to attempt a new route using protected sugars to improve the solubility in organic solvents which could facilitate the reaction workup and also opens new synthetic possibilities.

The synthesis of the glycolipids based on maltose was then accomplished using peracetylated maltose as the starting material (commercially available), which was amine-functionalized as shown in **scheme 3.5,** by reduction of the corresponding azide which has been previously synthesized. Maltosylazide **5** was synthesized in a stereoselective manner, to obtain the β isomer, by treating β-D-maltose octa-acetate with trimethylsilyl azide and tin tetrachloride, as a Lewis acid catalyst, employing the general procedure described by Paulsen.[21] The azide group was reduced to the amine by hydrogenation using Palladium hydroxide on carbon as catalyst to yield the acetylated maltosylamine **6**. The product was used without further purification because of its instability. The disappearance of azide was monitored by the IR signal to confirm the product formation. Compound **6** is used in the synthesis of the target amide derivatives by amidation with palmitic acid or N-palmitoylphenylalanine. Furthermore, this synthetic route allows the use of the β-maltosylazide for direct coupling of hydrophobic blocks in the preparation of glycoamphiphiles as will be described below.

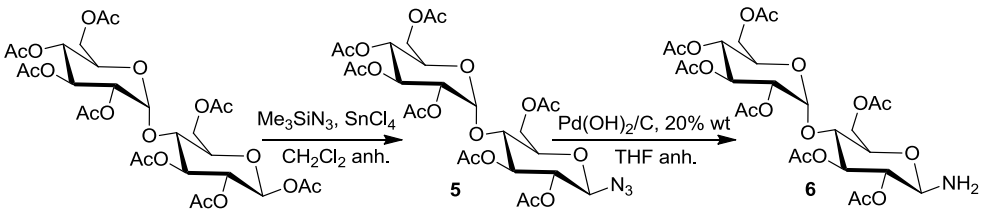

Scheme 3.5: Synthesis of the functionalized acetylated maltose derivatives.

On one hand, reaction of the peracetylated β-maltosylamine **6** with palmitic acid or a derivative of palmitic acid gives rise to the peracetylated precursor of **Malt-NH-C_{16} and Malt-NH-Phe-C_{16}**, see **scheme 3.6.** The synthesis of **Malt-NH-C_{16}** was recently published and according to this reference palmitoyl chloride was used for the condensation.[16a] On the other hand, compound **6** can react with *N*-palmitoylphenylalanine which was synthesized from phenylalanine and palmitic acid activated with N-hydroxysuccinimide, see **scheme 3.6.** DCC and hydroxybenzotriazole

were used for the condensation of these synthetic blocks for the synthesis of **OAc-Malt-NH-Phe-C_{16}**. Yields in both condensation reactions were around 45%. Peracetylated compounds are easy to dissolve, purify and characterize.

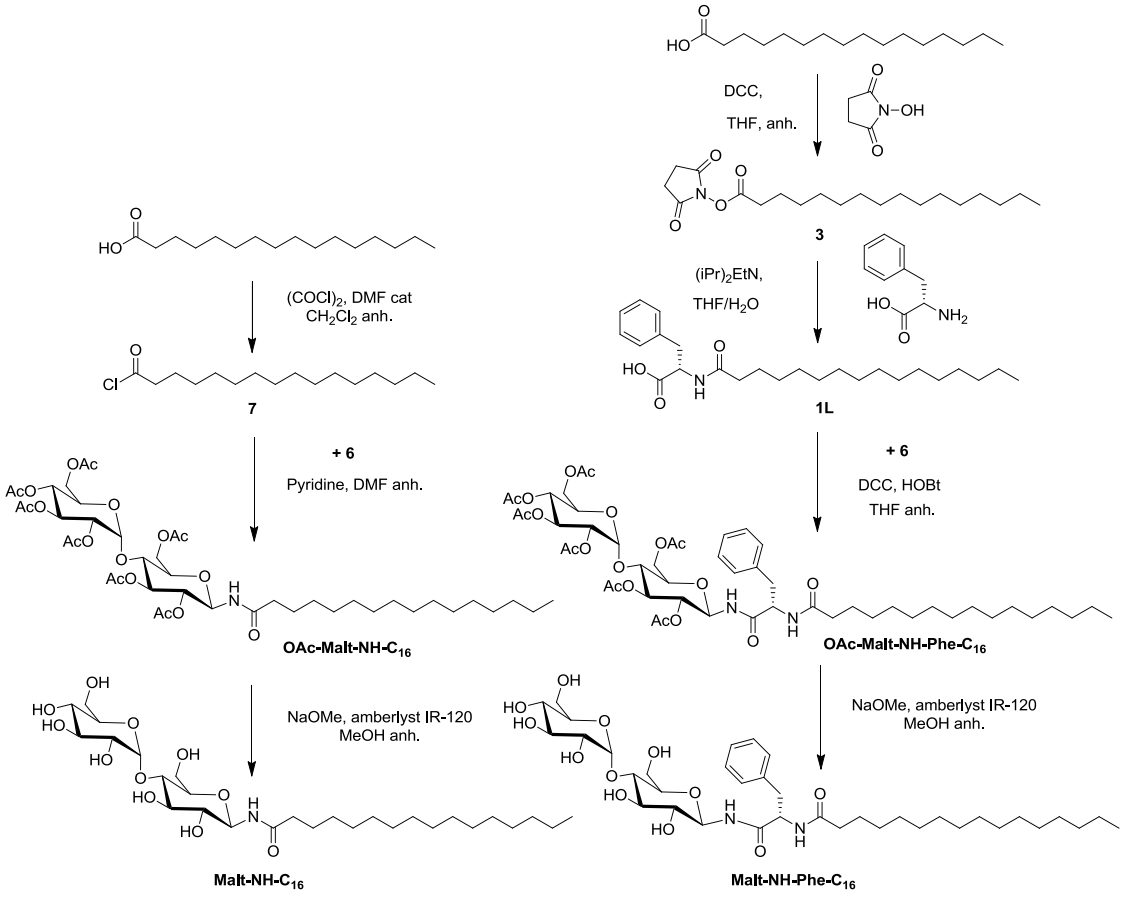

Scheme 3.6: Synthesis of **Malt-NH-C_{16}** and **Malt-NH-Phe-C_{16}**.

As mentioned above it is possible to take advantage of the azide group on compound **5.** The coupling of azide and alkynes through a copper-catalyzed 1,3-dipolar cycloaddition is widely used as efficient click reaction in the preparation of organic materials.[22] This cycloaddition generates a triazole ring that connects the sugar head and the hydrophobic tail. This fact opens up new possibilities for the design and preparation of amphiphilic glycolipids. Click reaction[23] was first described by Sharpless and this strategy is characterized by high yields, mild reaction conditions, and requires simple or no workup for obtaining the final product.

Thus in an alternative approach, a copper(I)-catalyzed azide-alkyne [3+2] cycloaddition was carried out by using compound **5** and propargyl derivatives of palmitic acid, as it is

shown in **scheme 3.7**. For this purpose the *N*-propargyl palmitic amide **8** and the *N*-propargyl amide derivative of (*N'*-palmitoyl)phenylalanine **9** were first synthesized. Click reaction was carried out in DMF using CuBr and pentamethyldiethylenetriamine (PMDETA) to give the desired product in around 90% yield.

In a final step, all the protected derivatives were deacetylated at RT according to Zemplen´s conditions using MeONa and Amberlyst IR120 in anhydrous MeOH, to give the final product in almost quantitative yield.

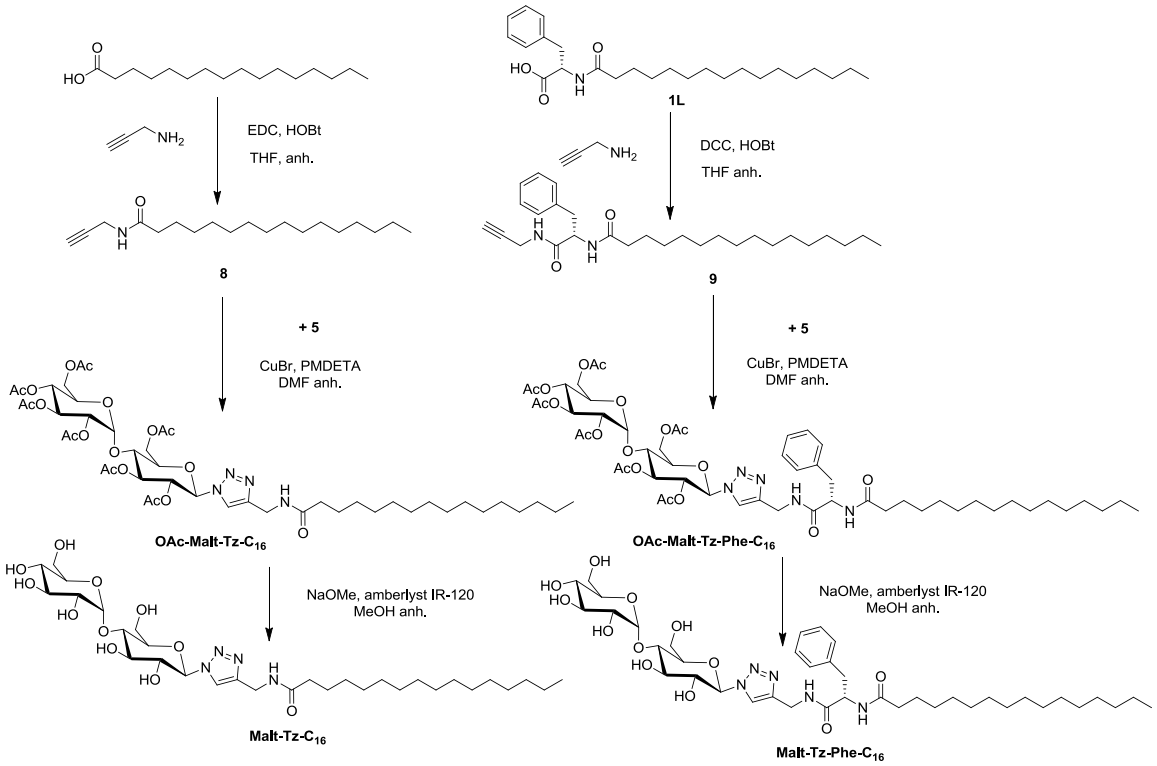

Scheme 3.7: Synthesis of **Malt-Tz-C_{16}** and **Malt-Tz-Phe-C_{16}**.

Final compounds **Malt-NH-C_{16}**, **Malt-NH-Phe-C_{16}**, **Malt-Tz-C_{16} and Malt-Tz-Phe-C_{16}** were characterized by ^{1}H NMR, ^{13}C NMR, IR and mass spectrometry. See experimental **section 3.7** for more detail.

2D NMR experiments as COSY, TOCSY, NOESY, HSQC and HMBC were performed in order to corroborate the chemical structure of the glycolipids.

Fig. 3.16 shows, as example, ^{1}H NMR experiment of **OAc-Malt-Tz-C_{16}** and **Malt-Tz-C_{16}**. The assignments of the sugar protons are supported by 2D experiments. In **Fig.**

3.17 the TOCSY experiment of **OAc-Malt-Tz-C_{16}** can be seen where by means of correlations of a whole spin system, protons from one cycle of the sugar can be distinguished from protons of the second cycle (see **section 3.6** for a detailed example of the structural characterization of a glycoamphiphilic product by NMR).

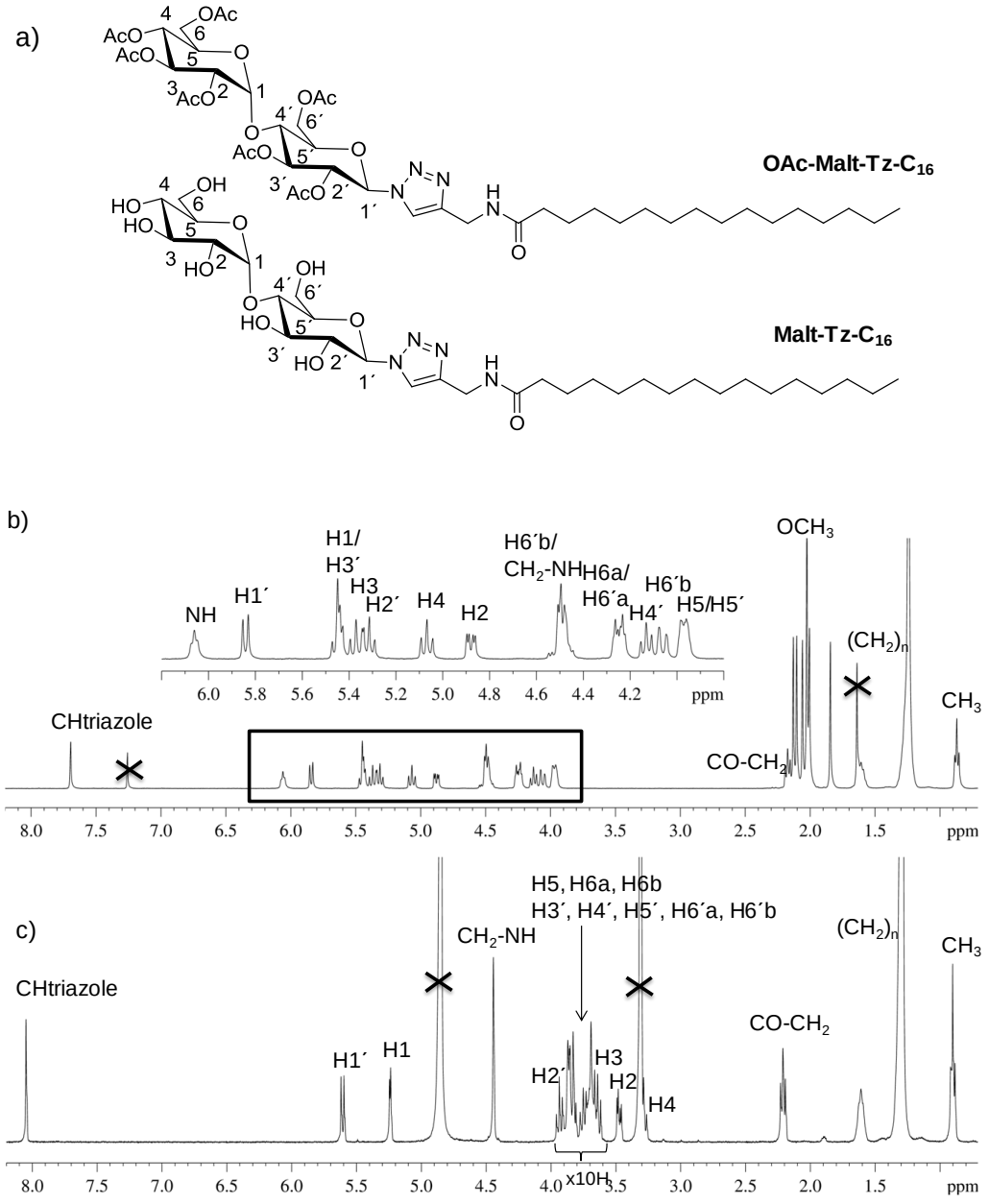

Figure 3.16: a) **OAc-Malt-Tz-C_{16}** and **Malt-Tz-C_{16}** chemical structure, b) ^{1}H NMR spectrum of **OAc-Malt-Tz-C_{16}** with $CDCl_3$ as solvent at 25ºC, c) ^{1}H NMR spectrum of **Malt-Tz-C_{16}** with MeOD as solvent at 50 ºC.

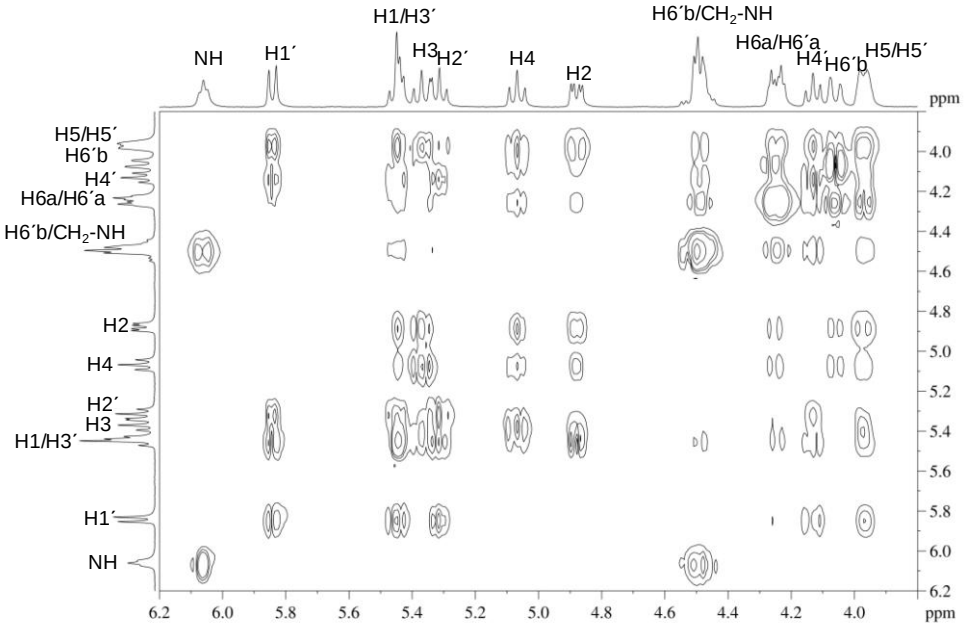

Figure 3.17: TOCSY spectrum of **OAc-Malt-Tz-C_{16}** with $CDCl_3$ as solvent at 25ºC and 90 ms of mixing time.

3.3.2. *Thermal properties*

As it was described in **Chapter 1** maltose derivatives linked by an ether bond to different alkyl chains were found to exhibit a bilayer smectic A phase. Maltose derivatives linked by an amide bond to aliphatic chains have also been studied and in particular, **Malt-NH-C_{16}** was previously reported as mesomorphic but the mesophase was not clearly assigned.[16a]

The thermal and mesomorphic properties of the synthesized amphiphilic glycolipids as well as the peracetylated precursors were studied by thermogravimetric analysis (TGA), polarizing optical microscopy (POM) and differential scanning calorimetry (DSC).

The thermogravimetric results are gathered in **Table 3.1**. The samples were dried and immediately analyzed; however small weight losses are observed around 100ºC, probably due to the hygroscopy of the sample. In peracetylated precursors weight loss associated to thermal decomposition was observed at temperatures close to 300ºC. Thermogravimetric curves for glycolipids display weight losses in the range 140-225 ºC. As example, in **Fig. 3.18** are shown the thermogravimetric curves of **OAc-Malt-Tz-Phe-C_{16}** and **Malt-Tz-Phe-C_{16}**.

Table 3.1: Thermogravimetric analysis of peracetylated precursors and glycolipids derived from maltose.

Compound	$T_{5\%lost}$	T_{onset}	T_{max}
OAc-Malt-NH-C_{16}	300ºC	330ºC	360ºC
OAc-Malt-NH-Phe-C_{16}	320ºC	335ºC	360ºC
OAc-Malt-Tz-C_{16}	315ºC	325ºC	345ºC
OAc-Malt-Tz-Phe-C_{16}	315ºC	325ºC	345ºC
Malt-NH-C_{16}	180ºC	258ºC	260ºC
Malt-NH-Phe-C_{16}	140ºC	190ºC	210ºC
Malt-Tz-C_{16}	225ºC	275ºC	310ºC
Malt-Tz-Phe-C_{16}	200ºC	275ºC	310ºC

$T_{5\%lost}$ = Temperatures at which 5% of the initial mass is lost. T_{onset} = Onset of decomposition process. T_{max} = Temperatures at which the rate of weight loss is maximum.

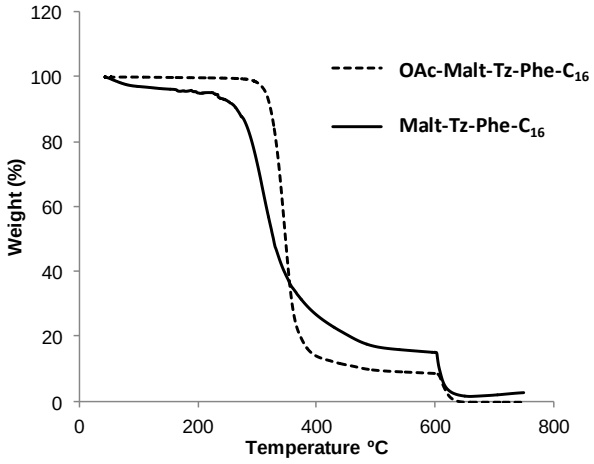

Fig. 3.18: Thermogravimetric curves of **OAc-Malt-Tz-Phe-C_{16}** and **Malt-Tz-Phe-C_{16}**.

The peracetylated precursors were studied by polarizing optical microscopy provided with a heating stage as a function of temperature and mesomorphic behavior was not observed. All compounds melted directly from a crystalline state into an isotropic liquid, see **Table 3.2**.

However, the final glycolipids exhibited textures which can be associated with thermotropic liquid crystalline behavior. The poorly defined birefringent texture of the viscous mesophase, see **Fig. 3.19,** cannot be unambiguously assigned. Nevertheless it can be postulated that the mesophase is lamellar based on previous results on thermotropic glycolipids having a similar structure.

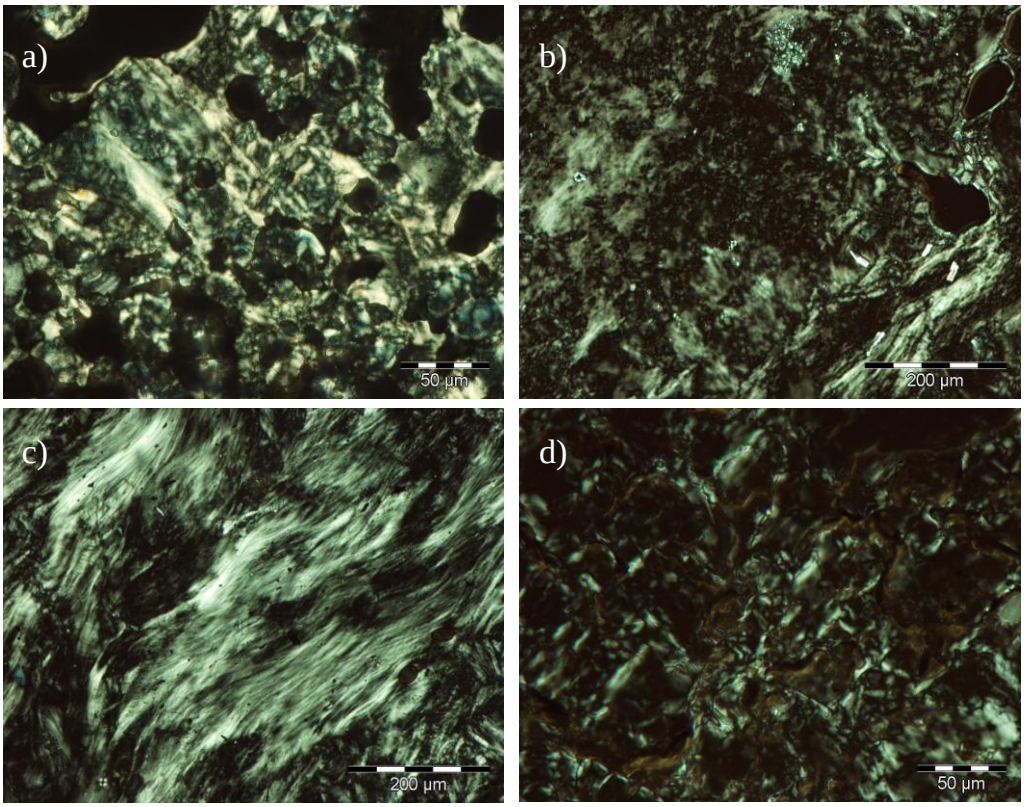

Fig. 3.19: Microphotograph of a) **Malt-NH-C_{16}** taken at 155 ºC, b) **Malt-NH-Phe-C_{16}** taken at 160 ºC, c) **Malt-Tz-C_{16}** taken at 130 ºC, d) **Malt-Tz-Phe-C_{16}** taken at 160 ºC.

Decomposition of glycolipids was observed by optical microscopy at temperatures around 170 ºC since the sample became brown, most probably due to the thermal decomposition of the sugar unit even at temperatures below the onset of the massive weight loss detected by thermogravimetry.

The DSC study of the glycolipids was performed by heating the compounds to 150 ºC (as maximum) in order to minimize the thermal decomposition of the samples (detected around 170 ºC by optical microscopy). Under these conditions the second and successive scans were reproducible. The transition data are gathered in **Table 3.2**. In all cases, broad transition peaks were observed and traces of water were detected, even

after drying under vacuum. Complex curves were obtained with changes in the baseline **(see Fig. 3.20)**.

Table 3.2: Thermal transitions of glycolipids and peracetylated precursors detected by DSC (10ºC/min).

Compound	Thermal transition (ºC) [ΔH kJ/mol]
OAc-Malt-NH-C_{16}	Cr 124 [18.7] I[a]
OAc-Malt-NH-Phe-C_{16}	Cr 170 [42.5] I[a]
OAc-Malt-Tz-C_{16}	Cr103 [15.1] I[a]
OAc-Malt-Tz-Phe-C_{16}	Cr 171[24.4] I[a]
Malt-NH-C_{16}	Cr 49 [6.2] Cr´ 67 [5.0] (cold crystallization 75) Cr´´ 144 [2.3] S_a[b]
Malt-NH-Phe-C_{16}	Cr 24 [3.7] (cold crystallization 80) Cr´ 127 [7.7] S_a[b]
Malt-Tz-C_{16}	Cr 31 [2.0] Cr´ 49 [6.2] (90)[c] S_A[b]
Malt-Tz-Phe-C_{16}	Cr 45 [3.0] Cr´ 142 [4.0] S_a[b]

[a] Data corresponding to the first heating scan. The heating cycles on protected glycolipids were only carried out up to 200 ºC [b] Data corresponding to the second heating scan. The heating cycles on glycolipids were only carried out up to 150 ºC to avoid decomposition, which occurs before isotropization. Cr = crystal, I = Isotropic phase, S_A = Smectic A phase (according to X-ray data). [c] See text.

Malt-NH-C_{16} was previously characterized by Branderburg and co-workers[16a] as a glassy material with a transition from a glass to a mesophase (the nature of the mesophase was not described) at around 141 ºC. On heating, however, this compound exhibits (once it has been cooled from 150 ºC) two endothermic peaks (probably due to crystalline polymorphism) followed by an exothermic transition that can be assigned to a cold crystallization. Finally, the compound melts at around 145 ºC into a highly viscous mesophase (according to POM). On cooling, this compound crystallizes at around 60 ºC. Consequently, the compound is crystalline up to ca. 145 ºC and it finally melts to give a mesomorphic phase in contrast to the previous described characterization, see **Fig. 3.20.a**.

The analog **Mal-NH-Phe-C_{16}** shows similar thermal behavior, but in this case the melting point of the crystalline solid formed by cold crystallization is around 130 ºC. The thermal behavior of **Malt-Tz-Phe-C_{16}** is similar except that cold crystallization is

not observed for this compound and the melting transition occurs at around 140 ºC. However, in the case of **Malt-Tz-C_{16}**, the peak corresponding to the melting transition is depressed and was observed at around 50 ºC. Above this temperature the sample is highly viscous and difficult to characterize by optical microscopy. Nevertheless, at temperatures above approximately 90 ºC the sample becomes more fluid and can be clearly described as liquid crystalline according to the optical observations, see **Fig. 3.20.b**.

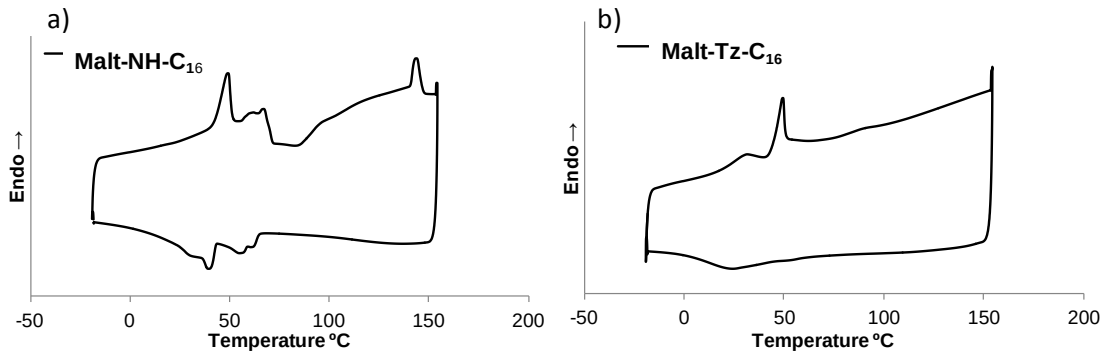

Fig. 3.20: a) Second cycle scan DSC profile in the solid state of **Malt-NH-C_{16},** b) Second cycle scan DSC profile in the solid state of **Malt-Tz-C_{16}.**

In all cases, decomposition was observed in the mesomorphic state at temperatures above approximately 170 ºC either by optical microscopy or DSC, when samples were heated up to this temperature. In this case the decomposition was observed as a modification of the baseline, see **Fig. 3.21**.

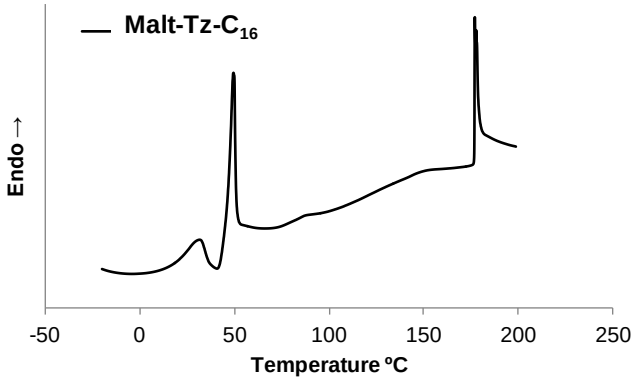

Fig. 3.21: Third cycle scan DSC profile in the solid state of **Malt-Tz-C_{16}** to 200ºC.

In order to identify the mesophase, XRD studies were carried out on the glycoamphiphile **Malt-Tz-C_{16}**, as a representative example, which exhibit mesomorphism at lower temperatures. X-ray patterns were recorded at 65 ºC for 4.5 h on samples previously heated to 150 ºC in order to develop the mesophase. Bragg reflexions in the low-angle region were found that were related to second, third and fifth order of a lamellar organization, see **Fig. 3.22**. The lamellar spacing was measured close to 51 Å, which indicates an interdigitated bilayer Smectic A phase. In Fig. **3.23** a proposed model is shown. The length of the aliphatic acid chain is approximately 18.4 Å, the sugar polar head 9.7 Å and the triazole has 6.6 Å (according to measurements accomplished in Chem3D Pro 12.0 program). In the high angle region a diffuse, broad maximum was found along with several slightly sharper peaks. These peaks were also observed when the experiment was performed at 150 ºC. This fact leads us to suggest that some degradation occurred during the experiment.

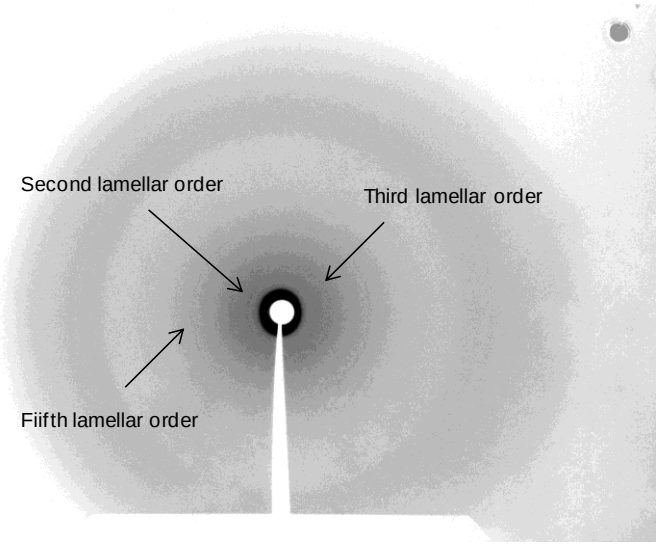

Fig. 3.22: XRD diffractogram of the **Malt-Tz-C_{16}**, the sample was heated until 150ºC and the experiment was recorded at 65ºC for 4.5 h.

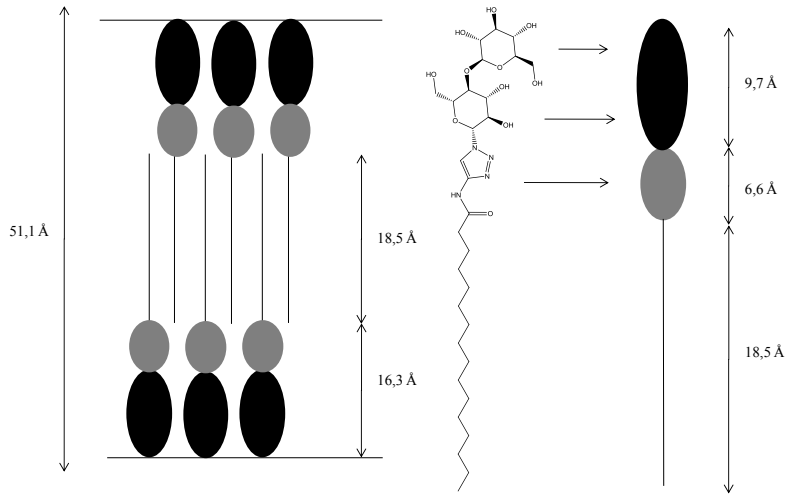

Fig. 3.23: Proposed organization of the **Malt-Tz-C_{16}** molecules on the lamellar phase.

A qualitative study of the lyotropic properties was also carried out by the contact method. **Malt-Tz-C_{16}** was selected to be tested because this compound presents solubility in water under heating, as it will be explained below. The sample was first heated to 120 ºC (mesophase) and then cooled to RT. A small amount of water was then placed on the slide at the edge of the cover glass and this completely surrounded the sample. The slide was placed again for a few seconds on the hot stage at 80 ºC and the phase behavior was immediately investigated by polarizing optical microscopy. A concentration effect was observed, as can be seen in **Fig. 3.24**. A birefringent texture appeared on a gradient of water from pure liquid to solid glass state. This is due to a lyotropic phase with a lamellar organization according to similar reported textures.[12] However, a precipitate finally appeared over time.

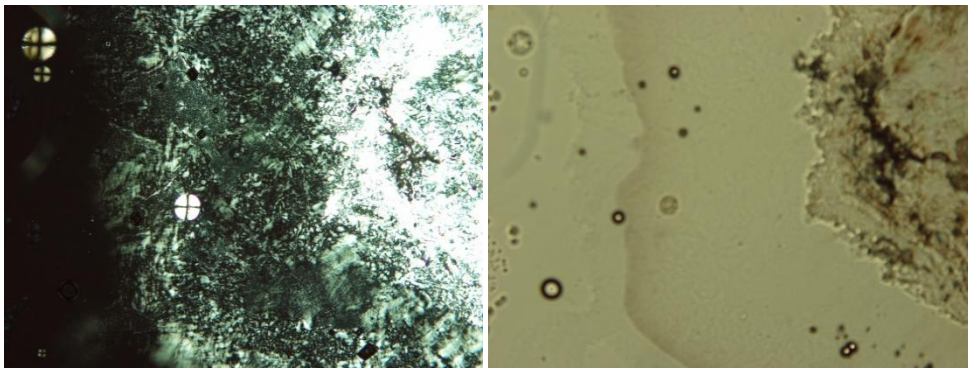

Fig. 3.24: Lyotropic phase observed by optical microscopy on a sample of **Malt-Tz-C_{16}** in water prepared by the contact method: a) with polarizers, b) without polarizers. The

concentration increases from left to right; the solid glycolipid sample is shown on the right side.

3.3.3. *Supramolecular Gels*

The solubility and gelation ability of **Malt-NH-C_{16}**, **Malt-NH-Phe-C_{16}**, **Malt-Tz-C_{16}** and **Malt-Tz-Phe-C_{16}** were examined in different solvents. With this aim, 5 mg of the corresponding glycoamphiphile was dissolved in about 0.1-1 mL of the solvent, i.e. in the range of 0.5-5 wt % (the gelator and the solvent were placed in a septum-capped test tube). Glycoamphiphiles are not soluble at RT in the selected solvents, except DMSO. However, in some of the solvents, the glycolipids eventually dissolved on heating. The solution was then cooled down to RT and a solution, a precipitate or a gel was observed depending on the system glycolipid-solvent. The formation of a gel was registered if the tube was turned upside down and the solution did not flow. The results are summarized in **Table 3.3** for mixtures with 1wt % of the sample.

Table 3.3: Solubility and gelation properties of synthesized glycolipids in different solvents at 1wt %, after heating and cooling down to RT.

Solvent	Malt-NH-C_{16}	Malt-NH-Phe-C_{16}	Malt-Tz-C_{16}	Malt-Tz-Phe-C_{16}
Hexane	I	I	I	I
Ethyl Acetate	I	I	I	I
Tetrahydrofuran	P	I	S	I
Dichloromethane	I	I	I	I
Acetone	I	I	I	I
Methanol	P	P (G^a)	S	P(G^a)
Water	I	I	G	G^b
Water/Methanol	P	G (3:2)^c	Not tested	G (3:1)^d
Dimethylsulfoxide	S	S	S	S

I = Insoluble, P = Precipitate, S = Solution, G = Gel. [a] Gels are formed at higher concentrations (2.5-5 wt %) and upon cooling in a fridge. [b] Inhomogeneous gel, see text. [c]5 mg in the mixture of 0.3 mL of water and 0.2 mL of methanol.[d]3 mg in the mixture of 0.3 mL of water and 0.1 mL of methanol.

It can be seen that only the compounds that contain a triazole ring give rise to gels in aqueous solution. **Malt-Tz-C_{16}** can gelate in water to form a homogeneous gel, at a

minimum concentration of 1 wt % and in the absence of other organic solvents. **Malt-Tz-Phe-C_{16}** also formed a stable gel in water at 1 wt % but it was found to be inhomogeneous as some precipitate was observed within the gel structure once it was cooled to RT. The addition of methanol as an organic solvent led to the formation of a homogeneous and stable gel (in a mixture of water/methanol 3:1). **Malt-NH-Phe-C_{16}** can also gelate in a mixture of water/methanol (3:2). In all cases, gels are thermoreversible, having a gel-sol transition at around 60-80 ºC, and they are stable at RT, see **Fig. 3.25**. **Malt-NH-C_{16}** did not form gels even with a 1:1 proportion of water and methanol. Compounds with phenylalanine (**Malt-NH-Phe-C_{16}** and **Malt-Tz-Phe-C_{16}**) can gelate in methanol at concentration of 2.5-5 wt %, and cooling the solution in a freezer.

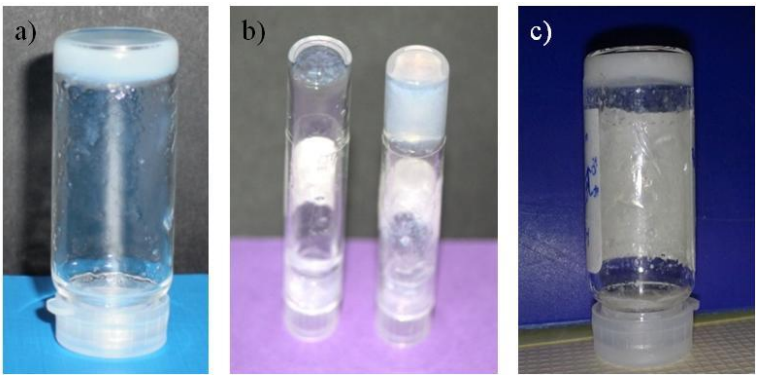

Fig. 3.25: a) Hydrogel of **Malt-Tz-C_{16}** (1 wt %), b) **Malt-Tz-Phe-C_{16}** gels (left: 1 wt % water, right: 3mg in 0.3 mL of water and 0.1 mL of methanol), c) **Malt-NH-Phe-C_{16}** gel (5mg in 0.3 mL of water and 0.2 mL of methanol).

Temperatures of gel to sol transition of the hydrogels were studied by DSC using aluminum sealed capsules. For **Malt-Tz-C_{16}** in a first experiment 5 wt % of solid was dispersed in water at RT and heated at 10ºC min^{-1}. On heating this mixture an endotherm was detected at 66 ºC. A thermal peak was not observed in the cooling scan. On the second heating, a broad peak was observed at around 65 ºC and this could be due to the gel-sol transition. In order to confirm that this peak corresponds to the gel-sol transition, a preformed hydrogel of **Malt-Tz-C_{16}** (1 wt %) was directly studied by DSC (5 ºC min^{-1}). An endothermic peak was detected at around 65 ºC but a peak was not

observed on cooling as in the first study. However, in the second heating scan the peak corresponding to the gel-sol transition was again observed, which confirms the reversibility of this transition**, see Fig. 3.26.a**.

The hydrogel derived from **Malt-Tz-Phe-C_{16}** at 1% wt was directly studied by DSC (5 ºC min^{-1}) and two peaks were detected on heating (see **Fig. 3.26.b** for the second thermal cycle, top). This observation could be due to the presence of a partial precipitate. The first peak could correspond to a solubilization transition similar to those observed for surfactants that display a Krafft Temperature.[24] A second endotherm is measured at higher temperature and this can correspond to the gel-sol transition of the gel. DSC measurements (5 ºC/min) on the gel formed in a water/methanol/water (3:1) mixture (see **Figure 3.26.b** for the second thermal cycle, bottom) show a peak at around 75 ºC corresponding to the gel-sol transition (a small transition can be detected at around 65 ºC, probably due to slight insolubility). DSC measurements (10 ºC min^{-1}) on a gel of **Malt-NH-Phe-C_{16}** obtained in a mixture of water/methanol (3:2) also show a single peak at around 80 ºC corresponding to the sol-gel transition. In all cases, subsequent heating scans confirmed the reversibility of these transitions.

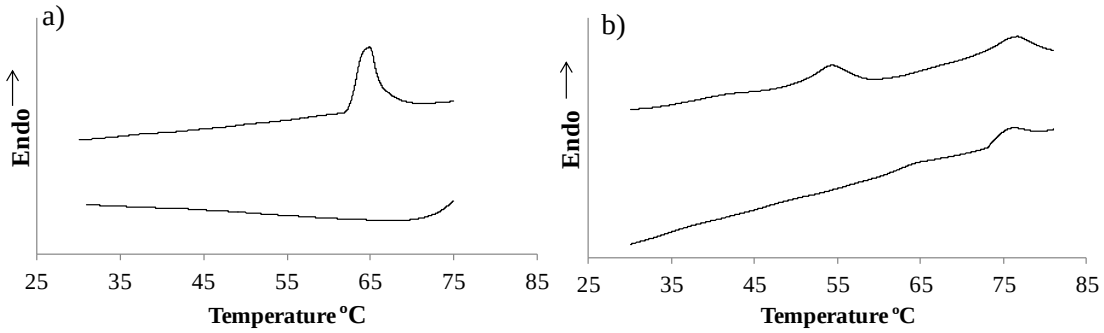

Fig. 3.26: Second DSC thermal cycle (5 ºCmin^{-1}, nitrogen atmosphere): a) gel of **Malt-Tz-C_{16}** at 1wt % water, heating scan (top) and cooling scan (bottom), b) gels of **Malt-Tz-Phe-C_{16}** at 1 wt % in water, heating scan (top) and at 1 wt % in a mixture of water/methanol 3:1, heating scan (bottom).

NMR experiments can also provide information about gel-sol transitions. **Malt-Tz-C_{16}** hydrogel at 1 wt % in D_2O was selected as example to study the gel-sol transition temperature. For this purpose ^{1}HNMR spectra were recorded at different temperatures.

On heating progressively the gel sample, the spectrum was fully resolved above 70 ºC (a clear solution is obtained around this temperature) as can be seen in **Fig. 3.27.**

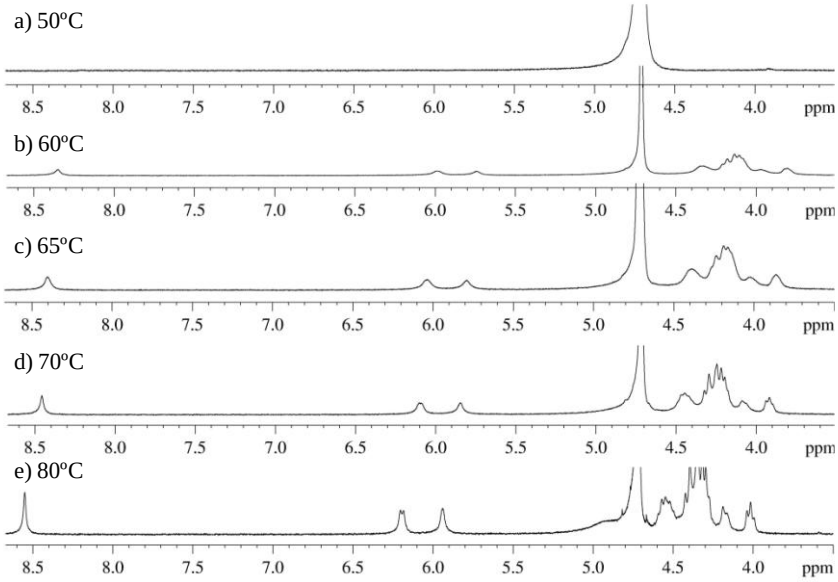

Fig. 3.27: ^{1}H NMR spectra of **Malt-Tz-C$_{16}$** hydrogel, 1 wt % (at RT) taken at different temperatures, around the gel-sol transition.

It has been reported that two of the driving forces that can favor gelation are H-bonding and π-π stacking of aromatic rings. In two of the synthesized compounds, **Malt-NH-Phe-C$_{16}$** and **Malt-Tz-Phe-C$_{16}$**, the phenyl group is remote from the axis of the molecule and can rotate freely and probably π-π stacking interactions are one of the interactions responsible for the directional self-assembly. Moreover the different gelation behavior between **Malt-Tz-C$_{16}$** and **Malt-NH-C$_{16}$** highlights the effect of the triazole ring. This group can also provide π-π stacking interactions. Otherwise, the triazole ring corresponds to a rigid fragment in the amphiphile structure which can favor directional interactions and help the formation of 1D or 2D aggregates (fibrils and tapes). Besides, the dipole moment exhibited by the 1,2,3-triazole ring increases the hydrophilic behavior and favor the preparation of hydrogels. In the case of **Malt-NH-Phe-C$_{16}$** and **Malt-Tz-Phe-C$_{16}$**, molecules are more hydrophobic and the presence of an organic co-solvent is required for complete solubilization and subsequent gel formation on cooling. Consequently, in the design of these gelators the presence of the triazole as a linking unit between the hydrophobic and hydrophilic parts seems to play an

important role both for the formation of the supramolecular network and also for ensuring an appropriate solubility in water.

Morphological gel characterization. The self-assembled structure of the gels derived from the synthesized glycoamphiphiles was studied by electron microscopy.

SEM measurements show a topological image of the xerogel obtained by drying the gel as in this technique a high vacuum is generally needed (environmental scanning electron microscopy –ESEM- allows the option of collection information from wet samples). Gel was fixed onto a glass and subsequently dried and coated with gold. Xerogels obtained from **Malt-Tz-C_{16}**, **Mal-Tz-Phe-C_{16}** and **Malt-NH-Phe-C_{16}** gels display an interconnected fibrillar structure where the diameter of the fibres changes depending on the sample. The microphotographs in **Fig 3.28** show this fibrillar network for all the studied compounds.

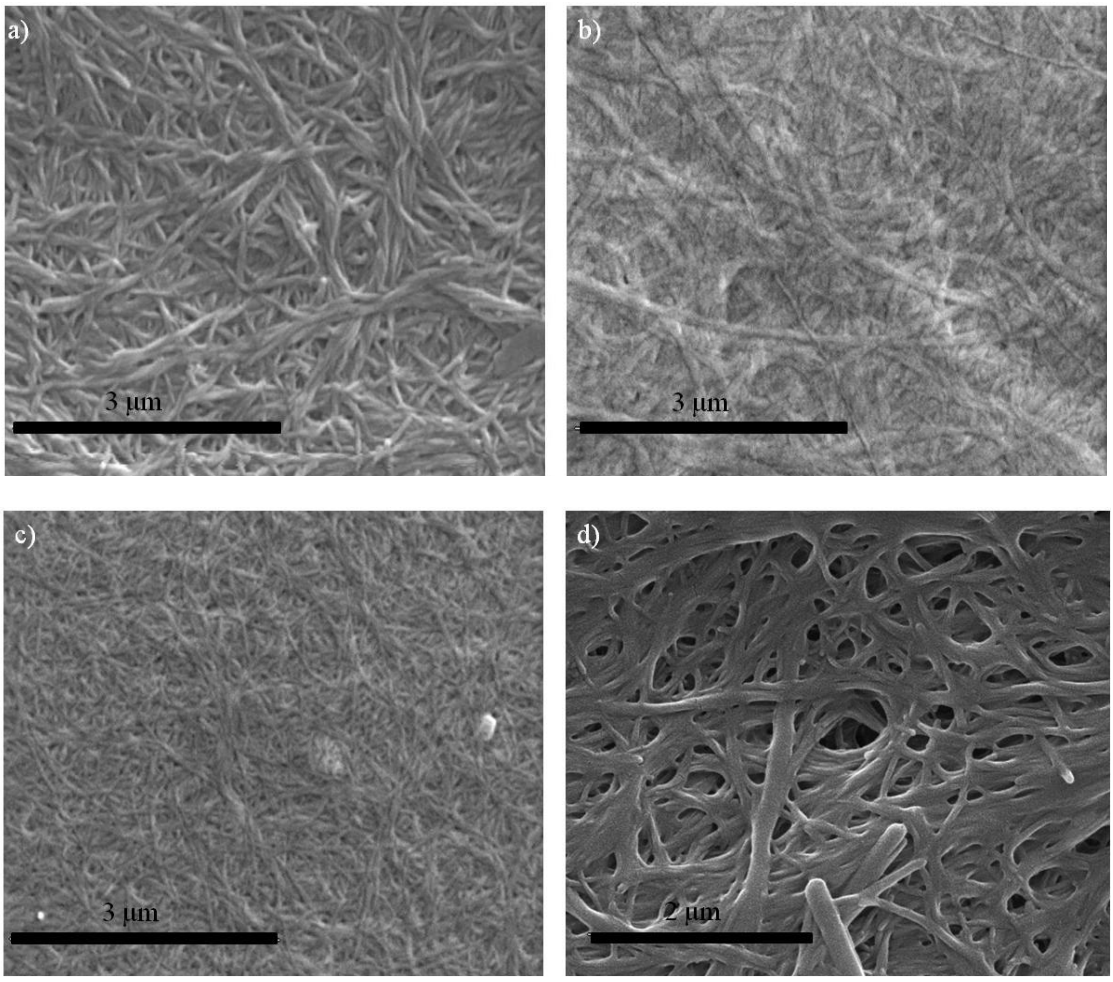

Fig. 3.28: a) SEM image of **Malt-Tz-C_{16}** (1 wt % water) xerogel, b) SEM image of **Malt-Tz-Phe-C_{16}** (1 wt % water) xerogel, c) SEM image of **Malt-Tz-Phe-C_{16}** (3 mg in

0.3 mL of water and 0.1 mL of methanol) xerogel, d) SEM image of **Malt-NH-Phe-C_{16}** (5 mg in 0.3 mL of water and 0.2 mL of methanol) xerogel.

In **Malt-Tz-C_{16}** the diameter of the observed fibers is around 80 nm and the length is in de order of several μm, see **Fig. 3.28.a**. Gels derived from compounds with phenylalanine, i.e. **Mal-Tz-Phe-C_{16}** (in water and in a mixture of methanol and water) and **Malt-NH-Phe-C_{16}** (in a mixture of methanol and water), display fibrillar structures with estimated diameters of around 80-200 nm, with lengths in the order of several μm, see **Fig. 3.28 b, c and d**.

In order to have a deeper insight into the fibers which form the fibrillar network, a dilution (0.1 wt %) of the different gels was measured by TEM, see **Fig. 3.29.** A drop of a sample was placed onto a carbon-carbon grid and later negatively stained with a uranyl acetate solution; also in this case the sample has to be dried.

In **Malt-NH-Phe-C_{16}** the fiber diameter was similar to the diameter observed by SEM, i.e. around 150 nm (**Fig. 3.29.d**), but in the cases of **Malt-Tz-Phe-C_{16}** and **Malt-Tz-C_{16}** the estimated diameters were smaller: around 15 nm for **Mal-Tz-Phe-C_{16}** in water (**Fig. 3.29.c**), 40-80 nm for **Mal-Tz-Phe-C_{16}** in mixture methanol/water and 40 nm for **Malt-Tz-C_{16}** (**Fig. 3.29.a**). This finding is consistent with the presence of bundles of fibers of tens of nanometers that are further interpenetrated to form the physical network and make the immobilization of the solvent possible. Furthermore, torsion was detected in the fibrillar structure studied. For instance, in **Malt-Tz-C_{16}** (**Fig. 3.29.b**) a twisted helical ribbon was observed in a dried sample of a 0.1% solution of the material in water.

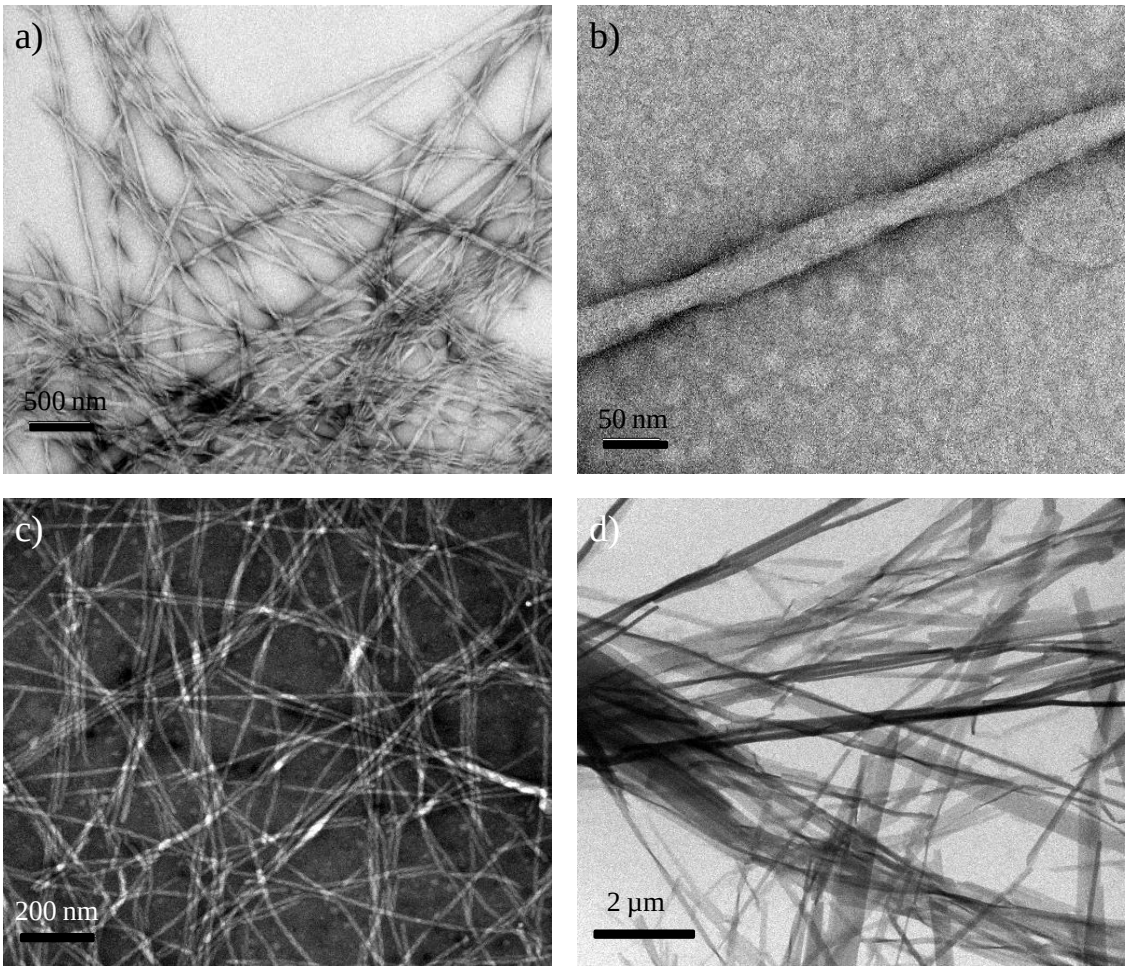

Fig. 3.29: a) TEM image of **Malt-Tz-C_{16}** (0.1 wt % water), b) TEM image of a single fiber of **Malt-Tz-C_{16}** (0.1 wt % water), c) TEM image of **Malt-Tz-Phe-C_{16}** (0. 1 wt % water), d) TEM image of **Malt-NH-Phe-C_{16}** (5 mg in 0.3 mL of water and 0.2 mL of methanol gel, diluted 10 times). TEM images were dried and negatively stained with a aqueous solution of uranyl acetate.

AFM measurements on **Malt-Tz-C_{16}** xerogel were also performed. A drop of the gel, placed onto graphite and subsequently dried with air, was directly observed. As it is shown in **Fig. 3.30**, fibers obtained from **Malt-Tz-C_{16}** have a twisted ribbon structure. If isolated fibers of **Malt-Tz-C_{16}** are observed a left handed orientation was detected. As example, a single fiber is showed in **Fig. 3.30.b.** Furthermore, when the thickness was measured along the fiber, different values were observed that are also in accordance with a helical arrangement of the ribbons instead of regular cylindrical fibers.

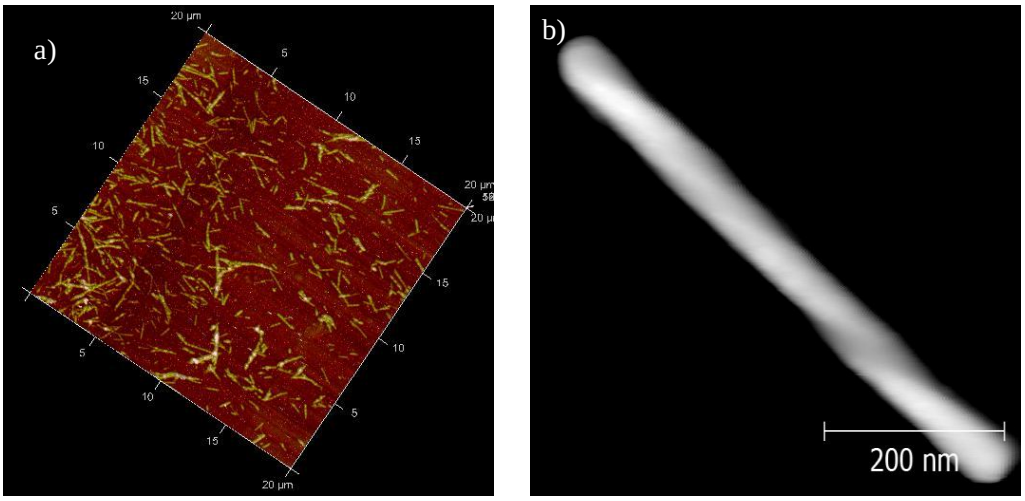

Fig. 3.30: AFM microphotographs of xerogel of **Malt-Tz-C$_{16}$** (1 wt %), b) single ribbon of **Malt-Tz-C$_{16}$** (1 wt %).

The drawback of the microscopic results described above is that the techniques require complete drying of the sample and consequently the structure could be modified. Moreover the stain has the potential of introducing artifacts interacting with the assemblies in a manner that can change their morphology.[9] Environmental scanning electron microscopy (ESEM) and cryo-transmission electron microscopy (Cryo-TEM) were used to study the native **Malt-Tz-C$_{16}$** hydrogel.

ESEM gives an insight on the micrometer structure under wet environmental conditions. **Fig. 3.31** shows microphotographs of a directly measured **Malt-Tz-C$_{16}$** hydrogel.

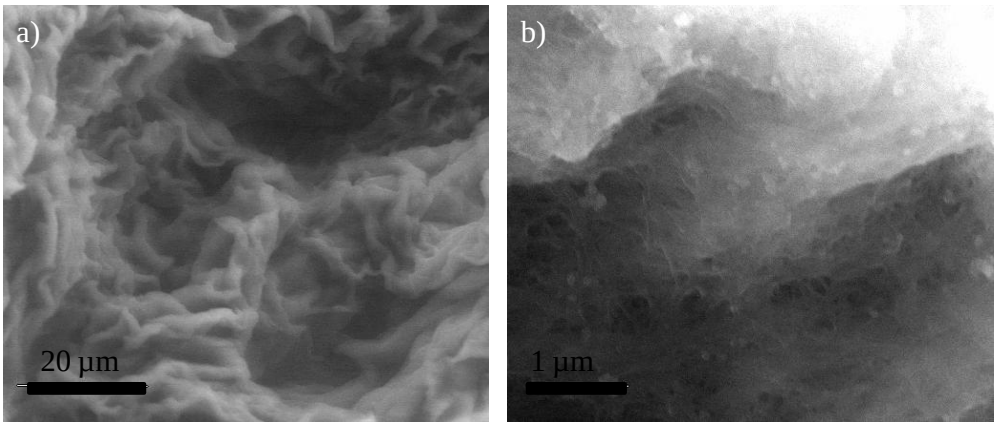

Fig. 3.31: Malt-Tz-C$_{16}$ 1 wt % ESEM microphotograph a) at 99.9% humidity and 3ºC and 759 Pa, b) at 5.0% humidity and 22.0ºC and 133 Pa.

The gel has a wrinkle brain-like texture at the scale of micrometers. When humidity decreases small fibers can be observed, which form the interpenetrated network, see **Fig. 3.31.b**. This technique also enables to observe the irregular holes of the structure.

An experiment was performed at a fixed temperature of 3 ºC while the humidity was decreasing from 99.9 % to 10 % in an established area, in order to observe possible changes promoted by drying. In a sample of **Malt-Tz-C_{16}** 1 wt % hydrogel no drastic modifications in the structure were detected, see **Fig. 3.32**. According to these results it can be concluded that the xerogel obtained by removing the solvent has morphology similar to wet structure of the gel.

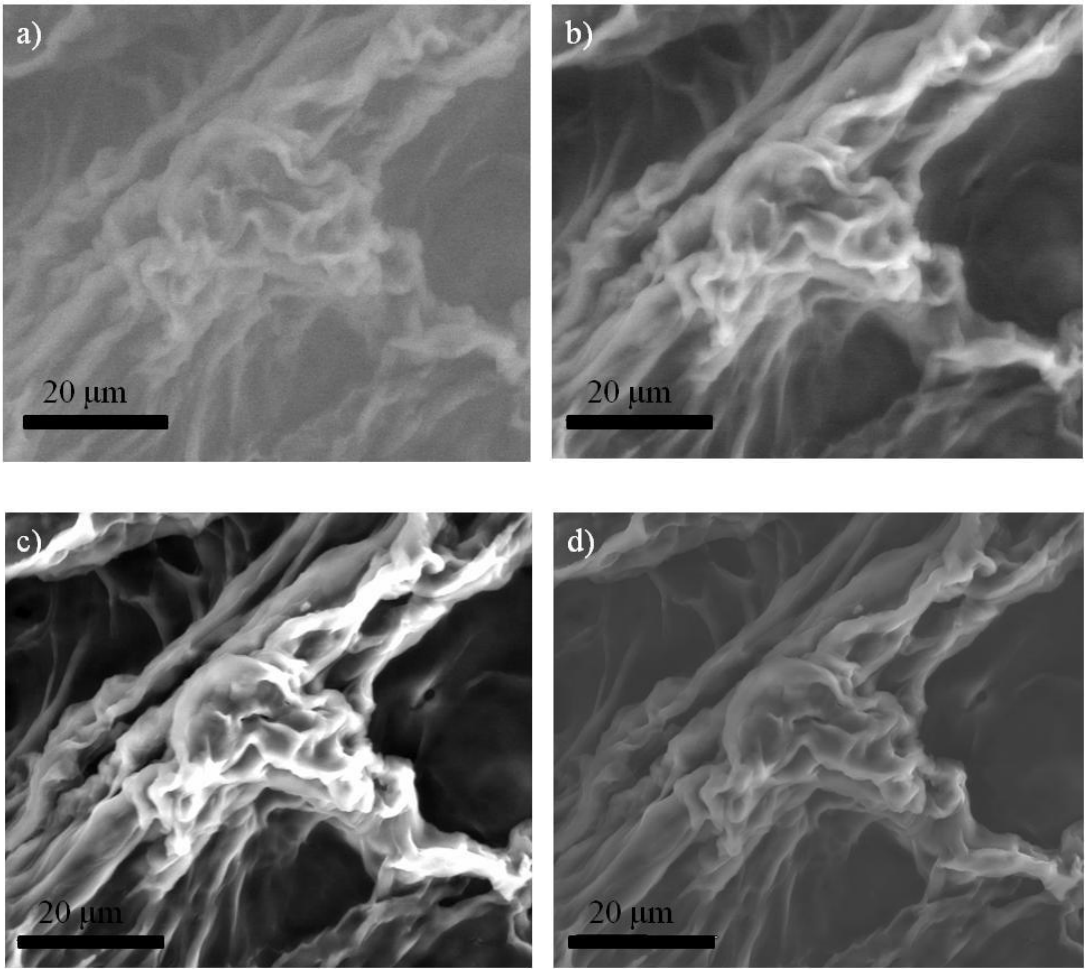

Fig. 3.32: Malt-Tz-C_{16} 1 wt % water ESEM microphotographs: a) at 99.9% humidity, 3ºC and 759 Pa b) at 65.8 % humidity, 3ºC and 500 Pa, c) at 20.0 % humidity, 3ºC and 152 Pa, d) at 10.0 % humidity, 3ºC and 76 Pa.

Cryo-TEM experiments were carried out also directly in the **Malt-Tz-C_{16}** 1 wt % hydrogel. The aqueous sample was flash-frozen in liquid ethane at the temperature of liquid nitrogen, creating thin vitrified ice films onto the grid and observed by TEM. Microphotographs of the gel are shown in **Fig. 3.33**. Ribbons resulting from the self-assembly of the amphiphile were detected by this technique.

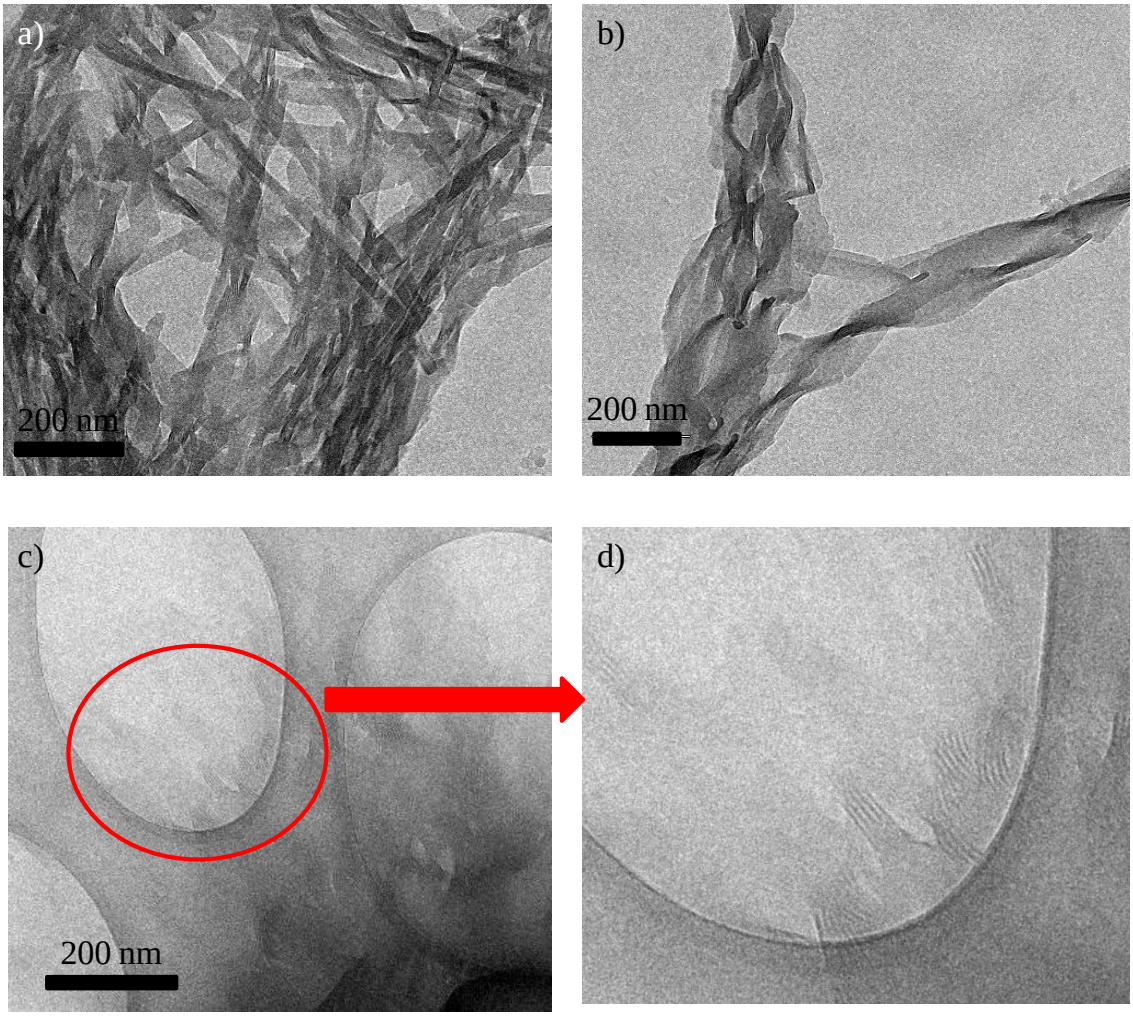

Fig. 3.33. Cryo-TEM images of **Malt-Tz-C_{16}** 1 wt % water gel: a), b) and c) twisted ribbon and d) close up of a part of the microphotograph c).

On studying the twisted part of a ribbon, it can be seen that their cross-sections show alternate dark and bright regions (as can be seen in the close up of **Fig. 3.33.d**) with a thickness of these regions of about 2 nm and 2.5 nm, respectively. A model, shown in **Fig. 3.34** is proposed to explain the assembly of **Malt-Tz-C_{16}** amphiphiles in water into ribbons and the resulting layered structure of the cross-section.

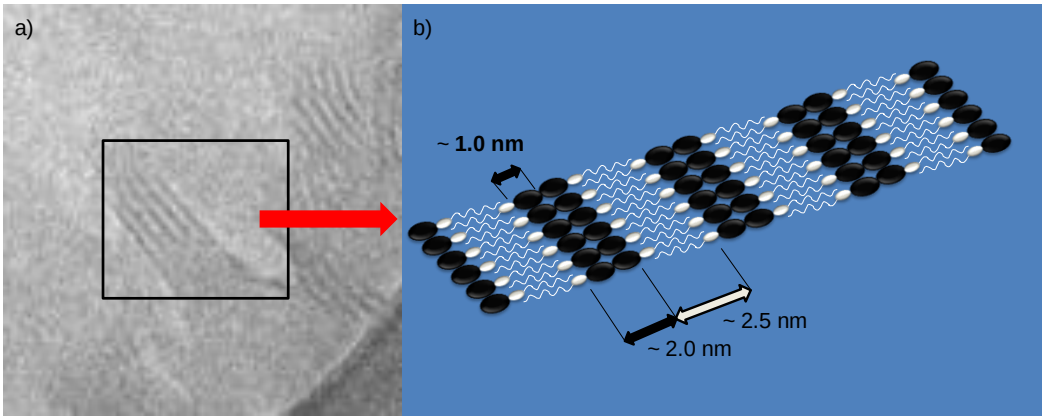

Fig. 3.34: a) Close up of microphotograph c) in **Fig. 3.33,** b) model proposed for the self-assembled **Malt-Tz-C_{16}** hydrogel.

This layered structure of the cross-section of ribbons is formed by alternating hydrophilic parts, consisting of a bilayer of sugar polar heads, and hydrophobic parts of interdigitated aliphatic domains. In fact, the theoretical length of the hydrophobic part is about 25 Å (18.5 Å for the palmitic chain and 6.6 Å for the amide and triazole ring, **see Fig. 3.23**), which is in accordance with the thickness of the bright motives of around 2.5 nm. In the same way the theoretical length of the disaccharide is around 10 Å. The thickness of the dark motive is around 2 nm, which is in accordance with a disaccharide bilayer.

X-ray diffraction experiments were performed on **Malt-Tz-C_{16}** sample. X ray diffraction patterns of a gel 1 wt % in water and lyophilized gel (xerogel) were recorded and compared, see **Table 3.4** and **Fig. 3.35**.

Table 3.4: Spacing measured by X-ray diffraction for **Malt-Tz-C_{16}** 1 wt % water and the lyophilized sample (xerogel).

GEL (100 mm)	XEROGEL (80 mm)
44.0 Å	44.8 Å
26.8 Å	15.4 Å
3.4 Å	4.0 Å
	3.6 Å

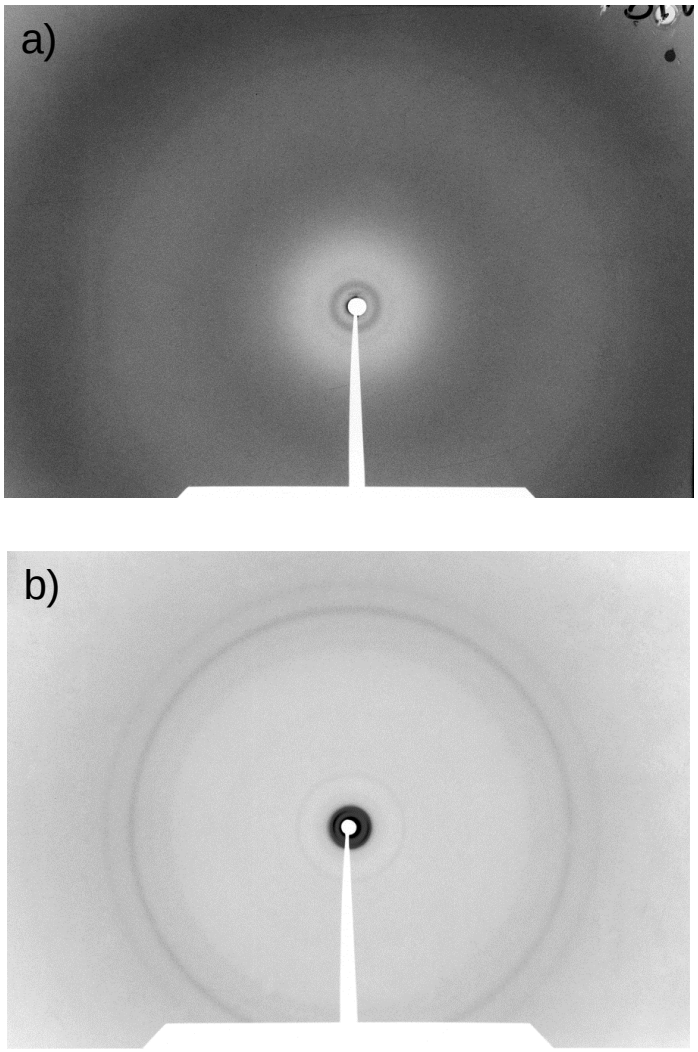

Fig. 3.35: XRD diffractograms of **Malt-Tz-C_{16}**: a) gel 1 wt %, b) lyophilized gel. The experiments were recorded at RT.

Information from the powder pattern obtained is the long *d* spacing which corresponds to the longest repeat distance in the structure. In both cases, this *d* spacing was around 44 Å. This pattern is larger than the length of one molecule (34.8 Å, see **Fig. 3.23**) but smaller than twice the extended molecular length. This result indicates that an interdigitated tilted bilayer was probably formed as it was observed in cryo-TEM. However, other reflections characteristic of the lamellar order were no clearly found for the gel. In the lyophilized sample (xerogel) only the third order reflection was found (15.4 Å).

Supramolecular Chirality. The twisted fibrillar structure observed by previous microscopic techniques can indicate a chiral supramolecular organization in the hydrogel of **Malt-Tz-C_{16}**. In order to confirm this possibility, circular dichroism (CD) measurements were carried out both in solution and hydrogel state of this compound and the results are collected in **Fig. 3.36**.

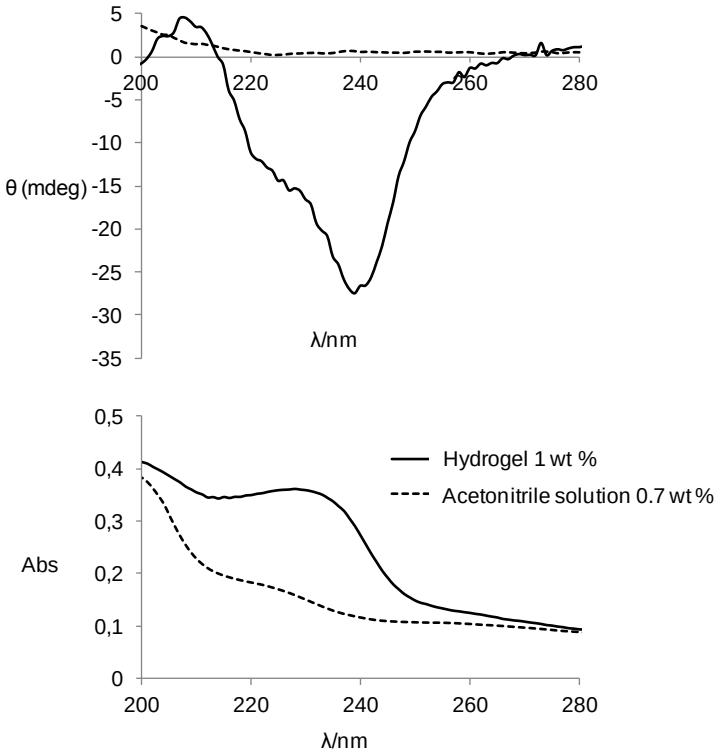

Fig. 3.36: CD (top) and UV-vis (botton) spectra of **Malt-Tz-C_{16}**: (a) dashed line: acetonitrile solution (0.7 wt %) and (b) solid line: hydrogel 1 wt % of **Malt-Tz-C_{16}**.

The λ_{max} value for a **Malt-Tz-C_{16}** solution 0.7 wt % in acetonitrile in the UV absorption spectrum appears at around 224 nm and the λ_{max} value for a **Malt-Tz-C_{16}** hydrogel at 1 wt % in the UV absorption spectrum appears at around 232 nm. This absorption can be assigned to the triazole group. A Cotton effect was not observed in the CD spectrum of a solution of the compound in acetonitrile. However, the hydrogel of this compound (1 wt %), when placed between two quartz discs, exhibited a negative Cotton effect where the θ_{min} value appeared at 236 nm which is very slightly displaced from the λ_{max} in the UV spectrum (232 nm). We confirmed that the contribution of the linear dichroism (LD) to the true CD spectrum is negligible by comparing several CD spectra recorded at different angles around the incident light beam. See **Characterization Techniques 7.**

Annex for experimental conditions. The Cotton effect for the gel sample supports the hypothesis that an ordered chiral structure is formed by self-assembly and gelification in aqueous solution.

In order to gain an insight into the supramolecular aggregates formed in water, a dilute solution containing 0.01% wt of **Mal-Tz-C$_{16}$** was studied by CD, see **Fig. 3.37.**

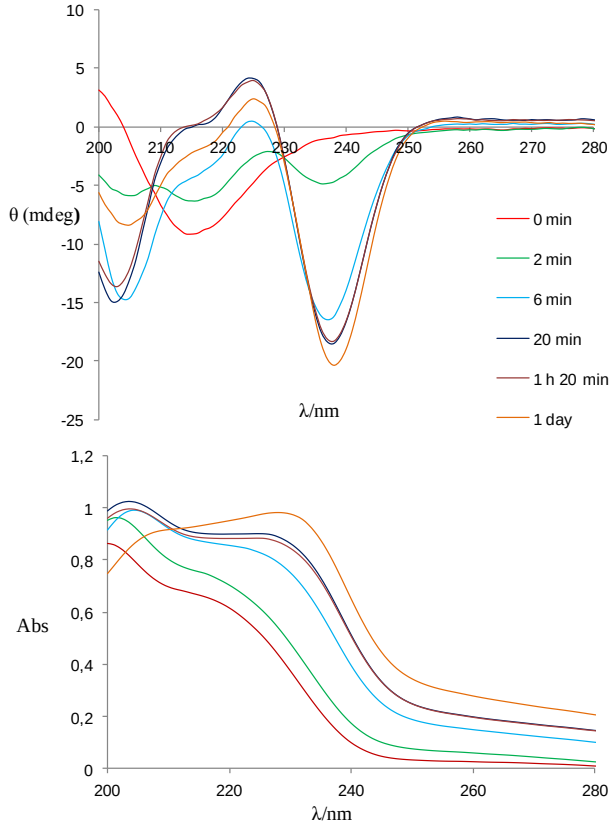

Figure 3.37: CD (top) and UV-vis (bottom) spectra of a solution of **Malt-Tz-C$_{16}$** (0.01 wt % in water) taken at different times once the solution has been previously heated to 80 ºC and left to cool to RT.

This solution was first heated to 80 ºC and then cooled down to RT. The evolution of the UV-vis and CD spectra was then registered. A displacement in the λ_{max} from 220 nm to 235 nm in the UV spectrum was observed and an evolution of the corresponding CD signal was also observed. A cloudy solution was eventually obtained due to aggregation. It can be observed that there is an evolution of the signal corresponding to the aggregates formed in solution (it should be remarked that in this concentration, gel formation does not take place). Despite the different experimental conditions, the final

CD spectrum exhibits as main band a negative Cotton effect at a similar wavelength as the one observed in the gel state and corresponding to the absorption of the triazole ring. This result may indicate a similar supramolecular arrangement of amphiphiles in a chiral fibrillar structure.

3.4. Glycolipids derived from cellobiose or lactose and palmitic acid

According to the results described above, amphiphilic glycolipids prepared by clicking a hydrophobic linear chain to a maltose polar head by copper(I)-catalyzed azide-alkyne [3+2] cycloaddition resulted to be hydrogelators. This click reaction[23] provides a satisfactory synthetic pathway to link parts with different polarity and the resulting triazole unit can afford a rigid fragment that favors the directional self-assembly in one dimension to build fibers. Moreover, the dipole moment of the triazole unit increases the hydrophilicity of the amphiphile, thus aiding the gelation process in water.[9, 25] Due to the good gelation properties of **Malt-Tz-C_{16}** as hydrogelator, this compound was selected as reference in order to modify the disaccharide polar head and study its influence o on the gelation properties see **Fig. 3.38**.

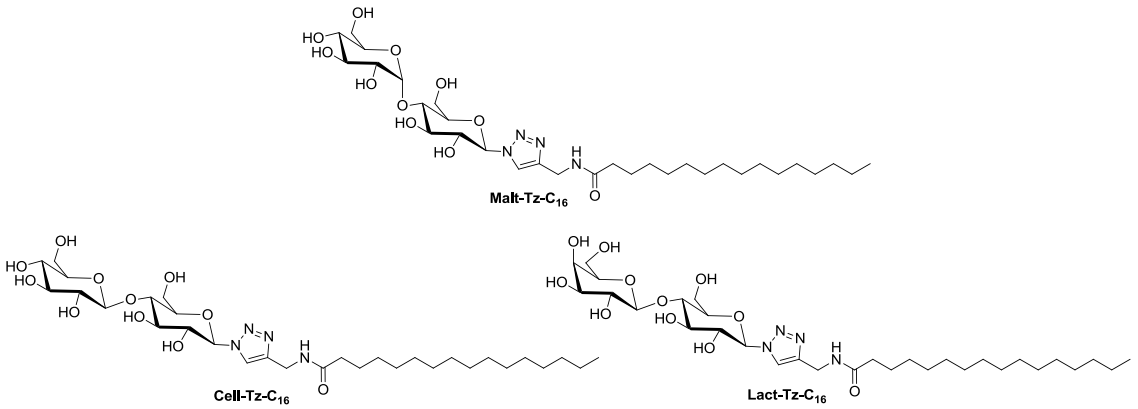

Figure 3.38. Chemical structure and nomenclature of the glycolipids.

In this section we prepared two new hydrogelators based on different disaccharide polar head. Cellobiose has a β (1→4) connection between two glucoses instead of the α (1→4) connection of maltose. In the case of lactose the terminal sugar ring is galactose instead of glucose. These disaccharides, with different stereochemistries also adopt

preferential conformations[26] that can induce different packing of the corresponding low molecular mass amphiphiles.

The liquid crystalline properties of the amphiphilic materials were also characterized. The fibrillar supramolecular structures formed by the self-assembly were studied by different microscopic techniques on the dried gel (xerogel) and hydrated conditions in order to characterize the micro and nano-structures.

3.4.1. *Synthesis*

Cell-Tz-C_{16} and **Lact-Tz-C_{16}** glycoamphiphiles were synthesized by click coupling of the disaccharide polar head and the aliphatic chain as was previously described for **Malt-Tz-C_{16}** and **Malt-Tz-Phe-C_{16}** and the synthetic pathway is shown in **Scheme 3.8**. The connecting group is a triazole ring bearing a neighboring amide group. The triazole ring was formed by a copper(I)-catalyzed azide-alkyne [3+2] cycloaddition using a disaccharide azide and *N*-propargylpalmitamide **8**.

The synthesis of the disaccharide-azides was performed using the corresponding peracetylated sugar as the starting material. Peracetylated lactose **10** was synthesized using sodium acetate and acetic anhydride and peracetylated cellobiose was commercially purchased. Glycosyl azides **11** and **12** were synthesized stereoselectively employing the general procedure described by Paulsen[21, 27] and previously used for maltosylazide **5**. Glycosyl azides react through a 1,3-dipolar cycloaddition with *N*-propargylpalmitamide **8**. The click reaction was carried out in DMF using CuBr and N-pentamethyldiethylenetriamine (PMDETA) to give the desired product. All of the protected derivatives were deacetylated at RT according to Zemplen´s conditions (MeONa and Amberlyst IR120 in anhydrous MeOH) to give the final product in almost quantitative yield.

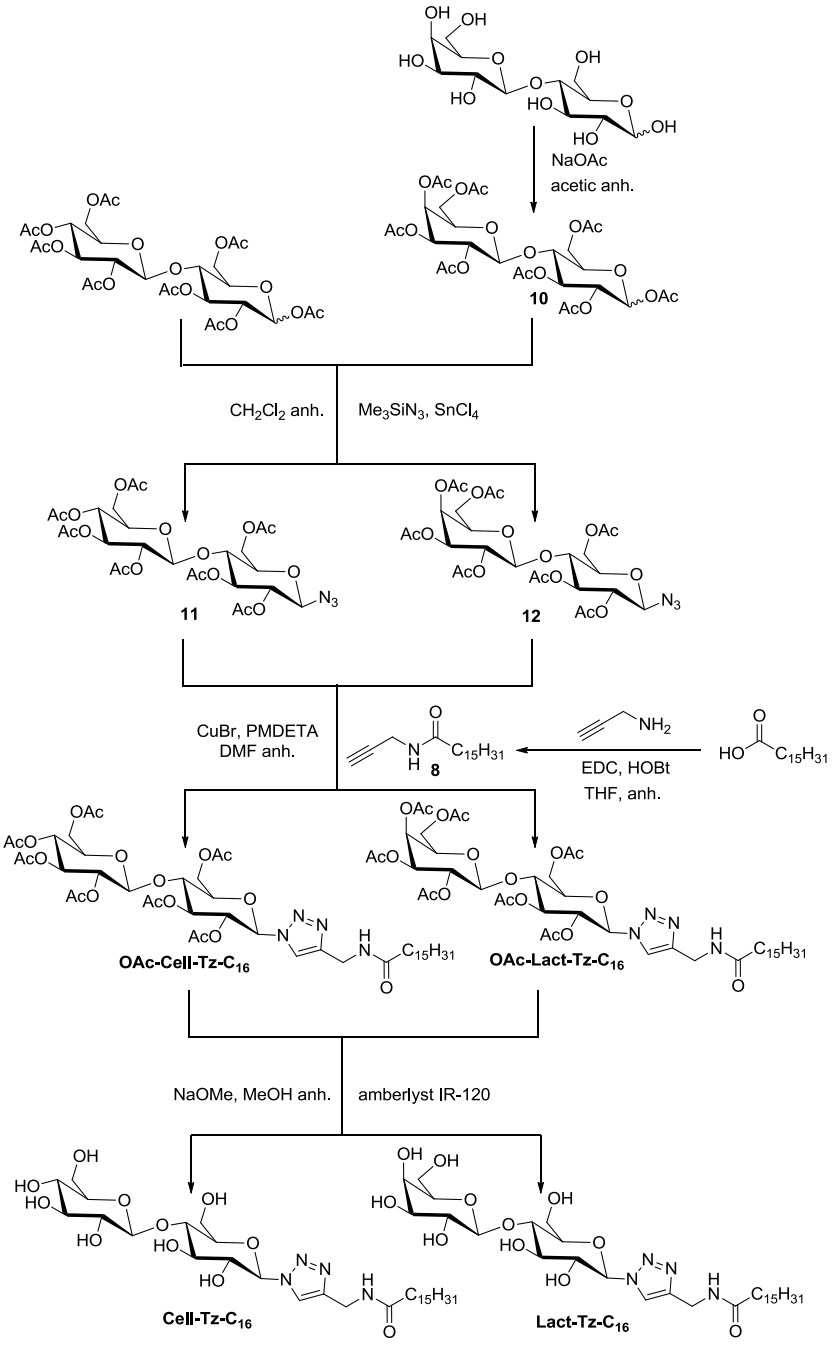

Scheme 3.8. Synthesis of **Cell-Tz-C_{16}** and **Lact-Tz-C_{16}**.

The peracetylated precursors and the glycoamphiphiles were fully characterized by ^{1}H and ^{13}C NMR, IR and mass spectrometry. ^{1}H NMR spectra of **OAc-Lact-Tz-C_{16}** and **Lact-Tz-C_{16}** are shown in **Fig. 3.39** as example.

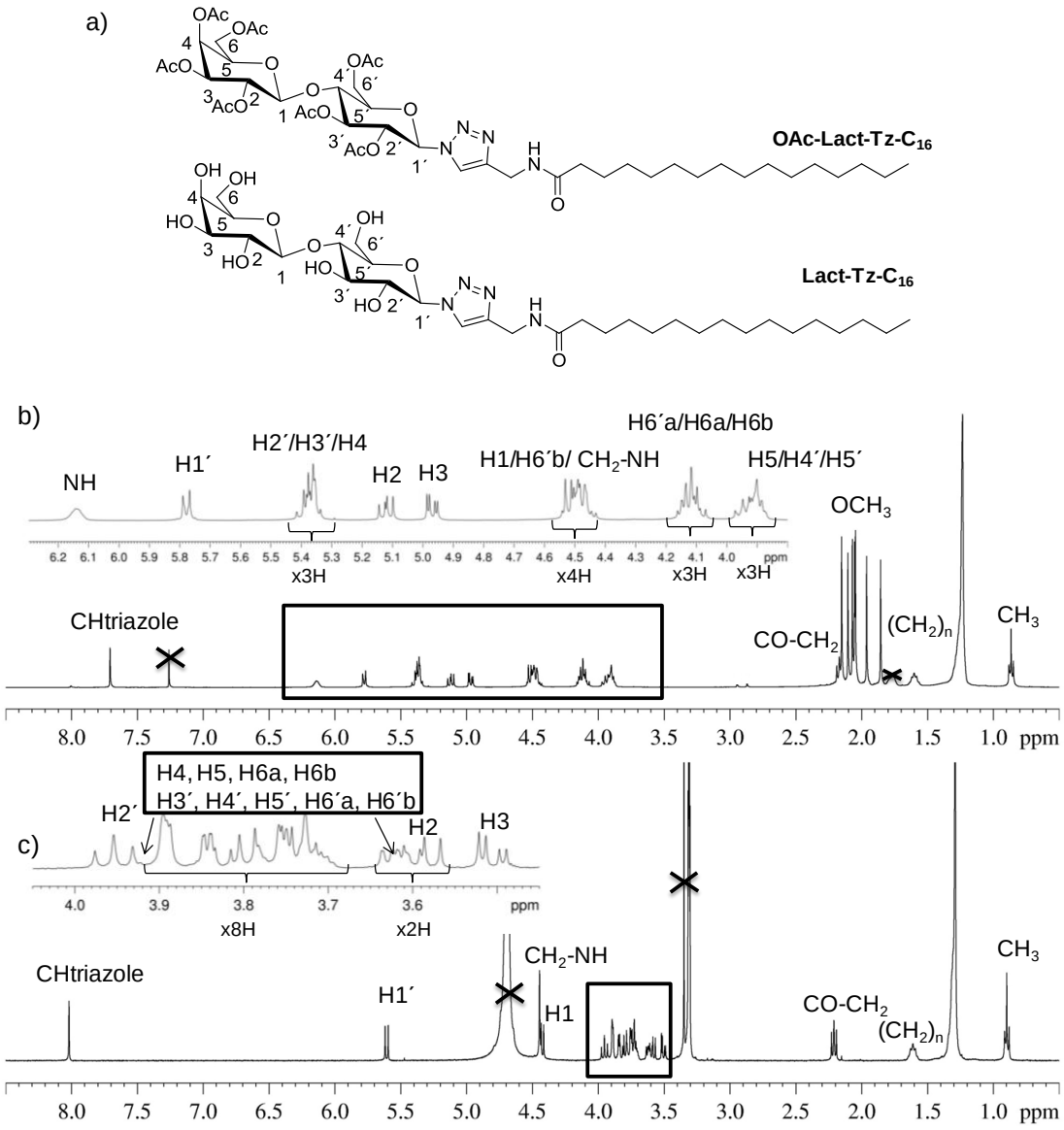

Figure 3.39: a) **OAc-Lact-Tz-C$_{16}$** and **Lact-Tz-C$_{16}$** chemical structure, b) ^{1}H NMR spectrum of **OAc-Lact-Tz-C$_{16}$** with $CDCl_3$ as solvent at 25ºC, c) ^{1}H NMR spectrum of **Lact-Tz-C$_{16}$** with MeOD as solvent at 50 ºC.

2D NMR experiments COSY, TOCSY, NOESY, HSQC and HMBC were also performed in order to corroborate the chemical structure of the glycolipids. It can be seen in **Fig. 3.39 and 3.40** that all of the sugar protons of **OAc-Lact-Tz-C$_{16}$** can be assigned. These assignments are supported, as example, by TOCSY experiments (Fig 3.40). For a full elucidation of **OAc-Cell-Tz-C$_{16}$** and **Cell-Tz-C$_{16}$** molecules see **section 3.6. structural characterization** where correlations and determination of signals are explained.

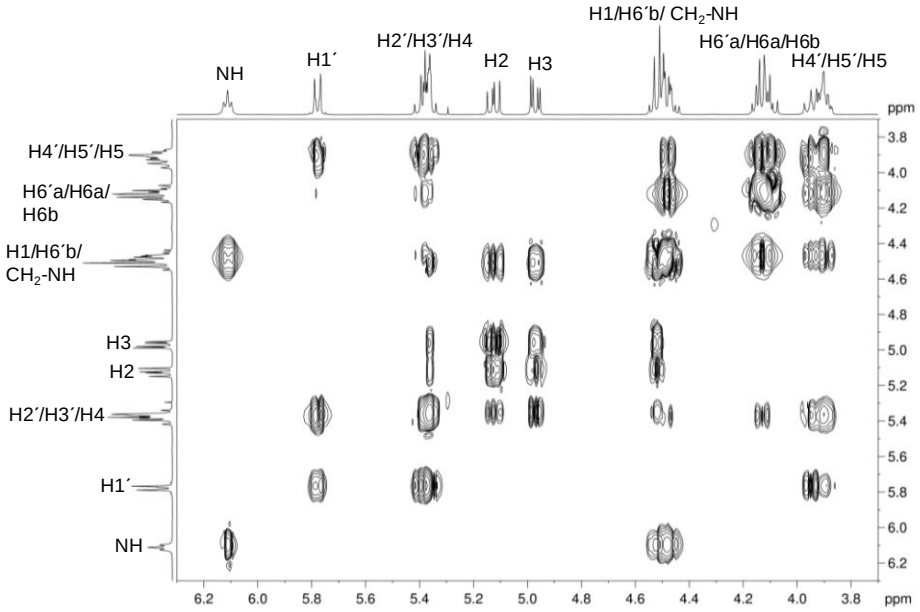

Fig. 3.40: TOCSY spectrum of **OAc-Lact-Tz-C_{16}** with $CDCl_3$ as solvent at 25ºC and 90 ms of mixing time.

3.4.2. *Thermal properties*

The mesomorphic properties of the synthesized amphiphilic glycolipids and the peracetylated precursors were studied by polarizing optical microscopy (POM) and differential scanning calorimetry (DSC).

Thermogravimetry of glycoamphiphile samples previously dried and immediately analyzed showed weight losses at temperatures due to a massive thermal decomposition process above 275 ºC while the peracetylated compound showed weight losses at temperatures around 310ºC, see **Table 3.5** and **Fig. 3.41**.

Table 3.5: Thermogravimetric analysis of peracetylated precursors and glycolipids.

Compound	$T_{5\%lost}$	T_{onset}	T_{max}
OAc-Cell-Tz-C_{16}	310ºC	323ºC	345ºC
OAc-Lact-Tz-C_{16}	305ºC	320ºC	345ºC
Cell-Tz-C_{16}	275ºC	302ºC	330ºC
Lact-Tz-C_{16}	278ºC	298ºC	330ºC

$T_{5\%lost}$ = Temperatures at which 5% of the initial mass is lost. T_{onset} = Onset of decomposition. T_{max} = Temperatures at which the maximum rate of weight loss is produced.

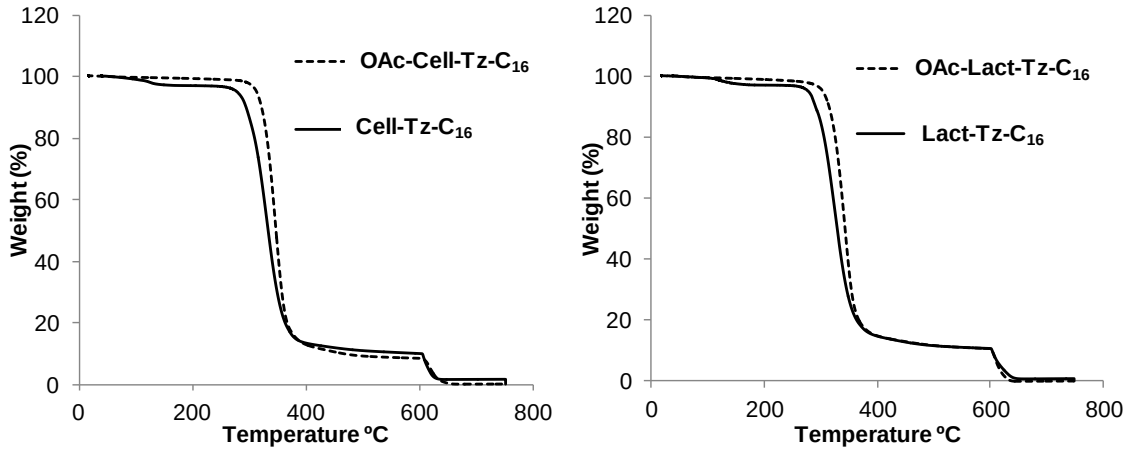

Fig. 3.41: Thermogravimetric curves of peracetylated compounds versus their corresponding glycoamphiphiles.

The peracetylated precursors were studied by polarizing optical microscopy (POM) as a function of temperature and mesomorphic behavior was not observed. DSC experiments confirm that **OAc-Cell-Tz-C_{16}** melts directly from a crystalline state to an isotropic liquid at 175 ºC, see **Table 3.6** and **Fig. 3.42**. Nevertheless, in the DSC study of **OAc-Lact-Tz-C_{16}** crystallization was not observed on cooling the molten state and a glassy material was obtained, see **Table 3.6**. DSC traces corresponding to the second or subsequent scans only exhibit a glass transition at 52 ºC, see **Fig. 3.42**.

Table 3.6: Thermal transitions of the synthesized glycolipids determined by DSC (10ºC.min^{-1})

Compound	Thermal transition (ºC) [ΔH kJ/mol]
OAc-Cell-Tz-C_{16}	Cr 175 [37.7] I[a]
OAc-Lact-Tz-C_{16}	g 52 I[a]
Cell-Tz-C_{16}	Cr 159 [1.9][b] S_A
Lact-Tz-C_{16}	Cr 147 [1.5][b] S_A

[a] The heating scans were carried out up to 200 ºC. Data from the second heating scan. [b] The heating scans were carried out up to 165 ºC to avoid decomposition. Data from the second cycle scan. Decomposition was observed in the third heating scan carried out up to 250 ºC. Decomposition temperatures are around 170–175 ºC. Cr = Crystal, I = Isotropic phase, S_A = Smectic A phase, g = Glassy state.

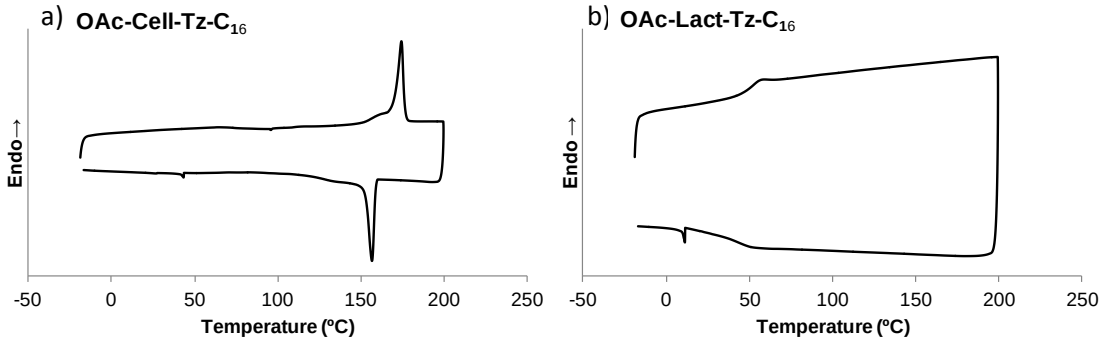

Fig. 3.42: DSC curves for the second scan in the solid state of a) **OAc-Cell-Tz-C_{16}**, b) **OAc-Lact-Tz-C_{16}.**

The glycolipids **Cell-Tz-C_{16}** and **Lact-Tz-C_{16}**, as with the previously reported **Malt-Tz-C_{16}**, exhibited birefringent textures associated with thermotropic liquid crystalline behavior. The poorly defined birefringent textures of the viscous mesophase (see **Fig. 3.43**) precluded unambiguous assignment of the mesophase by this method. However, according to previous results obtained on the maltose derivative, it can be assigned as smectic. This fact was subsequently confirmed by X ray diffraction experiments (see below). Samples become brown due to decomposition at temperatures above 170ºC.

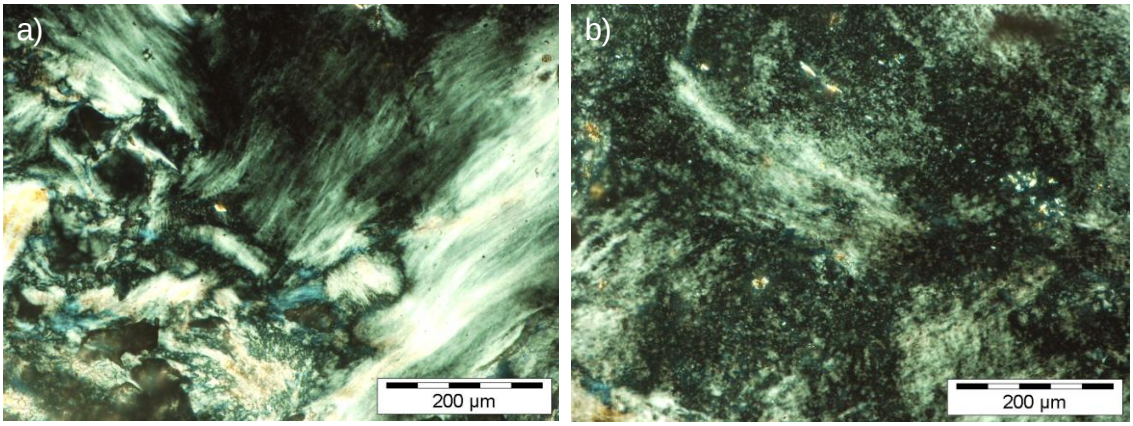

Fig. 3.43: Microphotograph of a) **Cell-Tz-C_{16}** taken at 165ºC, first heating, b) **Lact-Tz-C_{16}** taken at 165 ºC, first heating.

A DSC study of the glycolipids was performed by heating the compounds to 165 ºC in the first and second scans, before decomposition in the third scan, in order to minimize thermal decomposition of the samples, which was observed in this technique around

170–175ºC. In the third scan the sample was heated to 260 ºC. Under these conditions the second and third scans were reproducible and the transition data are gathered in **Table 3.7**.

As described above **Malt-Tz-C_{16}** was characterized and exhibits a peak corresponding to the melting transition at around 50 ºC. Above this temperature the sample is highly viscous and at temperatures above approximately 90 ºC the sample becomes more fluid and can be clearly characterized as liquid crystalline according to the optical observations. Similar behavior was observed for **Cell-Tz-C_{16}** and **Lact-Tz-C_{16}** although the mesophase appeared at a higher temperature, around 160 and 150 ºC, respectively, see **Fig. 3.44**. Textures were analogous to those observed for **Malt-Tz-C_{16}**. On heating samples up to 250 ºC, peaks corresponding to decomposition were observed at around 170–175 ºC, as was detected for **Malt-Tz-C_{16}**.

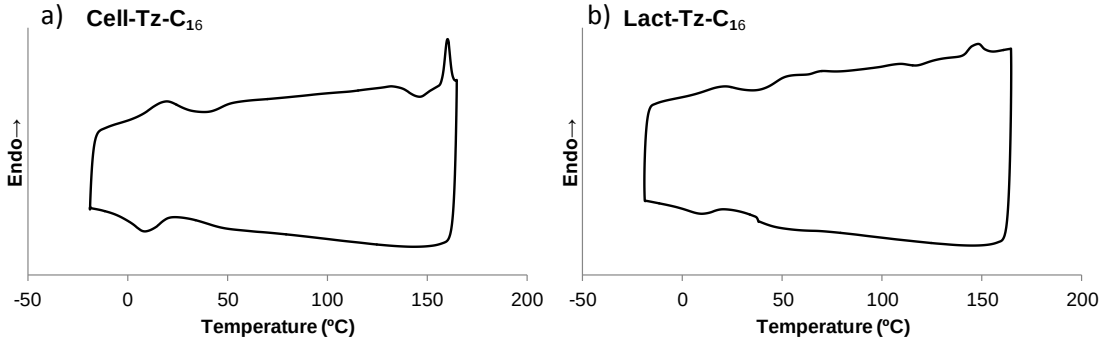

Fig. 3.44: DSC curves for the second scan in the solid state of (a) **Cell-Tz-C_{16}** and (b) **Lact-Tz-C_{16}**.

The smectic mesophase for **Cell-Tz-C_{16}** and **Lact-Tz-C_{16}** was confirmed by X ray diffraction (XRD), see **Fig. 3.45** for **Cell-Tz-C_{16}** and **Lact-Tz-C_{16}** powder. The lamellar spacing was measured close to 47 Å, which indicates an interdigitated SmA bilayer. Second and third order was also observed.

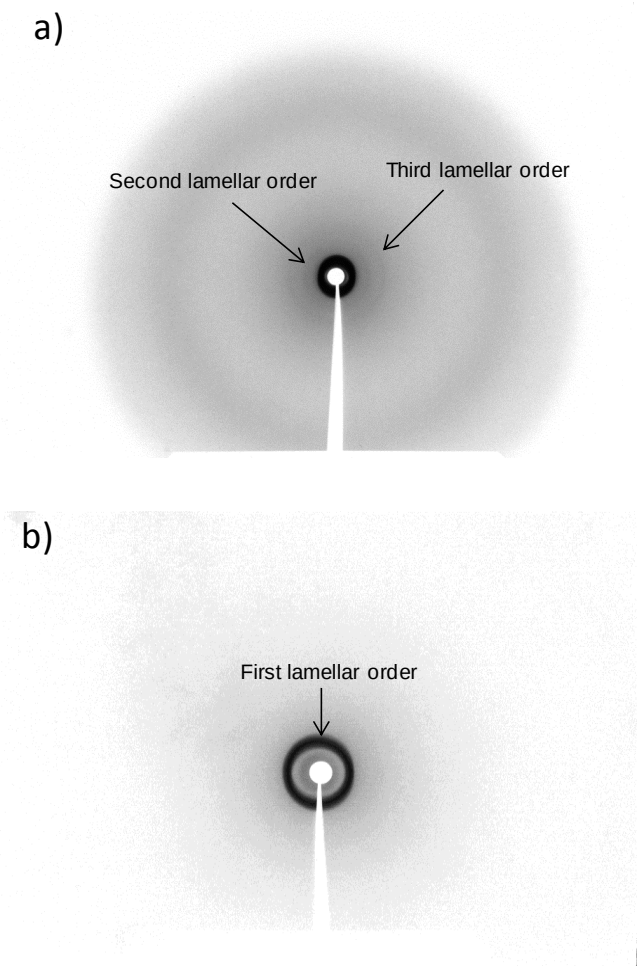

Fig. 3.45: a) X-ray patterns of **Cell-Tz-C_{16}** recorded at 160º C for 2.5 h, b) detail of the small angle region recorded at 160ºC for 1.5 h.

3.4.3. *Supramolecular Gels*

The solubility and gelation ability of **Cell-Tz-C_{16}** and **Lact-Tz-C_{16}** glycolipids were examined in different solvents by dissolving 5 mg of compound in about 0.1–1 mL of the solvent, i.e. 0.5–5 wt % (the gelator and the solvent were placed in a septum-capped test tube). The results are summarized in **Table 3.7**. Glycoamphiphiles are not soluble at RT in the selected solvents except for DMSO. However, in some of the selected solvents, the glycolipids eventually dissolved on heating. The solution was then cooled down to RT and a solution, a precipitate or a gel was observed depending on the solvent. The formation of a gel was registered if the tube was turned upside down and the solution did not flow. Results are compared with **Malt-Tz-C_{16}** compound described in **section 3.3.3**.

Table 3.7: Solubility and gelation properties of glycolipids in different solvents, after heating and cooling down to RT.[a]

Solvent	Cell-Tz-C_{16}	Lact-Tz-C_{16}	Malt-Tz-C_{16}
Hexane	I	I	I
Ethyl Acetate	I	I	I
Tetrahydrofuran	I	I	S
Dichloromethane	I	I	I
Acetone	I	I	I
Methanol	P	P	S
Water	G[b]	G[c]	G[c]
Dimethylsulfoxide	S	S	S

[a] I = Insoluble, P = Precipitate, S = Solution, G = Gel.[b] Gels are formed at 0.5 wt %. [c] Gels are formed at 1wt %.

Cell-Tz-C_{16} and **Lact-Tz-C_{16}** form hydrogels, see **Fig 3.46,** as the analog **Malt-Tz-C_{16}**.[28] Maltose and lactose derivatives both gel at a minimum concentration of 1 wt % while the cellobiose derivative gels at a minimum concentration of 0.5 wt %. In order to solubilize the glycolipids in water, solutions were first heated to 90–100 ºC and then cooled to RT. Hydrogels were obtained in the cooling process. In all cases the gels are stable at RT and thermoreversible. The sol state can be achieved again by reheating. Thus, the septum-capped test tube was heated in a heating block and the gel-sol transition occurs for **Cell-Tz-C_{16}** at 95 ºC and for **Lact-Tz-C_{16}** at 85 ºC.

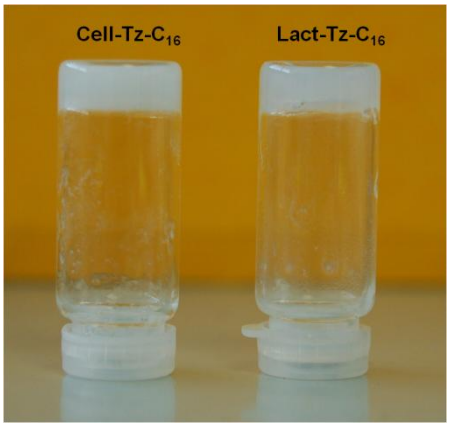

Fig. 3.46: Hydrogel of **Cell-Tz-C_{16}** (0.5 wt %) and **Lact-Tz-C_{16}** (1 wt %).

To better establish the gel-sol transition, hydrogels were studied by DSC (under a nitrogen atmosphere, 10 ºC min^{-1}). The hydrogel of **Cell-Tz-C_{16}** (0.5 wt %) shows a broad endothermic peak at around 90 ºC, see **Fig. 3.47**, which is consistent with the results obtained on heating the sample in a heating block and corresponds to the gel-sol transition. A thermal peak was not observed in the cooling scan, however, in the second (or subsequent) heating scans the peak at around 90 ºC was again observed, thus confirming the reversibility of this transition. In the case of **Lact-Tz-C_{16}**, peaks corresponding to the sol-gel transition were not clearly detected by DSC (under 10 ºC.min^{-1} or 5 ºC.min^{-1}). That fact is probably due to the fact that the transition occurs in a more extended temperature range and the low enthalpic content.

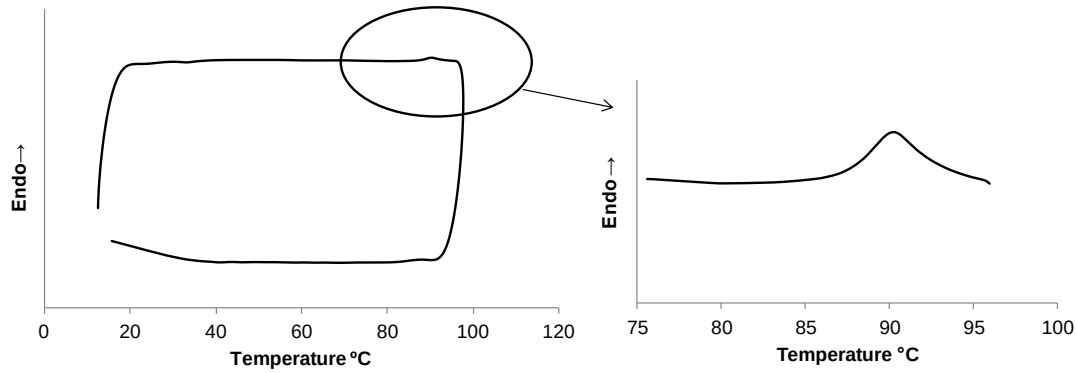

Fig. 3.47: Third DSC thermal cycle in a nitrogen atmosphere (10 ºC.min^{-1}) of **Cell-Tz-C_{16}** (0.5 wt %) hydrogel.

NMR experiments also provide information about gel-sol transitions. On progressive heating a gel sample in D_2O, the spectrum was fully resolved once the corresponding sol (clear solution) is obtained. **Cell-Tz-C_{16}** gel (0.5 wt % D_2O) was fully resolved at around 95ºC, see **Fig. 3.48** and **Lact-Tz-C_{16}** (1 wt % D_2O) gel was fully resolved at around 80ºC, see **Fig. 3.49**.

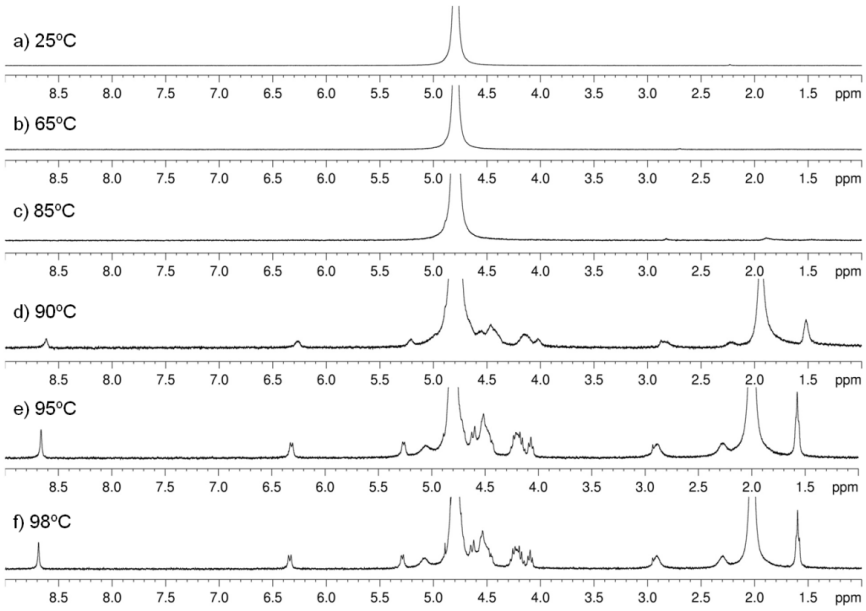

Fig. 3.48: ^{1}H NMR spectra of **Cell-Tz-C$_{16}$** hydrogel, 0.5 wt % D_2O, taken at different temperatures.

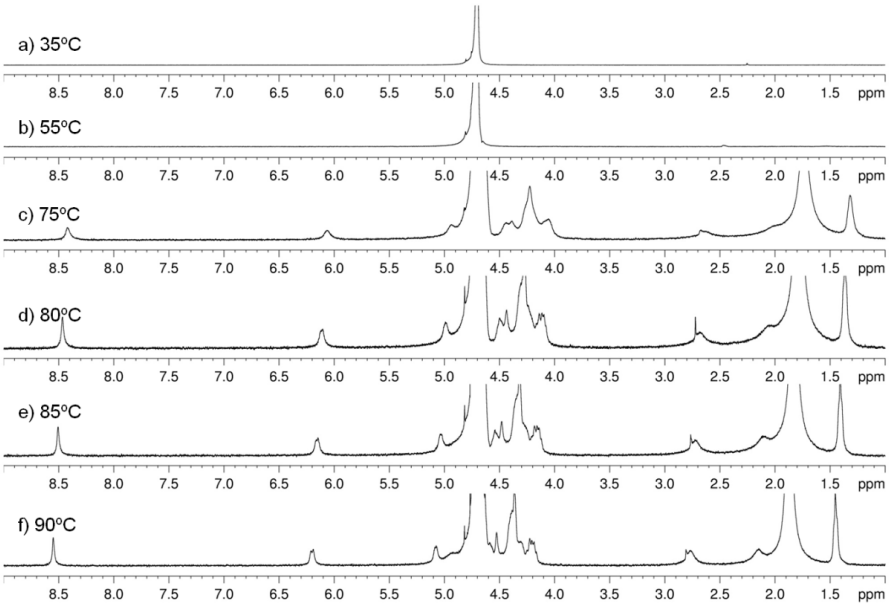

Fig. 3.49: ^{1}H NMR spectra of **Lact-Tz-C$_{16}$** hydrogel, 1 wt % D_2O, taken at different temperatures.

In the case of **Malt-Tz-C$_{16}$** it was reported that the gel-sol transition occurs by DSC at around 65 ºC, consequently **Cell-Tz-C$_{16}$** and **Lact-Tz-C$_{16}$** present a gel state with a higher temperature range. The nature of the sugar polar head and specially the nature of

the glycosidic linkage between the two units (α 1→4 for maltose, β 1→4 for cellobiose and lactose) seems to influence the stability of the supramolecular network that supports the gels and on the gel-sol temperature or minimum gel concentration.

It is known that two of the driving forces that can promote gel formation are π-π stacking of aromatic rings and H-bonding. The structure of the synthesized glycoamphiphiles contains a 1,2,3-triazole ring and an amide group, both of which could be responsible for the molecular aggregation and formation of the supramolecular gel. In an effort to confirm the participation of these groups in the supramolecular assembly, ^{1}H NMR experiments were performed by adding gradually water to a DMSO solution of the glycolipids, according to the experiment described by Suzuki and coworkers.[29]

For both compounds, **Cell-Tz-C$_{16}$** and **Lact-Tz-C$_{16}$,** the amphiphile was dissolved in DMSO-d$_6$ (approximately 3.0 mg in 0.40 mL) and gradual addition of 0.04 mL of water was performed. It was found that the signals corresponding to CH or CH$_2$ of the carbohydrate remains unchanged meanwhile a displacement of the rest of signals was observed. See **Fig. 3.50** for ^{1}H NMR experiments of **Lact-Tz-C$_{16}$** (3.4 mg in 0.40 mL DMSO-d$_6$) from 3.00 to 6.00 ppm.

As it is showed in **Fig. 3.51** for **Lact-Tz-C$_{16}$,** a singlet corresponding to the H of the triazole ring is located at 8.04 ppm and the signal corresponding to the NH group is located at around 8.27 ppm. The addition of water to the sample led to shielding of the signal due to the H of the triazole ring, a change that indicates the contribution of π-π stacking to the aggregation. Moreover, a simultaneous deshielding of the NH signal was also observed and this can be assigned to self-assembly through hydrogen bonding, as well as it happens with OH signals.

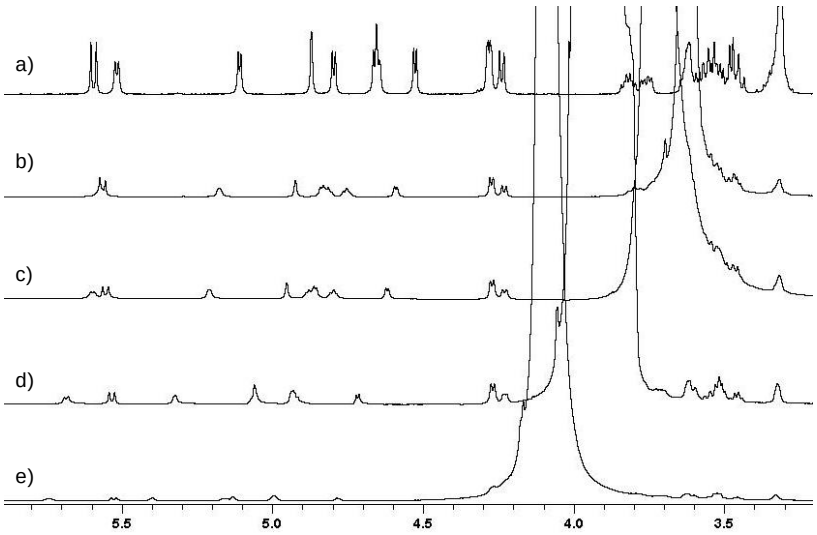

Fig. 3.50: ^{1}H NMR spectra from 3.00 to 6.00 ppm in DMSO-d_6 at 25ºC upon addition of water, (a) 3.4 mg of **Lact-Tz-C$_{16}$** in 0.40 mL DMSO-d_6, (b) addition of 0.04 mL H_2O, (c) addition of 0.08 mL H_2O, (d) addition of 0.12 mL H_2O, (e) addition of 0.16 mL H_2O.

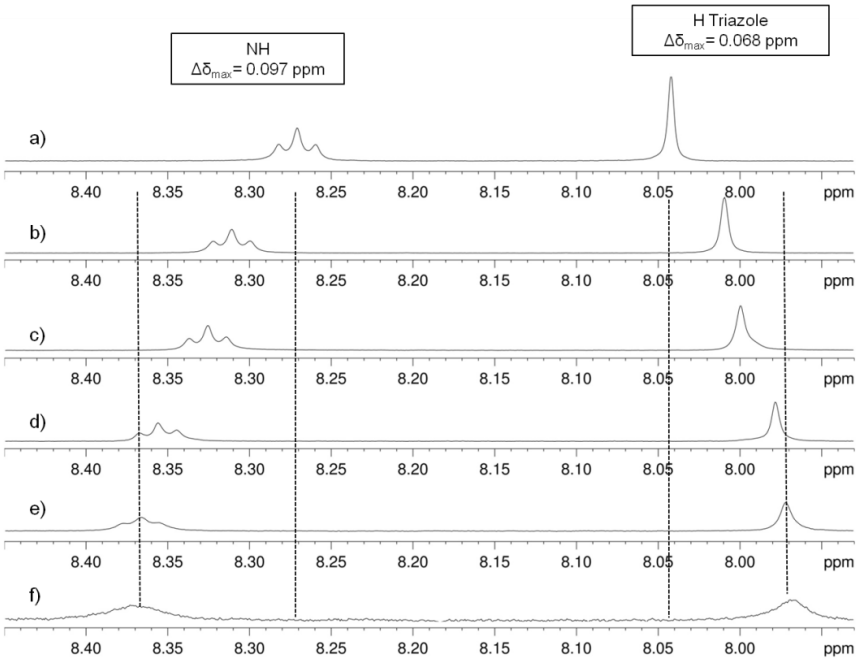

Fig. 3.51: ^{1}H NMR spectra from 7.95 to 8.50 ppm in DMSO-d_6 at 25ºC upon addition of water, (a) 3.4 mg of **Lact-Tz-C$_{16}$** in 0.40 mL DMSO-d_6, (b) addition of 0.04 mL H_2O, (c) addition of 0.08 mL H_2O, (d) addition of 0.12 mL H_2O, (e) addition of 0.16 mL H_2O, (f) addition of 0.18 mL H_2O.

In this experiment, the $\Delta\delta_{max}$ value for the H of the triazole is 0.068 ppm and $\Delta\delta_{max}$ for NH is 0.097 ppm when 0.16 mL of water (40%) was added. The signals did not shift further beyond this volume (see **Fig. 3.51 e** and **f**) and a gel-like structure, suspended in the solvent, is formed.

Same results are obtained for **Cell-Tz-C$_{16}$**, see **Fig. 3.52**. In this experiment the $\Delta\delta_{max}$ value for the H of the triazole is 0.069 ppm and $\Delta\delta_{max}$ for NH is 0.095 ppm when 0.16 mL of water (40%) was added.

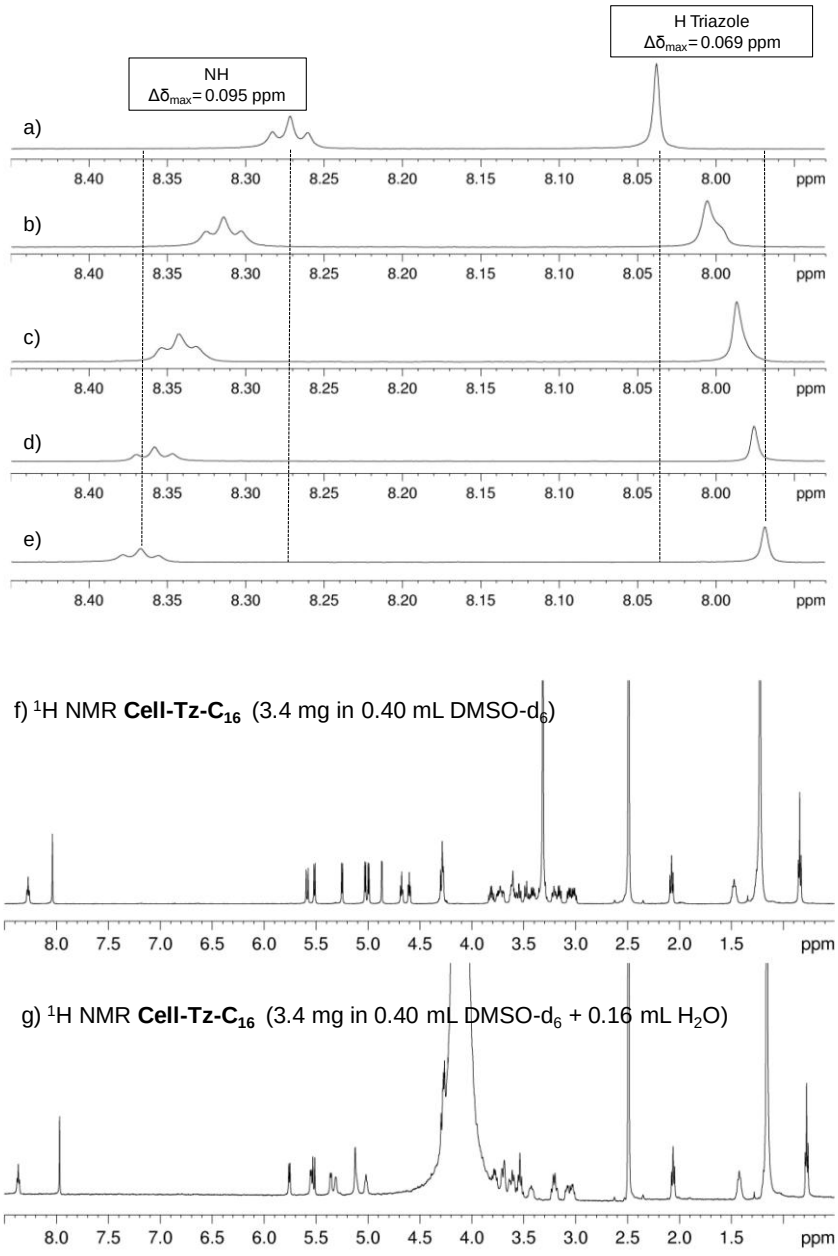

Fig. 3.52: ^{1}H NMR experiments in DMSO-d$_6$ at 25ºC upon water addition, a) 3.0 mg of **Cell-Tz-C$_{16}$** in 0.40 mL DMSO-d$_6$, b) addition of 0.04 mL H_2O, c) addition of 0.08 mL

H_2O, d) addition of 0.12 mL H_2O, e) addition of 0.16 mL H_2O , f) full spectrum of 3.0 mg of **Cell-Tz-C_{16}** in 0.40 mL DMSO-d_6, g) full spectrum of 3.0 mg of **Cell-Tz-C_{16}** in 0.40 mL DMSO-d_6 + 0.16 mL H_2O**.**

Consequently the amide groups have an important role in the design of hydrogelators, as is well known, but the presence of the triazole as the linking unit of the hydrophobic and hydrophilic parts of the synthesized glycoamphiphiles also plays a key role in the properties of these materials as hydrogelators.

Morphological gel characterization. The self-assembled microstructures of the xerogels derived from **Cell-Tz-C_{16}** and **Lact-Tz-C_{16}** were studied by SEM and TEM and additional experiments were performed by ESEM and cryo-TEM in order to better understand the swollen structure in water. AFM measurements were also performed in order to obtain topological information on the structure.

FESEM measurements on the xerogel obtained from **Cell-Tz-C_{16}** (0.5 wt % gel in water) show a supramolecular fibrillar network formed by bundles of ribbons with a width ranging from around 50 to 400 nm, and a length of several μm (**Fig. 3.53.a**). Similar ribbons are also observed for **Lact-Tz-C_{16}** (1.0 wt % gel in water), with a width ranging from around 40 to 150 nm and a length of several μm (**Fig. 3.53.b**). This physical network of ribbons is responsible for the immobilization of the solvent in hydrogels.

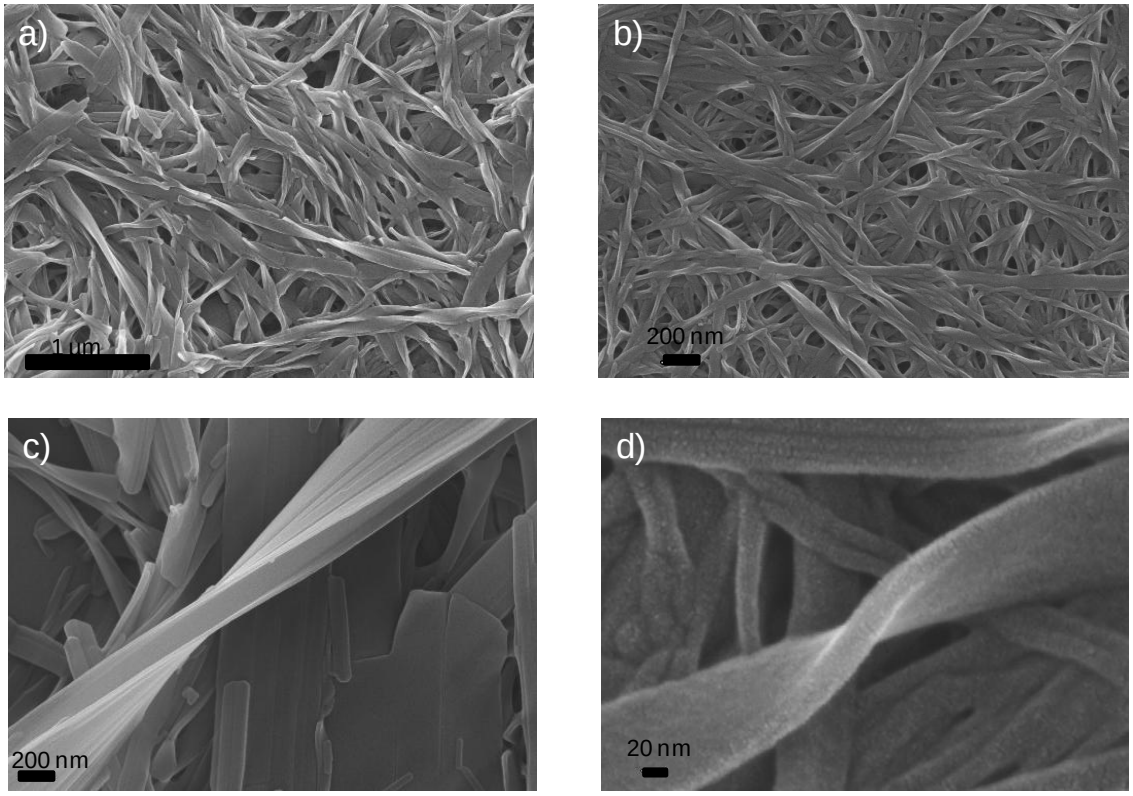

Fig. 3.53: a) FESEM image of **Cell-Tz-C_{16}** (0.5 wt % water) xerogel, b) FESEM image of **Lact-Tz-C_{16}** (1 wt % water) xerogel, c) FESEM image of a single ribbon of **Cell-Tz-C_{16}** (0.5 wt % water) xerogel, d) FESEM image of a single ribbon of **Lact-Tz-C_{16}** (1 wt % water) xerogel. The samples were coated with platinum.

When single ribbons are observed, torsion can be detected in both samples. Surprisingly, **Cell-Tz-C_{16}** ribbons exhibit a right-handed twist, as can be seen in **Fig. 3.53.c**, while the torsion in **Lact-Tz-C_{16}** ribbons leads to a left-handed twist, as can be seen in **Fig. 3.53.d**.

For TEM measurements, diluted samples of 0.05 wt % for **Cell-Tz-C_{16}** or 0.1 wt % for **Lact-Tz-C_{16}** (10 times more diluted than minimum gel concentration) were used and negatively stained with uranyl acetate. Microphotographs of the physical network and ribbons are shown in **Fig. 3.54**. Upon dilution, TEM microphotographs also display a physical network of twisted ribbons that have widths of around 60 to 150 nm for **Cell-Tz-C_{16}**, see **Fig. 3.54.a**. In **Lact-Tz-C_{16}** the ribbons seem to have a more regular width of around 40 nm, see **Fig. 3.54.b**.

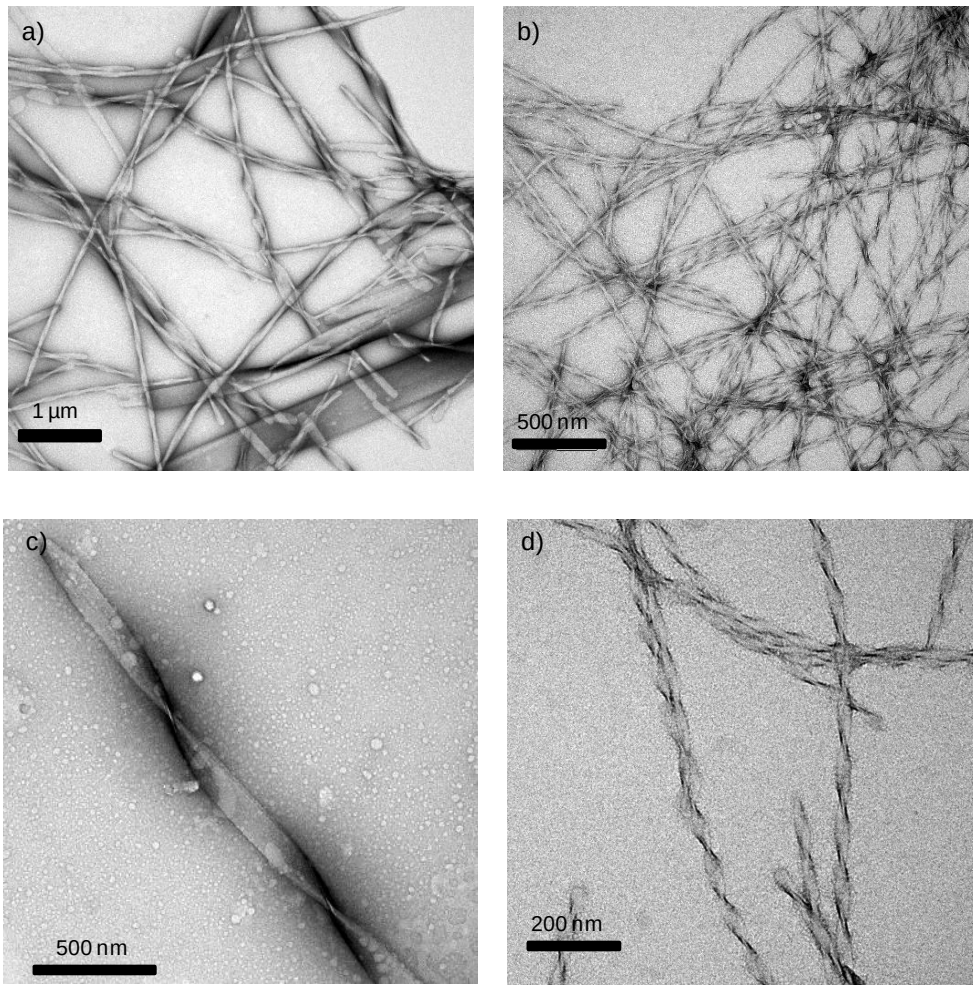

Fig. 3.54: a) TEM image of **Cell-Tz-C_{16}** (0.05 wt %), b) TEM image of **Lact-Tz-C_{16}** (0.1 wt % water), c) TEM image of a single ribbon of **Cell-Tz-C_{16}** (0.05 wt % water) with a right handed twist, d) TEM image of ribbons of **Lact-Tz-C_{16}** (0.1 wt % water) with a left handed twist. TEM images were taken on samples that were dried and negatively stained with uranyl acetate (1wt % water).

On careful observation of a single ribbon of **Cell-Tz-C_{16}**, see **Fig. 3.54.c** a right-handed twist is detected. In the single ribbon of **Lact-Tz-C_{16}**, see **Fig. 3.54.d** a left-handed twist can be observed. The space between two torsions (pitch) seems to be approximately regular within a single ribbon but differs from one fiber to another, especially as the width changes.

AFM measurements were performed on a drop of the gel placed onto graphite and subsequently dried with air. It can be observed in **Fig. 3.55** that the samples have opposite twisted ribbons in hydrogels from **Cell-Tz-C_{16}** and **Lact-Tz-C_{16}**, a situation in

accordance with the results obtained by electron microscopy. As an example, for a single ribbon of **Cell-Tz-C_{16}** the profiles of two different zones are represented in **Fig. 3.55.d**. The widths for the two profiles are around 125 nm. A height of 42 nm was determined at the highest point (profile 1, black) and 26 nm at the torsion (profile 2, red).

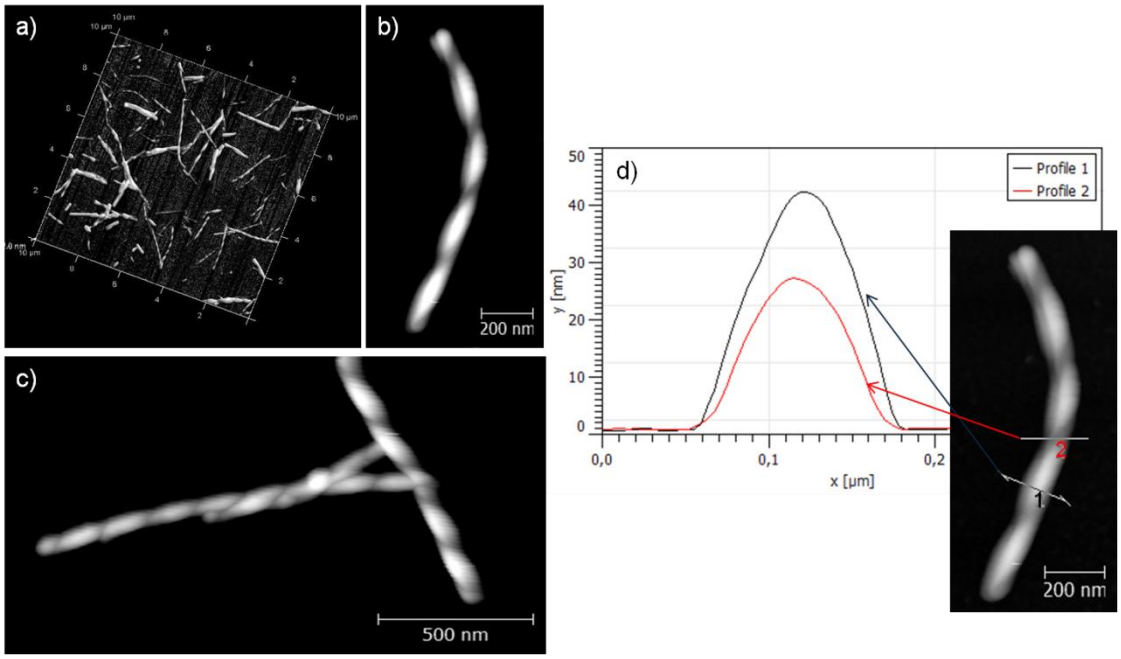

Fig. 3.55: AFM microphotographs of hydrogels a) **Cell-Tz-C_{16}** (0.5 wt %), b) single ribbon of **Cell-Tz-C_{16}** (0.5 wt %), c) single ribbons of **Lact-Tz-C_{16}** (1 wt %), d) profiles of two different zones of a single ribbon of **Cell-Tz-C_{16}** (0.5 wt %).

ESEM and cryo-TEM experiments were also carried out in order to better understand the structure in the native gel. ESEM measurements on the gels provide an insight into the structure under wet conditions. In the case of **Cell-Tz-C_{16}**, flat ribbons are directly observed, see **Fig. 3.56.a** while **Lact-Tz-C_{16}** shows a rough structure, see **Fig. 3.56.c**.

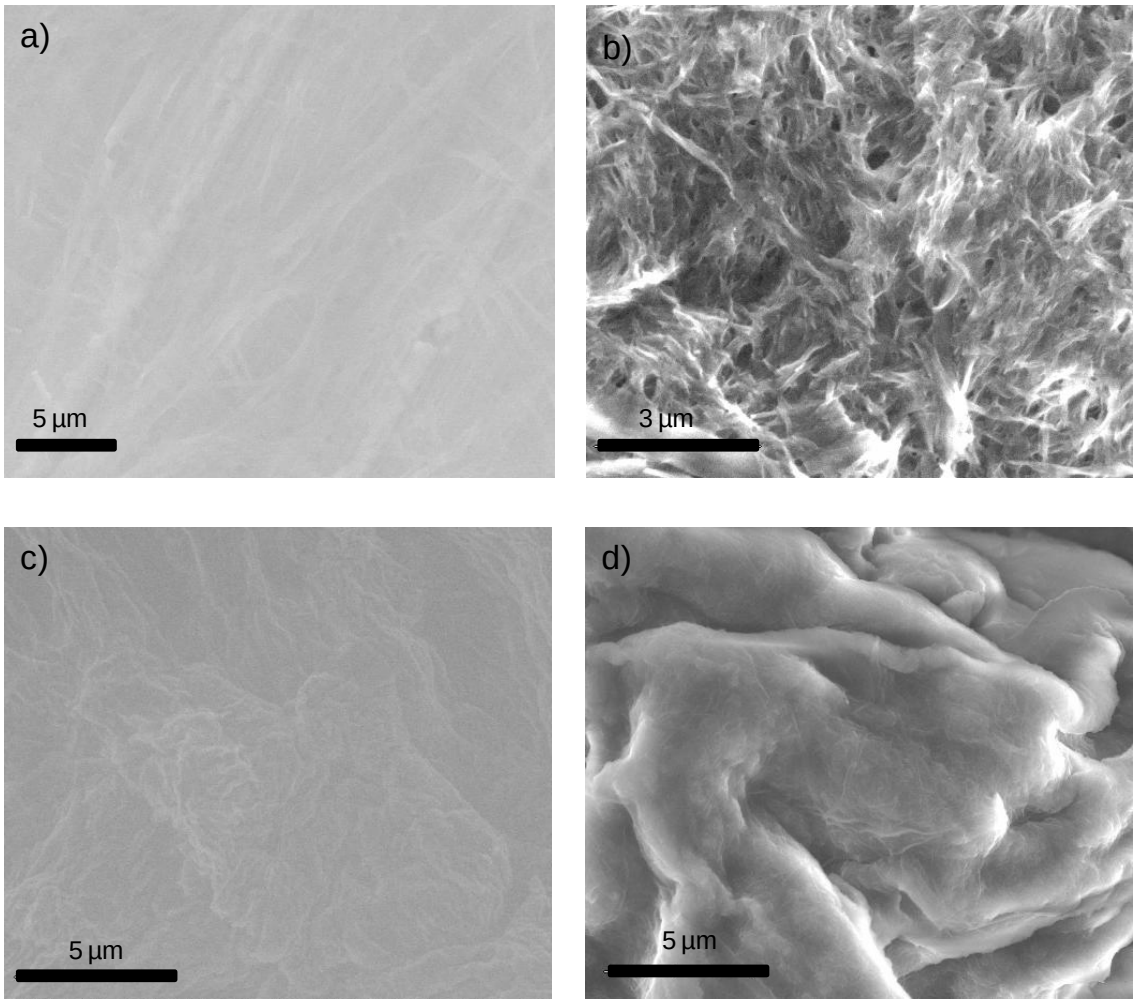

Fig. 3.56: a) ESEM image of **Cell-Tz-C_{16}** (0.5 wt % water) 99.9% humidity, 3.0 ºC, 759 Pa, b) ESEM image of **Cell-Tz-C_{16}** (0.5 wt % water) 20% humidity, 3.0 ºC, 152 Pa, c) ESEM image of **Lact-Tz-C_{16}** (1 wt % water) 99.9% humidity, 3.0 ºC, 759 Pa, d) ESEM image of **Lact-Tz-C_{16}** (1 wt % water) 20.0 % humidity, 3.0 ºC, 152 Pa.

Smaller fibers are detected as the gels are progressively dried. This technique also enables to observe holes in the structure (these holes are easier observed in **Cell-Tz-C_{16}** in comparison with **Lact-Tz-C_{16}**, see **Fig. 3.56 b and d**).

Significant changes were not observed on studying the same area in the samples while the humidity was progressively decreased. This fact shows that the supramolecular 3D network remains very similar when water is removed, see **Fig. 3.57** for **Lact-Tz-C_{16}** gel as example.

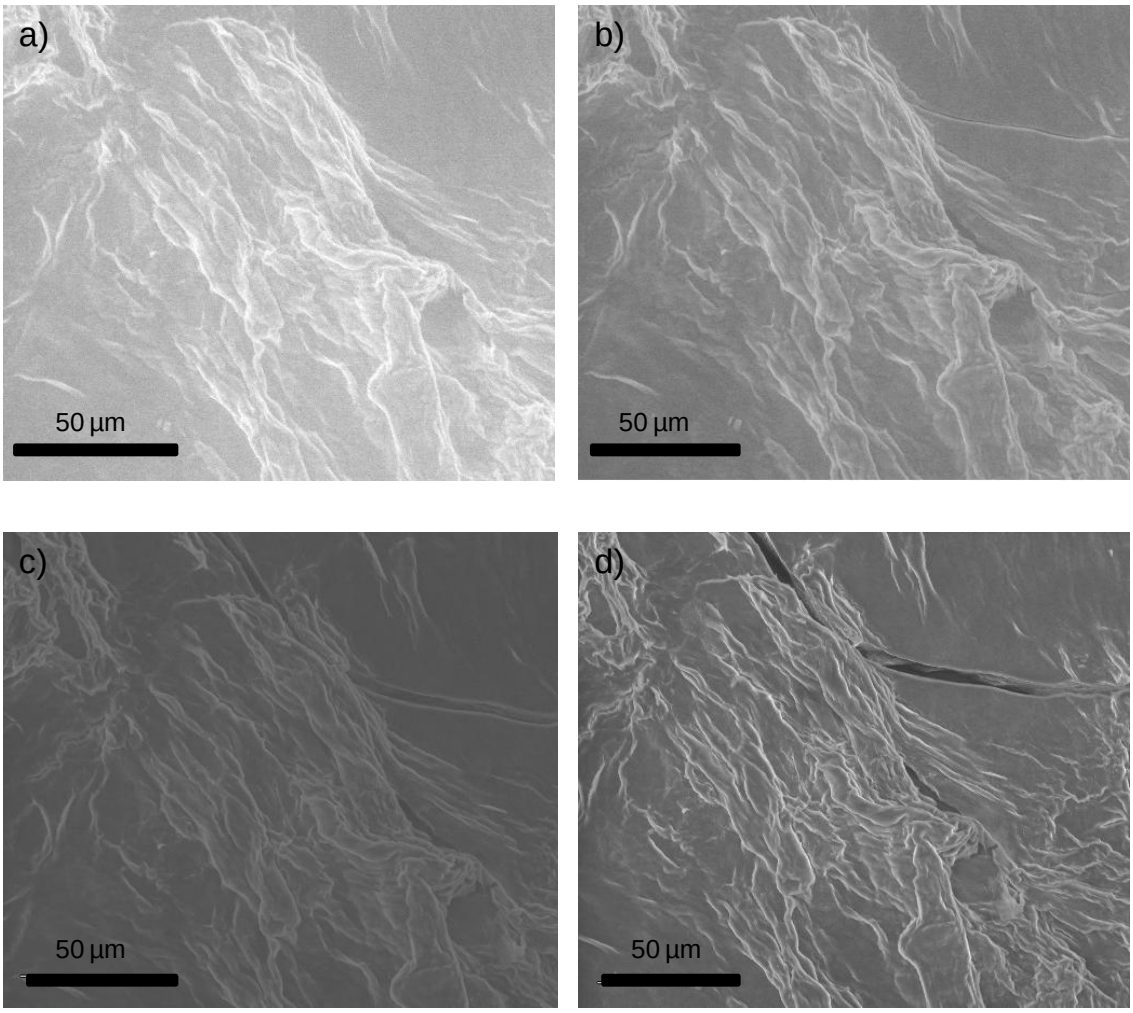

Fig. 3.57: ESEM image of **Lact-Tz-C_{16}** (1 wt % water): a) 80% humidity, 3.0 ºC, 607 Pa, b) 60% humidity, 3.0ºC, 459 Pa, c) 40% humidity, 3.0 ºC, 303 Pa, d) 20.0 % humidity, 3.0ºC, 150 Pa.

Cryo-TEM experiments were carried out directly on hydrogels vitrified in liquid ethane. The ribbons resulting from the self-assembly of the amphiphiles were also detected by this technique in both samples. Cryo-TEM microphotograph of **Cell-Tz-C_{16}** gel is shown in **Fig. 3.58**. On studying the twisted part of the ribbon, it can be seen that the cross-sections of the ribbon show alternate dark and bright regions, as can be seen in **Fig. 3.59 (**a close up of microphotograph **Fig. 3.58**) with a thickness of these regions of about 2 nm and 2.5 nm, respectively, as well as it was found in **Malt-Tz-C_{16}** gel. The model shown in **Fig. 3.59** is proposed to explain the assembly of amphiphiles into ribbons and the resulting layered structure of the cross-section.

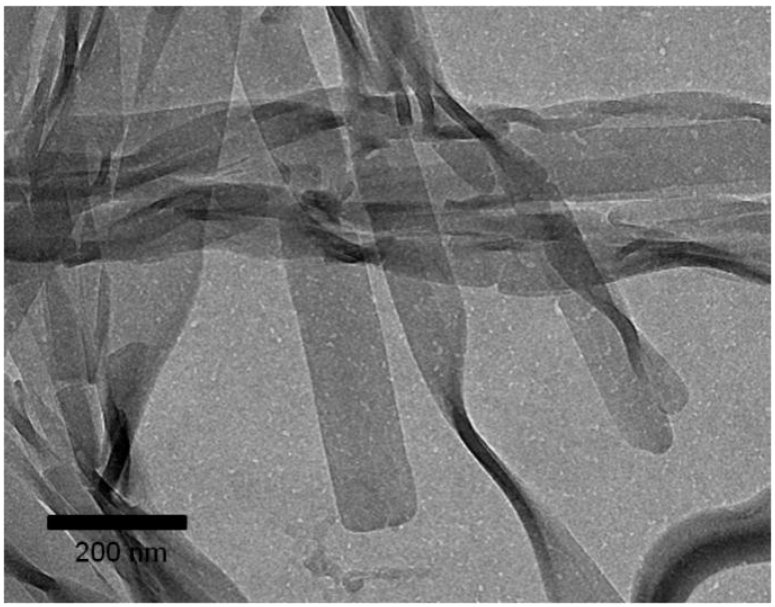

Fig. 3.58. Cryo-TEM image of **Cell-Tz-C_{16}** 0.5 wt % hydrogel.

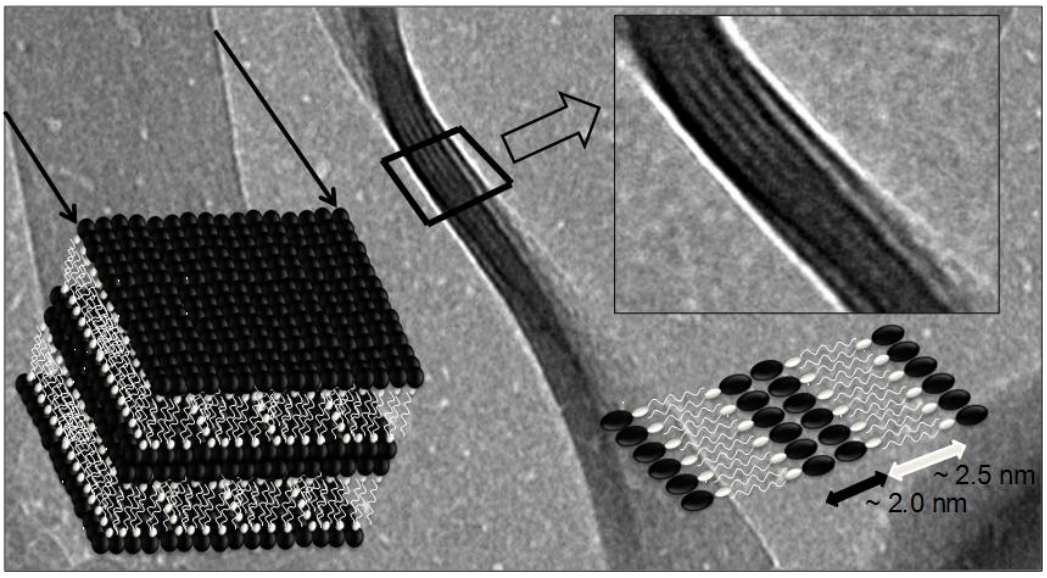

Fig. 3.59: Close up of Cryo-TEM image of **Cell-Tz-C_{16}** 0.5 wt % water gel and model proposed for molecular arrangement (bottom): Ribbons formed by alternating hydrophobic sugar regions and interdigitated hydrophobic regions. A close up of the cross-section of the ribbon is shown on the right corner (see below the model for this cross-section).

This layered structure of the cross-section of the ribbons is formed by alternating hydrophilic parts, consisting of a bilayer of sugar polar heads, and hydrophobic parts of interdigitated aliphatic domains. As was previously described, the theoretical length of the hydrophobic part of the synthesized glycoamphiphiles is about 25 Å (18.5 Å for the palmitic chain and 6.6 Å for amide and triazole ring), which is in accordance with the thickness of the bright motives of around 2.5 nm. In the same way the theoretical length of the disaccharide is around 10 Å. The thickness of the dark motive is around 2 nm, which is in accordance with a disaccharide bilayer.

Similar results were obtained for **Lact-Tz-C_{16}** gel. Twisted ribbons are observed with alternate dark and bright regions in the cross-section. However this technique does not differentiate the opposite direction of the torsion. In **Fig. 3.60**, we can see a close-up of a single ribbon which has the alternative dark and bright regions in the cross-section, with about 2 nm and 2.5 nm, respectively.

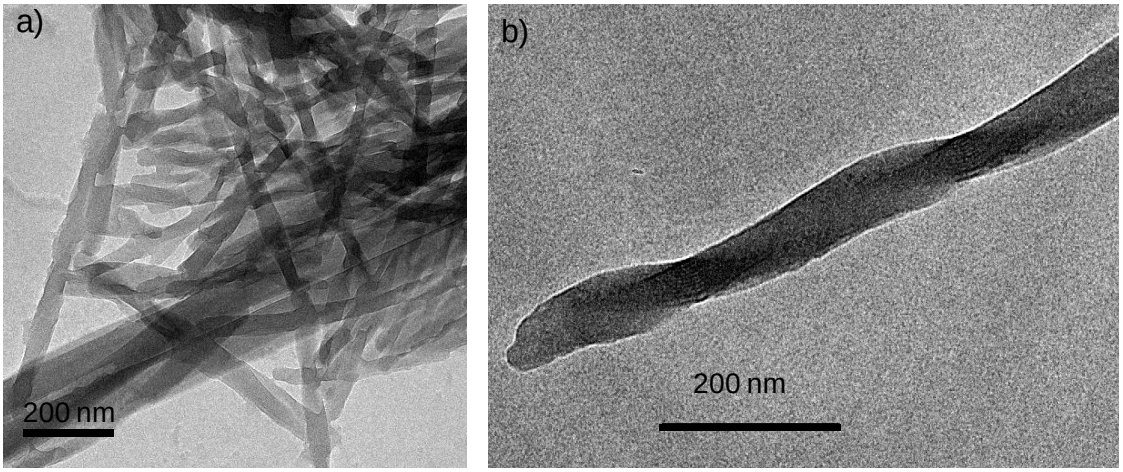

Fig. 3.60: a) Cryo-TEM image of **Lact-Tz-C_{16}** 1 wt % water gel, b) single ribbon of **Lact-Tz-C_{16}** 1 wt % water gel.

Supramolecular chirality. The twisted ribbons detected in hydrogel samples are a consequence of a chiral supramolecular arrangement of self-assembled amphiphiles. The opposite handedness of the ribbons, observed by the different microscopic techniques, seems to be consequence of an opposite supramolecular chirality.

In an attempt to confirm this opposite supramolecular chirality, circular dichroism (CD) measurements were carried out on the gels at their minimum gel concentration and the results are represented in **Fig. 3.61**.

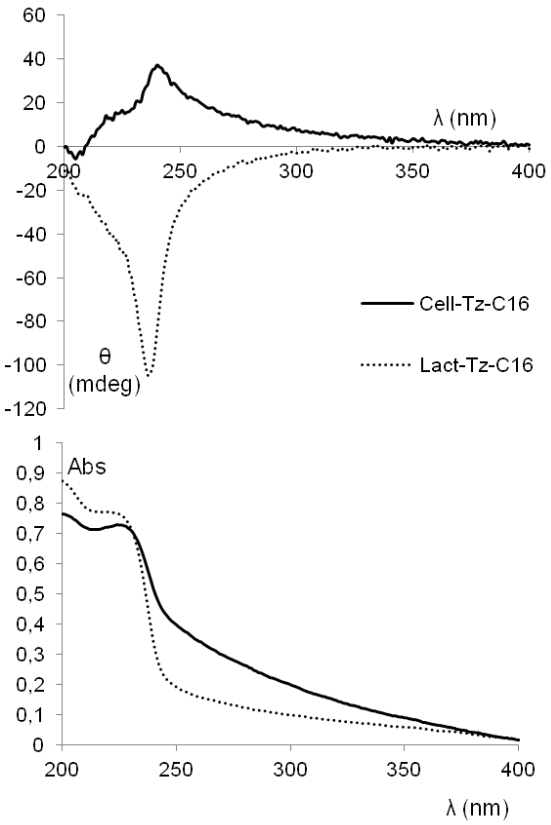

Fig. 3.61: CD (top) and UV-vis (bottom) spectra of hydrogels derived from: **Cell-Tz-C_{16}** (0.5 wt %), solid line and **Lact-Tz-C_{16}** (1 wt %) dashed line.

The λ_{max} value for a hydrogel of **Cell-Tz-C_{16}** at minimum gelator concentration (0.5 wt %) in the UV absorption spectrum appears at around 230 nm and this absorption can be assigned to the triazole group. The hydrogel of this compound (0.5 wt %), when placed between two quartz discs, exhibited a positive Cotton effect for which the θ_{max} value appeared to be slightly displaced from the λ_{max} in the UV spectrum to 240 nm. For the hydrogel derived from **Lact-Tz-C_{16}** at minimum gelator concentration (1 wt %) the λ_{max} (due to the triazole group) appears at 227 nm, but in this case the Cotton effect was negative. The θ_{min} value appeared to be displaced from the λ_{max} in the UV spectrum to 237 nm. For **Lact-Tz-C_{16}** compound, the signal of the Cotton effect matched those obtained for an aqueous gel of **Malt-Tz-C_{16}** at 1 wt %. It was confirmed that the

contribution of the linear dichroism (LD) to the CD spectrum is negligible by comparing several CD spectra recorded at different angles around the incident light beam. See **Characterization Techniques 7. Annex** for experimental conditions.

The opposite CD signals can be attributed to an opposite chiral supramolecular arrangement of the molecules, a structure that is the origin of the opposite handeness observed in the ribbons. This fact shows that the stereochemical arrangement of only one hydroxyl group (equatorial OH-4 in **Cell-Tz-C_{16}** *vs* axial OH-4 in **Lact-Tz-C_{16}**) or the arrangement of the glycosidic bond (β 1→4 in **Cell-Tz-C_{16}** vs α 1→4 in **Malt-Tz-C_{16}**) has a significant effect on the preferential conformation that drives the self-assembly and supramolecular organization of these molecules.

3.5. Summary and conclusions

✓ A mixture of isomers of sucrose esters have been synthesized which can act as gelators in water, using sucrose, phenylalanine and palmitic acid as starting materials.

- The rheological properties of the hydrogel prepared by stirring with Ultra-turrax homogenizer are similar to the previously described for gels of this material.
- From the results based on microscopic techniques we propose a fibrillar structure for **Suc-OOC-Phe-C_{16}** hydrogels, probably formed by an association of worm like aggregates.

✓ New amphiphiles based on disaccharides (maltose, cellobiose and lactose) as polar head groups, similar to sucrose esters, have been synthesized. Different synthetic routes were performed based on deprotected and protected sugars. Their liquid crystalline and gel-forming properties have been investigated. The resulting gel network morphology was studied by different microscopic techniques, either in the xerogel state by TEM, FESEM and AFM or in a wet

environment by cryo-TEM and ESEM. A supramolecular chirality was confirmed by CD.

- Copper(I)-catalyzed azide-alkyne [3+2] cycloaddition provided a satisfactory and versatile synthetic pathway to obtain glycoamphiphiles.
- The glycolipids give rise to thermotropic and lyotropic liquid crystalline phases.
- Glycolipids containing a triazole ring, obtained from the click coupling, as linking group of the hydrophilic and hydrophobic blocks give rise to stable hydrogels at RT.
- Glycolipids with phenylalanine are molecules more hydrophobic and the presence of an organic co-solvent is required for complete solubilization and subsequent gel formation on cooling.
- Temperatures of gel-sol transitions and minimum concentration depend on the chemical structure of the glycoamphiphile. Small structural differences promoted changes in gel properties.
- Gels are supported by a fibrillar network, which has been characterized and is composed by ribbons resulting from the supramolecular arrangement of glycoamphiphiles.
- Twisted ribbons with different thickness were characterized by different microscopic techniques.
- A chiral arrangement of amphiphiles in the gel structure was confirmed by CD.
- The handedness of the supramolecular arrangement of amphiphiles and the sense of the CD signal were found to depend on the sugar polar head.

3.6. Structural characterization

As example of the structural characterization of the glycoamphiphiles, a detailed explanation of **OAc-Cell-Tz-C_{16}** and **Cell-Tz-C_{16}** characterization is included in this section. 2D experiments as COSY, TOCSY, NOESY, HSQC and HMBC, were performed in order to elucidate their chemical structure.

First, H and C of sugar cycles of **OAc-Cell-Tz-C$_{16}$** and **Cell-Tz-C$_{16}$** have been named as it is specified in **Fig. 3.62**. For example, 1´ is indicated for identifying proton H1´and carbon C1´ which correspond to the first ring directly linked to the hydrophobic chain.

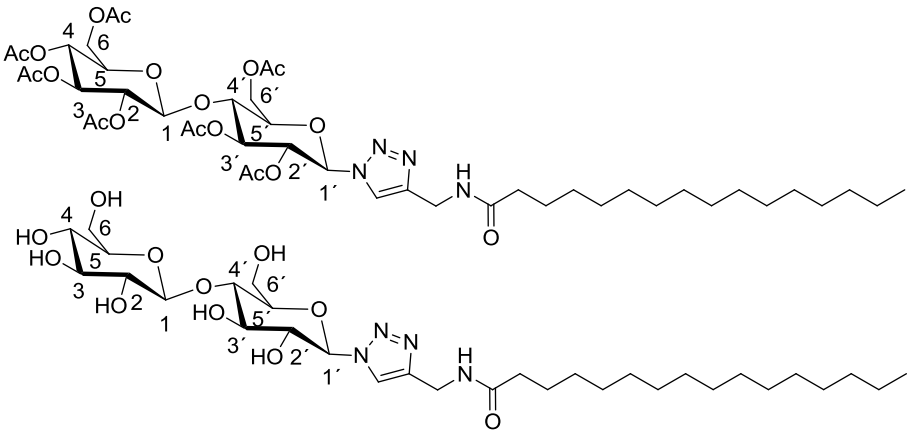

Fig. 3.62: OAc-Cell-Tz-C$_{16}$ and **Cell-Tz-C$_{16}$** chemical structure and nomenclature.

Structural characterization of OAc-Cell-Tz-C$_{16}$. ^{1}H NMR experiment of **OAc-Cell-Tz-C$_{16}$** was performed in $CDCl_3$ as solvent at RT. First, H corresponding to hydrophobic chain were identified, as well as CH_3 of the acetyl groups and the H from the triazole ring (see characterization below and **Fig. 3.63**, both in green). Region ranging from 3.50 to 6.50 ppm corresponds to H of the sugar and amide group. They were identified by 2D experiments as it is discussed below (see characterization and **Fig. 3.63** in red).

^{1}H NMR (400 MHz, $CDCl_3$, δ ppm): 0.87 (t, 3H, J = 6.8 Hz, -$(CH_2)_{12}$-C*H*$_3$), 1.19-1.35 (m, 24H, -(C*H*$_2$)$_{12}$-), 1.55-1.65 (m, 2H, CO-CH$_2$-C*H*$_2$-$(CH_2)_{12}$), 1.86 (s, 3H), 1.98 (s, 3H), 2.01 (s, 3H), 2.03 (s, 3H), 2.04 (s, 3H), 2.10 (s, 3H), 2.11 (s, 3H), C*H*$_3$-CO-O x7, 2.17 (t, 2H, J = 7.3 Hz, CO-C*H*$_2$-CH$_2$), 3.69 (ddd, 1H, $J_{4,5}$=9.6 Hz, $J_{5,6a}$= 2.1 Hz, $J_{5,6b}$= 4.3 Hz, *H5*), 3.84-3.98 (m, 2H, *H4´*, *H5´*), 4.06 (dd, 1H, $J_{5,6a}$ = 2.1 Hz, $J_{6a,6b}$ = 12.5 Hz, *H6a*), 4.12 (dd, 1H, $J_{5´,6´a}$=4.7 Hz, $J_{6´a,6´b}$=12.2 Hz, *H6´a*), 4.38 (dd, 1H, $J_{5,6b}$ = 4.3 Hz, $J_{6a,6b}$ = 12.5 Hz, *H6b*), 4.43-4.53 (m, 3H, *H6´b*, C = C-C*H*$_2$-NH), 4.55 (d, 1H, $J_{1,2}$ = 8.2 Hz, *H1*), 4.94 (dd, 1H, $J_{1,2}$ = 8.2 Hz, $J_{2,3}$ = 9.4 Hz, *H2*), 5.07 (dd, 1H, $J_{3,4}$ = 9.5 Hz, $J_{4,5}$ = 9.6 Hz, *H4*), 5.16 (dd, 1H, $J_{2,3}$ = 9.4 Hz, $J_{3,4}$ = 9.5 Hz, *H3*), 5.33-5.42 (m, 2H, *H2´*, *H3´*), 5.73- 5.81 (m, 1H, *H1´*), 6.11 (t, 1H, J = 5.6 Hz, -CH$_2$-N*H*-CO), 7.70 (s, 1H, N-C*H* = C-CH$_2$ triazole).

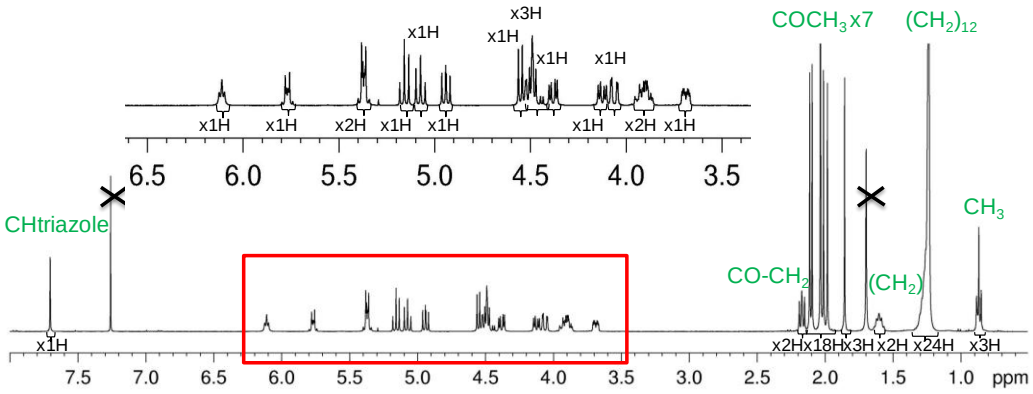

Fig. 3.63: ^{1}H NMR spectrum of **OAc-Cell-Tz-C$_{16}$** in $CDCl_3$ at RT.

In a second step, C1 was identified at 101.7 ppm and C1´ was identified at 85.9 ppm. C1 is deshielded comparing with C1´ because it is linked to two O atoms and C1´ it is linked to one O atom and one N atom. Then HSQC experiment was performed to identify H1 (4.55 ppm) and H1´ (5.73-5.81 ppm). In this experiment correlations between protons and carbons appear. NH (7.70 ppm) can be also identified by HSQC because it has not a correlation with C, see **Fig. 3.64.** The identification of C1, H1 and C1´, H1´ was also corroborated by HMBC. This experiment allows obtaining two dimensional heteronuclear chemical shift correlation maps between long-range coupled ^{1}H and ^{13}C. First, $C_{CH\ triazole}$ was identified by HSQC (121.2 ppm), see **Fig. 3.65,** red circle. Subsequently by HMBC the correlation of this carbon with H1´ confirmed the previous assignation, see **Fig. 3.66**, red square.

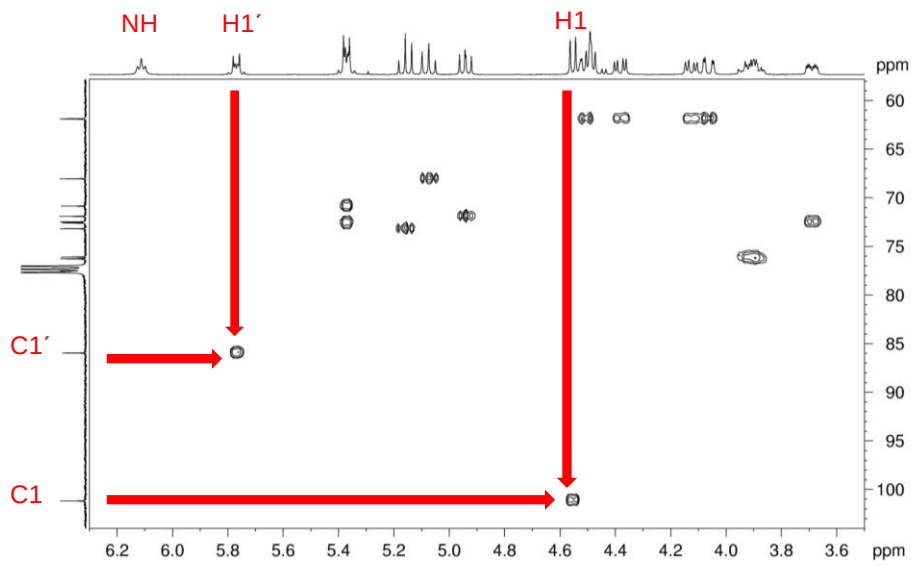

Fig. 3.64: HSQC NMR spectrum of **OAc-Cell-Tz-C_{16}** in $CDCl_3$ at RT.

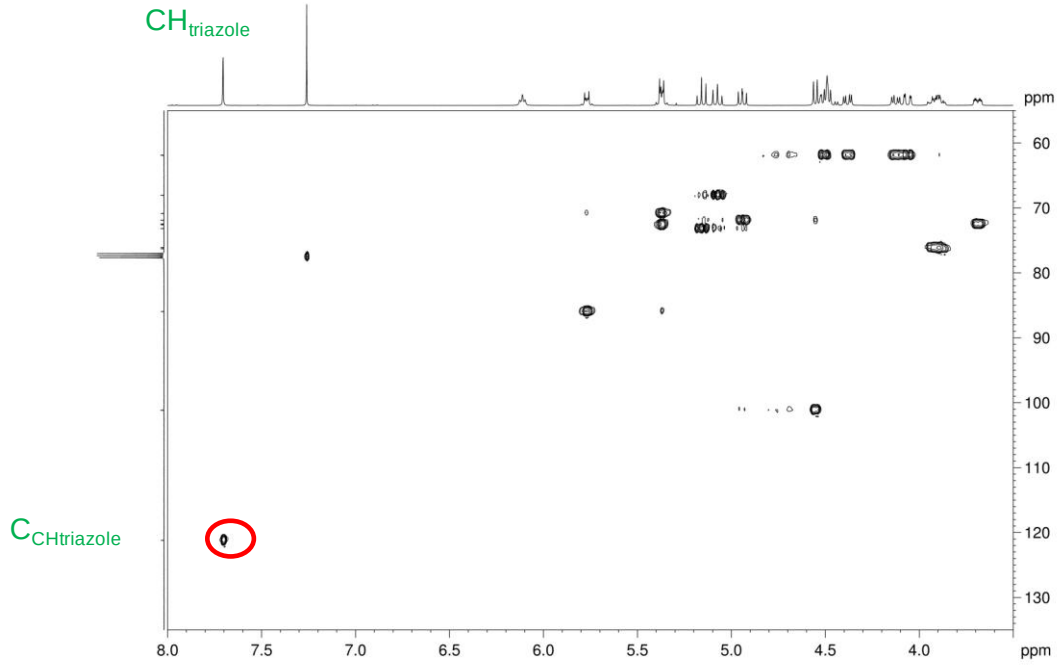

Fig. 3.65: HSQC NMR spectrum of **OAc-Cell-Tz-C_{16}** in $CDCl_3$ at RT.

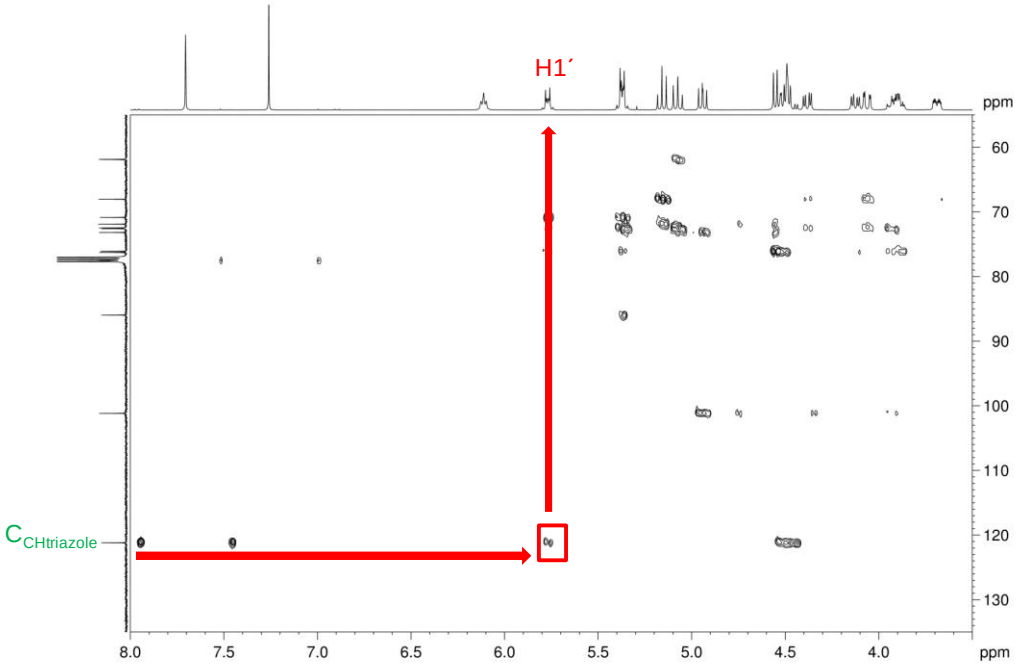

Fig. 3.66: HMBC NMR spectrum of **OAc-Cell-Tz-C_{16}** in $CDCl_3$ at RT.

With COSY experiment, H directly coupled to each other can be identified. Starting with H1 (4.55 ppm) and following a vertical to horizontal line, correlations with the neighbor H can be identified. H2 (4.94 ppm) is identified by the red-blue correlation line, see **Fig. 3.67**. From H2 (4.94 ppm), blue-violet correlation line identifies H3 (5.16 ppm). Violet-green correlation line identifies H4 (5.07 ppm). Green-black correlation line identifies **H5 (3.69 ppm).** Black-yellow correlation line identifies one of the H6 (4.38 ppm) and yellow-dark red correlation line identifies the other H6 (4.06 ppm).

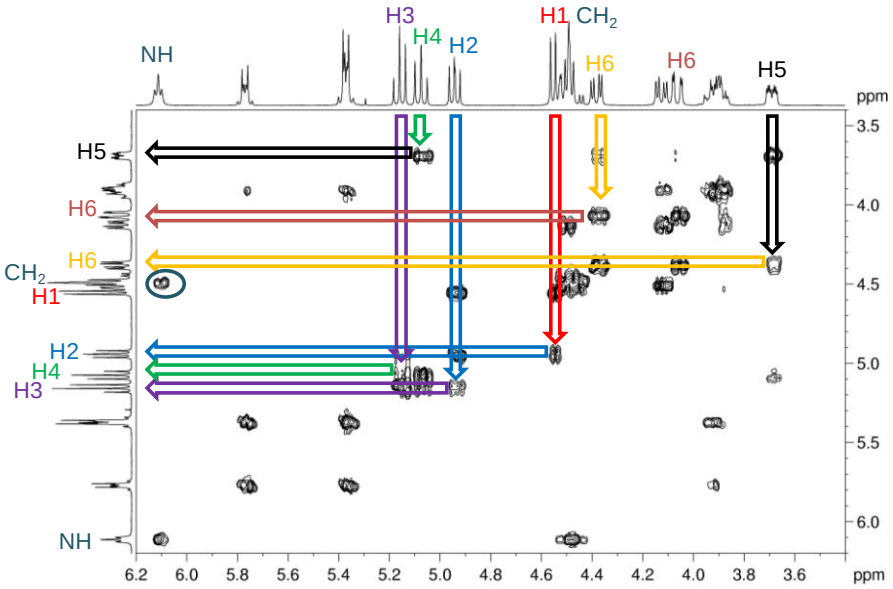

Fig. 3.67: COSY NMR spectrum of **OAc-Cell-Tz-C_{16}** in $CDCl_3$ at RT.

As it can be observed at **Fig. 3.67**, from 4.43 to 4.53 ppm there is a correlation with H amide, see dark blue circle. This correspond to a signal of CH_2 of C=C-CH_2-NH group.

In a TOCSY experiment, correlations are seen among all H in a spin system. Protons from cycle H1-H6 (H are in blue) were confirmed as well as protons from cycle´ H1´-H6´ (red circles), see **Fig. 3.68**.

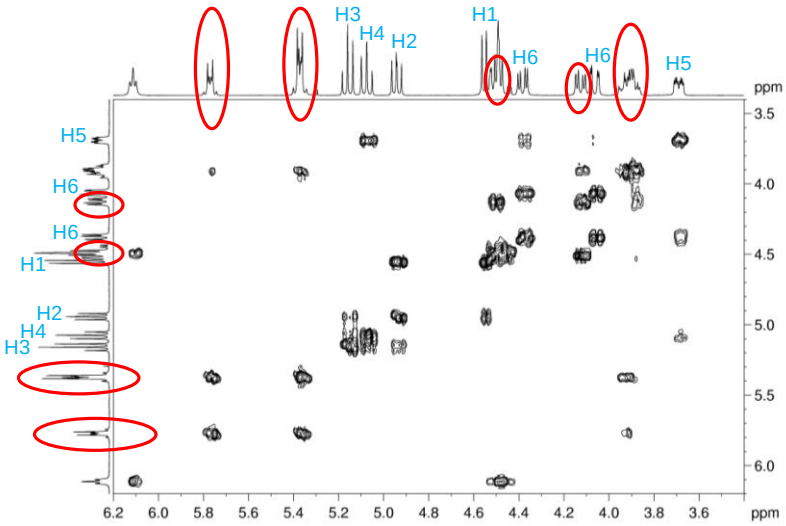

Fig. 3.68: TOCSY NMR spectrum of **OAc-Cell-Tz-C_{16}** in $CDCl_3$ at RT.

In a second step, H1´, H2´, H3´, H4, H5´and H6´ are identified. Nevertheless there are two H in the signal from 5.33 to 5.42 ppm and also two H are in the signal from 3.84 to 3.98 ppm, consequently identification is not evident. First, HSQC was again investigated. C6´was identified (61.9 ppm) and therefore H6´a (4.12 ppm) and H6´b (4.43-4.53 ppm), see **Fig. 3.69.**

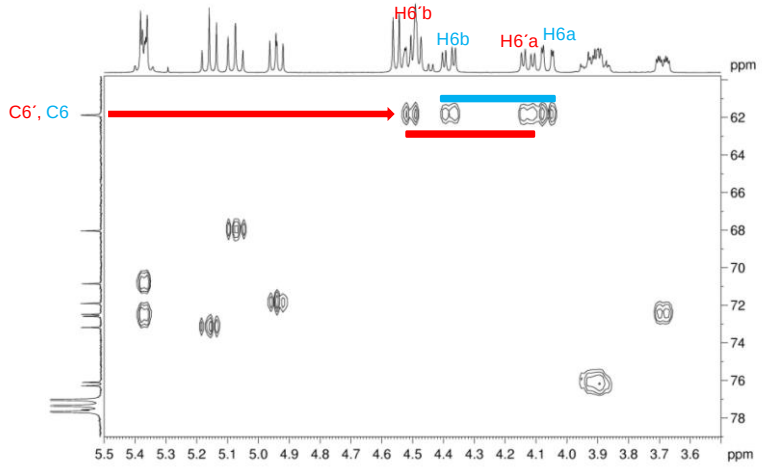

Fig. 3.69: HSQC NMR spectum of **OAc-Cell-Tz-C_{16}** in $CDCl_3$ at RT.

H5´ (3.84-3.98 ppm) and H2´ (5.33-5.42 ppm) were then identified by a COSY experiment, see Fig **3.70**.

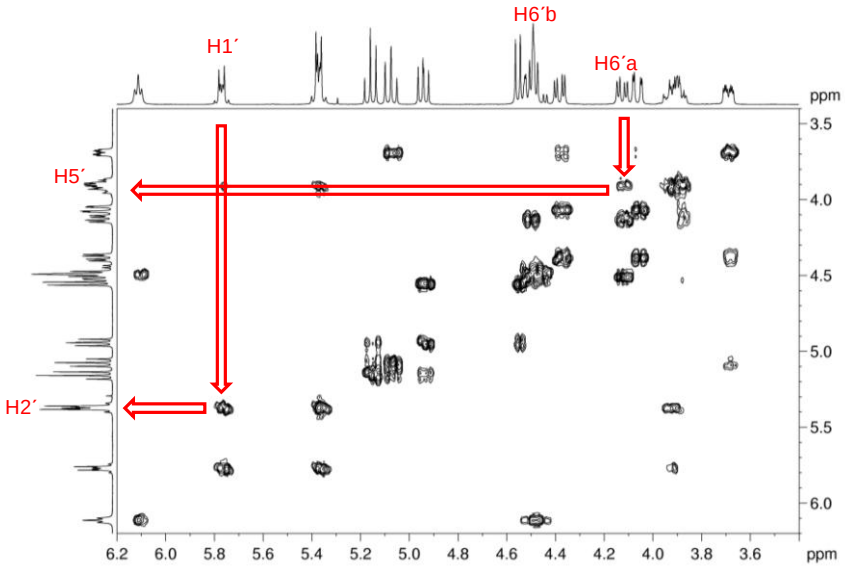

Fig. 3.70: COSY NMR spectum of **OAc-Cell-Tz-C_{16}**.

With this information there are two possibilities of assignation: 3.84-3.98 (m, 2H) corresponds to *H4´*, *H5´* and 5.33-5.42 (m, 2H) corresponds to *H2´*, *H3´* or 3.84-3.98 (m, 2H) corresponds to *H3´*, *H5´* and 5.33-5.42 (m, 2H) corresponds to *H2´*, *H4´*.

The cross peaks of a NOESY spectrum indicate which protons are close in space and the aim is to identify spins undergoing cross-relaxation. NOESY experiment was performed but no additional information was obtained, see **Fig. 3.71**.

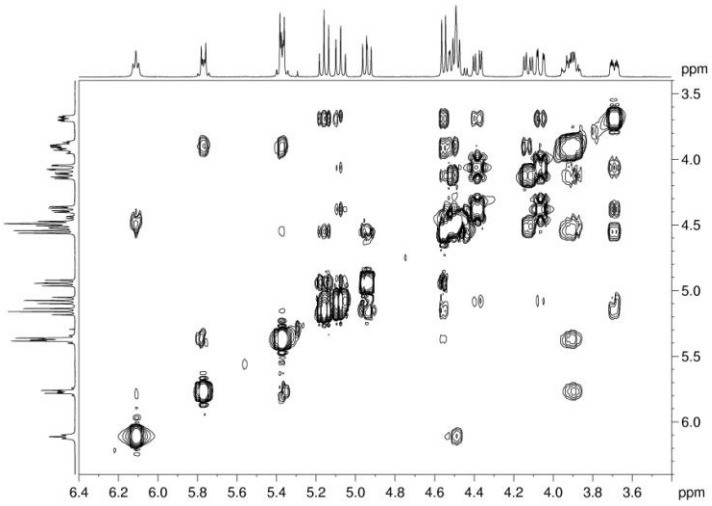

.

Fig. 3.71: NOESY NMR spectum of **OAc-Cell-Tz-C_{16}**.

HMBC can be used to verify the correct assignment of the H, studying the correlation among the C from the carbonyl of the peracetyl group and the corresponding H of the sugar. H3´ has correlation with a quaternary C of the acetyl group while H4´ has not this correlation, see **Fig. 3.72**.

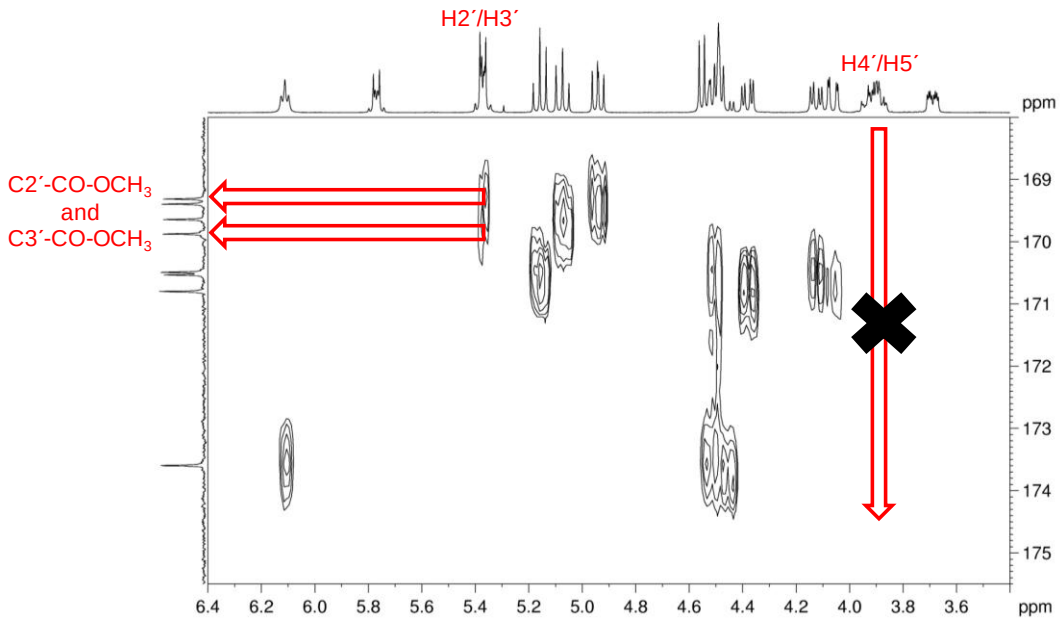

Fig. 3.72: HMBC NMR spectum of **OAc-Cell-Tz-C_{16}** in $CDCl_3$ at RT.

Therefore H2´/H3´ both appear in the signal from 5.33 to 5.42 ppm and H4´/H5´ in the signal from 3.84 to 3.98 ppm, with these identifications the H of the glycoamphiphiles were eventually assigned.

Once H were identified, C can be assigned by direct correlation by HSQC, see **Fig. 3.73**.

^{13}C NMR (100 MHz, $CDCl_3$, δ ppm): 14.4 -$(CH_2)_{12}$-CH_3, 20.5, 20.7, 20.8, 21.0, 21.1 CH_3-CO-O x7, 23.0 -$(CH_2)_{12}$-, 25.8 CO-CH_2-CH_2-$(CH_2)_{12}$, 29.6, 29.6, 29.7, 29.8, 29.9, 29.9, 30.0, 32.2, -$(CH_2)_{12}$-, 35.1 C-CH_2-NH, 36.9 CO-CH_2-CH_2, 61.9 x2 *C6*, *C6´*, 68.0 *C4*, 70.8 *C2´*or *C3´*, 71.9 *C2*, 72.5, 72.6 *C5*, *C2´*or *C3´*, 73.2 *C3*, 76.0 *C4´*, 76.3 *C5´*, 85.9 *C1´*, 100,1 *C1*, 121.2 *C*H triazole.

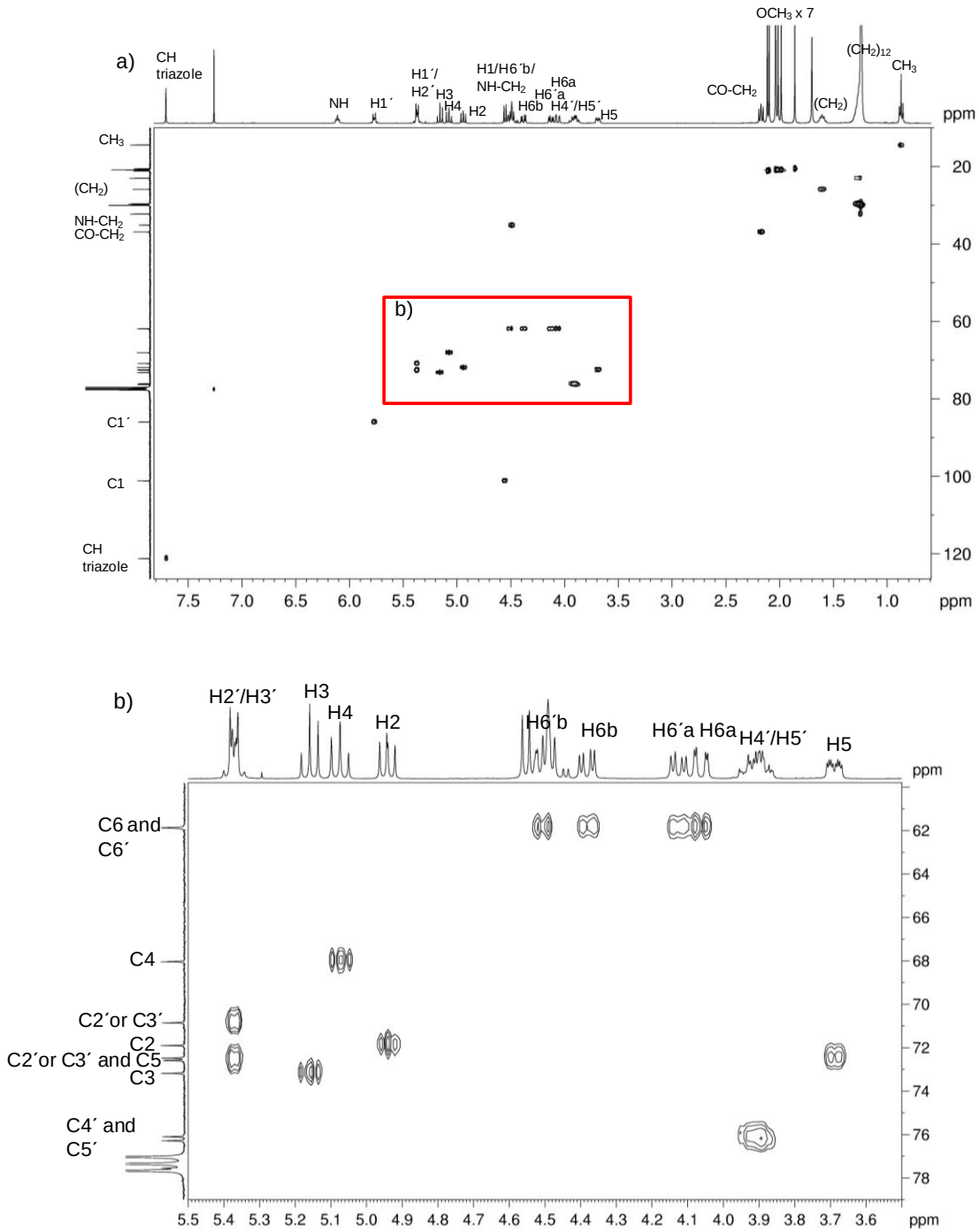

Fig. 3.73: a) HSQC NMR spectrum of **OAc-Cell-Tz-C_{16}**, b) close up of red square.

C4´ (76.0 ppm) and C5´ (76.3 ppm) could be distinguished by HMBC, as well as the quaternary *C* of acetyl (169.3, 169.4, 169.6, 169.8, 170.4, 170.5, 170.8 ppm), triazole and amide groups (173.6 ppm), see **Fig. 3.74.**

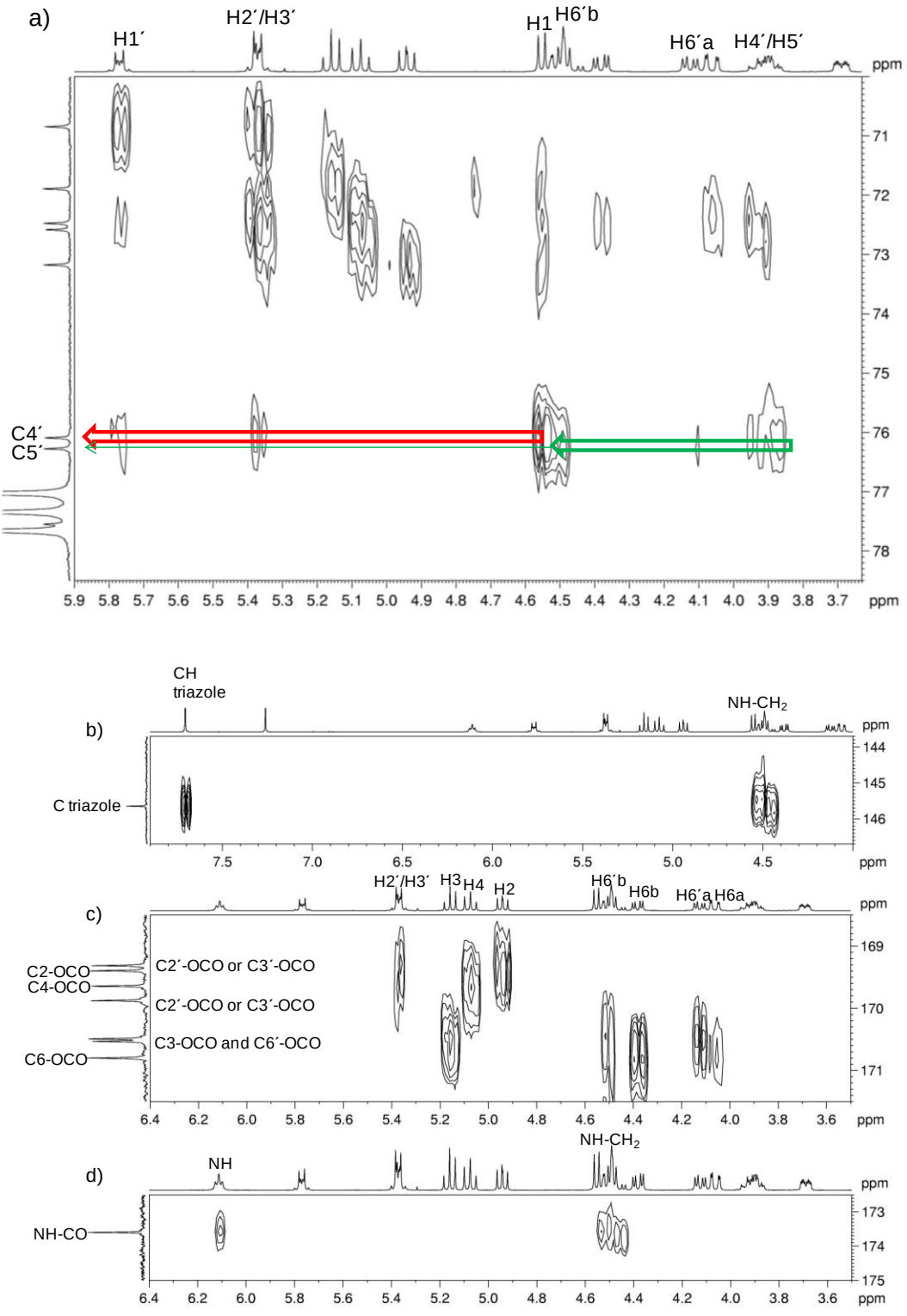

Fig. 3.74: HMBC NMR spectra of **OAc-Cell-Tz-C_{16}**: a) close up of region corresponding to C4´and C5´, b) close up of region corresponding to quaternary *C* of the triazole group, c) close up of region corresponding to quaternary *C* of acetyl groups, d) close up of region corresponding to quaternary *C* of the amide group.

*C*triazole (145.7 ppm), C2´-O-*C*O- / C3´-O-*C*O- (169.3 ppm), C2-O-*C*O- (169.4 ppm), C4-O-*C*O- (169.6 ppm), C2´-O-*C*O- / C3´-O-*C*O- (169.8 ppm), C3-O-*C*O / C6´-O-*C*O (170.4, 170.5 ppm), C6-O-*C*O (170.8 ppm), NH-*C*O-CH_2 (173.6 ppm).

Structural characterization of Cell-Tz-C_{16}. ^{1}H NMR experiment of **Cell-Tz-C_{16}** was performed in MeOD as solvent at 50ºC. H corresponding to hydrophobic chain were identified, as well as H from the triazole ring (see characterization and **Fig. 3.75** in green). Zone ranging from 3.50 to 6.50 ppm corresponds to sugar H. They were identified by 2D experiments as described below (see characterization and **Fig. 3.75** in red).

^{1}H NMR (400 MHz, MeOD, 50 ºC, δ ppm): 0.90 (t, 3H, J = 6.8 Hz, -$(CH_2)_{12}$-C*H*$_3$), 1.13-1.45 (m, 24H, -$(CH_2)_{12}$-CH_3), 1.56-1.66 (m, 2H, CO-CH_2-C*H*$_2$-$(CH_2)_{12}$), 2.21 (t, 2H, J = 7.3 Hz, CO-C*H*$_2$-CH_2), 3.27 (dd, 1H, $J_{1,2}$ = 7.3 Hz, $J_{2,3}$ = 8.4 Hz, *H2*), 3.32-3.46 (m, 3H), 3.65-3.80 (m, 4H), 3.85-3.92 (m, 3H), *H3´*, *H4´*, *H5´*, *H6´a*, *H6´b*, *H3*, *H4*, *H5*, *H6a*, *H6b*, 3.95 (dd, 1H, $J_{1´,2´}$ = 9.8 Hz, $J_{2´,3´}$ = 7.7 Hz, *H2´*), 4.45 (m, 2H, C-C*H*$_2$-NH) 4.48 (d, 1H, $J_{1,2}$ = 7.3 Hz, *H1*), 5.60 (d, 1H, $J_{1´,2´}$ = 9.2 Hz, *H1´*), 8.00 (s, 1H, C*H*triazole).

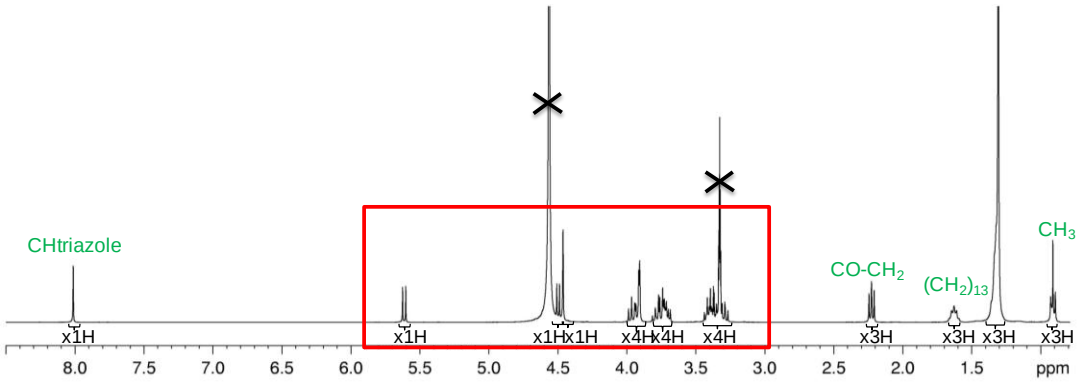

Fig. 3.75: ^{1}H NMR spectum of **Cell-Tz-C_{16}** in MeOD at 50ºC.

First, as in peracetylated compound, C1 (104.6 ppm) and C1´ (89.4 ppm) were identified by HSQC, see **Fig. 3.76** to further identify H1 (4.48 ppm) and H1´ (5.60 ppm). HMBC experiment, see **Fig. 3.77**, verifies the assignation of H1´, red square. H1 and H1´ are used as reference for the correlations among H by COSY. But in this case,

only H2 (3.27 ppm) and H2´ (3.95 ppm) can be determined because the rest of the H appear as multiplets (tree multiplets, each one integrating by 4 H), see **Fig. 3.78.**

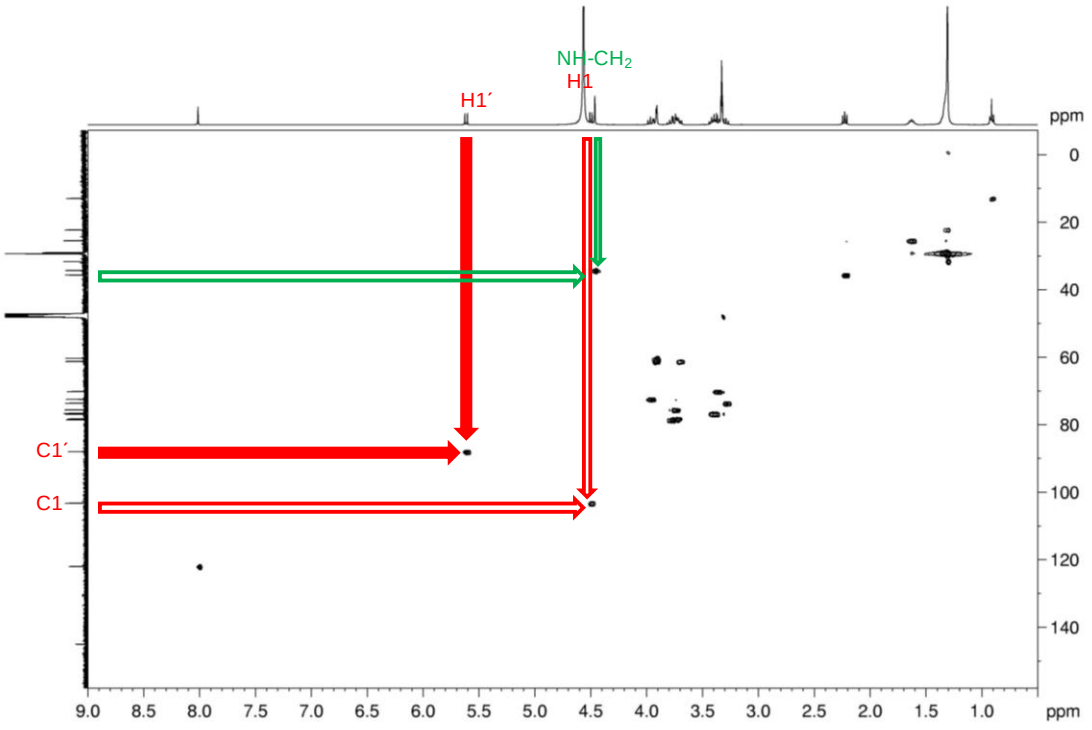

Figure 3.76: HSQC NMR spectum of **Cell-Tz-C_{16}** in MeOD at 50ºC.

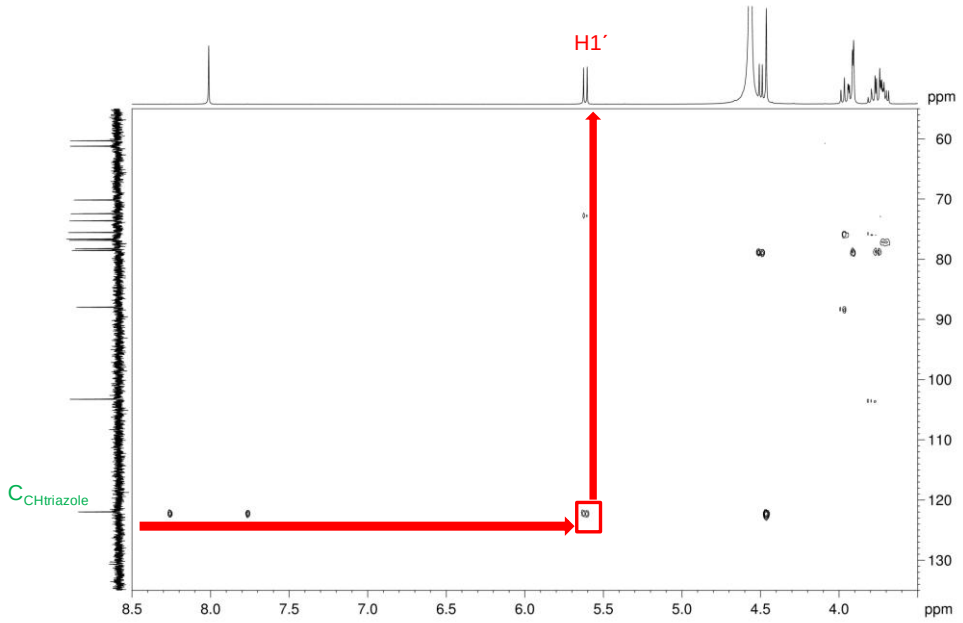

Figure 3.77: HMBC NMR spectum of **Cell-Tz-C_{16}** in MeOD at 50ºC.

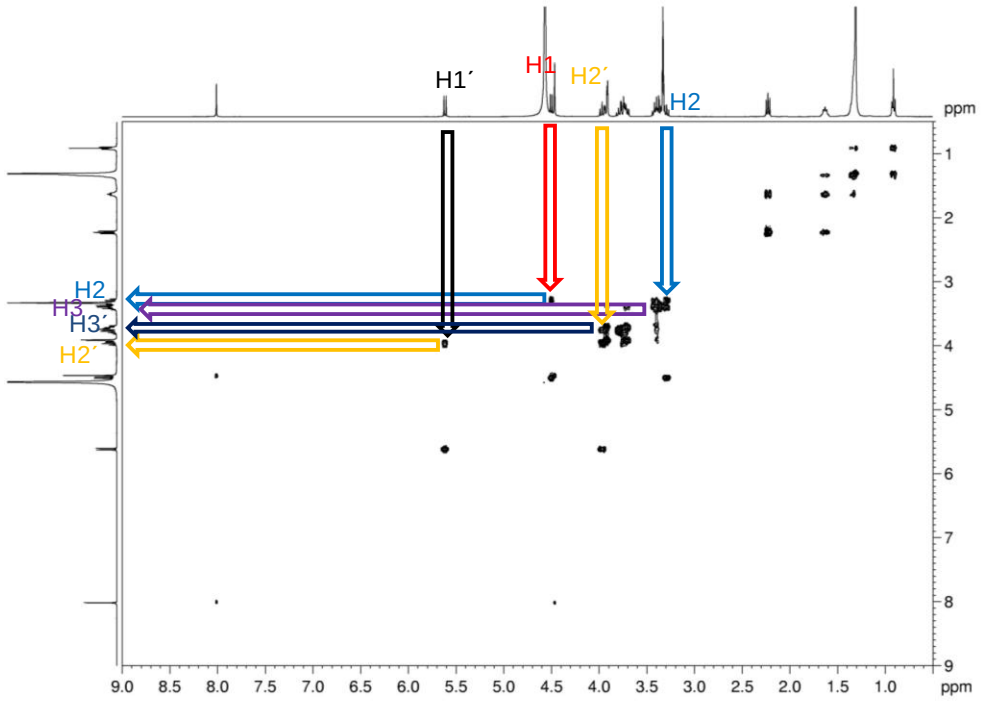

Fig. 3.78: COSY NMR expectum of **Cell-Tz-C_{16}** in MeOD at 50ºC.

TOCSY and NOESY were performed but no additional information was obtained, see **Fig. 3.79 and 3.80.**

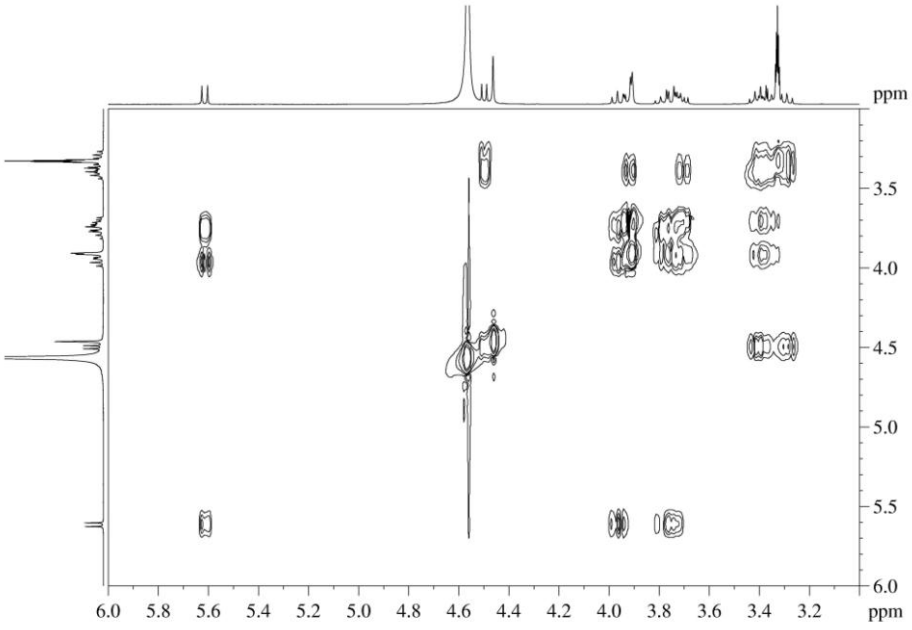

Fig. 3.79: TOCSY NMR spectum of **Cell-Tz-C_{16}** in MeOD at 50ºC.

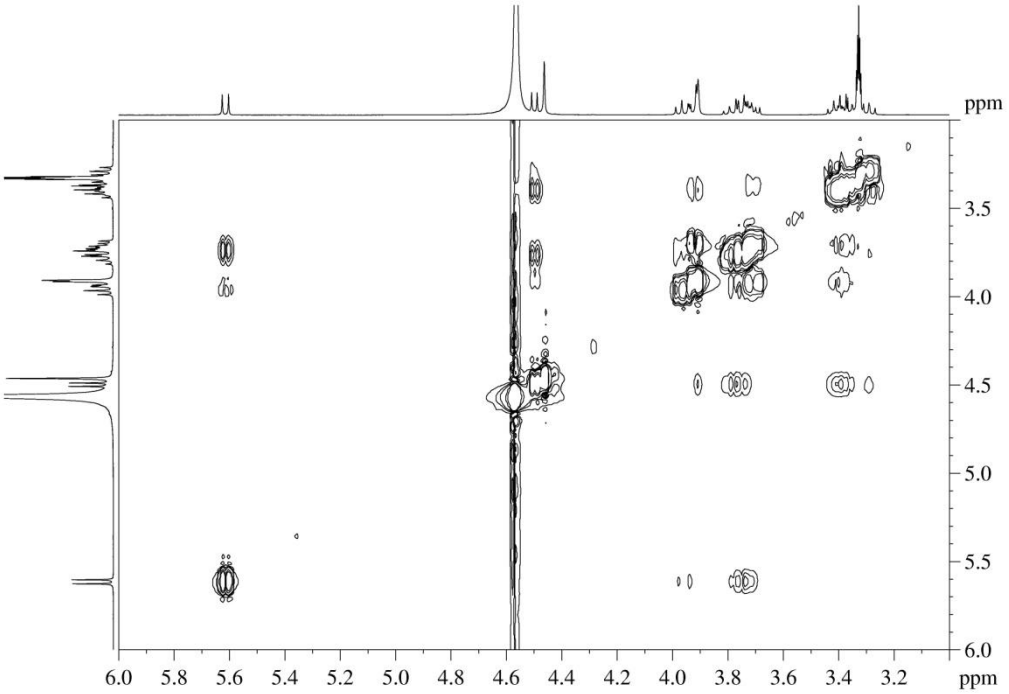

Fig. 3.80: NOESY NMR spectum of **Cell-Tz-C_{16}** in MeOD at 50ºC.

Once H were identified, C can be assigned by direct correlation by HSQC, see **Fig. 3.81**. ^{13}C NMR (125 MHz, MeOD, 55 ºC, δ ppm): 14.3 -$(CH_2)_{12}$-*C*H_3, 23.6 -(*C*H_2)$_{12}$-, 26.8 CO-CH_2-*C*H_2-$(CH_2)_{12}$, 30.4, 30.5, 30.7, 32.9 -CH_2-(*C*H_2)$_{12}$-, 35.6 C-*C*H_2-NH-, 37.0 CO-*C*H_2-CH_2, 61.7, 62.6, 71.5, 76.9, 78.0, 78.2, 79.6, 79.9 *C3´*,*C4´*, *C5´*,*C6´*, *C3*,*C4*, *C5*,*C6*, 73.8 *C2´*, 75.6 *C2*, 89.4 *C1´*, 104.6 *C1*, 123.4 *C*Htriazole, 146.4 *C*triazole, 176.3 NH-*C*O-CH_2.

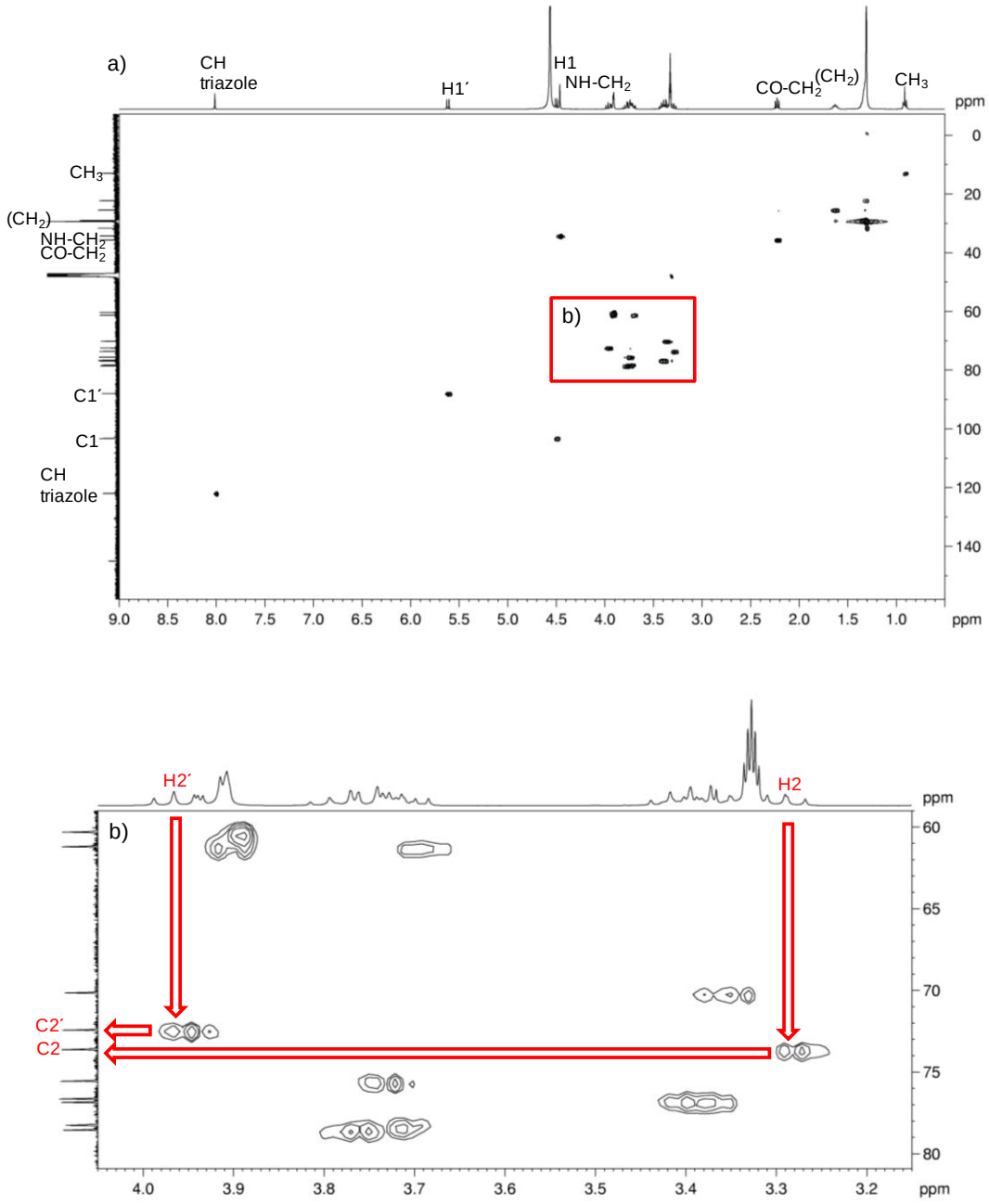

Fig. 3.81: a) HSQC NMR spectrum of **OAc-Cell-Tz-C_{16}** in MeOD at 50ºC, b) close up of red square region.

The quaternary C of triazole and amide group can be distinguised by HMBC, see **Fig. 3.82.**

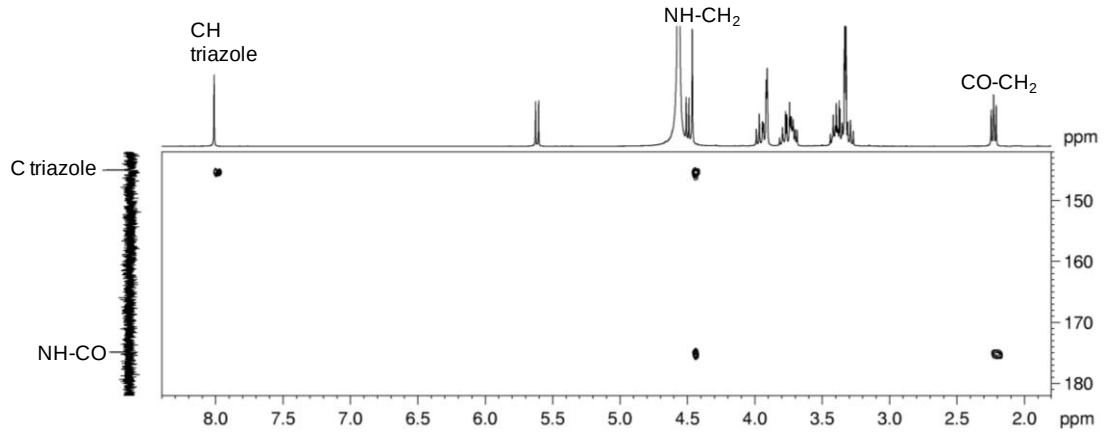

Figure 3.82: HMBC NMR spectum of **Cell-Tz-C_{16}** in MeOD at 50ºC.

3.7. Experimental section

Synthesis of *N*-Palmitoyl-D,L-phenylalanine ($C_{25}H_{41}NO_3$) **(1):**

Palmitic acid (2.00 g, 7.80 mmol) and *N*-hydroxysuccinimide (1.26 g, 10.92 mmol) were dissolved in 25 mL of THF and DCC (2.57 g, 12.48 mmol) was dissolved in 14 mL of THF. All these solutions were joined and stirred at RT for 96 h and the reaction was monitored by NMR until completion. When the first reaction was completed D,L-Phenylalanine (1.31 g, 6.59 mmol) and diisopropylethylamine (2.11 mL, 12.78 mmol) were dissolved in 64 mL of water and 32 mL of THF. The mixture was stirred at RT for 48 h. The reaction was monitored by ^{1}H NMR. The crude reaction was filtered and washed with THF. A solution of HCl (37%) was added in order to reach pH= 4. Part of the solvent was removed and then extracted with dichloromethane (3x100 mL). The organic solvent wasdried with anhydrous Na_2SO_4. The product was recrystallized with petroleum ether/dichloromethane (95/5). A white solid was obtained (1.14 g, 36%).

^{1}H NMR (300 MHz, $CDCl_3$, δ ppm): 0.88 (t, 3H, J= 7.2 Hz, C*H*$_3$- CH_2-), 1.58-1.25 (m, 26 H, -(C*H*$_2$)$_{13}$-), 2.17 (t, 2H, J=7.2 Hz, -C*H*$_2$-CO-), 3.29-3.09 (m, 2H, CH-C*H*$_2$- Car), 4.85 (ddd, 1H, J= 6.0 HZ, J= 6.0 HZ, J= 6.0 Hz, C*H*-CH_2- Car), 5.84 (d, 1H, J=6.0 Hz, N*H*), 7.15-7.33 (m, 5H, *Harom*).

^{13}C (75 MHz, $CDCl_3$, δ ppm): 14.8 -CH_2-*C*H_3, 23.4 -*C*H_2-CH_3, 26.3 –*C*H_2-CH_2-CH_3, 28.9, 29.3, 29.5, 29.7, 29.8, 29.8, 29.8 –(*C*H_2)$_{10}$-, 32.6 –*C*H_2-arom., 37.1 *C*H_2-CH_2-CO, 37.9 *C*H_2-CO, 53.7 CO-*C*H-NH, 127.8, 129.3, 130.0 *C*Harom, 174.8 CH-*C*O-NH, 175.4 -*C*O-OH.

ESI: 404.2 $[M+H]^+$.

IR (KBr, cm^{-1}): 3295, 2916, 2849, 1706, 1641, 1544, 698.

Synthesis of Suc-OOC-Phe-C$_{16}$ ($C_{37}H_{61}NO_{13}$):

A solution of sucrose (10.95 g, 31.99 mmol) was prepared in 80 mL of DMF and heated to reach a complete solution. *N*-Palmitoyl-D,L-phenylalanine (1.845 g, 4.57 mmol) and diisopropylethylamine (302 µl, 1.82 mmol) were dissolved in 20 mL of DMF. Sucrose solution was cooled at RT and added to the former solution. The mixture was cooled at 5° C for 10 min and DCC (1.42 g, 6.87 mmol) was added carefully. It was allowed to warm at RT and stirred for 46 h. The reaction was monitored by HPLC. The solvent was evaporated under reduced pressure and the product purified by flash chromatography with dichloromethane/acetone/methanol/water (67/15/15/3). The product was freeze-dried. The freeze-drying was carried out by redissolving the solid in water and freezing in liquid nitrogen. The block was broken in small pieces, in order to avoid the breaking of the vessel during the process due to tension on the glassware, introduced in the freeze-dried flask and kept in vacuum for 4 days. A white solid was obtained (0.72 g, 22%).

^{1}H NMR (300, MeOD, δ ppm): 0.84 (t, J=6.6 Hz, 3 H, C*H*$_3$-CH_2), 1.00-1.30 (m, 24H,-(C*H*$_2$)$_n$-), 1.38-1.43 (m, 2H, C*H*$_2$-CH_2-C=O), 2.10-2.17 (m, 2H, C*H*$_2$-C=O), 2.87-3.02 (m, 2H, C*H*$_2$-arom), 3.36-4.25 (m, *H*sucrose),4.59-4.65 (m, 1H, C*H*-NH), 5.34-5.47 (m, *H*sucrose), 5.57-5.60 (m, 1H, N*H*), 7.16-7.29 (m, 5H, *H*arom).

^{13}C NMR (100, MeOD, δ ppm): 13.1 -(CH_2)$_{12}$-*C*H_3, 22.4, 25.6, 28.8, 29.1, 29.3, 29.5, 29.5, 31.8, 35.5, 35.6, 36.8, 37.1, CO-*C*H_2-(*C*H_2)$_{13}$-CH_3, -CH-*C*H_2-arom , 53.6 -*C*H-CH_2-arom, 60.8, 62.1, 62.1, 62.3, 62.5, 62.8, 70.0, 70.2, 70.3, 70.7, 71.9, 72.9, 73.1, 73.3, 73.8, 73.9, 74.1, 74.4, 76.2, 76.5, 78.0, 82.1, 82.2, 82.5, 89.3, 89.5, 92.3, 104.0, 104.2, 104.5, 104.7, *C*maltose, 125.9, 126.4, 126.4, 127.7, 128.1, 128.1, 128.8, 128.9, 129.0, 129.2, 137.1, 137.3, C*H*arom, *C*arom, 171.5, 171.6, 174.9, 175.1 malt-NH-*C*O-CH, CH-NH-*C*O-CH_2.

*H*sucrose and ^{13}C were not completely assigned due to the mixture of isomers (see **ref 8b**).

HPLC column C8, eluent: THF/MeOH/H_2O: 40/40/20 + 0.5 ml/L AcOH, 0.8 mL/min.: tr (min) = 3.61 (solvent), 5.03 (mixture of monoesters).

MS (FAB+, NBA):750 $[M+Na]^+$.

IR (KBr, cm^{-1}): 3390 (broad), 2923, 2852, 1741, 1650, 1547, 1455, 1378, 1217, 1053, 1002, 930, 699.

Synthesis of Maltosylamine ($C_{12}H_{23}NO_{10}$) **(2):**

I. Carbonate method:

Maltose (500 mg, 1.46 mmol) was dissolved in 10 mL of DMSO and ammonium carbonate was added in intervals to keep the solution saturated. The reaction was monitored by TLC using a mixture of ethyl acetate/ acetic acid/ methanol/ water (4/3/3/2) as eluent. The reaction was kept for 48 h under argon and stirring at RT. The crude product was precipitated by addition of acetone and filtered under argon and immediately used. The product seems to be sensitive to air and the solvent of the next reaction was added immediately to continue the next reaction.

II. Carbamate method:

Maltose (509 mg, 1.48 mmol) was dissolved in 7.5 mL of anhydrous methanol and ammonium carbamate was progressively added to keep the solution saturated. The reaction was monitored by TLC using a mixture of ethyl acetate/ acetic acid/ methanol/ water (4/3/3/2) as eluent. The reaction was kept for 24 h under argon and stirring at 37 ºC. A white precipitate was obtained, filtered under argon and immediately used. The product was immediately used in the next reaction.

Synthesis of *N*-Palmitoyloxy succinimide ($C_{20}H_{35}NO_3$) **(3):**

Palmitic acid (5.13 g, 20 mmol) was dissolved in 30 mL of THF, *N*-hydroxysuccinimide (3.24 g, 28 mmol) was dissolved in 45 mL of THF and DCC (6.60 g, 32 mmol) was dissolved in 35 mL of THF. These solutions were mixed and stirred for 96 h at RT. The reaction was monitored by ^1H NMR. The reaction mixture was filtered and the solvent

was distilled off. The product was recrystallized from isopropanol to give a white powder (5.55 g, 78%).

^{1}H NMR (400 MHz, $CDCl_3$, δ ppm): 0.87 (t, 3H, J=6.8 Hz, -CH_2-C*H*$_3$), 1.25-1.42 (m, 24H, -(C*H*$_2$)$_{12}$-), 1.60-1.79 (m, 2H, -(CH_2)$_{12}$-C*H*$_2$-CH_2-CO-), 2.60 (t, 2H, J=7.5 Hz, -C*H*$_2$-CO-O-), 2.83 (s, 4H, -CO-C*H*$_2$ -C*H*$_2$-CO-).

^{13}C NMR (100 MHz, $CDCl_3$, δ ppm): 14.3 -CH_2-*C*H_3, 22.8 -*C*H_2-CH_3, 24.7 –*C*H_2-CH_2-CH_3, 25.7 *C*H_2-CO-N x2, 28.9, 29.3, 29.5, 29.7, 29.8, 29.8, 29.8 –(*C*H_2)$_{10}$-, 31.1 *C*H_2-CH_2-CO, 32.0 *C*H_2-CO, 168.9 CH_2-CH_2-*C*O-N, 169.3 CH_2-*C*O-N x2.

ESI: 376.3 $[M+K]^+$.

IR (KBr, cm^{-1}): 2955, 2920, 2850, 1822, 1788, 1726, 1210, 1070, 868, 654.

Synthesis of Malt-NH-C$_{16}$ ($C_{28}H_{53}NO_{11}$):

Compound **3** (36.0 mg, 0.10 mmol) was dissolved in 1.3 mL of anhydrous DMF, 1.0 mL of maltosylamine solution (0.29 mmol in 5.0 mL of anhydrous DMF), *N*,*N*-diisopropylethylamine (0.03 mL, 0.17 mmol) and dimethylaminopyridine (2.5 mg, 0.02 mmol) were mixed. Reaction was stirred at RT for 48 h and monitored by TLC with dichloromethane/ acetone/ methanol /water (56/20/20/1). Yield was lower than 5%, therefore purification was not performed.

Synthesis of the *N*-(*N´*-Palmitoyl-(S)-phenylalanyloxy)succinimide ($C_{29}H_{44}N_2O_5$) **(4):**

N-palmitoylphenylalanine (1.14 g, 2.82 mmol) was dissolved in 10 mL of THF, *N*-hydroxysuccinimide (0.46 g, 3.95 mmol) was dissolved in 15 mL of THF and DCC (0.94 g, 4.51 mmol) was dissolved in 20 mL of THF. All these solutions were joined and stirred for 48 h at RT. The reaction was monitored by ^{1}H NMR. The crude reaction was filtered and the solvent was distilled off. The product was recrystallized in oil petroleum/dichloromethane (95/5). A white solid was yield (1.12 g, 80%).

^{1}H NMR (300, CD_3OD, δ ppm): 0.88 (t, 3H, J= 7.2 Hz, C*H*$_3$-CH_2-), 1.58-1.25 (m, 26 H, -(C*H*$_2$)$_{13}$-, 2.17 (t, 2H, J=7.2 Hz, -C*H*$_2$-CO-), 2.85 (s, 4H, -C*H*$_2$-CO-), 3.29-3.09 (m, 2H, CH-C*H*$_2$-Car), 5.34-5.28 (m, 1H, C*H*-CH_2-), 5.70 (d, 1H, J=6.0 Hz, N*H*),7.31 -7.26 (m, 5H, *H*arom).

Synthesis of Malt-NH-Phe-C_{16} ($C_{37}H_{62}N_2O_{12}$):

Compound **4** (130.0 mg, 0.26 mmol) was dissolved in 3.55 mL solution of maltosylamine in pyridine (1.13 mmol in 4.8 mL of anhydrous pyridine, supposed previous reaction 100%). Crude reaction was stirred at RT and monitored by HPLC (methanol/ water (82/18) + 0.5 mL/L acetic acid, C8 column). Purification was made by flash chromatography: first chromatography in dichloromethane / acetone / methanol / water (56/20/20/4), and second chromatography in dichloromethane / acetone / methanol/ water (67/15/15/3). A white solid was obtained in a yield lower than 5%.

Compound **1** (0.500 g, 1.24 mmol) was dissolved in 16.5 mL of anhydrous DMF, 4.2 mL of maltosylamine solution (1.26 mmol in 5 mL of anhydrous DMF) and *N*-hydroxybenzotriazole (0.169 g, 1.25 mmol) in 6.5 mL of anhydrous DMF, were mixed. This solution was cooled to 0° C and then DCC (0.266 g, 1.29 mmol) in 6.5 mL of anhydrous DMF was added. The reaction was kept at 0ºC for 30 min. Crude reaction was stirred at RT and monitored by HPLC (methanol/ water (82/18) + 0.5 mL/L acetic acid, C8 column). Purification was made by flash chromatography: first chromatography in dichloromethane / acetone / methanol / water (56/20/20/4), and second chromatography in ethyl acetate /methanol / water (75/20/5). Finally reaction was purified by HPLC preparative. Preparative HPLC was performed using a X Bridge C18 column, 19 mm diameter and 150 mm height with a flow speed of 20 mL/min. Eluent conditions were: methanol 88% / trifluoroacetic acid (TFA, 1% water solution) 12 %, by isocratic method. A white solid was obtained with a final yield of around 5%.

^{1}H NMR (400 MHz, MeOD, 55 ºC, δ ppm): 0.89 (t, 3H, J = 6.5 Hz, -$(CH_2)_{12}$-C*H*$_3$), 1.20-1.29 (m, 24 H, -CH_2-(C*H*$_2$)$_{12}$-CH_3), 1.42-1.49 (m, 2H, -CH_2-C*H*$_2$-$(CH_2)_{12}$-), 2.14 (t, 2H, J = 7.3 Hz, -CO-C*H*$_2$-CH_2-), 2.89 (dd, 1H, $J_{CH\text{-}CH2a}$ = 9.4 Hz, $J_{CH2a\text{-}CH2b}$ = 14.0 Hz, -CH-(C*H*$_2$)$_b$-arom), 3.18 (dd, 1H, $J_{CH\text{-}CH2b}$ = 4.9 Hz, $J_{CH2a\text{-}CH2b}$ = 14.0 Hz, -CH-(C*H*$_2$)$_a$-arom), 3.27-3.88 (m, 11H, *H3´, H4´, H5´,H6´$_a$, H6´$_b$, H2, H3, H4, H5, H6$_a$, H6$_b$*), 3.37 (dd, 1H, $J_{H1'\text{-}H2'}$ = 9.1 Hz, $J_{H2'\text{-}H3'}$ = 9.2 Hz, *H2´*), 4.67 (dd, 1H, $J_{CH\text{-}CH2b}$ = 4.9 Hz $J_{CH\text{-}CH2a}$ = 9.4 Hz, -C*H*-CH_2-arom), 4.92 (d, 1H, $J_{H1'\text{-}H2'}$ = 9.1 Hz, *H1´*), 5.18 (d, 1H, $J_{H1\text{-}H2}$ = 3.5 Hz, *H1*), 7.17-7.26 (m, 5H, C*H*arom).

MS (FAB$^+$, NBA): 749 [M+Na]$^+$.

HPLC column C8, eluent: MeOH/H_2O: + 0.5 ml/L AcOH, 0.8 mL/min.: tr (min) = 3.91 (solvent), 10.97.

Synthesis of Hepta-O-acetyl-β-maltosyl azide ($C_{26}H_{35}N_3O_{17}$) **(5):**

Trimethylsilyl azide (543 µl, 4.13 mmol) and tin tetrachloride (173 µl, 1.48 mmol) were added, at RT and under argon, to a solution of β-D-maltose octaacetate (2.00 g, 2.95 mmol) in dry dichloromethane (6 mL, 0.5 M). The reaction mixture was stirred at RT and the reaction was monitored by TLC (6:4 hexane/ethyl acetate). After 24 h, dichloromethane was added and the solution was washed with saturated Na_2CO_3 and twice with water. The organic layer was dried over anhydrous $MgSO_4$, filtered and evaporated under reduced pressure. The product was purified by flash chromatography using hexane/ethyl acetate 6:4. A white solid was obtained (1.59 g, 80%).

^{1}H NMR (500 MHz, $CDCl_3$, δ ppm): 1.99 (s, 3H), 2.01 (s, 3H), C*H*$_3$-CO-O-C3/C*H*$_3$-CO-O-C3′, 2.02 (s, 3H), 2.04 (s, 3H) C*H*$_3$-CO-O-C2/C*H*$_3$-CO-O-C4, 2.03 (s,3H), 2.10 (s, 3H), 2.15 (s,3H) C*H*$_3$-CO-O-C2/C*H*$_3$-CO-O-C6/ C*H*$_3$-CO-O-C6′, 3.77 (ddd, 1H, $J_{5'-6'b}$= 2.5 Hz, $J_{5'-6'a}$=4.5 Hz, $J_{4'-5'}$=9.7 Hz, *H5′*), 3.94 (ddd, 1H, J_{5-6b}=2.4 Hz, J_{5-6a}=3.7 Hz, J_{5-4}=10.0 Hz, *H5*), 4.01 (ddd, 1H, $J_{3'-4'}$= 10.0 Hz, $J_{4'-5'}$= 9.7 Hz, *H4′*), 4.04 (dd, 1H, J_{5-6b}=2.4 Hz, J_{6a-6b}=12.5 Hz, *H6b*), 4.24 (dd, 1H, J_{5-6a}=3.7 Hz, J_{6a-6b}=12.5 Hz, *H6a*), 4.24 (dd, 1H, $J_{5'-6'a}$=4.5 Hz, $J_{6'a-6'b}$=12.2 Hz, *H6′a*), 4.50 (dd, 1H, $J_{5'-6'b}$=2.5 Hz, $J_{6'a-6'b}$=12.2 Hz, *H6′b*), 4.70 (d, 1H, $J_{1'-2'}$= 8.7 Hz, *H1′*), 4.78 (dd, 1H, $J_{1'-2'}$= 8.7 Hz, $J_{2'-3'}$= 9.0 Hz, *H2′*), 4.85 (dd, 1H, J_{1-2}=4.0 Hz, J_{2-3}= 10.5 Hz, *H2*), 5.05 (dd, 1H, J_{3-4}= 9.7 Hz, J_{4-5}= 10.0 Hz, *H4*), 5.25 (dd,1H, $J_{2'-3'}$= 9.0 Hz, $J_{3'-4'}$=10.0 Hz, *H3′*), 5.35 (dd, 1H, J_{3-4}= 9.7 Hz, J_{2-3}=10.5 Hz, *H3*), 5.40 (d, 1H, J_{1-2}= 4.0 Hz, *H1*).

^{13}C NMR (125 MHz, $CDCl_3$, δ ppm): 20.5, 20.6, 20.7, 20.8 *C*H$_3$-CO- x7, 61.5 *C6*, 62.5 *C6′*, 68.0 *C4*, 68.6 *C5*, 69.3 *C3*, 70.0 *C2*, 71.5 *C2′*, 72.4 *C4′*, 74.2 *C5′*, 75.1 *C3′*, 87.46 *C1′*, 95.7 *C1*, 169.4, 169.5 C2′-O-*C*O-/C4-O-*C*O-, 169.9, 170.1 C3-O-*C*O-/C3′-O-*C*O-, 170.1, 170.4, 170.5 C2-O-*C*O-/C6-O-*C*O/C6′-O-*C*O.

MALDI-TOF MS (DCTB): 684.2 $[M+Na]^+$.

IR (KBr, cm^{-1}): 2962, 2122, 1754, 1371, 1228, 1033, 896, 603.

Synthesis of Hepta-O-acetyl-β-maltosyl amine ($C_{26}H_{35}NO_{17}$) **(6):**

Compound **5** (1.00 g, 1.51 mmol) was dissolved in 10 mL of anhydrous THF under an argon atmosphere. Palladium hydroxide (20 wt % Pd on carbon wet, 104 mg, 10% wt) was added and the reaction mixture was stirred for 2 days at RT under an atmosphere of hydrogen. The catalyst was removed by filtration and the solvent was removed under reduced pressure. The disappearance of azide was monitored by the IR signal at 2122 cm^{-1}. The product was used without further purification.

MALDI-TOF MS (DCTB+NaTFA): 658.2 $[M+Na]^+$.

Synthesis of Palmitoyl chloride ($C_{16}H_{31}ClO$) **(7):**

Palmitic acid (295 mg, 1.15 mmol) was dissolved in 25 mL of anhydrous dichloromethane. Oxalyl chloride (0.30 mL, 2.81 mmol) and DMF (0.3 mL) were added. The reaction mixture was stirred overnight. The solvent was removed under reduced pressure. The acyl chloride formation was monitored by appearance of an IR signal at around 1800 cm^{-1}. The product was used without further purification.

Synthesis of OAc-Malt-NH-C_{16} ($C_{42}H_{67}NO_{18}$)**:**

Compound **6** was dissolved in 10 mL of anhydrous DMF. Pyridine (130 µL, 1.61 mmol) was added and the solution was cooled to 0 ºC. A solution of palmitoyl chloride **7** in 5 mL of anhydrous DMF was added. The reaction mixture was stirred for 48 h at RT and poured into 150 mL of water. The aqueous phase was extracted with 3 × 150 mL of dichloromethane. The combined organic phases were washed once with 150 mL of saturated Na_2CO_3 solution and 2 × 150 mL of water. The organic phase was dried with anhydrous $MgSO_4$. The solution was filtered and the solvent was removed under reduced pressure. The resulting syrup was purified by flash chromatography with dichloromethane/ethyl acetate 4:6 as eluent. A white solid was obtained (0.369 mg, 45%).

^{1}H NMR (400 MHz$CDCl_3$): 0.87 (t, 3H, J = 6.7 Hz, -$(CH_2)_{12}$-C*H*$_3$), 1.1-1.38 (m, 24H, CH_2-(C*H*$_2$)$_{12}$-CH_3), 1.52-1.62 (m, 2H, -CH_2-C*H*$_2$-$(CH_2)_{12}$), 1.99 (s, 3H), 2.00 (s, 3H), 2.02 (s, 3H), 2.06 (s, 3H), 2.09 (s, 3H), 2.12 (s, 3H), 2.16 (s, 3H) C*H*$_3$-CO-O x7, 2.10-2.20 (m, 2H, CO-C*H*$_2$-CH_2-), 3.72 (ddd, 1H, $J_{4'-5'}$ = 9.0 Hz, $J_{5'-6'a}$ = 4.3 Hz, $J_{5'-6'b}$ = 2.3 Hz, *H5´*), 3.85 (ddd, 1H, J_{4-5} = 9.9 Hz, J_{5-6a} = 3.8 Hz, J_{5-6b} = 2.2 Hz, *H5*), 3.89 (dd, 1H,

$J_{3'-4'}$ = 9.5 Hz, $J_{4'-5'}$ = 9.0 Hz, *H4´*), 3.97 (dd, 1H, J_{5-6b} = 2.2 Hz, J_{6b-6a} = 12.4 Hz, *H6b*), 4.15 (dd, 1H, J_{5-6a} = 3.8 Hz, J_{6a-6b} = 12.4 Hz, *H6a*), 4.17 (dd, 1H, $J_{5'-6'a}$ = 4.3 Hz, $J_{6'a-6'b}$ = 12.3 Hz, *H6´a*), 4.35 (dd, 1H, $J_{5'-6'b}$ = 2.3 Hz, $J_{6'a-6'b}$ = 12.3 Hz, *H6´b*), 4.68 (dd, 1H, $J_{1'-2'}$ = 9.4 Hz, $J_{2'-3'}$ = 9.5 Hz, *H2´*), 4.78 (dd, 1H, J_{1-2} = 4.0 Hz, J_{2-3} = 10.5 Hz, *H2*), 4.99 (dd, 1H, J_{3-4} = 9.8 Hz, J_{4-5} = 9.9 Hz, *H4*), 5.21 (dd, 1H, $J_{1'-2'}$ = 9.4 Hz, $J_{1'-NH}$ = 9.4 Hz, *H1´*), 5.26-5.33 (m, 3H, *H1*, *H3*, *H3´*), 5.97 (d, 1H, $J_{1'-NH}$ = 9.4 Hz, -*NH*-CO).

^{13}C NMR (100 MHz, $CDCl_3$): 14.1 -$(CH_2)_{12}$-*C*H_3, 20.6, 20.6, 20.7, 20.8 *C*H_3-CO-O x7, 22.7, 25.2, 29.0, 29.3, 29.3, 29.4, 29.6, 31.9, 36.7 -CO-C*H*$_2$-(C*H*$_2$)$_{13}$-CH_3, 61.4 *C6*, 62.8 *C6´*, 67.9 *C4*, 68.5 *C5*, 69.3 *C3*, 70.0 *C2*, 71.4 *C2´*, 72.7 *C4´*, 73.9 *C5´*, 75.0 *C3´*, 77.7 *C1´*, 95.6 *C1*, 169.5 CH_3-*C*O-O-C4, 169.6, 169.8, 170.4 CH_3-*C*O-O-C2/ CH_3-*C*O-O-C6/ CH_3-*C*O-O-C6´, 170.5, 170.7 CH_3-*C*O-O-C3/ CH_3-*C*O-O-C3´, 171.1 CH_3-*C*O-O-C2´, 173.2 NH-*C*O-CH_2.

MALDI-TOF MS (DCTB+NaTFA): 896.4$[M + Na]^+$.

Anal. Calcd for $C_{42}H_{67}NO_{18}$: C, 57.72; H, 7.73; N, 1.60. Found: C, 57.30; H, 7.57; N, 1.60.

IR (KBr, cm^{-1}): 3322 (broad), 2925, 2853, 1747, 1672, 1538, 1371, 1236, 1039, 900, 603.

Synthesis of *N*-Palmitoyl- (S)-phenylalanine ($C_{25}H_{41}NO_3$) **(1L):**

L-Phenylalanine (1.26 g, 7.63 mmol) and diisopropylethylamine (2.50 mL, 15.26 mmol) were dissolved in 100 mL of water and 50 mL of THF. A solution of compound **4** (2.70 g, 7.63 mmol) in 115 mL of THF was added. The mixture was stirred at RT for 6 h. The reaction was monitored by ^{1}H NMR. A solution of HCl (37%) was added to give pH = 4. The solvent was partially removed and the resulting aqueous phase was extracted with dichloromethane (3 × 100 mL). The organic layer was dried with anhydrous Na_2SO_4 and finally the solvent was evaporated. A white solid was obtained and recrystallized from petroleum ether/dichloromethane (95/5) (2.27 g, 78%).

^{1}H NMR (300 MHz, $CDCl_3$, δ ppm): 0.88 (t, 3H, J= 7.2 Hz, -CH_2-C*H*$_3$), 1.25-1.38 (m, 24 H, -(C*H*$_2$)$_{12}$-CH_3), 1.50-1.58 (m, 2H, CH_2-C*H*$_2$-$(CH_2)_{12}$-CH_3), 2.17 (t, 2H, J=7.2 Hz, -C*H*$_2$-CO-, 3.09-3.29 (m, 2H, CH-C*H*$_2$- arom), 4.85 (m, 1H, -C*H*-CH_2-arom), 5.84 (d, 1H, J=6.0 Hz, N*H*), 7.15-7.33 (m, 5H, C*H*arom).

^{13}C (75 MHz, $CDCl_3$, δ ppm): 14.8 -CH_2-*C*H_3, 23.4 -*C*H_2-CH_3, 26.3 –*C*H_2-CH_2-CH_3, 28.9, 29.3, 29.5, 29.7, 29.8, 29.8, 29.8 –(*C*H_2)$_{10}$-, 32.6 –*C*H_2-arom., 37.1 *C*H_2-CH_2-CO, 37.9 *C*H_2-CO, 53.7 CO-*C*H-NH, 127.8, 129.3, 130.0 *C*Harom, 174.8 CH-*C*O-NH, 175.4 -*C*O-OH.

ESI: 404.2 $[M+H]^+$.

IR (KBr, cm-1): 3295, 2916, 2849, 1706, 1641, 1544, 698.

Synthesis of OAc-Malt-NH-Phe-C$_{16}$ ($C_{51}H_{76}N_2O_{19}$)**:**

Compound **6** (700 mg, 1.10 mmol) was dissolved in 10 mL of anhydrous THF, *N*-palmitoyl-L-phenylalanine **1L** (680 mg, 1.68 mmol) and hydroxybenzotriazole (255 mg, 1.89 mmol) were added and the solution was cooled to 0 ºC. A solution of DCC (330 mg, 1.60 mmol) in 10 mL of anhydrous THF was added. The reaction mixture was stirred for 2 days at RT. The reaction was monitored by TLC using a mixture of hexane/ethyl acetate 1:1 as eluent. The mixture was filtered and the solvent was removed under reduced pressure. 150 mL of ethyl acetate were added and the organic phase was washed three times with 1M $KHSO_4$ solution, and three times with 1M $NaHCO_3$ solution. The organic layer was dried over anhydrous $MgSO_4$. The solution was filtered and the solvent was removed under reduced pressure. The resulting white solid was purified by flash chromatography with a mixture of hexane/ethyl acetate 1:1 and recrystallized from ethanol. A white solid was obtained (720 mg, 50%).

^{1}H NMR (500 MHz, $CDCl_3$, δ ppm): 0.87 (t, 3H, J = 7.0 Hz, -(CH_2)$_{12}$-C*H*$_3$), 1.25-1.40 (m, 24H, -CH_2-(C*H*$_2$)$_{12}$-CH_3), 1.46-1.60 (m, 2H, -C*H*$_2$-(CH_2)$_{12}$-CH_3), 1.93 (s, 3H), 1.99 (s, 6H), 2.02 (s, 3H), 2.05 (s, 3H), 2.10 (s, 3H), 2.15 (s, 3H) C*H*$_3$-CO-O- x7, 2.10-2.20 (m, 2H, CO-C*H*$_2$-CH_2), 2.97-3.15 (m, 2H, CH-C*H*$_2$-ar), 3.75-3.85 (m, 1H, *H5´*), 3.91-3.96 (m, 2H, *H4´*, *H5*), 4.03 (dd, 1H, $J_{5\text{-}6b}$ = 2.0 Hz, $J_{6a\text{-}6b}$ = 12.4 Hz, *H6b*), 4.20-4.26 (m, 2H, *H6a*, *H6´a*), 4.47 (dd, 1H, $J_{5\text{-}6´b}$ = 2.2 Hz, $J_{6´a\text{-}6´b}$ = 12.3 Hz, *H6´b*), 4.57 (m, 1H, NH-C*H*-CH_2-), 4.67 (dd, 1H, $J_{1´\text{-}2´}$ = 9.5 Hz, $J_{2´\text{-}3´}$ = 9.5 Hz, *H2´*), 4.84 (dd, 1H, $J_{1\text{-}2}$ = 4.0 Hz, $J_{2\text{-}3}$ = 10.5 Hz, *H2*), 5.06 (dd, 1H, $J_{3\text{-}4}$ = 10.0 Hz, $J_{4\text{-}5}$ = 10.0 Hz, *H4*), 5.20 (dd, 1H, $J_{1´\text{-}2´}$ = 9.5 Hz, $J_{1´\text{-}NH}$ = 9.1 Hz, *H1´*), 5.33 (dd, 1H, $J_{2´\text{-}3´}$ = 9.5 Hz, $J_{3´\text{-}4´}$ = 9.2 Hz, *H3´*), 5.35(dd, 1H, $J_{3\text{-}4}$ = 10.0 Hz, $J_{2\text{-}3}$ = 10.5 Hz, *H3*), 5.37 (d, 1H, $J_{1\text{-}2}$ = 4.0 Hz, *H1*), 5.77 (d, 1H, $J_{NH\text{-}CH}$ = 7.6 Hz, CH-N*H*-CO), 6.64 (dd, 1H, J $H_{1´\text{-}NH}$ = 9.1 Hz, malt-N*H*-CO), 7.16-7.11 (m, 2H, ar-C*H*-C-NH), 7.29-7.21 (m, 3H, ar-C*H* = C*H*-C*H* = ar).

^{13}C NMR (125 MHz, $CDCl_3$, δ ppm): 14.1 $(CH_2)_{13}$-*C*H_3, 20.5, 20.6, 20.7, 20.9, *C*H_3-CO-O x7, 22.7, 24.9, 25.4, 25.6, 29.1, 29.3, 29.3, 29.4, 29.6, 29.7, 31.9, 33.9 -*C*H_2-(*C*H_2)$_{12}$-CH_3, 36.4 CO-*C*H_2-CH_2-, 37.1 CH-*C*H_2-arom, 53.9 CO-*C*H-CH_2, 61.4 *C6*, 62.7 *C6´*, 67.9 *C4*, 68.6 *C5*, 69.3 *C3*, 70.0 *C2*, 71.2 *C2´*, 72.6 *C4´*, 73.9 *C5´*, 74.8 *C3´*, 77.8 *C1´*, 95.6 *C1*, 127.1, 128.7, 128.8, 129.1, 129.4 *C*Harom, 135.9 *C*arom, 169.5 CH_3-*C*O-O-C4, 169.7, 169.8 CH_3-*C*O-O-C3/CH_3-*C*O-O-C3´, 170.4, 170.5, 170.6 CH_3-*C*O-O-C2/CH_3-*C*O-O-C6/CH_3-*C*O-O-C6´, 170.9 CH_3-*C*O-O-C2´, 171.7 mal-NH-*C*O-CH, 173.3 NH-*C*O-CH_2-.

MALDI-TOF MS (DCTB+NaTFA): 1043.6 $[M + Na]^+$.

Anal. Calcd for $C_{51}H_{76}N_2O_{19}$: C, 59.99; H, 7.50; N, 2.74. Found: C, 59.60, H, 7.51, N, 2.99.

IR (KBr, cm^{-1}): 3332, 2918, 2849, 1745, 1689, 1649, 1533, 1371, 1226, 1040, 938, 611.

Synthesis of Malt-NH-C_{16} and Malt-NH-Phe-C_{16}:

The protected peracetylated glycolipids, **OAc-Malt-NH-C_{16}** or **OAc-Malt-NH-Phe-C_{16}** (149.7 mg, 0.146 mmol) was dissolved in 7.5 mL of anhydrous methanol and sodium methoxide (55.3 mg, 1.023 mmol) was added. The solution was stirred at RT until the reaction was complete (TLC, hexane/ethyl acetate 1:1). Amberlyst IR 120 (H^+ form) was added to exchange sodium ions. The resin was filtered off and the solvent was evaporated in vacuo to give a white solid (70-85%).

Malt-NH-C_{16} ($C_{28}H_{53}NO_{11}$)**:**

^{1}H NMR (400 MHz, MeOD, 55 ºC, δ ppm): 0.90 (t, 3H, J = 6.7 Hz, -$(CH_2)_{12}$-C*H*$_3$), 1.20-1.41 (m, 24H, CH_2-(C*H*$_2$)$_{12}$-CH_3), 1.56-1.67 (m, 2H, CH_2-C*H*$_2$-$(CH_2)_{12}$-), 2.23 (m, 2H, -CO-C*H*$_2$-CH_2-), 3.20-3.88 (m, 12H, *H2, H3, H4, H5, H6a, H6b, H2´, H3´, H4´,H5´,H6´a, H6´b)*, 4.89 (d, 1H, $J_{1´-2´}$ = 9.2 Hz, *H1´*), 5.16 (d, 1H, J_{1-2} = 3.7 Hz, *H1*).

^{13}C NMR (100 MHz, DMSO, δ ppm): 14.5 -$(CH_2)_{12}$-*C*H_3, 25.4 -CH_2-*C*H_2-$(CH_2)_{12}$-, 22.5, 29.1 29.2, 29.3, 29.4, 29.5, 29.5, 31.7, CH_2-(*C*H_2)$_{12}$-CH_3, 35.9 -CO-*C*H_2-CH_2-, 60.9, 61.2, 70.4, 72.4, 73.0, 73.7, 73.9, 77.2, 77.7, 79.6, *C2, C3, C4, C5, C6, C2´, C3´, C4´,C5´, C6´*, 80.1 *C1´*, 101.4 *C1*, 173.1 NH-*C*O-CH_2.

Micro-TOF MS: 580.3698 $[M + H]^+$ calcd 580.3691; 602.3521$[M + Na]^+$ calcd 602.3511.

IR (KBr, cm^{-1}): 3312 (broad), 2914, 2850, 1670, 1548, 1472, 1151, 1083, 1033, 715.

Malt-NH-Phe-C_{16} ($C_{37}H_{62}N_2O_{12}$)**:**

^{1}H NMR (400 MHz, MeOD, 55 ºC, δ ppm): 0.89 (t, 3H, J = 6.5 Hz, -$(CH_2)_{12}$-C*H*$_3$), 1.20-1.29 (m, 24 H, -CH_2-(C*H*$_2$)$_{12}$-CH_3), 1.42-1.49 (m, 2H, -CH_2-C*H*$_2$-$(CH_2)_{12}$-), 2.14 (t, 2H, J = 7.3 Hz, -CO-C*H*$_2$-CH_2-), 2.89 (dd, 1H, $J_{CH-CH2a}$ = 9.4 Hz, $J_{CH2a-CH2b}$ = 14.0 Hz, -CH-(C*H*$_2$)$_b$-arom), 3.18 (dd, 1H, $J_{CH-CH2b}$ = 4.9 Hz, $J_{CH2a-CH2b}$ = 14.0 Hz, -CH-(C*H*$_2$)$_a$-arom), 3.27-3.88 (m, 11H, *H3´, H4´, H5´,H6´$_a$, H6´$_b$, H2, H3, H4, H5, H6$_a$, H6$_b$*) 3.37 (dd, 1H, $J_{H1´-H2´}$ = 9.1 Hz, $J_{H2´-H3´}$ = 9.2 Hz, *H2´*), 4.67 (dd, 1H, $J_{CH-CH2b}$ = 4.9 Hz $J_{CH-CH2a}$ = 9.4 Hz, -C*H*-CH_2-arom), 4.92 (d, 1H, $J_{H1´-H2´}$ = 9.1 Hz, *H1´*), 5.18 (d, 1H, J_{H1-H2} = 3.5 Hz, *H1*), 7.17-7.26 (m, 5H, C*H*arom).

^{13}C NMR (100 MHz, MeOD, 55 ºC, δ ppm): 14.3 -$(CH_2)_{12}$-*C*H_3, 26.7 -CH_2-*C*H_2-$(CH_2)_{12}$-, 23.6, 30.3, 30.4, 30.6, 32.9 -CH_2-(*C*H_2)$_{12}$-CH_3, 36.9 -CO-*C*H_2-CH_2-, 38.8 -CH-*C*H_2-arom, 55.7 -*C*H-CH_2-arom, 62.2, 62.8, 71.7, 74.2, 74.8, 75.2, 78.45, 78.7, 80.9 *C2, C3, C4, C5, C6, C3´, C4´, C5´, C6´*, 73.7 *C2´*, 81.3 *C1´*, 102.8 *C1*, 127.7, 129.3, 130.4 C*H*arom, 138.3 *C*arom, 174.63 malt-NH-*C*O-CH, 176.1 CH-NH-*C*O-CH_2.

Micro-TOF MS: 727.4400 $[M + H]^+$ calcd 727.4375; 749.4234 $[M + Na]^+$, calcd 749.4194.

IR(KBr, cm^{-1}): 3323 (broad), 2919, 2850, 1645, 1540, 1147, 1081, 1034, 698.

Synthesis of *N*-propargyl palmitoylamide (8) and *N*-propargyl (*N´*-palmitoyl-(S)-phenylalanine)amide (9):

Palmitic acid or compound **1L** (1.0 g, 2.48 mmol) and hydroxybenzotriazole were dissolved in 20 mL of anhydrous tetrahydrofuran. Propargylamine (0.16 mL, 2.50 mmol) was added. The solution was cooled to 0 ºC. A solution of DCC (511 mg mg, 2.48 mmol) in 15 mL of anhydrous THF was added. The reaction mixture was stirred for 2 days at RT. The reaction was monitored by TLC with hexane/ethyl acetate 7:3 as eluent. The mixture was filtered and the solvent was removed under reduced pressure. 250 mL of dichoromethane were added and the organic phase was washed three times with 1M $KHSO_4$ solution, and three times with 1M $NaHCO_3$ solution. The organic layer

was dried over anhydrous $MgSO_4$. The solution was filtered and the solvent was removed under reduced pressure. The resulting white solid was purified by recrystallization from ethanol. A white solid was obtained (545 mg, yield 75% for compound 8 and 820 mg, yield 75% for compound 9).

***N*-Propargyl palmitoylamide** ($C_{19}H_{35}NO$) **(8):**

^{1}H NMR (300 MHz, $CDCl_3$, δ ppm): 0.87 (t, 3H, J=6,5 Hz, $–CH_2-CH_3$), 1.20-1.40 (m, 24H, $–CH_2-(CH_2)_{12}-$), 1.59-1.64 (m, 2H, $–CH_2-(CH_2)_{12}-$), 2.18 (t, 2H, J=7,5Hz, $-CO-CH_2-$), 2.22 (t, 1H, J=2,4 Hz, HC≡C-), 4.05 (dd, 2H, $J_{CH2-C≡CH}$= 2,5 Hz, J_{CH2-NH}=5,0 Hz, ≡C-CH_2-NH-), 5.63 (s, 1H, NH).

^{13}C NMR (75 MHz, $CDCl_3$, δ ppm): 14.1 $–CH_2-CH_3$, 25.6 $-CH_2-(CH_2)_{12}$, 22.7, 29.2, 29.3, 29.3, 29.4, 29.5, 29.6, 29.7, 29.7, 31.9, $-(CH_2)_{12}-$, ≡C-CH_2-NH, 36.5 $-CO-CH_2-(CH_2)_{13}$, 71.5 HC≡C, 79.7 HC≡C-CH_2, 172.7 NH-CO-CH_2.

Micro-TOF MS: 294.2773 $[M+H]^+$ calcd 293.2713; 316.2612 $[M+Na]^+$, calcd 316.2611.

IR (KBr, cm^{-1}): 3292, 3073, 2955, 2918, 2848, 1639, 1553, 1472, 1462, 1275, 729, 719, 689, 666, 631, 570.

***N*-Propargyl (*N´*-palmitoyl-(S)-phenylalanine)amide** ($C_{28}H_{44}N_2O_2$) **(9):**

^{1}H (300 MHz, $CDCl_3$, δ ppm): 0.88 (t, 3H, J=6.7 Hz, $–CH_2-CH_3$), 1.25-1.34 (m, 24H, $–CH_2-(CH_2)_{12}-$), 1.52-1.57 (m, 2H, $–CH_2-(CH_2)_{12}-$), 2.16 (t, 2H, J=8.0 Hz, $-CO-CH_2-$), 2.18 (t, 1H, J=2.5 Hz, HC≡C-), 3.00-3.13 (m, 2H, -CH-CH_2-Phe), 3.95 (dd, 2H, $J_{CH2-C≡CH}$= 2.5 Hz, J_{CH2-NH}=5.4 Hz, ≡C-CH_2-NH-), 4.64 (m, 1H, -CO-CH-CO-), 6.06 (d, 1H, J=7,7 Hz, -CH-NH-CO-), 6.13 (t, 1H, J=5,4 Hz, $–CH_2-$NH-CO-), 7.19-7.33 (m, 5Harom).

^{13}C (75 MHz, $CDCl_3$, δ ppm): 14.0 $–CH_2-CH_3$, 25.5 $-CH_2-(CH2)_{12}-$, 22.7, 29.1, 29.2, 29.3, 29.3, 29.4, 29.6, 29.6, 29.7, 30.8, 31.9 $-(CH_2)_{12}-$, ≡C-CH_2-NH, 36.6 $-CO-CH_2-(CH_2)_{13}$, 38.3 -CH-CH_2-Phe, 54.3 -CO-CH-NH-, 71.6 HC≡C, 78.9 ≡C-CH_2, 127.1, 128.7, 129.3 CHarom, 136.6 Carom, 170.7 –NH-CO-CH-CH_2-arom, 173.3 –NH-CO-$CH_2-(CH_2)_{12}$.

MALDI-TOF MS (DCTB+NaTFA): 463.3$[M+Na]^+$.

IR (KBr, cm^{-1}): 3285, 3067, 2953, 2917, 2850, 1656, 1634, 1543, 1237, 1228, 752, 727, 703, 689, 658, 501.

Synthesis of OAc-Malt-Tz-C_{16} and OAc-Malt-Tz-Phe-C_{16}:

N-Propargyl derivatives **8** or **9** (266 mg, 0.91 mmol), azide **5** (602 mg, 0.91 mmol), copper(I) bromide (27.7 mg, 0.19 mol) and N-pentamethyldiethylenetriamine (PMDETA) (38 µL, 0.18 mmol) were dissolved in anhydrous DMF (6mL) under an argon atmosphere. The mixture was stirred at RT for 2 days. The reaction was monitored by TLC with hexane/ethyl acetate 1:1 as eluent. The catalyst was removed by filtration and the solvent was removed under reduced pressure. The reaction was poured into 150 mL of water. The aqueous phase was extracted three times, each with 150 mL of dichloromethane/ethyl acetate 1:1. The organic phase was dried with anhydrous $MgSO_4$. The solution was filtered and the solvent was removed under reduced pressure. The resulting white solid was purified by flash chromatography using initially dichloromethane/ethyl acetate 1:1 and then increasing the polarity. A white solid was obtained (756 mg, 87% of **OAc-Malt-Tz-C_{16}** and 850 mg, 85% of **OAc-Malt-Tz-Phe-C_{16}**).

OAc-Malt-Tz-C_{16} ($C_{45}H_{70}N_4O_{18}$)**:**

^{1}H NMR (400 MHz, $CDCl_3$, δ ppm): 0.87 (t, 3H, J = 6.2 Hz, -$(CH_2)_{12}$-C*H*$_3$), 1.16-1.35 (m, 24H, -(C*H*$_2$)$_{12}$-), 1.55-1.66 (m, 2H, -C*H*$_2$-$(CH_2)_{12}$), 1.84 (s, 3H, C*H*$_3$-CO-O-C2´) 2.00 (s, 3H), 2.02 (s, 6H), 2.06 (s, 3H), 2.10 (s, 3H), 2.13 (s, 3H), C*H*$_3$-CO-O x7, 2.17 (t, 2H, J = 7.7 Hz, CO-C*H*$_2$-CH_2), 3.96-3.98 (m, 2H, *H5*, *H5´*), 4.05 (dd, 1H, $J_{6b\text{-}5}$ = 1.5 Hz, $J_{6a\text{-}6b}$ = 1.6 Hz, *H6b*), 4.13 (dd, 1H, $J_{3'\text{-}4'}$ = 9.3 Hz, $J_{4'\text{-}5'}$ = 9.3 Hz, *H4´*), 4.23-4.27 (m, 2H, *H6a*, *H6´a*), 4.44-4.54 (m, 3H, C = C-C*H*$_2$-NH, *H6´b*), 4.87 (dd, 1H, $J_{1\text{-}2}$ = 3.9 Hz, $J_{2\text{-}3}$ = 10.7 Hz, *H2*), 5.07 (dd, 1H, $J_{3\text{-}4}$ = 10.0 Hz, $J_{4\text{-}5}$ = 9.8 Hz, *H4*), 5.31 (dd, 1H, $J_{1'\text{-}2'}$ = 9.1 Hz, $J_{2'\text{-}3'}$ = 8.8 Hz, *H2´*), 5.37 (dd, 1H, $J_{2\text{-}3}$ = 10.7 Hz, $J_{3\text{-}4}$ = 10.0 Hz, *H3*), 5.43 (dd, 1H, $J_{2'\text{-}3'}$ = 8.8 Hz, $J_{3'\text{-}4'}$ = 9.3 Hz, *H3´*), 5.44 (d, 1H, $J_{1\text{-}2}$ = 3.9 Hz, *H1*), 5.84 (d, 1H, $J_{1'\text{-}2'}$ = 9.1 Hz, *H1´*), 6.06 (t, 1H, J = 4.7 Hz, -CH_2-N*H*-CO), 7.69 (s, 1H, N-C*H* = C-CH_2 triazole).

^{13}C NMR (100 MHz, $CDCl_3$, δ ppm): 14.1 -$(CH_2)_{12}$-*C*H_3, 20.2, 20.6, 20.7, 20.8, 20.8 *C*H_3-CO-O x7, 25.6 CH_2-*C*H_2-$(CH_2)_{12}$-, 22.7, 29.3, 29.4, 29.4, 29.5, 29.6, 29.7, 29.7, 31.9, 35.6 -(*C*H_2)$_{12}$-, CO-*C*H_2-CH_2, 34.8 C-*C*H_2-NH, 61.5 *C6*, 62.5 *C6´*, 67.9 *C4*, 68.8

C5, 69.2 *C3*, 70.0 *C2´*, 70.9 *C2*, 72.4 *C4´*, 75.1 *C3´*, 75.4 *C5´*, 85.3 *C1´*, 95.9 *C1*, 120.8 N-C*H*=C-Ntriazole, 145.3 CH=*C*-Ntriazole, 169.1, 169.4, 169.9 CH_3-*C*O-O-C2/ CH_3-*C*O-O-C6/ CH_3-*C*O-O-C6´, 169.9, 170.3 CH_3-*C*O-O-C3/ CH_3-*C*O-O-C3´, 170.5 CH_3-*C*O-O-C4, 170.6 CH_3-*C*O-O-C2´, 173.2 NH-*C*O-CH_2.

MALDI-TOF MS (DCTB+NaTFA): 977.5 $[M + Na]^+$.

Anal. Calcd for $C_{45}H_{70}N_4O_{18}$: C, 56.59; H, 7.39; N, 5.87. Found: C, 56.25; H, 7.28; N, 5.80.

IR (KBr, cm^{-1}): 3303, 2925, 2854, 1754, 1645, 1552, 1369, 1233, 1036.

OAc-Malt-Tz-Phe-C_{16} ($C_{54}H_{79}N_5O_{19}$)**:**

^{1}H NMR (400 MHz, $CDCl_3$, δ ppm): 0.87 (t, 3H, J = 6.8 Hz, -$(CH_2)_{12}$-C*H*$_3$), 1.14-1.40 (m, 24H, -(C*H*$_2$)$_{12}$-), 1.47-1.58 (m, 2H, -C*H*$_2$-$(CH_2)_{12}$-), 1.83 (s, 3H, C*H*$_3$-CO-O-C2´), 2.01 (s, 3H), 2.03 (s, 6H), 2.07 (s, 3H), 2.10 (s, 3H), 2.12 (s, 3H), C*H*$_3$-CO-O x6, 2.10-2.17 (m, 2H, CO-C*H*$_2$-CH_2), 2.98-3.10 (m, 2H, -CH-C*H*$_2$-Phe), 3.94- 4.01 (m, 2H, *H5*, *H5´*), 4.07 (dd, 1H, $J_{5\text{-}6b}$ = 1.8 Hz, $J_{6a\text{-}6b}$ = 12.4 Hz, *H6b*), 4.16 (dd, 1H, $J_{3'\text{-}4'}$ = 9.4 Hz, $J_{4'\text{-}5'}$ = 9.4 Hz, *H4´*), 4.23-4.28 (m, 2H, *H6a*, *H6´a*), 4.42 (d, 2H, J = 5.8 Hz, C-C*H*$_2$-NH), 4.51 (dd, 1H, $J_{5'\text{-}6'b}$ = 2.2 Hz, $J_{6'a\text{-}6'b}$ = 12.4 Hz, *H6´b*), 4.60-4.66 (m, 1H, -CO-C*H*-NH-), 4.88 (dd, 1H, $J_{1\text{-}2}$ = 3.9 Hz, $J_{2\text{-}3}$ = 10.5 Hz, *H2*), 5.07 (dd, 1H, $J_{3\text{-}4}$ = 9.7 Hz, $J_{4\text{-}5}$ = 10.0 Hz, *H4*), 5.32 (dd, 1H, $J_{1'\text{-}2'}$ = 9.4 Hz, $J_{2'\text{-}3'}$ = 9.2 Hz, *H2´*), 5.38 (dd, 1H, $J_{2\text{-}3}$ = 10.5 Hz, $J_{3\text{-}4}$ = 9.7 Hz, *H3*), 5.45 (dd, 1H, $J_{2'\text{-}3'}$ = 9.2 Hz, $J_{3'\text{-}4'}$ = 9.4 Hz, *H3´*), 5.46 (d, 1H, $J_{1\text{-}2}$ = 3.9 Hz, *H1*), 5.83 (d, 1H, $J_{1'\text{-}2'}$ = 9.4 Hz, *H1´*), 6.04 (d, 1H, J = 7.6 Hz, CH-N*H*-CO), 6.36 (t, 1H, J = 5.7 Hz, CH_2-N*H*-CO), 7.12-7.13 (m, 2H, <u>*H*arom</u>), 7.27-7.22 (m, 3H, *H*arom), 7.54 (s, 1H, N-C*H* = C).

^{13}C NMR (100 MHz, $CDCl_3$, δ ppm): 14.1 -$(CH_2)_{12}$-*C*H_3, 20.5, 20.6, 20.7, 20.8, *C*H_3-CO-O x7, 22.7 -(*C*H_2)$_{12}$-, 25.5 -*C*H_2-$(CH_2)_{12}$, 29.2, 29.3, 29.3, 29.4, 29.6, 29.7, 32.0 -(*C*H_2)$_{12}$-, 34.9 C-*C*H_2-NH, 36.5 CO-*C*H_2-CH_2, 38.2 CH-*C*H_2-Phe, 54.3 -CO-*C*H-CH_2, 61.5 *C6*, 62.5 *C6´*, 68.0 *C4*, 68.8 *C5*, 69.3 *C3*, 70.0 *C2*, 70.9 *C2´*, 72.5 *C4´*, 75.2 *C3´*, 75.5 *C5´*, 85.0 *C1´*, 96.0 *C1*, 120.8 N-*C*H=C-N triazole, 127.0, 128.9, 129.2 *C*Harom, 136.5 *C*arom, 144.9 CH=*C*-N triazole, 169.1 CH_3-*C*O-O-C2´, 169.3 CH_3-*C*O-O-C4, 169.8 CH_3-*C*O-O-C3, 169.9 CH_3-*C*O-O-C3´, 170.4 CH_3-*C*O-O-C2, 170.5, 170.3 CH_3-*C*O-O-C6/ CH_3-*C*O-O-C6´, 171.0 NH-*C*O-CH-, 173.2 NH-*C*O-CH_2-.

MALDI-TOF MS (DCTB): 1124.4 $[M + Na]^+$.

Anal. Calcd for $C_{54}H_{79}N_5O_{19}$: C, 58.84; H, 7.22; N, 6.35. Found: C, 58.24; H, 7.12; N, 6.28.

IR (KBr, cm^{-1}): 3306, 2923, 2852, 1753, 1640, 1546, 1370, 1234, 1037.

Synthesis of Malt-Tz-C_{16} and Malt-Tz-Phe-C_{16}:

The protected compound **OAc-Malt-Tz-C_{16}** or **OAc-Malt-Tz-Phe-C_{16}** (0.146 mmol) was dissolved in 7.5 mL of anhydrous methanol. Sodium methoxide (55.3 mg, 1.023 mmol) was added. The solution was stirred at RT until the reaction was complete (TLC, hexane/ethyl acetate 1:1). Amberlyst IR 120 (H^+ form) was added to exchange sodium ions, the resin was filtered off and the solvent was evaporated in vacuo. A white solid was obtained (85-90%).

Malt-Tz-C_{16} ($C_{31}H_{56}N_4O_{11}$)**:**

^{1}H NMR (400 MHz, MeOD, 55 ºC, δ ppm): 0.90 (t, 3H, J = 6.9 Hz, -$(CH_2)_{12}$-C*H*$_3$), 1.20-1.36 (m, 24H, -(C*H*$_2$)$_{12}$-CH_3), 1.56-1.60 (m, 2H, C*H*$_2$-CH_2-$(CH_2)_{12}$), 2.21 (t, 2H, J = 7.4 Hz, CO-C*H*$_2$-CH_2), 3.28 (dd, 1H, $J_{3\text{-}4}$ = 9.6 Hz, $J_{4\text{-}5}$ = 9.5 Hz, *H4*), 3.47 (dd, 1H, $J_{1\text{-}2}$ = 3.8 Hz, $J_{2\text{-}3}$ = 9.7 Hz, *H2*), 3.64 (dd, 1H, $J_{2\text{-}3}$ = 9.7 Hz, $J_{3\text{-}4}$ = 9.6 Hz, *H3*), 3.65-3.90 (m, 8H, *H5, H6a, H6b, H3´, H4´, H5´, H6´a, H6´b*), 3.93 (dd, 1H, $J_{1'\text{-}2'}$ = 9.1 Hz, $J_{2'\text{-}3'}$ = 9.0 Hz, *H2´*), 4.34 (s, 2H, C-C*H*$_2$-NH), 5.13 (d, 1H, $J_{1\text{-}2}$ = 3.8 Hz, *H1*), 5.50 (d, 1H, $J_{1'\text{-}2'}$ = 9.1 Hz, *H1´*), 7.95 (s, 1H, N-C*H*-C-triazole).

^{13}C NMR (100 MHz, MeOD, 55 ºC, δ ppm):13.0 -$(CH_2)_{12}$-*C*H_3, 22.3, 25.4, 28.9, 29.2, 31.6 -*C*H_2-(*C*H_2)$_{12}$-, 34.1 C-*C*H_2-NH-, 35.5 CO-*C*H_2-CH_2, 60.4, 61.3, 73.7, 76.8, 78.2, *C6, C3´,C4´, C5´,C6´*, 70.1 *C4*, 72.2 *C2´*, 72.8 *C2*, 73.5 *C3*, 78.9 *C5*, 88.0 *C1´*, 101.5 *C1*, 120.0 N-*CH*=Ctriazole, 145.0 CH=*C*-CH_2 triazole, 174.9 NH-*C*O-CH_2.

MicroTOF MS: 683.383 $[M+ Na]^+$, calcd: 683.384.

IR (KBr, cm^{-1}): 3313 (broad), 2917, 2849, 1643, 1543, 1464, 1429, 1241, 1050, 719.

Malt-Tz-Phe-C_{16} ($C_{40}H_{65}N_5O_{12}$)**:**

^{1}H NMR (400 MHz, MeOD, 55 ºC, δ ppm): 0.86 (t, 3H, J = 6.8 Hz, -$(CH_2)_{12}$-C*H*$_3$), 1.10-1.32 (m, 24H, CH_2-CH_2-(C*H*$_2$)$_{12}$), 1.38-1.48 (m, 2H, C*H*$_2$-CH_2-$(CH_2)_{12}$-), 2.15 (t,

2H, J = 7.5 Hz, CO-C*H*$_2$-CH$_2$), 2.89 (dd, 1H, $J_{CH-CH2a}$ = 8.9 Hz, $J_{CH2a-CH2b}$ = 13.9 Hz, CH-(C*H*$_2$)a-Phe), 3.11 (dd, 1H, $J_{CH-CH2b}$ = 6.4 Hz, $J_{CH2a-CH2b}$ = 13.9 Hz, CH-(C*H*$_2$)b-Phe), 3.34 (dd, 1H, J_{3-4} = 8.8 Hz, J_{4-5} = 9.0 Hz, *H4*), 3.52 (dd, 1H, J_{1-2} = 3.8 Hz, J_{2-3} = 9.6 Hz, *H2*), 3.67 (dd, 1H, J_{2-3} = 9.6 Hz, J_{3-4} = 8.8 Hz, *H3*), 3.70-3.93 (m, 9H, *H5, H6a, H6b, H2´, H3´,H4´,H5´,H6´a, H6´b*), 4.42 (s, 2H, C-C*H*$_2$-NH), 4.61 (dd, 1H, $J_{CH-CH2a}$ = 8.9 Hz, $J_{CH-CH2b}$ = 6.4 Hz, CO-C*H*-NH), 5.29 (d, 1H, J_{1-2} = 3.8 Hz, *H1*), 5.59 (d, 1H, $J_{1´-2´}$ = 8.8 Hz, *H1´*), 7.16-7.29 (m, 5H, *H*arom), 7.88 (s, 1H, N-C*H*=C-triazole).

^{13}C NMR (100 MHz, MeOD, 55 ºC, δ ppm): 13.0 -(CH$_2$)$_{12}$-*C*H$_3$, 25.3 CH$_2$-*C*H$_2$-(CH$_2$)$_{12}$-, 22.1, 28.5 28.7, 28.8, 28.9, 31.4 -(*C*H$_2$)$_{12}$-, 34.4 C-*C*H$_2$-NH-, 35.6 CO-*C*H$_2$-CH$_2$, 37.5 CH-*C*H$_2$-arom, 54.7 CO-*C*H-NH-, 60.6, 61.3, 73.3, 76.8, 78.2, 78.3 C5, *C6, C3´, C4´, C5´, C6´*, 70.2 *C4*, 72.3 *C2´*, 72.6 *C2*, 73.7 *C3*, 87.9 *C1´*, 101.1 *C1*, 122.4 N-*C*H=C triazole, 126.5 *C*arom, 128.2, 128.9, 136.9 *C*Harom, 144.8 CH=*C*-CH$_2$ triazole, 175.6 NH-*C*O-CH, 175.2 NH-*C*O-CH$_2$-.

Micro-TOF MS: 808.4666 $[M + H]^+$ calcd: 808.4702; 830.4495 $[M + Na]^+$, calcd: 830.4521.

IR (KBr, cm^{-1}): 3297 (broad), 2919, 2850, 1638, 1543, 1456, 1377, 1036, 699.

Octa-O-acetyl-lactose (C$_{28}$H$_{38}$O$_{19}$) **(10):**

To a refluxing suspension of anhydrous NaOAc (4.14 g, 50.46 mmol) in acetic anhydride (30 mL, 317.36 mmol) was added α-lactose monohydrate (4.54 g, 12.60 mmol). The reaction mixture was refluxed for 3 h and cooled to 100 °C, then immediately transferred into ice-water mixture and stirred vigorously until a gum formed. After decanting the water, the gum was dissolved in dichloromethane and then washed with saturated aqueous NaHCO$_3$ and water. The organic layer was dried over MgSO$_4$, filtered and evaporated under reduced pressure. The crude product was purified by column chromatography using hexane/ethyl acetate 1:1 to give a white solid (7.44 g, 87%).

^{1}H NMR (500 MHz, CDCl$_3$, 25 °C, δ ppm): (**1β**) 1.96 (s, 3H), 2.02 (s, 3H), 2.03 (s, 3H), 2.04 (s, 3H) 2.06 (s, 3H), 2.09 (s, 3H), 2.11 (s, 3H), 2,15 (s, 3H) C*H*$_3$-CO-O- x8, 3.75 (ddd, 1H, $J_{5´,6´b}$= 2.0 Hz, $J_{5´,6´a}$= 4.8 Hz, $J_{4´,5´}$= 9.8 Hz, *H5´*$_β$), 3.81 – 3.88 (m, 2H, *H5*$_β$, *H4´*$_β$), 4.04 – 4,16 (m, 3H, *H6a*$_β$, *H6b*$_β$, *H6´a*$_β$), 4.41 – 4.49 (m, 2H, *H6´b*$_β$, *H1*$_β$), 4.94 (dd, 1H, $J_{3,4}$= 3.4 Hz, $J_{2,3}$=10.5 Hz, *H3*$_β$), 5.04 (dd, 1H, $J_{1´,2´}$= 8.2 Hz, $J_{2´,3´}$= 8.7 Hz,

H2′$_\beta$), 5.10 (dd, 1H, $J_{1,2}$= 7.8 Hz, $J_{2,3}$= 10.5 Hz, *H2$_\beta$*), 5.23 (dd, 1H, $J_{2',3'}$= 8.7 Hz, $J_{3',4'}$=9.3 Hz, *H3′$_\beta$*), 5.34 (dd, 1H, $J_{3,4}$= 3.4 Hz, $J_{4,5}$= 1.1 Hz, *H4$_\beta$*), 5.66 (d, 1H, $J_{1',2'}$= 8.2 Hz, *H1′$_\beta$*). (**1α**) 1.96 (s, 3H), 2.00 (s, 3H), 2.05 (s, 3H), 2.05 (s, 3H) 2.06 (s, 3H), 2.12 (s, 3H), 2.15 (s, 3H), 2,17 (s, 3H) C*H$_3$*-CO-O- x8, 3,78- 3.90 (m, 2H, *H4′$_\alpha$, H5$_\alpha$*), 3.97 (m, 1H, *H5′$_\alpha$*), 4.05-4.18 (m, 2H, *H6a$_\alpha$, H6b$_\alpha$*), 4.12-4.18 (m, 1H, *H6′a$_\alpha$*), 4.43-4.51 (m, 2H, *H6′b$_\alpha$, H1$_\alpha$*), 4.94-4.97 (m, 1H, *H3$_\alpha$*), 5.00 (dd, 1H, $J_{1',2'}$= 3.7 Hz, $J_{2',3'}$= 10.5 Hz, *H2′$_\alpha$*), 5.10- 5.14 (m, 1H, *H2α*), 5.34-5.37 (m, 1H, *H4α*,), 5.45 (dd, 1H, $J_{2',3'}$= 10.5 Hz, $J_{3',4'}$=9.3 Hz, *H3′$_\alpha$*), 6.24 (d, 1H, $J_{1',2'}$= 3.7 Hz, *H1′α*).

^{13}C NMR (125 MHz, $CDCl_3$, 25 °C, δ ppm): (**1β**) 20.7, 20.7, 20.8, 20.9, 20.9, 21.0 *C*H$_3$-CO- x8, 61.0, 61.9 *C6$_\beta$, C6′$_\beta$*, 66.7 *C4$_\beta$*, 69.1 *C2$_\beta$*, 70.6 *C2′$_\beta$*, 70.9, 71.7, *C5$_\beta$, C3$_\beta$*, 72.8 *C3′$_\beta$*, 73.6 *C5′$_\beta$*, 75.8 *C4′$_\beta$*, 91.7 *C1′$_\beta$*, 101.6 *C1$_\beta$*, 169.0, 169.2 C2-O-*CO*-, C1′-O-*CO*-, 169.7, 169.8 C2′-O-*CO*-, C3′-O-*C*O-, 170.2, 170.3, 170.5, 170.5 C3-O-*C*O-, C4-O-*C*O-, C6-O-*C*O-, C6′-O-*C*O. (**1α**) 20.8, 21.1, 20,7, 21,1 *C*H$_3$-CO- x8, 60.9, 61.6, *C6$_\alpha$, C6′$_\alpha$*, 69.3, 69.8, 71.1, 75.9, *C$_{X\alpha}$* 69.5 *C3′$_\alpha$*, 70.8 *C5′$_\alpha$*, 89.1 *C1′$_\alpha$*, 101.3 *C1$_\alpha$*, 169.1, 169.3, 170.1 CH$_3$-O- *C*O-, other C cannot be assigned.

MALDI-TOF MS (DIT+NaTFA): 701.2 $[M + Na]^+$.

IR (KBr, cm^{-1}): 3481, 2983, 1754, 1371, 1219, 1048, 898, 601.

Synthesis of Hepta-O-acetyl-β-cellobiosyl azide (11) and Hepta-O-acetyl-β-lactosyl azide (12):

Trimethylsilyl azide (1.1 mL, 8.36 mmol) and tin tetrachloride (350 µl, 2.99 mmol) were added, at RT and under argon, to a solution of compound **10** or α-cellobiose octaacetate (4.01 g, 5.92 mmol) in dry CH_2Cl_2 (15 mL). The reaction mixture was stirred at RT and the reaction was monitored by TLC (1:1 hexane/ethyl acetate). After 24 h, dichloromethane was added and the solution was washed with saturated Na_2CO_3 and twice with water. The organic layer was dried over $MgSO_4$, filtered and evaporated under reduced pressure. The product was purified by flash chromatography using hexane/ethyl acetate 1:1. A white solid was obtained (3.19 g, 82%).

Hepta-O-acetyl-β-cellobiosyl azide ($C_{26}H_{35}N_3O_{17}$) **(11):**

^{1}H NMR (400 MHz, $CDCl_3$, 25 °C, δ ppm): 1.98 (s, 3H), 2.00 (s, 3H), 2.02 (s, 3H), 2.03 (s, 3H), 2.06 (s,3H), 2.08 (s, 3H), 2.14 (s,3H) C*H$_3$*-CO-O- x7, 3.61- 3.73 (m, 2H, *H5,*

H5´), 3.79 (dd, 1H, $J_{3',4'}$= 9.0 Hz, $J_{4',5'}$= 9.9 Hz, *H4´*), 4.03 (dd, 1H, $J_{5,6a}$= 2.3 Hz, $J_{6a,6b}$=12.9 Hz, *H6a*), 4.11 (dd, 1H, $J_{5',6'a}$=4.9 Hz, $J_{6'a,6'b}$=12.2 Hz, *H6´a*), 4.37 (dd, 1H, $J_{5,6b}$= 4.5 Hz, $J_{6a,6b}$=12.9 Hz, *H6b*), 4.48-4.56 (m, 2H, *H1, H6´b*), 4.61 (d, 1H, $J_{1',2'}$= 8.9 Hz, *H1´*), 4.86 (dd, 1H, $J_{1',2'}$= 8.9 Hz, $J_{2',3'}$= 8.4 Hz, *H2´*), 4.92 (dd, 1H, $J_{1,2}$= 7.9 Hz, $J_{2,3}$= 9.1 Hz, *H2*), 5.06 (dd, 1H, $J_{3,4}$= 9.4 Hz, $J_{4,5}$= 9.7 Hz, *H4*), 5.14 (dd, 1H, $J_{2,3}$= 9.1 Hz, $J_{3,4}$= 9.4 Hz, *H3*), 5.18 (dd,1H, $J_{2',3'}$= 8.4 Hz, $J_{3',4'}$= 9.0 Hz, *H3´*).

^{13}C NMR (100 MHz, $CDCl_3$, 25 °C, δ ppm): 20.6, 20.7, 20.7, 20.8, 20.9 *C*H_3-CO- x7, 61.6, 61.7 *C6, C6´,* 67.8 *C4*, 71.0 *C2´*, 71.7 *C2*, 72.2, 72.3, 73.0, 75.0 *C3, C5, C3´, C5´*, 76.1 *C4´*, 87.8 *C1´*, 100.8 *C1*, 169.2 C2-O- *C*O-, 169.4 C4-O- *C*O-, 169.6 *C2´*-O- *C*O-, 169.8 C3´-O- *C*O-, 170.3, 170.4, 170.6 C3-O- *C*O-, C6-O- *C*O-, C6´-O- *C*O-.

MALDI-TOF MS (DIT+NaTFA): 684.0 $[M + Na]^+$.

IR (KBr, cm^{-1}): 3474, 2954, 2879, 2121, 1748, 1371, 1238, 1066, 1046, 904, 600.

Hepta-O-acetyl-β-lactosyl azide ($C_{26}H_{35}N_3O_{17}$) **(12):**

^{1}H NMR (400 MHz, $CDCl_3$, 25 °C, δ ppm): 1.96 (s, 3H), 2.04 (s, 3H), 2.04 (s, 3H), 2.06 (s, 3H), 2.06 (s, 3H), 2.13 (s, 3H), 2.14 (s, 3H) C*H*$_3$-CO-O- x7, 3.70 (ddd, 1H, $J_{5',6'b}$= 5.1 Hz, $J_{5',6'a}$= 2.2 Hz, $J_{4',5'}$=9.9 Hz, *H5´*), 3.81 (dd, 1H, $J_{3',4'}$= 9.1 Hz, $J_{4',5'}$= 9.9 Hz, *H4´*), 3.87 (ddd, 1H, $J_{5,6b}$= 7.3 Hz, $J_{5,6a}$= 7.3 Hz, $J_{5,4}$= 0.9 Hz, *H5*), 4.05-4.14 (m, 3H, *H6a, H6b,H6´b*), 4.47-4.52 (m, 2H, *H1, H6´a*), 4.62 (d, 1H, $J_{1',2'}$= 8.8 Hz, *H1´*, 4.85 (dd, 1H, $J_{1',2'}$= 8.8 Hz, $J_{2',3'}$= 9.3 Hz, *H2´*), 4.95 (dd, 1H, $J_{3,4}$= 3.5 Hz, $J_{2,3}$=10.5 Hz, *H3*), 5.10 (dd, 1H, $J_{1,2}$=7.9 Hz, $J_{2,3}$= 10.5 Hz, *H2*), 5.20 (dd,1H, $J_{2',3'}$= 9.3 Hz, $J_{3',4'}$=9.1 Hz, *H3´*), 5.34 (dd, 1H, $J_{3,4}$= 3.5 Hz, $J_{4,5}$= 0.9 Hz, *H4*).

^{13}C NMR (100 MHz, $CDCl_3$, 25 °C, δ ppm): 20.6, 20.7, 20.7, 20.7 20.8, 20.9 *C*H_3-CO- x7, 60.9 *C6,* 61.8 *C6´*, 66.7 *C4*, 69.2 *C2*, 70.8, 71.0, 71.1 *C3, C5, C2´,* 72.6 *C3´*, 74.9 *C5´*, 75.9 *C4´*, 87.8 *C1´*, 101.2 *C1*, 169.2 C2-O-*C*O-, 169.6 C2´-O-*C*O-, 169.7 C3´-O-*C*O-, 170.1, 170.2 C3-O- *C*O-, C4-O- *C*O-, 170.4, 170.5 C6-O- *C*O-, C6´-O- *C*O-.

MALDI-TOF MS (DIT+NaTFA): 684.3 $[M + Na]^+$.

IR (KBr, cm^{-1}): 3481, 2983, 2122, 1753, 1372, 1230, 1057, 899, 602.

Synthesis of acetylated glycolipids OAc-Cell-Tz-$C_{16}$and OAc-Lact-Tz-C_{16}:

Propargyl derivative **8** (0.44 g, 1.50 mmol), azide derivative **11** or **12** (1.00 g, 1.51 mmol), copper(I) bromide (46.6 mg, 0.32 mol) and *N*-pentamethyldiethylenetriamine (PMDETA) (65 μL, 0.31 mmol) were dissolved in anhydrous DMF (10mL) under argon atmosphere. The mixture was stirred at RT for 2 days. The reaction was monitored by TLC with hexane/ethyl acetate 1:1 as eluent. The catalyst was then removed by filtration and the solvent was removed under reduced pressure. The reaction was poured into 150 mL of water. The aqueous phase was extracted three times, each with 200 mL of hexane/ethyl acetate 1:1. The organic phase was dried with anhydrous $MgSO_4$. The solution was filtered and the solvent was removed under reduced pressure. The resulting white solid was purified by flash chromatography using initially dichloromethane/ethyl acetate 1:1 and then increasing the polarity. A white solid was obtained (1.14 g, 80% of **OAc-Cell-Tz-C_{16},** 1.17 g, 81% of **OAc-Lact-Tz-C_{16}**).

OAc-Cell-Tz-C_{16} ($C_{45}H_{70}N_4O_{18}$):

^{1}H NMR (400 MHz, $CDCl_3$, 25 °C, δ ppm): 0.87 (t, 3H, J = 6.8 Hz, -$(CH_2)_{12}$-C*H*$_3$), 1.19-1.35 (m, 24H, -(C*H*$_2$)$_{12}$-), 1.55-1.65 (m, 2H, CO-CH_2-C*H*$_2$-$(CH_2)_{12}$), 1.86 (s, 3H), 1.98 (s, 3H), 2.01 (s, 3H), 2.03 (s, 3H), 2.04 (s, 3H), 2.10 (s, 3H), 2.11 (s, 3H) C*H*$_3$-CO-O x7, 2.17 (t, 2H, J = 7.3 Hz, CO-C*H*$_2$-CH_2), 3.69 (ddd, 1H, $J_{4,5}$=9.6 Hz, $J_{5,6a}$= 2.1 Hz, $J_{5,6b}$= 4.3 Hz,, *H5*), 3.84-3.98 (m, 2H, *H4′, H5′*), 4.06 (dd, 1H, $J_{5,6a}$ = 2.1 Hz, $J_{6a,6b}$ = 12.5 Hz, *H6a*), 4.12 (dd, 1H, $J_{5',6'a}$=4.7 Hz, $J_{6'a,6'b}$=12.2 Hz, *H6′a*), 4.38 (dd, 1H, $J_{5,6b}$ = 4.3 Hz, $J_{6a,6b}$ = 12.5 Hz, *H6b*), 4.43-4.53 (m, 3H, *H6′b*, C = C-C*H*$_2$-NH), 4.55 (d, 1H, $J_{1,2}$ = 8.2 Hz, *H1*), 4.94 (dd, 1H, $J_{1,2}$ = 8.2 Hz, $J_{2,3}$ = 9.4 Hz, *H2*), 5.07 (dd, 1H, $J_{3,4}$ = 9.5 Hz, $J_{4,5}$ = 9.6 Hz, *H4*), 5.16 (dd, 1H, $J_{2,3}$ = 9.4 Hz, $J_{3,4}$ = 9.5 Hz, *H3*), 5.33-5.42 (m, 2H, *H2′, H3′*), 5.73-5.73- 5.81 (m, 1H, *H1′*), 6.11 (t, 1H, J = 5.6 Hz, -CH_2-N*H*-CO), 7.70 (s, 1H, N-C*H* = C-CH_2 triazole).

^{13}C NMR (100 MHz, $CDCl_3$, 25 °C, δ ppm): 14.4 -$(CH_2)_{12}$-*C*H_3, 20.5, 20.7, 20.8, 21.0, 21.1 *C*H_3-CO-O x7, 23.0 -(*C*H_2)$_{12}$-, 25.8 CO-CH_2-*C*H_2-$(CH_2)_{12}$, 29.6, 29.6, 29.7, 29.8, 29.9, 29.9, 30.0, 32.2, -(*C*H_2)$_{12}$-, 35.1 C-*C*H_2-NH, 36.9 CO-*C*H_2-CH_2, 61.9 x2 *C6, C6′*, 68.0 *C4*, 70.8 *C2′*or *C3′*, 71.9 *C2,* 72.5, 72.6 *C5, C2′*or *C3′*, 73.2 *C3*, 76.0 *C4′*, 76.3 *C5′*, 85.9 *C1′*, 100,1 *C1*, 121.2 *C*H triazole, 145.7 *C*triazole, 169.3 C2′-O-*C*O- or C3′-O-*C*O-, 169.4 C2-O-*C*O-, 169.6 C4-O-*C*O-, 169.8 C2′-O-*C*O- or C3′-O-*C*O-, 170.4, 170.5 C3-O-*C*O, C6′-O-*C*O, 170.8 C6-O-*C*O, 173.6 NH-*C*O-CH_2.

MALDI-TOF MS (DIT+NaTFA): 977.4 $[M + Na]^+$.

Anal. Calcd for $C_{45}H_{70}N_4O_{18}$: C, 56.59; H, 7.39; N, 5.87. Found: C, 57.00; H, 7.75; N, 5.93.

IR (KBr, cm^{-1}): 3360, 3073, 2923, 2852, 1750, 1650, 1377, 1228, 1044, 906, 599.

OAc-Lact-Tz- C_{16} ($C_{45}H_{70}N_4O_{18}$)**:**

^{1}H NMR (400 MHz, $CDCl_3$, 25 °C, δ ppm): 0.87 (t, 3H, J = 6.8 Hz, -$(CH_2)_{12}$-C*H*$_3$), 1.20-1.36 (m, 24H, -(C*H*$_2$)$_{12}$-), 1.56-1.65 (m, 2H, CO-CH_2-C*H*$_2$-$(CH_2)_{12}$), 1.86 (s, 3H), 1.97 (s, 3H), 2.05 (s, 3H), 2.06 (s, 3H), 2.08 (s, 3H), 2.11(s, 3H), 2.16 (s, 3H) C*H*$_3$-CO-O x7, 2.18 (t, 2H, J = 7.3 Hz, CO-C*H*$_2$-CH_2), 3.85-3.99 (m, 3H, *H4´,H5, H5´*), 4.05-4.19 (m, 3H, *H6a, H6$_b$, H6´$_a$*), 4.42-4.57 (m, 4H, C-C*H*$_2$-NH, *H1, H6´$_b$*), 4.97 (dd, 1H, $J_{2,3}$ = 10.4 Hz, $J_{3,4}$ = 3.5 Hz, *H3*), 5.12 (dd, 1H, $J_{1,2}$ = 7.9 Hz, $J_{2,3}$ = 10.4 Hz, *H2*), 5.33-5.44 (m, 3H, *H2´, H3´, H4*), 5.78 (d, 1H, $J_{1',2'}$ = 9.2 Hz, *H1´*), 6.11 (t, 1H, J = 5.3 Hz, -CH_2-N*H*-CO), 7.71 (s, 1H, N-C*H* = C-CH_2 triazole).

^{13}C NMR (100 MHz, $CDCl_3$, 25 °C, δ ppm): 14.2 -$(CH_2)_{12}$-*C*H_3, 20.3, 20.6, 20.7, 20.8, 20.9 *C*H_3-CO-O x7, 22.8 CH_2-*C*H_2-$(CH_2)_{12}$-, 25.7 CO-CH_2-*C*H_2-$(CH_2)_{12}$, 29.4, 29.5, 29.5, 29.6, 29.7, 29.8, 29.8, 32.1, -(*C*H_2)$_{12}$-, 34.9 C-*C*H_2-NH, 36.7 CO-*C*H_2-CH_2, 60.9, 61.8 *C6, C6´*, 66.7 C4, 69.1 C2, 70.7, 70.9, 71.0, 72.5, 75.5, 75.9, *C2´, C3´, C4´, C5´, C3, C5*, 85.6 *C1´*, 101.2 *C1*, 120.8 *C*Htriazole, 145.5 *C*triazole, 169.2, 169.2, 169.6, 170.2, 170.2, 170.3, 170.5 CH_3-*C*O-O-, 173.4 NH-*C*O-CH_2.

MALDI-TOF MS (DIT+NaTFA): 977.4 $[M + Na]^+$.

Anal. Calcd for $C_{45}H_{70}N_4O_{18}$: C, 56.59; H, 7.39; N, 5.87. Found: C, 56.88; H, 7.73; N, 5.84.

IR (KBr, cm^{-1}): 3398, 2925, 2854, 1754, 1658, 1371, 1230, 1047, 919, 603.

Synthesis of glycolipids Cell-Tz-C_{16} and Lact-Tz-C_{16}:

The protected triazole-disaccharide-heptaacetate derivative (**OAc-Cell-Tz-C_{16}** or **OAc-Lact-Tz-C_{16}**) (401 mg, 0.42 mmol) was dissolved in 25 mL of anhydrous methanol. Sodium methoxide (160 mg, 2.96 mmol) was added. The solution was stirred at RT until the reaction was complete (TLC, dichoromethane/ethyl acetate 1:1). Amberlyst IR

120 (H^+ form) was added to exchange sodium ions, the resin was filtered off. A white solid was obtained (214 mg, 77% for **Cell-Tz-C$_{16}$**, 220 mg, 80% for **Lact-Tz-C$_{16}$**).

Cell-Tz-C$_{16}$ ($C_{31}H_{56}N_4O_{11}$)**:**

^{1}H NMR (500 MHz, MeOD, 50 °C, δ ppm): 0.90 (t, 3H, J = 6.8 Hz, -$(CH_2)_{12}$-C*H*$_3$), 1.13-1.45 (m, 24H, -(C*H*$_2$)$_{12}$-CH$_3$), 1.56-1.66 (m, 2H, CO-CH$_2$-C*H*$_2$-$(CH_2)_{12}$), 2.21 (t, 2H, J = 7.3 Hz, CO-C*H*$_2$-CH$_2$), 3.27 (dd, 1H, $J_{1,2}$ = 7.3 Hz, $J_{2,3}$ = 8.4 Hz, *H2*), 3.32-3.46 (m, 3H), 3.65-3.80 (m, 4H), 3.85-3.92 (m, 3H, *H3´, H4´, H5´, H6´a, H6´b, H3, H4, H5, H6a, H6b*), 3.95 (dd, 1H, $J_{1´,2´}$ = 9.8 Hz, $J_{2´,3´}$ = 7.7 Hz, *H2´*), 4.45 (m, 2H, C-C*H*$_2$-NH), 4.48 (d, 1H, $J_{1,2}$ = 7.3 Hz, *H1*), 5.60 (d, 1H, $J_{1´,2´}$ = 9.2 Hz, *H1´*), 8.00 (s, 1H, C*H*triazole).

^{13}C NMR (125 MHz, MeOD, 55 °C, δ ppm): 14.3 -$(CH_2)_{12}$-*C*H$_3$, 23.6 -(*C*H$_2$)$_{12}$-, 26.8 CO-CH$_2$-*C*H$_2$-$(CH_2)_{12}$, 30.4, 30.5, 30.7, 32.9 -CH$_2$-(*C*H$_2$)$_{12}$-, 35.6 C-*C*H$_2$-NH-, 37.0 CO-*C*H$_2$-CH$_2$, 61.7, 62.6, 71.5, 76.9, 78.0, 78.2, 79.6, 79.9 *C3´,C4´, C5´,C6´, C3,C4, C5,C6,* 73.8 *C2´*, 75.6 *C2*, 89.4 *C1´*, 104.6 *C1*, 123.4 *C*Htriazole, 146.4 *C*triazole, 176.3 NH-*C*O-CH$_2$.

MicroTOF MS: 661.3997 $[M+ H]^+$, calcd: 661.4018.

Anal. Calcd for $C_{31}H_{56}N_4O_{11}$.H_2O: C, 54.85; H, 8.61; N, 8.25. Found: C, 54.94; H, 8.88; N, 8.27.

IR (KBr, cm^{-1}): 3326, 2915, 2848, 1649, 1542, 1468, 1368, 1328, 1247, 1227, 1210, 1095, 1041, 997, 899, 997, 899, 831, 760, 719, 655.

Lact-Tz-C$_{16}$ ($C_{31}H_{56}N_4O_{11}$)**:**

^{1}H NMR (400 MHz, MeOD, 50 °C, δ ppm): 0.90 (t, 3H, J = 6.9 Hz, -$(CH_2)_{12}$-C*H*$_3$), 1.22-1.40 (m, 24H, -(C*H*$_2$)$_{12}$-), 1.56-1.66 (m, 2H, CO-CH$_2$-C*H*$_2$-$(CH_2)_{12}$), 2.21 (t, 2H, J = 7.3 Hz, CO-C*H*$_2$-CH$_2$), 3.50 (dd, 1H, $J_{2,3}$ = 9.7 Hz, $J_{3,4}$ = 3.3 Hz, *H3*), 3.59 (dd, 1H, $J_{1,2}$ = 7.8 Hz, $J_{2,3}$ = 9.7 Hz, *H2*), 3.82-3.86 (m, 1H, *H4*), 3.60-3.64 (m, 1H), 3.69-3.82 (m, 5H), 3.87-3.91 (m, 2H, *H3´,H4´, H5´, H6´$_a$, H6´$_b$, H5, H6$_a$, H6$_b$*), 3.95 (dd, 1H, $J_{1´,2´}$= 9.2 Hz, $J_{2´,3´}$= 8.9 Hz, *H2´*), 4.42 (d, 1H, $J_{1,2}$ = 7.8 Hz, *H1*), 4.44 (s, 1H, -C*H*$_2$-NH-CO), 5.60 (d, 1H, $J_{1´-2´}$ = 9.2 Hz, *H1´*), 8.02 (s, 1H, C*H* triazole).

^{13}C NMR (100 MHz, MeOD, 50 °C, δ ppm): 14.3 -$(CH_2)_{12}$-CH_3, 23.6 -$(CH_2)_{12}$-, 26.8 CO-CH_2-CH_2-$(CH_2)_{12}$-, 30.3, 30.3, 30.5, 30.6, 30.7, 32.9, -CH_2-$(CH_2)_{12}$-, 35.6 C-CH_2-NH-, 37.0 CO-CH_2-CH_2, 61.8, 62.6, 76.9, 77.1, 79.6, 80.1,C3′,*C4′, C5′,C6′, C5*, *C6*, 70.4 *C4*, 72.6 *C2*, 73.8 *C2′*, 75.0 *C3*, 89.1 *C1′*, 105.2 *C1*, 123.4 *C*Htriazole, 146.4 *C*triazole, 176.2 NH-*C*O-CH_2.

MicroTOF MS: 661.4008 $[M+ Na]^+$, calcd: 661.4018.

Anal. Calcd for $C_{31}H_{56}N_4O_{11}$.H_2O: C, 54.85; H, 8.61; N, 8.25. Found: C, 55.34; H, 8.96; N, 8.39.

IR (KBr, cm^{-1}): 3328, 2915, 2848, 1649, 1542, 1467, 1416, 1379, 1329, 1247, 1227, 1130, 1089, 1074, 1048, 998, 895, 758, 700, 645.

3.8. References

1. (a) Brunsveld, L.; Folmer, B. J. B.; Meijer, E. W.; Sijbesma, R. P., Supramolecular polymers. *Chem. Rev.* **2001,** *101* (12), 4071-4097; (b) De Greef, T. F. A.; Smulders, M. M. J.; Wolffs, M.; Schenning, A.; Sijbesma, R. P.; Meijer, E. W., Supramolecular Polymerization. *Chem. Rev.* **2009,** *109* (11), 5687-5754.
2. Sangeetha, N. M.; Maitra, U., Supramolecular gels: Functions and uses. *Chem. Soc. Rev.* **2005,** *34* (10), 821-836.
3. Weiss, R. G.; Terech, P., *Molecular gels*. Springer: Dordrecht, 2006.
4. (a) Pfannemuller, B.; Welte, W., Amphiphilic Properties of Synthetic Glycolipids Based on Amide Linkages. 1. Electron -Microscopic Studies on Aqueous Gels. *Chem. Phys. Lip.* **1985,** *37* (3), 227-240; (b) Fuhrhop, J. H.; Schnieder, P.; Rosenberg, J.; Boekema, E., The Chiral Bilayer Effect Stabilizes Micellar Fibers. *J. Am. Chem. Soc.* **1987,** *109* (11), 3387-3390; (c) Fuhrhop, J. H.; Schnieder, P.; Boekema, E.; Helfrich, W., Lipid Bilayer Fibers from Diastereomeric and Enantiomeric N-Octylaldonamides. *J. Am. Chem. Soc.* **1988,** *110* (9), 2861-2867.
5. (a) John, G.; Masuda, M.; Okada, Y.; Yase, K.; Shimizu, T., Nanotube formation from renewable resources via coiled nanofibers. *Adv. Mat.* **2001,** *13* (10), 715-718; (b) Jung, J. H.; John, G.; Masuda, M.; Yoshida, K.; Shinkai, S.; Shimizu, T., Self-assembly of a sugar-based gelator in water: Its remarkable diversity in gelation ability and aggregate structure. *Langmuir* **2001,** *17* (23), 7229-7232; (c) Yang, Z. M.; Liang, G. L.; Ma, M. L.; Abbah, A. S.; Lu, W. W.; Xu, B., D-glucosamine-based supramolecular hydrogels to improve wound healing. *Chem. Commun.* **2007,** (8), 843-845.
6. (a) Shimizu, T.; Masuda, M., Stereochemical effect of even-odd connecting links on supramolecular assemblies made of 1-glucosamide bolaamphiphiles. *J. Am. Chem. Soc.* **1997,** *119* (12), 2812-2818; (b) Jung, J. H.; Shinkai, S.; Shimizu, T., Spectral characterization of self-assemblies of aldopyranoside amphiphilic gelators: What is the essential structural difference between simple amphiphiles and bolaamphiphiles? *Chem.-a Eur. J.* **2002,** *8* (12), 2684-2690; (c) Shimizu, T., Bottom-up synthesis and morphological control of high-axial-ratio nanostructures through molecular self-assembly. *Pol. J.* **2003,** *35* (1), 1-22.
7. (a) Hamachi, I.; Kiyonaka, S.; Shinkai, S., Solid phase lipid synthesis (SPLS) for construction of an artificial glycolipid library. *Chem. Commun.* **2000,** (14), 1281-1282; (b) Kiyonaka, S.; Shinkai, S.; Hamachi, I., Combinatorial library of low molecular-weight organo- and hydrogelators based on glycosylated amino acid derivatives by solid-phase synthesis. *Chem.-a Eur. J.* **2003,** *9* (4), 976-983; (c) Mohan, S. R. K.; Hamachi, I., Synthesis of new supramolecular polymers based on glycosylated amino acid and their applications. *Curr. Org. Chem.* **2005,** *9* (5), 491-502.
8. (a) Bhattacharya, S.; Acharya, S. N. G., Pronounced hydrogel formation by the self-assembled aggregates of N-alkyl disaccharide amphiphiles. *Chem. Mat.* **1999,** *11* (12), 3504-3511; (b) Fitremann, J.; Bouchu, A.; Queneau, Y., Synthesis and gelling properties of N-palmitoyl-L-phenylalanine sucrose esters. *Langmuir* **2003,** *19* (23), 9981-9983.
9. Estroff, L. A.; Hamilton, A. D., Water gelation by small organic molecules. *Chem. Rev.* **2004,** *104* (3), 1201-1217.
10. (a) Kiyonaka, S.; Sugiyasu, K.; Shinkai, S.; Hamachi, I., First thermally responsive supramolecular polymer based on glycosylated amino acid. *J. Am. Chem. Soc.* **2002,** *124* (37), 10954-10955; (b) Kiyonaka, S.; Sada, K.; Yoshimura, I.; Shinkai, S.; Kato, N.; Hamachi, I., Semi-wet peptide/protein array using supramolecular hydrogel. *Nat. Mat.* **2004,** *3* (1), 58-64; (c) Yoshimura, I.; Miyahara, Y.; Kasagi, N.;

Yamane, H.; Ojida, A.; Hamachi, I., Molecular recognition in a supramolecular hydrogel to afford a semi-wet sensor chip. *J. Am. Chem. Soc.* **2004,** *126* (39), 12204-12205; (d) Tamaru, S.; Kiyonaka, S.; Hamachi, I., Three distinct read-out modes for enzyme activity can operate in a semi-wet supramolecular hydrogel. *Chem.-a Eur. J.* **2005,** *11* (24), 7294-7304; (e) Yamaguchi, S.; Yoshimura, L.; Kohira, T.; Tamaru, S.; Hamachi, I., Cooperation between artificial receptors and supramolecular hydrogels for sensing and discriminating phosphate derivatives. *J. Am. Chem. Soc.* **2005,** *127* (33), 11835-11841; (f) Koshi, Y.; Nakata, E.; Yamane, H.; Hamachi, I., A fluorescent lectin array using supramolecular hydrogel for simple detection and pattern profiling for various glycoconjugates. *J. Am. Chem. Soc.* **2006,** *128* (32), 10413-10422; (g) Matsumoto, S.; Yamaguchi, S.; Ueno, S.; Komatsu, H.; Ikeda, M.; Ishizuka, K.; Iko, Y.; Tabata, K. V.; Aoki, H.; Ito, S.; Noji, H.; Hamachi, I., Photo gel-sol/sol-gel transition and its patterning of a supramolecular hydrogel as stimuli-responsive biomaterials. *Chem.-a Eur. J.* **2008,** *14* (13), 3977-3986; (h) Matsumoto, S.; Yamaguchi, S.; Wada, A.; Matsui, T.; Ikeda, M.; Hamachi, I., Photo-responsive gel droplet as a nano- or pico-litre container comprising a supramolecular hydrogel. *Chem. Commun.* **2008,** (13), 1545-1547.

11. (a) Ikeda, M.; Ueno, S.; Matsumoto, S.; Shimizu, Y.; Komatsu, H.; Kusumoto, K. I.; Hamachi, I., Three-Dimensional Encapsulation of Live Cells by Using a Hybrid Matrix of Nanoparticles in a Supramolecular Hydrogel. *Chem.-a Eur. J.* **2008,** *14* (34), 10808-10815; (b) Wang, W. J.; Wang, H. M.; Ren, C. H.; Wang, J. Y.; Tan, M.; Shen, J.; Yang, Z. M.; Wang, P. G.; Wang, L., A saccharide-based supramolecular hydrogel for cell culture. *Carb. Res.* **2011,** *346* (8), 1013-1017.

12. Goodby, J. W.; Gortz, V.; Cowling, S. J.; Mackenzie, G.; Martin, P.; Plusquellec, D.; Benvegnu, T.; Boullanger, P.; Lafont, D.; Queneau, Y.; Chambert, S.; Fitremann, J., Thermotropic liquid crystalline glycolipids. *Chem. Soc. Rev.* **2007,** *36* (12), 1971-2032.

13. (a) Dorset, D. L.; Rosenbusch, J. P., Solid-State Properties Of Anomeric "1-O-Normal-Octyl-D-Glucopyranosides". *Chem. Phys. Lip.* **1981,** *29* (4), 299-307; (b) Goodby, J. W., Liquid-Crystal Phases Exhibited By Some Monossacharides. *Mol. Cryst. Liq. Cryst.* **1984,** *110* (1-4), 205-219; (c) Miethchen, R.; Holz, J.; Prade, H.; Liptak, A., Amphiphilic And Mesogenic Carbohydrates.2. Synthesis And Characterization Of Mono-O-(Normal-Alkyl)-D-Glucose Derivatives. *Tetrahedron* **1992,** *48* (15), 3061-3068.

14. (a) Fischer, S.; Fischer, H.; Diele, S.; Pelzl, G.; Jankowski, K.; Schmidt, R. R.; Vill, V., On The Structure Of The Thermotropic Cubic Mesophases. *Liq. Cryst.* **1994,** *17* (6), 855-861; (b) Molinier, V.; Kouwer, P. H. J.; Fitremann, J.; Bouchu, A.; Mackenzie, G.; Queneau, Y.; Goodby, J. W., Self-organizing properties of monosubstituted sucrose fatty acid esters: The effects of chain length and unsaturation. *Chem.-a Eur. J.* **2006,** *12* (13), 3547-3557; (c) Queneau, Y.; Gagnaire, J.; West, J. J.; Mackenzie, G.; Goodby, J. W., The effect of molecular shape on the liquid crystal properties of the mono-O-(2-hydroxydodecyl)sucroses. *J. Mat. Chem.* **2001,** *11* (11), 2839-2844.

15. (a) Auvray, X.; Petipas, C.; Anthore, R.; Ricolattes, I.; Lattes, A., RX-Diffraction Study of The Ordered Lyotropic Phases Formed by Sugar-Based Surfactants. *Langmuir* **1995,** *11* (2), 433-439; (b) Goodby, J. W.; Haley, J. A.; Mackenzie, G.; Watson, M. J.; Plusquellec, D.; Ferrieres, V., Amphitropic liquid-crystalline properties of some novel alkyl furanosides. *J. Mat. Chem.* **1995,** *5* (12), 2209-2220; (c) Ho, M. S.; Hsu, C. S., Synthesis and self-assembled nanostructures of novel chiral amphiphilic liquid crystals containing -beta-galactopyranoside end-groups.

Liq. Cryst. **2010,** *37* (3), 293-301; (d) Smits, E.; Engberts, J.; Kellogg, R. M.; VanDoren, H. A., Thermotropic and lyotropic liquid crystalline behaviour of 4-alkoxyphenyl beta-D-glucopyranosides. *Liq. Cryst.* **1997,** *23* (4), 481-488; (e) Vandoren, H. A.; Vandergeest, R.; Deruijter, C. F.; Kellogg, R. M.; Wynberg, H., The Scope and Limitations of Liquid-Crystalline Behavior in Monosaccharide Amphiphiles-Comparison of the Thermal-Behavior of Several Homologous Series of D-Glucose Derived Compounds with an Amino-Linked Alkyl Chain. *Liq. Cryst.* **1990,** *8* (1), 109-121; (f) Vandoren, H. A.; Wingert, L. M., The Relationship Between The Molecular-Structure of Polyhydroxy Amphiphiles and Their Aggregation Behavior in Water .1. The Conctact Preparation Method as a Tool For Empirical-Studies. *Recueil Des Travaux Chimiques Des Pays-Bas-Journal of the Royal Netherlands Chemical Society* **1994,** *113* (4), 260-265.

16. (a) Gerber, S.; Wulf, M.; Milkereit, G.; Vill, V.; Howe, J.; Roessle, M.; Garidel, P.; Gutsmann, T.; Brandenburg, K., Phase diagrams of monoacylated amide-linked disaccharide glycolipids. *Chem. Phys. Lip.* **2009,** *158* (2), 118-130; (b) Ma, Y. D.; Takada, A.; Sugiura, M.; Fukuda, T.; Miyamoto, T.; Watanabe, J., Thermotropic Liquid-Crystals Based On Oligosaccharides- N-Akyl-1-O-Beta-D-Cellobiosides. *Bull. Chem. Soc. Jap.* **1994,** *67* (2), 346-351; (c) von Minden, H. M.; Brandenburg, K.; Seydel, U.; Koch, M. H. J.; Garamus, V.; Willumeit, R.; Vill, V., Thermotropic and lyotropic properties of long chain alkyl glycopyranosides. Part II. Disaccharide headgroups. *Chem. Phys. Lip.* **2000,** *106* (2), 157-179.

17. Marlène, L., Synthese et etude des propietes d´un derive du saccharose. *Ecole Doctorale de Chimie Universite Paul Sabatier* **2004**.

18. Bensimon, A.; Simon, A.; Chiffaudel, A.; Croquette, V.; Heslot, F.; Bensimon, D., Alignment and sensitive detection of DNA by a moving Interface. *Science* **1994,** *265* (5181), 2096-2098.

19. (a) Meinjohanns, E.; Meldal, M.; Paulsen, H.; Dwek, R. A.; Bock, K., Novel sequential solid-phase synthesis of N-linked glycopeptides from natural sources. *J. Chem. Soc.-Perkin Trans. 1* **1998,** (3), 549-560; (b) Vetter, D. Methods for the solid phase synthesis of glycoconjugates. WO 95/18971.

20. (a) Hackenberger, C. P. R.; O'Reilly, M. K.; Imperiali, B., Improving glycopeptide synthesis: A convenient protocol for the preparation of beta-glycosylamines and the synthesis of glycopeptides. *J. Org. Chem.* **2005,** *70* (9), 3574-3578; (b) Likhosherstov, L. M.; Novikova, O. S.; Shibaev, V. N., New efficient synthesis of beta-glucosylamines of mono- and disaccharides with the use of ammonium carbamate. *Doklady Chem.* **2002,** *383* (4-6), 89-92; (c) Somsak, L.; Felfoldi, N.; Konya, B.; Huse, C.; Telepo, K.; Bokor, E.; Czifrak, K., Assessment of synthetic methods for the preparation of N-beta-D-glucopyranosyl-N '- substituted ureas, -thioureas and related compounds. *Carb. Res.***2008,** *343* (12), 2083-2093.

21. Gyorgydeak, Z.; Szilagyi, L.; Paulsen, H., Synthesis, Structure and Reactions of Glycosyl Azides. *J. Carb. Chem.* **1993,** *12* (2), 139-163.

22. Lahann, J., *Click Chemistry for Biotechnology and Material Science*. Willey: Chischester, 2009.

23. (a) Dedola, S.; Nepogodiev, S. A.; Field, R. A., Recent applications of the Cu-I-catalysed Huisgen azide-alkyne 1,3-dipolar cycloaddition reaction in carbohydrate chemistry. *Org. & Biomol. Chem.* **2007,** *5* (7), 1006-1017; (b) Kolb, H. C.; Finn, M. G.; Sharpless, K. B., Click chemistry: Diverse chemical function from a few good reactions. *Ang. Chem.-Int. Ed.* **2001,** *40* (11), 2004-2021; (c) Tornoe, C. W.; Christensen, C.; Meldal, M., Peptidotriazoles on solid phase: 1,2,3 -triazoles by regiospecific copper(I)-catalyzed 1,3-dipolar cycloadditions of terminal alkynes to azides. *J. Org. Chem.* **2002,**

67 (9), 3057-3064; (d) Wu, P.; Feldman, A. K.; Nugent, A. K.; Hawker, C. J.; Scheel, A.; Voit, B.; Pyun, J.; Frechet, J. M. J.; Sharpless, K. B.; Fokin, V. V., Efficiency and fidelity in a click-chemistry route to triazole dendrimers by the copper(I)-catalyzed ligation of azides and alkynes. *Ang. Chem.-Int. Ed.* **2004,** *43* (30), 3928-3932.

24. Shinoda, K.; Yamaguchi, N.; Carlsson, A., Physical Meaning of the Krafft Point - Observation of Melting Phenomenon of Hydrated Solid Surfactant at the Krafft Point. *J. Phys. Chem.* **1989,** *93* (20), 7216-7218.

25. Juwarker, H.; Lenhardt, J. M.; Castillo, J. C.; Zhao, E.; Krishnamurthy, S.; Jamiolkowski, R. M.; Kim, K. H.; Craig, S. L., Anion Binding of Short, Flexible Aryl Triazole Oligomers. *J. Org. Chem.* **2009,** *74* (23), 8924-8934.

26. (a) da Silva, C. O.; Nascimento, M. A. C., Ab initio conformational maps for disaccharides in gas phase and aqueous solution. *Carb. Res.* **2004,** *339* (1), 113-122; (b) French, A. D.; Johnson, G. P.; Cramer, C. J.; Csonka, G. I., Conformational analysis of cellobiose by electronic structure theories. *Carb. Res.* **2012,** *350*, 68-76; (c) Momany, F. A.; Schnupf, U.; Willett, J. L.; Bosma, W. B., DFT study of alpha-maltose: influence of hydroxyl orientations on the glycosidic bond. *Struct. Chem.* **2007,** *18* (5), 611-632.

27. Bianchi, A.; Bernardi, A., Traceless staudinger ligation of glycosyl azides with triaryl phosphines: Stereoselective synthesis of glycosyl amides. *J. Org. Chem.* **2006,** *71* (12), 4565-4577.

28. Clemente, M. J.; Fitremann, J.; Mauzac, M.; Serrano, J. L.; Oriol, L., Synthesis and Characterization of Maltose-based Amphiphiles as Supramolecular Hydrogelators *Langmuir* **2011,** *27*, 15236-15247.

29. Suzuki, M.; Yumoto, M.; Kimura, M.; Shirai, H.; Hanabusa, K., A family of low-molecular-weight hydrogelators based on L-lysine derivatives with a positively charged terminal group. *Chem.-a Eur. J.* **2003,** *9* (1), 348-354.

4. SUPRAMOLECULAR GELS DERIVED FROM AZOBENZENE GLYCOAMPHIPHILES

4.1. Introduction

Research on supramolecular gels based on low molecular weight gelators (LMWG) has increased in recent years due to their potential applications[1] as biomaterials, smart materials and electronic devices. These applications in the field of materials are based in the fact that these supramolecular gels are responsive to external stimuli, taking into account the reversibility of the weak interactions which form the 3D structure of the gel.[2] These interactions are supposed to be weaker and easily reversible in the case of gels based on low molecular mass gelators compared to supramolecular polymeric gels. The type of response depends on the applied stimulus and can affect the supramolecular structure at different hierarchical levels. For instance, by triggering adequate modifications, these materials can be cycled between free-flowing liquids and non-flowing materials. However other modifications can also be promoted, for example, in the chemical or physical properties, such as color or conductivity or swelling and shrinking by extension or contraction of the network.[3]

Changes in these supramolecular materials can be triggered by chemical or physical stimuli yielding to smart materials. Different supramolecular gels have been reported to be chemo-responsive by a host-guest complexation,[4] a metal-ion interaction[5] and pH changes.[6] Apart from the response to temperature and mechanical stress, among the different physical stimuli, light is attractive because it is a remote stimulus that can promote spatially controlled changes. As photoactive gels there are several examples of luminescent gels[7] and phototunable gels, having a structure transformation through a photochemical process of a photochromic unit. The photochromic unit can be the gelator itself or a co-gelator. The gel response is a consequence of the ability of the photochromic unit to alternate between two different chemical forms with light; the two forms displaying different absorption spectra. Most often, the mechanisms involved at the molecular level are *trans-cis* isomerization, tautomerization and electrocycling ring closures and openings. The photoinduced response in gels can be irreversible or reversible.[8] Azo dye systems are used in supramolecular assemblies to trigger reversible environmental changes, due to the reversible *trans-cis* photochemical isomerization experienced by azobenzenes, where the *cis* isomer can promote a structural change or disruption of the structure.[9]

Examples of *trans*-isomer organogels giving rise to a photo-stationary state of *trans-cis* mixtures which provide a sol state, have been described on aza-crown-appended cholesterol derivatives[10] and recently on hydrazine[11] and lipid derivatives.[12] By contrast, in organogels derived from bis-ureido-azobenzene derivatives, the *trans-cis* isomerization is blocked in the gel state.[13] Most reported examples are related to organogels, due to the difficulty of incorporating a hydrophobic photoresponsive part in water soluble aggregates. However, a few photoresponsive hydrogels based on peptide derivatives have also been reported.[14] Azobenzene chromophores can also be incorporated into glyco-amphiphilic structures. Changes under irradiation in their structure[15] or gel-sol transition[16] have been described for sugar-based azo-gelators.

Multi-component supramolecular gels[17] have also been previously studied because the mixture of components allows tailoring the properties of the resulting gel. If two components, which are themselves gelators, are used, either co-gels or self-sorting gels can be formed.[18] Azo mixtures have been studied by the potential light control of the gel structure through azo isomerisation.[19] As example, the co-assembly of an azobenzene derivative with gels having a chiral nanotube structure has been studied, in which reversible changes have been regulated by light switching.[20] Furthermore, mixtures of amphiphiles based on sugars have been also described as self-sorting gels.[21]

On the other hand, as it has been concluded in previous chapters, click chemistry is an effective reaction to link a hydrophilic sugar head and a hydrophobic chain in order to prepare amphiphilic molecules. The triazole ring gives additional π-π stacking and its dipolar moment increases the hydrophilicity of the amphiphile, contributing to the formation of hydrogels. Now we are going to introduce in the structure an azobenzene group at different positions of the hydrophobic chain, using maltose as sugar polar head, in order to obtain photoactive gels, see **Fig. 4.1**. The liquid crystalline behavior, chiral supramolecular structures and light-response capability of these gels have been explored. Furthermore, hydrogel formed by a mixture of gelators of similar structure have been formed in order to investigate if the chiral arrangement can be modulated by light as remote stimulus.

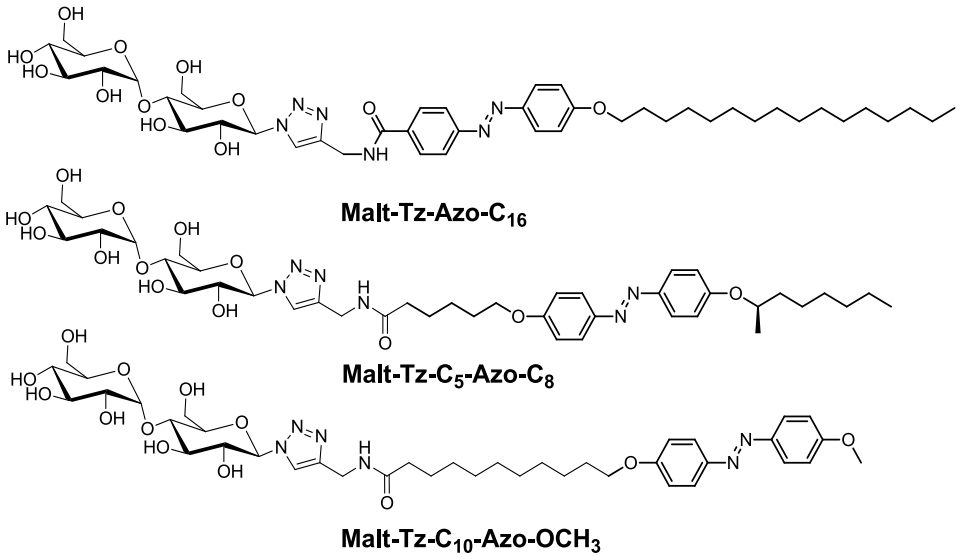

Fig. 4.1: Chemical structure of the synthesized azo-glycolipids.

4.2. Results and discussion

4.2.1. *Synthesis*

As starting materials were used peracetylated maltose, as the sugar block precursor, and the azobenzene-containing carboxylic acids shown in **Fig. 4.2**.

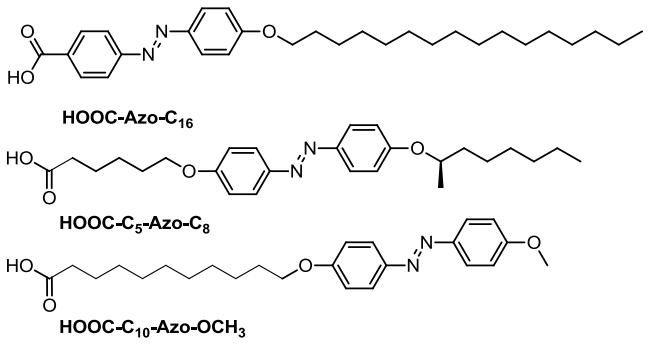

Fig. 4.2: Chemical structure and nomenclature of the azobenzene blocks.

Compounds **HOOC-Azo-C_{16}** and **HOOC-C_5-Azo-C_8** were synthesized following **Scheme 4.1** and **Scheme 4.2** respectively. **HOOC-C_{10}-Azo-OCH_3** was provided by the Liquid Crystal and Polymer group at Zaragoza University (Eva Blasco).

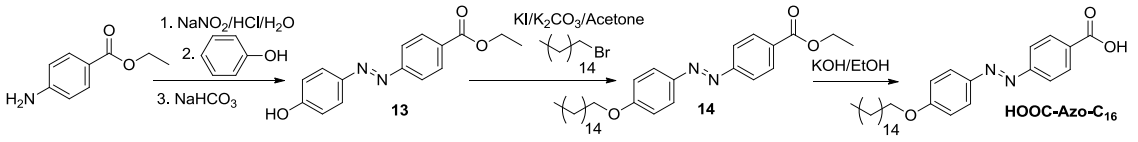

Scheme 4.1: Synthesis of **HOOC-Azo-C_{16}**.

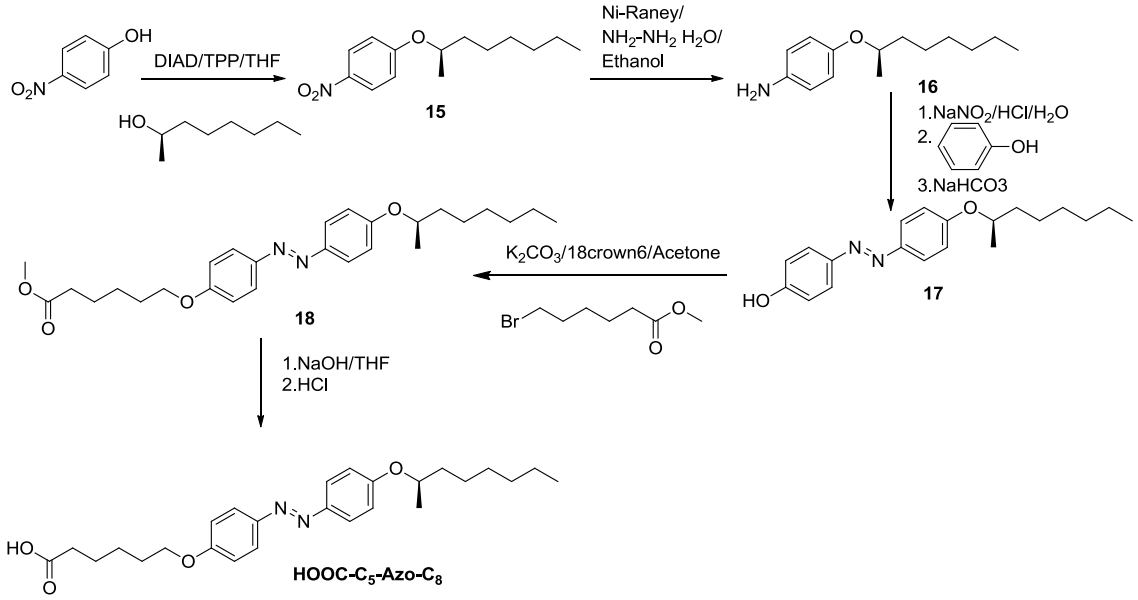

Scheme 4.2: Synthesis of **HOOC-C_5-Azo-OC_8**.

Compounds were prepared by an azo coupling reaction[22] using sodium phenoxide and ethyl p-aminobenzoate for **HOOC-Azo-C_{16}**, (R)-2-octyloxyaniline (**15**) for **HOOC-C_5-Azo-C_8** and p-methoxyaniline for **HOOC-C_{10}-Azo-OCH_3**, respectively. Compound (R)-2-octyloxyaniline (**16**) was prepared from 4-nitrophenol by etherification with (S)-2-octanol and further reduction of the nitro group. The carboxylic aliphatic chains were introduced by a Williamson reaction, followed by the hydrolysis of the ester group to yield the aimed acid.

The glyco azo-amphiphiles were synthesised by click coupling of β-maltosylazide and the *N*-propargylamides derived from the azobenzenes shown in **Figure 4.2** using a copper(I)-catalysed azide-alkyne [3+2] cycloaddition, see **Scheme 4.3**.

The resulting triazole ring connects the maltose polar head with the hydrophobic part. The hydrophobic part consists of an azobenzene group and an alkyl chain with the

azobenzene at different positions: directly linked to the triazole (**Malt-Tz-Azo-C_{16}**), in the middle of the chain (**Malt-Tz-C_5-Azo-C_8**) or at the end of the chain (**Malt-Tz-C_{10}-Azo-OCH_3**.

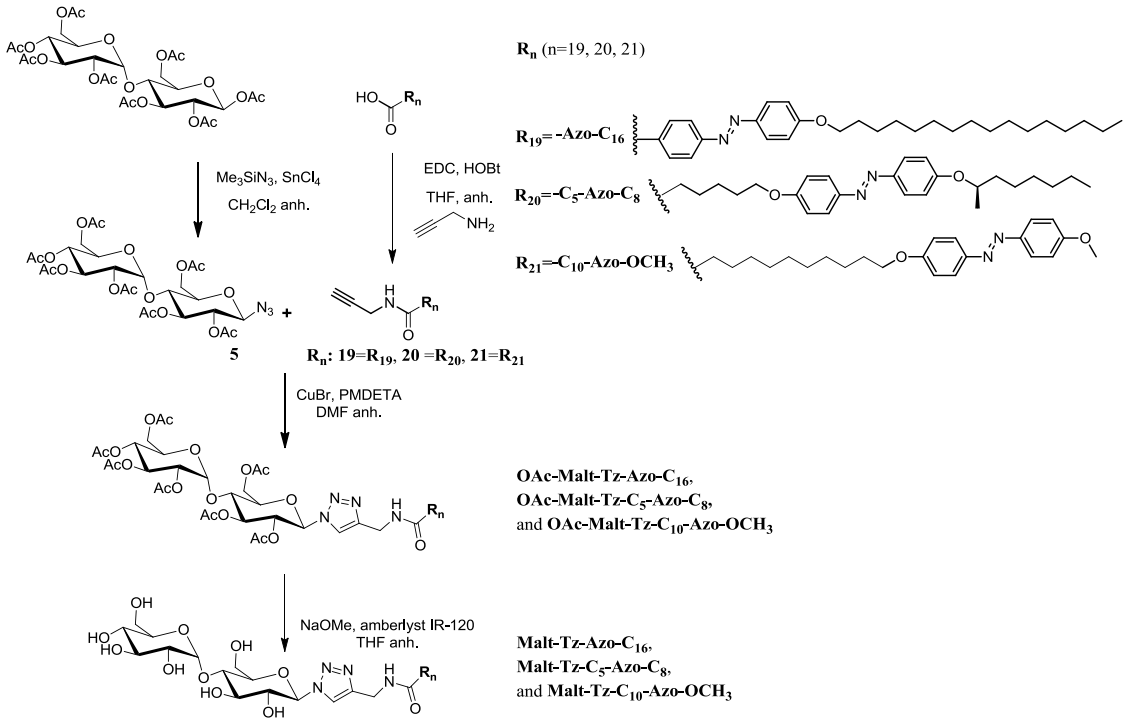

Scheme 4.3: Synthesis of **Malt-Tz-Azo-C_{16}**, **Malt-Tz-C_5-Azo-C_8**, and **Malt-Tz-C_{10}-Azo-OCH_3**.

As was described in **Chapter 3**, β-maltosylazide **5** was synthesized in a stereoselective manner by treating β-maltose octa-acetate with trimethylsilyl azide and tin tetrachloride, as a Lewis acid catalyst, employing the general procedure described by Paulsen. To introduce the alkyne, the propargylamide derivatives **19, 20** and **21,** were synthesized using EDC as coupling agent and hydroxybenzotriazole. The click coupling reaction azide-alkyne was carried out in DMF using CuBr and *N*-pentamethyldiethylenetriamine (PMDETA) to give the azo-glycosyl products in 80-90% yield. All of the protected derivatives were deacetylated at room temperature with MeONa and Amberlyst IR120 in anhydrous THF to give the final product at a yield of 75-90%.

Peracetylated compounds and azo-glycoamphiphiles were characterized by ^{1}H NMR, ^{13}C NMR, IR and mass spectrometry (see experimental section). Peracetylated compounds (**OAc-Malt-Tz-Azo-C_{16}**, **OAc-Malt-Tz-C_5-Azo-C_8** and **OAc-Malt-Tz-C_{10}-**

Azo-OCH$_3$) and azo-glycoamphiphilic compounds (**Malt-Tz-Azo-C$_{16}$**, **Malt-Tz-C$_5$-Azo-C$_8$**, and **Malt-Tz-C$_{10}$-Azo-OCH$_3$**) were characterized by additional 2D NMR experiments (COSY, TOCSY, NOESY, HSQC and HMBC) to corroborate their chemical structure.

As an example of the characterization studies, **Fig. 4.3** shows ^{1}H NMR experiments on **OAc-Malt-Tz-C$_{10}$-Azo-OCH$_3$** and **Malt-Tz-C$_{10}$-Azo-OCH$_3$**, and **Fig. 4.4** shows a 2D TOCSY experiment on **OAc-Malt-Tz-C$_{10}$-Azo-OCH$_3$** where all the sugar ring protons can be assigned.

a) **OAc-Malt-Tz-C$_{10}$-Azo-OCH$_3$** and **Malt-Tz-C$_{10}$-Azo-OCH$_3$**

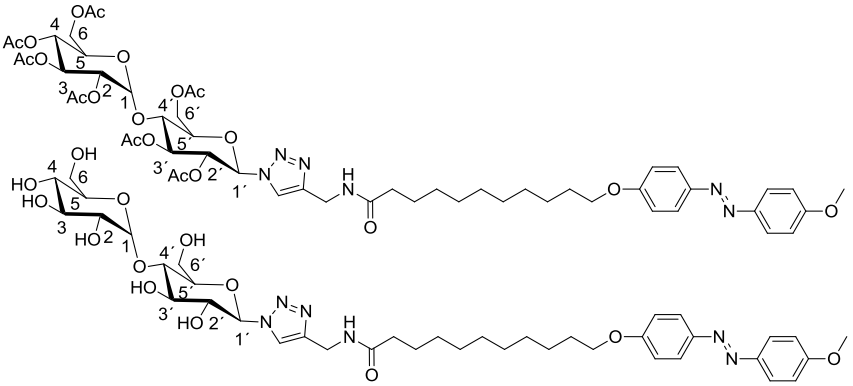

b) ^{1}H NMR **OAc-Malt-Tz-C$_{10}$-Azo-OCH$_3$**

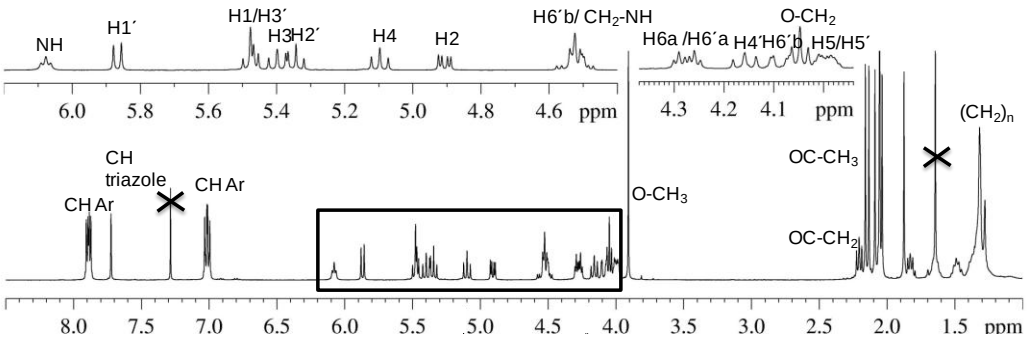

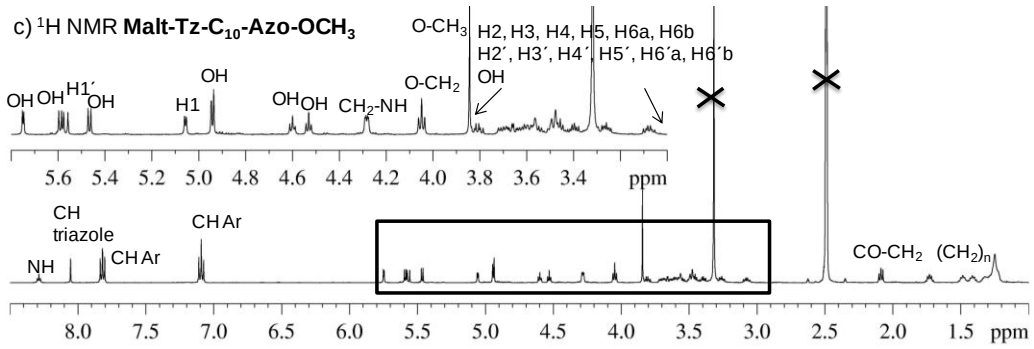

Fig. 4.3: a) **OAc-Malt-Tz-C$_{10}$-Azo-OCH$_3$** and **Malt-Tz-C$_{10}$-Azo-OCH$_3$** chemical structure and nomenclature, b) ^{1}H NMR spectrum of **OAc-Malt-Tz-C$_{10}$-Azo-OCH$_3$** with $CDCl_3$ as solvent at 25ºC, c) ^{1}H NMR spectrum of **Malt-Tz-C$_{10}$-Azo-OCH$_3$** with DMSO as solvent at 25ºC.

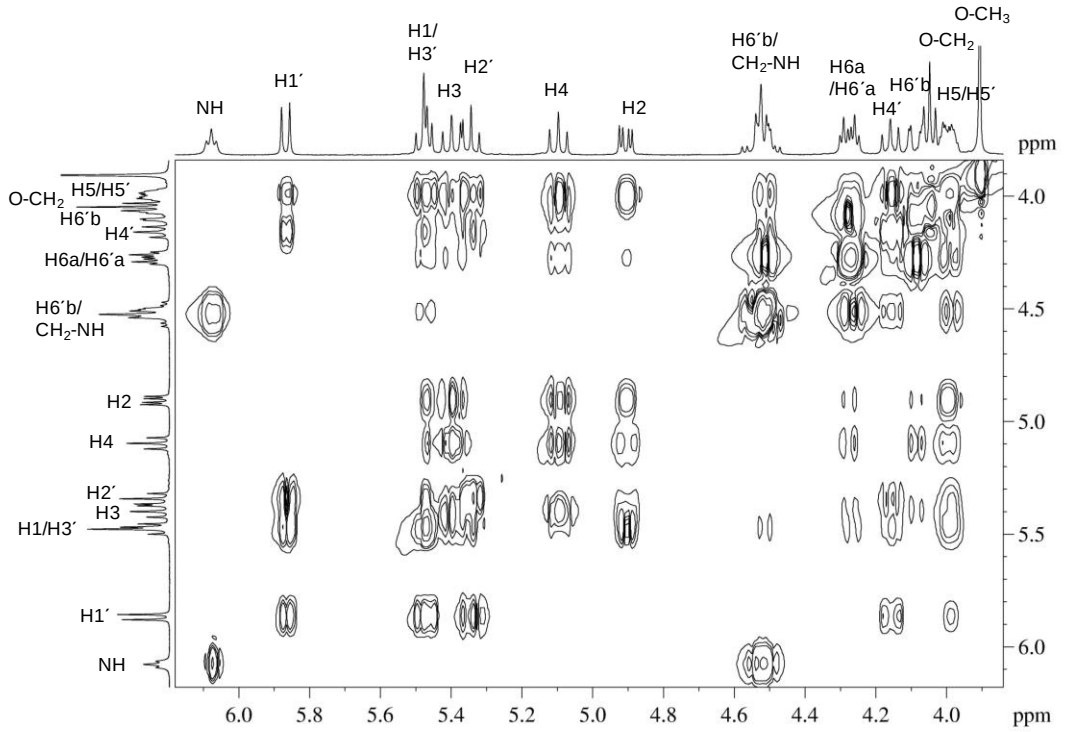

Fig. 4.4: TOCSY experiment of **OAc-Malt-Tz-C$_{10}$-Azo-OCH$_3$** with $CDCl_3$ as solvent at 25ºC and 60 ms of mixing time.

The exact masses of the azo-glycoamphiphiles were determined by mass spectrometry, see **Fig. 4.5** for MicroTOF mass spectrometry of **Malt-Tz-C_{10}-Azo-OCH_3** as an example, and the results also confirmed the proposed structures of these materials.

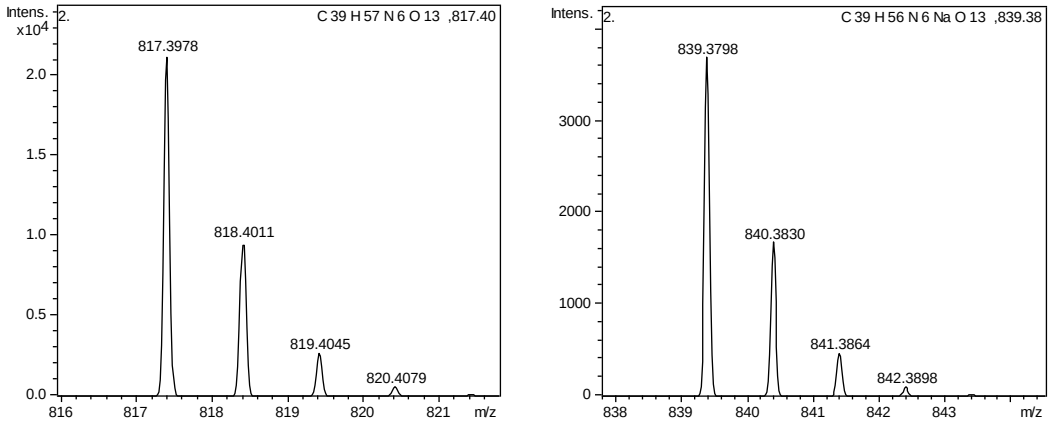

Fig. 4.5: MicroTOF Mass Spectrometry of **Malt-Tz-C_{10}-Azo-OCH_3**.

4.2.2. *Thermal properties*

The thermal properties of the synthesized azo-glycolipids were studied by thermogravimetric analysis (TGA), polarizing optical microscopy (POM) and differential scanning calorimetry (DSC).

In peracetylated precursors, 5% weight losses were observed at temperatures close to 300ºC. However, thermogravimetric curves for deprotected azo-glycolipids display 5% weight losses at temperatures of 170-245ºC (in samples previously dried and immediately analyzed). See **Table 4.1** and **Fig. 4.6**.

Table 4.1: Thermogravimetric analysis of peracetylated precursors and azo-glycolipids.

Compound	$T_{5\%lost}$	T_{onset}	T_{max}
OAc-Malt-Tz-Azo-C_{16}	315ºC	320ºC	340ºC
OAc-Malt-Tz-C_5-Azo-C_8	315ºC	320ºC	336ºC
OAc-Malt-Tz-C_{10}-Azo-OCH_3	315ºC	320ºC	335ºC
Malt-Tz-Azo-C_{16}	215ºC	240ºC	260ºC
Malt-Tz-C_5-Azo-C_8	245ºC	273ºC	285ºC
Malt-Tz-C_{10}-Azo-OCH_3	170ºC	218ºC	258ºC

$T_{5\%lost}$ = Temperatures at which 5% of the initial mass is lost. T_{onset} = Onset of decomposition. T_{max} = Temperatures at which the maximum rate of weight loss is produced.

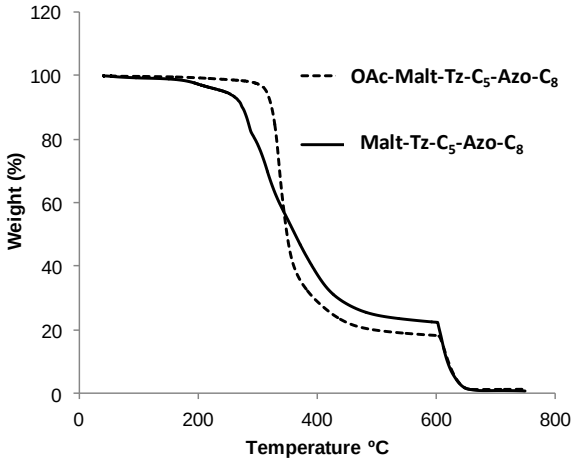

Fig. 4.6: Thermogravimetric curves of **OAc-Malt-Tz-C_5-Azo-C_8** and **Malt-Tz-C_5-Azo-C_8**.

The peracetylated precursors were studied by polarized optical microscopy and DSC as a function of temperature. Mesomorphic behavior was not observed in these peracetylated precursors. **OAc-Malt-Tz-Azo-C_{16}** and **OAc-Malt-Tz-C_{10}-Azo-OCH_3**, melt directly from a crystalline state into an isotropic liquid. **OAc-Malt-Tz-C_5-Azo-C_8** is an amorphous solid having a glass transition around 57ºC (DSC), see **Fig. 4.7**.

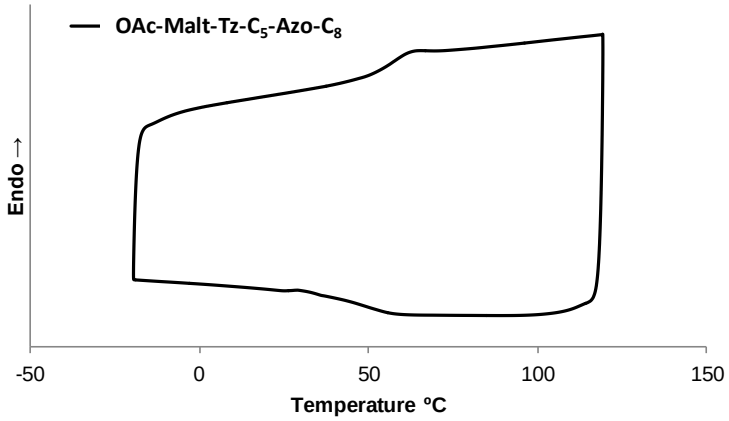

Fig. 4.7: DSC curve for the second scan in the solid state of **OAc-Malt-Tz-C_5-Azo-C_8**.

Decomposition of azo-glycolipids was observed by optical microscopy at temperatures above 170ºC and the sample became brown, most probably due to decomposition of the sugar units. In DSC experiments, when the azo-glycolipids were heated up to 200ºC, decomposition at around 170-175ºC was observed for **Malt-Tz-Azo-C_{16}** and **Malt-Tz-C_5-Azo-C_8**; while for **Malt-Tz-C_{10}-Azo-OCH_3**, the decomposition started at 120ºC as a

decrease of the baseline. As consequence, DSC studies of the azo-glycolipids were performed by heating the compounds up to 120ºC (maximum) to prevent the thermal decomposition of the samples, see **Table 4.2**. Under these conditions, the second and successive scans were reproducible. Compounds are crystalline except **OAc-Malt-Tz-C_5-Azo-C_8** that only exhibits a glass transition (in the first heating exhibits an endothermic peak at approximately 110ºC, which is not observed in successive scans).

Table 4.2: Thermal characterization of peracetylated compounds and azo-glycolipid compounds.

Compound	Thermal transition (ºC) [ΔH kJ/mol][a]
OAc-Malt-Tz-Azo-C_{16}[b]	Cr 171 [48.3] I
OAc-Malt-Tz-C_5-Azo-C_8[b]	g 57 I
OAc-Malt-Tz-C_{10}-Azo-OCH_3[b]	Cr 132 [38.4] I
Malt-Tz-Azo-C_{16}[c]	Cr 58 [5.2] Cr ´79 [3.3] Cr´´ 140[d] S_m
Malt-Tz-C_5-Azo-C_8[c]	g 78 Sm
Malt-Tz-C_{10}-Azo-OCH_3[c]	g 67 Sm+dec

[a]DSC thermal cycles were carried out in nitrogen atmosphere (10ºC/min). [b]The heating cycles were carried out up to 200ºC. Data corresponding to the second heating scan. [c]The first and second heating cycles were carried out up to 120ºC. Data corresponding to the second heating scan. [d]Data from polarized light microscopy. Cr = crystal, I = isotropic liquid, g = glassy state, Sm = smectic phase.

From the DSC measurements, **Malt-Tz-Azo-C_{16}** has a thermal transition at around 80ºC; however, above this temperature, the sample is highly viscous and difficult to study by optical microscopy. Nevertheless, using optical microscopy, the sample becomes more fluid at temperatures above approximately 140ºC, and it can be characterized as a liquid crystal according to the optical observations. In DSC (sample heated up to 200ºC) a peak was not clearly observed in this region although a broad transition cannot be ruled out. **Malt-Tz-C_5-Azo-C_8** has a glass transition (no clear endothermic or exothermic peaks were observed in the first heating), observed by DSC measurement, at around 78º C and also exhibits a birefringent texture corresponding to a highly viscous mesophase above this glass transition, see **Fig. 4.8**. **Malt-Tz-C_{10}-Azo-OCH_3** is semicrystalline as obtained. Once heated above 120ºC (endothermic peak at

120ºC) the compound does not crystallize on cooling and exhibits a glass transition (at around 70ºC) in the second and subsequent heating scans. The textures of all compounds were similar and difficult to be unambiguously assigned.

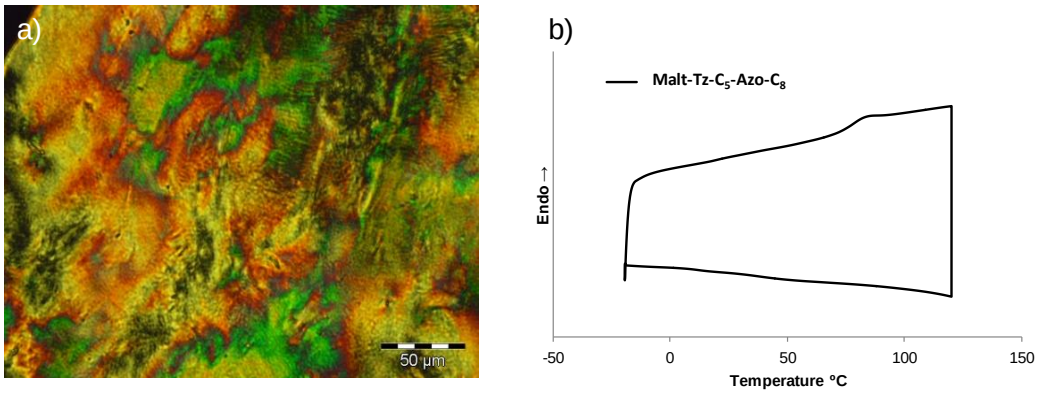

Fig. 4.8: a) Microphotograph of **Malt-Tz-C_5-Azo-C_8** taken at 130º C at first heating cycle, b) DSC curves for the second heating and cooling scan of **Malt-Tz-C_5-Azo-C_8**.

In an effort to identify the mesophase by XRD, several attempts were made to obtain oriented fibers of the compounds. A fiber of **Malt-Tz-C_5-Azo-C_8** compound was obtained around 160ºC; at lower temperatures any fibre can be drawn. However, oriented fibres of **Malt-Tz-Azo-C_{16}** and **Malt-Tz-C_{10}-Azo-OCH_3** could not be obtained. X-ray patterns of the **Malt-Tz-C_5-Azo-C_8** fibre were recorded at room temperature for 15h, see **Fig. 4.9**. Bragg reflections were found in the low-angle region corresponding to the second, third and fourth lamellar orders. The lamellar spacing obtained is close to 61.6Å which is larger than the length of one molecule (44.1Å according to measurements accomplished in Chem3D Pro 12.0 program), but smaller than twice the extended molecular length. This result indicates that an interdigitated bilayer is probably formed. In the high angle region a diffuse, broad maximum was found.

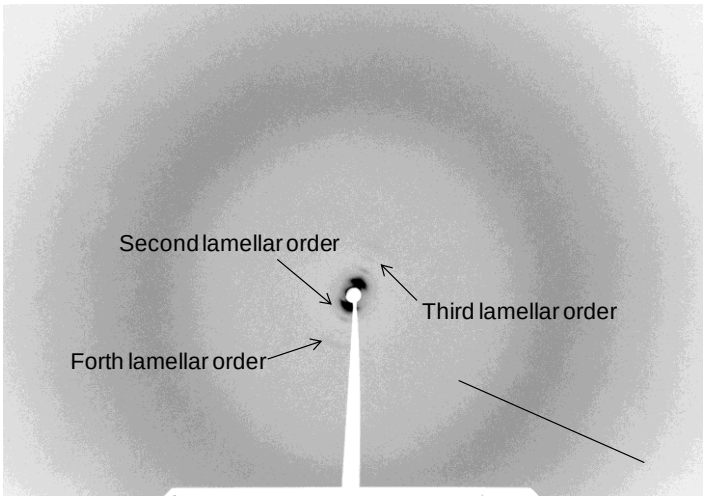

Fig. 4.9: a) X-ray pattern of a fibre of**Malt-Tz-C_5-Azo-C_8** recorded at RT for 15 h (fibre axis indicated in the figure).

4.2.3. *Supramolecular Gels*

The solubility and gelation abilities of the azo-glycolipids were examined in different solvents by dissolving the compound in the corresponding solvent with a concentration in the range of 0.5-5 wt % (the gelator and the solvent were placed in a septum-capped test tube). **Malt-Tz-Azo-C_{16}** and **Malt-Tz-C_{10}-Azo-OCH_3** azo-glycoamphiphiles are not soluble at room temperature (RT) in any of the selected solvents, except DMSO. However, the **Malt-Tz-C_5-Azo-C_8** compound has a different behavior: it is soluble at RT in solvents such as chloroform, THF, DMF, DMSO, methanol and the DMSO/water mixture. This compound is not soluble in water; however if the aqueous solution is heated, the compound is finally solubilized and remains soluble when the aqueous solution is cooled down to RT (2.5 wt %). The results for the three compounds in the selected solvents are summarized in **Table 4.3**. If the compound was not soluble at RT, the mixtures were first dissolved by heating and then cooling to RT. Under this process a solution, a precipitate or a gel was observed depending on the solvent. The formation of a gel was registered if the tube was turned upside down and the solution did not flow.

Table 4.3: Solubility and gelation properties of the synthesized azo-glycolipids in different solvents tested at different concentrations (0.5-5.0 wt %), after heating and cooling down to RT.

Solvent	Malt-Tz-Azo-C_{16}	Malt-Tz-C_5-Azo-C_8	Malt-Tz-C_{10}-Azo-OCH_3
Toluene	I	I	I
Choroform	I	S	I
THF	P	S	P
Dodecanol	I	I	I
Acetone	I	I	I
DMF	P	S	P
DMSO	S	S	S
Methanol	I	S	I
Water	G (5.0 wt %)	S[a]	I
DMSO/Water	G (1.5 wt %, 1:1 wt)	S	G (2.0 wt %, 1:1 wt)

I=Insoluble, P = Precipitate, S = Solution, NT = Not Tested, G= Gel (minimum gelation concentration). [a]Soluble by previous heating at 2.5 wt % in water.

Malt-Tz-Azo-C_{16} compound gelates in water in a minimum gelation concentration of 5.0 wt % to form a gel in the absence of other organic solvents. This gel is opaque, but becomes a little transparent in a DMSO/water mixture, as can be seen in **Fig. 4.10**.

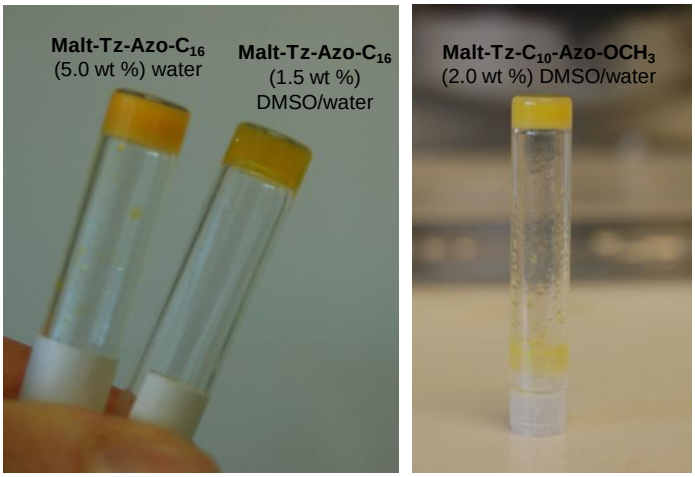

Fig. 4.10: Left: gels of **Malt-Tz-Azo-C_{16}** 5.0 wt % water and 1.5 wt % DMSO/water (1:1 wt). Right: gel of **Malt-Tz-C_{10}-Azo-OCH_3**, 2.0 wt % DMSO/water (1:1 wt).

The minimum gelation concentration decreases to 1.5 wt % for the mixture of the two solvents (DMSO/water, 1:1 wt). **Malt-Tz-C_{10}-Azo-OCH_3** also formed a gel in a DMSO/water mixture (1:1 wt) at 2.0 wt % as minimum gelation concentration; this gel is also opaque.

These molecules have a highly hydrophobic tail and the presence of an organic co-solvent such as DMSO, in addition to water, is required for complete solubilisation on cooling and subsequent gel formation. In all the cases, the gels are stable at RT and thermoreversible. Sol states were reached by heating the septum-capped test tube in a block heater, for **Malt-Tz-Azo-C_{16}** (5.0 wt % water) at 90ºC, **Malt-Tz-Azo-C_{16}** (1.5 wt % DMSO/water 1:1 wt) at 85ºC and for **Malt-Tz-C_{10}-Azo-OCH_3** (2.0 wt % DMSO/water 1:1 wt) at 100ºC. However, **Malt-Tz-C_5-Azo-C_8** compound cannot form a gel even in mixtures of solvents.

To corroborate the presence of π-π stacking and H-bonding interactions, ^{1}H-NMR experiments were performed to study the groups involved in the self-assembly. An experiment was carried out starting from a DMSO solution of **Malt-Tz-C_{10}-Azo-OCH_3** and subsequent addition of water.

For example, **Fig. 4.11** shows the the 8.50 to 6.90 ppm region of the ^{1}H NMR spectra of the **Malt-Tz-C_{10}-Azo-OCH_3** compound (2.9mg) in 0.40mL of DMSO-d_6 at RT (and successive addition of water) and **Fig. 4.12** shows the region from 6.00 to 3.00 ppm. The spectra were recorded upon successive additions of 0.04 mL of water to the initial DMSO-d_6 solution. The signals corresponding to CH or CH_2 of the carbohydrate remains unchanged (see **Fig. 4.12**) meanwhile a displacement of the rest of signals was observed. Several signals exhibited a shift upon addition of water up to 0.16 mL. Upon addition of more water the signals did not exhibit additional shift and the intensity decreased. A shielding was found for the H signal of the triazole ring ($\Delta\delta(H_{Tz)}$ = 0.072 ppm) and for the H signals of the azobenzene aromatic ring ($\Delta\delta(H_{arom})$ = 0.036 ppm in both signals). These latter protons have a similar shift in DMSO-d_6 solution, but become unequally shifted as the aggregation takes place, due to parallel displacement of the rings minimizing the unfavorable electrostatic effects in the π-π stacked arrangements. This supports the contribution of π-π stacking to the aggregation of the amphiphiles promoted by water addition.

A simultaneous deshielding for the NH signal is detected ($\Delta\delta(H_{NH})$ = 0.075 ppm) as well as in the OH signals which can be assigned to H-bonding interactions. These facts are in accordance with self-assembly upon addition of water that finally led to a swollen gel aggregate macroscopically detected in the NMR tube.

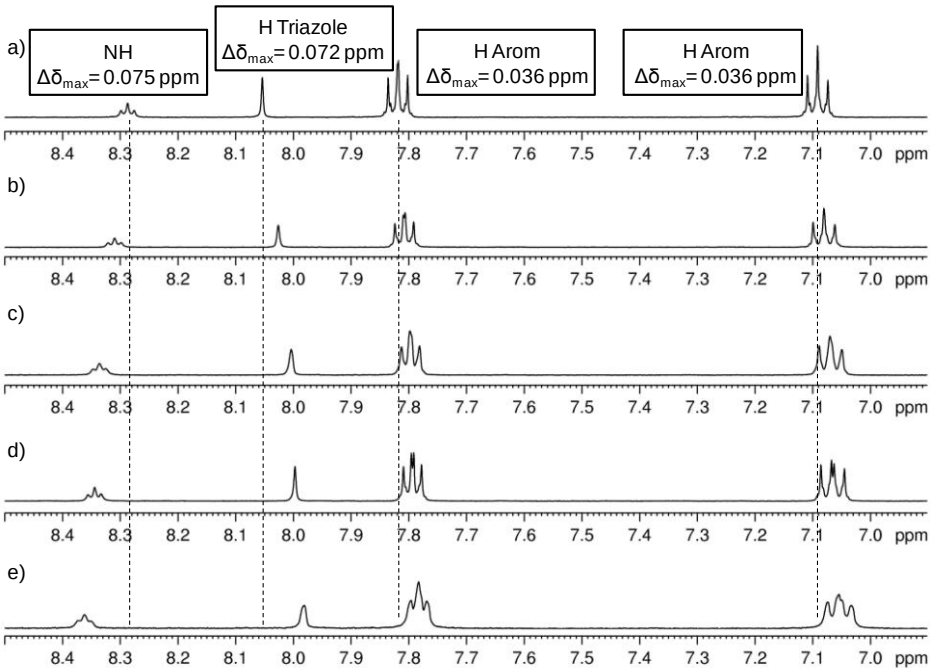

Fig. 4.11: 8.50 to 6.90 ppm region of the ^{1}H NMR spectra in DMSO-d_6 upon successive addition of water, (a) 2.9 mg of **Malt-Tz-C_{10}-Azo-OCH_3** in 0.40 mL DMSO-d_6, (b) addition of 0.04 mL H_2O to **(a)** [1:0.1 DMSO/water], (c) addition of 0.08 mL H_2O to **(a)** [1:0.2 DMSO/water], **(**d) addition of 0.12 mL H_2O to **(a)** [1:0.3 DMSO/water], (e) addition of 0.16 mL H_2O to **(a)** [1:0.4 DMSO/water]**.**

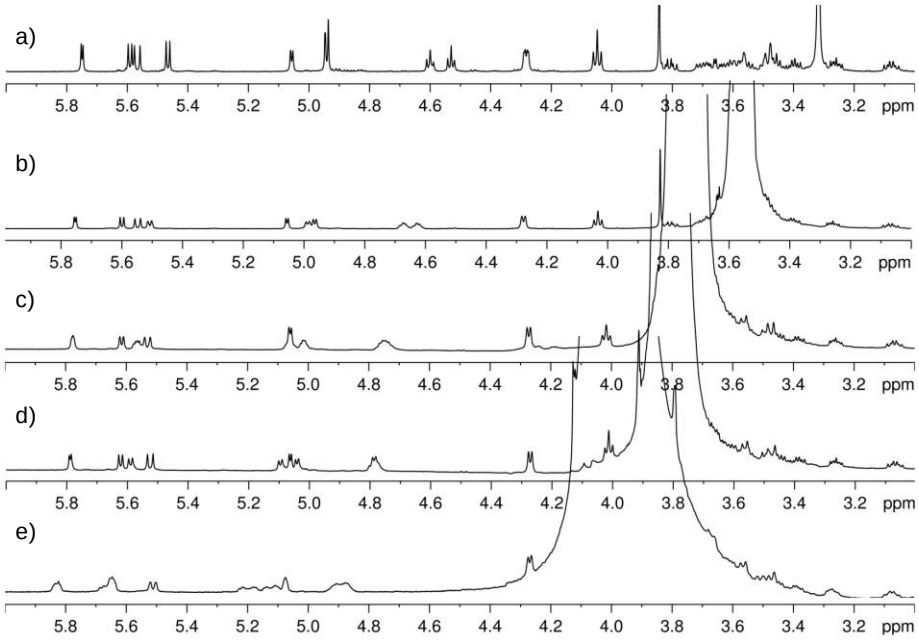

Figure 4.12: 6.00 to 3.00 ppm region of the ^{1}H NMR spectra in DMSO-d_6 upon successive addition of water. (a) 2.9 mg of **Malt-Tz-C_{10}-Azo-OCH_3** in 0.40 mL DMSO-d_6, (b) addition of 0.04 mL H_2O to **(a)** [1:0.1 DMSO/water], (c) addition of 0.08 mL H_2O to **(a)** [1:0.2 DMSO/water], **(**d) addition of 0.12 mL H_2O to **(a) [**1:0.3 DMSO/water], (e) addition of 0.16 mL H_2O to **(a)** [1:0.4 DMSO/water]**.**

The position of the azobenzene group seems to have an influence of the solubility and gel ability. When the azobenzene group is located in the middle (**Malt-Tz-C_5-Azo-C_8**), the compound is soluble in several organic solvents and surprisingly soluble in water, and no gels were obtained in the solvents studied. If it is directly linked to the sugar polar head, the compound (**Malt-Tz-Azo-C_{16}**) gelates in water, but when the azobenzene is at the end of the hydrophobic chain (**Malt-Tz-C_{10}-Azo-OCH_3**), the gel had to be formed in a mixture of a solubilising solvent, DMSO, and a non-solubilising solvent, water.

Morphological gel characterization. The self-assembled structure of the gels derived from **Malt-Tz-Azo-C_{16}** and **Malt-Tz-C_{10}-Azo-OCH_3** were studied by electron microscopy (SEM and TEM) on dried gels under vacuum (xerogels).

SEM measurements of the xerogels show bundles of fibres which form the 3D network responsible for the gel structure, see **Fig. 4.13**. The fibres of the **Malt-Tz-Azo-C_{16}** gel, either in water or in a mixture of 1:1 wt DMSO/water, show diameters of around 40-60nm, see **Fig. 4.13.a and b**. However, fibres from gels in water seem to be shorter than for the mixture of solvents, where they are several μm in length. Moreover, some wider fibres of around 100nm in diameter can also be measured in the gel from the mixture of solvents. **Malt-Tz-C_{10}-Azo-OCH_3** xerogel images show fiber with a broad range of diameters (some of them are close to 1 μm, fibres of around 80 nm can also be observed; however most of the fibers are mainly around 200-250 nm), see **Fig. 4.13c**.

Torsion was observed for a single **Malt-Tz-C_{10}-Azo-OCH_3** ribbon, which is shown in **Fig. 4.13.d.** This torsion could be related to the molecular chirality of the molecules, which is traduced into the chiral helicity of the supramolecular arrangement.

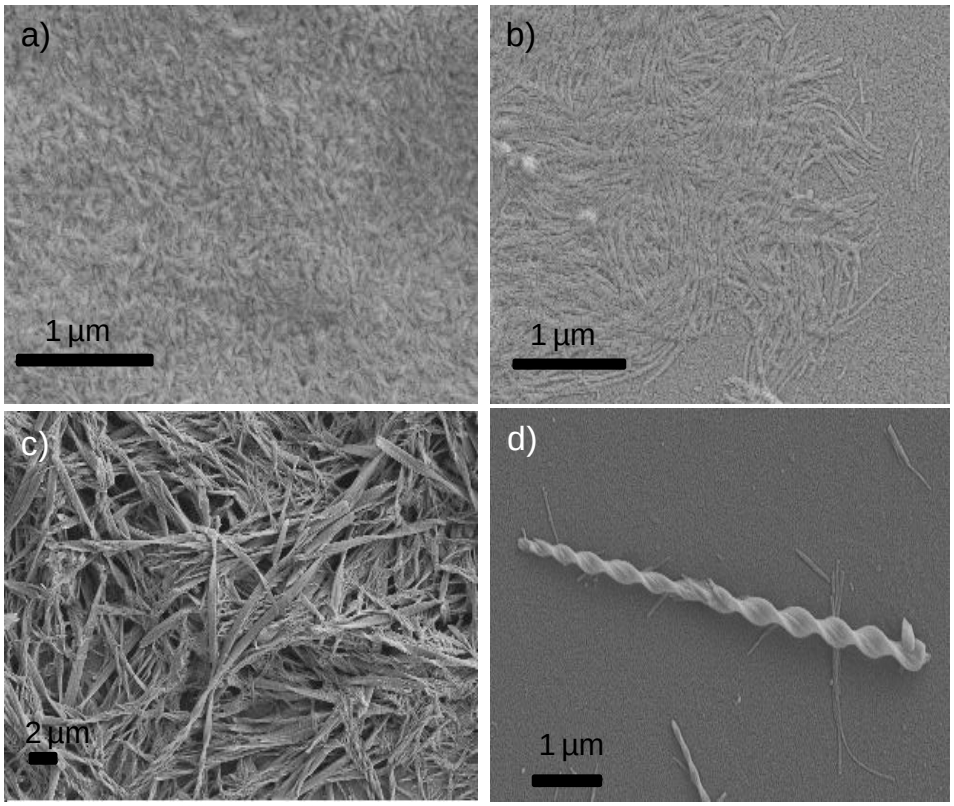

Fig. 4.13: a) SEM image of **Malt-Tz-Azo-C_{16}** xerogel (5.0 wt % water), b) SEM image of **Malt-Tz-Azo-C_{16}** xerogel (1.5 wt % DMSO/water 1:1 wt), c) SEM image **Malt-Tz-C_{10}-Azo-OCH_3** xerogel (2.0 wt % DMSO/water 1:1 wt), d) SEM image of a single twisted ribbon of **Malt-Tz-C_{10}-Azo-OCH_3** xerogel (2.0 wt % DMSO/water 1:1 wt).

Fibrillar structures were also observed by TEM, see **Fig. 4.14**. However, in this technique, a dried dilute solution of the gel must be used (0.1 wt % in water or DMSO/water) and negative staining with uranyl acetate was done. The observed fibres were over 10-20 nm in diameter for the **Malt-Tz-Azo-C_{16}** and **Malt-Tz-C_{10}-Azo-OCH_3**.

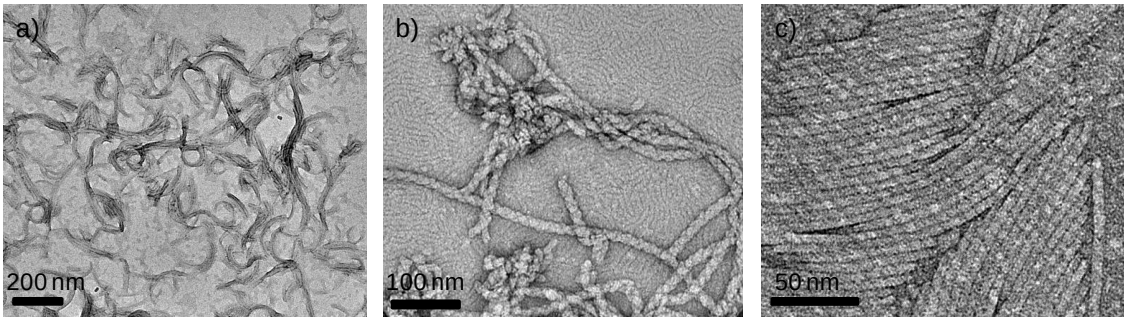

Fig. 4.14: a) TEM image of **Malt-Tz-Azo-C_{16}** (0.1 wt % water), b) TEM image of **Malt-Tz-Azo-C_{16}** (0.1 wt % DMSO/water 1:1 wt), c) TEM image of **Malt-Tz-C_{10}-Azo-OCH_3** (0.1 wt % DMSO/water 1:1 wt).

4.2.4 *Study and control of the chiral supramolecular arrangement*

The presence in the supramolecular gels of photoactive units as the azobenzene moieties should allow the control of their nanostructure and subsequently of the gel properties. If a chiral organisation is expected in the gel, CD spectroscopy is of great interest to characterise the chiral assemblies and potential changes in the organisation. For this purpose, UV-vis and CD spectra of the azo-gelators, were registered simultaneously both in DMSO solution and in gel state.

In DMSO solution, $5x10^{-5}$ M, λ_{max} in the UV absorption spectrum appears at 362 nm for all the compounds, **Malt-Tz-Azo-C_{16}**, **Malt-Tz-C_5-Azo-C_8** and **Malt-Tz-C_{10}-Azo-OCH_3**, see **Fig. 4.15.** The solutions were CD silent. These spectroscopic results seem to evidence that azobenzene chromophores are mainly isolated in the DMSO solutions, with a low aggregation detected.

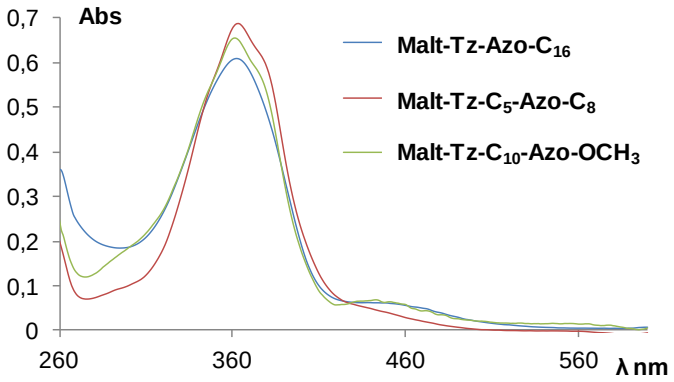

Fig. 4.15: Absorption spectra of **Malt-Tz-Azo-C_{16}**, **Malt-Tz-C_5-Azo-C_8** and **Malt-Tz-C_{10}-Azo-OCH_3** in DMSO solution ($5x10^{-5}$ M).

The absorption spectrum of **Malt-Tz-C_{10}-Azo-OCH_3** gel (2 wt % DMSO/water, 1:1 wt), see **Fig. 4.16**, exhibits a λ_{max} at 335 nm, which is blue shifted with respect to the $\lambda_{máx}$ of the free azobenzene units in DMSO solution. That points to the existence of H-aggregates of azobenzene moieties. Moreover, a negative Cotton effect is detected in the CD spectrum corresponding with the absorption band of azobenzene H aggregates. Unfortunately, the UV-vis and CD spectra of the **Malt-Tz-Azo-C_{16}** gel (1.5 wt % DMSO/water, 1:1 wt) could not be performed probably due to the sample crystallization in the silica sandwich.

The presence of azobenzene groups can be used to induce modifications on the supramolecular structure of the gel by irradiation with UV light. However, after UV irradiation at 365nm for 150 min (see **Characterization Techniques 7. Annex** for experimental conditions), no changes were detected in the UV-vis and CD spectra of **Malt-Tz-C_{10}-Azo-OCH_3** gel (2.0 wt % DMSO/water, 1:1 wt); see **Fig. 4.16**. The gel is stable under these conditions, indicating that *trans-cis* isomerisation of the azobenzene groups does not occur, probably because the dense packing of the azobenzene groups prevents the *trans-cis* isomerization.[23]

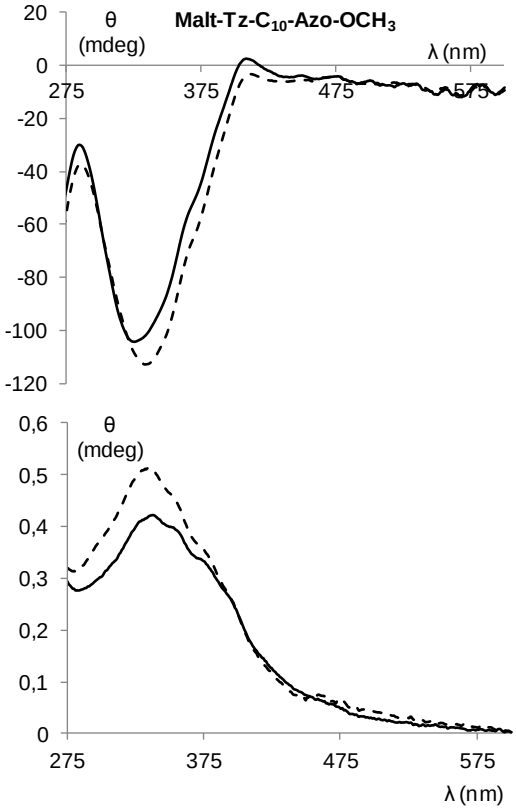

Fig. 4.16: CD spectrum (top) and absorption (bottom) spectra of **Malt-Tz-C_{10}-Azo-OCH_3** gel (2.0 wt % DMSO/water (1:1)) without irradiation, solid line, and irradiated at 365 nm for 150 min, dashed line.

To obtain hydrogels with a lower ratio of azo-derivatives, multi-component supramolecular gels have been formed. With this aim, we prepared mixtures with an azo-glycolipid (**Malt-Tz-C_5-Azo-C_8** or **Malt-Tz-Azo-C_{16}**) and the previously described hydrogelator **Malt-Tz-C_{16},** having a similar structure but without photochromic units, see **Fig. 4.17.**

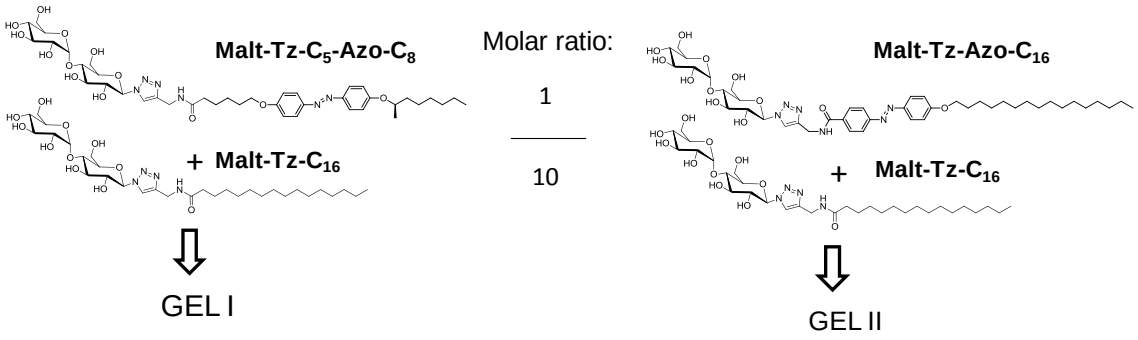

Fig. 4.17: Chemical structure of compounds used for preparing **Gel I** and **Gel II.**

Malt-Tz-C_5-Azo-C_8 and **Malt-Tz-Azo-C_{16}** azo-glycolipids were selected because of their solubility or ability to gelify in water. **Malt-Tz-C_{10}-Azo-OCH_3** was not used because it is not soluble in water. In these cases, CD and absorption spectra were recorded from 200 to 600 nm to investigate both regions corresponding to triazole and azobenzene groups, in contrast to the gels made from DMSO/water mixtures, where only the azobenzene group region can be observed.

Gel I was formed by **Malt-Tz-C_5-Azo-C_8** and **Malt-Tz-C_{16}** in a 1:10 molar ratio, at 1wt % of **Malt-Tz-C_{16}** hydrogelator in water. In mixtures with an increasing amount of **Malt-Tz-C_5-Azo-C_8** azo-compound, no gel formation was observed. To compare the influence of the azoamphiphile, **Gel II** was formed by **Malt-Tz-Azo-C_{16}** and **Malt-Tz-C_{16}**, in the same ratio (1:10 molar ratio), at 1 wt % of the **Malt-Tz-C_{16}** hydrogelator in water.

A solution of **Malt-Tz-C_5-Azo-C_8** in water ($4.5x10^{-5}$ M) and having a similar absorption to **Gel I** exhibits a maximum absorption of the π-π^* band of the azobenzene groups at 343 nm; the maximum is blue-shifted with respect to the observed for isolated azobenzene. Moreover, a CD signal was observed in this water solution of **Malt-Tz-C_5-Azo-C_8**. These results indicate that azobenzene chromophores are aggregated (H-aggregation) and this aggregation is the origin of the CD signal, see **Fig. 4.18**.

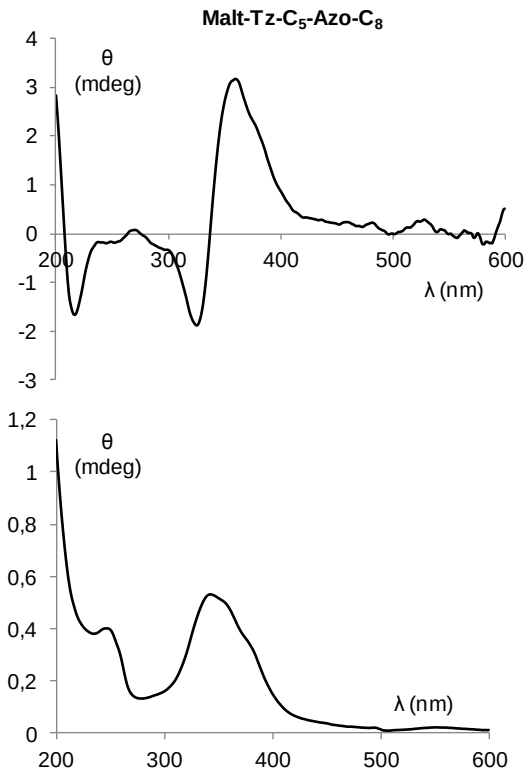

Fig. 4.18: CD and absorption spectra of a water solution of **Malt-Tz-C_5-Azo-C_8** (4.5x 10^{-5} M).

The π-π* band of the azobenzene units in the UV-vis spectra of **Gel I** (**Malt-Tz-C_5-Azo-C_8** as photoactive compound) and **Gel II** (**Malt-Tz-Azo-C_{16}** as photoactive compound) show a hypsochromic shift in relation to the band of free azobenzene chromophores, suggesting a H-aggregation, see **Fig. 4.19 (bottom)** for **Gel I** and **Fig. 4.20 (bottom)** for **Gel II**. Both gels show CD signals due to the triazole and azobenzene groups; however there are some notable differences; see **Fig. 4.19 (top)** for **Gel I** and **Fig. 4.20 (top)** for **Gel II**. At a shorter wavelength, **Gel I** exhibits a Cotton effect around 240 nm due to the absorption band of the triazole group, which is directly bonded to the chiral sugar unit (maltose). At a longer wavelength, a negative Cotton effect associated with the π–π* absorption band of the azobenzene moiety is also detected. Moreover, the CD spectrum of the fresh **Gel II** seems to show two positive couplets, corresponding to triazole groups (shorter wavelength) and azobenzene units (longer wavelength). Surprisingly, after storing **Gel II** for 6h, the ellipticity values of

the negative bands increase and a new CD band is detected at 365nm. A reorganisation of the sample probably occurs in the sandwich formed under measurement conditions.

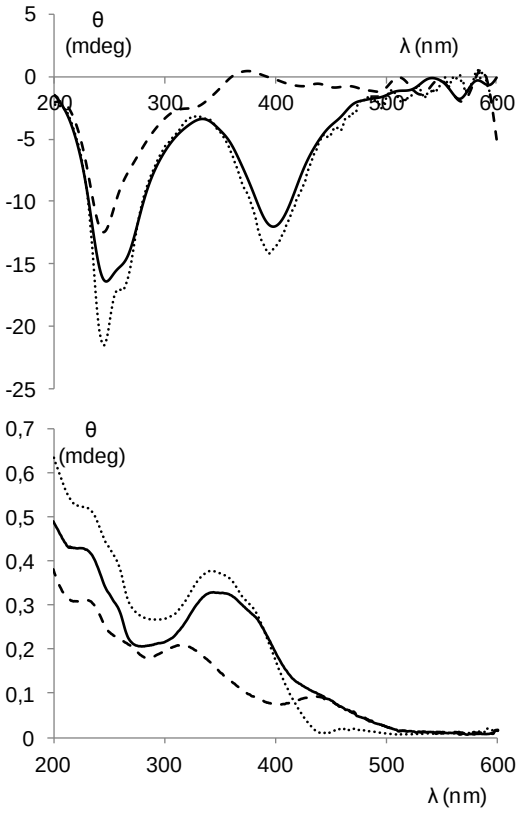

Fig. 4.19: CD (top) and absorption (bottom) spectra of fresh **Gel I**, solid line; irradiated for 2 min with UV light at 365 nm; dashed line; after 24h storage in darkness, dotted line.

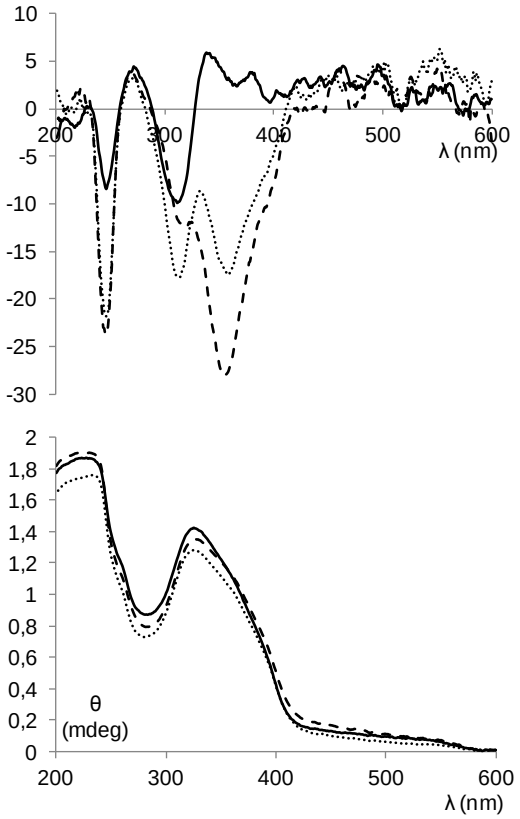

Fig. 4.20: (b) CD (top) and absorption (bottom) spectrum of fresh **Gel II**, solid line; after 6 h in the sandwich without irradiation, dotted line, irradiated for 150 min with UV light at 365 nm, dashed line.

Both **Gel I** and **Gel II** were irradiated with UV light at 365nm (see **Characterization Techniques 7. Annex** for experimental conditions), to evaluate the effect on the supramolecular organisation of the *trans-cis* isomerisation of the azobenzene groups. The UV-vis spectra of **Gel I** (see **Fig. 4.19 dashed line**) after 365 nm irradiation, clearly shows the presence of a *cis*-azobenzene isomer: the π–π* absorption band at 365nm of the *trans* isomer decreases and the band is blue shifted meanwhile an increase of the n–π* absorption band at 450 nm is detected. The photostationary state is reached after irradiation for 2 min. The photoisomerisation reduces the *trans*-azoisomer concentration, thus the negative CD signal related to the azobenzene group disappears, while the negative signal corresponding to the triazole only decreases. It can be deduced that gel-sol transition does not occur as the signals did not disappear. This was macroscopically corroborated by irradiation of the gel on a flask: gel disruption was not

detected and only a colour change from red to yellow was obtained, probably due to partial disruption of the azobenzene aggregates, which is in accordance with the disappearance of the CD signal corresponding to the chiral supramolecular aggregation of azobenzene units. When the sample was kept for 24h in the dark, a total recovery of the initial UV-vis and CD spectra was obtained.

However, after irradiation for 150 min, the **Gel II** showed no evidence of *trans-cis* isomerisation, but the CD band at around 300-350 nm exhibit a modification (see **Fig. 4.20 dashed line**). This fact can be probably due to a photoinduced reorganisation of the chiral supramolecular structure, or a simple reorganisation over time involving the azobenzene groups. By storing the sample for 24h in the dark, the CD and absorption signals were not modified.

Gel I works as a photoresponsive soft material, meanwhile **Gel II** has no response to light. This fact can be due to the different location of the azobenzene. In case of the **Malt-Tz-C_5-Azo-C_8**, component of **Gel I**, the azobenzene unit is in the middle of the hydrophobic part and separated from the sugar moiety by means of a methylenic chain, which may favour the isomerisation. However, the azo-amphiphile derivative in **Gel II** has the azobenzene unit directly linked to the sugar polar head and triazole units involved in the H-bonding and π–π interactions (among others) that support the gel. The proximity to this rigid part probably hinders an effective isomerisation

4.3. Summary and conclusions

- ✓ Three maltose-based azo-amphiphiles have been synthesized, liquid crystalline and gel-forming properties have been determined. Azobenzene chromophore was placed at different positions of the hydrophobic chain and a maltose sugar head. Chiral supramolecular assemblies have been characterized by NMR, electron microscopy and CD. The light-response of azo-amphiphiles in supramolecular gels has been studied. Also azo-gels which contained mixtures of the azo-amphiphilic compounds and a similar structural hydrogelator have been investigated.

- Copper(I)-catalysed azide-alkyne [3+2] cycloaddition reaction is useful to link hydrophobic, chromophoric blocks and sugar polar heads.
- The maltose-based azo-amphiphiles give rise to thermotropic smectic phases.
- When the azobenzene group is located in the middle of the hydrophobic block (**Malt-Tz-C_5-Azo-C_8**), the compound is soluble in several solvents, but has not the ability to form gels.
- When the azobenzene is directly linked to the sugar polar head, the compound (**Malt-Tz-Azo-C_{16}**) is able to form gels in water as well as in a mixture of DMSO/water, but when the azobenzene is at the end of the hydrophobic chain (**Malt-Tz-C_{10}-Azo-OCH_3**), the gel had to be formed in a mixture of DMSO/water.
- Torsion on the resulting self-assembled fibrillar network was observed by electron microscopy and a chiral arrangement was confirmed by CD.
- No changes under irradiation with UV light were obtained in the DMSO/water gels of the pure compounds probably due to the packing and ordering of hydrophobic blocks.
- The 3D network of **Malt-Tz-C_{16}** hydrogel was successfully doped with a similar structure having a photoresponsive unit (**Gel I** and **Gel II**). Reversible modifications were detected in CD under irradiation with UV light for **Gel I**. The CD signal related to the azobenzene group disappeared when *trans-cis* isomerization takes place. This indicates that some reversible structural modifications have been promoted in the chromophoric moieties while the gel structure remained unchanged. A macroscopic color change has also been observed on this gel.

4.4. Experimental Section

Synthesis of ethyl 4-hydroxy-4´-(ethyloxycarbonyl)azobenzene ($C_{15}H_{14}N_2O_3$) **(13):**

Ethyl 4-aminobenzoate (9.26 g) was dissolved in 45 mL of water and cooled in a water-ice bath. 20 mL of HCl (37%) solution was added dropwise and later a $NaNO_2$ (4.68 g in 30 mL of water) solution, also dropwise. 6.30 g of phenol (66.94 mmol) was added 30 min later, and for 1 hour the mixture was stirred at 5° C. The product precipitated upon addition of a concentrated $NaHCO_3$ aqueous solution to achieve pH 7-8. It was filtered and washed with water. The product was finally purified by flash chromatography with dichloromethane as eluent. A red solid was obtained (6.55 g, 45%).

^{1}H NMR (400 MHz, $CDCl_3$, 25ºC, δ ppm): 1.42 (t, 3H, J=7.2 Hz, C*H*$_3$-CH$_2$), 4.41 (q, 2 H, J=7.2 Hz, C*H*$_2$-CH$_3$), 5.63 (s, 1H, O*H*), 6.99-6.95 (m, 2H, C*H*arom), 7.92-7.88 (m, 4H, C*H*arom), 8.19-8.16 (m, 2H, C*H*arom).

^{13}C (100 MHz, $CDCl_3$, δ ppm): 14.4 *C*H$_3$-CH$_2$, 61.5 *C*H$_2$-O-, 116.1, 122.5, 125.7, 130.7, *C*Har, 131.5, 147.2, 155.4, 159.3, *C*ar, 166.7, *C*O.

ESI$^+$: 271.1 $[M + H]^+$, 293.0 $[M + Na]^+$.

IR (KBr, cm^{-1}): 3397, 1693, 1599, 1592, 1504, 1402, 1280, 1134, 846, 773.

Synthesis of 4-(hexadecyloxy)-4´-(ethyloxyoxycarbonyl)azobenzene ($C_{31}H_{46}N_2O_3$) **(14):**

5.40 g of compound **13** (20 mmol) was dissolved in acetone (140 mL), under Ar atmosphere, KI (0.83 g, 1.85 mmol) and K_2CO_3 (5.52 g, 40 mmol) was added. The mixture was refluxed and the alkyl bromide (7.33 mL, 24 mmol) was added dropwise. The mixture was stirred for 24 hours. The reaction was monitored by TLC (hexane/ethyl acetate, 7:3). The solvent was partially removed; dichloromethane (300 mL) was added and the organic solution was washed three times with water and dried with anhydrous $MgSO_4$. The product was recrystallized in ethanol yielding an orange solid (8.50 g, 85%).

^{1}H NMR (400 MHz, $CDCl_3$, 25ºC, δ ppm): 0.88 (t, 3 H, J=7.2 Hz, C*H*$_3$-$(CH_2)_{15}$-), 1.50-1.28 (m, 33 H, C*H*$_3$-CH_2-O-, -(C*H*$_2$)$_{15}$-), 1.86-1.79 (m, 2H, O-CH_2-C*H*$_2$-$(CH_2)_{15}$), 4.05 (t, 2H, J=6.8 Hz, O-C*H*$_2$-CH_2), 4.41 (q, 2H, J= 7.2 Hz, CH_3-C*H*$_2$-O), 7.02-7.00 (m,2H, C*H*arom), 7.95-7.89 (m, 4H, C*H*arom), 8.18-8.16 (m, 2H, C*H*arom).

Synthesis of 4-(hexadecyloxy)-4´-(hydroxycarbonyl)azobenzene HOOC-Azo-C_{16} ($C_{29}H_{42}N_2O_3$):

Compound **14** (8.50 g, 17.22 mmol) and KOH (6.97 g, 120.54 mmol) were dissolved in ethanol (220 mL) and stirred and heated under reflux for 24 hours. The reaction is monitored by TLC with dichloromethane as eluent. 150 mL of water was added. The product precipitated upon addition of HCl (37%) in order to reach pH aprox. 2. It was filtered and washed with water. It was obtained as an orange powder which was recrystallized in acetic acid (7.27g, 90%).

^{1}H NMR (400MHz, DMSO-d_6, 70ºC, δ ppm): 0.85 (t, 3H, J= 6.8 Hz, –$(CH_2)_{12}$-C*H*$_3$), 1.17-1.52 (m, 24H, -(C*H*$_2$)$_{12}$-CH_3), 1.69-1.80 (m, 2H, –O-CH_2-C*H*$_2$-), 4.10 (t, 2H, J=6,6 Hz, –O-*CH*$_2$-CH_2-), 7.10-7.14 (m, 2H, *Har*), 7.86-7.92 (m, 4H, *Har*), 8.09-8.12 (m, 2H, *Har*).

^{13}C NMR (100 MHz, DMSO-d_6, 70ºC, δ ppm): 14.2 –$(CH_2)_{12}$-*C*H_3, 22.4, 25.8, 29.0, 29.0, 29.3, 29.3, 29.3, 31.6 -(*C*H_2)$_{15}$-, 68.7 –O-*C*H_2, 115.4, 122.5, 125.3, 130.9 *C*Har, 132.8, 146.8, 155.2, 162.6, *C*ar, 167.1 *C*OOH.

ESI: 467.2 $[M+H]^+$.

IR (KBr, cm^{-1}): 2953, 2919, 2868, 2850, 1680, 1601, 1582, 1501, 1470, 1418, 1404, 1303, 1290, 1248, 1143, 1107, 1026, 941, 864, 838, 809, 775, 721, 544.

Synthesis of 4-((R)- 2-methylheptyloxy) nitrobenzene ($C_{14}H_{21}NO_3$) **(15):**

(S)-2-Octanol (6.35 mL, 40 mmol), *p*-nitrophenol (5.56 g, 40 mmol), and diisopropylazodicarboxylate (7.87 mL, 40 mmol) were dissolved in dry THF (34 mL) under Ar atmosphere and cooled in a water-ice bath. Then, a solution of triphenylphosphine (10.55 g, 40 mmol) in 15 mL of dry THF was added dropwise under stirring. The mixture was stirred at room temperature overnight, the precipitate was filtered off, and the solution was washed twice with a saturated Na_2CO_3 solution, twice with water, and then with brine. The organic phase was dried, concentrated, and purified

by flash chromatography using hexane/ethyl acetate (8:2) as eluent to yield the desired compound as viscous yellowish oil (9.05 g, 90%).

^{1}H NMR (400 MHz, $CDCl_3$, 25ºC, δ ppm): 0.81 (t, 3H, J= 7.0 Hz, C*H*$_3$-CH_2), 1.26 (d, 3H, J= 6.1 Hz, C*H*$_3$-CH-O), 1.55-1.88 (m, 10H, -(C*H*$_2$)-), 4.35-4.45 (m, 1H, C*H*-O), 6.81-6.87 (m, 2H, C*H*arom), 8.07-8.12 (m, 2H, C*H*arom).

Synthesis of 4-((R)- 2-methylheptyloxy) aniline ($C_{14}H_{23}NO$) **(16):**

Compound **15** (5.04 g, 20.1 mmol) was dissolved in ethanol (40 mL) and 1.95 mL hydrazine monohydrate (98%) (40.2 mmol) was added dropwise. After heating the solution to 40° C, 1 g of activated Raney nickel was added in portions until no further reaction was observed. The resulting mixture was filtered from Raney nickel and ethanol was removed under reduced pressure. The crude was dissolved in 35 mL of diethylether and washed with water, brine and dried over anhydrous $MgSO_4$. The solvent was distilled off giving the desired aniline as yellow oil (3.78 g, 85%) which was used without further purification.

IR (Nujol, cm^{-1}): 3430, 3352, 3219, 2971, 2918, 2875, 1604, 1509, 1464, 1230.

Synthesis of 4-hydroxy-4´-((R)-2-methylheptyloxy)azobenzene ($C_{20}H_{26}N_2O_2$) **(17):**

A 2.5 M $NaNO_2$ solution (9.00 mL, 22.11 mmol) was added dropwise at a temperature below 5 °C to a heterogeneous mixture of aniline derivative **16** (4.44 g, 20.1 mmol) in 11 mL of 5 M HCl. The mixture was held at 5 °C and added carefully to a solution of of phenol (1.90 g, 20.1 mmol) in 20.00 mL of 2 M NaOH. The product precipitated upon addition of NaCl. It was collected with a Büchner funnel and purified by flash chromatography using dichloromethane as an eluent to yield the required product as yellow-orange crystalline leaflets (4.92 g, 75%).

^{1}H NMR (400 MHz, $CDCl_3$, 25ºC, δ ppm): 0.81 (t, 3H, J=7.0 Hz, C*H*$_3$-CH_2), 1.26 (d, 3H, J= 6.1 Hz, C*H*$_3$-CH-O), 1.55-1.88 (m, 10H, -(C*H*$_2$)-), 4.35-4.45 (m, 1H, C*H*-O), 6.81-6.93 (m, 4H, C*H*arom), 7.72-7.81 (m, 4H, C*H*arom).

Synthesis of 4-[5-(methyloxycarbonyl)pentyloxy]-4´-[-((R)- 2-methylheptyloxy)azobenzene ($C_{27}H_{38}N_2O_4$) **(18) :**

A mixture of 18-crown-6 (0.40 g, 1.5 mmol), finely ground K_2CO_3 (4.60 g, 33.28 mmol), compound **17** (4.92 g, 14 mmol), and methyl-6-bromohexanoate (4.63 g, 22.2 mmol) in acetone (100 mL) was stirred vigorously and heated under reflux for 24 h. The mixture was filtered and concentrated in vacuum. The crude product was recrystallized from methanol, yielding the required compound as an orange solid (5.72 g, 90%).

^{1}H NMR (400 MHz, $CDCl_3$, 25ºC, δ ppm): 0.81 (t, 3H, J=7.0 Hz, C*H*$_3$-CH_2), 1.27 (d, 3H, J= 6.1 Hz, C*H*$_3$-CH-O), 1.15-1.83 (m, 16H, -(C*H*$_2$)-), 2.30 (t, 2H, J= 7.6 Hz, CO-C*H*$_2$-CH_2-), 3.62 (s, 3H, C*H*$_3$-O), 3.97 (t, 2H, J=6,2 Hz, O-C*H*$_2$-CH_2-), 4.34-4.42 (m, 1H, C*H*-O), 6.87-6.95 (m, 4H, C*H*arom), 7.76-7.83 (m, 4H, C*H*arom).

Synthesis of 4-[5-(hydroxycarbonyl)pentyloxy]-4´-[-((R)- 2-methylheptyloxy)azobenzene HOOC-C_5-Azo-C_8 ($C_{26}H_{36}N_2O_4$):

Compound **18** (4.87 g, 10.74 mmol) was added to a NaOH solution (55.00 mL, 3 M). THF (9.00 mL) was then added until a homogeneous suspension was formed. The reaction mixture was stirred at room temperature for 4 days, during which the reaction was monitored with TLC. Once complete hydrolysis, the suspension was neutralized with a solution of HCl (5 M) at 0 °C, yielding the crude product as an orange solid that was filtered off and washed with acetone. The crude product was recrystallized twice from ethanol to yield the desired acid (3.075 g, 68%).

^{1}H NMR (400MHz, DMSO-d_6, 50ºC, δ ppm): 0.85 (t, 3H, J= 6.8 Hz, –(CH_2)$_5$-C*H*$_3$), 1.26 (d, 3H, J=6.4 Hz, –CH-C*H*$_3$), 1.20-1.80 (m, 16H, -(C*H*$_2$)-), 2.24 (t, 2H, J=7.3 Hz, –C*H*$_2$-COOH), 4.05 (t, 2H, J=6.4 Hz, –O-C*H*$_2$-CH_2-), 4.55 (m, 1H, –O-C*H*-CH_3), 7.07-7.10 (m, 4H, *Har*), 7.79-7.82 (m, 4H, *Har*).

^{13}C NMR (100 MHz, DMSO-d_6, 50ºC, δ ppm): 13.9 -CH_2-*C*H_3, 19.4 *C*H_3-O- 21.9, 24.2, 24.7, 25.0, 28.3, 28.6, 31.2, 33.5, 35.7, -(*C*H_2)-, CO-*C*H_2-CH_2-, 67.7 O-*C*H_2-CH_2, 73.4 -O-*C*H-CH_3, 114.9, 115.7, 124.0, 124.1 *C*Har x8, 145.8, 146.0, 160.0, 160.8 *C*ar x4, 174.4 NH-*C*O-Car.

ESI: 441.1 $[M+H]^+$, 463.1 $[M+Na]^+$.

IR (KBr, cm^{-1}): 2936, 2859, 2868, 1706, 1600, 1578, 1498, 1473, 1464, 1314, 1257, 1241, 1206, 1146, 1111, 1059, 1042, 1006, 972, 961, 935, 854, 845, 553.

Synthesis of 4-(methyloxy)-4´-[10-(hydroxycarbonyl)decyloxy]azobenzene HOOC-C_{10}-Azo-OCH_3 ($C_{24}H_{32}N_2O_4$):

This compound was provided by the Liquid Crystal and Polymer group (Eva Blasco), University of Zaragoza.

^{1}H NMR (400MHz, DMSO-d_6, 45ºC, δ ppm): 1.17-1.53 (m, 14H, -(C*H*$_2$)$_7$-), 1.68-1.77 (m, 2H, C*H*$_2$-CH$_2$-O), 2.15 (t, 2H, J= 7.6 Hz, –C*H*$_2$-CO), 3.84 (s, 3H, O-C*H*$_3$), 4.05 (t, 2H, J=6.8 Hz, –O-C*H*$_2$-CH$_2$-), 7.03-7.12 (m, 4H, C*Har*), 7.76-7.85 (m, 4H, C*Har*).

^{13}C NMR (100 MHz, DMSO-d_6, 45ºC, δ ppm): 25.0, 25.9, 29.0, 29.1, 29.2, 29.3 -(*C*H$_2$)$_8$-, 34.4 CH$_2$-*C*H$_2$-CO, 56.0 -O-*C*H$_3$, 68.5 -O-*C*H$_2$-CH$_2$-, 115.0, 115.5, 124.5, 124.5, *C*Har, 146.7, 146.8, 161.4, 161.9 *C*ar, 174.9 *C*O-NH.

ESI: 413.1 $[M+H]^+$, 435.1 $[M+Na]^+$.

IR (KBr, cm^{-1}): 2936, 2916, 2848, 1709, 16202, 1582, 1497, 1469, 1465, 1317, 1296, 1278, 1246, 1151, 1107, 1029, 1018, 843, 823, 558.

For synthesis of hepta-O-acetyl-β-maltosyl azide **5**, see **experimental section 3.7**.

Synthesis of *N*-propargyl amide azo-derivatives (19), (20) and (21):

Azobenzene acids (**HOOC-Azo-C_{16}**, **HOOC-C_5-Azo-C_8**, **HOOC-C_{10}-Azo-OCH_3**) (1.05 g, 2.25 mmol) and hydroxybenzotriazole (0.35 g, 2.60 mmol) were dissolved in 20 mL of anhydrous THF. Propargylamine (0.16 mL, 2.50 mmol) was added. The solution was cooled to 0 ºC. A solution of 1-Ethyl-3-(3-dimethylaminopropyl)carbodiimide hydrochloride (EDC) (418 mg, 2.18 mmol) in 15 mL of anhydrous THF was added. The reaction mixture was stirred for 2 days at room temperature (or at 40ºC in case of **19**). The reaction was monitored by TLC with hexane/ethyl acetate 7:3 as eluent. The mixture was filtered and the solvent was removed under reduced pressure. 250 mL of dichoromethane were added and the organic phase was washed three times with 1M $KHSO_4$ solution, and three times with 1M $NaHCO_3$ solution. The organic layer was dried over anhydrous $MgSO_4$. The solution was filtered and the solvent was removed under reduced pressure. The resulting white solid was purified by recrystallization or

flash chromatography. A red solid was obtained (yield around 40-70% depending on the compound).

($C_{34}H_{49}N_3O_2$) **(19)**:

The reaction was heated at 40º. The product was purified by recrystallization with ethyl acetate in 40% of yield.

^{1}H (300 MHz, $CDCl_3$, 25ºC, δ ppm): 0.91 (t, 3H, J=6.8 Hz, -C*H*$_3$), 1.17-1.56 (m, 26H, -CH_2-(C*H*$_2$)$_{13}$-CH_3), 1.76-1.89 (m, 2H, -O-CH_2-C*H*$_2$-), 2.30 (t, 1H, J=2.5 Hz, *H*C≡C-,) 4.06 (t, 2H, J=6.8 Hz, –O-C*H*$_2$-CH_2-), 4.30 (m, 2H, HC≡C-C*H*$_2$-NH), 6.26 (t, 1H, J=5.0 Hz, CH_2-N*H*-CO), 6.99-7.03 (m, 2H, *Har*), 7.87-7.97 (m, 6H, *Har*).

^{13}C (75 MHz, $CDCl_3$, 25ºC, δ ppm): 13.9 *C*H_3, 22.6, 25.9, 29.2, 29.3, 29.3, 29.5, 29.5, 29.6, 29.6, 29.9, 31.9 -(*C*H_2)$_{14}$-CH_3, ≡C-*C*H_2-NH, 68.5 O-*C*H_2-(CH_2)$_{14}$, 71.9 H*C*≡C-, 79.37 HC≡*C*, 114.8, 122.6, 125.1, 127.9 *C*Har x8, 134.9, 146.9, 154.8, 162.3, *C*ar , 166.4 NH-*C*O-Car.

ESI: 504.2 $[M+H]^+$, 526.1 $[M+Na]^+$.

IR (KBr, cm^{-1}): 3279, 3263, 2935, 2917, 2873, 2848, 1639, 1603, 1585, 1545, 1502, 1495, 1472, 1463, 1317, 1298, 1251, 1152, 1146, 1106, 1025, 858, 841, 823, 719, 680, 634, 553.

($C_{29}H_{39}N_3O_3$) **(20)**:

The reaction was stirred at room temperature. The product was purified by flash chromatography with hexane/ethyl acetate 7:3 as eluent in 70% of yield.

^{1}H NMR (400MHz, DMSO-d_6, 25ºC, δ ppm): 0.90 (t, 3H, J= 6.5 Hz, –(CH_2)$_5$-C*H*$_3$), 1.35 (d, 3H, J=6.4 Hz, –CH-C*H*$_3$), 1.24-1.91 (m, 16H, -(C*H*$_2$)-), 2.21-2.30 (m, 3H, *H*C≡C-, –C*H*$_2$-CO), 4.00-4.12 (m, 4H, –O-C*H*$_2$-CH_2-, HC≡C-C*H*$_2$-NH), 4.46 (m, 1H, –O-C*H*-CH_3), 5.67 (s, 1H, CH_2-N*H*-CO), 6.94-7.04 (m, 4H, *Har*), 7.85-7.88 (m, 4H, *Har*).

^{13}C (100 MHz, DMSO-d_6, 25ºC, δ ppm): 14.0 CH_2-*C*H_3, 19.7 *C*H_3-O- 22.6, 25.2, 25.5, 25.7, 28.9, 29.2, 31.7, 36.2, 36.4, -(*C*H_2)-, ≡C-*C*H_2-NH, CO-*C*H_2-CH_2-, 67.9 O-*C*H_2-CH_2, 71.6 H*C*≡C-, 74.2 –O-*C*H-CH_3, 79.3 HC≡*C*, 114.6, 115.8, 124.2, 124.3 *C*Har x8, 146.8, 147.0, 160.3, 161.0 *C*ar, 172.1 NH-*C*O-Car.

ESI: 478.3 $[M+H]^+$, 500.2 $[M+Na]^+$, 516,2 $[M+K]^+$

IR (KBr, cm^{-1}): 3273, 2931, 2853, 1625, 1598, 1577, 1544, 1496, 1464, 1384, 1311, 1296, 1249, 1145, 1130, 1061, 971, 840, 550.

($C_{27}H_{35}N_3O_3$) **(21)**:

The reaction was stirred at room temperature. The product was purified by recrystallization with ethyl acetate in 40% of yield.

^1H (300 MHz, $CDCl_3$, 25ºC, δ ppm): 1.22-1.72 (m, 12H, -(CH_2)$_6$-), 1.76-1.89 (m, 2H, -O-CH_2-CH_2), 2.20 (t, 2H, J=7.0 Hz, –CH_2-CO), 2.24 (t, 1H, J=2.6 Hz, *H*C≡C-), 3.09 (s, 3H, -O-CH_3), 4.01-4.09 (m, 4H, -O-CH_2-CH_2-, HC≡C-CH_2-NH), 5.57 (s, 1H, CH_2-N*H*-CO), 6.97-7.05 (m, 4H, *Har*), 7.84-7.92 (m, 4H, *Har*).

^{13}C (75 MHz, $CDCl_3$, 25ºC, δ ppm): 25.5, 25.9, 29.1, 29.2, 29.2, 29.2, 29.3, 29.3, 29.4 -(CH_2)$_6$-, HC≡C-CH_2-NH, 36.4 –CH_2-CO, 55.6 -O-CH_3, 68.3 -O-CH_2-CH_2-, 71.5 HC≡C-, 79.7 HC≡C-, 11.4, 114.6, 124.3, 124.3 *C*Har, 146.9, 147.1, 161.2, 161.5 *C*ar, 172.6 NH-*C*O.

ESI: 450.3 $[M+H]^+$, 472.1 $[M+Na]^+$.

IR (KBr, cm^{-1}): 3290, 2935, 2917, 2849, 1643, 1602, 1583, 1546, 1497, 1470, 1463, 1421, 1318, 1296, 1249, 1152, 1107, 1029, 843, 823, 666, 640, 558.

Synthesis of acetylated maltose conjugates OAc-Malt-Tz-Azo-C_{16}, OAc-Malt-Tz-C_5-Azo-C_8, and OAc-Malt-Tz-C_{10}-Azo-OCH_3:

The appropriate azobenzene derivative (0.83 mmol), peracetylated β-maltosylazide (562 mg, 0.85 mmol), copper(I) bromide (27.1 mg, 0.19 mol) and *N*-pentamethyldiethylenetriamine (PMDETA) (35 µL, 0.17 mmol) were dissolved in anhydrous dimethylformamide (6mL) under an argon atmosphere. The mixture was stirred at room temperature for 2 days. The reaction was monitored by TLC with hexane/ethyl acetate 1:1 as eluent. The catalyst was removed by filtration and the solvent was removed under reduced pressure. The reaction was poured into 150 mL of water. The aqueous phase was extracted with 3x150 mL of hexane/ethyl acetate 1:1. The organic phase was dried with anhydrous $MgSO_4$. The solution was filtered and the solvent was removed under reduced pressure. The resulting solid was purified by flash

chromatography using initially dichloromethane/ethyl acetate 6:4 and then increasing the polarity. A red solid was obtained (82-90%).

OAc-Malt-Tz-Azo-C_{16} ($C_{58}H_{80}N_6O_{19}$):

^{1}H (400 MHz, $CDCl_3$, 25ºC, δ ppm): 0.87 (t, 3H, J=6.7 Hz, -$(CH_2)_{11}$-C*H*$_3$), 1.18-1.40 (m, 22H, -CH_2-(C*H*$_2$)$_{11}$-CH_3), 1.41-1.52 (m, 2H, -C*H*$_2$-$(CH_2)_{11}$-CH_3), 1.78-1.86 (m, 2H, –O-CH_2-C*H*$_2$-), 1.85 (s, 3H, C*H*$_3$-CO-O-C2´), 2.01 (s, 3H), 2.03 (s, 3H), 2.06 (s, 3H), 2.10 (s, 3H), 2.12 (s, 3H), 2.17 (s, 3H) *CH*$_3$-CO-O-, 3.97-3.99 (m, 2H, *H5´*, *H5*), 4.05-4.10 (m, 4H, –O-C*H*$_2$-CH_2, *H4´*, *H6b*), 4.23-4.27 (m, 2H, *H6a*, *H6´a*), 4.49 (dd, 1H, $J_{5´,6´b}$=1,8 Hz, $J_{6´a,6´b}$=12.5 Hz, *H6´b*), 4.69-4.79 (m, 2H, NH-C*H*$_2$-triazole), 4.88 (dd, 1H, $J_{1,2}$= 3.9 Hz, $J_{2,3}$= 10.5 Hz, *H2*), 5.07 (dd, 1H, $J_{3,4}$= 9.8 Hz, $J_{4,5}$= 9.8 Hz, *H4*), 5.34 (dd, 1H, $J_{1´,2´}$= 9.1 Hz, $J_{2´,3´}$=9.3 Hz, *H2´*), 5.37 (dd, 1H, $J_{2,3}$=10.5 Hz, $J_{3,4}$= 9.8 Hz, *H3*), 5.44 (d, 1H, $J_{1,2}$=3.9 Hz, *H1*), 5.46 (dd, 1H, $J_{2´,3´}$=9.3 Hz, $J_{3´,4´}$=9.1 Hz, *H3´*), 5.87 (d, 1H, $J_{1´,2´}$= 9.1 Hz, *H1´*), 6.91 (t, 1H, J=5.5 Hz, -N*H*-CO), 6.99-7.01 (m, 2H, *Har*), 7.81 (s, 1H, C*H*-triazole), 7.90-7.93 (m, 6H, *Har*).

^{13}C (100 MHz, $CDCl_3$, 25ºC, δ ppm): 14.1 $(CH_2)_{14}$-*C*H_3, 20.2, 20.6, 20.7, 20.8, 20.8, *C*H_3-CO-O- 22.7, 26.0, 29.2, 29.4, 29.5, 29.5, 29.6, 29.7, 30.9, 31.9 -(*C*H_2)$_{14}$-CH_3, 35.4 triazole-*C*H_2-NH, 61.5 *C6*, 62.4 *C6´*, 67.9 *C4*, 68.4 O-C*H*$_2$-$(CH_2)_{14}$, 68.8 *C5*, 69.2 *C3*, 70.0 *C2*, 70.9 *C2´*, 72.4 *C4´*, 75.0 *C3´*, 75.4 *C5´*, 85.4 *C1´*, 95.9 *C1*, 114.8 *C*Har, 121.2 *C*H triazole, 122.6, 125.2, 127.9 *C*Har, 134.9 *C*ar, 145.1 CHtriazole-*C*triazole-CH_2, 146.8, 154.6, 162.3 *Car*, 166.8 NH-*C*O-Car, 169.1 CH_3-*C*O-O-C2´, 169.4 CH_3-*C*O-O-C4, 169.9, 169.9 CH_3-*C*O-O-C3/C3´, 170.3, 170.5, 170.6 CH_3-*C*O-O-C2/C6/C6´.

MALDI-TOF (DCTB+NaTFA): 1187,6 $[M+Na]^+$.

IR (KBr, cm^{-1}): 3351, 2922, 2851, 1749, 1644, 1604, 1532, 1503, 1470, 1370, 1234, 1141, 1036, 859.

OAc-Malt-Tz-C_5-Azo-C_8 ($C_{55}H_{74}N_6O_{20}$):

^{1}H (400 MHz, $CDCl_3$, 25ºC, δ ppm): 0.90 (t, 3H, J=7.0 Hz, -$(CH_2)_5$-C*H*$_3$), 1.27- 1.89 (m, 16H, -(C*H*$_2$)-), 1.35 (d, 3H, J= 6.2 Hz, C*H*$_3$-CH-O), 1.87 (s, 3H), 2.03 (s, 3H), 2.04 (s, 3H), 2.05 (s, 3H), 2.08 (s, 3H), 2.13 (s, 3H), 2.15 (s, 3H) C*H*$_3$-CO-O-, 2.26 (t, 2H, J=7,6 Hz, CO-C*H*$_2$-$(CH_2)_3$), 3.96- 4.02 (m, 2H, *H5*, *H5´*), 4.04 (t, 2H, J=6.4 Hz, –O-C*H*$_2$-CH_2), 4.05-4.11 (m, 1H, *H6b*), 4.15 (dd, 1H, $J_{3´,4´}$= 8.8 Hz, $J_{4´,5´}$= 9.8 Hz, *H4´*),

4.25-4.30 (m, 2H, *H6a*, *H6´a*), 4.43-4.58 (m, 4H, *H6´b*, O-C*H*-CH_3-, Ctriazole-CH_2-NH-), 4.90 (dd, 1H, $J_{1,2}$= 3.9 Hz, $J_{2,3}$= 10.5 Hz, *H2*), 5.09 (dd, 1H, $J_{3,4}$= 9.9 Hz, $J_{4,5}$= 9.9 Hz, *H4*), 5.34 (dd, 1H, $J_{1´,2´}$= 9.3 Hz, $J_{2´,3´}$=9.5 Hz, *H2´*), 5.39 (dd, 1H, $J_{2,3}$=10.5 Hz, $J_{3,4}$= 9.9 Hz, *H3*), 5.46 (d, 1H, $J_{1,2}$=3.9 Hz, *H1*), 5.47 (dd, 1H, $J_{2´,3´}$=9.5 Hz, $J_{3´,4´}$=8.8 Hz, *H3´*), 5.87 (d, 1H, $J_{1´,2´}$= 9.3 Hz, *H1´*), 6.11 (t, 1H, J=5.7 Hz, CH_2-N*H*-CO), 6.98-6.99 (m, 4H, *H*ar), 7.73 (s, 1H, C*H*-triazole), 7.85-7.80 (m, 4H, *H*ar).

^{13}C (100 MHz, $CDCl_3$, 25ºC, δ ppm): 14.1 $(CH_2)_5$-CH_3, 19.7 CH-CH_3, 20.2 CH_3-CO-O-C2´, 20.6, 20.7, 20.8, 20.8, CH_3-CO-O- 22.6, 25.2, 25.5, 25.7, 28.9, 29.2, 31.8 -(CH_2)-, 34.9 Ctriazole-CH_2-NH, 36.3 –CO-CH_2-CH_2-, 36.4 CH_3-CH-CH_2-, 61.4 *C6*, 62.4 *C6´*, 67.9 *C4*, O-CH_2-CH_2, 68.8 *C5*, 69.2 *C3*, 70.0 *C2*, 70.9 *C2´*, 72.4 *C4´*, 74.2 O-*CH*-CH_3, 75.1 *C3´*, 75.4 *C5´*, 85.3 *C1´*, 95.9 *C1*, 114.8, 115.2 *C*Har, 120.7 *C*Htriazole, 124.3, 124.3, *C*Har, 145.2 CHtriazole-*Ctriazole*-CH_2, 146.8, 147.0, 160.4, 160.9 *Car*, 169.1 CH_3-*C*O-O-C2´, 169.4 CH_3-*C*O-O-C4, 169.9, 169.9 CH_3-*C*O-O-C3/C3´, 170.3, 170.5, 170.6 CH_3-*C*O-O-C2/C6/C6´, 172.8 NH-*C*O-CH_2.

MALDI-TOF (DCTB+NaTFA): 1161,5 [(M+Na].

IR (KBr, cm^{-1}): 3326, 2935, 2858, 1748, 1599, 1499, 1373, 1234, 1147, 1036, 841.

OAc-Malt-Tz-C_{10}-Azo-OCH_3 ($C_{53}H_{70}N_6O_{20}$):

^{1}H (400 MHz, $CDCl_3$, 25ºC, δ ppm): 1.31- 1.72 (m, 14H,–(CH_2)$_7$-), 1.77- 1.87 (m, 2H, –O-CH_2-CH_2-(CH_2)-), 1.87 (s, 3H, CH_3-CO-O-C2´), 2.03 (s, 3H), 2.05 (s, 6H), 2.09 (s, 3H), 2.01 (s, 3H), 2.16 (s, 3H) CH_3-CO-O-, 2.20 (t, 2H, J= 7,5 Hz, CO-CH_2-CH_2-), 3.91 (s, 3H, -O-CH_3), 3.97-4.02 (m, 2H, *H5*, *H5´*), 4.05 (t, 2H, J= 6,8 Hz, –O-CH_2-CH_2), 4.06-4.12 (m, 1H, *H6b*), 4.16 (dd, 1H, $J_{3´,4´}$= 9.1 Hz, $J_{4´,5´}$= 9.1 Hz, *H4´*), 4.25-4.30 (m, 2H, *H6a*, *H6´a*), 4.47-4.58 (m, 3H, *H6´b*, Ctriazole-CH_2-NH-), 4.91 (dd, 1H, $J_{1,2}$= 4.2 Hz, $J_{2,3}$= 10.6 Hz, *H2*), 5.10 (dd, 1H, $J_{3,4}$= 9.8 Hz, $J_{4,5}$= 9.8 Hz, *H4*), 5.34 (dd, 1H, $J_{1´,2´}$= 9.1 Hz, $J_{2´,3´}$= 9.1 Hz, *H2´*), 5.40 (dd, 1H, $J_{2,3}$= 9.8 Hz, $J_{3,4}$= 9.8 Hz, *H3*), 5.46-5.50 (m, 2H, *H1*, *H3´*), 5.86 (d, 1H, $J_{1´,2´}$= 9.1Hz, *H1´*), 6.08 (t, 1H, J= 5.6Hz, CH_2-*NH*-CO), 6.99-7.03 (m, 4H, *Har*), 7.72 (s, 1H, C*H*-triazole), 7.87-7.90 (m, 4H, *Har*).

^{13}C (100 MHz, $CDCl_3$, 25ºC, δ ppm): 20.2 *C*H_3-CO-O-C2´, 20.6, 20.7, 20.8, 20.8, *C*H_3-CO-O- 25.5, 26.0, 29.2, 29.3, 29.3, 29.3, 29.4, 29.5, -(*C*H_2)-, 34.8 Ctriazole-*C*H_2-NH, 36.5 –CO-*C*H_2-CH_2-, 55.6 –O-*C*H_3, 61.4 *C6*, 62.4 *C6´*, 67.9 *C4*, 68.3 O-*C*H_2-CH_2, 68.8 *C5*, 69.2 *C3*, 70.0 *C2*, 71.0 *C2´*, 72.4 *C4´*, 75.1 *C3´*, 75.4 *C5´*, 85.3 *C1´*, 95.9 *C1*, 114.2,

115.6 *C*Har, 120.8 *C*Htriazole, 124.3, 124.3 *C*Har, 145.3 CHtriazole-*C*triazole-CH_2, 146.9, 147.1 *Car* 161.2 *Car*-O-CH_2, 161.5 *Car*-O-CH_3, 169.1 CH_3-*C*O-O-C2´, 169.4 CH_3-*C*O-O-C4, 169.9, 169.9 CH_3-*C*O-O-C3/C3´, 170.3, 170.5, 170.6 CH_3-*C*O-O-C2/C6/C6´, 173.2 NH-*C*O-CH_2.

MALDI-TOF (DCTB+NaTFA): 1133,5 $[M+Na]^+$.

IR (KBr, cm^{-1}): 3360, 2926, 2851, 1748, 1652, 1601, 1582, 1501, 1370, 1238, 1147, 1038, 840.

Synthesis of azo-glycosyl conjugates Malt-Tz-Azo-C_{16}, Malt-Tz-C_5-Azo-C_8 and **Malt-Tz-C_{10}-Azo-OCH_3:**

The peracetylated derivatives **OAc-Malt-Tz-Azo-C_{16}**, **OAc-Malt-Tz-C_5-Azo-C_8** and **OAc-Malt-Tz-C_{10}-Azo-OCH_3** (0.17 mmol) were dissolved in 7.5 mL of anhydrous THF. Sodium methoxide (81.0 mg, 1.50 mmol) was added. The solution was stirred at room temperature until the reaction was complete (TLC, dichloromethane/ethyl acetate 1:1). Amberlyst IR 120 (H^+ form) was added to exchange sodium ions to reach pH= 6-7, the resin was filtered off and the solvent was evaporated in vacuo. The resulting solid was purified by flash chromatography using initially dichloromethane/methanol 9:1 and then increasing the polarity. A red solid was obtained (75-90%).

Malt-Tz-Azo-C_{16} ($C_{44}H_{66}N_6O_{12}$):

^{1}H (400 MHz, DMSO-d_6, 25ºC, δ ppm): 0.85 (t, 3H, J=7.0 Hz, -$(CH_2)_{13}$-C*H*$_3$), 1.20-1.40 (m, 26H, -CH_2-(C*H*$_2$)$_{13}$-CH_3), 1.73-1.76 (m, 2H, -C*H*$_2$-$(CH_2)_{13}$-CH_3), 3.04-3.87 (m, 12H, *H2*, *H3*, *H4*, *H5*, *H6a*, *H6b*, *H2´*, *H3´*, *H4´*, *H5´*, *H6´a*, *H6´b*), 4.09 (t, 2H, J=6.4 Hz, O-C*H*$_2$-CH_2), 4.56 (d, 2H, J=5.5 Hz, Ctriazole-C*H*$_2$-NH), 5.04 (d, 1H, $J_{1,2}$= 3.6 Hz, *H1*), 5.56 (d, 1H, $J_{1´,2´}$= 9.2 Hz, *H1´*), 7.12- 7.15 (m, 2H, *Har*), 7.68-7.93 (m, 4H, *Har*), 8.08-8.09 (m, 2H, *Har*), 8.18 (s, 1H, C*H*-triazole), 9.28 (t, 1H, J=5.5 Hz, CH_2-N*H*-CO).

^{13}C (100 MHz, DMSO-d_6, 25ºC, δ ppm): 14.4 $(CH_2)_{14}$-*C*H_3, 22.5, 25.8, 28.9, 29.2, 29.4, 29.5, 31.7, -(*C*H_2)$_{14}$-CH_3, 35.4 triazole-*C*H_2-NH, 60.70, 61.3, 70.4, 71.5, 73.1, 73.7, 74.1, 77.1, 78.6, 79.7 *C2*, *C3*, *C4*, *C5*, *C6*, *C3´*, *C4´*, *C5´*, *C6´*, 68.5 O-*C*H_2-$(CH_2)_{14}$, 71.5 *C2´*, 87.7 *C1´*, 101.7 *C1*, 115.6 *C*Har, 122.4 *C*Htriazole, 125.3, 129.1 *C*Har, 135.5 *C*ar, 145.4 CHtriazole-*C*triazole-CH_2, 146.5, 153.9, 162.4 *Car*, 165.4 NH-*C*O-ar.

MicrOTOF-Q: $[M+Na]^+$ 893.461 calcd.: 893.463.

IR (KBr, cm-1): 3320 (wide band), 2918, 2849, 1577, 1418, 1251, 1040, 850.

Malt-Tz-C_5-Azo-C_8 ($C_{41}H_{60}N_6O_{13}$):

^{1}H (400 MHz, MeOD, 25ºC, δ ppm): 0.92 (t, 3H, J=6.8 Hz, -$(CH_2)_5$-C*H*$_3$), 1.31- 1.88 (m, 16H, -C*H*$_2$-), 1.35 (d, 3H, J= 5.8 Hz, C*H*$_3$-CH-O), 2.29 (t, 2H, J=7.4 Hz, CO-C*H*$_2$-$(CH_2)_3$-), 3.29- 3.91 (m, 10H, *H3*, *H4*, *H5*, *H6a*, *H6b*, *H3´*, *H4´*, *H5´*, *H6´a*, *H6´b*), 3.48 (dd, 1H, $J_{1,2}$=3.8 Hz, $J_{2,3}$= 9.7 Hz, *H2*), 3.95 (dd, 1H, $J_{1´,2´}$= 9.1 Hz, $J_{2´,3´}$= 9.1 Hz, *H2´*), 4.08 (t, 2H, J= 6.5 Hz, –O-C*H*$_2$-), 4.47 (s, 2H, Ctriazole-C*H*$_2$-NH-), 4.51-4.60 (m, 1H, O-C*H*-CH_3), 5.24 (d, 1H, $J_{1,2}$= 3.8 Hz, *H1*), 5.62 (d, 1H, $J_{1´,2´}$= 9.1 Hz, *H1´*), 7.02-7.06 (m, 4H, *Har*), 7.83-7.86 (m, 4H, *Har*), 8.08 (s, 1H, C*H*-triazole).

^{13}C (100 MHz, MeOD, 25ºC, δ ppm): 13.0 CH_2-*C*H_3, 18.6 O-CH-*C*H_3, 22.2, 25.1, 25.2, 25.3, 28.6, 29.0, 29.5, 31.6 -(*C*H_2)-, 34.2 Ctriazole-*C*H_2-NH, 35.4 –CO-*C*H_2-CH_2-, 36.2 CH_3-CH-*C*H_2-, 67.8 O-*C*H_2-CH_2, 72.2 *C2´*, 72.8 *C2*, 60.4, 61.3, 70.1, 73.5, 73.7, 73.8, 76.8, 78.2, 78.9 *C3*, *C4*, *C5*, *C6*, *C3´*, *C4´*, *C5´*, *C6´*-O-*C*H-CH_3, 88.0 *C1´*, 101.5 *C1*, 114.4, 115.4 *C*H ar, 122.0 *C*Htriazole, 123.9, 123.9 *C*Har, 145.0 CHtriazole-*C*triazole-CH_2, 146.6, 146.8, 160.5, 161.3 *C*ar, 174.7 NH-*C*O-CH_2.

MicrOTOF MS: 845.4309 $[M+H]^+$, 867.4118 $[M+Na]^+$. Calcd: 845.4218 $[M+H]^+$, 867.4110 $[M+Na]^+$.

IR (KBr, cm^{-1}): 3364, 2928, 2857, 1652, 1598, 1498, 1248, 1148, 1039, 840.

Malt-Tz-C_{10}-Azo-OCH_3 ($C_{39}H_{56}N_6O_{13}$):

^{1}H (400 MHz, DMSO-d_6, 25ºC, δ ppm: 1.27- 1.56 (m, 14H, –(C*H*$_2$)$_7$)-, 1.71- 1.78 (m, 2H, –O-CH_2-C*H*$_2$-(CH_2)-), 2.11 (t, 2H, J= 7.4 Hz, CO-C*H*$_2$-CH_2), 3.07- 3.90 (m, 12H, *H2*, *H3*, *H4*, *H5*, *H6a*, *H6b*, *H2´*, *H3´*, *H4´*, *H5´*, *H6´a*, *H6´b*), 3.85 (s, 3H, ar-O-C*H*$_3$), 4.05 (t, 2H, J= 6.0 Hz, –O-C*H*$_2$-CH_2), 4.30 (d, 2H, J= 3.9 Hz, Ctriazole-C*H*$_2$-NH-), 4.54-4.60 (m, 1H, O*H*), 4.60-4.67 (m, 1H, O*H*), 4.95-5.02 (m, 2H, O*H*), 5.07 (d, 1H, J_{1-2}=2.6 Hz, *H1*), 5.50-5.51 (m, 1H, O*H*), 5.58-5.63 (m, 2H, *H1´*,O*H*), 5.79-5.80 (m, 1H, O*H*), 7.09-7.13 (m, 4H, *Har*), 7.82-7.85 (m, 4H, *Har*), 8.08 (s, 1H, C*H*-triazole), 8.33 (t, 1H, J= 5.6 Hz, CH_2-N*H*-CO).

^{13}C (100 MHz, DMSO-d_6, 25ºC, δ ppm): 25.6, 25.9, 29.1, 29.2, 29.2, 29.3, 29.4, 29.5, -(*C*H_2)-, 34.5 Ctriazole-*C*H_2-NH, 35.7 –CO-*C*H_2-CH_2-, 56.1 –O-*C*H_3, 68.4 O-*C*H_2-CH_2, 60.7, 61.2, 70.3, 72.0, 72.9, 73.7, 74.0, 77.2, 78.4, 79.6 *C2*, *C3*, *C4*, *C5*, *C6*, *C2´*, *C3´*,

C4´, *C5´*, *C6´*, 87.6 *C1´*, 101.4 *C1*, 115.0, 115.4 *C*Har, 122.3 *C*Htriazole, 124.6, 124.6 *C*Har, 145.5 CHtriazole-Ctriazole-CH_2, 146.5, 146.7 *C*ar**,** 161.4 *C*ar-O-CH_2**,** 161.9 *C*ar-O-CH_3**,** 172.6 NH-*C*O-CH_2.

MicrOTOF MS: 817.3968 $[M+H]^+$, 839.3773 $[M+Na]^+$. Calcd: 817.3978 $[M+H]^+$, 839.3797 $[M+Na]^+$.

IR (KBr, cm^{-1}): 3376 (wide band), 2920, 2850, 1642, 1582, 1602, 1253, 1148, 1025, 840.

4. 5. References

1. (a) Babu, S. S.; Prasanthkumar, S.; Ajayaghosh, A., Self-Assembled Gelators for Organic Electronics. *Ang. Chem.-Int. Ed.* **2012,** *51* (8), 1766-1776; (b) Hirst, A. R.; Escuder, B.; Miravet, J. F.; Smith, D. K., High-Tech Applications of Self-Assembling Supramolecular Nanostructured Gel-Phase Materials: From Regenerative Medicine to Electronic Devices. *Ang. Chem.-Int. Ed.* **2008,** *47* (42), 8002-8018; (c) Sangeetha, N. M.; Maitra, U., Supramolecular gels: Functions and uses. *Chem. Soc. Rev.* **2005,** *34* (10), 821-836.

2. (a) Terech, P.; Weiss, R. G., Low molecular mass gelators of organic liquids and the properties of their gels. *Chem. Rev.* **1997,** *97* (8), 3133-3159; (b) Abdallah, D. J.; Weiss, R. G., Organogels and low molecular mass organic gelators. *Adv. Mat.* **2000,** *12* (17), 1237-1247; (c) Estroff, L. A.; Hamilton, A. D., Water gelation by small organic molecules. *Chem. Rev.* **2004,** *104* (3), 1201-1217; (d) Smith, D. K., Molecular gels - underpinning nanoscale materials with organic chemistry - Preface. *Tetrahedron* **2007,** *63* (31), 7283-7284; (e) Banerjee, S.; Das, R. K.; Maitra, U., Supramolecular gels 'in action'. *J. Mat. Chem.* **2009,** *19* (37), 6649-6687; (f) Smith, D. K., Lost in translation? Chirality effects in the self-assembly of nanostructured gel-phase materials. *Chem. Soc. Rev.* **2009,** *38* (3), 684-694; (g) Steed, J. W., Supramolecular gel chemistry: developments over the last decade. *Chem. Commun.* **2011,** *47* (5), 1379-1383.

3. De Jong, J. J. D.; Feringa, B. L.; Van Esch, J., Responsive Molecular Gels. In *Molecular Gels*, Weiss, R. G.; Terech, P., Eds. Springer: Dordrecht, 2006; pp 895-927.

4. (a) Chang, S. K.; Hamilton, A. D., Molecular Recognition of Biologically Interesting Substrates- Synthesis of an Artificial Receptor for Barbiturates Employing 6 Hydrogen-Bonds. *J. Am. Chem. Soc.* **1988,** *110* (4), 1318-1319; (b) Hanabusa, K.; Miki, T.; Taguchi, Y.; Koyama, T.; Shirai, H., 2-Component, Small- Molecule Gelling Agents. *J. Chem. Soc.-Chem. Commun.* **1993,** (18), 1382-1384; (c) Inoue, K.; Ono, Y.; Kanekiyo, Y.; Ishi-i, T.; Yoshihara, K.; Shinkai, S., Design of new organic gelators stabilized by a host-guest interaction. *J. Org. Chem.* **1999,** *64* (8), 2933-2937.

5. Piepenbrock, M. O. M.; Lloyd, G. O.; Clarke, N.; Steed, J. W., Metal- and Anion-Binding Supramolecular Gels. *Chem. Rev.* **2010,** *110* (4), 1960-2004.

6. (a) Pozzo, J. L.; Clavier, G. M.; Desvergne, J. P., Rational design of new acid-sensitive organogelators. *J. Mat. Chem.* **1998,** *8* (12), 2575-2577; (b) Deng, W.; Thompson, D. H., pH and cation-responsive supramolecular gels formed by cyclodextrin amines in DMSO. *Soft Matt.* **2010,** *6* (9), 1884-1887.

7. (a) Ihara, H.; Sakurai, T.; Yamada, T.; Hashimoto, T.; Takafuji, M.; Sagawa, T.; Hachisako, H., Chirality control of self-assembling organogels from a lipophilic L-glutamide derivative with metal chlorides. *Langmuir* **2002,** *18* (19), 7120-7123; (b) Terech, P.; Coutin, A., Organic solutions of monomolecular organometallic threads. Nonlinear rheology and effects of end-capping species. *J. Phys. Chem. B* **2001,** *105* (24), 5670-5676.

8. Del Guerzo, A.; Pozzo, J. L., Photoresponsive Gels. In *Molecular Gels*, Weiss, R. G.; Terech, P., Eds. Springer: Dordrecht, 2006; pp 817-855.

9. Griffith. J, Selected Aspects of Photochemistry .2. Photochemistry of Azobenzene and its Derivatives. *Chem. Soc. Rev.* **1972,** *1* (4), 481-493.

10. (a) Jung, J. H.; Ono, Y.; Shinkai, S., Organogels of azacrown-appended cholesterol derivatives can be stabilized by host-guest interactions. *Tetrahedron Lett.* **1999,** *40* (48), 8395-8399; (b) Murata, K.; Aoki, M.; Nishi, T.; Ikeda, A.; Shinkai, S., New Cholesterol-Based Gelators with Light-Responsive and Metal-Responsive Functions. *J. Chem. Soc.-Chem. Commun.* **1991,** (24), 1715-1718; (c) Murata, K.;

Aoki, M.; Shinkai, S., Sol-Gel Phase-Transition of Switch-Functionalized Cholesterol as detected by Circular Dichroism. *Chem. Lett.* **1992,** (5), 739-742; (d) Murata, K.; Aoki, M.; Suzuki, T.; Harada, T.; Kawabata, H.; Komori, T.; Ohseto, F.; Ueda, K.; Shinkai, S., Thermal and Ligth control of the Sol-Gel Phase-Transition in Cholesterol-Based Organic Gels- Novel Helical Aggregation Modes as detected by Circular-Dichroism and Electron-Microscopic Observation. *J. Am. Chem. Soc.* **1994,** *116* (15), 6664-6676.

11. Ran, X.; Wang, H. T.; Zhang, P.; Bai, B. L.; Zhao, C. X.; Yu, Z. X.; Li, M., Photo-induced fiber-vesicle morphological change in an organogel based on an azophenyl hydrazide derivative. *Soft Matt.* **2011,** *7* (18), 8561-8566.

12. Duan, P. F.; Li, Y. G.; Li, L. C.; Deng, J. G.; Liu, M. H., Multiresponsive Chiroptical Switch of an Azobenzene-Containing Lipid: Solvent, Temperature, and Photoregulated Supramolecular Chirality. *J. Phys. Chem. B* **2011,** *115* (13), 3322-3329.

13. (a) de Loos, M.; van Esch, J.; Kellogg, R. M.; Feringa, B. L., Chiral recognition in bis-urea-based aggregates and organogels through cooperative interactions. *Ang. Chem.-Int. Ed.* **2001,** *40* (3), 613-616; (b) van der Laan, S.; Feringa, B. L.; Kellogg, R. M.; van Esch, J., Remarkable polymorphism in gels of new azobenzene bis-urea gelators. *Langmuir* **2002,** *18* (19), 7136-7140.

14. Huang, Y. C.; Qiu, Z. J.; Xu, Y. M.; Shi, J. F.; Lin, H. K.; Zhang, Y., Supramolecular hydrogels based on short peptides linked with conformational switch. *Org. & Biomol. Chem.* **2011,** *9* (7), 2149-2155.

15. Kobayashi, H.; Friggeri, A.; Koumoto, K.; Amaike, M.; Shinkai, S.; Reinhoudt, D. N., Molecular design of "super" hydrogelators: Understanding the gelation process of azobenzene-based sugar derivatives in water. *Org. Lett.* **2002,** *4* (9), 1423-1426.

16. (a) Lin, Y. Y.; Wang, A. D.; Qiao, Y.; Gao, C.; Drechsler, M.; Ye, J. P.; Yan, Y.; Huang, J. B., Rationally designed helical nanofibers via multiple non-covalent interactions: fabrication and modulation. *Soft Matt.* **2010,** *6* (9), 2031-2036; (b) Rajaganesh, R.; Gopal, A.; Das, T. M.; Ajayaghosh, A., Synthesis and Properties of Amphiphilic Photoresponsive Gelators for Aromatic Solvents. *Org. Lett.* **2012,** *14* (3), 748-751; (c) Ogawa, Y.; Yoshiyama, C.; Kitaoka, T., Helical Assembly of Azobenzene-Conjugated Carbohydrate Hydrogelators with Specific Affinity for Lectins. *Langmuir* **2012,** *28* (9), 4404-4412.

17. Buerkle, L. E.; Rowan, S. J., Supramolecular gels formed from multi-component low molecular weight species. *Chem. Soc. Rev.* **2012,** *41* (18), 6089-102.

18. (a) Jeong, Y.; Friggeri, A.; Akiba, I.; Masunaga, H.; Sakurai, K.; Sakurai, S.; Okamoto, S.; Inoue, K.; Shinkai, S., Small-angle X-ray scattering from a dual-component organogel to exhibit a charge transfer interaction. *J. Coll. Interf. Sci.* **2005,** *283* (1), 113-122; (b) Botterhuis, N. E.; Karthikeyan, S.; Veldman, D.; Meskers, S. C. J.; Sijbesma, R. P., Molecular recognition in bisurea thermoplastic elastomers studied with pyrene-based fluorescent probes and atomic force microscopy. *Chem. Commun.* **2008,** (33), 3915-3917; (c) Moffat, J. R.; Smith, D. K., Controlled self-sorting in the assembly of 'multi-gelator' gels. *Chem. Commun.* **2009,** (3), 316-318; (d) Das, A.; Ghosh, S., A generalized supramolecular strategy for self-sorted assembly between donor and acceptor gelators. *Chem. Commun.* **2011,** *47* (31), 8922-8924; (e) Garcia Velazquez, D.; Luque, R., Spontaneous Orthogonal Self-Assembly of a Synergetic Gelator System. *Chem.-a Eur. J.* **2011,** *17* (14), 3847-3849; (f) Smith, M. M.; Smith, D. K., Self-sorting multi-gelator gels-mixing and ageing effects in thermally addressable supramolecular soft nanomaterials. *Soft Matt.* **2011,** *7* (10), 4856-4860; (g) Kohno, K.; Morimoto, K.; Manabe, N.; Yajima, T.; Yamagishi, A.; Sato, H., Promotion effects of optical antipodes on the formation of helical fibrils: chiral perfluorinated gelators.

Chem. Commun. **2012,** *48* (32), 3860-3862; (h) Li, D.; Liu, J.; Chu, L.; Liu, J.; Yang, Z., A novel mixed-component molecular hydrogel system with excellent stabilities. *Chem. Commun.* **2012,** *48* (49), 6175-6177; (i) Lloyd, G. O.; Piepenbrock, M.-O. M.; Foster, J. A.; Clarke, N.; Steed, J. W., Anion tuning of chiral bis(urea) low molecular weight gels. *Soft Matt.* **2012,** *8* (1), 204-216.

19. (a) Liao, X. J.; Chen, G. S.; Liu, X. X.; Chen, W. X.; Chen, F.; Jiang, M., Photoresponsive Pseudopolyrotaxane Hydrogels Based on Competition of Host-Guest Interactions. *Ang. Chem.-Int. Ed.* **2010,** *49* (26), 4409-4413; (b) Park, J. S.; Jeong, S.; Ahn, B.; Kim, M.; Oh, W.; Kim, J., Selective response of cyclodextrin-dye hydrogel to metal ions. *J. Incl. Phenom. Macrocyclic Chem.* **2011,** *71* (1-2), 79-86; (c) Yagai, S.; Karatsu, T.; Kitamura, A., Melamine-barbiturate/cyanurate binary organogels possessing rigid azobenzene-tether moiety. *Langmuir* **2005,** *21* (24), 11048-11052; (d) Yagai, S.; Nakajima, T.; Kishikawa, K.; Kohmoto, S.; Karatsu, T.; Kitamura, A., Hierarchical organization of photoresponsive hydrogen-bonded rosettes. *J. Am. Chem. Soc.* **2005,** *127* (31), 11134-11139; (e) Zhou, Y. F.; Xu, M.; Yi, T.; Xiao, S. Z.; Zhou, Z. G.; Li, F. Y.; Huang, C. H., Morphology-tunable and photoresponsive properties in a self-assembled two-component gel system. *Langmuir* **2007,** *23* (1), 202-208.

20. Cao, H.; Jiang, J.; Zhu, X. F.; Duan, P. F.; Liu, M. H., Hierarchical co-assembly of chiral lipid nanotubes with an azobenzene derivative: optical and chiroptical switching. *Soft Matt.* **2011,** *7* (10), 4654-4660.

21. Fuhrhop, J. H.; Boettcher, C., Stereochemistry and Curvature Effects In Supramolecular Organization and Separation Processes of Micellar N-Alkylaldonamide Mixtures. *J. Am. Chem. Soc.* **1990,** *112* (5), 1768-1776.

22. (a) Haro, M.; del Barrio, J.; Villares, A.; Oriol, L.; Cea, P.; Lopez, M. C., Supramolecular architecture in Langmuir and Lanigmuir-Blodgett films incorporating a chiral azobenzene. *Langmuir* **2008,** *24* (18), 10196-10203; (b) Vera, F.; Tejedor, R. M.; Romero, P.; Barbera, J.; Ros, M. B.; Serrano, J. L.; Sierra, T., Light-driven supramolecular chirality in propeller-like hydrogen-bonded complexes that show columnar mesomorphism. *Ang. Chem.-Int. Ed.* **2007,** *46* (11), 1873-1877; (c) Zhou, Y. F.; Yi, T.; Li, T. C.; Zhou, Z. G.; Li, F. Y.; Huang, W.; Huang, C. H., Morphology and Wettability tunable two-dimensional superstructure assembled by hydrogen bonds and hydrophobic interactions. *Chem. Mat.* **2006,** *18* (13), 2974-2981.

23. del Barrio, J.; Tejedor, R. M.; Chinelatto, L. S.; Sanchez, C.; Pinol, M.; Oriol, L., Photocontrol of the Supramolecular Chirality Imposed by Stereocenters in Liquid Crystalline Azodendrimers. *Chem. Mat.* **2010,** *22* (5), 1714-1723.

5. AMPHIPHILIC MOLECULES BASED ON POLYETHYLENE GLYCOL AND AZOBENZENE DERIVATIVES

5.1. Introduction

As it has been previously remarked, supramolecular gels are sensitive to external stimuli due to the reversibility of the supramolecular interactions that support the gel structure. As a consequence, when a photoresponsive group is inserted in the gel structure, the supramolecular assembly can be stimulated by light.[1] Related to the studies described in **Chapter 4**, herein we reported the incorporation of photoresponsive azobenzene units in new amphiphilic molecules. In this case, a polar head different from sugars has been selected in order to explore its influence on the gelation process and properties of derived gels. In particular, we have selected poly(ethylene glycol) (PEG) chains as polar heads. This type of hydrophilic units was previously used in our labs to synthesize amphiphilic block copolymers having the ability to self-assemble into different photoresponsive nano-objects in aqueous solutions.[2] As hydrophobic part, we have selected L-phenylalanine connected to a photoresponsive azobenzene unit having a fatty terminal chain.

On the one hand, PEG is a widely used polymer due to its solubility in water and other organic solvents and commercially available in a range of different molecular weights and functionalities at one or both endings of the polymeric chain. PEG has been widely investigated for applications in Biomedicine or in Nanobiomedicine due to its biocompatibility and its ability to prolong the lifetime of biological compounds in the body. Pegylation, the covalent attachment of PEG, has been used to modify peptides and proteins.[3] PEG derivatives have also been explored as soft materials as they have the ability to form gels,[4] especially due to the supramolecular interactions formed,[5] being either a part of a block copolymer[6] or a crosslinked system.[7] Incorporation of different molecular weight PEG moieties makes possible the modulation of hydrophilic/hydrophobic ratio and therefore the different aggregates formation.

On the other hand, amino acids, like phenylalanine, are widely used in gelator structures, especially to obtain supramolecular hydrogelators,[8] not only due to their potential biocompatibility, as for PEG derivatives, but also by their ability to self-assembly in structures which can promote fibrillar objects and subsequent interpenetrated networks to entrap the solvent and gelate.[9]

In the case of supramolecular gels, a number of interesting polymer-peptide conjugates have been prepared based on PEG, which arrange in fibers or tapes comprising by peptide cores and PEG shells[10] and form hydro[11] and organogels[12], see **Fig. 5.1**.

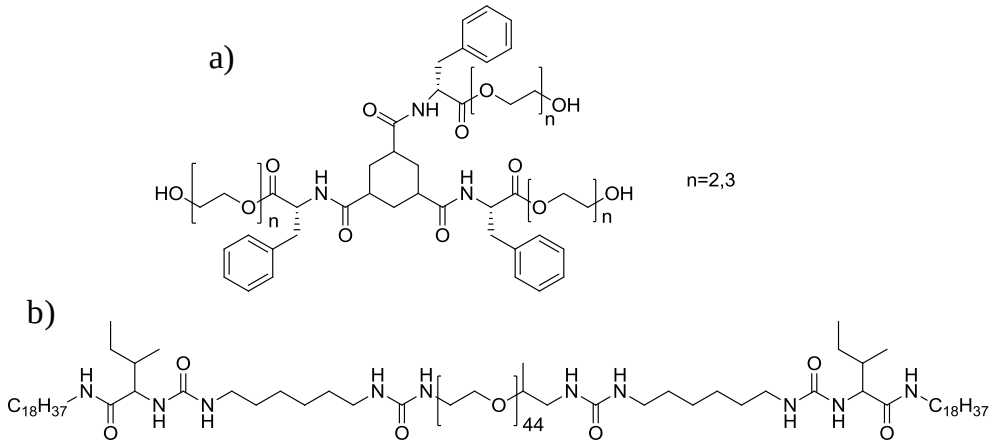

Fig. 5.1: Chemical structure of examples of PEG and amino acid derivatives which forms: a) hydrogels[11] and b) organogels.[12]

Here, we report the synthesis and characterization of different amphiphilic molecules consisting of different hydrophilic heads and a hydrophobic part based on **Phe-Azo-C_{18}**, see **Fig. 5.2**. This molecule derives from the condensation of two parts, L-phenylalanine and an azobenzene compound, **HOOC-Azo-C_{18}**. The structure of these molecules can be adequate to promote supramolecular gel formation because they have amide groups which can provide H-bonding, phenyl groups which can help the self-assembly via a π-π arrangement, as well as long hydrophobic chains which can promote van der Waals interactions. As hydrophilic part, PEG chains of two different molecular weights were used in order to check the importance of hydrophilic/hydrophobic ratio in aggregation properties and maltose was also introduced as a disaccharide polar head, in accordance to our previous work, in order to compare gelation properties of both hydrophilic moieties, see **Fig. 5.2**. The thermal and gelation properties of these photoresponsive and amphiphlic compounds are reported.

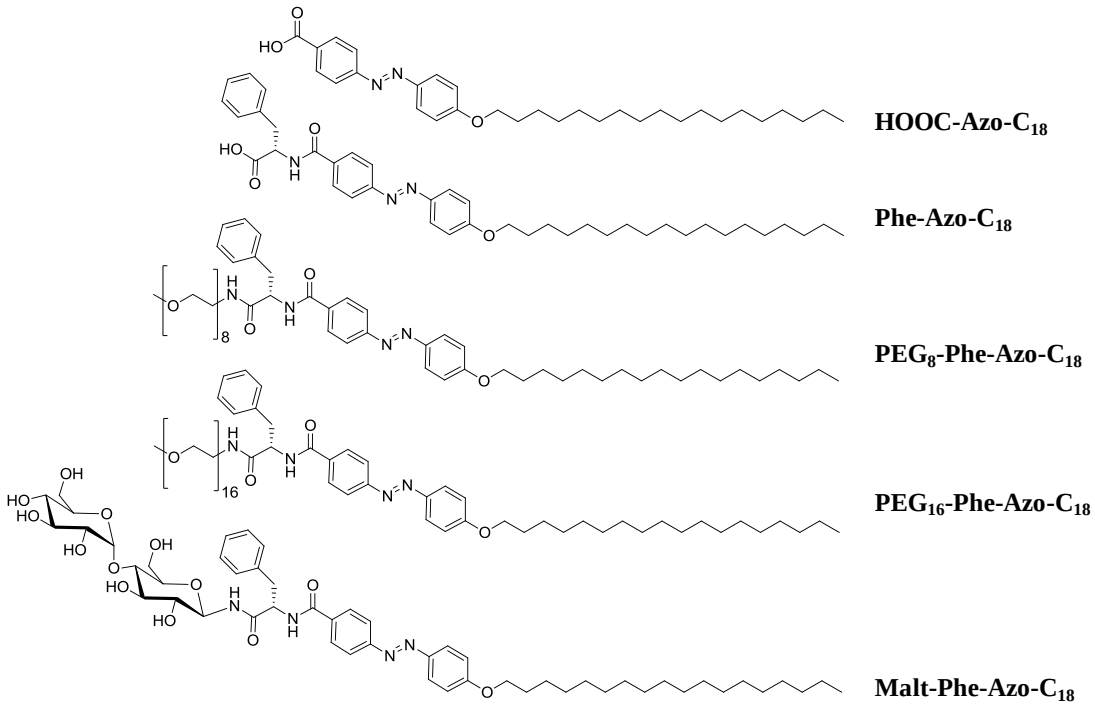

Fig. 5.2: Chemical structure of the synthesized materials.

5.2. Results and discussion

5.2.1. *Synthesis*

The synthesis of the amphiphiles was approached according to the synthetic pathway described in **Scheme 5.1** and **Scheme 5.2**. The azobenzene carboxylic acid, **HOOC-Azo-C_{18}** was used as starting material. This compound was prepared following a similar pathway to that used to synthesize **HOOC-Azo-C_{16}**, see **Chapter 4**, **Scheme 4.1**. The azo coupling was made by reaction of sodium phenoxide and ethyl *p*-aminobenzoate to obtain compound **13** (see **Scheme 4.1**, **Chapter 4**). The carboxylic aliphatic chain was introduced by means of a Williamson reaction and subsequent hydrolysis of **22** gave rise to the desired acid compound **HOOC-Azo-C_{18}**. This acid was used as precursor of **Phe-Azo-C_{18}** which was obtained by previous activation of **HOOC-Azo-C_{18}** with *N*-hydroxysuccinimide, (compound **23**), and further reaction with L-phenylalanine. This reaction was made in a mixture of water/THF to enhance the solubility of both compounds. In the last synthetic step, **Phe-Azo-C_{18}** was subsequently coupled with amine-ended polyethylene glycol to obtain **PEG_n-Phe-Azo-C_{18} (n=8 or 16,** according to commercial data) or with maltose to obtain **Malt-Phe-Azo-C_{18}**, see **Scheme 5.1** and

Scheme 5.2, respectively. **PEG_n-Phe-Azo-C_{18} (n=8 or 16)** were synthesized using 1-Ethyl-3-(3-dimethyl aminopropyl) carbodiimide hydrochloride (EDC), hydroxybenzotriazole and THF as solvent. Commercial poly(ethyleneglycol)s having an amino terminal group were used for the synthesis of **PEG_8-Phe-Azo-C_{18}** (monodisperse amino-PEG with a MW=383.48) and for **PEG_{16}-Phe-Azo-C_{18}** (amino-PEG with a MW average of MW=750).

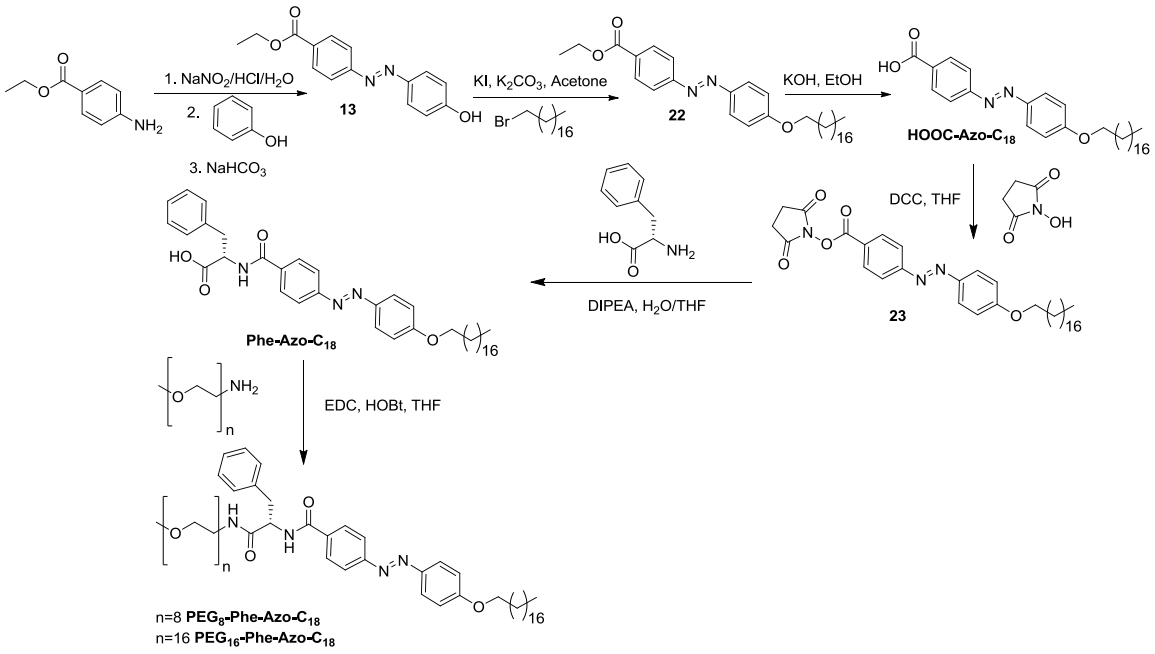

Scheme 5.1: Synthesis of **HOOC-Azo-C_{18}**, **Phe-Azo-C_{18}** and **PEG_n-Phe-Azo-C_{18} (n=8 or 16)**. Compound **13** was described in **Scheme 4.1**, **Chapter 4**.

Malt-Phe-Azo-C_{18} was synthesized using acetylated maltosylamine (compound **6**, see **Scheme 3.5**, **Chapter 3**) as starting material. Subsequently amide synthesis was made with a chloride derivative of **Phe-Azo-C_{18}** and maltosylamide in a DMF/THF mixture yielding the peracetylated compound **OAc-Malt-Phe-Azo-C_{18}**. This compound was deprotected using MeONa in a mixture of MeOH and THF to obtain the aimed **Malt-Phe-Azo-C_{18}** according to the Zemplen´s conditions described in **Chapter 3**.

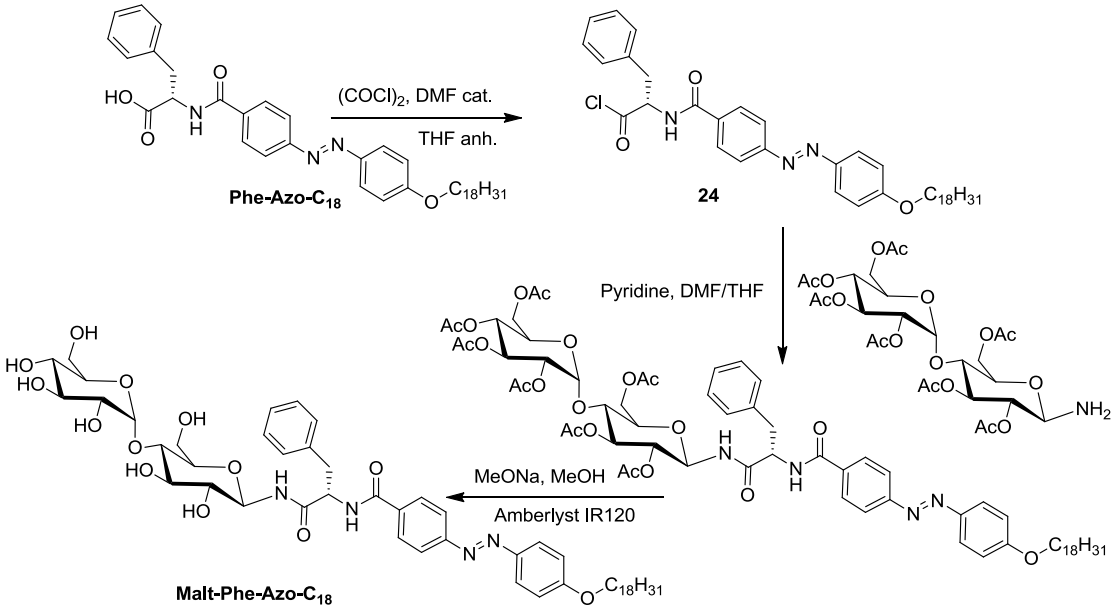

Scheme 5.2: Synthesis of **Malt-Phe-Azo-C_{18}**.

All the compounds were adequately characterized by ^{1}H NMR, ^{13}C NMR, IR and mass spectrometry, see **experimental section 5.4**.

MALDI-TOF mass spectrometry experiments of **PEG_8-Phe-Azo-C_{18}** and **PEG_{16}-Phe-Azo-C_{18}** (see **Fig. 5.3**) showed that in the case of **PEG_8-Phe-Azo-C_{18}** the sample is monodisperse, whereas in **PEG_{16}-Phe-Azo-C_{18}** there is a pattern of peaks separated about 44 (-[O-CH_2-CH_2]-) due to the polydispersity of the starting and commercial **Methyl-PEG_{16}-amine** used in the synthesis of **PEG_{16}-Phe-Azo-C_{18}**. According to that, **PEG_{16}-Phe-Azo-C_{18}** has a dispersity of degrees of polymerization of the PEG chain ranging from n=13 to n=24. **Malt-Phe-Azo-C_{18}** shows a normal isotopic distribution.

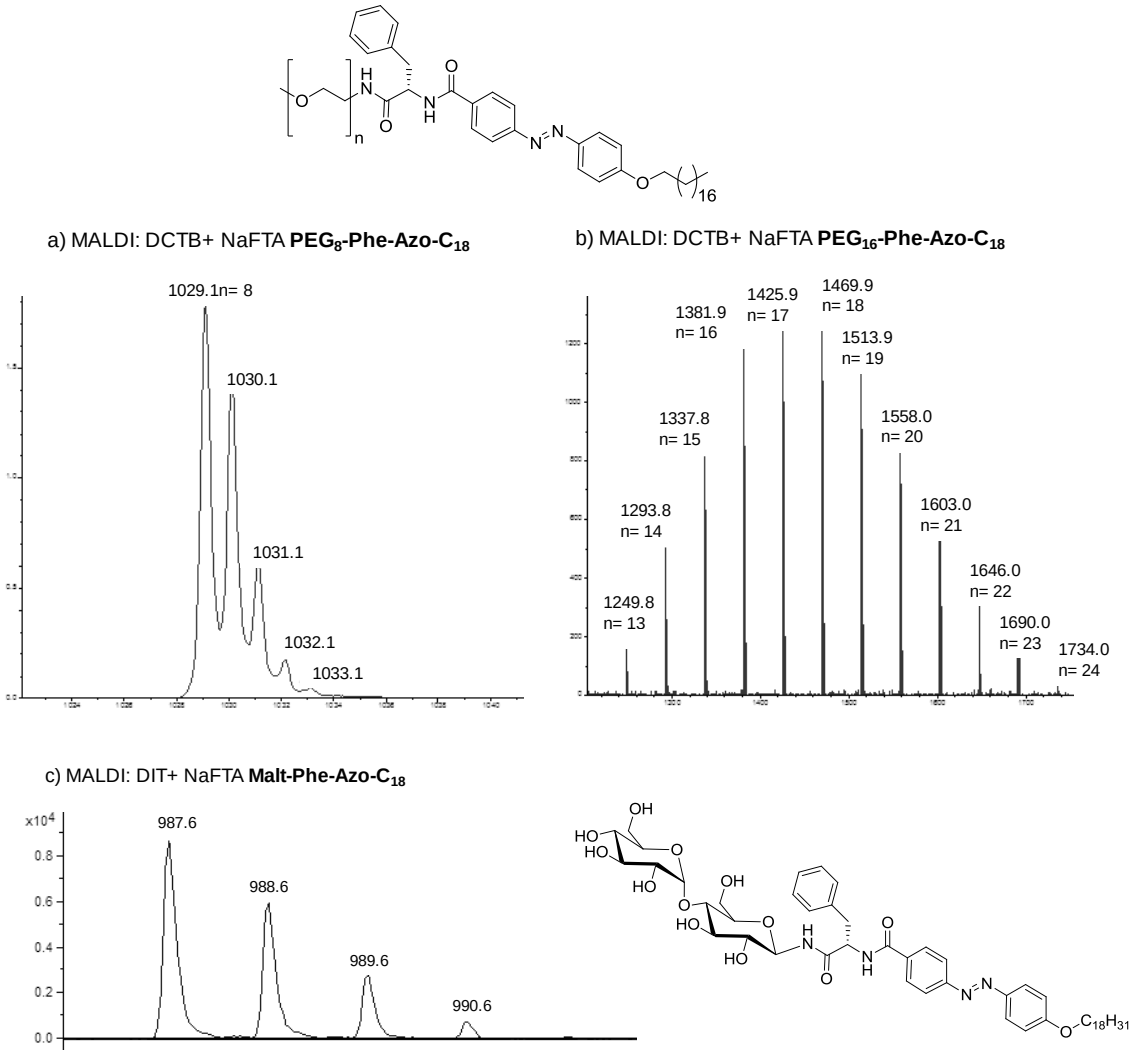

Fig. 5.3: a) MALDI (DCTB+ NaFTA) of **PEG$_8$-Phe-Azo-C$_{18}$**, b) MALDI (DCTB+ NaFTA) of **PEG$_{16}$-Phe-Azo-C$_{18}$**, c) MALDI (DIT+ NaFTA) of **Malt-Phe-Azo-C$_{18}$**.

^{1}H NMR spectrum and structural determination of **PEG$_8$-Phe-Azo-C$_{18}$**, **PEG$_{16}$-Phe-Azo-C$_{18}$**, **OAc-Malt-Phe-Azo-C$_{18}$** and **Malt-Phe-Azo-C$_{18}$** are shown in **Fig. 5.4**. **PEG$_8$-Phe-Azo-C$_{18}$** and **PEG$_{16}$-Phe-Azo-C$_{18}$** spectra corroborate the chemical structure of PEG derivatives. **OAc-Malt-Phe-Azo-C$_{18}$** and **Malt-Phe-Azo-C$_{18}$** compounds were characterized by additional two-dimensional NMR experiments (COSY, TOCSY, NOESY, HSQC and HMBC) as was done in similar glycoamphiphilic compounds in previous chapters. A total deprotection of the maltose groups was confirmed by ^{1}H NMR when spectra of **OAc-Malt-Phe-Azo-C$_{18}$** and **Malt-Phe-Azo-C$_{18}$** are compared, see **Fig. 5.4**. In **OAc-Malt-Phe-Azo-C$_{18}$** compound, a complete assignment of the sugar

protons could be done. As an example, a TOCSY experiment is shown in **Fig. 5.5.** However, the complete assignment of sugar protons was not possible in **Malt-Phe-Azo-C_{18}** where only H1 and H1´ were assigned.

a) **PEG_8-Phe-Azo-C_{18}** ($CDCl_3$, RT)

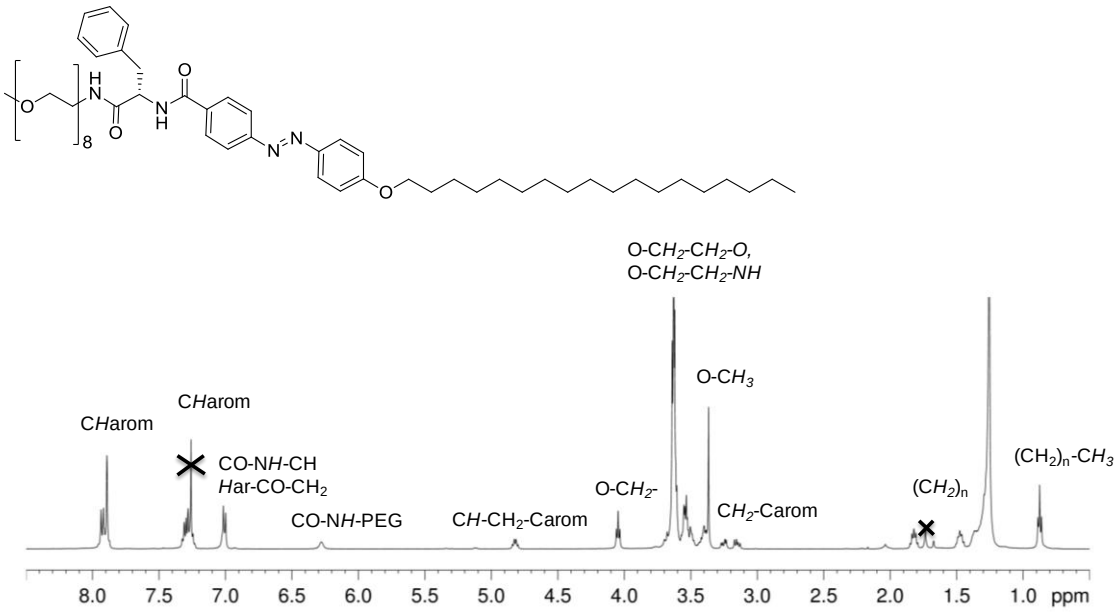

b) **PEG_{16}-Phe-Azo-C_{18}** ($CDCl_3$, RT)

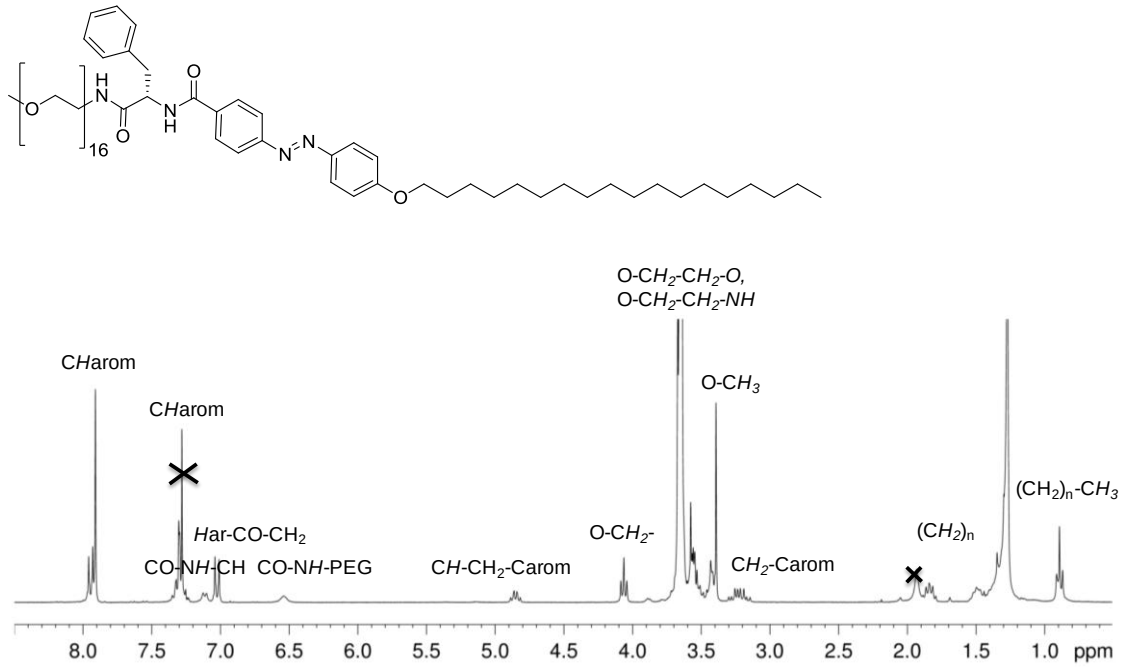

c) **OAc-Malt-Phe-Azo-C_{18}** ($CDCl_3$, RT)

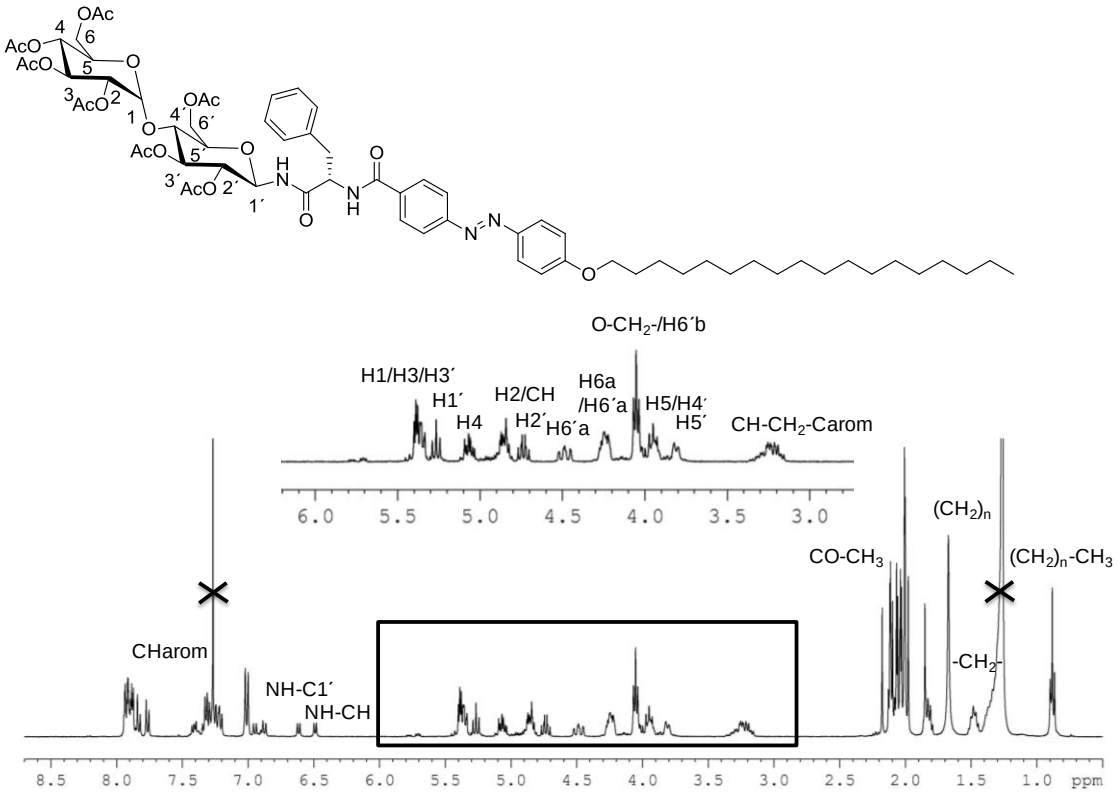

d) **Malt-Phe-Azo-C_{18}** (DMSO-d_6 , 80ºC)

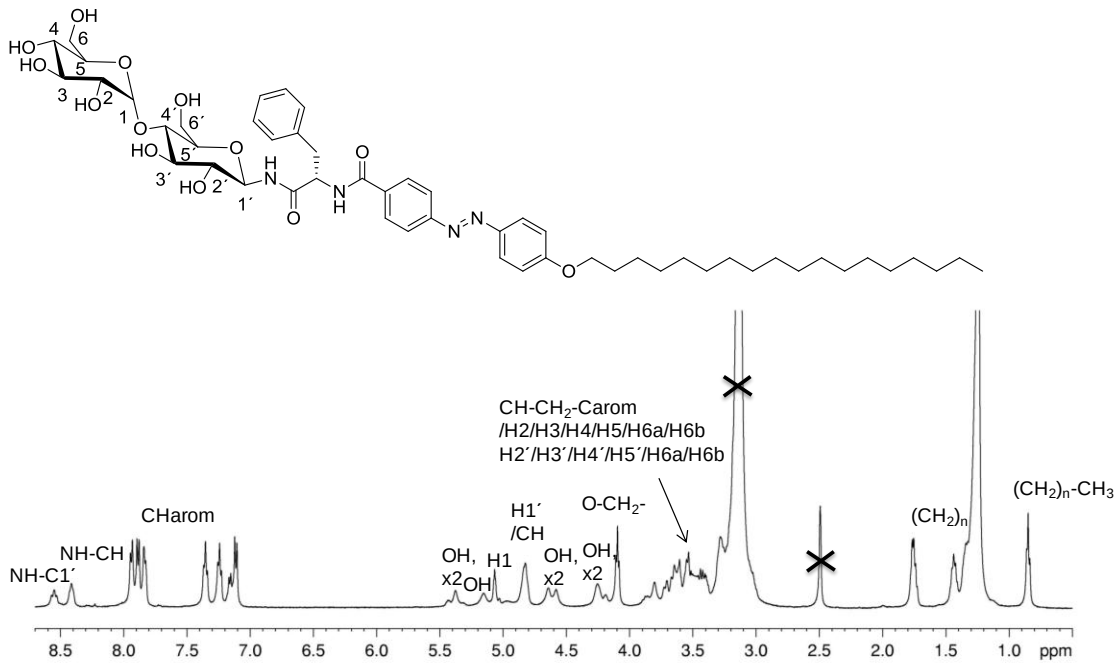

Fig. 5.4: ^{1}H NMR of a) **PEG_8-Phe-Azo-C_{18}**, b) **PEG_{16}-Phe-Azo-C_{18}**, c) **OAc-Malt-Phe-Azo-C_{18}** and d) **Malt-Phe-Azo-C_{18}**.

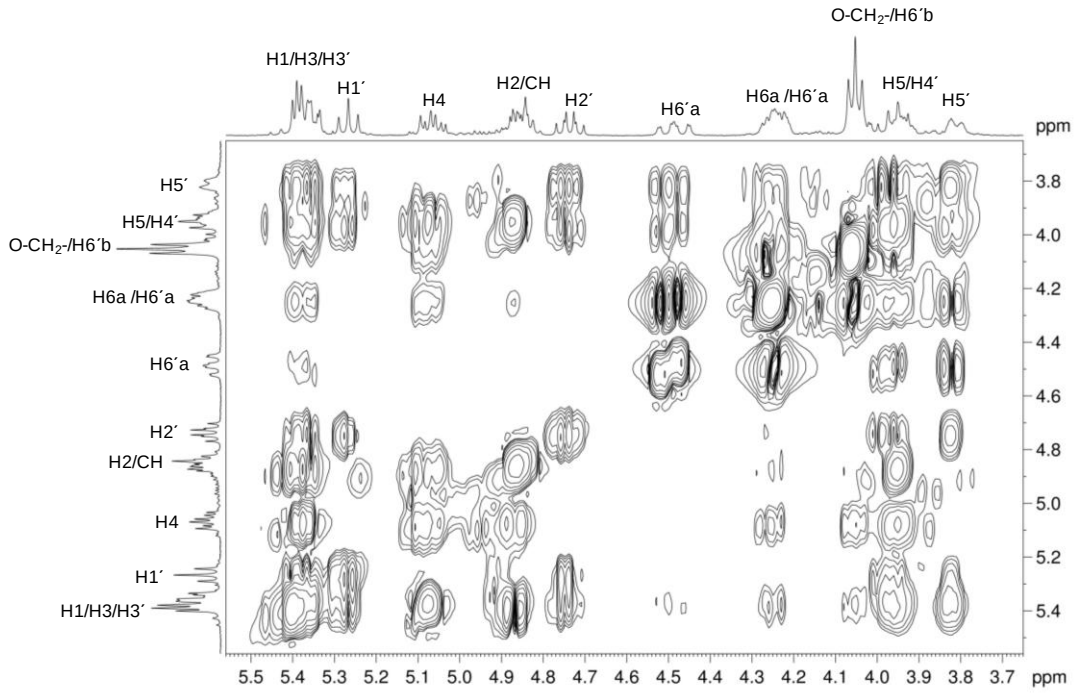

Fig. 5.5: TOCSY spectrum of **OAc-Malt-Phe-Azo-C_{18}** with $CDCl_3$ as solvent at 25ºC and 60 ms of mixing time.

5.2.2. *Thermal properties*

The thermal properties of the synthesized amphiphilic azocompounds were studied by thermogravimetric analysis (TGA), polarizing optical microscopy provided with a thermal stage (POM) and differential scanning calorimetry (DSC).

Weight losses were observed in thermogravimetry at temperatures ranging from 200 to 325 ºC as it has been summarized in **Table 5.1**. Acid compound **HOOC-Azo-C_{18}** has high stability while introduction of L-phenylalanine makes that the temperature at which 5 % of the initial mass is lost decreases from 325ºC to 250ºC (first decomposition process of that compound). However, linking a PEG moiety increases the thermal stability. Temperatures for 5 % weight loses for **PEG_8-Phe-Azo-C_{18}** and **PEG_{16}-Phe-Azo-C_{18}** are around 310ºC. In the case of **Malt-Phe-Azo-C_{18}** thermal stability is lower than the PEG-analogs as it can be expected from the introduction of a sugar polar head.[13]

Table 5.1: Thermogravimetric analysis of azocompounds.

Compound	$T_{5\%lost}$	T_{onset}	T_{max}
HOOC-Azo-C_{18}	325ºC	340ºC	360ºC
Phe-Azo-C_{18}	250ºC	245ºC 370ºC	280ºC 430ºC
PEG_8-Phe-Azo-C_{18}	305ºC	325ºC	345ºC
PEG_{16}-Phe-Azo-C_{18}	315ºC	320ºC 380ºC	340ºC 395ºC
Malt-Phe-Azo-C_{18}	220ºC	235ºC	250ºC

$T_{5\%lost}$ = Temperatures at wich 5% of the initial mass is lost. T_{onset} = Onset of thermal decomposition process. T_{max} = Temperatures at which the maximum rate of weight loss is produced.

Regarding the mesomorphic properties, in the case of **HOOC-Azo-C_{18}** mesomorphism was observed in accordance with the previously reported data in bibliography.[14] Different smectic mesophases were observed. The mesomorphic properties of this compound can be related with the tendency of carboxylic acids to dimerize by H-bonding giving rise to a supramolecular mesogen with a high aspect ratio. However, the derivative **Phe-Azo-C_{18}** is not mesogenic, as consequence of the phenyl lateral ring that decrease this aspect ratio, as well as the lateral amide hydrogen bonding. The final amphiphiles **PEG_8-Azo-Phe-C_{18}** and **PEG_{16}-Azo-Phe-C_{18}** and the sugar derivative **Malt-Phe-Azo-C_{18}** do not present mesogenic behavior.

The compounds were studied by DSC technique in order to characterize thermal transitions. The results of **Phe-Azo-C_{18}**, **PEG_8-Azo-Phe-C_{18}**, **PEG_{16}-Azo-Phe-C_{18}** and **Malt-Phe-Azo-C_{18}** are gathered in **Table 5.2. HOOC-Azo-C_{18}** thermal transitions agree with those reported in bibliography.[14]

Table 5.2: Thermal transitions of the synthesized amphiphiles determined by DSC ($10^{o}C.min^{-1}$).

Compound	Thermal transition (ºC) [ΔH kJ/mol][a]
Phe-Azo-C_{18}	Cr 137 [5.6] Cr´ 153 [28.3] I
PEG_8-Phe-Azo-C_{18}	Cr 87 [1.0] Cr´ 97 [2.7] Cr´´ 116 [32.6] I
PEG_{16}-Phe-Azo-C_{18}	Cr 27[53.4] Cr´ 84 [4.2] Cr´´ 106 [33.5] I
Malt-Phe-Azo-C_{18}	Cr 112 [22.8] Cr´ 175 Dec

[a] Data corresponding to the second heating and cooling scan. Cr = crystal, I = isotropic phase, Dec=decomposition.

Phe-Azo-C_{18} melts from crystalline state to isotropic liquid at 153 ºC. The melting transition from crystalline to isotropic state of **PEG_8-Azo-Phe-C_{18}** and **PEG_{16}-Azo-Phe-C_{18}** is detected at temperatures around 110ºC. Different polymorphic transitions are observed in these products until melting. In the case of the sugar derivative, **Malt-Phe-Azo-C_{18}**, the sample was previously dried and immediately analyzed. When this compound was studied by optical microscopy, the sample becomes brown above melting transition due to decomposition of the sugar units. On a DSC experiment performed until 200ºC, decomposition was detected at around 175ºC as confirmed by a decrease of the baseline. A polymorphic transition was detected at 112ºC.

5.2.3. *Supramolecular Gels*

The solubility and gelation ability of the synthesized compounds were examined in different solvents by dissolving 5 mg of compound in about 50-1000 mg of the corresponding solvent, i.e. 0.5-10 wt % (the gelator and the solvent were placed in a septum-capped test tube). The final results obtained at room temperature (RT) on the selected solvents are summarized in **Table 5.3**. **HOOC-Azo-C_{18}** and **Malt-Tz-Azo-C_{18}** were not initially soluble at RT for any of the tested solvents. However, **Phe-Azo-C_{18}** was soluble at RT only in chloroform and PEG derivatives (**PEG_8-Azo-Phe-C_{18}** and **PEG_{16}-Azo-Phe-C_{18}**) are soluble at RT in different organic solvents, see **Table 5.3**. In particular, **PEG_{16}-Azo-Phe-C_{18}** was soluble in most of the used organic solvents. If the compound was not soluble at RT, mixtures were first heated and then cooled down to RT. A solution, precipitate or a gel was then observed depending on the solvent, see

Table 5.3. The formation of a gel was confirmed if the tube was turned upside down and the solution did not flow.

Table 5.3. Solubility and gelation properties of synthesized compounds in different solvents.

Solvent	HOOC-Azo-C_{18}	Phe-Azo-C_{18}	PEG_8-Phe-Azo-C_{18}	PEG_{16}-Phe-Azo-C_{18}	Malt-Phe-Azo-C_{18}
Hexane	I	I	I	I	I
Toluene	P	Gel (5 wt %)	S	S	I
Dichloromethane	I	Gel (5 wt %)	S	S (heat)	I
Chloroform	I	S	S	S	I
THF	P	S (heat)	S	S	Gel (1.3 wt %)
1-Dodecanol	Gel (5 wt %)	Gel (10 wt %)	Gel (5 wt %)	I	Gel (0.5 wt %)
Acetone	I	P	Gel (8 wt %)	S	I
DMF	Gel (2 wt %)	S (heat)	S	S	S (heat)
DMSO	Gel (6 wt %)	Gel (10 wt %)	Gel (5 wt %)	S	P
Methanol	I	I	Gel (5 wt %)	S	I
Water	I	I	I	I	I

I = Insoluble, P = Precipitate after solubilization upon heating and cooling down to room temperature, S(heat) = Solution after heating and cooling down to room temperature, S = Soluble at room temperature without heating, G = Gel (minimum gel concentration).

All compounds are able to form organogels in different solvents (at different minimum concentrations) except **PEG_{16}-Phe-Azo-C_{18}**. **HOOC-Azo-C_{18}** is able to form gels in a minimum concentration lower than 10 wt % in DMSO (6 wt %), 1-dodecanol (5 wt %) and DMF (2 wt %). **Phe-Azo-C_{18}** was able to form gels in DMSO and 1-dodecanol in a minimum concentration of 10 wt %. In toluene and in dichloromethane, the minimum concentration decreases to 5 wt %. **PEG_8-Phe-Azo-C_{18}** forms gels in 1-dodecanol, DMSO and methanol at a minimum concentration of 5 wt % and in acetone at 8 wt %. **Malt-Tz-Azo-C_{18}** form gels in THF in a minimum concentration of 1.3 wt % and the lowest concentration was reached in 1-dodecanol at 0.5 wt %. All gels are orange in color due to the azobenzene group, as can be seen for the examples selected in **Fig. 5.6,** an opaque gel of **Phe-Azo-C_{18}** in dichloromethane at 5 wt % and a transparent gel of **Malt-Phe-Azo-C_{18}** in THF at 1.3 wt %.

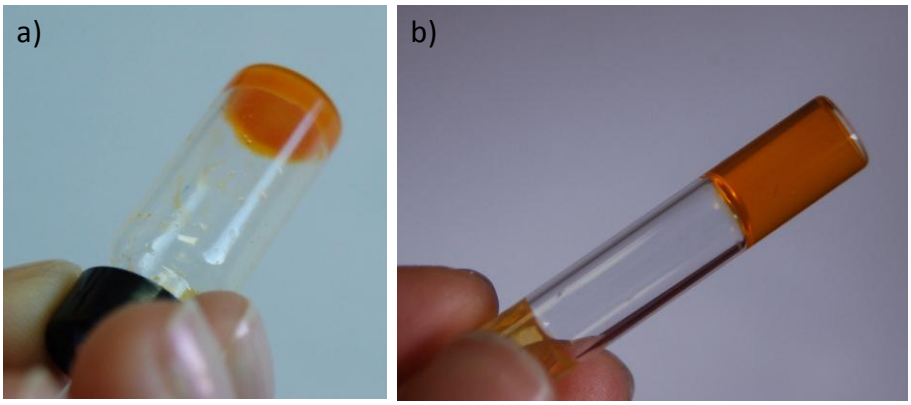

Fig 5.6: Gels of the synthesized compounds: a) opaque gel of **Phe-Azo-C_{18}** in dichloromethane at 5 wt %, b) transparent gel of **Malt-Phe-Azo-C_{18}** in THF at 1.3 wt %.

The obtained gels are stable at RT and thermoreversible. In contrast to azo-sugar derivatives synthesized in **Chapter 4**, they are not soluble in water or mixtures of water-DMSO even on heating. Synthesized azobenzene derivatives are able to gelify in 1-dodecanol except **PEG_{16}-Phe-Azo-C_{18}** which is not soluble.

Morphological gel characterization. In order to investigate the supramolecular organization of the gels derived from the synthesized amphiphiles, xerogels (gels dried under vacuum) were first obtained from these compounds and studied under microscopic techniques.

Xerogels of **HOOC-Azo-C_{18}**, **Phe-Azo-C_{18}**, **PEG_8-Phe-Azo-C_{18}** and **Malt-Phe-Azo-C_{18}** were first investigated by SEM in 1-dodecanol at their minimum gel concentration, see **Fig. 5.7**. For **HOOC-Azo-C_{18}** sample, non-well defined structures were observed, see **Fig. 5.7.a**. Ribbons, having lengths and widths of around several micrometers are detected for **PEG_8-Phe-Azo-C_{18}**, see **Fig. 5.7.c**. However, for **Phe-Azo-C_{18}** and **Malt-Phe-Azo-C_{18}** widths of the ribbons are at the nanometer scale. For **Phe-Azo-C_{18}** sample, measured ribbons have widths ranging from 50 to 200 nm, see **Fig. 5.7.b** and for **Malt-Phe-Azo-C_{18}** they have widths ranging from 90 to 160 nm, see **Fig. 5.7.d**.

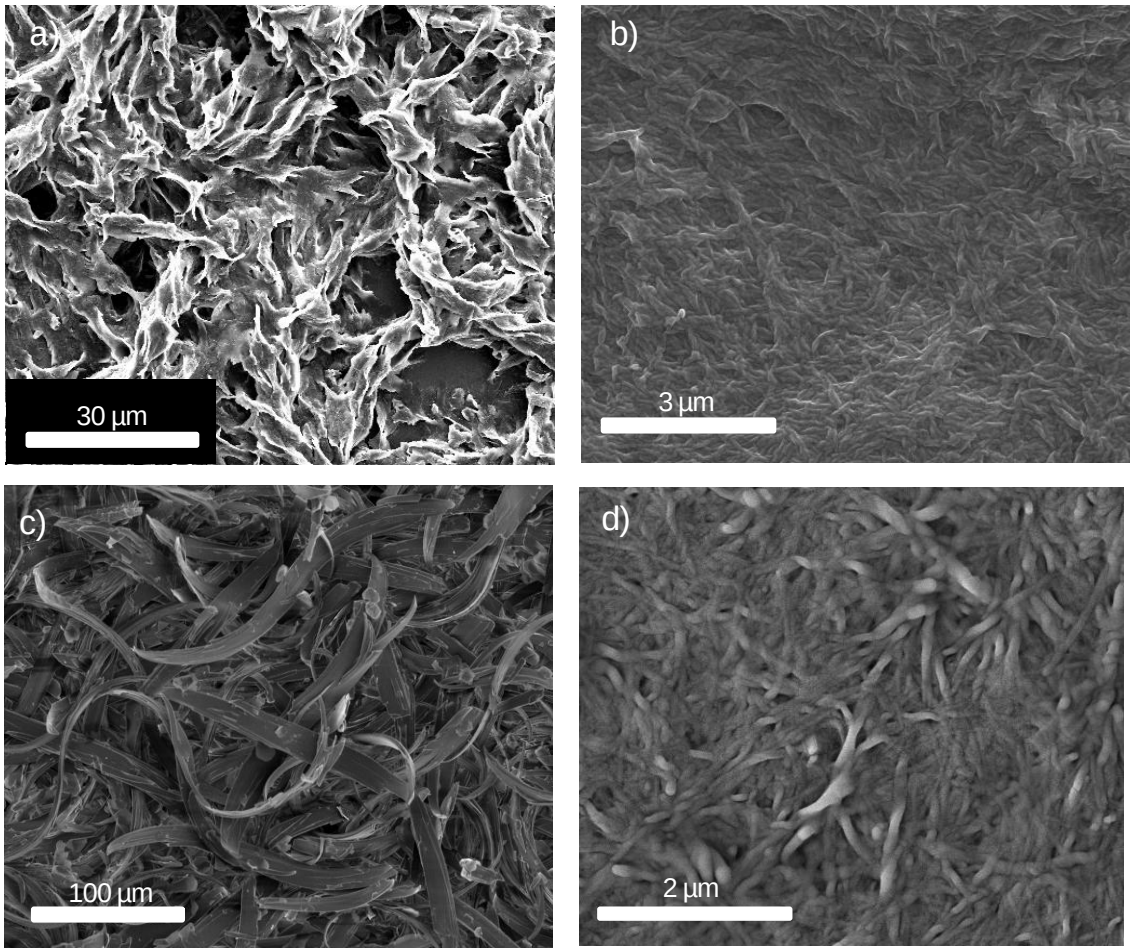

Fig. 5.7: a) SEM image of xerogel obtained from **HOOC-Azo-C_{18}** at 5 wt % in 1-dodecanol, b) SEM image of xerogel obtained from **Phe-Azo-C_{18}** at 10 wt % in 1-dodecanol, c) SEM image of xerogel obtained from **PEG_8-Phe-Azo-C_{18}** at 5 wt % in 1-dodecanol, d) SEM image of xerogel obtained from **Malt-Phe-Azo-C_{18}** at 0.5 wt % in 1-dodecanol.

Xerogels of **HOOC-Azo-C_{18}**, **Phe-Azo-C_{18}** and **PEG_8-Phe-Azo-C_{18}** were also studied in DMSO, a solvent in which compounds synthesized give rise to gels, except **Malt-Phe-Azo-C_{18}**. Compounds were also measured at their minimum gel concentrations; see SEM images in **Fig. 5.8.** In **HOOC-Azo-C_{18}** a "cabbage like" structure[15] was observed, see **Fig. 5.8.a**, while in the case of the xerogel from 1-dodecanol non-well defined structures were formed. For **Phe-Azo-C_{18}**, in contrast to 1-dodecanol xerogel (both are formed at 10 wt %), ribbons with lengths and widths of several micrometers are observed, see **Fig. 5.8.b**. Finally in the case of **PEG_8-Phe-Azo-C_{18}** measured ribbons

have around 150 – 200 nm of width and they are smaller than the observed in gels from 1-dodecanol (both are formed at 5 wt %).

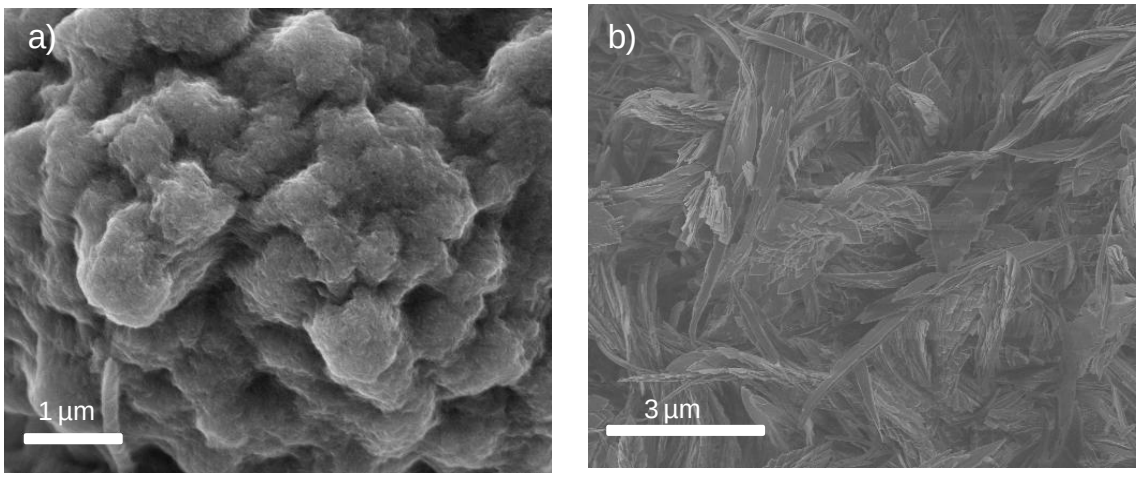

Fig. 5.8: a) SEM image of xerogel obtained from **HOOC-Azo-C_{18}** at 6 wt % in DMSO, b) SEM image of xerogel obtained from **Phe-Azo-C_{18}** at 10 wt % in DMSO.

Furthermore xerogels of **Phe-Azo-C_{18}** were also studied in two additional solvents as dichloromethane and toluene. Both gels were formed at the minimum gel concentration of 5 wt %, see **Fig. 5.9**. In this case, no differences in both solvents were found. An interpenetrated structure was observed with non regular pores and measured ribbons had widths ranging from 100 to 250 nm, similarly to the structures detected in 1-dodecanol.

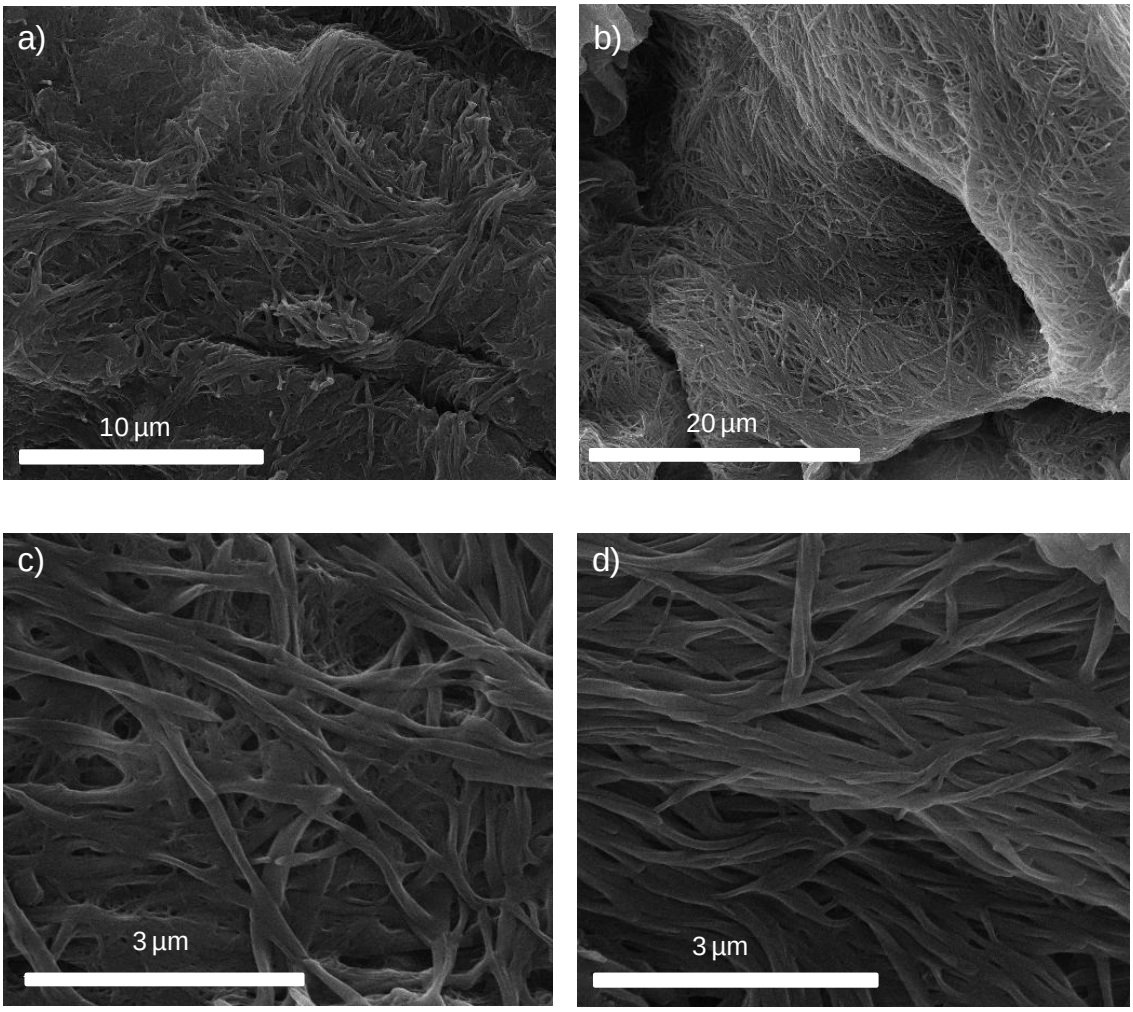

Fig. 5.9: a) and c) SEM image of xerogel obtained from **Phe-Azo-C_{18}** at 5 wt % in dichloromethane, b) and d) SEM image of xerogel obtained from **Phe-Azo-C_{18}** at 5 wt % in toluene.

Diluted and negative stained samples of the amphiphiles were also studied by TEM. The self-assembled microstructures of **HOOC-Azo-C_{18}**, **Phe-Azo-C_{18}**, **PEG_8-Phe-Azo-C_{18}** and **Malt-Phe-Azo-C_{18}** were investigated in 1-dodecanol. Concentration of the solutions were 0.5 wt %, 1 wt %, 0.5 wt % and 0.05 wt % respectively (10 times more diluted than minimum gel concentration); see **Fig. 5.10.** Microphotographs of **HOOC-Azo-C_{18}** sample showed ribbons with widths of around 0.5 micrometers see **Fig. 5.10.a**. For **Phe-Azo-C_{18}** sample, twisted ribbons were observed and measured widths were around to 20-30 nm, see **Fig. 5.10.b** with a torsion pitch around 50 nm, see close up in **Fig. 5.10.b**. Ribbons were also observed for **PEG_8-Phe-Azo-C_{18}**. In this case,

measurements were around 100 to 300 nm, see **Fig. 5.10.c**. For **Malt-Phe-Azo-C_{18}**, widths were around 50 to 150 nm, see **Fig. 5.10.d.**

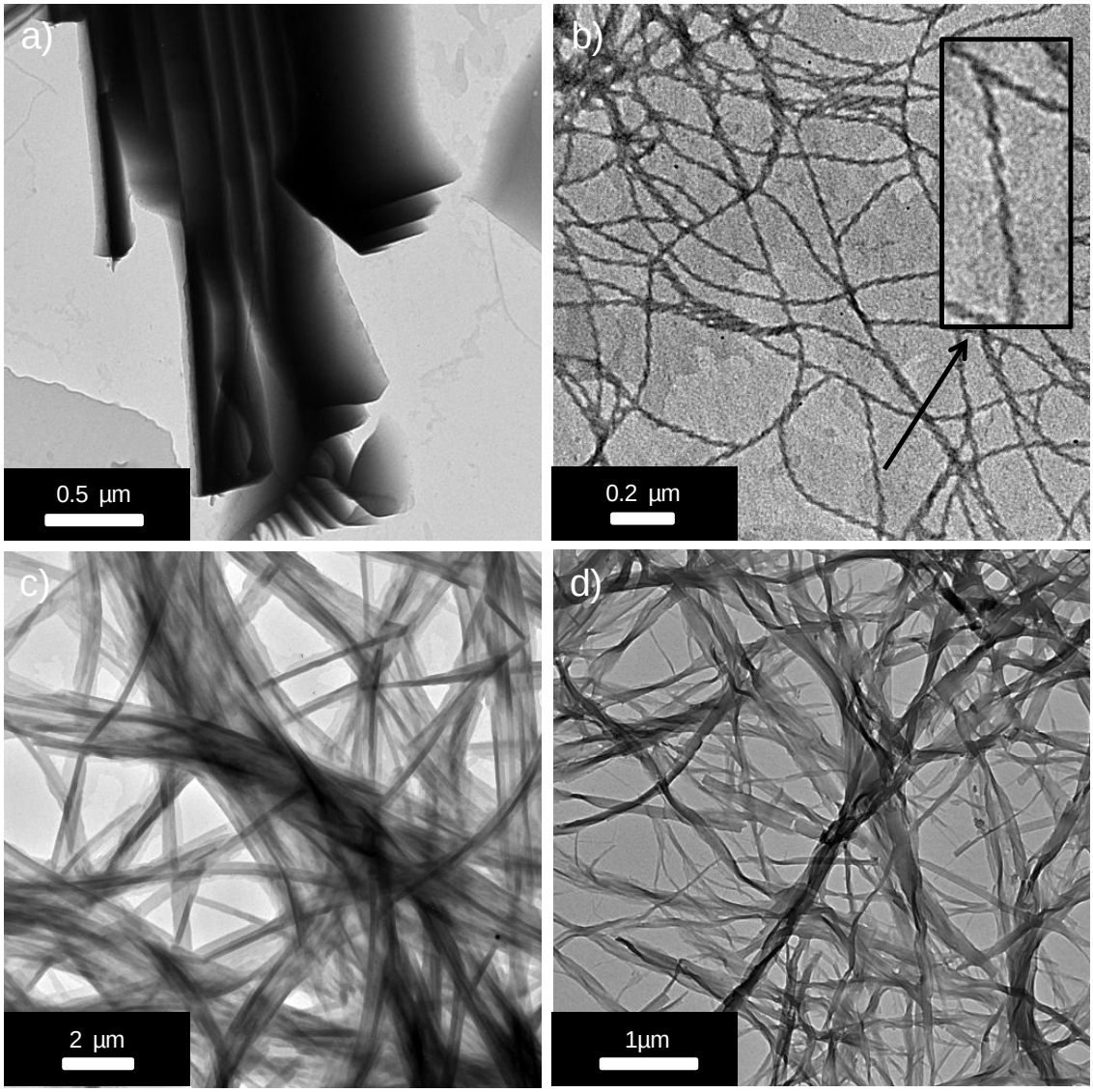

Fig. 5.10: a) TEM image of **HOOC-Azo-C_{18}** at 0.5 wt % in 1-dodecanol, b) TEM image of **Phe-Azo-C_{18}** at 1 wt % in 1-dodecanol, c) TEM image of **PEG_8-Phe-Azo-C_{18}** at 0.5 wt % in 1-dodecanol, d) TEM image of **Malt-Phe-Azo-C_{18}** at 0.05 wt % in 1-dodecanol.

As it has been previously described, **PEG_8-Phe-Azo-C_{18}** derivative was able to self-assembly and formed supramolecular gels meanwhile gels could not be obtained for the analog **PEG_{16}-Phe-Azo-C_{18}**. Aggregation studies were then carried out in both PEG derivatives in order to study the supramolecular organization of these compounds.

First of all**, PEG_8-Phe-Azo-C_{18}** compound was studied in DMSO, where this compound forms a gel at a concentration of 5 wt% and consequently should aggregate in this solvent even at a lower concentration. For the study of supramolecular aggregation, diluted samples at 0.25 wt % and 0.1 wt % were prepared and heated to complete solubilization and then cooled to obtain clear solutions. No turbidity was observed at naked eyes. Solution at 0.1 wt % in DMSO was studied by TEM. A drop of the solution was placed onto a copper grid and negative stained by uranyl acetate. As it can be seen at **Fig. 5.11**, planar ribbons were again observed with widths of around 150 – 200 nm.

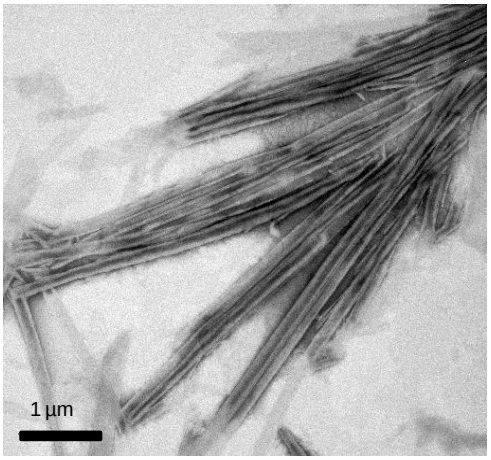

Fig. 5.11: a) TEM image of **PEG_8-Phe-Azo-C_{18}** at 0.1 wt % in DMSO.

PEG_{16}-Phe-Azo-C_{18} compound is not able to gel neither in DMSO nor in a mixture of DMSO/water. It is soluble in DMSO but turbidity in the mixture of DMSO/water was observed, which indicates that aggregation takes place. Therefore a study of the supramolecular aggregation can be carried out in order to establish a possible self-assembly of this compound as an amphiphilic molecule. A solution in DMSO (good solvent) was first prepared and water was progressively and carefully added to that solution. Turbidity was monitored as a means of detecting aggregation.[2b, 16]

The sample was first dissolved in DMSO (0.5 wt %) and Mili-Q water was carefully added to the solution (20 µL of water to 1.0 mL of solution) with slight shaking. Turbidity of the solution was measured after every addition of water at a wavelength of 650 nm (at this wavelength there is no absorption of the azobenzene chromophore and there is no turbidity in the initial clear solution) using a quartz cell (path length 1 cm) with a Unicam UV/vis spectrophotometer. The solution was left to equilibrate till the

turbidity remains constant. The cycle of water addition, equilibration and turbidity measurement was continued until the increase in turbidity upon water addition was very small. Beyond 38 wt % addition of water the turbidity remains almost stable, see **Fig. 5.12**.

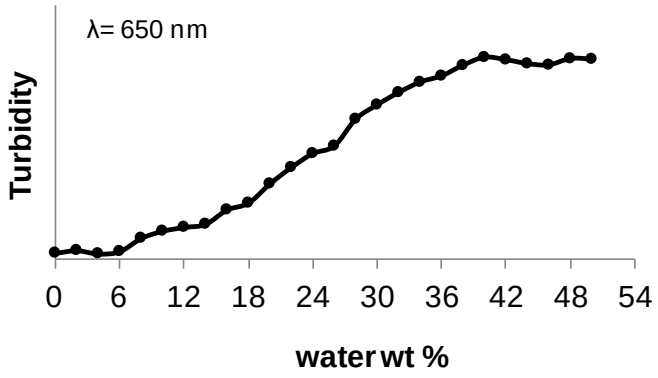

Fig. 5.12: Turbidity curve of **PEG_{16}-Phe-Azo-C_{18}** solution in a mixture of DMSO/water represented as a function of the amount of water added to the solution (wt %). The initial turbidity value, corresponding to this curve for a 100 wt % DMSO solution, is zero.

The solution was then dialyzed against water for 2 days to remove the organic solvent using a regenerated cellulose membrane with a molecular weight cutoff of 1000 a. m. u. The morphological analysis of the dialyzed aggregate solution was then performed by TEM on a sample stained with uranyl acetate, see **Fig. 5.13**.

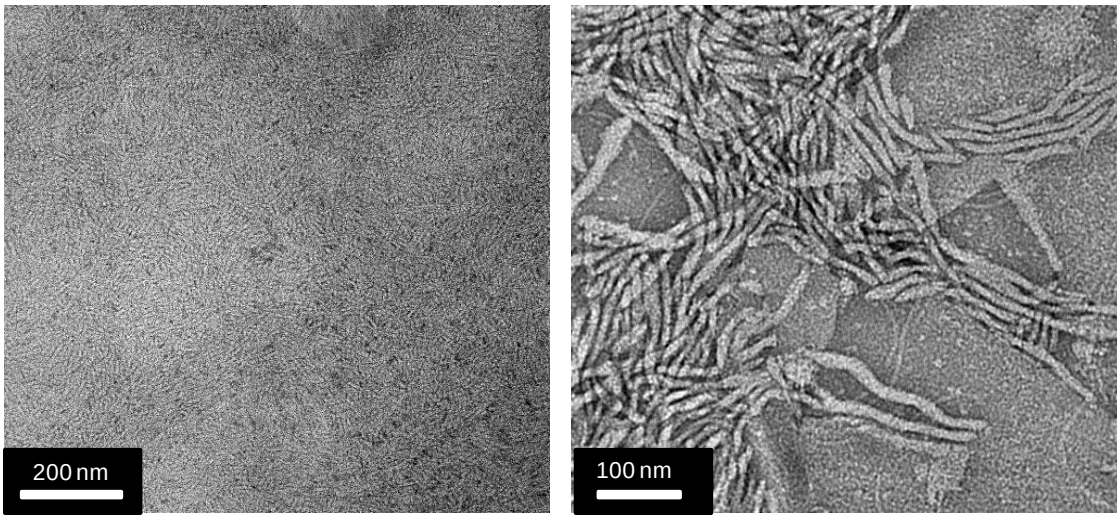

Fig. 5.13: TEM images of a **PEG_{16}-Phe-Azo-C_{18}** sample.

Fibrillar structures were found with widths around 10-20 nm. These structures are thinner than structures observed in **PEG_8-Phe-Azo-C_{18}**. In fact, **PEG_{16}-Phe-Azo-C_{18}** is able to self-assembly in a mixture of DMSO/water solvents although the network resulting of these self-assembly is not able to form a gel. The hydrophobic/hydrophilic balance seems to play a crucial role in the self-assembly and the dimensions of the aggregates of these amphiphilic molecules. In the case of **PEG_8-Phe-Azo-C_{18}**, having a higher hydrophobic content than **PEG_{16}-Phe-Azo-C_{18}** (60/40 molecular weight hydrophobic/hydrophilic block ratio), the network is consistent enough to entrap the solvent. Meanwhile for **PEG_{16}-Phe-Azo-C_{18}**, with a higher hydrophilic content (44/56 molecular weight hydrophobic/hydrophilic block ratio taking as reference n=16), the aggregates cannot form a consistent network to entrap the solvent.

5.2.4. *Irradiation experiments*

Azobenzene group is used in the field of materials science due to the reversible *trans-cis* photochemical isomerization. Irradiation experiments were performed in order to investigate a possible photoresponse of the compounds, either in solution or in gel state.

Experiments in DMSO solution (10^{-4} M) of **PEG_8-Phe-Azo-C_{18}** and **PEG_{16}-Phe-Azo-C_{18}** were performed under irradiation at 365 nm (see **Characterization Techniques 7. Annex** for experimental conditions), around the maximum corresponding to the π–π* transition of the *trans* isomer. Behavior under photoirradiation was first studied in solution and subsequently studies under photoirradiation in DMSO of **PEG_8-Phe-Azo-C_{18}** in gel state will be described in the following section.

Evolution of the sample was monitored by UV-vis absorption and *trans-cis* isomerization was checked, see **Fig. 5.14**. The shape of the absorption band of both compounds in DMSO (10^{-4} M) before irradiation is very similar, an approximately symmetrical band corresponding to *trans*-azobenzenes having a maximum at 365 nm corresponding to the π-π* transition, which is in accordance with a relatively low aggregation. Under irradiation, **PEG_8-Phe-Azo-C_{18}** exhibits a decrease of the absorbance at λ_{max} due to the decrease of the *trans*-isomer and the absorbance at 445 nm, corresponding to the n–π* transition, increases due to the appearance of the *cis*-isomer. In 6 min, a photostationary state can be considered to be reached, see **Fig. 5.14.a**. For a 10^{-4} M solution of **PEG_{16}-Phe-Azo-C_{18}** in DMSO, the same behavior of

the signal under irradiation was observed but, in this case, the photostationary state was observed at 4 min, see **Fig. 5.14.b.** Partial recovery of the initial UV-vis spectrum was achieved when samples were kept in the dark for 24 h.

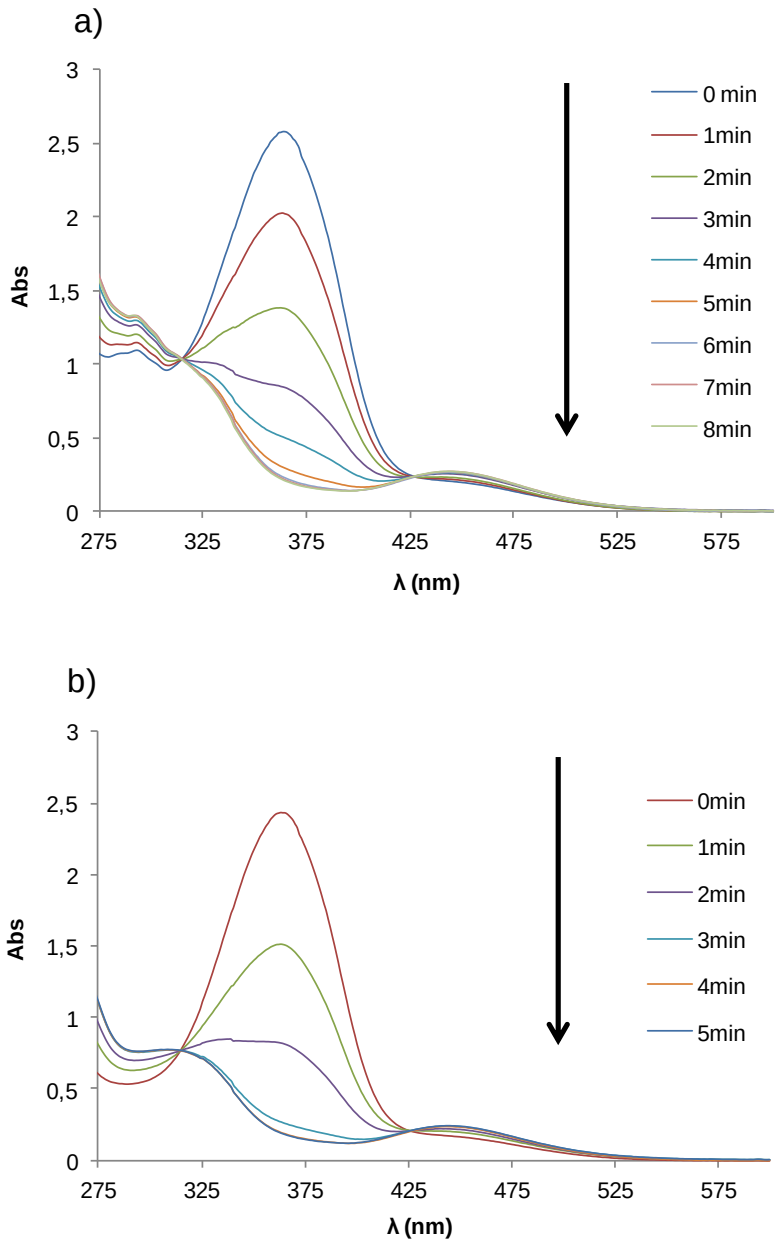

Fig. 5.14: a) Absorption spectra of a 10^{-4} M solution of **PEG_8-Phe-Azo-C_{18}** in DMSO under irradiation at 365 nm as a function of time, b) Absorption spectra of a 10^{-4} M solution of **PEG_{16}-Phe-Azo-C_{18}** in DMSO under irradiation at 365 nm as a function of time.

Studies by electronic circular dichroism (CD) were performed in order to get more insight into the chiral supramolecular organization as well as the possibility to control

the chiral structure by light. **PEG_8-Phe-Azo-C_{18}** gel, 5 wt % in DMSO and **Malt-Phe-Azo-C_{18}** gel, 0.5 wt % in 1-dodecanol were selected to register their CD spectrum. **Malt-Phe-Azo-C_{18}** was not soluble in DMSO and gel in 1-dodecanol was selected because the minimum concentration of gelification (0.5 wt %) is obtained for this solvent. A small amount of the gel was sandwiched between two quartz discs and measured (see **Characterization Techniques 7. Annex** for experimental conditions). We confirmed that the contribution of the linear dichroism (LD) to the CD spectra is negligible by comparing several CD spectra recorded at different angles around the incident light beam.

UV-vis absorption spectra in gel state of **PEG_8-Phe-Azo-C_{18}** at 5 wt % in DMSO shows a broader curve compared with solution and the λ_{max} value appears at around 362 nm, see **Fig. 5.15.a**. The λ_{max} value for a **Malt-Phe-Azo-C_{18}** organogel at 0.5 wt % in 1-dodecanol appears at around 339 nm, see **Fig. 5.15.b**. The maximums are blue-shifted due to the H-aggregation of azobenzene chromophores.

In the case of **PEG_8-Phe-Azo-C_{18}** gel at 5 wt % in DMSO, under UV irradiation (see **Fig. 5.15.a**) at 365 nm for 25 min (using the same irradiation conditions as in solution) a decrease in the *trans*-azobenzene UV band was observed. After irradiation for 45 min, UV-vis spectrum is more similar to the one exhibited by the *cis*-isomer, however, the *trans* to *cis* isomerization was clearer appreciated when the sample was irradiated for 3h. The photoisomerization was more hindered in the case of gel, due to the stronger self-assembly of the chromophores compared to solution. For **Malt-Phe-Azo-C_{18}** gel at 0.5 wt % in 1-dodecanol under irradiation at 365 nm, a photostationary state was reached after 10 min, see **Fig. 5.15.b**. Partial recovery of the initial UV-vis spectrum was achieved when gel samples were kept in the dark for 24 h.

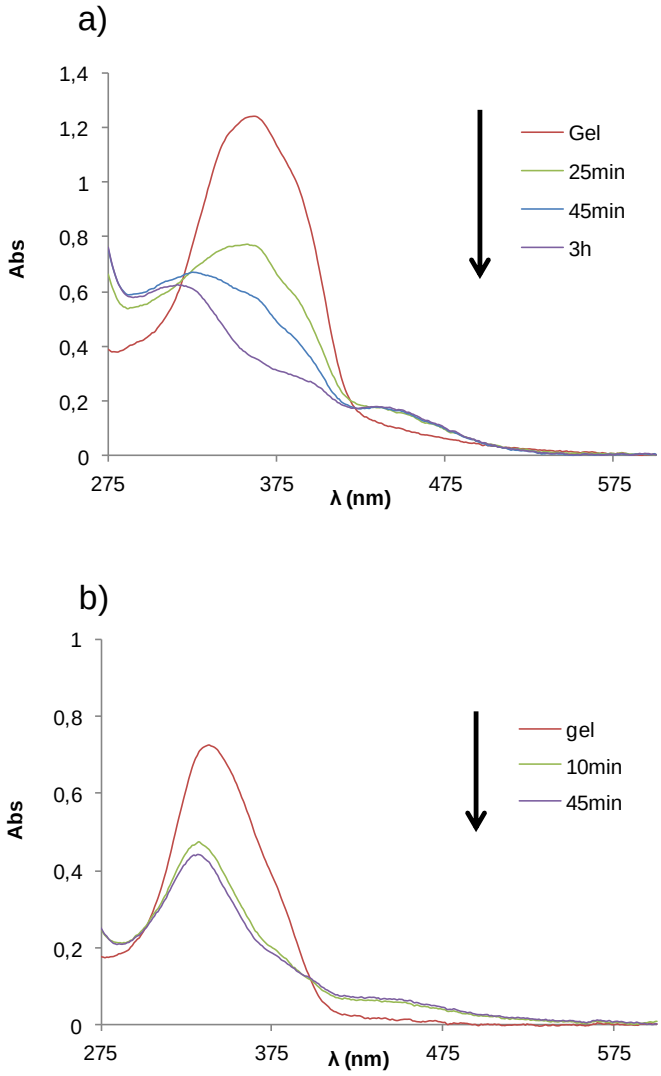

Fig. 5.15: a) Absorption spectra of **PEG$_8$-Phe-Azo-C$_{18}$** gel (5 wt % in DMSO) measured at RT, without irradiation, after 25 min of irradiation, after 45 min of irradiation and after 3 h of irradiation. b) Absorption spectra of **Malt-Phe-Azo-C$_{18}$** gel (0.5 wt % in 1-dodecanol) measured at RT, without irradiation, after 10 min of irradiation, after 45 min of irradiation.

As we can see in the CD spectra of these gels, see **Fig. 5.16**, for the organogel of **PEG$_8$-Phe-Azo-C$_{18}$** at 5 wt % in DMSO, a positive exciton coupling band was observed (see **Fig. 5.16.a)**, as well as for **Malt-Phe-Azo-C$_{18}$** gel at 0.5 wt % in 1-dodecanol (see **Fig. 5.16.b)**.

A decrease in the CD band was observed under UV irradiation at 365 nm for 3h for **PEG_8-Phe-Azo-C_{18}** gel at 5 wt % in DMSO (see **Fig. 5.16.a)**. Moreover the intersection for the CD signal was slightly displaced. UV irradiation at 365nm was also studied in **Malt-Phe-Azo-C_{18}** at 0.5 wt % in 1-dodecanol gel and only a slight decrease of the CD signal was observed in the photostationary state at 10 min (see **Fig. 5.16.b)**. In both cases, modifications in the CD signal along the isomerization were observed but disappearance of the aggregates was not fully obtained as there was not a complete disappearance of the signal. Once irradiated, the gel samples recovered its original CD spectra after 24h at darkness.

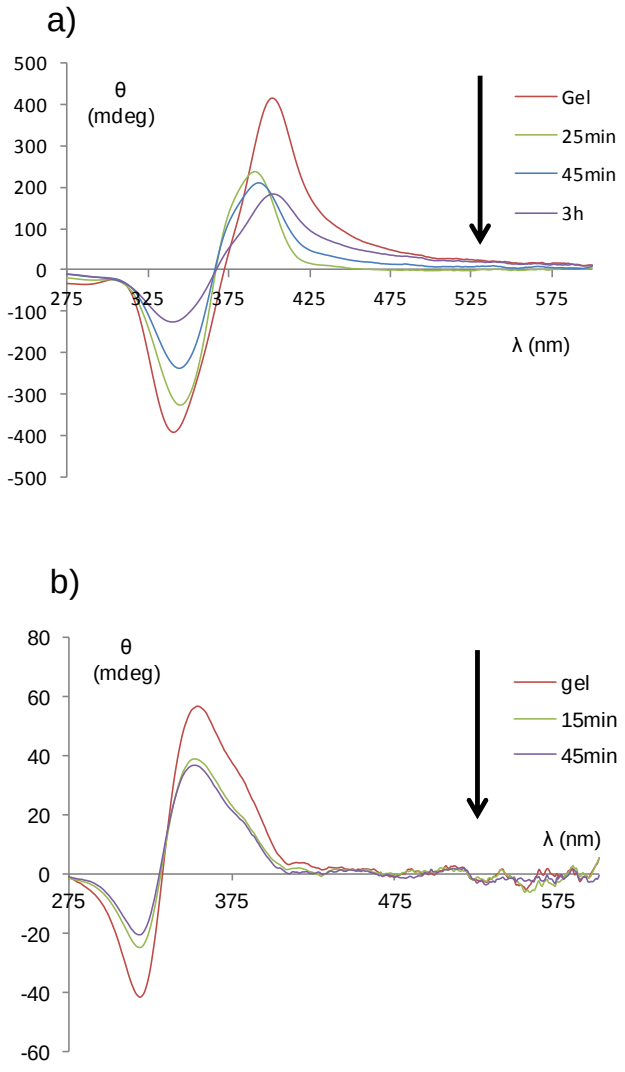

Fig 5.16: CD spectra of: a) **PEG_8-Phe-Azo-C_{18}** gel (5 wt % in DMSO) measured at RT, without irradiation, after 25min of irradiation, after 45min of irradiation, after 3 h of irradiation. b) **Malt-Phe-Azo-C_{18}** gel (0.5 wt % in 1-dodecanol) measured at RT, without irradiation, after 10 min of irradiation, after 45 min of irradiation.

Disruption of gels. Irradiation of the **PEG$_8$-Phe-Azo-C$_{18}$** gel (5 wt % in DMSO) and **Malt-Phe-Azo-C$_{18}$** gel (0.5 wt % in 1-dodecanol) were performed using a cuvette 1mm thickness in order to observe at naked eye if there was a sol-gel transition under irradiation. This transition was observed, in both cases, by using the same irradiation conditions as in CD studies. For **PEG$_8$-Phe-Azo-C$_{18}$** gel (5 wt % in DMSO), after 45 min of irradiation a partial dark red solution was observed at the bottom of the cuvette and after 3h almost all the gel was in sol state, see **Fig. 5.17.a**. Once irradiated, the sample did not totally gelify after 24h at darkness, however some aggregates were observed. Gel was recovered after approximately 96 h and sol state was again obtained under irradiation at 365 nm. For **Malt-Phe-Azo-C$_{18}$** gel (0.5 wt % in 1-dodecanol) a sol-gel transition was reached after 10 min of irradiation at 365 nm. Gel was formed again after approximately 6 h and sol state was again obtained under irradiation at 365 nm.

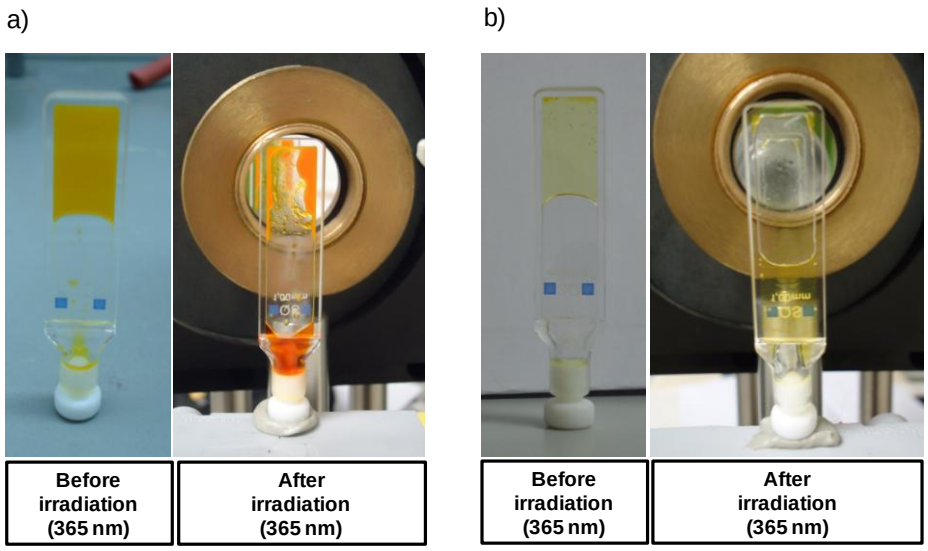

Fig 5.17: a) **PEG$_8$-Phe-Azo-C$_{18}$** gel (5 wt % in DMSO) before irradiation and after 3h of irradiation at 365 nm. b) **Malt-Phe-Azo-C$_{18}$** gel (0.5 wt % in 1-dodecanol) before irradiation and after 10 min of irradiation at 365 nm.

5.3. Summary and conclusions

- ✓ Amphiphilic molecules, based on a phenyl azobenzene hydrophobic chain, have been synthesized with different polar heads, as a phenylalanine group, a PEG derivative or maltose. Liquid crystalline and gel-forming properties have been determined. Chiral supramolecular assemblies have been characterized by electron microscopy and CD. The light-response of azo-amphiphiles compounds has been studied in solution and gel state.

    - Only **HOOC-Azo-C_{18}** exhibited liquid crystal properties. No mesomorphic behavior was found for **Phe-Azo-C_{18}, PEG_8-Phe-Azo-C_{18}**, **PEG_{16}-Phe-Azo-C_{18}** and **Malt-Phe-Azo-C_{18}** derivatives.

    - **HOOC-Azo-C_{18}, Phe-Azo-C_{18}, PEG_8-Phe-Azo-C_{18}** and **Malt-Phe-Azo-C_{18}** form gels in different organic solvents.

    - The hydrophobic/hydrophilic ratio is a key factor in the gel formation as detected in compounds with different molecular weight of PEG. While **PEG_8-Phe-Azo-C_{18}** is able to form organogels, gelation of **PEG_{16}-Phe-Azo-C_{18}** was not possible despite of forming fibrillar structures in solution.

    - By different microscopic techniques the resulting self-assembled fibrillar network was characterized and a supramolecular chiral arrangement was confirmed by CD.

    - **PEG_8-Phe-Azo-C_{18}** gel at 5 wt % in DMSO and **Malt-Phe-Azo-C_{18}** gel at 0.5 wt % in 1-dodecanol showed a gel-sol photoresponse to irradiation at UV light.

5.4. Experimental Section

For the synthesis of compound **13** ($C_{15}H_{14}N_2O_3$)**,** see **Chapter 4**, **Experimental Section 4.4**.

Synthesis of the ethyl 4-(octadecyloxy)-4'-(ethyloxycarbonyl)azobenzene ($C_{33}H_{50}N_2O_3$) **(22):**

Compound **13** (1.84 g, 7.4 mmol) was dissolved in acetone (30 mL), under an argon atmosphere, KI (0.28 g, 1.85 mmol) and K_2CO_3 (1.89 g, 1.48 mmol) was added. Once the solvent is refluxing the octadecyl bromide (2.72 g, 8.88 mmol) was added dropwise. The mixture was stirred for 24 hours. The reaction was monitored by TLC (hexane/ethyl acetate, 7:3). The solvent was partially removed. Dichloromethane (60 mL) was added and washed three times with water and dried with anhydrous $MgSO_4$. The product was recrystallized in ethanol yielding an orange solid (2.08 g, 55%).

^{1}H NMR (400 MHz, $CDCl_3$, δ ppm): 0.88 (t, 3 H, J=7.2 Hz, C*H*$_3$-$(CH_2)_{15}$-), 1.50-1.28 (m, 33 H, C*H*$_3$-CH_2-O-, -(C*H*$_2$)$_{15}$-), 1.86-1.79 (m, 2H, $(CH_2)_{15}$-C*H*$_2$-CH_2-O), 4.05 (t, 2H, J=6.8 Hz, -CH_2 -C*H*$_2$-O), 4.41 (q, 2H, J= 7.2 Hz, O-C*H*$_2$-CH_3), 7.02-7.00 (m, 2H, C*H*ar), 7.95-7.89 (m, 4H, C*H*ar), 8.18-8.16 (m, 2H, C*H*ar).

^{13}C (100 MHz, $CDCl_3$, δ ppm): 14.1, 14.3 *C*H_3-CH_2 x2, 22.7, 26.0, 29.2, 29.4, 29.6, 29.6, 29.7, 29.7, 31.9 *C*H_2 x16, 61.2, 68.4 O-*C*H_2 x2, 114.8, 122.3, 125.1, 130.5, *C*Har, 131.5, 146.8, 155.3, 162.4, 166.2 *C*ar, *C*O.

ESI$^+$: 523.4 $[M + H]^+$, 545.4 $[M + Na]^+$.

IR (KBr, cm^{-1}): 2916, 2848, 1715, 1601, 1584, 1472, 1463, 1283, 1251, 1142, 1106, 1020, 866, 841, 773, 695, 553.

Synthesis of 4-(octadecyloxy)-4'-(hydoxycarbonyl)azobenzene HOOC-Azo-C_{18} ($C_{31}H_{46}N_2O_3$)**:**

Compound **22** (2.08 g, 3.9 mmol) and KOH (1.58 g, 27.3 mmol) were dissolved in ethanol (50 mL) and stirred and heated under reflux for 24 hours. The reaction is monitored by TLC with dichloromethane as eluent. 70 mL of water was added. The product precipitated upon addition of HCl (37%) until pH 2. It was filtered and washed

with water. It was obtained as an orange powder which was recrystallized in acetic acid (1.55 g, 80%).

^{1}H NMR (400 MHz, DMSO, 90°C, δ ppm): 0.87 (t, 3H, J=7.2 Hz, C*H*$_3$-CH$_2$-), 1.47-1.27 (m, 30 H, –(C*H*$_2$)$_{15}$-), 1.80-1.76 (m,2H, (CH$_2$)$_{15}$-C*H*$_2$-CH$_2$-O-), 4.13 (t, 2H, J=6.4 Hz, CH$_2$-C*H*$_2$-O-), 7.13-7.11 (m, 2H, C*Har*), 7.91-7.86 (m, 4H, C*Har*), 8.12-8.10 (m, 2H, C*Har*).

^{13}C (100 MHz, DMSO, 90°C, δ ppm): 14.0, *C*H$_3$, 22.3, 25.8, 28.9, 29.1, 29.3, 29.3, 31.6, *C*H$_2$, 68.9 O-*C*H$_2$, 115.7, 122.4, 125.2, 130.8, *C*Har, 132.9, 147.0, 155.3, 162.6, 167.7 *C*ar, *C*O.

ESI^{+}: 495.4 [M + H]$^{+}$.

IR (KBr, cm^{-1}): 2918, 2849, 1680, 1602, 1583, 1501, 1471, 1419, 1290, 1249, 1143, 837, 544.

Synthesis of 4-(octadecyloxy)-4'-(succinimidyl-*N*-oxycarbonyl)azobenzene ($C_{35}H_{49}N_3O_5$) **(23):**

HOOC-Azo-C$_{18}$ (2.49 g, 5.04 mmol) was dissolved in 240 mL of anhydrous THF. This solution was heated until the benzoic acid was dissolved and a ***N***-hydroxysuccinimide (0.81 g, 7.13 mmol) in 40 mL of THF solution was added. The mixture was cooled to room temperature and then placed in a water-ice bath. Dicyclohexylcarbodiimide (DCC) (6.60 g, 32 mmol) was dissolved in 35 mL of THF and added to the mixture and was stirred for 96 h at room temperature. The reaction mixture was filtered and the solvent was distilled off. The product was recrystallized from isopropanol to obtain a red solid (2.56 g, 86%).

^{1}H NMR (400 MHz, CDCl$_3$, δ ppm): 0.87 (t, 3H, J=6.1 Hz, C*H*$_3$-CH$_2$-), 1.18-1.52 (m, 30 H, –(C*H*$_2$)$_{15}$-), 1.78-1.87 (m,2H, (CH$_2$)$_{15}$-C*H*$_2$-CH$_2$-O-), 2.92 (s, 4H, C*H*succ), 4.05 (t, 2H, J=6.5 Hz, CH$_2$-C*H*$_2$-O-), 6.99-7.05 (m, 2H, C*Har*), 7.92-7.99 (m, 4H, C*Har*), 8.24-8.29 (m, 2H, C*Har*).

^{13}C (100 MHz, CDCl$_3$, δ ppm): 14.1, *C*H$_3$-CH$_2$, 22.7, 25.7, 26.0, 29.2, 29.4, 29.6, 29.6, 29.7, 29.7, 31.9 *C*H$_2$ x16, 68.4 O-*C*H$_2$, 114.8, 122.7, 125.5, 131.7, *C*Har, 125.8, 146.8, 156.5, 161.5, 162.7, *C*ar, 169.2,*C*O succ x2.

ESI$^+$: 592.4 $[M + H]^+$.

IR (KBr, cm^{-1}): 2918, 2848, 1775, 1733, 1583, 1500, 1467, 1244, 1208, 1081, 1003, 863, 686, 549.

Synthesis of Phe-Azo-C_{18} ($C_{40}H_{55}N_3O_4$):

L-Phenylalanine (0.66 g, 3.99 mmol) and diisopropylethylamine (1.40 mL, 8.12 mmol) were dissolved in 25 mL of water and 30 mL of THF. A solution of **23** (2.40 g, 4.06 mmol) in 100 mL of THF was added. The mixture was stirred at room temperature for 60 h. The reaction was monitored by TLC using hexane/ethyl acetate 1:1 as eluent. A solution of HCl (37%) was added until pH = 4. The solvent was partially removed and the resulting aqueous phase was extracted with dichloromethane (3 × 250 mL). The organic layer was dried with anhydrous $MgSO_4$ and finally the solvent was evaporated. The product was purified by flash chromatography using dichloromethane and increasing the polarity with methanol. A red solid was obtained (1.502 g, 58%).

^{1}H(300 MHz, $CDCl_3$, δ ppm): 0.88 (t, 3H, J= 6.7 Hz, CH_2-C*H*$_3$), 1.26-1.50 (m, 30H, -(C*H*$_2$)$_{15}$-), 1.78-1.87 (m, 2H, –O-CH_2-C*H*$_2$), 3.24-3.46 (m, 2H, –CH-C*H*$_2$-ar), 4.05 (t, 2H, J=6.6 Hz, -O-C*H*$_2$-CH_2-), 5.07-5.17 (m, 1H, -C*H*-CH_2-ar), 6.59 (d, 1H, J=7.2 Hz, N*H*-CO-), 6.99-7.02 (m, 2H, *Har*-C-O-CH_2-), 7.22-7.73 (m, 6H, *Har*), 7.80-7.94 (m, 5H, *Har*).

^{13}C (75 MHz, $CDCl_3$, δ ppm): 14.1 CH_2-*C*H_3, 22.7, 26.0, 29.2, 29.4, 29.5, 29.6, 29.7, 29.7, 31.9,-*C*H_2-, 37.2 –CH-*C*H_2-ar, 53.7 -*C*H-CH_2-ar, 68.5 O-*C*H_2-CH_2-, 114.8, 122.7, 125.2, 127.4, 128.0, 128.8, 129.4 *C*Har, 134.3, 135.5, 146.8, 155.8, 162.3 *C*ar, 167.0 NH-*C*O, 174.3 *C*OOH.

MALDI-TOF (DCTB+NaTFA): 686.7 $[M+2Na]^+$, 664.6 $[M+Na]^+$, 642.6 $[M+H]^+$.

Anal. Calcd. for **$C_{40}H_{55}N_3O_4$**: C, 74.85; H, 8.64; N, 6.55. Found: C, 74.75; H, 8.65; N, 6.44.

IR (KBr, cm^{-1}): 3316, 2919, 2850, 1644, 1527, 1252, 1143, 838.

Synthesis of PEG_8-Phe-Azo-C_{18} and PEG_{16}-Phe-Azo-C_{18}:

Phe-Azo-C_{18} (305 mg, 0.47 mmol) and hydroxybenzotriazole (80 mg, 0.59 mmol) were dissolved in 20 mL of anhydrous THF. Methyl-PEGn-amine (n=8, from Fisher

Scientific or 16, from Fluka) (200 mg, 0.52 mmol) was added. The solution was cooled to 0 ºC. 1-Ethyl-3-(3-dimethyllaminopropyl)carbodiimide hydrochloride (101 mg, 0.52 mmol) was added. The reaction mixture was stirred for 2 days at room temperature. The reaction was monitored by TLC with hexane/ethyl acetate 1:9 as eluent. The mixture was filtered and the solvent was removed under reduced pressure. 250 mL of dichloromethane were added and the organic phase was washed three times with 1M $KHSO_4$ solution, and three times with 1M $NaHCO_3$ solution. The organic layer was dried over anhydrous $MgSO_4$. The solution was filtered and the solvent was removed under reduced pressure. The product was purified by flash chromatography using dichloromethane and increasing the polarity with methanol. A red solid was obtained (0.401 mg, 85% for **PEG_8-Phe-Azo-C_{18}**, 315 mg, 84% **PEG_{16}-Phe-Azo-C_{18}**).

PEG_8-Phe-Azo-C_{18}

^{1}H(500 MHz, $CDCl_3$ δ ppm): 0.87 (t, 3H, J= 6.7Hz, CH_2-C*H*$_3$), 1.16-1.53 (m, 30H, -(C*H*$_2$)$_{15}$-), 1.78-1.85 (m, 2H, -O-CH_2-C*H*$_2$), 3.10-3.29 (m, 2H, -CH-C*H*$_2$-ar), 3.36 (s, 3H,–O-C*H*$_3$), 3.32-3.73 (m, 32H, –(O-C*H*$_2$-C*H*$_2$)$_7$-O, -O-C*H*$_2$-C*H*$_2$-NH-), 4.05 (t, 2H, J= 6,5Hz, -O-C*H*$_2$-CH_2-), 4.77-4.86 (m, 1H, -C*H*-CH_2-ar), 6.28 (s, 1H, CH_2-CH_2-N*H*-CO), 6.97-7.07 (m, 3H, *Har*-C-O-CH_2-, ar-CH-N*H*-CO), 7.20-7.37 (m, 5H, *Har*), 7.85-7.99 (m, 6H, *Har*).

^{13}C (125 MHz, $CDCl_3$ δ ppm): 14.1 CH_2-*C*H_3, 22.7, 26.0, 29.2, 29.4, 29.4, 29.5, 29.5, 29.6, 29.7, 31.9 -*C*H_2-, 38.9 –CH-*C*H_2-ar, 39.4 –O-CH_2-*C*H_2-NH, 55.1 -*C*H-CH_2-ar, 59.0 -O-*C*H_3, 68.5 O-*C*H_2-CH_2-, 69.5, 70.3, 70.5, 70.5, 71.9 –(O-*C*H_2-*C*H_2)n-O, -O-*C*H_2-*C*H_2-NH-, 114.7, 122.6, 125.0, 127.0, 128.0, 128.7, 129.4 *C*Har, 134.9, 136.7, 146.8, 154.6, 162.2, 166.2, 170.6 *C*ar, ar-*C*H-NH-CO, CH_2-CH_2-NH-*C*O-.

MALDI-TOF (DCTB+NaTFA): 1029.8 [M (n=8) +Na]$^+$.

Anal. Calcd for $C_{57}H_{90}N_4O_{11}$: C, 67.96; H, 9.01; N, 5.56. Found: C, 68.08 ; H, 9.59 ; N, 5.58.

IR (KBr, cm^{-1}): 3301, 2920, 2850, 1636, 1530, 1251, 1143, 1105, 859, 837, 698.

PEG_{16}-Phe-Azo-C_{18}

^{1}H(300 MHz, $CDCl_3$ δ ppm): 0.81 (t, 3H, J= 6.7Hz, CH_2-C*H*$_3$), 1,04-1,40 (m, 30H, -(C*H*$_2$)$_{15}$-), 1.70-1.81 (m, 2H, –O-CH_2-C*H*$_2$), 3.04-3.22 (m, 2H, –CH-C*H*$_2$-ar), 3.31 (s,

3H, –O-C*H*$_3$), 3.32-3.70 (m, nH, –(O-C*H*$_2$-C*H*$_2$)n-O, -O-C*H*$_2$-C*H*$_2$-NH-), 3.98 (t, 2H, J= 6.5Hz, -O-C*H*$_2$-CH$_2$-), 4.73-4.84 (m, 1H, -C*H*-CH$_2$-ar), 6.60 (s, 1H, CH$_2$-CH$_2$-N*H*-CO-), 6.92-6.95 (m, 2H, *Har*-CO-CH$_2$-), 7,04 (d, 1H, J= 7.6 Hz, ar-CH-N*H*-CO), 7.16-7.26 (m, 5H, *Har*), 7.82-7.87 (m, 6H, *Har*).

^{13}C (100 MHz, $CDCl_3$, δ ppm): 14.1 CH$_2$-*C*H$_3$, 22.7, 26.0, 29.2, 29.4, 29.4, 29.5, 29.5, 29.6, 29.7, 31.9,-*C*H$_2$-, 38.9 –CH-*C*H$_2$-ar, 39.4 –O-CH$_2$-*C*H$_2$-NH, 54.9 -*C*H-CH$_2$-ar, 59.1 –O-*C*H$_3$, 68.5 O-*C*H$_2$-CH$_2$-, 69.5, 70.3, 70.5, 71.9 –(O-*C*H$_2$-*C*H$_2$)n-O, -O-*C*H$_2$-CH$_2$-NH-, 114.7, 122.5, 125.0, 126.9, 128.0, 128.5, 129.4 *C*Har, 134.3, 136.7, 146.8, 154.6, 162.2, 166.2, 170.6 Car, ar-*C*H-NH-CO, CH$_2$-CH$_2$-NH-*C*O-.

MALDI-TOF (DCTB+NaTFA): 1249.8 [M (n=13) +Na]$^+$, 1293.8 [M (n=14) +Na]$^+$, 1337.8 [M (n=15) +Na]$^+$, 1381.9 [M (n=16) +Na]$^+$, 1425.9 [(M (n=17) +Na]$^+$, 1469.9 [M (n=18) +Na]$^+$, 1513.9 [M (n=19) +Na]$^+$, 1558.0 [M (n=20) +Na]$^+$, 1603.0 [M (n=21) +Na]$^+$, 1646.0 [M (n=22) +Na]$^+$, 1690.0 [M (n=23) +Na]$^+$, 1734.0 [M (n=24) +Na]$^+$.

IR (KBr, cm^{-1}): 3300, 2920, 2850, 1636, 1531, 1251, 1144, 1107, 838.

Synthesis and characterization of Hepta-O-acetyl-β-maltosyl azide ($C_{26}H_{35}N_3O_{17}$) (**5**) and **Synthesis of Hepta-O-acetyl-β-maltosyl amine** ($C_{26}H_{37}NO_{17}$) **(6)** were previously described in **Chapter 3**, please see **Experimental Section 3.7** for data.

Synthesis of *N*-[4- (4´-octadecyloxyphenylazido)phenylcarbonyl L-phenylalanyl chloride (24):

Phe-Azo-C$_{18}$ (740 mg, 1.15 mmol) was dissolved in 25 mL of anhydrous THF. Oxalyl chloride (0.30 mL, 2.81 mmol) and anhydrous DMF (0.3 mL) were added. The reaction mixture was stirred overnight. The solvent was removed under reduced pressure. The product was used without further purification.

Synthesis of acetylated maltose conjugate OAc-Malt-Phe-Azo-C$_{18}$ ($C_{66}H_{90}N_4O_{20}$)**:**

Compound **6** (0.94 mmol) was dissolved in 10 mL of anhydrous DMF. Pyridine (0.1 mL, 1.24 mmol) was added and the solution was cooled to 0 ºC. A solution of compound **7** (1.15 mmol) in 10 mL of anhydrous DMF and 15 mL of THF was added. 20 mL of THF were added to complete solubilization. The reaction mixture was stirred for 48 h at room temperature and poured into 150 mL of water. The aqueous phase was extracted with 3 × 150 mL of hexane/ethyl acetate 1:1. The organic phase was dried

with anhydrous $MgSO_4$. The solution was filtered and the solvent was removed under reduced pressure. The resulting product was purified by flash chromatography with dichloromethane/ethyl acetate 8:2 as eluent. A red solid was obtained (646.2 mg, 54%).

^{1}H NMR (500 MHz, $CDCl_3$): 0.88 (t, 3H, J = 6.8 Hz, -$(CH_2)_{15}$-C*H*$_3$), 1.19-1.53 (m, 30H, CH_2-(C*H*$_2$)$_{15}$-CH_3), 1.78-1.87 (m, 2H, –CH_2-C*H*$_2$-$(CH_2)_{15}$), [1.85, 1.97, 2.00, 2.02, 2.03, 2.04, 2.05, 2.06, 2.09, 2.11, 2.12, 2.18] (s, 21H), 3.14-3.36 (m, 2H, CH-C*H*$_2$-Car-), 3.77-3.85 (m, 1H, *H5´*), 3.91-3.99 (m, 2H, *H5*, *H4´*), 4.05 (t, 2H, J = 7.3 Hz, –O-C*H*$_2$-CH_2), 3.99-4.08 (m, 1H, *H6b*), 4.19-4.31 (m, 2H, *H6a*, *H6´a*), 4.43-4.50 (m, 1H, *H6´a*), 4.68-4.78 (m, 1H, *H2´*), 4.79-4.90 (m, 2H, NH-*CH*-CH_2, *H2*), 5.01-5.11 (m, 1H, *H4*), 5.27 (dd, 1H, $J_{1´,2´}$= 8.9 Hz, $J_{1´,NH}$ = 8.9 Hz, *H1´*), 5.32-5.41 (m, 3H, *H1*, *H3*, *H3´*), 6.52 (dd, 1H, J=7.5 Hz, J= 69.2 Hz, N*H*-CH), 6.86 (dd, J=8.9 Hz, J= 41.5 Hz, N*H*-C1), 6.88-7.04 (m, 2H, *Har*), 7.18-7.35 (m, 4H, *Har*), 7.36-7.45 (m, 1H, *Har*), 7.73-7.79 (m, 1H, *Har*), 7.81-7.85 (m, 1H, *Har*), 7.85-7.97 (m, 4H, *Har*).

^{13}C NMR (125 MHz, $CDCl_3$): 14.1 -$(CH_2)_{15}$-*C*H_3, 20.5, 20.6, 20.6, 20.8, 20.8, 20.8, 22.6, 26.0, 29.1, 29.3, 29.5, 29.5, 29.6, 29.6, 31.9 (*C*H_3-CO-O), -(*C*H_2)$_{16}$-, 37.3, 37.4 CH-*C*H_2-Car, 54.5 *C*H-CH_2-Car, 61.4 *C6*, 62.6 *C6´*, 67.9 *C4*, 68.4 –O-CH_2-CH_2, 68.5 *C5*, 69.3 *C3/C3´*, 70.0 *C2*, 70.8, 71.1 *C2´*, 72.5, 72.6 *C4´*, 73.9 *C5´*, 74.8, 74.9 *C3/C3´*, 77.7, 78.0 *C1´*, 95.5 *C1*, 114.8, 122.6, 125.1, 127.3, 127.4, 127.9, 128.0, 128.8, 128.9, 129.2, 129.5, *C*Har, 134.2, 134.3, 135.6, 135.8, 146.7, 154.8, 162.3, *C*ar, 166.7, 166.8 CH-NH-*C*O-Car, 169.4, 169.7, 169.8, 170.4, 170.5, 170.6 CH_3-*C*O-O-CH_3, Car, 170.9, 171.1 C1´-NH-*C*O, 171.4 *C*ar-CH_2.

MALDI-TOF MS (DIT+NaTFA): 1281.2 $[M + Na]^+$.

IR (KBr, cm^{-1}): 3335, 2920, 2850, 1750, 1639, 1526, 1370, 1239, 1033, 859, 601.

Anal. Calcd for $C_{42}H_{67}NO_{18}$: C, 62.94; H, 7.20; N, 4.45. Found: C, 63.44 ; H, 7.56 ; N, 4.45.

Synthesis of Malt-Phe-Azo-C$_{18}$ ($C_{52}H_{76}N_4O_{13}$)**:**

OAc-Malt-Phe-Azo-C$_{18}$ (131.1 mg, 0.10 mmol) were dissolved in 5 mL of anhydrous methanol. Sodium methoxide (50.0 mg, 0.92 mmol) was then added. The solution was stirred at room temperature until the reaction was complete (TLC, dichloromethane/ethyl acetate 1:1). Amberlyst IR 120 (H^+ form) was added to exchange

sodium ions until pH 7-6. The resin was filtered off and the solvent was evaporated in vacuum to give a red solid (58 mg, 60%).

^{1}H NMR (500 MHz, DMSO, δ ppm): 0.85 (t, 3H, J = 6.7 Hz, -$(CH_2)_{15}$-C*H*$_3$), 1.17-1.49 (m, 30H, CH_2-(C*H*$_2$)$_{15}$-CH_3), 1.70-1.78 (m, 2H, –CH_2-*C*H_2-$(CH_2)_{15}$), 2.99-3.92 (m, 14H, CH-*C*H_2-Car-, *H2*, *H3*, *H4*, *H5*, *H6a*, *H6b*, *H2´*, *H3´*, *H4´*, *H5´*, *H6´a*, *H6´b*), 4.09 (t, 2H, J = 6.4 Hz, –O-C*H*$_2$-CH_2), 4.16-4.31 (m, 2H, O*H*), 4.49-4.72 (m, 2H, O*H*), 4.77-4.90 (m, 2H, NH-C*H*-CH_2, *H1´*), 5.01-5.09 (m, 1H, *H1*), 5.09-5.22 (m, 1H, O*H*), 5.29-5.45 (m, 2H, O*H*), 7.06-7.41 (m, 7H, *Har*), 7.78-7.99 (m, 6H, *Har*), 8.36-8.46 (m, 1H, N*H*-CO), 8.56 (t, 1H, N*H*-C1´).

^{13}C NMR (125 MHz, DMSO, δ ppm): 13.5 -$(CH_2)_{12}$-*C*H_3, 21.7, 25.2, 28.4, 28.7, 31.0 -CO-*C*H_2-(*C*H_2)$_{13}$-CH_3, 37.3 CH-*C*H_2-Car, 54.6, 54.7 *C*H-CH_2-Car, 68.1, –O-*C*H_2-CH_2, 61.0, 70.2, 71.7, 72.0, 72.2, 72.4, 73.3, 76.9, 77.1, 79.3, *C2*, *C3*, *C4*, *C5*, *C6*, *C2´*, *C3´*, *C4´*, *C5´*, *C6´*, 79.9 *C1´*, 100.6 *C1*, 115.0, 121.6, 124.6, 125.9, 127.8, 128.3, 129.0 *C*Har, 135.6, 137.9, 138.0, 146.2, 153.6, 165.4, 171.6 *C*ar, CH-NH-*C*O-Car, C1´-NH-*C*O.

MicroTOF MS: 987.5253 $[M+ Na]^+$, calcd: 987.5403.

IR (KBr, cm^{-1}): 3307, 2917, 2849, 1635, 1539, 1250, 1034, 856, 836.

5.5. References

1. Weiss, R. G.; Terech, P., *Molecular gels*. Springer: Dordrecht, 2006.
2. (a) del Barrio, J.; Oriol, L.; Alcala, R.; Sanchez, C., Azobenzene-Containing Linear-Dendritic Diblock Copolymers by Click Chemistry: Synthesis, Characterization, Morphological Study, and Photoinduction of Optical Anisotropy. *Macromol.* **2009,** *42* (15), 5752-5760; (b) del Barrio, J.; Oriol, L.; Sanchez, C.; Serrano, J. L.; Di Cicco, A.; Keller, P.; Li, M.-H., Self-Assembly of Linear-Dendritic Diblock Copolymers: From Nanofibers to Polymersomes. *J. Am. Chem. Soc.* **2010,** *132* (11), 3762-3769.
3. Roberts, M. J.; Bentley, M. D.; Harris, J. M., Chemistry for peptide and protein PEGylation. *Adv. Drug Del. Rev.* **2002,** *54* (4), 459-476.
4. (a) Adams, D. J.; Topham, P. D., Peptide conjugate hydrogelators. *Soft Matt.* **2010,** *6* (16), 3707-3721; (b) Peppas, N. A.; Bures, P.; Leobandung, W.; Ichikawa, H., Hydrogels in pharmaceutical formulations. *Eur. J. Pharm. Biopharm.* **2000,** *50* (1), 27-46; (c) Peppas, N. A.; Keys, K. B.; Torres-Lugo, M.; Lowman, A. M., Poly(ethylene glycol)-containing hydrogels in drug delivery. *J. Controlled Release* **1999,** *62* (1-2), 81-87; (d) Suzuki, M.; Hanabusa, K., Polymer organogelators that make supramolecular organogels through physical cross-linking and self-assembly *Chem. Soc. Rev.* **2010,** *39* (12), 455-463; (e) Tomatsu, I.; Peng, K.; Kros, A., Photoresponsive hydrogels for biomedical applications. *Adv. Drug Del. Rev.***2011,** *63* (14-15), 1257-1266.
5. (a) Dankers, P. Y. W.; van Luyn, M. J. A.; Huizinga-van der Vlag, A.; van Gemert, G. M. L.; Petersen, A. H.; Meijer, E. W.; Janssen, H. M.; Bosman, A. W.; Popa, E. R., Development and in-vivo characterization of supramolecular hydrogels for intrarenal drug delivery. *Biomat.* **2012,** *33* (20), 5144-5155; (b) Tamiaki, H.; Ogawa, K.; Enomoto, K.; Taki, K.; Hotta, A.; Toma, K., Supramolecular gelation of alcohol and water by synthetic amphiphilic gallic acid derivatives. *Tetrahedron* **2010,** *66* (9), 1661-1666.
6. (a) Jeong, B.; Bae, Y. H.; Kim, S. W., Thermoreversible gelation of PEG-PLGA-PEG triblock copolymer aqueous solutions. *Macromol.* **1999,** *32* (21), 7064-7069; (b) Lowman, A. M.; Morishita, M.; Kajita, M.; Nagai, T.; Peppas, N. A., Oral delivery of insulin using pH-responsive complexation gels. *J. Pharm. Sci.* **1999,** *88* (9), 933-937; (c) Da, J.; Hogen-Esch, T. E., Poly(N,N-dimethylacrylamide)s with perfluorocarbon pendent groups connected through poly(ethylene glycol) tethers give physical gels in organic solvents. *Macromol.* **2003,** *36* (25), 9559-9563; (d) Li, Z.; Yin, H.; Zhang, Z.; Liu, K. L.; Li, J., Supramolecular Anchoring of DNA Polyplexes in Cyclodextrin-Based Polypseudorotaxane Hydrogels for Sustained Gene Delivery. *Biomacromol.* **2012,** *13* (10), 3162-3172; (e) Zhu, W.; Li, Y.; Liu, L.; Chen, Y.; Xi, F., Supramolecular hydrogels as a universal scaffold for stepwise delivering Dox and Dox/cisplatin loaded block copolymer micelles. *Int. J. Pharm.* **2012,** *437* (1-2), 11-9.
7. Peng, K.; Tomatsu, I.; van den Broek, B.; Cui, C.; Korobko, A. V.; van Noort, J.; Meijer, A. H.; Spaink, H. P.; Kros, A., Dextran based photodegradable hydrogels formed via a Michael addition. *Soft Matt.* **2011,** *7* (10), 4881-4887.
8. Hirst, A. R.; Escuder, B.; Miravet, J. F.; Smith, D. K., High-Tech Applications of Self-Assembling Supramolecular Nanostructured Gel-Phase Materials: From Regenerative Medicine to Electronic Devices. *Ang. Chem.-Int. Ed.* **2008,** *47* (42), 8002-8018.
9. Tzokova, N.; Fernyhouph, C. M.; Topham, P. D.; Sandon, N.; Adams, D. J.; Butler, M. F.; Armes, S. P.; Ryan, A. J., Soft Hydrogels from Nanotubes of Poly(ethylene oxide) -Tetraphenylalanine Conjugates Prepared by Click Chemistry. *Langmuir* **2009,** *25* (4), 2479-2485.

10. (a) Borner, H. G.; Smarsly, B. M.; Hentschel, J.; Rank, A.; Schubert, R.; Geng, Y.; Discher, D. E.; Hellweg, T.; Brandt, A., Organization of self-assembled peptide-polymer nanofibers in solution. *Macromol.* **2008,** *41* (4), 1430-1437; (b) Hamley, I. W.; Ansari, A.; Castelletto, V.; Nuhn, H.; Rosler, A.; Klok, H. A., Solution self-assembly of hybrid block copolymers containing poly(ethylene glycol) and amphiphilic beta-strand peptide sequences. *Biomacromol.* **2005,** *6* (3), 1310-1315; (c) Hentschel, J.; Krause, E.; Borner, H. G., Switch-peptides to trigger the peptide guided assembly of poly(ethylene oxide)-peptide conjugates into tape structures. *J. Am. Chem. Soc.* **2006,** *128* (24), 7722-7723.
11. (a) Jing, P.; Rudra, J. S.; Herr, A. B.; Collier, J. H., Self-assembling peptide-polymer hydrogels designed from the coiled coil region of fibrin. *Biomacromol.* **2008,** *9* (9), 2438-2446; (b) Brizard, A.; Stuart, M.; van Bommel, K.; Friggeri, A.; de Jong, M.; van Esch, J., Preparation of nanostructures by orthogonal self-assembly of hydrogelators and surfactants. *Ang. Chem.-Int. E.* **2008,** *47* (11), 2063-2066.
12. Suzuki, M.; Yanagida, R.; Setoguchi, C.; Shirai, H.; Hanabusa, K., New polymer organogelators with L-isoleucine and L-valine as a gelation-causing segment: Organogelation by a combination of supramolecular polymer and conventional polymer. *J. Pol. Sci. Part a-Pol. Chem.* **2008,** *46* (1), 353-361.
13. Goodby, J. W.; Gortz, V.; Cowling, S. J.; Mackenzie, G.; Martin, P.; Plusquellec, D.; Benvegnu, T.; Boullanger, P.; Lafont, D.; Queneau, Y.; Chambert, S.; Fitremann, J., Thermotropic liquid crystalline glycolipids. *Chem. Soc. Rev.* **2007,** *36* (12), 1971-2032.
14. Sano, M.; Kunitake, T., Influence of phase and chain-length of Liquid-Crystals on wetting phenomena of graphite. *Langmuir* **1992,** *8* (1), 320-323.
15. Zhou, Y. F.; Yi, T.; Li, T. C.; Zhou, Z. G.; Li, F. Y.; Huang, W.; Huang, C. H., Morphology and Wettability tunable two-dimensional superstructure assembled by hydrogen bonds and hydrophobic interactions. *Chem. Mat.* **2006,** *18* (13), 2974-2981.
16. Zhang, L. F.; Eisenberg, A., Structures of "crew-cut" aggregates of polystyrene-b-poly(acrylic acid) diblock copolymers. *Macromol. Symp.* **1997,** *113*, 221-232.

6. CONCLUSION

Once presented the main conclusions of the different chapters, the following general conclusions can be obtained from this work:

- Glycoamphiphilic compounds based on disaccharides are molecules of interest to obtain different soft materials based on supramolecular gels. Variations in the molecular structure make possible variations in gel properties.

- Copper(I)-catalysed azide-alkyne [3+2] cycloaddition is a versatile synthetic tool for the preparation of glycoamphiphilic compounds and the presence of the triazole linking unit improves the gelation ability in water.

- Chiral supramolecular aggregation of the glycoamphiphiles, which is responsible of the entangled 3D-network to form the gel, is determined by the sugar unit of the structure.

- Supramolecular gels based on glyco and PEG azoderivatives give rise to photoresponsive materials. Chiroptical properties can be modulated by light and in some cases gel to sol state transition can be reached.

7. ANNEX

7.1. Characterization Techniques

^{1}H and ^{13}C NMR spectra were recorded on a BRUKER AV-400 (operating at 400 MHz for ^{1}H and 100 MHz for ^{13}C) or AV-500 (operating at 500 MHz for ^{1}H and 125 MHz for ^{13}C) spectrometer.
IR spectra were measured on Thermo NICOLET Avatar 360 FT-IR spectrophotometer using KBr pellets.

Mass Spectrometry was performed using a ESI Brüker Esquire 300+, a MALDI+/TOF Brüker Microflex system with a different matrix depending on the compound and MicroTOF Brüker equipment for exact mass measurements.

Elemental analysis was performed using a Perkin Elmer CHN2400 microanalizer.

The mesogenic behavior was studied by optical microscopy with an Olympus BH-2 polarizing microscope equipped with a Linkam THMS hot-stage central processor and a CS196 cooling system.

Differential scanning calorimetry (DSC) was performed using a DSC Q2000 from TA Instruments with samples sealed in aluminum pans and a scanning rate of 10 or 5 ºC/min under nitrogen atmosphere. Temperatures were read at the maximum of the transition peaks and glass transition at the midpoint of the jump of the baseline.

Thermogravimetric analysis (TGA) was performed using a TGA Q5000IR fromTA Instruments at a rate of 10 ºC/min under nitrogen atmosphere (at 600ºC, nitrogen atmosphere was changed and air was used).

XRD measurements were performed with an evacuated Pinhole camera (Anton-Paar) operating with a point-focused Ni-filtered Cu-Kα beam. Sample was held in Lidemann glass capillaries and the patterns were collected on flat photographic films perpendicular to the X-ray beam.

Circular Dichroism was measured using a Jasco J-180 equipment. The CD spectra of the samples were registered by rotating the sandwich every 60 degrees around the light beam axis. Sample preparation for CD measurement: **Malt-Tz-Azo-C_{16}** and **Malt-Tz-C_{10}-Azo-OCH_3** gels were heated up to the sol state and a drop of hot solution was placed and sandwiched between two quartz plates with a 25 μm spacer. Once cooled to

room temperature the gel is reformed. **Malt-Tz-C_{16}**, **Cell-Tz-C_{16}**, **Lact-Tz-C_{16}**, **Gel I** and **Gel II** were placed onto the sandwich at RT. **PEG_8-Phe-Azo-C_{18}** gel (5 wt % in DMSO) was placed onto the sandwich at RT with a 25 μm spacer and **Malt-Phe-Azo-C_{18}** gel (0.5 wt % in dodecanol) was placed onto the sandwich at RT with a 100 μm spacer. Spacers were selected in order to reach an absorption sample below 2.

Irradiation with UV light was carried out using an Hg lamp (1000 W, Oriel) with a IR water filter and an absorption filter 365 nm ± 5nm. Power used was 3.4 ± 0.3 mW/cm^2.

SEM measurements were performed using a JEOL JSM 6400 at the laboratory of 'Servicio de Microscopia de la Universidad de Zaragoza'. The sample was fixed onto glass and coated with gold. FESEM measurements were performed using a Carl Zeiss MERLIN^{TM} equipment at the laboratory of 'Servicio de Microscopia de la Universidad de Zaragoza'. The sample was fixed onto glass and coated with platinum. ESEM measurements were performed using a QUANTA FEG 250 equipment at the Laboratory of Advanced Microscopy (LMA) of the INA (Instituto de Nanociencia de Aragón). TEM measurements were performed using a TECNAI G^2 20 (FEI COMPANY), 200 kV, at the Laboratory of Advanced Microscopy (LMA) of the 'Instituto de Nanociencia de Aragon'. For TEM sample preparation, a drop of the solution (gel diluted depending on the sample) was placed on a copper grid and left to dry for 15 min. The copper grid was then placed again over a drop of 1% uranyl acetate solution as a negative stain for 30 s and was then left to dry. CryoTEM measurements were performed in this microscope with a cryo-holder. AFM measurements were performed using a VEECO MULTIMODE 8, mode tapping and tips 20-80 nN/m and υ 300 kHz at Laboratory of Advanced Microscopy (LMA) of the INA (Instituto de Nanociencia de Aragón).

7.2. ^{1}H NMR of final products

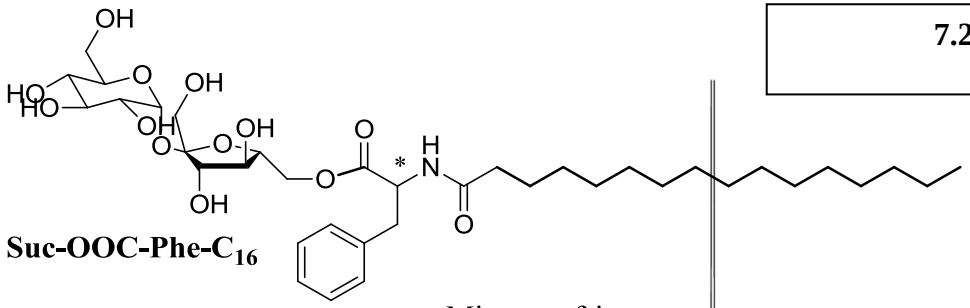

Suc-OOC-Phe-C_{16}

Mixture of isomers

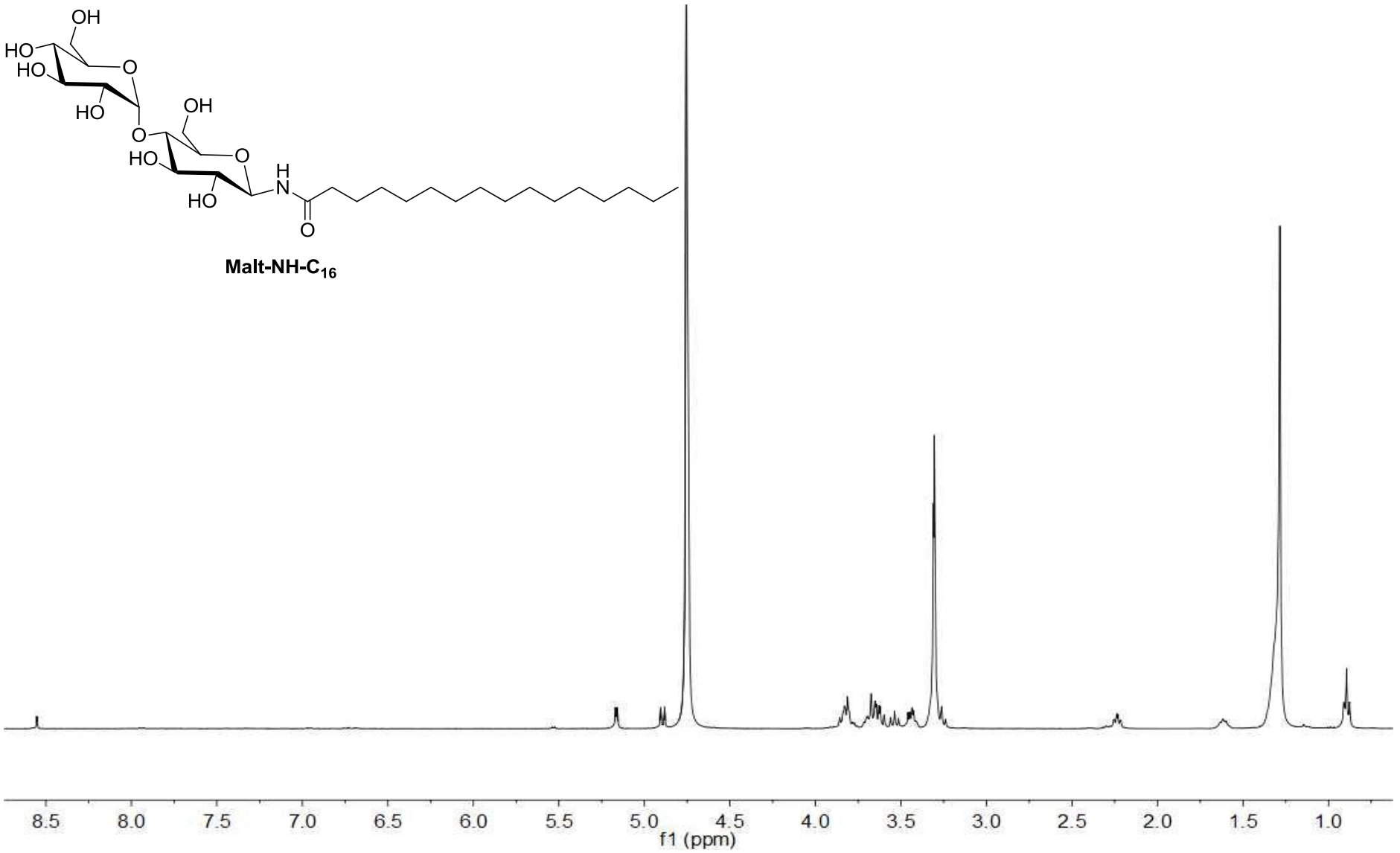
OH
HO
HO
O
HO
OH
O
HO
O
H
N
HO
O
Malt-NH-C16
8.5
8.0
7.5
7.0
6.5
6.0
5.5
5.0
4.5
4.0
3.5
3.0
2.5
2.0
1.5
1.0
f1 (ppm)

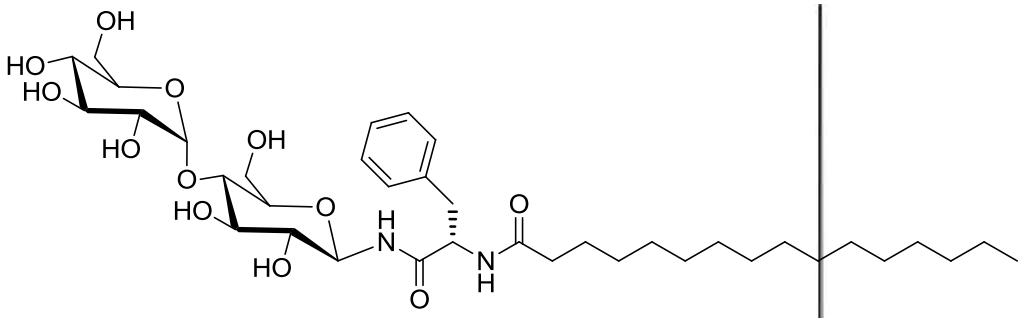

Malt-NH-Phe-C_{16}

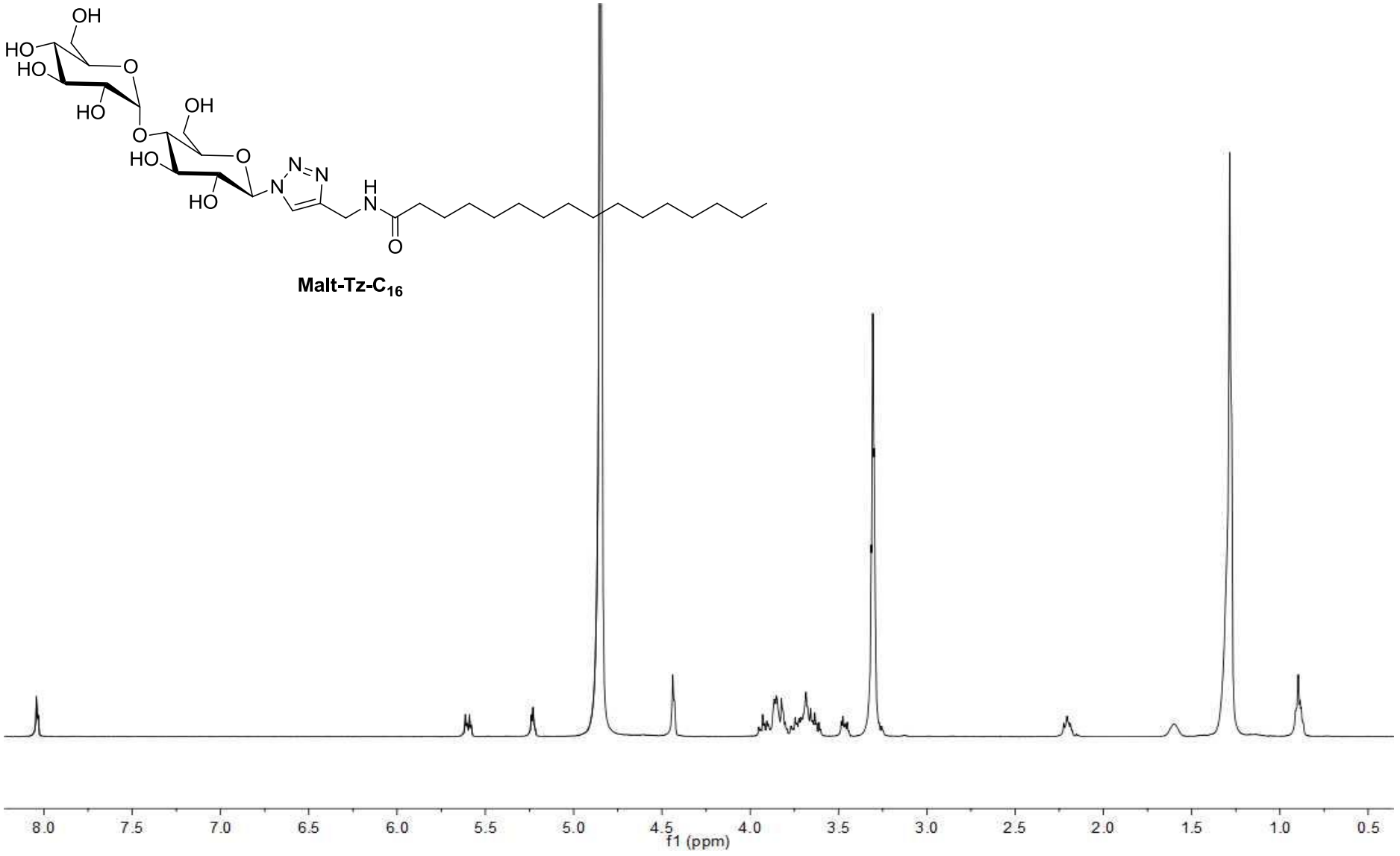
OH
HO
HO
HO
O
OH
O
HO
HO
O
N
N
N
H
N
O
8.0
7.5
7.0
6.5
6.0
5.5
5.0
4.5
4.0
3.5
3.0
2.5
2.0
1.5
1.0
0.5
f1 (ppm)

Malt-Tz-C_{16}

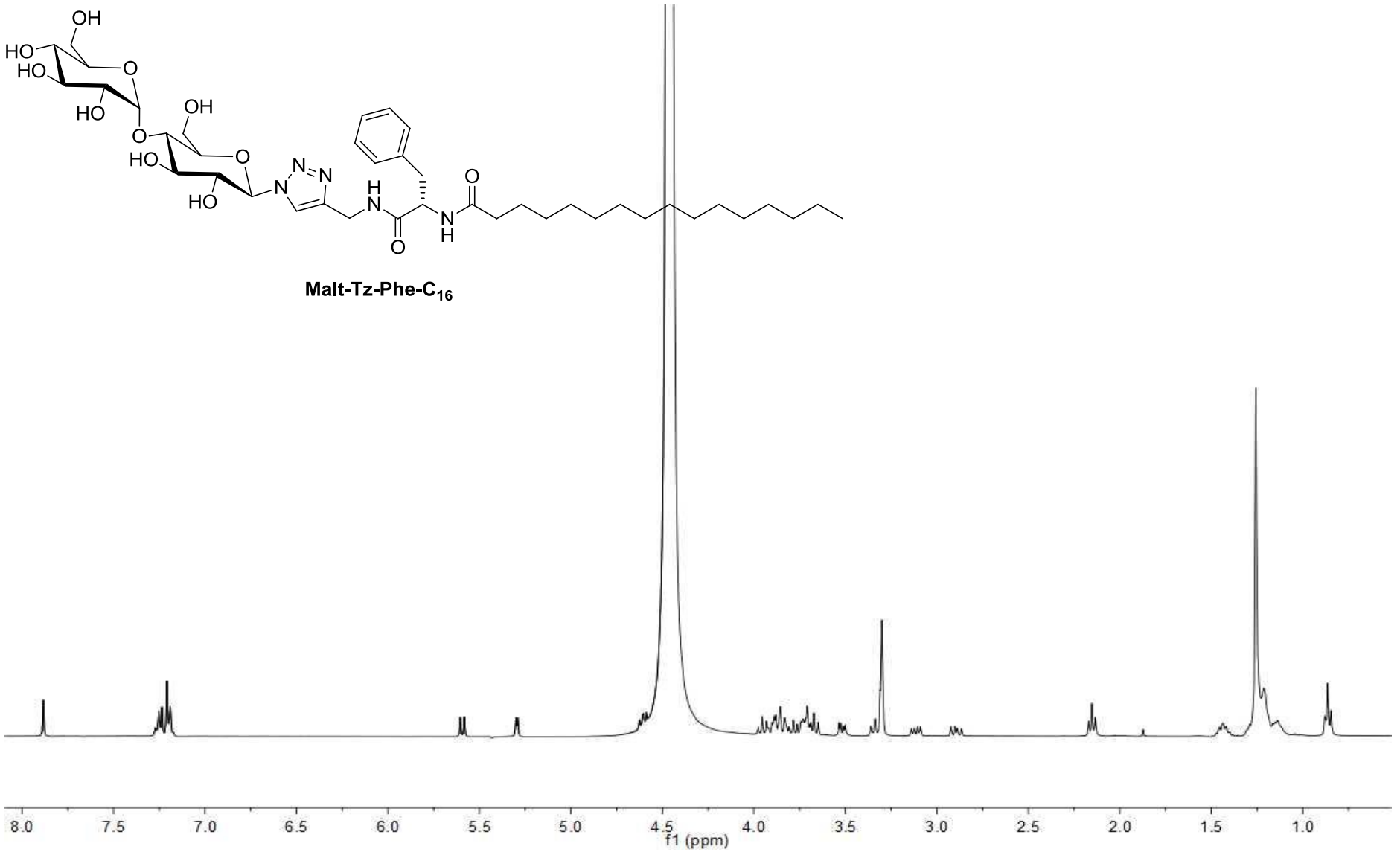

Malt-Tz-Phe-C_{16}

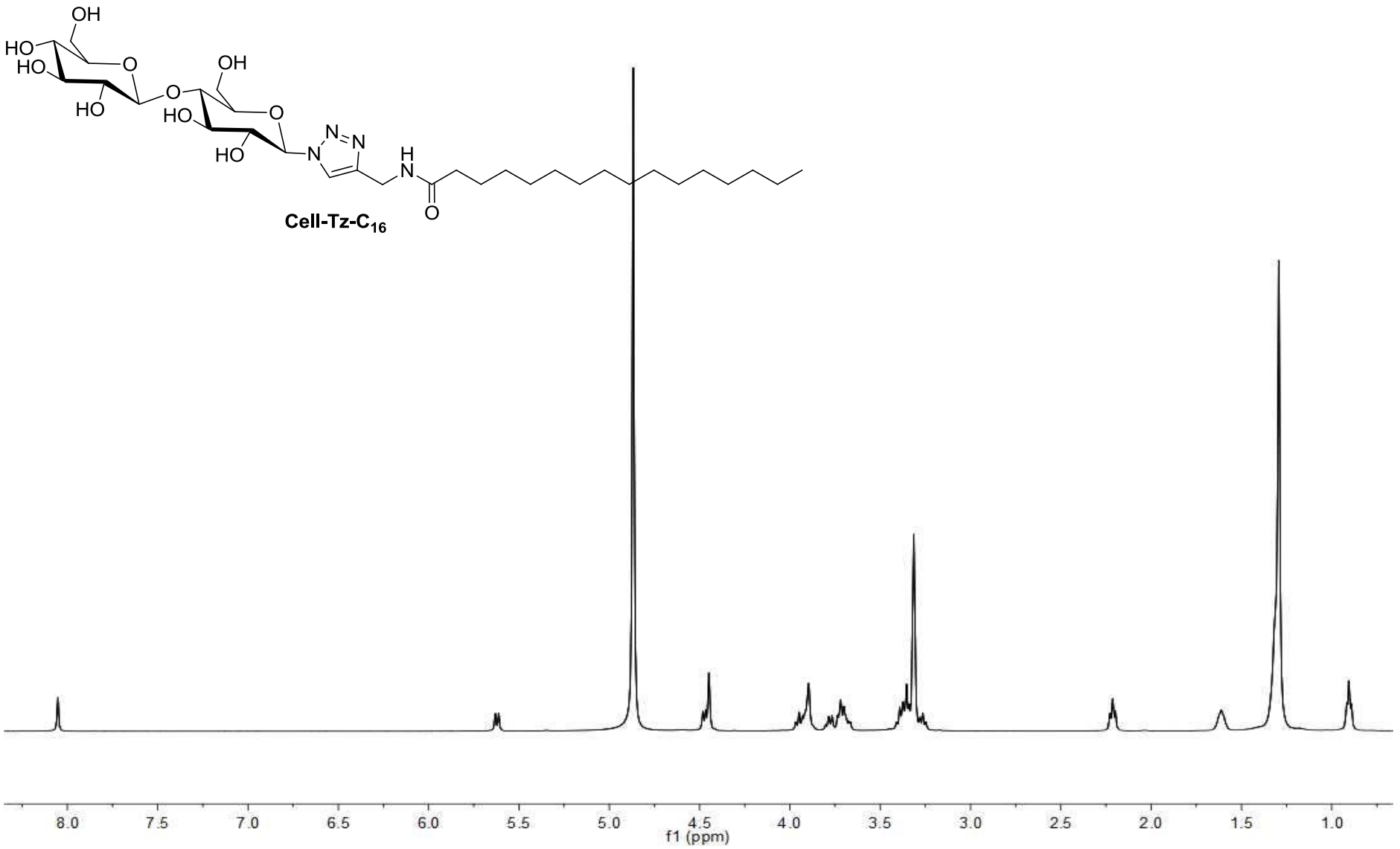
OH
HO
HO
HO
O
O
OH
HO
HO
O
N
N
N
H
N
O
Cell-Tz-C16
8.0
7.5
7.0
6.5
6.0
5.5
5.0
4.5
4.0
3.5
3.0
2.5
2.0
1.5
1.0
f1 (ppm)

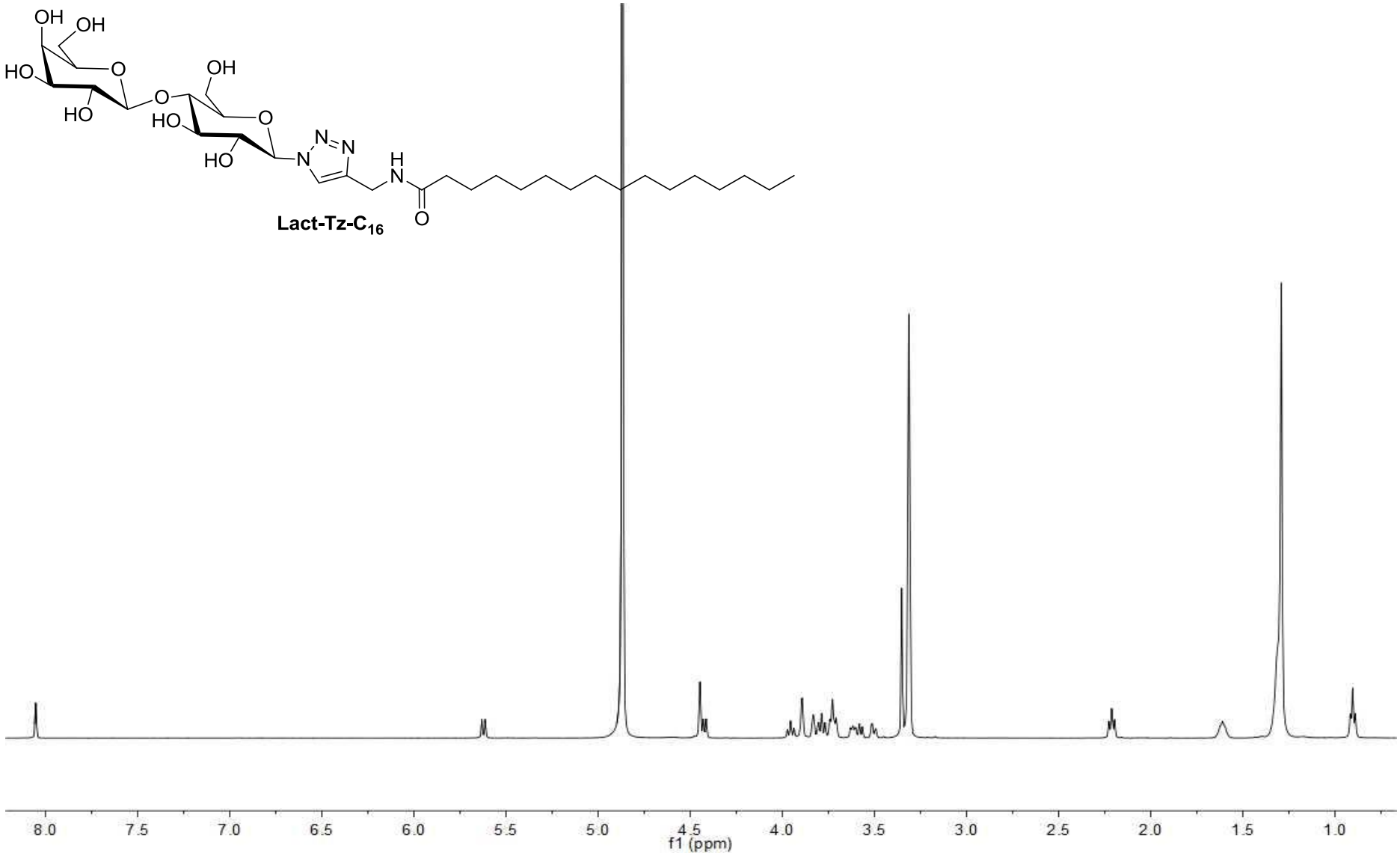
OH
OH
HO
O
HO
O
OH
HO
O
HO
N
N
N
H
N
O
8.0
7.5
7.0
6.5
6.0
5.5
5.0
4.5
4.0
3.5
3.0
2.5
2.0
1.5
1.0
f1 (ppm)

Lact-Tz-C_{16}

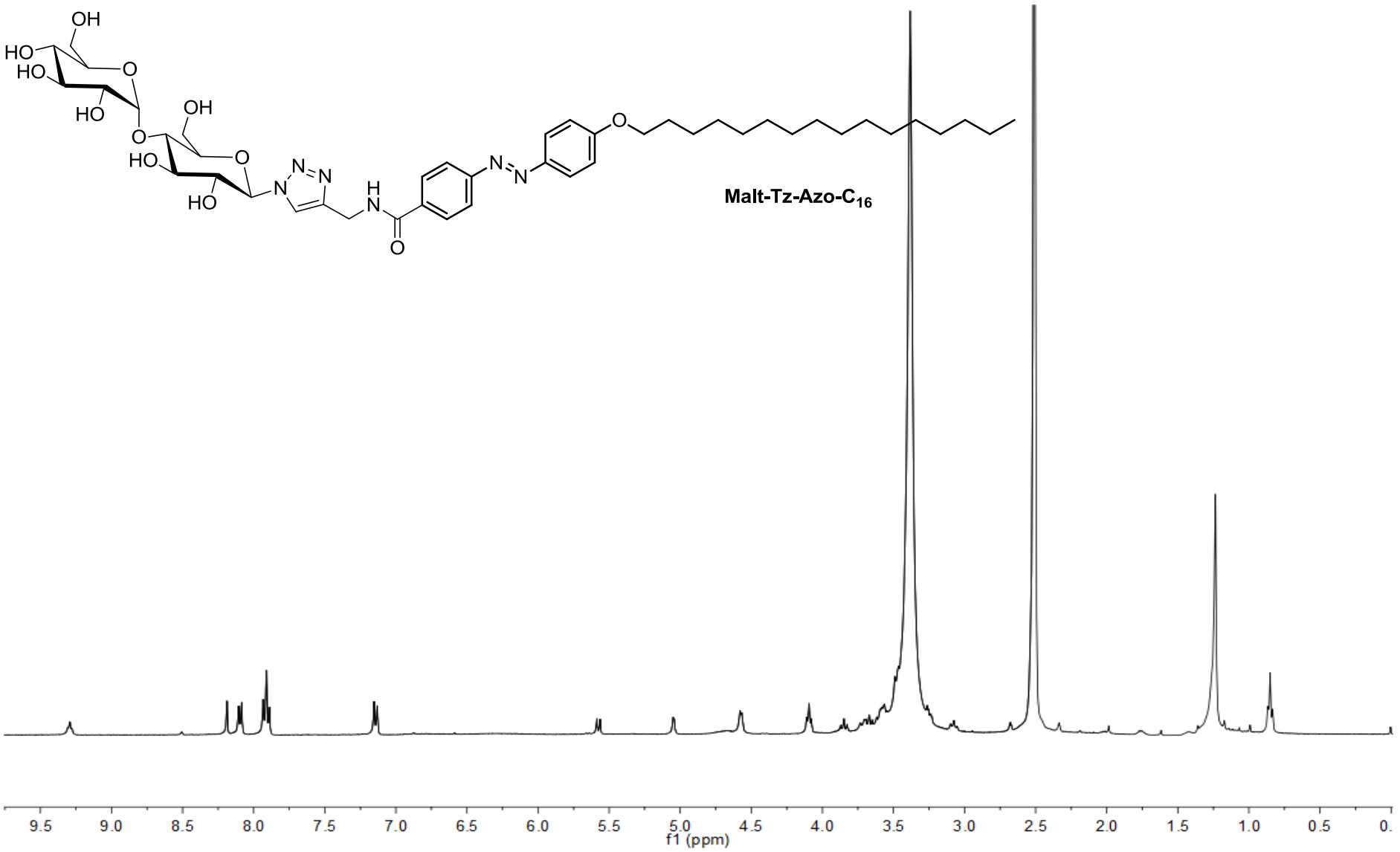
Malt-Tz-Azo-C16
9.5
9.0
8.5
8.0
7.5
7.0
6.5
6.0
5.5
5.0
4.5
4.0
3.5
3.0
2.5
2.0
1.5
1.0
0.5
f1 (ppm)

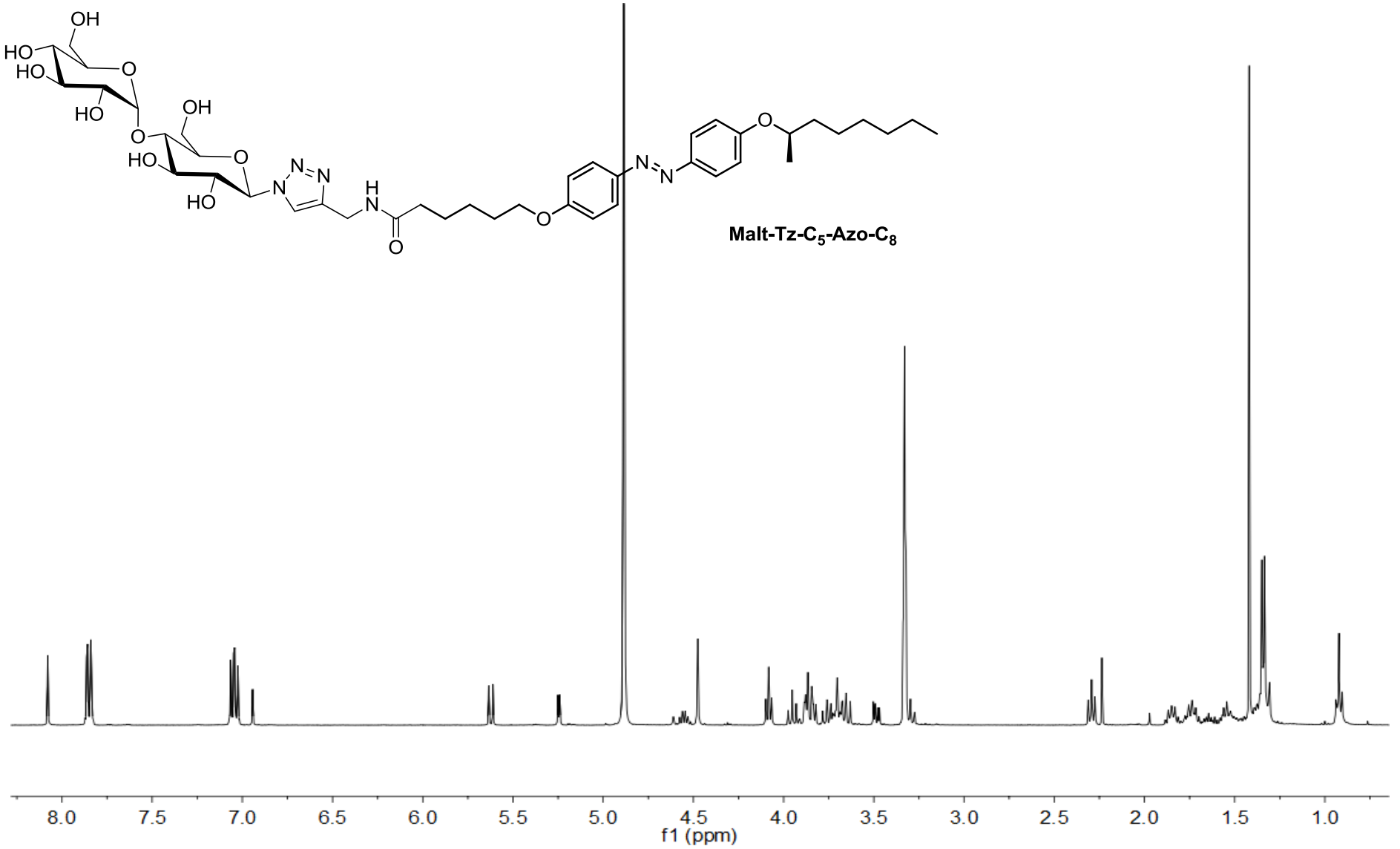
OH
HO
HO
HO
O
OH
O
HO
HO
N
N
N
H
N
O
O
N
N
O
Malt-Tz-C5-Azo-C8
8.0
7.5
7.0
6.5
6.0
5.5
5.0
4.5
4.0
3.5
3.0
2.5
2.0
1.5
1.0
f1 (ppm)

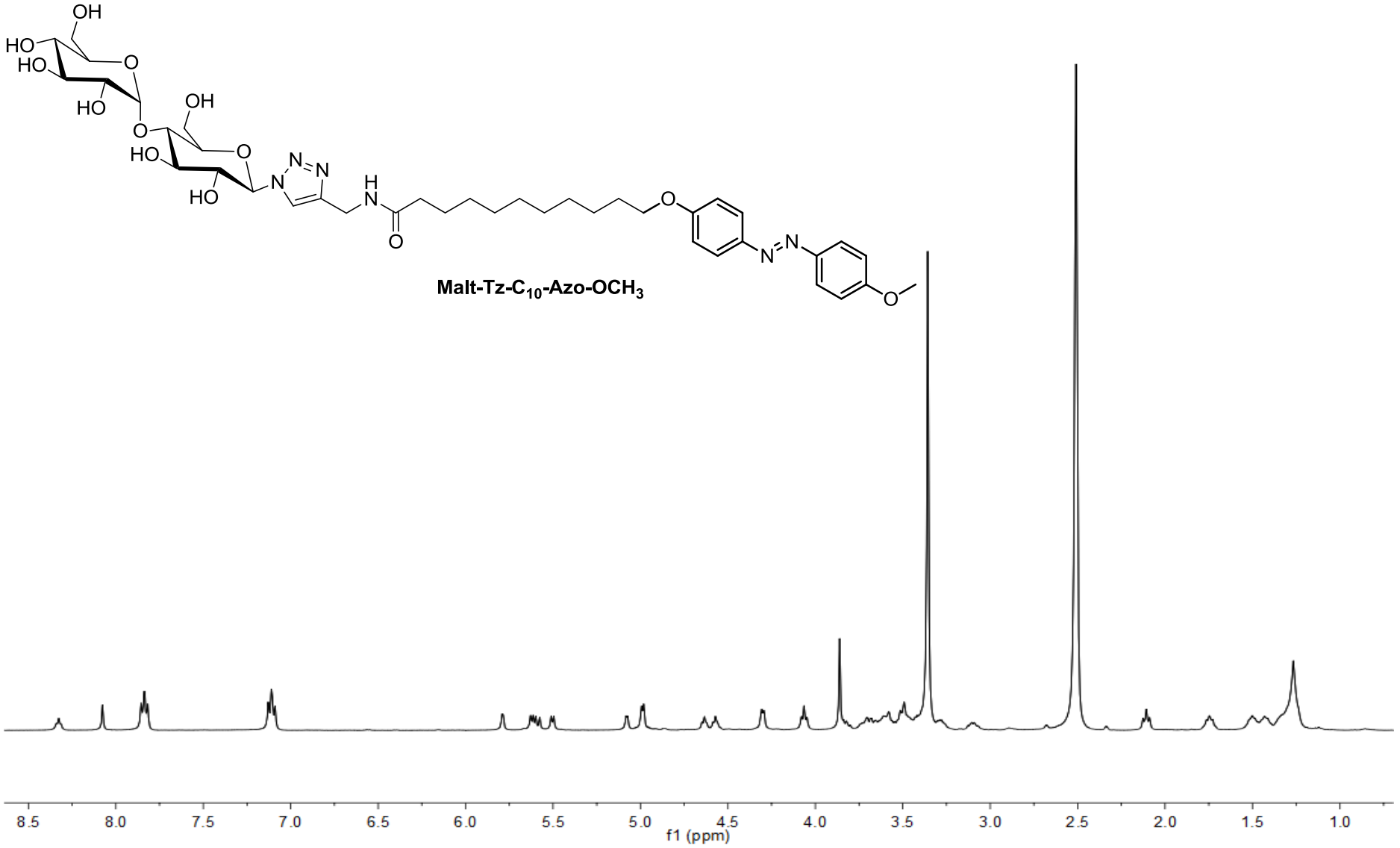
OH
HO
HO
HO
O
OH
O
HO
HO
N
N
N
H
N
O
O
N
N
O
Malt-Tz-C10-Azo-OCH3
8.5
8.0
7.5
7.0
6.5
6.0
5.5
5.0
4.5
4.0
3.5
3.0
2.5
2.0
1.5
1.0
f1 (ppm)

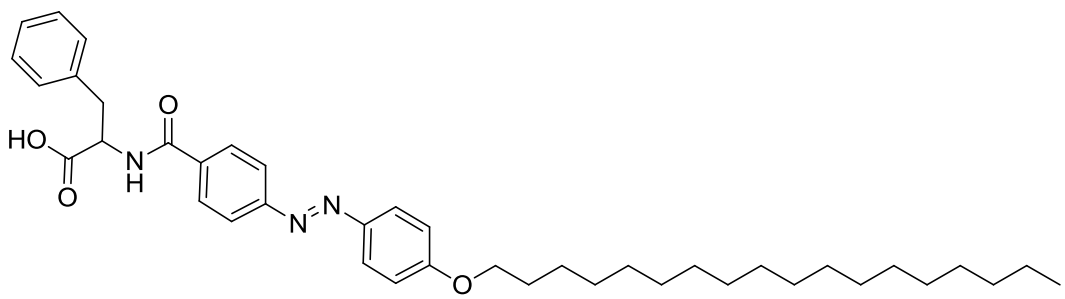

Phe-Azo-C_{18}

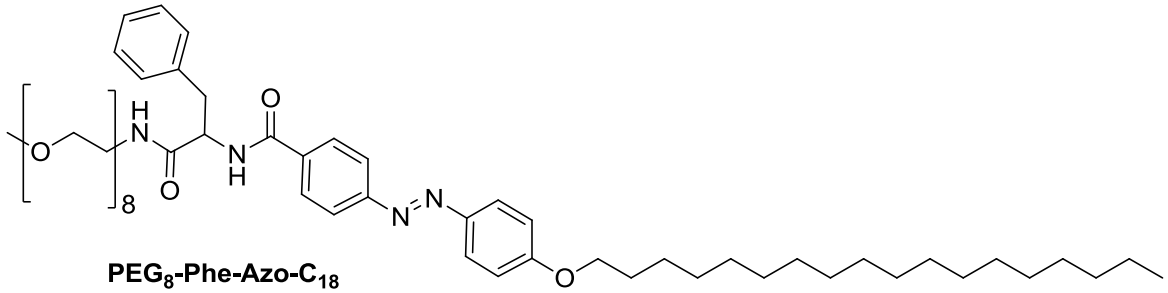

PEG_8-Phe-Azo-C_{18}

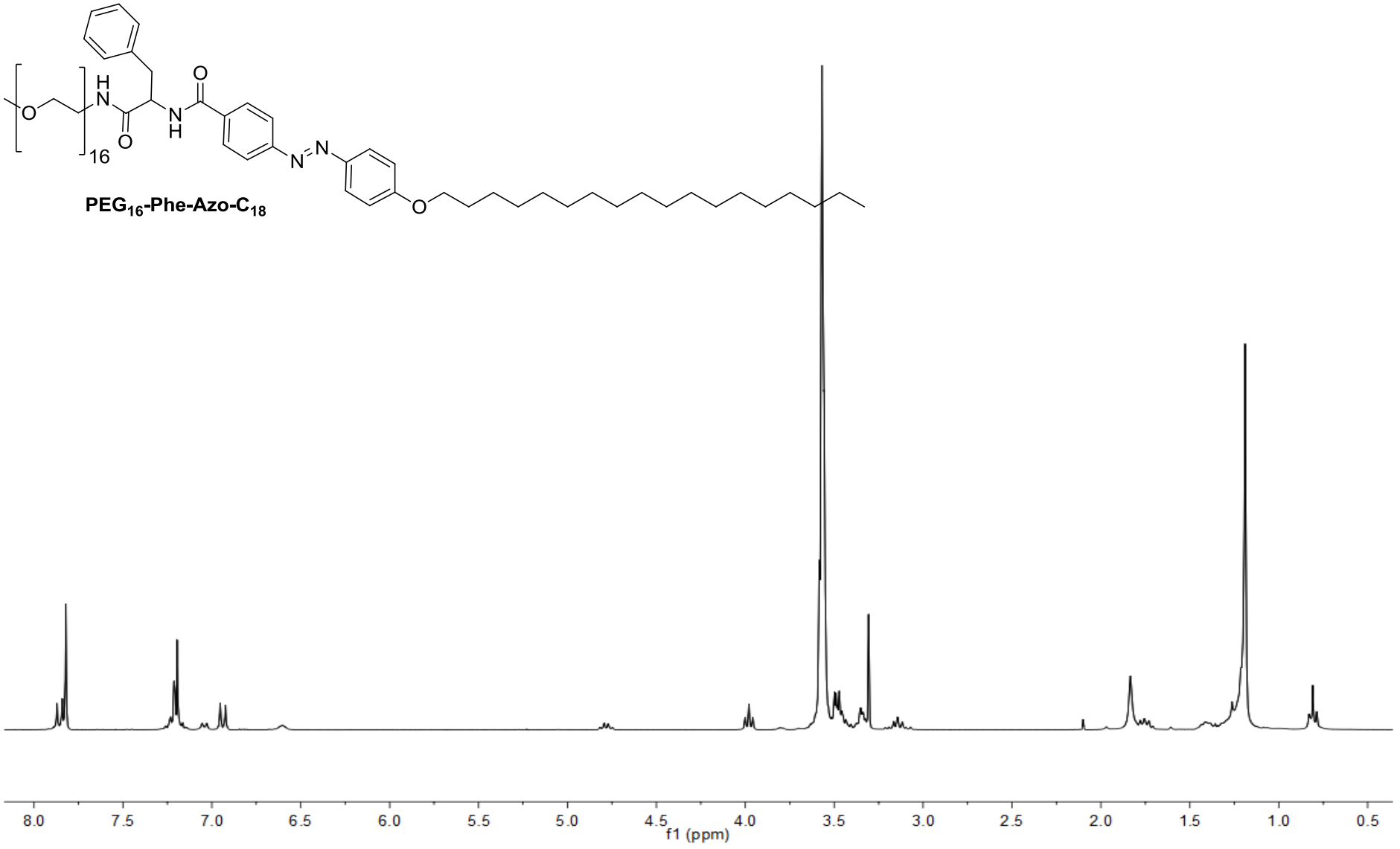
PEG16-Phe-Azo-C18
8.0
7.5
7.0
6.5
6.0
5.5
5.0
4.5
4.0
3.5
3.0
2.5
2.0
1.5
1.0
0.5
f1 (ppm)

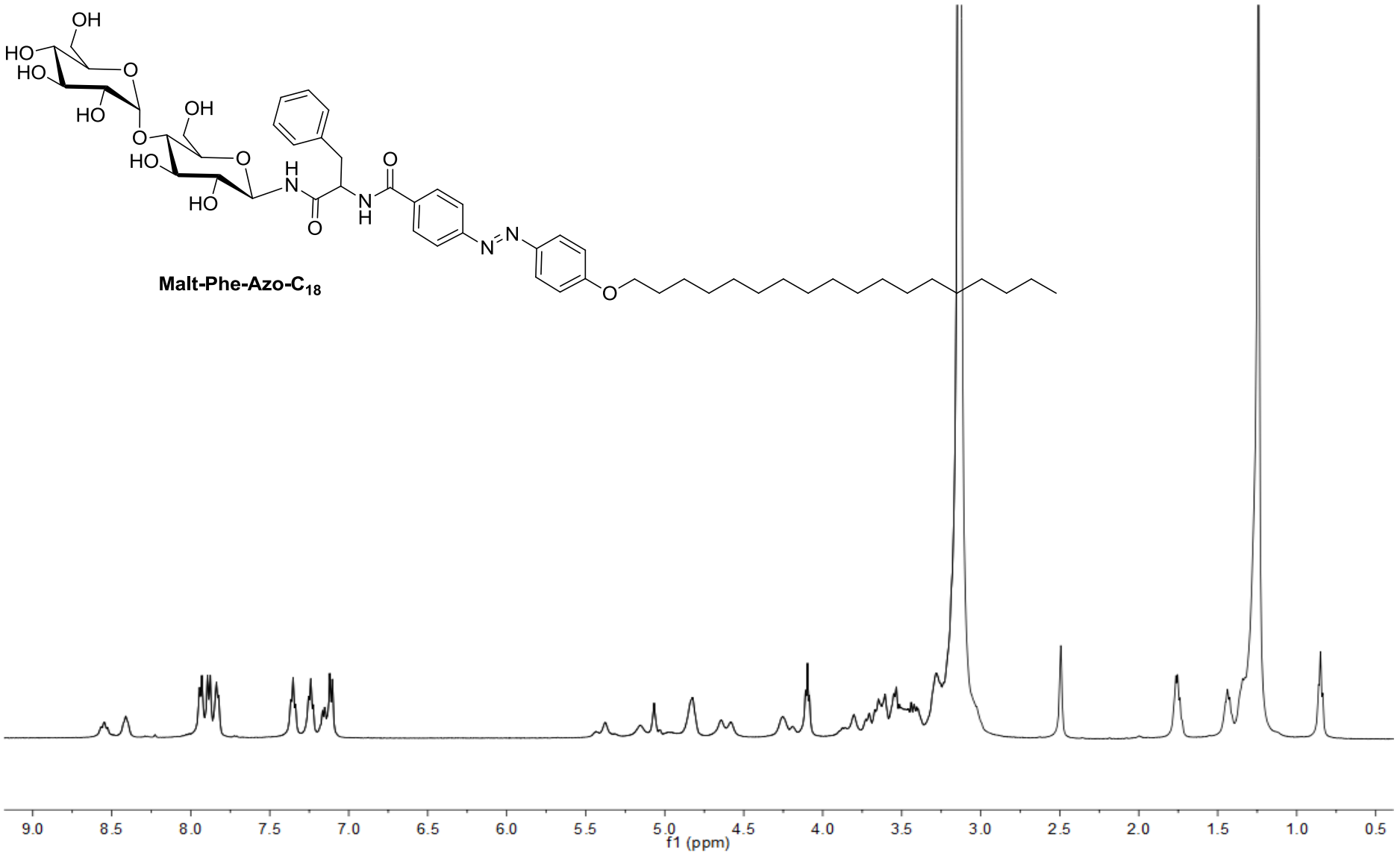
OH
HO
HO
HO
O
OH
O
HO
HO
H
N
O
N
H
O
N
N
O
Malt-Phe-Azo-C18
9.0
8.5
8.0
7.5
7.0
6.5
6.0
5.5
5.0
4.5
4.0
3.5
3.0
2.5
2.0
1.5
1.0
0.5
f1 (ppm)

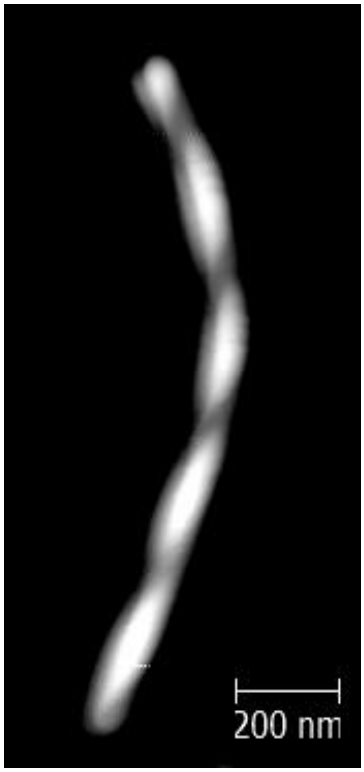

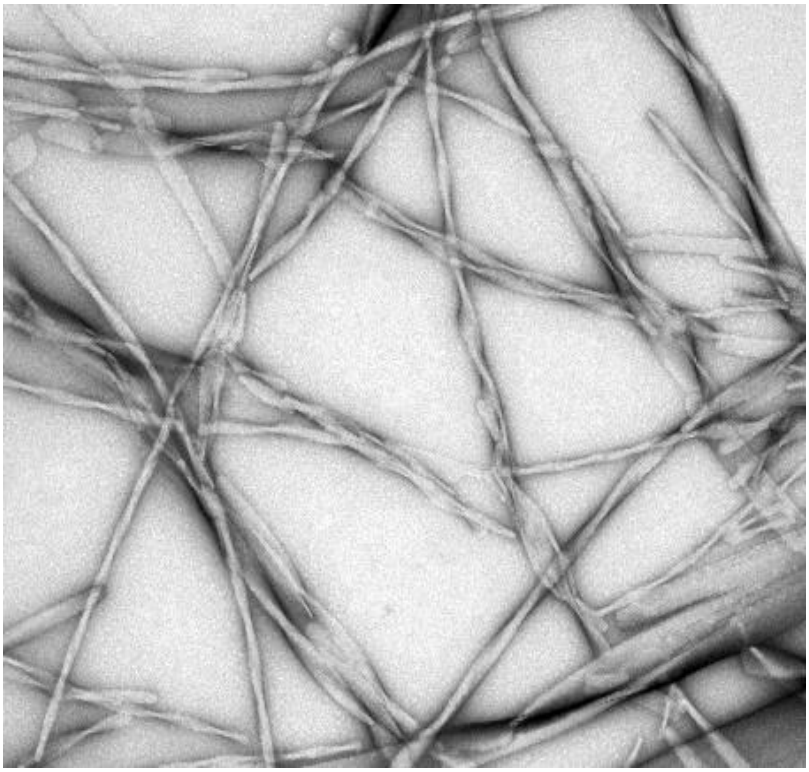

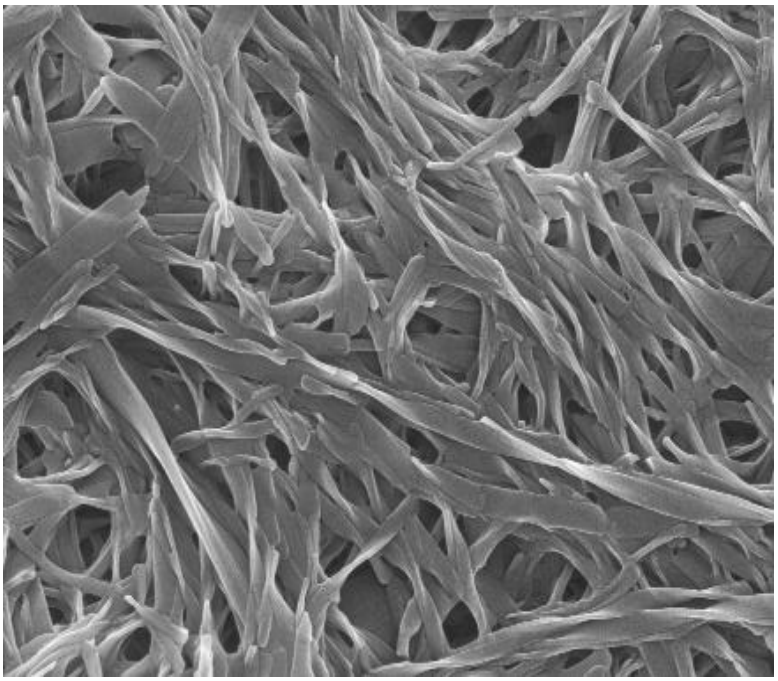

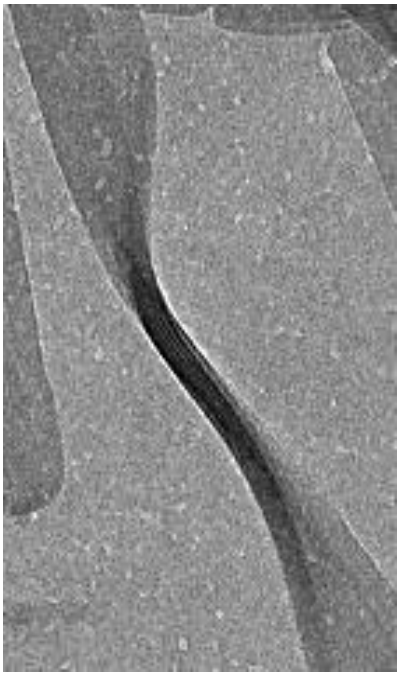

CSIC
1542
Departamento de Química Orgánica
Universidad Zaragoza
cnrs dépasser les frontières
Université de Toulouse
Université Paul Sabatier TOULOUSE III
icma Instituto de Ciencia de Materiales de Aragón
MARIE CURIE ACTIONS
IMRCP